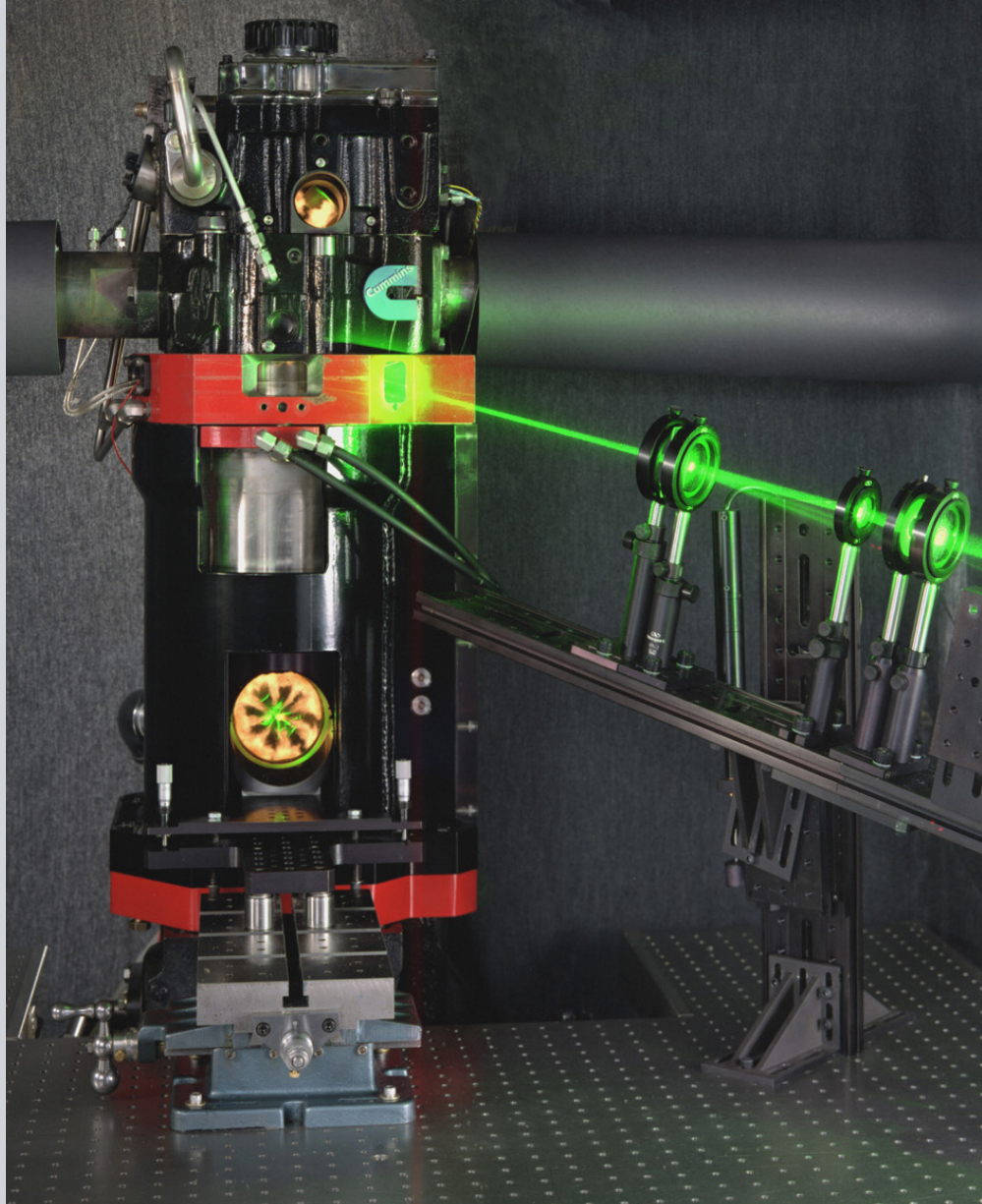


# Advanced Combustion Engines

## 2016 Annual Report

Vehicle Technologies Office



## Disclaimer

This report was prepared as an account of work sponsored by an agency of the United States government. Neither the United States government nor any agency thereof, nor any of their employees, makes any warranty, express or implied, or assumes any legal liability or responsibility for the accuracy, completeness, or usefulness of any information, apparatus, product, or process disclosed or represents that its use would not infringe privately owned rights. Reference herein to any specific commercial product, process, or service by trade name, trademark, manufacturer, or otherwise does not necessarily constitute or imply its endorsement, recommendation, or favoring by the United States government or any agency thereof. The views and opinions of authors expressed herein do not necessarily state or reflect those of the United States government or any agency thereof.

## Acknowledgments

We would like to express our sincere appreciation to Alliance Technical Services, Inc. and Oak Ridge National Laboratory for their technical and artistic contributions in preparing and publishing this report.

In addition, we would like to thank all the participants for their contributions to the programs and all the authors who prepared the project abstracts that comprise this report.

# Nomenclature

## List of Acronyms, Abbreviations, and Definitions

1D	one-dimensional
1MN	1-methylnaphthalene
3D	three-dimensional
3D-CFD	three-dimensional computation fluid dynamics
4SP	four-step protocol
6MR	six-membered ring
Å	angstrom
AC	alternating current
ACE	Advanced Combustion Engine
ACEC	Advanced Combustion and Emissions Control
Ag	silver
AHRR	apparent heat release rate
AIChE	American Institute of Chemical Engineers
AKI	Anti-Knock Index
Al	aluminum
Al <sub>2</sub> O <sub>3</sub>	aluminum oxide
ALCC	ASCR Leadership Computing Challenge
AMR	adaptive mesh refinement
ANL	Argonne National Laboratory
ANR	ammonia-to-NO <sub>x</sub> ratio
APS	Advanced Photon Source
ARC	affordable Rankine cycle
ASCR	Advanced Scientific Computing Research
ASI	after start of injection
ASME	American Society of Mechanical Engineers
ASOI	after start of injection
ASOIm	after start of the main injection
ATDC, aTDC	after top dead center
atm	atmosphere

ATP	Advanced Technology Powertrain
a.u.	arbitrary units
AVFL	Advanced Vehicle/Fuel/Lubricants
BFV	Bradley Fighting Vehicle
BMEP	brake mean effective pressure
BPF	band-pass filter
BPV	bypass valve
BSCO	brake specific carbon monoxide
BSFC	brake specific fuel consumption
BSHC	brake specific hydrocarbon
BTDC	before top dead center
BTE	brake thermal efficiency
$C_2H_4$	ethylene
$C_3H_6$	propene
$C_3H_8$	propane
ca.	circa
Ca	calcium
CA	crank angle
CA5	crank angle at which 5% of the heat has been released
CA50	crank angle at which 50% of the heat has been released
CAD	computer-aided design
CAD	crank angle degrees
CAN	controller area network
CAS	combustion analysis system
cc	cubic centimeter
CCC	$CuO-Ce_3O_4-CeO_2$
CCD	charge-coupled device
CDC	conventional diesel combustion
CEMA	chemical explosive mode analysis
$CeO_2$	cerium(IV) oxide
CFA	Certification Fuel, Batch A

CFD	computational fluid dynamics
CF-E0	Tier II certification gasoline
CFR	constant pressure flow rig
CH <sub>4</sub>	methane
CHA	chabazite zeolite
CHT	conjugate heat transfer
CI	compression ignition
CLEERS	Crosscut Lean Exhaust Emissions Reduction Simulations
CMC	conditional moment closure
CMOS	complementary metal-oxide semiconductor
CMT	CMT-Motores Térmicos
CN	coordination number
CNG	compressed natural gas
CNL	combustion noise level
CO	carbon monoxide
CO <sub>2</sub>	carbon dioxide
Co <sub>3</sub> O <sub>4</sub>	cobalt(II,II) oxide
COV	coefficient of variation
COV <sub>IMEP</sub>	coefficient of variation in indicated mean effective pressure
CP	cyclopentane
CPU	central processing unit
CR	compression ratio
CRADA	cooperative research and development agreement
CRC	Coordinating Research Council
CT	computed tomography
Cu	copper
Cu/GMR6	commercial ceria–zirconia-supported copper catalyst
CuO	copper(II) oxide
Cu/SAPO-34	copper-containing silicoaluminophosphate
Cu-SSZ-13	copper ion-exchanged aluminosilicate zeolite
CV	combustion vessel

CZ	ceria–zirconia
DAQ	data acquisition
dBA	A-weighted decibels
DBI	diffuse back illumination
dBTD	degrees before top dead center
DC	direct current
DC	dynamic NH <sub>3</sub> capacity
DDI-PFS	double direct injection partial fuel stratification
DEF	diesel exhaust fluid
deg	degree
DFE	double fine electrode
DFT	density functional theory
DG	degreened
DI	direct injection
D-LTC	diesel low temperature combustion
DME	dimethyl ether
DM-TJI	dual-mode turbulent jet ignition
DNS	direct numerical simulation
DOC	diesel oxidation catalyst
DOE	United States Department of Energy
DOEs	design of experiments
DPF	diesel particulate filter
DRGEP	directed relation graph with error propagation
DRIFTS	diffuse reflectance infrared Fourier transform spectroscopy
dur	duration
Dyno	dynamometer
E10	10% ethanol, 90% gasoline blend
E20	20% ethanol, 80% gasoline blend
E30	30% ethanol, 70% gasoline blend
ECN	Engine Combustion Network
ECP	ethylcyclopentane

EFA	Exhaust Filtration Analysis
e.g.	<i>exempli gratia</i> (for example)
EGR	exhaust gas recirculation
EINO <sub>x</sub>	normalized NO <sub>x</sub> emission index
EMST	Euclidean Minimum Spanning Tree
ENG	engine
EOI	end of injection
ERC	Engine Research Center at University of Wisconsin-Madison
etc.	<i>et cetera</i> (and so forth)
FA	field-aged
FACE	Fuels for Advanced Combustion Engines
FD9A	Fuels for Advanced Combustion Engines Diesel #9, Batch A
Fe	iron
FE	fuel economy
FEA	finite element analysis
FEM	finite element method
Fe/SSZ-13	iron ion-exchanged aluminosilicate zeolite
FMDF	filtered mass density function
FMEP	friction mean effective pressure
fps	frames per second
FSN	Filter Smoke Number
FTIR	Fourier transform infrared spectroscopy
FTP	Federal Test Procedure
fvL	product of soot volume fraction and line-of-sight path length
$f_{v,max}$	maximum soot concentration
FWHM	full width at half maximum
FY	fiscal year
GC	gas chromatography
GCI	gasoline compression ignition
GDCI	gasoline direct injection compression ignition
GDI	gasoline direct injection

GdZr	gadolinium zirconate
GHSV	gas hourly space velocity
g/kg	grams per kilogram
g/kWh	grams per kilowatt-hour
g/L	grams per liter
GM	General Motors
GOC	gasoline oxidation catalyst
GPF	gasoline particulate filter
GPU	graphical processing unit
GUI	graphical user interface
h	hour
H <sub>2</sub>	diatomic hydrogen
H <sub>2</sub> O	water
HAADF	high-angle annular dark-field imaging
HAB	height above burner
HC	hydrocarbon
HCCI	homogeneous charge compression ignition
HCHO	formaldehyde
HCl	hydrogen chloride
HCT	hydrocarbon trap
HDV	heavy-duty vehicle
HECC	high efficiency clean combustion
HEUI	hydraulically activated, electronically controlled, unit injector
HFIR	High Flux Isotope Reactor
HHX	hot side heat exchanger
HIL	hardware-in-the-loop
HIT	homogeneous ignition temperature
HMN	2,2,4,4,6,8,8-heptamethylnonane
HP	horsepower
HPC	high-performance computing
HP EGR	high pressure exhaust gas recirculation

HR	heat release
HRM	homogeneous relaxation model
HRR	heat release rate
HSE	Heyd-Scuseria-Ernzerhof
HT	hydrothermally
HT-GCI	high temperature gasoline compression ignition
IC	internal combustion
ICC	in-cylinder catalyst
ICE	internal combustion engine
ID	ignition delay
i.e.	<i>id est</i> (that is)
IFPEN	IFP Energies nouvelles
Ign	ignition
IHT	inverse heat transfer
IMEP	indicated mean effective pressure
IMEP <sub>g</sub>	gross indicated mean effective pressure
in	inch
I/O	input/output
IR	infrared
IVC	intake valve closing
K	Kelvin
KH-RT	Kelvin–Helmholtz Rayleigh–Taylor
kHz	kilohertz
kg/m <sup>3</sup>	kilograms per cubic meter
kPa	kilopascal
kW	kilowatt
L	liter
L4	inline four cylinder
LBL	line-by-line
LDV	light-duty vehicle
LE	Lagrangian–Eulerian

LED	light-emitting diode
LES	large eddy simulation
LFE	Laminar Flow Element
LHT	low heat transfer
LLNL	Lawrence Livermore National Laboratory
LMO	lanthanum manganite ( $\text{LaMnO}_3$ )
LNT	lean- $\text{NO}_x$ trap
LP-EGR	low pressure exhaust gas recirculation
LSMO	lanthanum strontium manganese oxide
LTAT	low temperature aftertreatment
LTC	low temperature combustion
LTC-D	low temperature combustion diesel
LTGC	low temperature gasoline combustion
LT-GCI	low temperature gasoline compression ignition
LTP	low temperature plasma
LWP	long wave pass
MBT	maximum brake torque
MCE	multi-cylinder engine
MCP	methylcyclopentane
MDV	medium-duty vehicle
min	minute
MIT	Massachusetts Institute of Technology
mJ	millijoule
MJEI-EMC	micro-jet enhanced ignition components with embedded micro-chamber
mL/s	milliliters per second
mm	millimeter
Mn	manganese
$\text{MnO}_2$	manganese(IV) oxide
MPa	megapascal
mpg	miles per gallon
MPI	Message Passing Interface

m/s	meters per second
ms	millisecond
MSU	Michigan State University
MTU	Michigan Technological University
$N_2$	diatomic nitrogen
NBCX	<i>n</i> -butylcyclohexane
NDE	NO <sub>x</sub> desorption efficiency
NEI	<i>n</i> -eicosane
NG/D	natural gas/diesel
NH <sub>3</sub>	ammonia
NHXD	<i>n</i> -hexadecane
NI	National Instruments
NiO	nickel(II) oxide
NIST	National Institute of Standards and Technology
nm	nanometer
N·m	Newton-meter
NMEP	net mean effective pressure
NMR	nuclear magnetic resonance
NO	nitric oxide
NOD	<i>n</i> -octadecane
NO <sub>x</sub>	oxides of nitrogen
NSE	NO <sub>x</sub> storage efficiency
NSF	National Science Foundation
NSFC	net specific fuel consumption
NSR	NO <sub>x</sub> storage-reduction
NTC	negative temperature coefficient
NVO	negative valve overlap
O	atomic oxygen
O <sub>2</sub>	diatomic oxygen
OASC	optically accessible spark calorimeter
OBD	on-board diagnostics

OH	hydroxide
OLCF	Oak Ridge Leadership Computing Facility
ORC	organic Rankine cycle
ORNL	Oak Ridge National Laboratory
P	phosphorus
<i>P</i>	pressure
PAH	polycyclic aromatic hydrocarbon
$P_c$	compressed pressure
PC	personal computer
PCD	passive cavitation detector
Pd	palladium
PDF	probability density function
PFI	port fuel injection
PFS	partial fuel stratification
PGM	platinum group metal
PIMS	photoionization mass spectrometry
$P_{in}$	intake pressure
$P_{inj}$	injection pressure
PIV	particle image velocimetry
PLIF	planar laser-induced fluorescence
PM	particulate matter
PMC	photon Monte Carlo
PMW	pulse-width modulation
PNA	passive NO <sub>x</sub> adsorber
PNNL	Pacific Northwest National Laboratory
ppm	parts per million
PRF	primary reference fuel
psi	pounds per square inch
Pt	platinum
PT	pressure transducer
PW	pulse width

RANS	Reynolds-averaged Navier–Stokes
RCCI	reactivity controlled compression ignition
RCM	rapid compression machine
RD5-87	87 Anti-Knock Index regular grade gasoline
Re	Reynolds number
RF	radio frequency
RFCDI	radio frequency corona discharge ignition
RI	ringing intensity
ROI	rate of injection
RON	Research Octane Number
rpm	revolutions per minute
RSD	rainbow schlieren deflectometry
RTE	radiative transfer equation
S	sulfur
SA	spark assist
SCCM	standard cubic centimeter per minute
SCE	single-cylinder engine
SCR	selective catalytic reduction
SEM	scanning electron microscopy
SFSM	sequential function specification method
Si	silicon
SIDI	spark ignition direct injection
SMD	Sauter mean diameter
SNL	Sandia National Laboratories
SO <sub>2</sub>	sulfur dioxide
SOC	start of combustion
SOI	start of injection
SpaciMS	spatially resolved capillary inlet mass spectrometry
SPH	smoothed particle hydrodynamics
SPPS	solution precursor plasma sprayed
SSB	secondary streamer breakdown

ST	shock tube
std. dev.	standard deviation
STEM	scanning transmission electron microscopy
STEM-EDS	scanning transmission electron microscopy–energy dispersive X-ray spectroscopy
$t$	time
$T$	temperature
T50	temperature at which 50% is removed
T-50	50% rise time
T90	temperature at which 90% is removed
TALIF	two-photon absorption laser induced fluorescence
TBC	thermal barrier coating
$T_c$	compressed temperature
TC	total NH <sub>3</sub> capacity
TCC	transparent combustion chamber
TCI	turbulence–chemistry interaction
TCR	thermochemical recuperation
TCSRI	turbulence–chemistry–soot–radiation interactions
TDC	top dead center
TDEC	<i>trans</i> -decalin
TE	thermal efficiency
TE	thermoelectric
TEC	thermoelectric converter
TEG	thermoelectric generator
TEM	transmission electron microscopy
TESF	Tabulated Equivalent Strain Flamelet Model
TET	tetralin
TFM	Tabulated Flamelet Model
TGDI	turbo gasoline direct injection
THC	total hydrocarbon
$T_{in}$	intake temperature
TiO <sub>2</sub>	titanium dioxide

TJI	turbulent jet ignition
TMB	1,2,4-trimethylbenzene
TPD	temperature programmed desorption
TPS	Transient Plasma Systems, Inc.
TWC	three-way catalyst
UC	unused NH <sub>3</sub> capacity
UConn	University of Connecticut
U.S.	United States
US06	Supplementary Federal Test Procedure (aggressive, high speed drive cycle)
USAXS	ultra-small X-ray scattering
USCAR	United States Council for Automotive Research
U.S. DRIVE	United States Driving Research and Innovation for Vehicle efficiency and Energy sustainability
UV	ultraviolet
V	volt
VCR	variable compression ratio
VFD	variable-frequency drive
VLE	visible laser extinction
VOF	volume of fluid
vs.	versus
VSL	constant-volume vessel
VVL	variable valve lift
W	watt
w/	with
WHR	waste heat recovery
w/o	without
WSR	well-stirred reactor
wt%	weight percent
XANES	X-ray absorption near edge structure
XES	X-ray emission spectroscopy
XRD	X-ray diffraction
YSI	Yield Sooting Index

YSZ	yttria-stabilized zirconia
YSZ-SP	yttria-stabilized zirconia with structured porosity
Zero-RK	Zero Order Reaction Kinetics software package
Zn	zinc
ZnO	zinc oxide
ZrF <sub>4</sub>	zirconium fluoride
ZrO <sub>2</sub>	zirconium dioxide
zT	figure of merit

### **List of Symbols**

°	degree
°C	degrees Celsius
°CA	crank angle degrees
>	greater than
λ	ratio of actual air–fuel ratio to stoichiometric air–fuel ratio
<	less than
μm	micrometer
μs	microsecond
%	percent
ϕ	fuel–air equivalence ratio
±	plus or minus
×	times

# Executive Summary

On behalf of the Vehicle Technologies Office (VTO) of the U.S. Department of Energy (DOE), we are pleased to introduce the Fiscal Year (FY) 2016 Annual Progress Report for the Advanced Combustion Engine (ACE) program. The VTO mission is to develop more energy-efficient and environmentally friendly highway transportation technologies that can enable the United States to use significantly less petroleum, and reduce greenhouse gas and other regulated emissions while meeting or exceeding drivers' performance expectations. Improving the efficiency of internal combustion engines (ICEs) is one of the most promising and cost-effective approaches to increasing the fuel economy of the United States vehicle fleet over the next several decades. The ACE program supports VTO's mission by addressing critical technical barriers to commercializing higher efficiency, very low emission advanced combustion engines for passenger and commercial vehicles that meet future federal emissions regulations. Advanced fuel formulations that can incorporate non-petroleum-based blending agents may be utilized to enhance combustion efficiency as well as reduce transportation use of petroleum. These advanced combustion engines can reduce the United States transportation petroleum consumption and achieve economic, environmental, and energy security benefits inasmuch as the Energy Information Administration Annual Energy Outlook 2016 reference case scenario forecasts that even in 2040, over 96% of all highway transportation vehicles sold will still have ICEs.

The ACE program undertakes research and development (R&D) activities to improve the efficiency of engines for highway transportation vehicles. The program supports a well-balanced R&D effort that spans fundamental research, applied technology development, and prototype demonstration. The ACE program includes collaborations with industry, national laboratories, and universities in these activities to address critical technology barriers and R&D needs of advanced combustion engines for both passenger and commercial vehicle applications.

Two initiatives launched in FY 2010, the SuperTruck initiative and the Advanced Technology Powertrains for Light-Duty Vehicles (ATP-LD initiative), successfully achieved their FY 2015 goals. All four SuperTruck projects exceeded the FY 2015 goals of a 50% brake thermal efficiency and 50% freight efficiency improvement. The ATP-LD projects achieved the FY 2015 goal of increasing the fuel economy of passenger vehicles by at least 25% using only engine/powertrain improvements. All vehicle fuel economy improvements were achieved while meeting Environmental Protection Agency (EPA) emission standards.

The ACE R&D program subsequently set the following goals for advanced combustion engines to achieve passenger and commercial vehicle fuel economy improvements:

- By 2020, increase the efficiency of ICEs for passenger vehicles resulting in fuel economy improvements of 35% for gasoline vehicles and 50% for diesel vehicles, compared to baseline 2009 gasoline vehicles.
- By 2020, increase the efficiency of ICEs for commercial vehicles from 42% (2009 baseline) to 55% (a 30% improvement) with demonstrations on commercial vehicle platforms.

The program goals have to be achieved while meeting future federal regulations on pollutant emissions that impact air quality. For example, the U.S. EPA Tier 3 emission regulations for passenger cars require over 70% reduction of NO<sub>x</sub>, particulate matter, and hydrocarbon emissions from present day Tier 2 levels.

This report highlights progress achieved by the ACE program during FY 2016. The Introduction outlines the nature, current focus, and recent progress of the ACE program. Also included are 63 abstracts of industry, university, and national laboratory projects that provide an overview of the exciting work being conducted to address critical technical barriers and challenges to commercializing higher efficiency, and cleaner advanced ICEs for light-duty passenger vehicles and medium- to heavy-duty commercial vehicles. We are encouraged by the technical progress realized under this dynamic program in FY 2016, but we also remain cognizant of the significant technical hurdles that lay ahead, especially those to further improve efficiency while meeting the light-duty EPA Tier 3 emission standards and future heavy-duty engine standards for the full useful life of these vehicles.

VTO competitively awards funding through FOA selections and projects are fully funded through the duration of the project in the year the funding is awarded. The future work for direct funded work at the national laboratories is subject to change based on annual appropriations.

Gurpreet Singh, Program Manager  
Advanced Combustion Engine Program  
Vehicle Technologies Office

Roland M. Gravel  
Vehicle Technologies Office

Kenneth C. Howden  
Vehicle Technologies Office

Leo Breton  
Vehicle Technologies Office

# Table of Contents

Acknowledgments . . . . .	i
Nomenclature . . . . .	ii
Executive Summary . . . . .	xvi
I. Introduction . . . . .	1
I.1    Program Overview and Status . . . . .	1
I.2    Technical Highlights . . . . .	5
I.3    Honors and Special Recognitions/Patents . . . . .	18
II. Combustion Research . . . . .	20
II.1    Light-Duty Diesel Combustion . . . . .	21
II.2    Heavy-Duty Low-Temperature and Diesel Combustion & Heavy-Duty Combustion Modeling . . . . .	26
II.3    Spray Combustion Cross-Cut Engine Research . . . . .	32
II.4    Low-Temperature Gasoline Combustion (LTGC) Engine Research . . . . .	36
II.5    Gasoline Combustion Fundamentals . . . . .	42
II.6    Advancements in Fuel Spray and Combustion Modeling with High Performance Computing Resources . . . . .	46
II.7    Fuel Injection and Spray Research Using X-Ray Diagnostics . . . . .	54
II.8    Large Eddy Simulation Applied to Advanced Engine Combustion Research . . . . .	59
II.9    RCM Studies to Enable Gasoline-Relevant Low Temperature Combustion . . . . .	63
II.10    Chemical Kinetic Models for Advanced Engine Combustion . . . . .	68
II.11    Model Development and Analysis of Clean and Efficient Engine Combustion . . . . .	72
II.12    Improved Solvers for Advanced Combustion Engine Simulation . . . . .	76
II.13    2016 KIVA-hpFE Development: a Robust and Accurate Engine Modeling Software . . . . .	81
II.14    Accelerating Predictive Simulation of Internal Combustion Engines with High Performance Computing . . . . .	88

## II. Combustion Research (Continued)

II.15	Use of Low Cetane Fuel to Enable Low Temperature Combustion . . . . .	92
II.16	High Efficiency GDI Engine Research . . . . .	96
II.17	High Dilution Stoichiometric Gasoline Direct-Injection (GDI) Combustion Control Development . . . 100	
II.18	High-Efficiency Clean Combustion in Light-Duty Multi-Cylinder Diesel Engines. . . . .	104
II.19	Stretch Efficiency—Exploiting New Combustion Regimes. . . . .	109
II.20	Cummins-ORNL Combustion CRADA: Characterization and Reduction of Combustion Variations . . 115	
II.21	Neutron Radiography of Advanced Transportation Technologies . . . . .	119
II.22	Ignition and Combustion Characteristics of Transportation Fuels under Lean-Burn Conditions for Advanced Engine Concepts . . . . .	125
II.23	A Comprehensive Investigation of Unsteady Reciprocating Effects on Near-Wall Heat Transfer in Engines . . . . .	131
II.24	Development of a Dynamic Wall Layer Model for LES of Internal Combustion Engines . . . . .	136
II.25	Collaborative Research: NSF/DOE Partnership on Advanced Combustion Engines: Advancing Low Temperature Combustion and Lean Burning Engines for Light- and Heavy-Duty Vehicles with Advanced Ignition Systems and Fuel Stratification. . . . .	140
II.26	Progress Report: NSF/DOE Partnership on Advanced Combustion Engines – Modeling and Experiments of a Novel Controllable Cavity Turbulent Jet Ignition System. . . . .	145
II.27	Collaborative Research: NSF/DOE Partnership on Advanced Combustion Engines: A Universal Combustion Model to Predict Premixed and Non-Premixed Turbulent Flames in Compression Ignition Engines. . . . .	150
II.28	NSF/DOE Partnership on Advanced Combustion Engines: Thermal Barrier Coatings for the LTC Engine – Heat Loss, Combustion, Thermal vs. Catalytic Effects, Emissions, and Exhaust Heat . . . . 157	
II.29	Radiation Heat Transfer and Turbulent Fluctuations in IC Engines – Toward Predictive Models to Enable High Efficiency . . . . .	164
II.30	Sooting Behavior of Conventional and Renewable Diesel Fuel Compounds and Mixtures. . . . .	167
II.31	Micro-Jet Enhanced Ignition with a Variable Orifice Fuel Injector for High Efficiency Lean-Burn Combustion . . . . .	172
II.32	Development and Validation of Predictive Models for In-Cylinder Radiation and Wall Heat Transfer. . . . .	175

## II. Combustion Research (Continued)

II.33	Model Development for Multi-Component Fuel Vaporization and Flash Boiling. . . . .	179
II.34	Evaporation Submodel Development for Volume of Fluid (eVOF) Method Applicable to Spray-Wall Interaction Including Film Characteristics with Validation. . . . .	183
II.35	Development and Validation of a Lagrangian Soot Model Considering Detailed Gas Phase Kinetics and Surface Chemistry . . . . .	190
II.36	Development and Validation of Physics-Based Sub-Models of High Pressure Supercritical Fuel Injection at Diesel Conditions. . . . .	195
II.37	Development of a Physics-Based Combustion Model for Engine Knock Prediction. . . . .	199
II.38	Development and Multiscale Validation of Euler-Lagrange-Based Computational Methods for Modeling Cavitation Within Fuel Injectors . . . . .	203
II.39	Development and Validation of a Turbulent Liquid Spray Atomization Submodel for Diesel Engine Simulations. . . . .	208
III.	Emission Control R&D. . . . .	213
III.1	Joint Development and Coordination of Emission Control Data and Models: Cross-Cut Lean Exhaust Emissions Reduction Simulations (CLEERS) Analysis and Coordination . . . . .	214
III.2	CLEERS Aftertreatment Modeling and Analysis. . . . .	220
III.3	Enhanced High and Low Temperature Performance of NO <sub>x</sub> Reduction Catalyst Materials. . . . .	227
III.4	Thermally Stable Ultra-Low Temperature Oxidation Catalysts . . . . .	232
III.5	Low Temperature Emissions Control . . . . .	237
III.6	Emissions Control for Lean-Gasoline Engines . . . . .	245
III.7	Cummins-ORNL SmartCatalyst CRADA: NO <sub>x</sub> Control and Measurement Technology for Heavy-Duty Diesel Engines . . . . .	250
III.8	Ash-Durable Catalyzed Filters for Gasoline Direct Injection (GDI) Engines. . . . .	255
III.9	Fuel-Neutral Studies of PM Transportation Emissions . . . . .	259
III.10	Next-Generation SCR Dosing System Investigation . . . . .	264
III.11	Metal Oxide-Based Nano-array Catalysts for Low Temperature Diesel Oxidation. . . . .	267
III.12	NSF/DOE Advanced Combustion Engines: Collaborative Research: GOALI: Understanding NO <sub>x</sub> SCR Mechanism and Activity on Cu/Chabazite Structures throughout the Catalyst Life Cycle . .	274

III. Emission Control R&D (Continued)	
III.13 Tailoring Catalyst Composition and Architecture for Conversion of Pollutants from Low Temperature Diesel Combustion Engines . . . . .	279
III.14 Low Temperature NO <sub>x</sub> Storage and Reduction Using Engineered Materials . . . . .	283
IV. High-Efficiency Engine Technologies. . . . .	288
IV.1 Volvo SuperTruck Powertrain Technologies for Efficiency Improvement . . . . .	289
IV.2 Navistar SuperTruck Advanced Combustion Development . . . . .	293
IV.3 Ultra-Efficient Light-Duty Powertrain with Gasoline Low Temperature Combustion . . . . .	298
IV.4 Improved Fuel Efficiency Through Adaptive Radio Frequency Controls and Diagnostics for Advanced Catalyst Systems . . . . .	303
IV.5 Affordable Rankine Cycle . . . . .	310
IV.6 High Efficiency Variable Compression Ratio Engine with Variable Valve Actuation and New Supercharging Technology: VCR Technology for the 2020 to 2025 Market Space . . . . .	314
IV.7 Lean Miller Cycle System Development for Light-Duty Vehicles . . . . .	318
IV.8 Enabling Technologies for Heavy-Duty Vehicles – Cummins 55% BTE . . . . .	322
V. Solid State Energy Conversion . . . . .	326
V.1 Gentherm Thermoelectric Waste Heat Recovery Project for Passenger Vehicles . . . . .	327
V.2 Development of Cost-Competitive Advanced Thermoelectric Generators for Direct Conversion of Vehicle Waste Heat into Useful Electrical Power. . . . .	331
VI. Index of Primary Contacts . . . . .	336
VII. Project Listings by Organization . . . . .	339

(This page intentionally left blank)

# I. Introduction

## I.1 Program Overview and Status

### Developing Advanced Combustion Engine Technologies

The mission of the Vehicle Technologies Office (VTO) of the U.S. Department of Energy (DOE) is to develop more energy-efficient and environmentally friendly highway transportation technologies that can enable the United States to use significantly less petroleum and to reduce greenhouse gas and other regulated emissions while meeting or exceeding drivers' performance expectations. The Advanced Combustion Engine (ACE) R&D program supports VTO's mission by addressing critical technical barriers to commercializing higher efficiency, very low emissions advanced combustion engines for passenger and commercial vehicles that meet future federal emission regulations.

Dramatically improving the efficiency of internal combustion engines (ICEs) is one of the most promising and cost-effective approaches to increasing the fuel economy of the United States vehicle fleet over the next several decades. ICEs already offer outstanding drivability and reliability to over 240 million highway transportation vehicles in the United States, and future technology improvements are expected to make them substantially more efficient and cleaner. Engine efficiency improvements alone can potentially increase the fuel economy of passenger vehicles by 35% to 50% and commercial vehicles by 30% with accompanying carbon dioxide (the primary greenhouse gas) reduction. Advanced fuel formulations that can incorporate non-petroleum-based blending agents may be used to enhance combustion efficiency and reduce petroleum use. Even greater vehicle fuel economy improvement is expected when more efficient engines are coupled with advanced hybrid electric powertrains. Since the Energy Information Administration Annual Energy Outlook 2016 reference case scenario forecasts that even in 2040, over 96% of all highway transportation vehicles sold will still have ICEs, advanced combustion engines will continue to reduce United States transportation petroleum consumption and achieve economic, environmental, and energy security benefits.

The ACE R&D program set the following goals for advanced combustion engines to achieve fuel economy improvements for passenger and commercial vehicles:

- By 2020, increase the efficiency of ICEs for passenger vehicles resulting in fuel economy improvements of 35% for gasoline vehicles and 50% for diesel vehicles, compared to baseline 2009 gasoline vehicles.
- By 2020, increase the efficiency of ICEs for commercial vehicles from 42% (2009 baseline) to 55% (a 30% improvement) with demonstrations on commercial vehicle platforms.

The program goals have to be achieved while meeting future U.S. Environmental Protection Agency (EPA) regulations on pollutant emissions that impact air quality. The expected EPA Tier 3 emissions regulation for passenger cars requires over 70% reduction of oxides of nitrogen ( $\text{NO}_x$ ), particulate matter (PM), and hydrocarbon (HC) emissions from present-day Tier 2 levels.

The ACE program undertakes research and development (R&D) activities to improve the efficiency of engines for highway transportation vehicles. The program supports a well-balanced R&D effort that spans fundamental research, applied technology development, and prototype demonstration. The ACE program collaborates with industry, national laboratories, and universities in these activities to address critical technology barriers and R&D needs of advanced combustion engines for passenger and commercial vehicle applications.

Two initiatives launched in Fiscal Year (FY) 2010, namely the SuperTruck initiative and the Advanced Technology Powertrains for Light-Duty Vehicles (ATP-LD), successfully achieved their goals in FY 2015. Two new ATP-LD projects that were competitively selected and awarded cost-shared contracts in FY 2015 continued in FY 2016 to accomplish the FY 2020 goal for passenger vehicles. Four SuperTruck projects were competitively selected and awarded cost-shared contracts in FY 2016 to accomplish the FY 2020 goal for commercial vehicles.

Competitively selected teams of suppliers and vehicle manufacturers, under contract awards (with 20% to 50% private cost share), continued in FY 2016 to develop and demonstrate innovations capable of achieving breakthrough engine and powertrain system efficiencies while meeting federal emission standards for passenger and commercial vehicles that include long-haul tractor trailers. These projects address the technical barriers inhibiting wider use of these advanced enabling engine technologies in the mass market.

Three-year university research grants totaling \$12 million (equally split between DOE and the National Science Foundation) were awarded in FY 2013 and continued through FY 2016. These grants were competitively selected through an FY 2012 joint solicitation under a Memorandum of Understanding between DOE/VTO and the National Science Foundation. Under these grants, the universities are partnered with industry and national laboratories to advance transformative ideas to develop the enabling understanding for improving the efficiency of ICEs. The grants cover a diverse array of topics that bring to bear experiments, modeling, and analyses to enable more efficient low temperature combustion processes in ICEs. Among the universities/university team(s) receiving grants, nine are focused on improving engine combustion efficiency and three are focused on reducing emissions. Eight university projects to develop computational fluid dynamics models for sprays, heat transfer, and soot that were competitively awarded under a program-wide solicitation continued in FY 2016 to complement the national laboratory efforts in combustion research. Two of the three projects initiated in FY 2011 continued in FY 2016 to develop thermoelectric generators with cost-competitive advanced thermoelectric materials that will improve passenger vehicle fuel economy.

This introduction outlines the nature, current focus, and recent progress of the ACE program. The R&D activities are planned in conjunction with the U.S. DRIVE (Driving Research and Innovation for Vehicle efficiency and Energy sustainability) and the 21st Century Truck Partnership. ACE R&D activities are closely coordinated with the relevant activities of the Fuel and Lubricant Technologies program and the Materials Technology program, also within VTO, due to the importance of clean fuels and advanced materials in achieving high efficiency and low emissions in engines.

### **Current Technical Focus Areas and Objectives**

The VTO ACE program focuses on R&D of advanced engine combustion strategies that will increase the efficiency beyond current state-of-the-art engines and reduce engine-out emissions of  $\text{NO}_x$  and PM to near-zero levels. Engine combustion research focuses on three major combustion strategies: (a) low temperature combustion (LTC), including homogeneous charge compression ignition, pre-mixed charge compression ignition, and reactivity controlled compression ignition; (b) lean-burn (or dilute) gasoline combustion; and (c) clean diesel combustion. In parallel, research is underway to increase emission control systems efficiency and durability to comply with emission regulations at an acceptable cost and with reduced dependence on precious metals.

The ACE program objectives are the following:

- Further the fundamental understanding of advanced combustion strategies that simultaneously show higher efficiencies and very low emissions, as well as the effects of critical factors such as fuel spray characteristics, in-cylinder air motion, heat transfer, and others. Address critical barriers associated with gasoline- and diesel-based advanced engines as well as renewable fuels.
- Improve the effectiveness and durability of emission control (exhaust aftertreatment) devices to complement advanced combustion strategies, as well as reduce their dependence on precious metals to reduce cost, which is another barrier to penetration of advanced combustion engines in the passenger and commercial vehicle markets.
- Improve integration of advanced engine/emissions technologies with hybrid electric systems for greater vehicle fuel economy with lowest possible emissions.
- Develop precise and flexible engine controls, and sensors for control systems and engine diagnostics, to facilitate adjustments of parameters that allow advanced combustion engines to operate over a wider range of engine speed and load conditions.
- Further advance engine technologies such as turbo-machinery, flexible valve systems, advanced combustion systems, and fuel system components to reduce parasitic losses and other losses to the environment, and incorporate technologies such as bottoming cycles or thermoelectric generators to recover energy from the engine exhaust.

The ACE program maintains close collaboration with industry through a number of working groups and teams and utilizes these networks for setting goals, adjusting priorities of research, and tracking progress. These collaborative groups include the Advanced Combustion and Emission Control Tech Team of the U.S. DRIVE Partnership and the Engine Systems Team of the 21st Century Truck Partnership. Focused efforts are carried out under the Advanced Engine Combustion Memorandum of Understanding (which includes auto manufacturers, engine companies, fuel suppliers,

national laboratories, and universities) and the Cross-Cut Lean Exhaust Emission Reduction Simulation (CLEERS) activity for the Advanced Engine Cross-Cut Team.

### **Technology Status and Key Barriers**

Significant advances in engine combustion, emission controls, and advanced engine technologies continue to increase the thermal efficiency of ICEs with simultaneous reduction in emissions. With these advances, gasoline and diesel engines continue to be attractive engine options for conventional vehicles. In addition, these engines can be readily adapted to use natural gas and biofuels such as ethanol and biodiesel, and can be integrated with hybrid and plug-in hybrid electric vehicle powertrains.

LTC strategies such as homogeneous charge compression ignition, pre-mixed charge compression ignition, and reactivity controlled compression ignition exhibit high efficiency with significant reductions in engine-out emissions of  $\text{NO}_x$  and PM to levels that remove or reduce the requirements for exhaust aftertreatment. Progress in LTC strategies continues to expand the operational range, covering speed and load combinations consistent with light-duty and heavy-duty drive cycles. Significant R&D effort has focused on allowing independent control of the intake and exhaust valves relative to piston motion and on other improvements in air handling and engine controls. These address major challenges of fuel mixing, conditioning of intake air, combustion timing control, and expansion of the operational range. Many of these technologies are transitioning to the vehicle market.

Spark-ignition (SI) gasoline engines power the majority of the United States light-duty vehicle fleet and generally operate with stoichiometric combustion to allow use of highly cost-effective three-way catalysts for emission control. Engine technology advances in recent years contributing to substantial improvements in gasoline engine efficiency include direct fuel injection, flexible valve systems, improved combustion chamber design, and reduced mechanical friction. Lean-burn gasoline engines have been introduced in countries with less stringent emission regulations. These engines have higher efficiencies at part load but require more costly lean- $\text{NO}_x$  emission controls to meet the more stringent United States emission regulations. Advances in lean-burn gasoline emission controls are critical for introducing this higher efficiency technology in the United States market.

Attaining the high efficiency potential of lean-burn gasoline technology requires a better understanding of the dynamics of fuel-air mixture preparation; the challenge is in creating combustible mixtures near the spark plug and away from cylinder walls in an overall lean environment. Research focuses on developing a comprehensive understanding of intake air flows and fuel sprays, as well as their interactions with the combustion chamber surfaces over a wide operating range and generating appropriate turbulence to enhance flame speed. Improved simulation tools are being developed for optimizing the lean-burn systems over the wide range of potential intake systems, piston geometries, and injector designs. Another challenge is the reliable ignition and combustion of lean (dilute) fuel-air mixtures. Robust, high-energy ignition systems and mixture control methods are also being developed to reduce combustion variability at lean and highly boosted conditions. Several new ignition systems have been proposed (e.g., high-energy plugs, plasma, corona, laser, etc.) and need to be investigated.

Diesel engines are also well-suited for light-duty vehicle applications, delivering fuel economies that are considerably higher than comparable SI engines. Key developments in combustion and emission controls combined with the availability of low-sulfur diesel fuel have enabled manufacturers to achieve the mandated emission levels and introduce additional diesel-powered models to the United States market. DOE research has contributed to all of these areas. However, diesels in passenger cars have limited market penetration in the United States primarily due to the cost of the added components required to reduce emissions; hence, research continues on increasing engine efficiency and reducing the cost of emissions compliance.

The heavy-duty diesel is the most common engine for commercial vehicles because of its high efficiency and outstanding durability. When R&D efforts over the last decade focused on meeting increasingly stringent heavy-duty engine emission standards, efficiency gains were modest. After meeting EPA 2010 emission standards for  $\text{NO}_x$  and PM, efforts turned to improving the engine efficiency. Continued aggressive R&D to improve boosting, thermal management, and the reduction and/or recovery of rejected thermal energy has resulted in current heavy-duty diesel engine efficiencies in the 43–45% range. Advanced combustion regimes and demonstrated waste heat recovery technologies can potentially improve overall engine efficiency to 55%.

Urea selective catalytic reduction (urea-SCR) technology has been used for  $\text{NO}_x$  control in Tier 2 light-duty vehicles, heavy-duty engines, and other diesel engine applications in the United States. Strategies have been developed and implemented to supply the urea–water solution (given the name “diesel exhaust fluid”) for vehicles. Using urea-SCR, light-duty manufacturers have been able to meet the Tier 2, Bin 5 emissions standard. All heavy-duty diesel vehicle manufacturers have adopted urea-SCR since it has a broader temperature range of effectiveness than competing means of  $\text{NO}_x$  reduction and allows the engine/emission control system to achieve higher fuel efficiency. Although urea-SCR is a relatively mature catalyst technology, more support research is needed to aid formulation optimization and minimize degradation effects such as HC fouling.

Due to the low exhaust temperature (150°C) of advanced engines, emissions of  $\text{NO}_x$  and PM are a significant challenge for lean-burn technologies, including conventional and advanced diesel combustion strategies for light- and heavy-duty engines as well as lean-burn gasoline engines. Advanced LTC strategies have significantly lower  $\text{NO}_x$  and PM engine-out emission levels but higher HC and carbon monoxide (CO) emissions, requiring additional controls which are often a challenge with the low exhaust temperature characteristic of these combustion modes.

The direct injection technology utilized for most advanced gasoline engines produces PM emissions that, although smaller in mass than diesel particulates, may still represent significant emissions in terms of particulate number counts. PM emissions from dilute combustion gasoline engines are not fully understood; their morphology and chemical composition are also affected by combustion. There is a need to develop filtration systems for smaller diameter PM that are durable and with low fuel economy penalty. Fuel economy penalties are caused by increased backpressure and the need to regenerate the filter. The PM aftertreatment effectiveness can be sensitive to fuel sulfur or other contaminants (e.g., ash), extended durability needs to be established, and the feasibility of meeting future more stringent United States regulations has to be confirmed.

Complex and precise engine and emission controls require sophisticated feedback systems employing new types of sensors. A major advancement in this area for light-duty engines has been the introduction of in-cylinder pressure sensors integrated into the glow plug. Start-of-combustion sensors (other than the aforementioned pressure sensor) have been identified as a need, and several development projects have been completed. Sensors are also beneficial for the emission control system.  $\text{NO}_x$  and PM sensors are under development and require additional advances to be cost-effective, accurate, and reliable. Upcoming regulations with increased requirements for onboard diagnostics will also challenge manufacturers trying to bring advanced fuel-efficient solutions to market. The role of sensors and catalyst diagnostic approaches will be key elements of emission control research in the next few years.

Cost is a primary limitation to further adoption of current light-duty diesels. Complex engine and exhaust gas recirculation systems, and the larger catalyst volumes associated with lean  $\text{NO}_x$  traps (LNTs) and diesel particulate filters, result in higher overall costs in comparison to conventional gasoline vehicle systems. LNTs are particularly cost-sensitive because they require platinum group metals, and the cost of these materials is high and volatile due to limited sources that are primarily mined in foreign countries. Improvements in the temperature range of operation for LNTs are also desired to reduce cost and enable success in the lean-gasoline engine application. Both LNTs and diesel particulate filters result in extra fuel use, or a “fuel penalty,” as they require fueling changes in the engine for regeneration processes. Aggressive research has substantially decreased the combined fuel penalty for both devices to less than 4% of total fuel flow; further reductions are possible. Since LNTs have a larger impact on fuel consumption than urea-SCR, most light-duty vehicle manufacturers appear to prefer SCR although urea replenishment is more of a challenge for light-duty customers as compared to heavy-duty vehicle users. Another improvement being pursued for LNT technology is to pair them with SCR catalysts. The advantage is that the SCR catalyst uses the  $\text{NH}_3$  produced by the LNT, so no urea is needed. Formulation and system geometries are being researched to reduce the overall precious metal content of LNT+SCR systems to reduce cost and make the systems more feasible for light-duty vehicles.

Waste heat recovery approaches (e.g., bottoming cycles) are being implemented in heavy-duty diesel vehicles and explored for light-duty diesel and gasoline applications. In current gasoline passenger vehicles, roughly over 70% of the fuel energy is lost as waste heat from an engine operating at full power—about 35% to 40% is lost in the exhaust gases and another 30% to 35% is lost to the engine coolant. Experiments have shown that bottoming cycles have the potential to improve vehicle fuel economy by as much as 10%, and thermoelectric generators can directly convert energy in the engine’s exhaust to electricity for operating auxiliary loads and accessories.

## I.2 Technical Highlights

The following projects highlight progress made in the Advanced Combustion Engine R&D program during FY 2016.

### Combustion Research

The objective of these projects is to develop a greater understanding of engine combustion and how emissions form within the engine. The focus in FY 2016 continued to be on advancing the fundamental understanding of combustion and related in-cylinder processes to achieve higher efficiency and very low engine-out emissions. This was accomplished through modeling of combustion, in-cylinder combustion experiments using optical and other imaging techniques, and parametric studies of engine operating conditions. The following describes what was accomplished in FY 2016.

- Sandia National Laboratories is providing the physical understanding of the in-cylinder combustion processes needed to minimize the fuel consumption and the carbon footprint of automotive diesel engines while maintaining compliance with emission standards. In FY 2016 they: (1) determined the impact of pilot-main dwell on late cycle in-cylinder flow behavior using a newly developed velocimetry technique; (2) experimentally confirmed that with a stepped-lip piston design, indicated efficiency improvements of up to 3% are possible with a simultaneous reduction in soot and  $\text{NO}_x$  emissions; and (3) demonstrated differences in in-cylinder flow resulting from a change in piston design from a conventional re-entrant bowl design to a stepped-lip bowl design. (Busch, report II.1)
- Sandia National Laboratories is developing fundamental understanding of how in-cylinder controls can improve efficiency and reduce pollutant emissions of advanced low-temperature combustion technologies. In FY 2016 they: (1) showed the new engine in-cylinder Spray B liquid length, vapor penetration, ignition delay, and lift-off generally agreed well with constant-volume vessel data; (2) showed progress on development of laser dispersion diagnostics for quantitative in-cylinder scalar dissipation measurement and development of robust coatings for infrared heat transfer imaging diagnostics; and (3) developed new insight on validation of soot models by comparing predicted and measured soot luminosity, including new transfer function. (Musculus, report II.2)
- Sandia National Laboratories is facilitating improvement of engine spray combustion modeling, accelerating the development of cleaner, more efficient engines. In FY 2016 they: (1) organized monthly web meetings for the Engine Combustion Network and developed plans for the next workshop; (2) developed a high-speed diagnostic to quantify the velocity field between plumes of gasoline Spray G, and performed measurements to understand sources of plume interaction and spray collapse; and (3) quantified spray spreading angle, liquid penetration, and ignition and combustion behavior of diesel Spray C (cavitation) and Spray D injectors. (Pickett, report II.3)
- Sandia National Laboratories is providing the fundamental understanding (science-base) required to overcome the technical barriers to the development of practical low-temperature gasoline combustion engines by industry. In FY 2016 they: (1) completed installation and shakedown testing of new spark plug capable, low-swirl cylinder head (Head #2); (2) conducted performance mapping of Head #2 and compared with Head #1 for both premixed and early direct inject fueling—multiple parameters were evaluated and compared; (3) demonstrated crank angle for 50% burn (CA50) control over a wide range (from strong knock to near misfire) using partial fuel stratification produced by a double direct injection (DDI-PFS) with variable injection timing to adjust the fuel stratification and shift CA50; (4) showed that DDI-PFS can substantially increase robustness (i.e., increased exhaust gas recirculation tolerance and allowable CA50 range), and that it can increase stability to extend the load range for some conditions; (5) demonstrated spark-assisted low temperature gasoline combustion for CA50 control and increased tolerance to variation in intake temperature with no increase in  $\text{NO}_x$  emissions; (6) evaluated

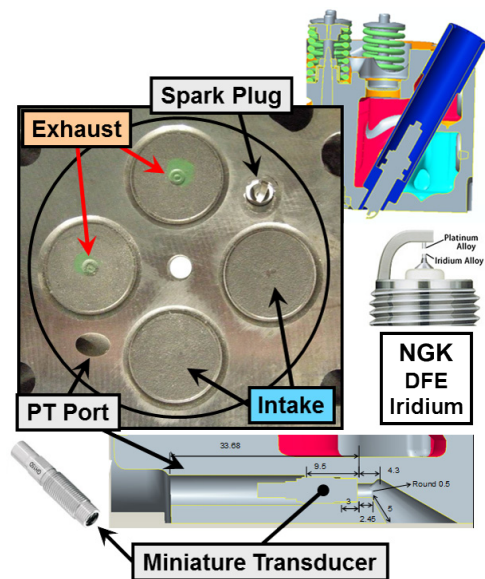
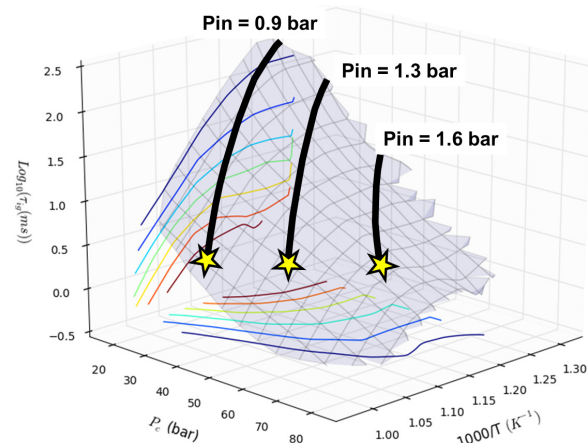


Photo of the new spark plug capable cylinder head and schematics showing the method of mounting the spark plug and the installation of the miniature pressure transducer (PT) through the firedock (Dec, report II.4)

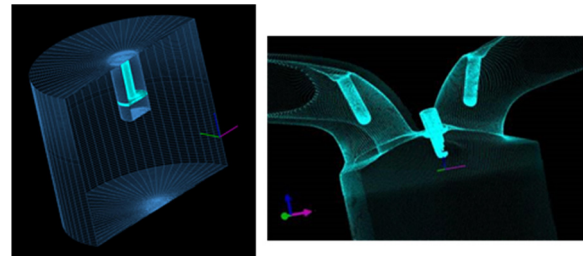
the performance of RD5-87 (87 Anti-Knock Index, E10) regular gasoline and compared to the high-octane, E0 certification gasoline (CF-E0); and (7) collaborated with Lawrence Livermore National Laboratory on development of a kinetic mechanism for RD5-87 and related rapid compression machine measurements at Argonne National Laboratory, and with GM on computational fluid dynamics modeling. (Dec, report II.4)

- Sandia National Laboratories is expanding the fundamental knowledgebase of fluid flow, thermodynamics, and combustion processes needed to achieve clean and fuel-efficient gasoline engines. In FY 2016 they: (1) clarified how in-cylinder generated reformate addition accelerates main-period auto-ignition for low-load, low temperature gasoline combustion; (2) performed first quantitative measure of atomic oxygen from low temperature plasma discharges in air at pressures above 1 atm via two-photon absorption laser induced fluorescence; (3) identified mechanisms responsible for arc transition when close-coupled low temperature plasma are used; and (4) tested rebuilt optically accessible gasoline engine. (Ekoto, report II.5)
- Argonne National Laboratory is developing physics-based nozzle flow and spray models, high-fidelity turbulence models for engine applications, reduced chemical-kinetic models, and high-performance computing tool development on codes used by the industry for internal combustion engine applications. In FY 2016 they: (1) developed a robust approach for predicting in-nozzle flow features for both diesel and gasoline injector applications; (2) developed an approach to couple the flow from inside the injector to the ensuing spray; (3) developed an engineering approach to capture shot-to-shot variation in-nozzle flow and sprays using a random number seed perturbation; (4) developed a high-fidelity turbulence–chemistry interaction model based on tabulating the flamelets; and (5) developed an approach to perform capacity computing, i.e., high-throughput computing on the Mira supercomputer. (Som, report II.6)
- Argonne National Laboratory is studying the fuel injection process by performing detailed, quantitative measurements both inside and outside fuel injector nozzles. In FY 2016 they: (1) achieved a spatial resolution  $<3 \mu\text{m}$  for X-ray tomography of fuel injection nozzles and is now being used by academic and industry partners; (2) characterized Engine Combustion Network Spray C and Spray D injectors and shared the data with the simulations community; and (3) completed simultaneous measurements of the fuel density inside a metal spray nozzle along with fuel distribution outside the nozzle. (Powell, report II.7)
- Sandia National Laboratories is combining unique state-of-the-art simulation capability based on the large eddy simulation technique and applying high-resolution large eddy simulation and first-principles models at conditions unattainable using direct numerical simulation to complement key experiments and bridge the gap between basic and applied research. In FY 2016 they: (1) tested and demonstrated use of a coupled model framework for large eddy simulation that simultaneously treats high-pressure thermodynamics, transport, and turbulence–chemistry interactions; and (2) quantified the combined effects of broadband (small-scale) turbulence and transient mixing dynamics on the development of ignition kernels and combustion. (Oefelein, report II.8)
- Argonne National Laboratory is collaborating with combustion researchers within DOE's Offices of Basic Energy Sciences and Vehicle Technologies Office programs to develop and validate predictive chemical kinetic models for a range of transportation-relevant fuels. In FY 2016 they: (1) acquired additional measurements for research-grade gasoline, blends of this full boiling range fuel with ethanol from E0 to E30 (30% ethanol, 70% gasoline blend), and single-component surrogate candidates, including ignition delay times as well as extents of low- and intermediate-temperature heat release; and (2) continued development of new approaches to accurately quantify uncertainty in the Lawrence Livermore National Laboratory detailed chemical kinetic model for gasoline, and estimated the extent of uncertainty at representative conditions. (Goldsborough, report II.9)



Ignition delay times as a function of inverse temperature and pressure for Fuels for Advanced Combustion Engines Fuel F, where the temperature–pressure trajectories from three engine cycles are overlaid on the surface (Goldsborough, report II.9)

- Lawrence Livermore National Laboratory is developing detailed chemical kinetic models for fuel components used in surrogate fuels for compression ignition, homogeneous charge compression ignition, and reactivity controlled compression ignition engines. In FY 2016 they: (1) developed an improved 2,2,4,4,6,8,8-heptamethylnonane kinetic model; (2) finished development of a complete mechanism for diesel component decalin, including low and high temperature chemistry; (3) validated and improved the chemical kinetic models for Fuels for Advanced Combustion Engines gasoline Fuels F and G using University of Connecticut rapid compression machine experimental data; and (4) updated toluene mechanism and improved its behavior in fuel blends. (Pitz, report II.10)
- Lawrence Livermore National Laboratory is gaining fundamental and practical insight into high-efficiency clean combustion (HCCI) regimes through numerical simulations and experiments, and developing and applying numerical tools to simulate high-efficiency clean combustion by combining multidimensional fluid mechanics with chemical kinetics. In FY 2016 they: (1) performed first “bottom up” uncertainty analysis of HCCI engine experimental measurements and analysis input quantities; (2) developed detailed uncertainty propagation for experimental HCCI engine performance measurements for comparison with simulations; (3) improved robustness of work-sharing methods for graphical processing unit chemistry calculations in parallel computational fluid dynamics; and (4) collaborated with Oak Ridge National Laboratory and General Motors to deploy graphical processing unit chemistry solver on Titan supercomputer for 8,000,000 core-hour Advanced Scientific Computing Research Leadership Computing Challenge award for virtual engine design and calibration. (Whitesides, report II.11)
- Lawrence Livermore National Laboratory is accelerating development and deployment of high-efficiency clean combustion engine concepts through deeper understanding of complex fluid and chemistry interactions. In FY 2016 they: (1) guided the correction of several new mechanisms developed for use in the Advanced Combustion Engine and Co-Optima programs, resulting in faster, more accurate combustion simulations; (2) created several mechanism debugging tools to uncover new errors leading to more robust fuel chemistry models for engine simulation; (3) deployed the first version of the mechanism debugging website for further testing on the internal Lawrence Livermore National Laboratory network; and (4) created the first framework for code verification and validation of the new flame solver using the adaptive preconditioner approach. (McNenly, report II.12)
- Los Alamos National Laboratory is developing algorithms and software for the advancement of speed, accuracy, robustness, and range of applicability of the KIVA internal engine combustion modeling—to be more predictive, and providing KIVA software that is easier to maintain and is easier to add models to than the current KIVA. In FY 2016 they: (1) finished developing a large eddy simulation turbulence model that is capable of spanning transition to turbulence and hence boundary layers; (2) finished developing the KIVA-hpFE to be parallel using Message Passing Interface to facilitate speed of solution of more fully resolved domains and parallel solution method for the moving parts, reactive chemistry, and sprays, showing  $\sim 30\times$  speed-up over serial version; (3) developed implicit solution system for diffusive and stress forces for an extra  $10\times$  speed-up per processor in some cases, giving a  $300\times$  speed-up over the original serial version; (4) started parallelization the *hp*-adaptive finite element methods; (5) continued development of the three-dimensional overset grid system to quickly utilize ‘stl’ file type from grid generator for quick/automatic overset parts surface generation; (6) developed a volume of fluid method for use in spray modeling to be more predictive modeling capability on initial break-up; (7) implemented higher fidelity reactive chemistry packages such as Chemkin-Pro and ZeroRK; and (8) continued validation and verification adding capabilities for many benchmark problems. (Carrington, report II.13)
- Oak Ridge National Laboratory is developing and applying innovative strategies that maximize the benefit of high-performance computing resources and predictive simulation to support accelerated design and development of advanced engines to meet future fuel economy and emissions goals. In FY 2016 they: (1) developed and validated



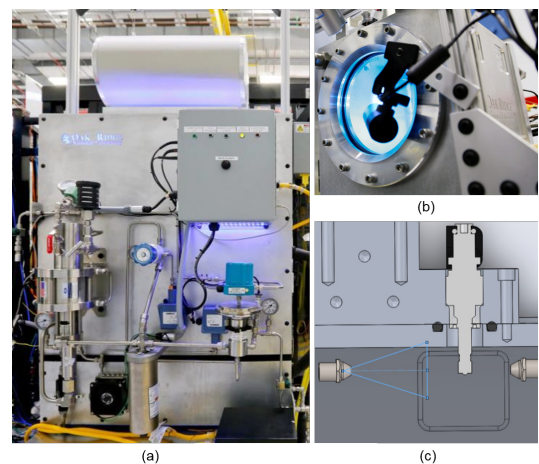
Engine parts to be overlaid onto the grid. (a) Valve overlaying the grid as constructed in GridPro and (b) Sandia's direct injection, spark ignition four-valve engine with spark and injection ports ready for overlaid parts (Carrington, report II.13)

computational fluid dynamics model of a light-duty gasoline direct injection engine; and (2) studied the impact of increasing detailed chemistry on emissions predictions. (Edwards, report II.14)

- Argonne National Laboratory is optimizing engine operating conditions to use low cetane fuel to achieve clean, high-efficiency engine operation and demonstrating the use of low-temperature combustion as an enabling technology for high-efficiency vehicles. In FY 2016 they: (1) determined nozzle inclusion angle effects upon high load combustion noise, particulate matter and  $\text{NO}_x$ ; (2) determined injection strategy requirements to enable transient operation; (3) quantified boost sensitivity of E10 (10% ethanol, 90% gasoline mixture); and (4) continued to develop a strategy for gasoline compression ignition operation for entire speed and load range on E10. (Ciatti, report II.15)
- Argonne National Laboratory is quantifying efficiency potential and combustion stability limitations of advanced gasoline direct injection engines, extending the lean and exhaust gas recirculation dilution tolerance of light-duty gasoline direct injection engines, and developing a three-dimensional computational fluid dynamics methodology to analyze and predict cyclic variability in gasoline direct-injection engines. In FY 2016 they: (1) successfully used X-ray diagnostics to visualize the spark event and characterize the thermal properties of the ignition plasma quantitatively; (2) extended the dilution tolerance with nano-pulse delivery system from Transient Plasma Systems, Inc. with increased pulse repetition rate with respect to conventional ignition and identified opportunities for future improvement; (3) implemented characteristics of the ignition discharge in the ignition model and demonstrated with numerical results that the expanded model is capable of describing the ignition behavior for conventional spark systems; and (4) showed stability and efficiency improvements with numerical simulations by adjusting the laser focal length and protruding the ignition point further in the combustion chamber. (Scarcelli, report II.16)
- Oak Ridge National Laboratory is improving light-duty vehicle fuel economy by developing control strategies that enable high-efficiency, high-dilution, gasoline direct injection engine operation. In FY 2016 they: (1) developed a low order model that effectively simulates the dynamics of cyclic combustion variations for dilute engine operations; (2) implemented model in online engine control system and evaluated differences in model performance between offline simulations and online next cycle predictions; and (3) quantified sensitivity of engine operation to fueling changes at dilute conditions. (Kaul, report II.17)
- Oak Ridge National Laboratory is developing and evaluating the potential of high-efficiency clean combustion strategies with production viable hardware and aftertreatment on multi-cylinder engines. In FY 2016 they: (1) demonstrated 25% increase in dynamometer fuel economy with reactively controlled compression ignition (RCCI) over light-duty drive cycle on transient experiments; (2) developed experimental multi-mode RCCI map suitable for drive cycle simulations; (3) explored the concept of low-delta RCCI in which the difference in reactivity between the high reactivity fuel and the low-reactivity fuel is narrowed; (4) characterized the challenge of emission control at low temperatures associated with high-efficiency combustion concepts including particulate matter; (5) utilized cycle simulation models for evaluating air handling system effects on advanced combustion regimes; and (6) developed thermodynamic models for comparing advanced combustion regimes. (Curran, report II.18)
- Oak Ridge National Laboratory is defining and analyzing specific advanced pathways to improve the energy conversion efficiency of internal combustion engines with emphasis on thermodynamic opportunities afforded by new approaches to combustion. In FY 2016 they: (1) demonstrated thermochemical recuperation under fuel-rich conditions with the catalytic reforming process in the bench flow reactor with a mix of partial oxidation and steam reforming; (2) determined that while sulfur tolerance does impact the  $\text{H}_2/\text{CO}$  ratio during catalytic reforming, the performance of the reforming process is recovered when sulfur is removed from the feed gas; and (3) demonstrated a fuel consumption benefit of over 10% using the catalytic reforming process on the engine at the Advanced Combustion and Emissions Control part-load efficiency point. (Szybist, report II.19)
- Oak Ridge National Laboratory is improving engine efficiency through better combustion uniformity, developing and applying diagnostics to resolve combustion uniformity drivers, understanding origins of combustion non-uniformity and develop mitigation strategies, and addressing critical barriers to engine efficiency and market penetration. In FY 2016 they: (1) developed the new Exhaust Measurement Apparatus for fast simultaneous measurement of  $\text{O}_2$ ,  $\text{H}_2\text{O}$ , temperature, and pressure; (2) measured intra-valve event exhaust transients in engine applications which provide for quantifying cylinder-to-cylinder and cycle-to-cycle combustion variations; (3) specified methodology for integrating

CO measurement into the EGR Probe; and (4) submitted two archival publications, two conference papers, and four oral presentations. (Partridge, report II.20)

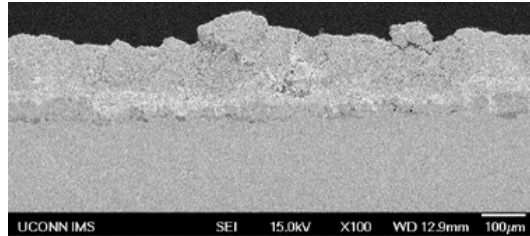
- Oak Ridge National Laboratory is developing high-fidelity neutron imaging capabilities and employing the technique to aid improved design and control of complex advanced combustion systems, and help to guide model validation and input. In FY 2016 they: (1) performed dynamic imaging of fluid dynamics inside gasoline direct injection-based injectors; (2) recorded fuel injection dynamic neutron images using Engine Combustion Network conditions; (3) recorded computed tomography scan of Spray G-type injector in collaboration with Argonne National Laboratory; and (4) performed gasoline direct injection-generated particulate study in gasoline particulate filters. (Toops, report II.21)
- Michigan Technological University is characterizing low temperature combustion of dimethyl ether (DME) through experiment. In FY 2016 they: (1) performed DME and diesel engine bench test with various exhaust gas recirculation levels; (2) explored DME spray and combustion characteristics with multi-hole injector under nonvaporizing, vaporizing, and combusting conditions; (3) provided a fundamental understanding of DME low temperature combustion via combustion vessel experiment; (4) demonstrated engine performance of DME; and (5) built and validated computational fluid dynamics simulations for both combustion vessel tests and engine tests. (Lee, report II.22)
- The University of New Hampshire is using collaborative experiments and numerical simulations to investigate unsteady reciprocating effects on heat transfer in piston engines. In FY 2016 they: (1) acquired near-wall profiles of velocity (using micro-scale particle image velocimetry) and temperature (using planar laser-induced fluorescence) in a motored engine near top dead center; (2) acquired fields of velocity in pulsatile boundary layer flow for various forcing parameters; and (3) identified that an internal shear layer, which emerges just prior to flow deceleration, is the key mechanistic trigger for transition to turbulence in reciprocating flow. (White, report II.23)
- Stanford University is conducting detailed measurements and developing advanced modeling capabilities to improve current understanding about heat transfer, thermal stratification, and non-equilibrium coupling processes in the near-wall region of internal combustion engines that are operated under low-temperature combustion conditions. In FY 2016 they: (1) derived and applied non-equilibrium wall model for thermal boundary layer; (2) performed high-quality heat flux measurements at motored and fired engine conditions; (3) compared model predictions against measurements for wall heat flux; and (4) assessed performance of algebraic models and correlations for heat flux predictions, showing significant discrepancies in capturing peak heat flux. (Ihme, report II.24)
- The University of California, Berkeley is demonstrating extension of engine load and speed limits using partial fuel stratification (PFS) compared to homogeneous charge compression ignition, and developing validated models of PFS. In FY 2016 they: (1) computationally estimated that PFS strategies can result in multiple high-efficiency (>43%) operating points with different combinations of intake pressure, intake temperature, exhaust gas recirculation (EGR), and injection timing; (2) experimentally demonstrated an extension of the EGR dilute limits (16% to 25% at low loads of 8 bar brake mean effective pressure [BMEP], 10% to 15% at high loads of 20 bar BMEP) using a radio frequency corona discharge injection system in a gasoline direct injection single-cylinder research engine, resulting in a maximum reduction in brake specific NO<sub>x</sub> of 73% and maximum reduction in brake specific fuel consumption of 4%; (3) developed a small reduced mechanism for multiple gasoline surrogates containing ethanol under homogeneous charge compression ignition/PFS engine operating conditions using the newly developed reduction approaches with high accuracy; and (4) successfully performed the stratified flame simulation studies for methane, propane, and



System used to study intra-nozzle fluid dynamics of fuel injection include the (a) high pressure fuel delivery system and (b) the aluminum spray chamber with optical viewport. The spray chamber is designed with (c) directed fans to minimize fuel buildup on the chamber walls and the injector. (Toops, report II.21)

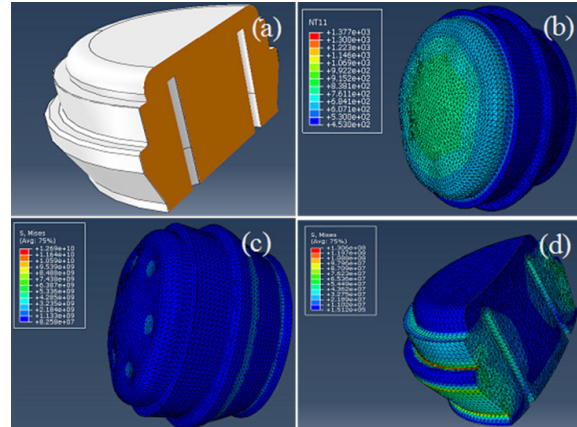
n-heptane, concluding that flame speed enhancement in stratified mixtures is due to preferential diffusion of hydrogen molecules and radicals from the burned gas into the fresh gas. (Dibble, report II.25)

- Michigan State University is examining the active radicals generated in the turbulent jet ignition (TJI) process through both rapid compression machine and optically accessible engine experiments and developing a new large eddy simulation modeling technique to model the TJI system. In FY 2016 they: (1) tested the DM-TJI (dual-mode TJI) system in the rapid compression machine with iso-octane and demonstrated the effects of pre-chamber main/chamber fueling ratio on combustion under ultra-lean conditions; (2) tested the DM-TJI system with liquid gasoline in the single-cylinder engine at a range of lean and dilute conditions with a thermal efficiency greater than 46% achieved; (3) developed and tested a model-based closed-loop combustion control system for the single-cylinder liquid-fueled DM-TJI engine; and (4) conducted large eddy simulation/filtered mass density function and Reynolds-averaged Navier-Stokes modeling of THJ in a coupled pre-chamber rapid compression machine for a series of TJI configurations to study the effects of various flow/flame parameters. (Toulson, report II.26)
- The University of Connecticut is developing a predictive turbulent combustion model that is universally applicable to mixed regimes of combustion including elements of both premixed and non-premixed flames in the presence of local limit phenomena such as extinction and autoignition. In FY 2016 they: (1) developed a dynamic adaptive combustion modeling framework based on chemical explosive mode analysis (CEMA); (2) developed an explicit CEMA approximation to enable efficiency on-the-fly CEMA in three-dimensional simulations; (3) implemented the dynamic adaptive model into the CONVERGE software for engine combustion simulations; (4) developed a tabulated flamelet model for large eddy simulation of engine combustion, which can be potentially integrated into the universal modeling framework; (5) developed a statistical averaging method for large eddy simulation spray flames; and (6) performed three-dimensional direct numerical simulation of a turbulent n-dodecane temporal jet in counterflowing air and a turbulent lifted dimethyl ether jet flame, both cases involve with negative temperature coefficient effect. (Lu, report II.27)
- Clemson University is elucidating the impact of thermal barrier coatings on low-temperature combustion (LTC) efficiency, operating range and emissions; developing ceramic and metallic piston coatings that increase thermal and combustion efficiency without decreasing volumetric efficiency; and developing simulation tools to predict temperature gradients and coating surface temperature swings. In FY 2016 they: (1) developed and refined the “Fuel Match/Phase Match” operational procedure; (2) assessed candidate materials for in-cylinder catalytic coatings based on literature review and communication with Oak Ridge National Laboratory; (3) refined yttria-stabilized zirconia with structured porosity (YSZ-SP) spray parameters including utilization of a dense top coat; (4) assessed YSZ-SP impact on LTC emissions, heat transfer, and efficiency, including lessons learned regarding coating morphology and durability; (5) assessed impact of the YSZ thermal barrier coatings on surface temperature and heat flux via the inverse heat condition sequential function specification method solver; (6) completed simulation analysis of surface temperature sensitivity to coating thermal and physical properties; and (7) developed a novel low-conductivity coating based on gadolinium zirconate material. (Filippi, report II.28)
- The Pennsylvania State University is quantifying effects of radiative heat transfer and turbulent fluctuations in composition and temperature on combustion, emissions, and heat losses in internal combustion engines; developing computational fluid dynamics-based models to capture these effects in simulations of in-cylinder processes in internal combustion engines; and exercising models to explore advanced combustion concepts for internal combustion engines to develop next-generation high-efficiency engines. In FY 2016 they: (1) continued coupled simulations using different spectral models and radiative transfer equation solvers; (2) coupled soot and radiative models with a transported probability density function method to account for effects of unresolved turbulent fluctuations in engines; and (3) performed photon Monte Carlo/line-by-line/probability density function simulations of a high-pressure turbulent spray flame where experimental measurement are available, which provided new insights into earlier radiation measurements for this flame. (Haworth, report II.29)



Third generation YSZ-SP coating with optimized porosity and higher thickness (Filippi, report II.28)

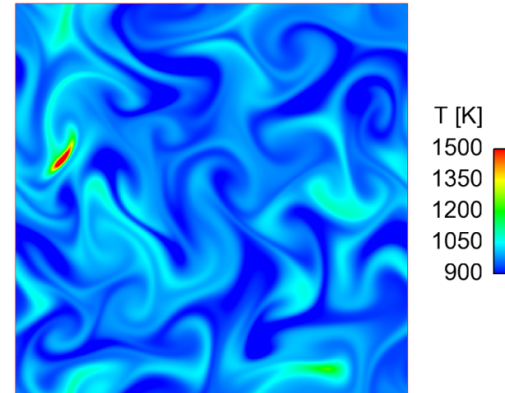
- Yale University is developing a knowledge base that allows surrogate mixtures to be formulated that match the sooting behavior of any given real diesel fuel. In FY 2016 they: (1) measured sooting tendencies of 25 components of proposed diesel surrogates, including all nine components of the first generation Coordinating Research Council surrogates; (2) measured sooting tendencies for all of the Coordinating Research Council surrogate mixtures and several reference diesel fuels; (3) developed two procedures for predicting the sooting tendencies of surrogate mixtures; (4) posted the measured two-dimensional soot and temperature data to the internet to maximize its availability to the research community; and (5) involved two high school students and two undergraduates in scanning transmission electron microscopy research. (Pfefferle, report II.30)
- The University of Illinois at Urbana–Champaign is designing and configuring an alpha version of the micro-jet enhanced ignition components with embedded micro-chamber which only needs one direct injection fuel injector without modifying cylinder head structure and spark plug. In FY 2016 they: (1) purchased and installed optical engine components, including optical mirror, piston rings, and optical piston head; (2) installed ignition coil and spark energy booster; (3) modified the LabVIEW code for injection and spark control parameters; (4) fully assembled the optical engine; (5) finalized the injector design; (6) performed preliminary metal engine combustion analysis; and (7) obtained combustion traces. (Lee, report II.31)
- The Pennsylvania State University is quantifying the relative importance of turbulent boundary layer wall heat transfer, radiative transfer, and boundary layer/radiation couplings in engines. In FY 2016 they: (1) implemented multiple wall heat transfer and radiation models in OpenFOAM, and exercised models to guide the design of the engine experiments; (2) implemented a baseline wall heat transfer model in RAPTOR; (3) procured the infrared camera for the University of Michigan engine laboratory; and (4) planned the FY 2017 metal engine experiments. (Haworth, report II.32)
- The University of Illinois at Urbana–Champaign is designing and developing a multi-component fuel droplet and wall film vaporization model using both discrete and continuous thermodynamics methods. In FY 2016 they: (1) obtained promising results performing one-way coupling validation of single-component gasoline-type fuel in gasoline direct injection systems for the multi-component flash boiling model; (2) performed preliminary set of flash boiling simulations for different fuels including iso-octane, ethanol, and binary blends of iso-octane and ethanol; (3) established the workflow for KIVA sprays simulation and tested the capability of the current models; and (4) developed the modular droplet evaporation model. (Lee, report II.33)
- Michigan Technological University is proposing research to develop, implement, and validate a volume of fluid modeling approach including vaporization integrated into computational fluid dynamics codes to provide accurate and predictive simulation of spray–wall interactions without extensive need of parameters tuning. In FY 2016 they: (1) completed finite element analysis of metal impinging window for heat, displacement and local load capabilities, and finalized locations of heaters and thermocouples; (2) finished two different drawings of metal impinging windows (with and without heaters); (3) finished the design and drawing of injector window with an off axis (1 in) injector mount; (4) designed single-hole injector nozzles with 120° full-included angle with two different fuel injector nominal nozzle outlet diameters (100  $\mu\text{m}$  and 200  $\mu\text{m}$ ); (5) established collaboration work of impingement research with Istituto Motori in Italy; (6) developed and implemented automated tools for extraction of liquid droplet information and physical properties at location of interest within the simulated sprays; (7) completed data acquisition layout for temperature and heat flux measurement; (8) conducted the first spray–wall interaction test with seven-hole diesel injector; (9) validated the state-of-the-art spray models in the CONVERGE framework; and (10) developed capabilities to extract the required



(a) Impingement window final design/configuration; (b) temperature distribution; (c) von Mises stress distribution; (d) von Mises stress distribution with 350 bar load (Lee, report II.34)

pre-impingement droplet characteristics from Lagrangian–Eulerian computational fluid dynamics simulations. (Lee, report II.34)

- The University of Wisconsin–Madison is improving soot modeling capabilities in government sponsored and commercial computational fluid dynamics codes to enable the engine industry to design high-efficiency, clean engines for transportation applications. In FY 2016 they: (1) identified detailed reaction mechanism containing polycyclic aromatic hydrocarbon chemistry up to benzo[a]pyrene; (2) implemented benzo[a]pyrene and ethanol chemistry into an existing toluene reference fuel mechanism to enable simulation of fuels ranging from ethanol containing gasoline to high aromatic content diesel fuel; (3) compared mechanism predictions to data from the literature; (4) developed framework to model soot using a Lagrangian approach; and (5) performed high-speed imaging of conventional and low temperature diesel combustion at several injection pressures and range of start of injection timings. (Kokjohn, report II.35)
- The University of Alabama is producing a validated real-fluid property code which can be integrated with computational fluid dynamics solvers to improve their accuracy in simulating high-pressure diesel sprays. In FY 2016 they: (1) designed and commissioned for construction a constant pressure flow rig for non-reacting experiments; (2) optimized high-speed rainbow schlieren deflectometry optical setup for diagnostics in constant pressure flow rig facility; (3) modified and developed schlieren analysis codes to obtain equivalence ratio and liquid penetration depth; (4) evaluated various existing equations of state and methodologies to assess their appropriateness and accuracy in describing correlations between the thermal properties and their corresponding transport properties at the high-pressure conditions; (5) developed a stand-alone numerical module to calculate thermo-physical properties based on the selected real-fluid model, or to interpolate the database of real-fluid thermal properties available; and (6) validated the developed real-fluid property with the available property data. (Agrawal, report II.36)
- The Ohio State University is developing a predictive combustion model for engine knock, which can capture turbulence–chemistry interactions in a physics-based way and incorporate detailed chemistry into large eddy simulation of in-cylinder turbulent reacting flows. In FY 2016 they: (1) developed a base computational code for the combustion model; (2) generated and analyzed direct numerical solution data for turbulent premixed flame propagation; (3) generated detailed chemistry direct numerical solution data for end-gas ignition; and (4) acquired experimental in-cylinder sampling hardware, and operating conditions were fully defined. (Kim, report II.37)
- Boston University is developing and validating physics-based mathematical submodels for use in standard multiphase computational fluid dynamics software to enable better prediction of cavitation within fuel injectors. In FY 2016 they: (1) selected and validated an appropriate open-source Lagrangian code modeling cavitation; (2) implemented and partially validated necessary physics to model air/water bubble dynamics; (3) developed controlled cavitation experiments for flow ranges of Reynolds number = 15,000–25,000 to test inside acrylic orifices of varying dimensions and geometry; (4) demonstrated two viable methods of detecting and characterizing cavitation; and (5) imagined fuel flow and cavitation in real fuel injector at Oak Ridge National Laboratory using the High Flux Isotope Reactor. (Ryan, report II.38)
- Georgia Institute of Technology is demonstrating a new spray atomization submodel for engine computational fluid dynamics codes with improved capability to accurately predict local spray morphology and global spray characteristics over a wide range of engine operating conditions, including conditions relevant for advanced combustion engines. In FY 2016 they: (1) demonstrated that measured nozzle area-contraction coefficient is not highly sensitive to backpressure, including that nozzle cavitation should not confound atomization physics under target experimental conditions; (2) demonstrated axi-symmetry of spray produced by target Engine Combustion Network (ECN) Spray



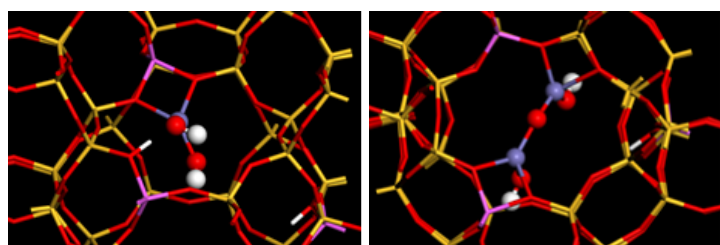
Temperature field in direct numerical simulation of end-gas ignition in homogeneous isotropic turbulence (Kim, report II.37)

D injector; (3) measured two-dimensional distributions of liquid mass within ECN Spray D at target experimental conditions; (4) demonstrated consistency between visible laser extinction and diffuse back illumination measurement techniques for quantifying optical thickness distribution; (5) measured two-dimensional distributions of optical thickness within ECN Spray D at target experimental conditions; (6) completed ultra-small angle X-ray scattering measurements of Sauter mean diameter in Spray D at target experimental conditions; and (7) demonstrated predictive capabilities and inaccuracies of literature spray atomization submodels implemented within a consistent open-source computational fluid dynamics framework. (Genzale, report II.39)

### Emission Control R&D

The following project highlights summarize the advancements made in emission control technologies to both reduce exhaust emissions and reduce the energy penalty of emission control system operation. In FY 2016, work continued on lean oxides of nitrogen traps (LNTs) and urea-selective catalytic reduction (urea-SCR) to reduce oxides of nitrogen ( $\text{NO}_x$ ) emissions. The focus of activities was on making these devices more efficient, more durable, and less costly. For particulate matter control, the focus was on more efficient methods of filter regeneration to reduce impact on engine fuel consumption.

- Oak Ridge National Laboratory is supporting industry in the development of accurate simulation tools for the design of catalytic emissions control systems that will enable advanced high-efficiency combustion engines to meet emissions regulations while maximizing fuel efficiency. In FY 2016 they: (1) facilitated Cross-Cut Lean Exhaust Emissions Reduction Simulations (CLEERS), which continue to have strong domestic and international participation (typically 30–50 participants, over half from industry); (2) provided regular update reports to the DOE Advanced Combustion Engine Cross-Cut Team; (3) organized the 2016 DOE Cross-Cut Workshop on Lean Emissions Reduction Simulation (CLEERS Workshop) in Ann Arbor, Michigan, on April 6–8, 2016; (4) maintained the CLEERS website ([www.cleers.org](http://www.cleers.org)); (5) supported the Advanced Combustion & Emissions Control Low Temperature Aftertreatment Team in developing an evaluation protocol for low temperature oxidation catalysts; (6) developed measurement and modeling strategies that accurately capture the effects of operating temperature,  $\text{NH}_3$  concentration,  $\text{H}_2\text{O}$  concentration, and hydrothermal aging on the  $\text{NH}_3$  storage capacity of a commercial small pore copper zeolite selective catalytic reduction (SCR) catalyst; (7) demonstrated that the  $\text{NH}_3$  isotherm measurement and modeling strategies work for a second, very different, commercial small pore copper SCR catalyst formation; and (8) hosted a visiting graduate student from Politecnico di Milano, who conducted detailed surface spectroscopy experiments aimed at elucidating key mechanistic steps in the SCR of NO by  $\text{NH}_3$  at low temperatures and at measuring the reactivity of  $\text{NH}_3$  adsorbed at different sites in the SCR catalyst. (Pihl, report III.1)
- Pacific Northwest National Laboratory is promoting the development of improved computational tools for simulating realistic full-system performance of lean-burn engines and associated emissions control systems, and providing the practical and scientific understanding and analytical base required to enable the development of efficient, commercially viable emissions control solutions for ultra-high-efficiency vehicles. In FY 2016 they: (1) submitted three journal publications and five presentations (four invited); (2) studied Fe-ion positioning in Fe/SSZ-13 with chemical titration and density functional theory calculation; (3) characterized fresh, low-temperature and high-temperature hydrothermally aged Cu/SAPO-34 catalysts with two-dimensional electron paramagnetic resonance spectroscopy; (4) studied active site and framework Al migration during Cu-SSZ-13 hydrothermal aging with kinetics and  $\text{Co}^{2+}$  titration; (5) initiated research on effects of extra framework Al species to selective catalytic reduction kinetics; (6) developed ammonia storage and oxidation kinetics models for a commercial Cu-SSZ-13 catalyst and correlated the same for different catalyst aging conditions that represent its lifecycle; (7) implemented a generalized optimization algorithm on Pacific Northwest National Laboratory's parallel computing workspace; (8) studied nature of Pd in zeolite supported Pd passive  $\text{NO}_x$  adsorbers with X-ray photoelectron spectroscopy and chemical titrations; (9) completed round-robin testing for validation of low temperature oxidation



Optimized structures of  $[\text{Fe}(\text{OH})_2]^+$  and  $[\text{HO}-\text{Fe}-\text{O}-\text{Fe}-\text{OH}]^{2+}$  active centers in Fe/SSZ-13 (Wang, report III.2)

catalyst test protocol with Advanced Combustion and Emissions Control Low Temperature Aftertreatment team; (10) completed low temperature trap protocol with Advanced Combustion and Emissions Control Low Temperature Aftertreatment team; and (11) scanned specimens from three different locations within a commercial selective catalytic reduction-coated diesel particulate filter. (Wang, report III.2)

- Pacific Northwest National Laboratory is identifying approaches to significantly improve both the high and low temperature performance, and the stability of catalytic  $\text{NO}_x$  reduction technologies via a pursuit of a more fundamental understanding of the various roles for multiple catalytic materials, the mechanisms for these roles, and the effects of high temperatures on the performance of these catalyst component materials in their various roles. In FY 2016 they: (1) carried out several synthesis efforts at Pacific Northwest National Laboratory to prepare model aluminosilicate zeolite and beta-based catalysts; (2) characterized catalysts after incorporation of Cu and Fe by nuclear magnetic resonance, Mossbauer, electron paramagnetic resonance, and Fourier transform infrared spectroscopies; (3) performed baseline reactivity measurements on these catalysts in preparation for mechanistic studies of high and low temperature performance loss; and (4) submitted three journal publications, one patent, and four public presentations (two invited). (Gao, report III.3)
- Pacific Northwest National Laboratory is investigating a number of candidate low-temperature oxidation catalysts as fresh materials, and after realistic laboratory and engine aging. They will obtain a better understanding of fundamental characteristics and various aging factors in both thermal and chemical aspects that impact the long-term performance of these candidate low temperature oxidation catalysts. In FY 2016 they: (1) determined that sulfur poisoning causes irreversible deactivation of the Cu/GMR6 catalyst; (2) determined the presence of  $\text{SO}_2$  in the simulated diesel exhaust initiates the formation of sulfates; and (3) determined the presence of sulfates influences both the active phase ( $\text{CuO}_2$ ) and the support (GMR6). (Szanyi, report III.4)
- Oak Ridge National Laboratory is developing emission control technologies that achieve >90% reduction of pollutants at low temperatures (<150°C) to enable fuel-efficient engines with low exhaust temperatures to meet new U.S. Environmental Protection Agency Tier 3 emission regulations that require ~80% less  $\text{NO}_x$  and hydrocarbon emissions than current standards. A low cost catalyst with no CO-HC inhibition discovered in FY 2014 studies has demonstrated hydrothermal aging durability and improved hydrocarbon oxidation performance in combination with platinum group metal catalysts. In FY 2016 Oak Ridge National Laboratory: (1) identified new mixed metal oxide candidate that has improved hydrocarbon activity (Sn–Mn–Ce and Mn–Ce); (2) measured sulfur tolerance of  $\text{CuO}-\text{Co}_3\text{O}_4-\text{CeO}_2$ ; (3) employed new core@shell technique to maximize  $\text{ZrO}_2$  surface for platinum group metal catalysis shown to yield improved activity especially for total hydrocarbons; (4) successfully implemented nano-on-nano technique with Pd dispersed on nanoparticles of Ce–Zr dispersed on  $\text{Al}_2\text{O}_3$ ; (5) determined key attributes of silver–zeolite hydrocarbon trap; and (6) demonstrated NO adsorption on Pd/ZSM-5. (Toops, report III.5)
- Oak Ridge National Laboratory is assessing and characterizing catalytic emission control technologies for lean-gasoline engines. They will identify strategies for reducing the costs, improving the performance, and minimizing the fuel penalty associated with emission controls for lean-gasoline engines. In FY 2016 they: (1) completed evaluation of a matrix of three-way catalyst (TWC) formulations under cold start conditions and demonstrated that  $\text{NH}_3$  can be produced at >80% efficiency beginning at 150°C; (2) demonstrated that the optimal  $\text{NH}_3:\text{NO}_x$  ratio is 1.13 at TWC and selective catalytic reduction temperatures of 470°C and 350°C, respectively, to achieve minimal  $\text{NO}_x$ ,  $\text{NH}_3$ , and  $\text{N}_2\text{O}$  tailpipe emissions; and (3) with a scanning transmission electron microscope, measured the distribution of platinum group metal particle sizes on TWCs aged for 25, 50, and 100 h with an accelerated aging protocol performed on the bench flow reactor; and (4) conducted investigations of the impacts of sulfur on TWC function after hydrothermal aging. (Parks, report III.6)
- Oak Ridge National Laboratory is researching the fundamental chemistry of automotive catalysts, identifying strategies for enabling self-diagnosing catalyst systems, and addressing critical barriers to market penetration. In FY 2016 they: (1) assessed spatially distributed performance of two separate field-aged catalyst samples relative to each other and the same catalyst in the degreened state; (2) assessed Cummins predictive selective catalytic reduction model via intra-catalyst spatially resolved capillary inlet mass spectrometry data; (3) demonstrated practical method for catalyst state assessment; and (4) submitted two archival publications, one journal cover feature, and one oral presentation. (Partridge, report III.7)

- Argonne National Laboratory is determining the performance of three-way catalyst-coated gasoline particulate filters (TWC/GPFs) with variation of filter/coating design parameters. In FY 2016 they: (1) explored extensive impacts of ash loading on TWC and GPF performance; and (2) provided an optimized TWC/GPF concept with respect to catalyst coating and filter design. (Seong, report III.8)
- Pacific Northwest National Laboratory is seeking to shorten development time of filtration technologies for future engines and developing modeling approaches relevant to the likely key challenge for gasoline particulate filtration—high number efficiency at high exhaust temperatures. In FY 2016 they: (1) assembled a large set of consistent filtration data using a number of different filter materials and covering a range of engine operating conditions; (2) developed a simple straight cylindrical pore filter model that qualitatively predicted many of the trends observed in the data; (3) performed three-dimensional flow simulations in filter wall reconstructions from micro X-ray computed tomography data and compared to experimental results; and (4) began development of constricted tube unit collector filtration models, which may offer some advantages over the more commonly used spherical unit collector models. (Stewart, report III.9)
- Pacific Northwest National Laboratory is helping fuel-efficient lean gasoline and diesel engines meet the current and future emission regulations with effective, inexpensive, and reliable  $\text{NO}_x$  emission control technologies, and developing the next generation selective catalytic reduction dosing system for improved low temperature performance, convenient handling and distribution of ammonia carriers, and reduced overall system volume, weight, and cost. In FY 2016 they: (1) completed detailed evaluation of 15 compositions; (2) developed composites that mitigate volume expansion issues from 350 vol% to 19 vol%; (3) quantified HCl generated during ammonia release; and (4) evaluated composites and mitigated HCl generated from ~600 ppm to <1 ppm. (Karkamkar, report III.10)
- The University of Connecticut is synthesizing, characterizing, and developing a new class of cost-effective and high performance metal oxide nanostructure array-based monolithic catalysts for hydrocarbon oxidation under lean burn conditions at low temperatures (<150°C). In FY 2016 they: (1) demonstrated  $\text{ZnO}/\text{perovskite}/\text{Pt}$  core-shell metal oxide nano-array catalysts with tunable propane oxidation activities; (2) demonstrated  $\text{TiO}_2/\text{Pt}$  nano-array catalysts with good low temperature CO and  $\text{C}_3\text{H}_6$  oxidation performance under U.S. DRIVE protocalled low temperature combustion diesel simulated exhaust gas conditions; (3) demonstrated  $\text{TiO}_2/\text{Pt}$  nano-array catalysts with superb low temperature CO,  $\text{C}_2\text{H}_4$ , and  $\text{C}_3\text{H}_6$  oxidation performance in U.S. DRIVE protocalled conventional diesel combustion simulated exhaust gas conditions; (4) evaluated hydrothermal durability of various metal oxide nano-array-based monolithic catalysts; and (5) formulated and assembled large-scale nano-array-based monolithic catalysts ready for selective transient cyclic tests and engine tests. (Gao, report III.11)
- Purdue University is synthesizing Cu-SSZ-13 catalysts that are exceptionally well-defined at the microscopic level, including control of number and type of active sites. In FY 2016 they: (1) showed that Cu exchange sites exist as  $\text{NH}_3$ -solvated ions at 200°C standard selective catalytic reduction (SCR) conditions and that  $\text{NH}_3$  solvation mobilizes Cu ions; (2) showed that standard SCR (per Cu) at 200°C is independent of Cu loading, Cu speciation, and zeolite framework type at commonly used Cu loading levels; (3) developed infrared and ultraviolet-visible spectroscopies as a means to distinguish Cu(II) and Cu(II)OH exchange sites; (4) developed synthetic methods to prepare SSZ-13 zeolites with tunable framework Al distribution and corresponding variations in Cu(II)/Cu(II)OH site ratios; (5) developed models to correlate features in Cu X-ray spectra with Cu coordination and oxidation state; and (6) showed that at low Cu loadings, standard SCR rates at 200°C vary with the square of Cu density, implicating a Cu dimer as transient SCR intermediate. (Ribeiro, report III.12)

**HCl Outlet Concentration as a Function of Ammonia Release Temperature for Magnesium Chloride and Novel Composites Developed and Tested at Pacific Northwest National Laboratory (Karkamkar, report III.10)**

Material	Temp* (°C)	Amount of HCl (ppm)
$\text{MgCl}_2$	400	580
$\text{Mg}(\text{NH}_3)_6\text{Cl}_2$	250	20
$\text{Mg}(\text{NH}_3)_6\text{Cl}_2:\text{X}$ (1:1)	400	<1
$\text{Mg}(\text{NH}_3)_6\text{Cl}_2:\text{X}$ (1:1)	400	<1
$\text{Mg}(\text{NH}_3)_6\text{Cl}_2:\text{X}$ (2:1)	250	<1
$\text{Mg}(\text{NH}_3)_6\text{Cl}_2:\text{X}$ (3:1)	250	<1

- The University of Houston is predicting binary and ternary metal alloy catalyst compositions for enhanced CO, NO, and hydrocarbon oxidation from first principles density functional theory and verification through kinetic and mechanistic studies, and developing enhanced low-temperature CO, hydrocarbon, and NO oxidation catalysts through zoning and profiling of metal and ceria components. In FY 2016 they: (1) developed a micro-kinetic model that could predict experimentally observed inverse hysteresis behavior during co-oxidation of CO and propylene; (2) predicted a zoned catalyst to lower the temperature required for 90% conversion by 40°C; (3) predicted density functional theory calculations for a bimetallic catalyst that avoids NO<sub>x</sub> oxidation of CO and hydrocarbons, such that higher NO<sub>x</sub> yields can be achieved at lower temperature; and (4) used a rapid cycling of reductant via a NO<sub>x</sub> storage/reduction process to show NO<sub>x</sub> reduction could be achieved 50°C lower than under conventional cycling modes. (Epling, report III.13)
- The University of Kentucky Center for Applied Energy Research is improving the low-temperature performance of catalyst-based oxides of nitrogen (NO<sub>x</sub>) mitigation systems by designing materials that can function as either passive NO<sub>x</sub> adsorbers or low-temperature lean-NO<sub>x</sub> trap catalysts. In FY 2016 they: (1) prepared a patent application; (2) performed bench reactor studies on 0.9% Pt-0.9% Pd/Ce<sub>0.2</sub>Zr<sub>0.8</sub>O<sub>2</sub>, both before and after hydrothermal aging; (3) showed CO exerted almost no impact on NO<sub>x</sub> storage efficiency at 160°C but significantly improved NO<sub>x</sub> storage performance at 120°C and 80°C; and (4) performed diffuse reflectance infrared Fourier transform spectroscopy measurements indicating that both nitrate and nitrite species were generated on 0.9% Pt-0.9% Pd/Ce<sub>0.2</sub>Zr<sub>0.8</sub>O<sub>2</sub> during NO storage. (Crocker, report III.14)

### High-Efficiency Engine Technologies

The objective of these projects is to research and develop technologies for more efficient clean advanced engine/powertrain systems to improve passenger and commercial vehicle fuel economy. The following describe what was accomplished in FY 2016.

- Volvo is identifying concepts and technologies that have potential to achieve 55% brake thermal efficiency (BTE) in a heavy-duty diesel engine and demonstrating a heavy-duty diesel engine capable of achieving 50% BTE at the end of the SuperTruck project. In FY 2016: (1) simulation tools have been refined and used together to lead design decisions and make accurate predictions of new combustion regimes required for the 55% BTE target; (2) computational fluid dynamics combustion models were validated against single-cylinder engine test data with primary reference fuel 87 surrogate fuel; (3) the design of concepts achieving 55 % BTE have been progressed and simulated, and practical implementations have been identified; (4) the engine installed the SuperTruck demonstrator was previously proven capable of stable operation at 48% BTE without waste heat recovery; (5) gas jet modeling has been able to shed new insight on the physics of multiple injections, interaction between adjacent injection plumes, and jet–wall interactions; and (6) a novel “wave piston” combustion system, which was developed earlier in this project, has moved into production at Volvo, providing both improved fuel economy and lowered emissions. (Amar, report IV.1)
- Navistar Inc. is developing a heavy-duty diesel engine capable of achieving 50% or better brake thermal efficiency (BTE) on a dynamometer under a load representative of a level road at 65 mph. In FY 2016 they: (1) delivered the engine calibrations for ST1 vehicle testing; (2) completed the demonstration of greater than 50% BTE on a dynamometer; (3) examined in-cylinder combustion process to identify opportunities for 55% BTE; (4) developed detailed friction models for valvetrain and cranktrain in GT-POWER; (5) completed low pressure exhaust gas recirculation (LP EGR) evaluation for NO<sub>x</sub> reduction with no negative impact on BTE; (6) completed the evaluation of three parasitic reduction technologies; (7) completed the dual-fuel investigation with LP EGR; and (8) advanced the conjugate heat transfer modeling for in-cylinder heat transfer simulation. (Zukouski, report IV.2)
- Delphi is developing, implementing, and demonstrating a low temperature combustion scheme called Gasoline Direct-Injection Compression Ignition (GDCI). The project will demonstrate a 35% fuel economy improvement over the baseline vehicle while meeting Tier 3 emissions levels. In FY 2016 they: (1) resolved Gen1 vehicle fuel economy testing issues; (2) designed and implemented improvements to engine controls and calibration on Gen1.8 vehicle for improved fuel economy and emissions; (3) completed Gen1.8 vehicle testing with a hydrocarbon trap aftertreatment system; (4) characterized and evaluated the fuel economy, emissions, and performance of Gen2 GDCI engine on dynamometer; (5) performed detailed emissions characterization of the Gen2 GDCI engine at Delphi with Oak Ridge National Laboratory; (6) completed Gen2 vehicle update and started break-in and steady-state calibration development; (7) designed and fabricated new Gen3 GDCI engines for dynamometer and vehicle testing; (8) packaged the Gen3

powertrain, new thermal management, and new aftertreatment in the test vehicle; and (9) developed the Gen3 aftertreatment system using simulation. (Confer, report IV.3)

- Filter Sensing Technologies is developing radio frequency (RF) sensors and evaluate RF sensing feasibility for selective catalytic reduction (SCR), three-way catalyst, and hydrocarbon trap applications. In FY 2016 they: (1) developed RF sensor hardware and software, including custom antennas for catalyst bench tests as well as full-size, heavy-duty system applications; (2) setup and conducted catalyst bench reactor studies to evaluate RF sensing feasibility for specific catalyst systems and formulations; (3) initiated fleet vehicle RF sensor evaluations with full-size SCR systems ahead of schedule and with more vehicles than originally planned; (4) investigated error sources, quantified their potential impacts on the RF sensor accuracy, and developed sensor correction methods where necessary; and (5) developed initial RF sensor calibration functions and evaluated sensor performance through bench reactor tests with carefully controlled gas compositions. (Sappok, report IV.4)
- Eaton is quantifying the available energy in the engine exhaust for a waste heat recovery (WHR) system, and optimizing the WHR architecture through an optimized number of heat exchangers and optimized expander design with optimized engine coolant composition. In FY 2016 they: (1) completed engine baseline experiments and analyzed the potential WHR architecture and boundary conditions of the affordable Rankine cycle (ARC) system; (2) evaluated the ARC system benefits based on WHR analysis; (3) attained the technical target of 5% fuel economy improvement from ARC architecture through preliminary analytical modeling; (4) identified ARC system components (expander, working fluid, heat exchanger, and working fluid pump); (5) completed Roots expander computational fluid dynamics and analysis for ARC specifications and concluded the need for an alternative positive displacement expander technology for ARC demonstration; and (6) evaluated the engine coolant feasibility of WHR working fluid using laboratory-scale coolant degradation analysis. (Subramanian, report IV.5)
- Envera LLC is developing a high-efficiency variable compression ratio (VCR) engine having variable valve actuation and an advanced high-efficiency supercharger to obtain up to a 40% improvement in fuel economy when replacing current production V8 engines with the new small displacement VCR engine. In FY 2016, the VCR hardware was built and assembled. There are no issues with the VCR mechanical assembly. (Mendler, report IV.6)
- General Motors demonstrated a new combustion concept combining lean stratified operation with Miller cycle in a gasoline engine and integrating with engine downsizing, advanced thermal management, 12 V start/stop, friction reduction mechanisms, and lean aftertreatment exhaust system. In FY 2016 they: (1) successfully demonstrated baseline homogeneous stoichiometric targets for the single-cylinder engine; (2) optimized piston, port, and injector spray details to achieve the target spray that avoids collapse; (3) demonstrated viable fuel consumption levels during stratified operation at the  $\text{NO}_x$  target of 10 g/kg fuel; (4) developed and calibrated computational fluid dynamics models to support understanding of the cylinder spray, mixing, and combustion phenomena and guided design changes; (5) developed boost and aftertreatment system using one-dimensional models to address the challenges of low-temperature lean exhaust, and defined single-cylinder engine boundary conditions; (6) analyzed the overall system cost for commercial viability; and (7) designed the initial multi-cylinder engine for dynamometer testing, including advanced thermal management. (Sczomak, report IV.7)
- Cummins Inc. is using a diesel engine system to demonstrate in a test cell peak engine system efficiency of 55% brake thermal efficiency, and will develop and demonstrate an advanced, highly integrated combustion and aftertreatment system to achieve 2010 emissions compliance. In FY 2016 they: (1) designed, procured, and tested a high-efficiency variable flow and pressure lube pump; (2) designed, developed, and tested an air handling controls system for dual loop exhaust gas recirculation architecture; (3) designed, developed, and tested a low parasitic valvetrain system incorporating roller bearing elements and lightweight components; (4) designed, developed, and tested an optimized



Gen3 engine mockup in test vehicle  
(Confer, report IV.3)

exhaust manifold for pulsation utilization; (5) designed and developed a low heat transfer power cylinder system; and (6) designed, developed, and tested an optimized low friction power cylinder system. (Kocher, report IV.8)

### Solid State Energy Conversion

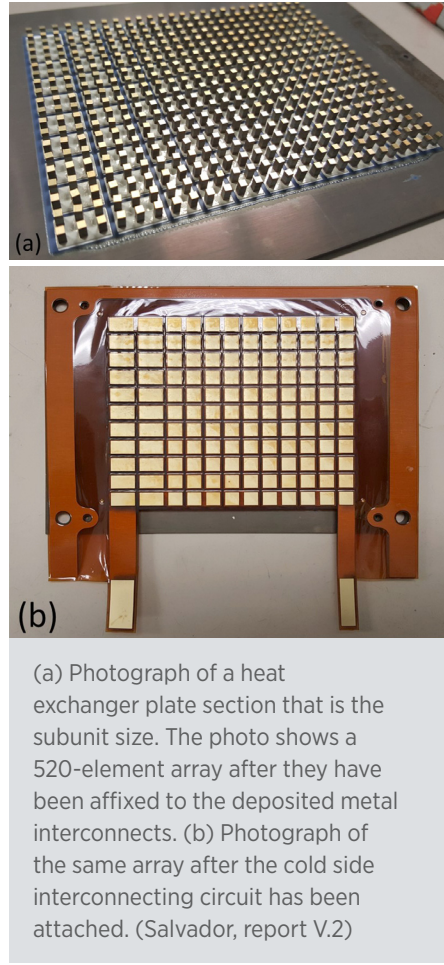
The following are FY 2016 highlights in the development of thermoelectric generators that can directly convert to electricity, the energy in the exhaust of advanced combustion engines. Research was focused on developing practical systems that are suitable for future vehicle production.

- Gentherm Inc. is preparing a detailed production cost analysis for a thermoelectric generator for passenger vehicle volumes of 100,000 units per year and a discussion of how costs will be reduced in manufacturing. In FY 2016 they performed vehicle-level testing. (Jovovic, report V.1)
- General Motors is overcoming major obstacles to the commercialization of automotive thermoelectric generator (TEG) systems, developing an overall TEG system including all necessary vehicle controls and electrical systems and fully integrating onto a light-duty vehicle, and demonstrating fuel economy improvement of 5% over the US06 drive cycle. In FY 2016 they: (1) developed and implemented a method for printing dielectric thick films directly onto the surface of stainless steel heat exchangers; (2) developed a diffusion bonding technique to attach metal standoffs to skutterudite elements; (3) developed a high pressure, low temperature method to join the thermoelectric elements to the printed dielectric/thick film metal layer; (4) finalized the subunit and system level design of the final TEG prototype; (5) designed and fabricated all fixtures, screens, and alignment jigs required to build the final generator prototype; (6) acquired, modified, and began baseline testing on the demonstration vehicle; (7) acquired, tested, and based on the test results, modified commercially available direct current-to-direct current converters for the final generator testing; and (8) estimated the fuel economy impacts of the generator using a combination of validated TEG models and vehicle unified models. (Salvador, report V.2)

### I.3 Honors and Special Recognitions/Patents

#### Honors and Special Recognitions

1. SAE Excellence in Oral Presentation Award (2016), Scott Skeen. (Pickett, report II.3)
2. DOE Office of Energy Efficiency & Renewable Energy Special Recognition Award for research on diesel engine and homogeneous charge compression ignition-like combustion. Presented by DOE at the Annual Merit Review, June 2016 (Dec, report II.4)
3. United States Council for Automotive Research (USCAR) Team Award for work on the U.S. DRIVE Advanced Combustion and Emission Control (ACEC) Fuels Roadmap Subteam. (Dec, report II.4)
4. Sibendu Som: 2016 Outstanding Postdoctoral Supervisor Award, Argonne National Laboratory. (Som, report II.6)
5. Sibendu Som: 2016 ASME Internal Combustion Engine Division “Outstanding Presenter” award. (Som, report II.6)
6. Pacesetter Award, Argonne National Laboratory. Awarded to Christopher Powell, Daniel Duke, Alan Kastengren, Katarzyna Matusik. “For excellence in achievement and performance which truly surpasses normal job expectations,” July 2016. (Powell, report II.7)



7. "Best Oral Presentation Award," Awarded by ILASS Europe, Brighton, UK. For the Paper "Time-Resolved X-Ray Radiography of Cavitation in a Metal Nozzle," D. Duke, A. Kastengren, A. Swantek, K. Matusik, R. Payri, J.P. Viera, C.F. Powell. September 2016. (Powell, report II.7)
8. 2016 R&D 100 Award Winner for Zero-RK in Software/Services Category. (Whitesides, report II.11)
9. Oak Ridge Leadership Computing Facility User Conference Best Poster Award (with Oak Ridge National Laboratory [ORNL] and General Motors [GM]). (Whitesides, report II.11)
10. M.J. McNenly and R.A. Whitesides, "Zero-RK," R&D 100 Winner – Software & Services, R&D Magazine, November 2015. (McNenly, report II.12)
11. GM, ORNL, and Lawrence Livermore National Laboratory received an Advanced Scientific Computing Research Leadership Computing Challenge award for 16,000,000 h on Titan to support simulation of Partial Fuel Stratification strategies in FY 2017. (Edwards, report II.14)
12. General Electric, Argonne National Laboratory, and ORNL received an Advanced Scientific Computing Research Leadership Computing Challenge award of 25,000,000 h on Mira to support simulation of cyclic variability in dual-fuel engines in FY 2017. (Edwards, report II.14)
13. GM and ORNL received Best Poster award at the 2016 Oak Ridge Leadership Computing Facility Users Meeting. (Edwards, report II.14)
14. The ACEC Low Temperature Aftertreatment Team, in which Josh Pihl is a participant, received a USCAR Team Award at the USCAR Annual Recognition Luncheon on May 26, 2016. (Pihl, report III.1)
15. Best Poster Award at Gordon Research Conference on Catalysis, Colby-Sawyer, New Hampshire, June 2016 (C. Paolucci). (Ribeiro, report III.12)
16. AIChE CRE Division Travel Award, San Francisco, CA, November 2016 (J. R. Di Iorio). (Ribeiro, report III.12)
17. Dow Chemical Company Travel Award for the ISCRE 24 Meeting, Minneapolis, MN, June 2016 (A. Shih). (Ribeiro, report III.12)
18. Yuying Song received the Colt Refining Award from the International Precious Metals Institute. (Epling, report III.13)
19. Dan Ruth (2015) Dr. John P. Karidis Department Head's Award for Research Achievement in Mechanical Engineering, The Pennsylvania State University. (Amar, report IV.1)
20. ASME Internal Combustion Engine Division Student Presentation Award, "Direct Measurements of Ammonia Storage on Selective Catalytic Reduction (SCR) Systems using Radio Frequency Methods," ASME, Greenville, SC, 2016. (Sappok, report IV.4)

### **Invention and Patent Disclosures**

1. U.S. Patent Application Filed, No. 14/855,809: Dec, J.E., and Renzi, R., September 2015. (Dec, report II.4)
2. C.H.F. Peden, F. Gao, Y. Wabg, M. Kollar, J. Szanyi. "Catalysts for enhanced reduction of NOx gases and processes for making and using same." US 2016/0107119 A1. (Gao, report III.3)
3. S.Y. Chen, J.K. He, P.X. Gao and S. Suib, Fabrication of manganese oxide based nanorod arrays on 3D substrates, University of Connecticut Invention Disclosure, 2016, submitted. (Gao, report III.11)
4. D. Scapens, D. Harris, J.G. Darab, M. Crocker, Y. Ji, patent application pending. (Crocker, report III.14)
5. Patent Application #62360769, Rankine Waste Heat Recovery Control Using Zeotropic Mixture. (Subramanian, report IV.5)
6. Three patent applications have been filed for the GM Lean-Miller Cycle project since inception. (Sczomak, report IV.7)

## II. Combustion Research

The Vehicle Technologies Office (VTO) funds research focused on developing a greater understanding of engine combustion and how emissions form within engine cylinders as well as how combustion and emissions depend on factors such as fuel spray characteristics, in-cylinder air motion, and type of fuel. This greater understanding will help researchers develop higher efficiency advanced combustion engine strategies such as low temperature combustion, dilute (lean burn) gasoline combustion, and clean diesel combustion that produce very low engine-out emissions of oxides of nitrogen and particulate matter. All the combustion approaches and associated critical technical issues VTO addresses are compatible with the industry trend toward engine downsizing and boosting to improve vehicle fuel economy. In addition, VTO also supports research on materials that can withstand high operating temperatures and pressures needed to capitalize on these engines' potential benefits.

## II.1 Light-Duty Diesel Combustion

### Overall Objectives

- Provide the physical understanding of the in-cylinder combustion processes needed to minimize the fuel consumption and the carbon footprint of automotive diesel engines while maintaining compliance with emissions standards and meeting customer expectations
- Develop efficient, accurate computational models that enable numerical optimization and design of fuel-efficient, clean engines
- Provide accurate data obtained under well-controlled and characterized conditions to validate new models and to guide optimization efforts

### Fiscal Year (FY) 2016 Objectives

- Characterize the impact of pilot injections on late-cycle in-cylinder flow behavior
- Measure efficiency and emissions benefits of a stepped-lip piston compared to a conventional, re-entrant piston bowl
- Refine and utilize computational fluid dynamics capabilities to characterize the impact of a stepped-lip piston bowl geometry on in-cylinder flow structure

### FY 2016 Accomplishments

- Determined the impact of pilot-main dwell on late-cycle in-cylinder flow behavior using a newly developed velocimetry technique
- Experimentally confirmed that with a stepped-lip piston design, indicated efficiency improvements of up to 3% are possible with a simultaneous reduction in soot and  $\text{NO}_x$  emissions
- Demonstrated differences in in-cylinder flow resulting from a change in piston design from a conventional re-entrant bowl design to a stepped-lip bowl design ■

### Introduction

Direct injection diesel engines have the highest proven brake fuel efficiency of any reciprocating internal combustion engine technology. Calibrating a modern diesel engine requires balancing tradeoffs between the emission of pollutants such as nitrogen oxides ( $\text{NO}_x$ ), soot, unburned hydrocarbons, and CO; fuel economy; combustion noise; and exhaust enthalpy for aftertreatment

### Stephen Busch

Sandia National Laboratories

P.O. Box 969

Livermore, CA 94551-0969

Phone: (925) 294-2216

Email: [sbusch@sandia.gov](mailto:sbusch@sandia.gov)

DOE Technology Development Manager:

Leo Breton

Subcontractor:

University of Wisconsin Engine Research Center,  
Madison, WI

systems. Diesel powertrains have made remarkable progress in terms of specific torque (peak torque output per liter of engine displacement) while meeting increasingly stringent emissions regulations. Further improvements to diesel engine design will necessitate a more complete understanding of in-cylinder mixing and combustion processes, and how various aspects of engine design and calibration impact the tradeoffs mentioned above.

The first objective for this year was to change the delay between a single pilot injection and a main injection, and then to characterize the impact of this delay on in-cylinder flow late during the cycle, when mixing is critical to oxidize partially burned fuel and soot. Second, a piston with a stepped-lip bowl was tested in the research engine and compared with the conventional, re-entrant piston to determine the impact that this geometrical change has on efficiency and emissions. Finally, using a newly developed computational fluid dynamics code, changes in in-cylinder flow resulting from the change in piston geometry have been simulated and analyzed.

### Approach

The overall research approach involves carefully coordinated experimental, modeling, and simulation efforts. Detailed optical measurements of flow, mixture preparation, and combustion processes are made in an optical research engine facility based on a General Motors 1.9-L automotive diesel engine. Careful attention is also paid to obtaining accurate boundary conditions to facilitate comparisons with simulations, including intake flow rate and thermodynamic properties, and

wall temperatures. Close geometric and thermodynamic correspondence between the optical engine and a traditional, all-metal test engine allow the combustion and, engine-out emissions behavior of the test engine to be closely matched. These measurements are closely coordinated and compared with the predictions of numerical simulations.

The experimental and numerical efforts are mutually complementary. Detailed experimental measurements guide the development, evaluation, and refinement of the models used in the computer simulations. The simulation results can in turn be used to obtain a more detailed understanding of the in-cylinder flow and combustion physics—a process that is difficult if only limited measurements are possible. This combined approach addresses both of the principal goals of this project: (1) development of the physical understanding to guide, and (2) the simulation tools to refine the design of optimal, clean, high-efficiency diesel combustion systems.

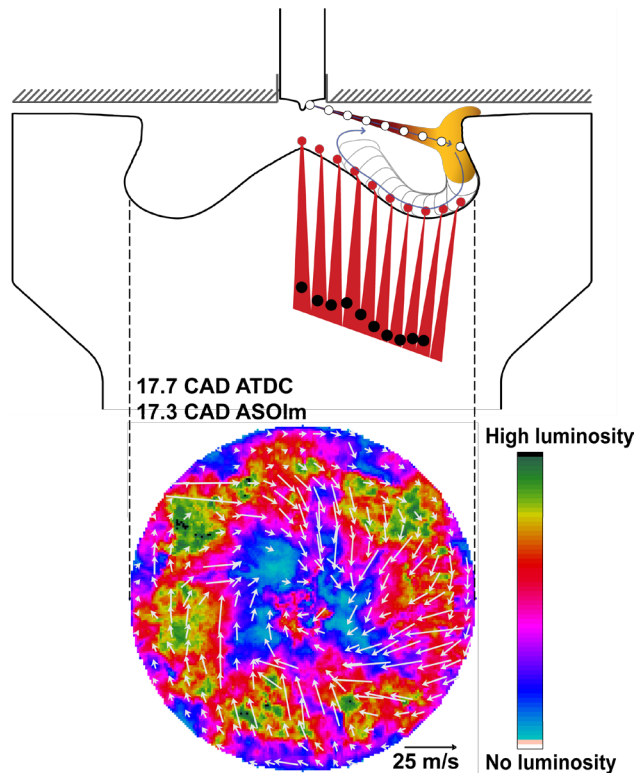
## Results

In light-duty, direct injection diesel engines, in-cylinder gas flow plays an important role in the mixture preparation, combustion, and pollutant formation processes. Complex interactions between tangential (swirl) and radial (squish and injection-driven) flows establish energetic and long-lived vertical plane flow structures in the piston bowl near top dead center. The development of these flow structures is supported by the piston bowl geometry, and the largest structures transport fuel, both unburned and partially burned, and soot to oxygen-containing regions. Fluid deformation caused by the large-scale structures generates additional turbulence that enhances mixing and promotes the oxidation of unburned fuel and soot particles [1]. Direct fuel injection near the end of the compression stroke has a significant impact on these flow structures, but also on the redistribution of angular momentum in the combustion chamber. This redistribution of angular momentum can create unstable radial profiles of angular momentum that have been identified as an important source of enhanced late-cycle turbulence [2], which is critical for the oxidation of soot. Proper combustion chamber design supports the development of desirable flow structures in the combustion chamber that are reported to be capable of improving soot and  $\text{NO}_x$  emissions with a modest gain in efficiency [3].

In this work, a velocimetry technique is applied to characterize the evolution of flow patterns that develop during combustion in the piston bowl of a light-duty optical diesel engine. Natural combustion luminosity,

which is dominated by soot luminosity during much of the combustion event, is imaged through the bottom of an extended optical piston using a high-speed complimentary metal-oxide-semiconductor camera. Advanced image processing methods are developed and combined with combustion image velocimetry techniques (see Dembinski and Angstrom [4]) to provide semi-quantitative information about the radial flow evolution in the bowl during the main combustion (see depiction in Figure 1). A variation of the delay, or dwell, between the pilot and main injections is performed to investigate how dwell may impact radial flow in the bowl attributed to vertical plane flow structures, particularly during the later stages of combustion.

Figure 2 shows the development of radial flow near the bottom of the piston bowl as a function of crank angle for each of the cases tested. It is observed that the inward radial flow reaches its highest amplitude shortly after the end of the main injection, after which the radial flow



CAD – crank angle degrees; ATDC – after top dead center; ASOI – after start of the main injection

Figure 1. Example of a natural luminosity image (shown in false color) taken through the bottom of the optical piston. High speed photography combined with an advanced ray tracing-based image distortion correction technique makes it possible to derive flow information from a sequence of images.

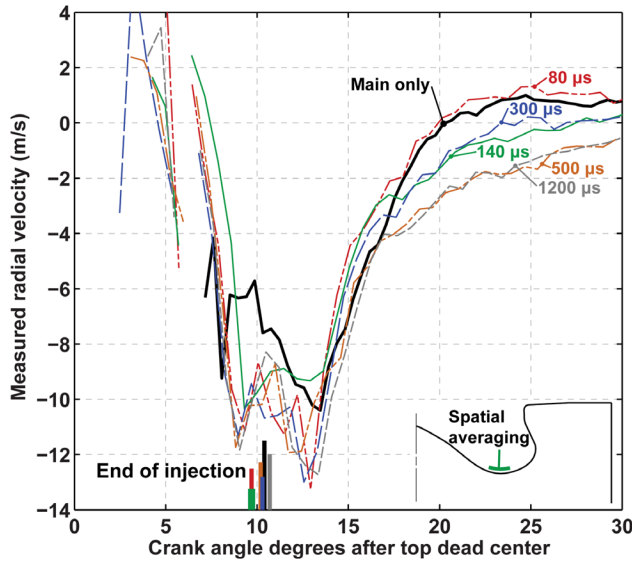


Figure 2. Radial flow as a function of crank angle for several different pilot-main delay (dwell) times. Changing the dwell by a fraction of a millisecond can have a dramatic impact on the flow in the cylinder even after the end of the main injection.

decreases in intensity. Although the mass of fuel injected during the pilot injection is 15–20 times less than the amount of fuel injected during the main injection, the dwell between the pilot and the main impacts the flow in the cylinder well after the end of the main injection. The impact becomes apparent approximately 7 CAD after the end of the main injection (see Figure 2).

The mechanisms by which this radial velocity decay takes place are not well understood; future numerical simulations will be performed to provide insight about how pilot-main dwell can impact late cycle turbulent flow and mixing in the combustion chamber.

In order to assess the impact that piston bowl geometry can have on efficiency and emissions, two different piston bowl designs are tested in the research engine: the conventional re-entrant bowl shown in Figure 1, and a stepped-lip bowl comparable to the one presented in Styron et al. [5]. Engine operation with the two piston designs is first compared in terms of fuel consumption (Figure 3) and pollutant emissions, namely soot and  $\text{NO}_x$  emissions (Figure 4).

While peak efficiency is not improved through use of the stepped-lip piston, fuel economy can be improved by as much as 3% for some injection timings. The mechanisms responsible for this fuel economy improvement are the subject of ongoing research efforts. A fundamental understanding of these mechanisms will potentially enable

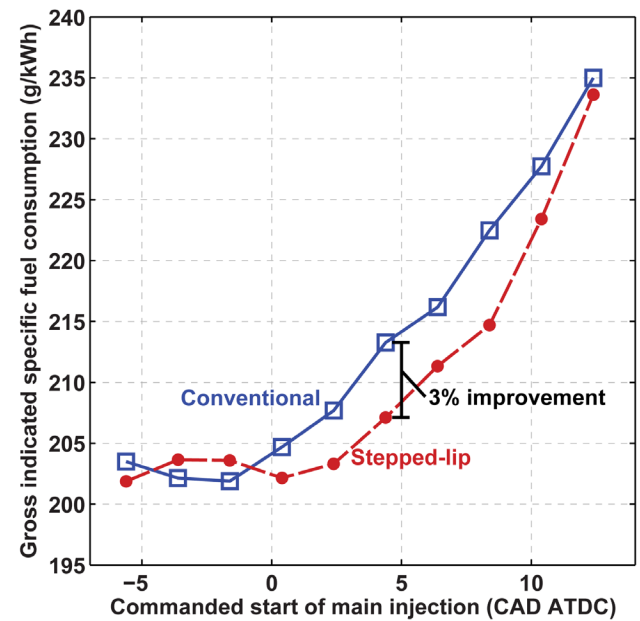


Figure 3. Indicated specific fuel consumption for operation with a conventional re-entrant and a stepped-lip piston. For some injection timings, the efficiency can be improved by as much as 3% by using the stepped-lip piston.

higher peak efficiencies through improved combustion chamber design.

In addition to improvements in fuel economy, use of the stepped-lip piston can result in substantial reductions in engine-out soot emissions (Figure 4). These benefits are in agreement with results found in the literature [6]. Ongoing thermodynamic analyses, combined with further experimental optical investigations, will provide more insight into the mechanisms responsible for the observed improvements in fuel economy and engine-out soot emissions. Additionally, computational simulation efforts are being devoted to understanding how in-cylinder flow, mixture preparation, combustion, and pollutant formation processes are changed by the stepped-lip piston.

To this end, experimental measurements of in-cylinder flow (shown in last year's annual report) were used to refine computational modeling efforts. This year, the computational models have been exercised to compare and contrast the in-cylinder flow patterns that result from the use of the two piston bowl geometries. One important finding of the work is depicted in Figure 5.

The in-cylinder flow structures that form as a result of competition between centrifugal forces and squish flow near the end of the compression stroke are depicted for both piston geometries in Figure 4. A highly organized toroidal vortex is clearly visible in conventional re-entrant

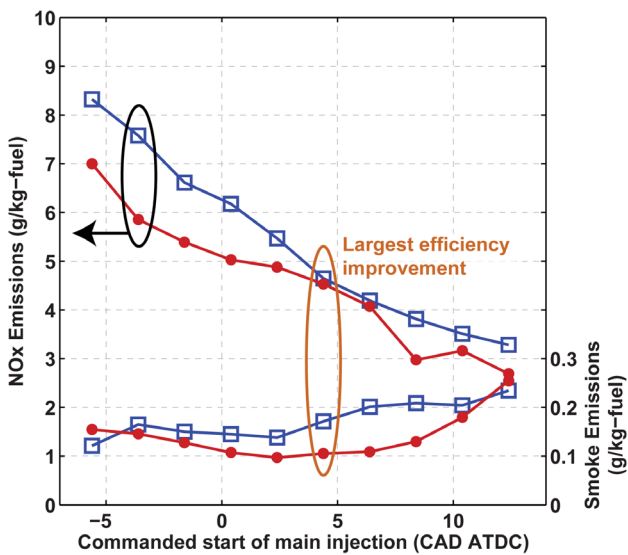


Figure 4. With a stepped-lip piston, soot emissions can be significantly reduced as fuel economy is improved.

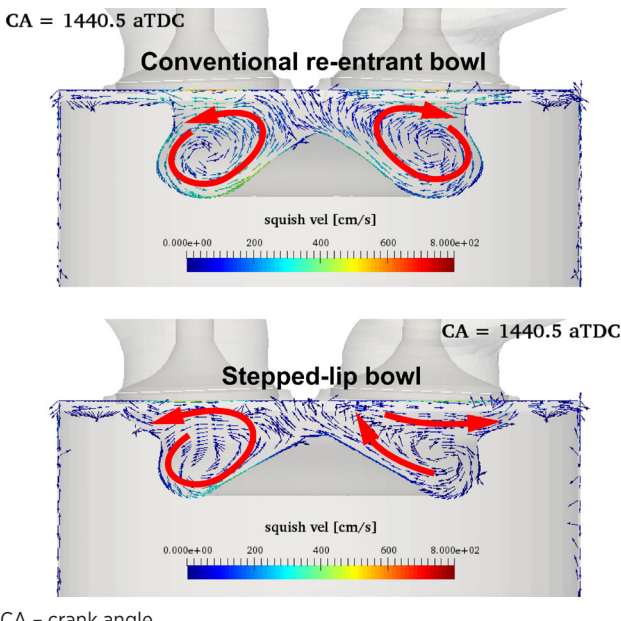
bowl, as has been reported in the literature [1]. With the stepped-lip bowl, significant asymmetries are observed in the vertical plane flow structures. The physical phenomena responsible for the asymmetrical flow structure are the focus of current research. Future efforts will be focused on interactions between the fuel injection and the bowl geometry, as well as on the resulting impact on in-cylinder flow.

## Conclusions

- Engine calibration parameters such as pilot-main dwell can have an impact on late-cycle in-cylinder flow behavior.
- Stepped-lip piston designs can improve fuel economy by as much as 3% while significantly reducing engine-out soot emissions.
- With the stepped-lip piston, vertical plane flow structures near top dead center are characterized by a higher degree of azimuthal asymmetry than for the conventional re-entrant piston bowl.

## References

1. Miles, P.C., Turbulent Flow Structure in Direct-Injection, Swirl-Supported Diesel Engines, in *Flow and Combustion in Reciprocating Engines*, C. Arcoumanis, Kamimoto, T., Editor. 2008, Springer-Verlag: Berlin Heidelberg. p. 173–256 DOI: 10.1007/978-3-540-68901-0\_4.
2. Miles, P.C., et al., *Late-Cycle Turbulence Generation in Swirl-Supported, Direct-Injection Diesel Engines*. SAE Technical Paper 2002-01-0891, 2002, DOI: 10.4271/2002-01-0891.
3. Andersson, Ö., et al., Development of the Euro 5 Combustion System for Volvo Cars' 2.4.I Diesel Engine. 2009, SAE Technical Paper 2009-01-1450, 2009, DOI: 10.4271/2009-01-1450.
4. Dembinski, H.W.R. and Angstrom, H.-E., “Optical Study of Swirl during Combustion in a CI Engine with Different Injection Pressures and Swirl Ratios Compared with Calculations,” SAE Technical Paper 2012-01-0682, 2012, DOI: 10.4271/2012-01-0682.
5. Styron, J., Baldwin, B., Fulton, B., Ives, D. and Ramanathan, S., “Ford 2011 6.7L Power Stroke® Diesel Engine Combustion System Development,” SAE Technical Paper 2011-01-0415, 2011, DOI: 10.4271/2011-01-0415.
6. Kurtz, E.M. and Styron, J., “An Assessment of Two Piston Bowl Concepts in a Medium-Duty Diesel Engine,” SAE Int. J. Engines 5(2):344-352, 2012, DOI: 10.4271/2012-01-0423



CA – crank angle

Figure 5. Vertical plane flow structures that form in the combustion chamber at the end of the compression stroke as a result of competition between swirling flow and squish flow. Flow patterns with the stepped-lip piston are less symmetrical than with the conventional re-entrant bowl.

## FY 2016 Publications/Presentations

1. Busch, S., Zha, K., Warey, A., Pesce, F., Peterson, R., "On the Reduction of Combustion Noise by a Close-Coupled Pilot Injection in a Small-Bore Direct Injection Diesel Engine," ASME J. Eng. Gas Turbines Power, V138, No. 10, pp. 102804-1-102804-13, 2016. Originally presented at ASME 2015 ICEF, November 8–11, 2015.
2. Zha, K., Busch, S., Park, C. and Miles, P.C., "A Novel Method for Correction of Temporally- and Spatially-Variant Optical Distortion in Planar Particle Image Velocimetry," Measurement Science and Technology 27 (8): 1-16, 2016, doi: 10.1088/0957-0233/27/8/085201.
3. Perini, F., Reitz, R.D., Zha, K., Busch, S., Warey, A., Peterson, R., "Modeling the effects of pilot injection strategies on combustion noise and soot emissions in a light duty optical Diesel engine," THIESEL 2016, September 13–16, 2016, Valencia, Spain.
4. Busch, S., Park., C., Warey, A., Pesce, F., Peterson, R., "A Study of the Impact of Pilot-Main Dwell on Late-Cycle Flow in the Piston Bowl of a Light-Duty Optical Diesel Engine," Proceedings of the 12th International Symposium on Combustion Diagnostics, May 10–11, 2016, Baden-Baden, Germany.
5. Zha, K., Perini, F., Busch, S., Park, C., Reitz, R., Kurtz, E., Warey, A., Peterson, R.C., "Piston Geometry Effects on Compression Stroke Swirling Flow in a Light-Duty Optical Diesel Engine," Presentation at SAE World Congress, April 12, 2016, Detroit, MI.

## II.2 Heavy-Duty Low-Temperature and Diesel Combustion & Heavy-Duty Combustion Modeling

### Overall Objectives

This project includes diesel combustion research at Sandia National Laboratories (SNL) and combustion modeling at the University of Wisconsin. The overall objectives are:

- Develop fundamental understanding of how in-cylinder controls can improve efficiency and reduce pollutant emissions of advanced low-temperature combustion technologies
- Quantify the effects of fuel injection, mixing, and combustion processes on thermodynamic losses and pollutant emission formation
- Improve computer modeling capabilities to accurately simulate these processes

### Fiscal Year (FY) 2016 Objectives

The objectives for FY 2016 focus on improving understanding of direct injection spray/jet processes on mixing and emissions and continuing to develop capabilities measure heat transfer effects on efficiency.

- Provide in-cylinder engine data and uncertainty estimates for the Engine Combustion Network (ECN) using the three-hole Spray B injector (SNL)
- Measure how end of injection mixing, including scalar dissipation, affects ignition in diesel jets (SNL)
- Improve capabilities for wall heat transfer measurements (SNL)
- Improve computer model simulation and analysis tools to complement experimental measurements (University of Wisconsin)

### FY 2016 Accomplishments

- New engine in-cylinder Spray B liquid length, vapor penetration, ignition delay, and lift-off generally agree well with constant-volume vessel data
  - Slower than expected vapor penetration could be due to hole-to-hole variation
  - Detailed uncertainty analysis, including sensitivity analysis relative to reference condition to reduce uncertainty, aids model validation

### Mark P.B. Musculus

Combustion Research Facility  
Sandia National Laboratories  
P.O. Box 969, MS9053  
Livermore, CA 94551-0969  
Phone: (925) 294-3435  
Email: mpmusu@sandia.gov

DOE Technology Development Manager:  
Leo Breton

- Showed progress on development of laser dispersion diagnostics for quantitative in-cylinder scalar dissipation measurement and development of robust coatings for infrared (IR) heat transfer imaging diagnostics
- Developed new insight on validation of soot models by comparing predicted and measured soot luminosity, including new transfer function; also progress on Spray B and post-injection modeling ■

### Introduction

Regulatory drivers and market demands for lower pollutant emissions, lower carbon dioxide emissions, and lower fuel consumption motivate the development of clean and fuel-efficient engine operating strategies. Most current production engines use a combination of both in-cylinder and exhaust aftertreatment strategies to achieve these goals. The emissions and efficiency performance of in-cylinder strategies depend strongly on flow and mixing processes associated with fuel injection.

The ECN is a forum and database for collaboration on engine combustion [1]. The existing ECN dataset is primarily for a single-hole Spray A injector operated in constant-volume combustion chambers. While these data are useful in a more fundamental sense, data that include the additional factors that affect in-cylinder processes with multi-hole injectors in practical reciprocating engines have been unavailable. In the previous fiscal year, this project reported new vapor penetration data for the multi-hole ECN Spray B injector in an optical engine. This year, a full in-cylinder dataset using multiple spray and combustion diagnostics was completed for the ECN

[2] and is featured in this report. Due to space constraints, other FY 2016 activities related to development of a scalar dissipation and heat transfer diagnostics are not detailed here.

## Approach

This project uses an optically accessible, heavy-duty, direct injection diesel engine (Figure 1). A large window in the piston crown provides primary imaging access to the piston bowl, and other windows at the cylinder wall provide cross-optical access for laser diagnostics or imaging.

The experiments use several in-cylinder optical measurements. For illustrative purposes, Figure 1 shows one of three imaging setups. The setup in Figure 1 uses two cameras to image ultraviolet (UV) OH\* chemiluminescence and visible-light broadband luminosity from the diesel flame. A band-pass filter (BPF) with a 10-nm full width at half maximum (FWHM) centered at a wavelength of 310 nm is placed in front of the UV camera to isolate OH\* chemiluminescence from soot emission. A long wave pass (LWP) beam splitter with a cutoff near 355 nm reflects UV light to the intensified high-speed complementary metal-oxide semiconductor

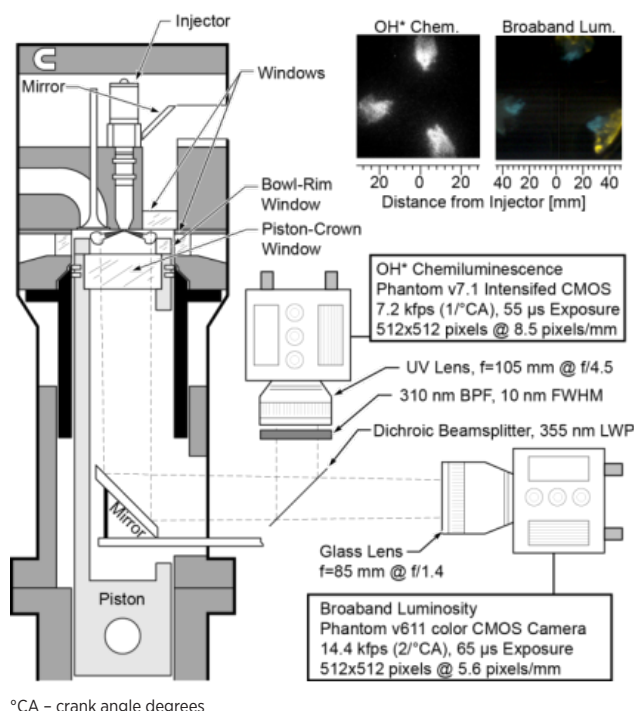


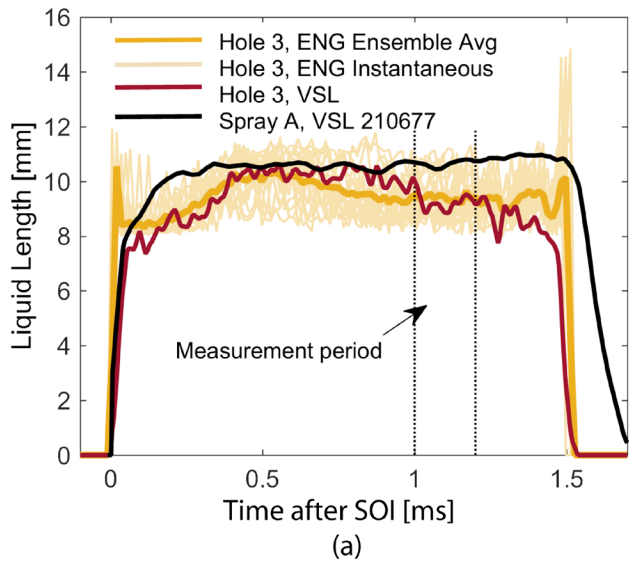
Figure 1. Schematic diagram of the optically accessible, heavy-duty, direct injection diesel engine and optical setup with OH\* chemiluminescence and natural luminosity cameras. Top right: sample images.

(CMOS) camera for OH\* chemiluminescence imaging, and transmits visible light to the high-speed color CMOS camera for broadband luminosity imaging. Other diagnostics not shown here include: imaging of elastic Mie scattering from liquid fuel droplets illuminated by a high-power pulsed light-emitting diode (LED) near 630 nm to measure liquid fuel penetration; a pass-through schlieren diagnostic using a second blue-color LED with emission near 455 nm coupled with a high-speed CMOS camera to measure vapor-fuel penetration; and an IR imaging diagnostic to measure vapor fuel penetration indicated by thermal emission from hot fuel jets.

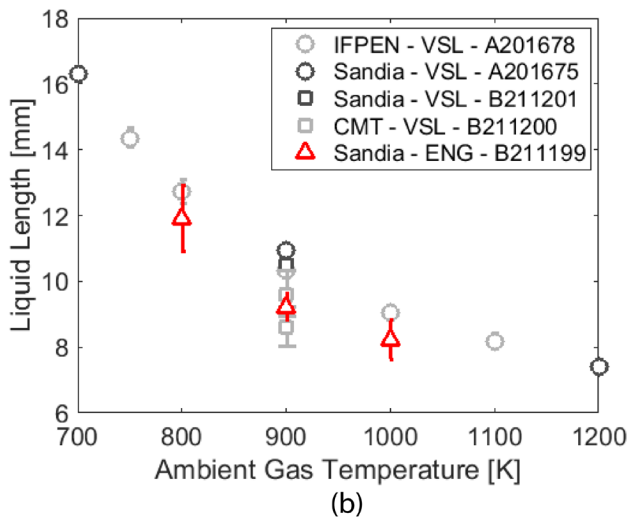
## Results

Figure 2a shows a comparison of the instantaneous and ensemble-averaged liquid length for Hole 3 of the Spray B injector as measured in the engine (ENG), compared to measurements in constant-volume combustion vessels (VSL), as well as a comparison to the single-hole Spray A injector. Conditions for the test are indicated in the caption. Compared to Spray A, the liquid length for Spray B shows higher variability during injection and from one injection to the next, and both in the engine and in vessels. Although an obvious quasi-steady period for the liquid length measurement was not clearly attained, the period between 1.0 ms and 1.2 ms after the start of injection (SOI) was relatively steady in the ensemble average, and is taken as the characteristic liquid length. Figure 2b shows a comparison of this characteristic liquid length over a temperature sweep for a number of facilities and injectors, as indicated in the figure caption. In general, the mean liquid length is shorter for the three-hole Spray B injector compared to the single-hole Spray A injector, in both engines and vessels. However, measurements in different facilities and with different injectors are often within the experimental error bars in Figure 2b.

Shown in Figure 3a are comparisons of ensemble-averaged lift-off lengths for all three holes of the Spray B injector measured in the engine, as well as instantaneous measurements for Hole 3 only, for the conditions indicated in the figure caption. The variation from hole to hole for the ensemble-averaged data span from 1 mm to 3 mm for this condition, and the variation in the instantaneous data spans approximately 7 mm. Figure 3b shows comparisons to measurements in constant-volume combustion vessels (VSL) of the ensemble-averaged lift-off length measured in the engine (ENG) for Hole 3 during the quasi-steady measurement period from 1.0 ms to 1.2 ms, as indicated in Figure 3a, for a sweep in ambient temperature. Over the temperature sweep, the mean lift-off lengths for Spray A and Hole 3 of Spray B,

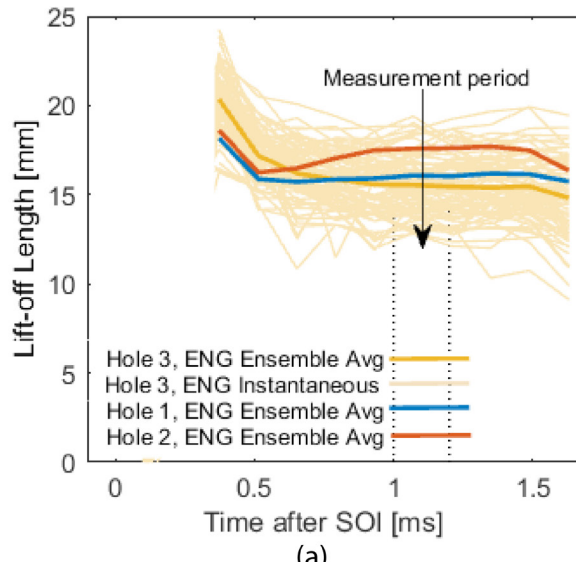


(a)

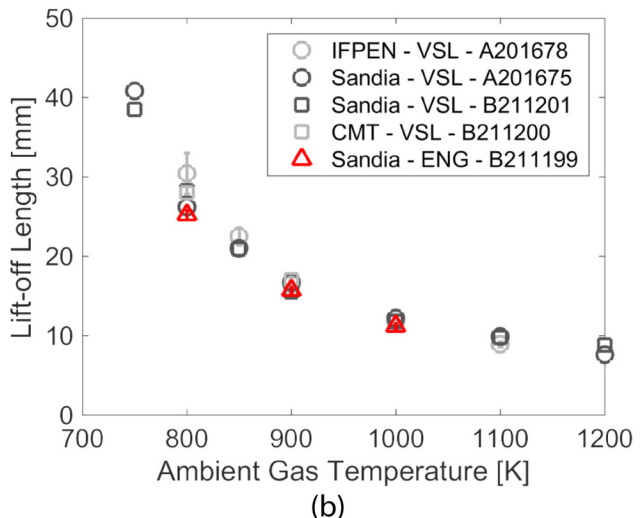


(b)

Figure 2. (a) Ensemble-averaged liquid length for nonreacting conditions (0% O<sub>2</sub>) at 900 K and 22.8 kg/m<sup>3</sup> ambient conditions with 1,500 bar rail pressure for Hole 3 of Spray B in the engine (ENG) vs. data previously acquired from Hole 3 of the same Spray B injector measured in the Sandia constant-volume vessel (VSL), and the Spray A injector #210677 in the Sandia vessel [1]. Instantaneous profiles from the engine show the measurement fluctuations. (b) Effect of ambient gas temperature on the liquid length for different sources (Sandia: Sandia National Laboratories, IFPEN: IFP Energies nouvelles, CMT: CMT-Motores T  rmicos), different facilities (VSL: constant-volume combustion vessel, ENG: engine), and different injectors (indicated by A or B spray type and serial number). The results obtained in this report are represented by red triangles, and other data are archived from ECN [1].



(a)



(b)

Figure 3. (a) Ensemble-averaged lift-off length for ambient conditions of 900 K and 22.8 kg/m<sup>3</sup> and 15% O<sub>2</sub> with 1,500 bar rail pressure for all three holes of Spray B in the engine (ENG). Instantaneous profiles for Hole 3 provide a visual estimate of the measurement fluctuations. (b) Effects of ambient temperature on lift-off length measured in the engine (ENG, red triangles) and constant-volume vessels (VSL) for different sources and injectors as indicated in the Figure 2 caption.

and across different facilities, generally agree within the experimental error bars.

A comparison of the vapor penetration measured using the schlieren technique is shown in Figure 4 for Spray B in both the engine and a constant-volume combustion vessel, as well as for Spray A in a combustion vessel. Operating conditions are indicated in the figure caption. The in-cylinder density of the engine measurement is limited by the intake flow capacity of the nitrogen supply

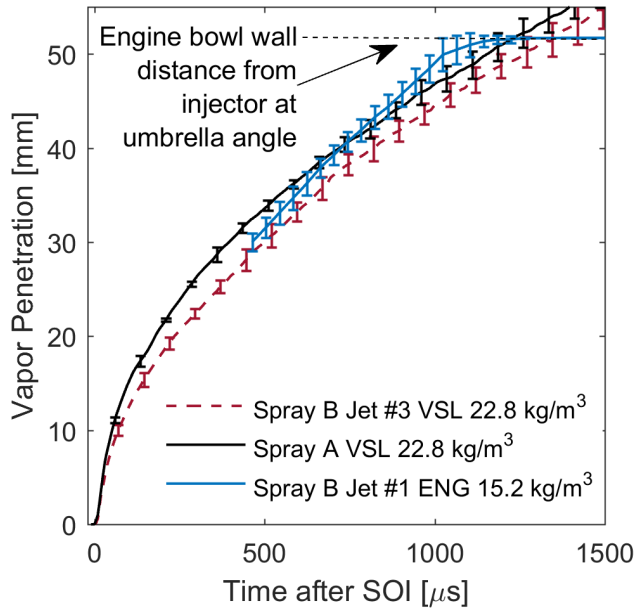


Figure 4. Ensemble-averaged vapor penetration for Spray B in the engine (ENG, blue) under nonreacting conditions at an ambient density of  $15.2 \text{ kg/m}^3$  and in the Sandia vessel (VSL, red) at  $22.8 \text{ kg/m}^3$ . Reference data for Spray A at  $22.8 \text{ kg/m}^3$  in the Sandia vessel (VSL, black) also included.

in the engine facility to create non-combusting conditions (100% nitrogen), so the density in the engine ( $15.2 \text{ kg/m}^3$ ) is not directly comparable to the available constant-volume combustion vessel (for a density of  $22.8 \text{ kg/m}^3$ ). Although the different data overlap in Figure 4, the penetration rate in the engine is slower than expected, since the jets should penetrate about 20% more rapidly at the lower density according to established scaling relationships [3]. The reasons for the slow penetration are not clear, but could be due to hole-to-hole variations, since engine penetration data were only available for Hole 1, while constant-volume combustion vessel data are for Hole 3. Hole-to-hole variations are observed in other data, for instance in the ensemble-averaged lift-off measurements, for which data from all three holes are available. Figure 3a shows ensemble-averaged lift-off length variations among the holes as large as 20%, which is a similar magnitude as the difference between measured penetration rate for Hole 1 in the engine versus for Hole 3 in the constant-volume vessels.

Finally, in separate efforts to improve the ability to compare optical soot luminosity data from experiments to simulations, as well as to help interpret experimental soot luminosity data in terms of in-cylinder soot mass, calculated soot luminosity from computer simulations was analyzed in detail. Figure 5 shows a comparison between model predictions of the product of soot volume

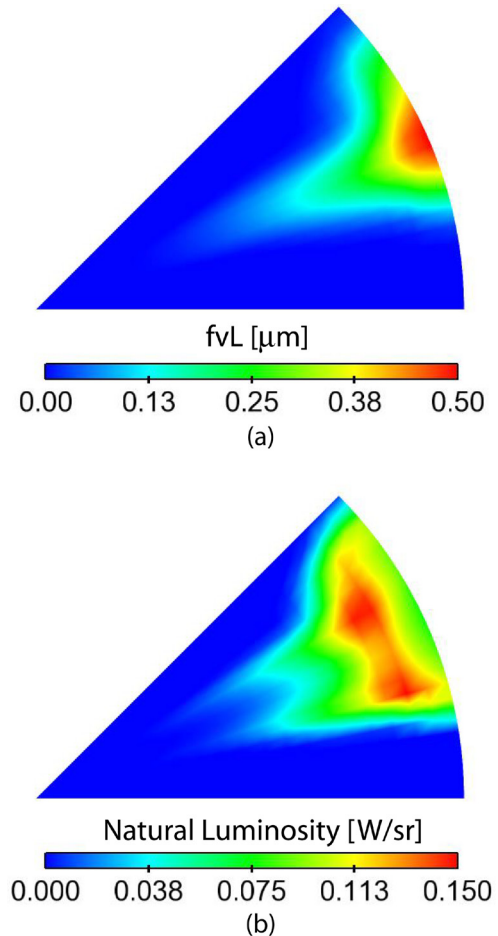


Figure 5. Example line-of-sight images from computer simulations of diesel combustion in a  $45^\circ$  sector, with the injector at the bottom left of the images and the bowl wall on the right. (a) Distribution of the product of soot volume-fraction and line-of-sight path length (fvL). (b) Distribution of the line-of-sight integrated soot natural luminosity.

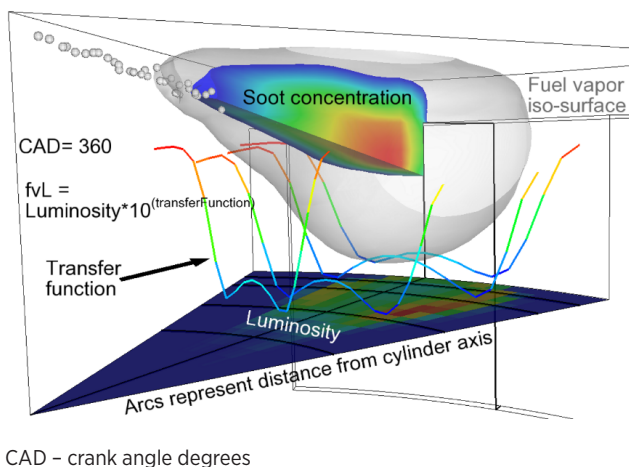
fraction and line-of-sight path length (fvL) and natural luminosity for one diesel jet in the piston bowl. The fvL is predicted using soot formation and oxidation submodels, and is quantitative for soot mass. The natural luminosity is calculated cell by cell using radiant emission from soot, accounting for absorption/emission along the line of sight as well as the camera spectral sensitivity. Natural luminosity is not quantitative for soot, but the calculation provides an estimate of how a natural luminosity image would appear in an experiment. A comparison of the images in Figure 5 shows a clear difference between the quantitative soot fvL and the soot natural luminosity, which is what hinders direct comparison between model soot predictions and experimental soot natural luminosity images. With the new calculation method, a generalized transfer function was derived to convert fvL to luminosity for comparison to experiments. As shown graphically

by the line plots in Figure 6, the transfer function has a characteristic “omega” shape that allows it to be applied even to experimental images of natural luminosity to aid interpretation of measured soot luminosity intensities in terms of more quantitative soot fvL. Future work will provide direct comparisons of experimental and model results using the new transfer function.

## Conclusions

The recent research described in this report provides improved understanding of in-cylinder processes required by industry to build cleaner, more efficient, heavy-duty engines. Specific conclusions include:

- Liquid length, vapor penetration, ignition delay, and lift-off measured in the engine show generally good agreement with ECN data, providing confidence in the applicability of models validated in constant-volume vessels for engine simulation. More study is required to resolve some differences in vapor penetration, which could be due to hole-to-hole variation.
- Comparisons of quantitative in-cylinder soot and resulting natural luminosity as predicted by computer simulations led to the development of a transfer function that helps to compare model predictions to experimental data for validation, as well as to help



CAD – crank angle degrees

Figure 6. Example fuel vapor iso-surface (gray) and soot concentration cross section (color, top) for computer simulation of diesel combustion for one spray in a sector mesh, with the injector at the top left and the piston-bowl bottom and wall in the bottom-right. Line plots show the natural-luminosity-to-fvL transfer function at selected radial distances from the cylinder axis, and the color contour map along the piston bowl (bottom) shows the resulting calculated line-of-sight soot natural luminosity distribution that would be viewed by the camera.

interpret experimental soot luminosity imaging in terms of quantitative soot distributions.

- Progress on development of laser dispersion diagnostics for quantitative in-cylinder scalar dissipation measurement will help to reveal how end-of-injection mixing processes affect ignition and combustion, potentially offering new avenues for combustion phasing control. Progress on heat transfer diagnostic development will provide new tools for understanding how in-cylinder processes can be controlled to reduce heat transfer losses for improved engine efficiency.

## References

1. Engine Combustion Network, [www.sandia.gov/ecn/](http://www.sandia.gov/ecn/).
2. “Measurements of liquid length, vapor penetration, ignition delay, and flame lift-off length for the Engine Combustion Network ‘Spray~B’ in a 2.34L optical heavy-duty diesel engine,” W.E. Eagle, L-M. Malbec, M.P.B. Musculus, SAE Technical Paper 2016-01-0743, SAE World Congress and Exposition, April 2016.
3. “Effects of gas density and vaporization on penetration and dispersion of diesel sprays,” J.D. Naber and D.L. Siebers, SAE Technical Paper 960034, SAE Transactions 105(3):82–111, 1996.

## FY 2016 Publications/Presentations

1. “Parametric comparison of well-mixed and flamelet n-dodecane spray combustion with engine experiments at well controlled boundary conditions,” A. Maghbouli, T. Lucchini, G. D’Errico, A. Onorati, L-M. Malbec, M.P.B. Musculus, W.E. Eagle, SAE Technical Paper 2016-01-0577, SAE World Congress and Exposition, April 2016.
2. “Measurements of liquid length, vapor penetration, ignition delay, and flame lift-off length for the Engine Combustion Network ‘Spray~B’ in a 2.34L Optical Heavy-Duty Diesel Engine,” W.E. Eagle, L-M. Malbec, M.P.B. Musculus, SAE Technical Paper 2016-01-0743, SAE World Congress and Exposition, April 2016.
3. “Effect of post injections on mixture preparation and unburned hydrocarbon emissions in a heavy-duty diesel engine,” J. O’Connor, M. Musculus, L. Pickett, Combust. Flame 170:111–123, 2016.
4. “Measurements of liquid length, vapor penetration, ignition delay and flame lift-off length for the Engine Combustion Network ‘Spray B’ in a 2.34 L optical heavy-duty engine,” W.E. Eagle, L-M. Malbec, M.P.B. Musculus, AEC Program Review Meeting, February 2016.

5. "Applying advanced CFD analysis tools to study differences between start-of-main and start-of-post injection flow, temperature and chemistry fields due to combustion of main-injected fuel," SAE Technical Paper 2015-24-2436, ICE2015 - 12th International Conference on Engines & Vehicles, Capri, Italy, September 2015.
6. "Influence of injection duration and ambient temperature on the ignition delay in a 2.34L optical diesel engine," L.M. Malbec, W.E. Eagle, M.P.B. Musculus, and P. Schihl, SAE Tech. Paper 2015-01-1830, 2015 JSAE/SAE Powertrains Fuels and Lubricants International Meeting, Kyoto, Japan, September 2015.
7. "IR Emission imaging of fuel vapor penetration with comparison to schlieren and LIF for ECN Spray B," W.E. Eagle, L-M. Malbec, M.P.B. Musculus, AEC Program Review Meeting, August 2016.
8. "Evaluating temperature and fuel stratification for heat-release rate control in a reactivity-controlled compression-ignition engine using optical diagnostics and chemical kinetics modeling," S.L. Kokjohn, M.P.B. Musculus, R.D. Reitz, Combustion and Flame 162(6):2729–2742, June 2015.
9. "Comparing vapor penetration measurements from IR thermography of C-H stretch with schlieren during fuel injection in a heavy-duty diesel engine," W.E. Eagle, L-M. Malbec, M.P.B. Musculus, 9th U.S. National Combustion Meeting, Cincinnati, Ohio, May 2015.

## II.3 Spray Combustion Cross-Cut Engine Research

### Overall Objectives

- Facilitate improvement of engine spray combustion modeling, accelerating the development of cleaner, more efficient engines

### Fiscal Year (FY) 2016 Objectives

- Lead a multi-institution, international, research effort on engine spray combustion called the Engine Combustion Network (ECN), with focus on diesel and gasoline sprays
- Characterize the velocity field and plume–plume interaction of gasoline Spray G at various operating conditions
- Compare spray mixing, evaporation, and combustion with cavitating and non-cavitating diesel injectors

### FY 2016 Accomplishments

- Organized monthly web meetings for the ECN and developed plans for the next workshop; led experimental/modeling exchange on gasoline and diesel targets to identify the state of art and in spray combustion modeling and remedy known weaknesses; facilitated the exchange by revamping the ECN website and data archive
- Developed a high-speed diagnostic to quantify the velocity field between plumes of gasoline Spray G, and performed measurements to understand sources of plume interaction and spray collapse
- Quantified spray spreading angle, liquid penetration, ignition, and combustion behavior of diesel Spray C (cavitation) and Spray D injectors ■

### Introduction

All future high-efficiency engines will have fuel directly sprayed into the engine cylinder. Engine developers agree that a major barrier to the rapid development and design of these high-efficiency, clean engines is the lack of accurate fuel spray computational fluid dynamic (CFD) models. The spray injection process largely determines the fuel–air mixture processes in the engine, which subsequently drives combustion and emissions in both direct injection gasoline and diesel systems. More predictive spray combustion models will enable rapid design and optimization of future high-efficiency engines, providing more affordable vehicles and also saving fuel.

### Lyle M. Pickett

Sandia National Laboratories  
P.O. Box 969, MS 9053  
Livermore, CA 94551-9053  
Phone: (925) 294-2166  
Email: LMPicke@sandia.gov

DOE Technology Development Manager:  
Leo Breton

### Approach

To address this barrier, we have established a multi-institution collaboration, called the Engine Combustion Network, to both improve spray understanding and develop predictive spray models. By providing highly leveraged, quantitative datasets (made available online [1]) CFD models may be evaluated more critically and in a manner that has not happened to date. Productive CFD evaluation requires new experimental data for the spray and the relevant boundary conditions, but it also includes a working methodology to evaluate the capabilities of current modeling practices. Activities include the gathering of experimental and modeling results at target conditions to allow a side-by-side comparison and expert review of the current state of the art for diagnostics and engine modeling. Significant progress has been made for both diesel and gasoline injection systems.

For brevity, we will highlight a few of the key advancements from our experimental spray combustion facility, with a particular emphasis on multi-hole gasoline fuel injectors and the ECN target injector Spray G [2,3]. Past work to characterize this injector has suggested that plumes move dynamically during injection and collect into one jet at the end of injection. The collapse or merging of individual plumes of direct injection gasoline injector is of fundamental importance to engine performance because of its impact on fuel–air mixing. However, the mechanics of plume interaction and spray collapse are not fully understood and are difficult to predict. This year we developed a high-speed (100 kHz) particle image velocimetry (PIV) to quantify the aerodynamics between plumes with full temporal evolution of plume interaction and potential collapse in transient individual injection events. This unique dataset is available for comparison with advanced Reynolds-averaged Navier–Stokes and large eddy simulation

models. We have also made significant progress understanding diesel combustion from fuel injectors made to intentionally induce cavitation, but this work will not be reviewed here because of space limitations. Please see a detailed reference on the subject in Westlye et al. [4].

## Results

In preparation for velocimetry between plumes of the multi-hole fuel injector, we first assessed the liquid boundaries of individual plumes using diffused back illumination extinction imaging and determined that it would be possible to position the PIV laser sheet between liquid plumes. As shown in Figure 1, the laser sheet was passed between plumes, thereby avoiding direct illumination of liquid sprays. The holes are drilled with an angle of  $37^\circ$  relative to the injector axis, permitting some separation between plumes if the plumes do not merge together. In order to make the data on plume interaction and collapse as useful as possible, the measurement position was also placed close to the injector in the near-field of the spray from approximately 13–19 mm as shown in Figure 2. Although liquid plumes are in the path of the signal collection, and impair the measurement, the plumes are not in the same plane as the laser sheet, and it was possible to distinguish the planar data from interferences caused by the out-of-plane liquid spray plumes.

Examples of the processed velocimetry on top of the raw PIV images are given in Figure 3, at the standard Spray G operating conditions with an injection duration of 800  $\mu\text{s}$ . During the early phase of injection, a strong upward recirculation flow is established. Out-of-plane liquid from Plume-Pairs 1 and 4 and 8 and 5 is visible in the raw images at 400  $\mu\text{s}$ , and could interfere from the actual signal along the laser plane. However, image processing algorithms designed to utilize the temporal sequence of data (available every 10  $\mu\text{s}$ ) effectively limit rogue velocity vectors even though the liquid spray moves in

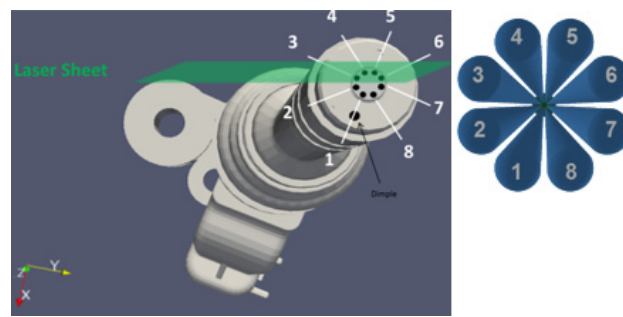


Figure 1. Illustration of the laser sheet alignment in regard to the gasoline Spray G injector plume orientation [1]

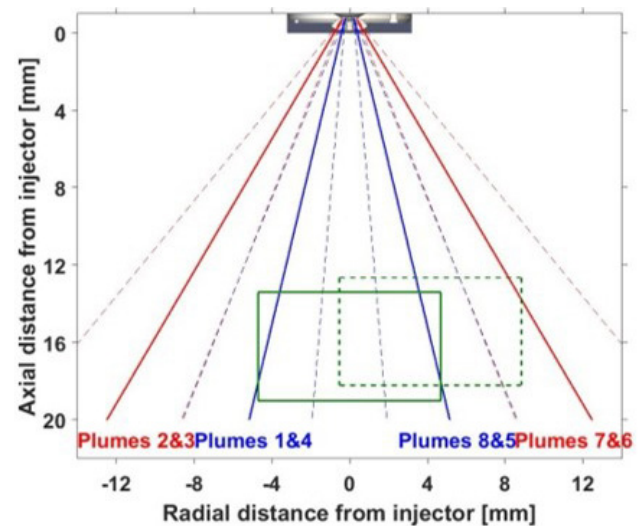


Figure 2. Scaled illustration of the viewing area between the plumes of the gasoline spray injector. Plume centers and edges on projection are indicated by solid and dashed lines, respectively.

the opposite direction to the gas between plumes at this time. The upward gas flow is momentary as eventually neighboring plumes contract into the central region and reverse the flow direction, as shown at 1,400  $\mu\text{s}$ .

The ensemble-averaged measurement of velocity at the centerline with an axial distance of 15 mm is shown in Figure 4, with labels indicating different phases generally observed for the centerline region. The central recirculation zone begins to develop even prior to the penetration of liquid plumes to that axial location, and continues to increase in magnitude until approximately 300  $\mu\text{s}$ . Recirculation persists at near steady values until 700  $\mu\text{s}$ , whereupon the velocity decelerates and eventually changes direction towards a positive axial flow. The change in recirculation velocity is an indicator that the plumes are beginning to interact and will eventually collapse.

The temporal behavior of the interacting plumes is illustrated further by considering variations at measurement positions outside of the central region and between plumes. Continuing to focus on the 15-mm axial position, the ensemble-averaged axial velocities for each cross-stream radial position are rendered in color and plotted as an “image” with time as vertical axis after start of injection (ASI) in Figure 5. The horizontal axis includes the central and offset radial measurement positions to extend to nearly a 9-mm position. The plot shows that plumes make contact at a radial position of 6 mm following a brief recirculation period that breaks down by 300  $\mu\text{s}$ . After this timing, the radial position of

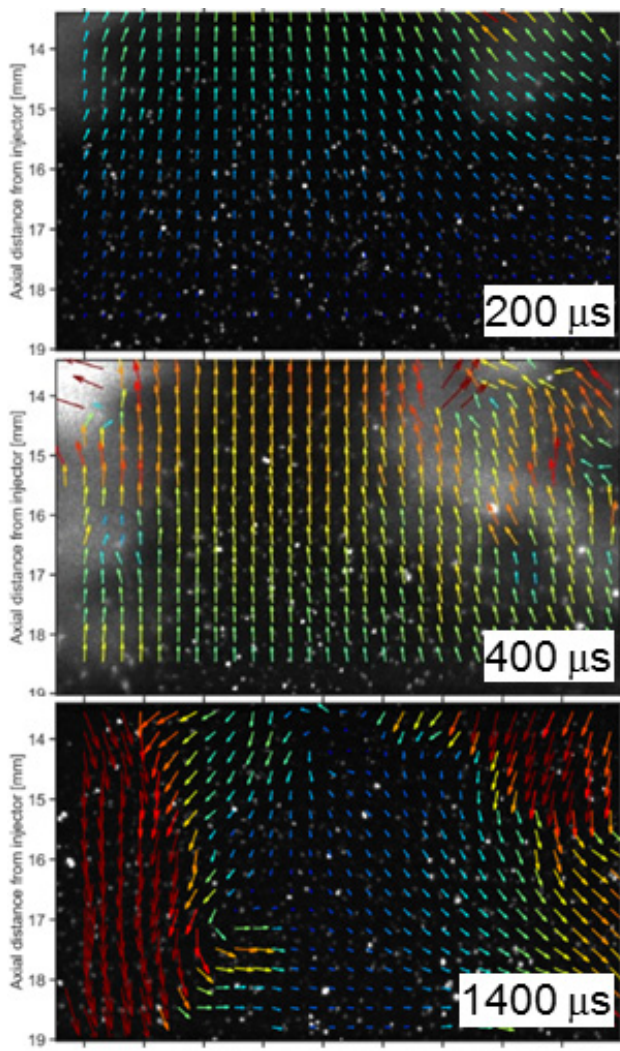


Figure 3. Velocity vectors overlaid on raw PIV images at specific times after the start of injection. Fuel injection: 200 bar, iso-octane; ambient: 573 K,  $3.5 \text{ kg/m}^3$ , 0%  $\text{O}_2$  [1].

the merging jets continues to encroach upon the centerline position until the flow is reversed at the centerline. Even though injection ends prior to the flow reversal at the centerline, the period after the end of injection is relevant to fuel delivery and combustion as this is the timing when spark ignition typically occurs.

Other operating conditions have also been explored, including the effect of ambient temperature, gas density and injection duration. Increasing ambient temperature or density, with enhanced vaporization and momentum exchange, accelerates plume interaction. Plume interaction is also inherently transient, as longer injection durations progressively show more interaction between plumes with the consequence of variable fuel plume delivery direction with time.

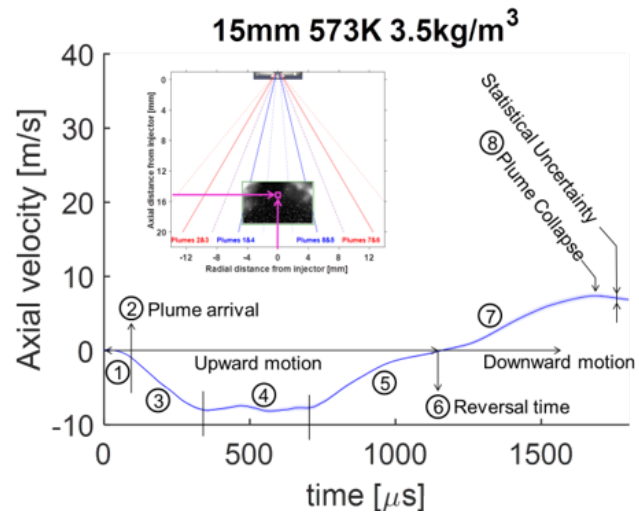


Figure 4. Ensemble-averaged velocity at the centerline, 15-mm axial position. Same conditions as Figure 3.

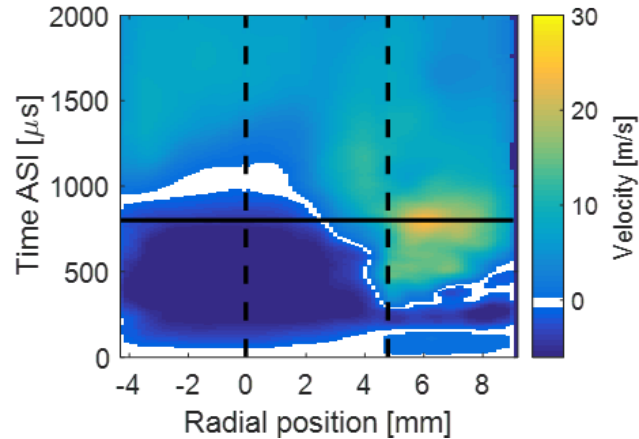


Figure 5. Temporal evolution of axial velocity for the 15-mm axial position between plumes

## Conclusions

Research this year has highlighted how realistic multi-hole sprays can affect mixing and combustion processes, using gasoline and diesel targets of the ECN. The experimental data provided is now being used by the ECN community to improve CFD models that will be used to optimize future engine designs. Future work will focus on mixing dynamics that lead to the formation of rich mixture and problematic particulate formation for gasoline engines.

## Acknowledgements

PIV research was facilitated by visiting researcher Dr. Panos Sphicas from Imperial College London.

Construction of the high-speed, pulse-burst laser was led by Dr. Jonathan Frank and enabled by funding provided by Sandia National Laboratories laboratory-directed research and development program.

## References

1. Engine Combustion Network, <https://ecn.sandia.gov/>.
2. Manin J., Skeen S.A., Pickett L.M., Jung Y., Parrish S.E., Markle L.E., "Experimental Characterization of DI Gasoline Injection Processes," SAE 2015-01-1894, 2015.
3. Itani L., Bruneaux G., Hermant L., Schulz C., "Investigation of the Mixing Process and the Fuel Mass Concentration Fields for a Gasoline Direct-injection Spray at ECN Spray G Conditions and Variants," JSAE20159330 / SAE2015-01-1902.
4. Westlye F.R., Battistoni M., Skeen S.A., Manin J., Pickett L.M., and Ivarsson A., "Penetration and combustion characterization of cavitating and non-cavitating fuel injectors under diesel engine conditions," SAE 2016-01-0680, 2016.
5. "Boundary condition and fuel composition effects on injection processes of high-pressure sprays at the microscopic level." J. Manin, M. Bardi, L.M. Pickett, and R. Payri. International Journal of Multiphase Flow 83:267–278, 2016.
6. "Penetration and combustion characterization of cavitating and non-cavitating fuel injectors under diesel engine conditions," Fredrik R. Westlye, Michele Battistoni, Scott A. Skeen, Julien Manin, Lyle M. Pickett, and Anders Ivarsson. SAE 2016-01-0680, 2016.
7. "A Progress Review on Soot Experiments and Modeling in the Engine Combustion Network (ECN)." Scott A. Skeen, Julien Manin, Lyle M. Pickett, Emre Cenker, Gilles Bruneaux, Katsufumi Kondo, Tets Aizawa, Fredrik Westlye, Kristine Dalen, Anders Ivarsson, Tiemin Xuan, Jose M. Garcia-Oliver, Yuanjiang Pei, Sibendu Som, Wang Hu, Rolf D. Reitz, Tommaso Lucchini, Gianluca D'Errico, Daniele Farrace, Sushant S. Pandurangi, Yuri M. Wright, Muhammad Aqib Chishty, Michele Bolla, and Evatt Hawkes. SAE Int. J. Engines 9 (2), 2016.
8. "Effect of Post Injections on Mixture Preparation and Unburned Hydrocarbon Emissions in a Heavy-Duty Diesel Engine," J. O'Connor, M.P.B. Musculus, L.M. Pickett, Combust. Flame 170:111–123, 2016.

## FY 2016 Publications

1. "Understanding the ignition mechanism of high-pressure spray flames," Rainer N. Dahms, Guenter A. Pazcko; Scott A. Skeen; Lyle M. Pickett, Proc. Combust. Inst., accepted 2016.
2. "Characterization of Spray A flame structure for parametric variations in ECN constant-volume vessels using chemiluminescence and laser-induced fluorescence," N. Maes, M. Meijer, N. Dam, B. Somers, H.B. Toda, G. Bruneaux., S. Skeen, L.M. Pickett, J. Manin, Combust. Flame, accepted 2016.
3. "Onset and progression of soot in high-pressure n-dodecane sprays under diesel engine conditions," Sushant S. Pandurangi, Michele Bolla, Yuri M Wright, Konstantinos Boulouchos, Scott A Skeen, Julien Manin, and Lyle M. Pickett, International Journal of Engine Research, 1468087416661041, first published on August 1, 2016.

## II.4 Low-Temperature Gasoline Combustion (LTGC) Engine Research

### Overall Objectives

- Provide the fundamental understanding (science-base) required to overcome the technical barriers to the development of practical low-temperature gasoline combustion (LTGC) engines by industry

### Fiscal Year (FY) 2016 Objectives

- Conduct LTGC engine performance mapping with new low-swirl, spark plug capable cylinder head (Head #2), and compare with previous head (Head #1)
- Determine the potential for controlling combustion phasing (crank angle for 50% burn [CA50]) using partial fuel stratification produced by a double direct injection (DDI)-partial fuel stratification (PFS)
- Investigate the ability of DDI-PFS to improve the robustness of LTGC operation for exhaust gas recirculation tolerance and load limits
- Demonstrate CA50 control of LTGC using spark assist (SA) and investigate operational limits for SA at naturally aspirated conditions
- Evaluate performance with a research-quality, regular-grade, 87 Anti-Knock Index (AKI), E10 gasoline (RD5-87) for both PFS and premixed fueling, and compare with previous Tier 2 certification gasoline (CF-E0) data
- Support modeling: chemical kinetics at Lawrence Livermore National Laboratory (LLNL) and related rapid compression machine experiments at Argonne National Laboratory, and computational fluid dynamics (CFD) modeling at General Motors (GM)

### Accomplishments

- Completed installation and shakedown testing of new spark plug capable, low-swirl cylinder head (Head #2)
- Conducted performance mapping of Head #2 and compared with Head #1 for both premixed and early direct inject (DI) fueling; multiple parameters evaluated and compared
  - Applied energy loss analysis tools developed in FY 2015 to understand differences between the heads
- Demonstrated CA50 control over a wide range (from strong knock to near misfire) using DDI-PFS with

### John E. Dec

Sandia National Laboratories  
MS 9053, P.O. Box 969  
Livermore, CA 94551-0969  
Phone: (925) 294-3269  
Email: jedec@sandia.gov

DOE Technology Development Manager:  
Leo Breton

variable injection timing to adjust the fuel stratification and shift CA50

- Showed that DDI-PFS can substantially increase robustness (i.e., increased exhaust gas recirculation tolerance and allowable CA50 range), and that it can increase stability to extend the load range for some conditions
- Demonstrated spark-assisted LTGC for CA50 control and increased tolerance to variation in intake temperature ( $T_{in}$ ) with no increase in  $NO_x$  emissions
  - Showed the low equivalence ratio ( $\phi$ ) limit for SA at naturally aspirated conditions
- Evaluated the performance of RD5-87 (87 AKI, E10) regular gasoline and compared to the high-octane, E0 certification gasoline (CF-E0)
- Collaborated with LLNL on the development of a kinetic mechanism for RD5-87 and related rapid compression machine measurements at Argonne National Laboratory, and with GM on CFD modeling ■

### Introduction

Improving the efficiency of internal combustion engines is critical for meeting global needs to reduce petroleum consumption and  $CO_2$  emissions, needs reflected in the mandate for 54 mpg vehicles by 2025. LTGC engines, including HCCI and stratified variants of HCCI, have a strong potential for contributing to these goals since they have high thermal efficiencies and ultra-low  $NO_x$  and particulate emissions. Furthermore, with intake pressure boost, LTGC can achieve loads comparable to turbocharged diesel engines. Perhaps most importantly, LTGC provides a means for producing

high-efficiency engines that operate on light distillates, thus complementing diesel engines which use middle distillates, for more effective overall utilization of crude oil supplies and lower total CO<sub>2</sub> production.

Although substantial progress has been made in recent years on extending the low- and high-load limits of LTGC over the desired operating range, rapid control of combustion phasing remains a key technical challenge. To address this challenge, two control techniques have been studied over the past year. First, with DDI-PFS, changes in the second injection timing and fuel fraction can be used adjust the reactivity of the charge mixture (i.e., the chemical kinetic rates of autoignition) to change combustion phasing. Second, SA uses a spark plug to create a weak flame (weak due to high charge dilution) that burns a small fraction of the total charge, but drives the main charge into autoignition at the desired time. The results of these studies are presented along with other related studies of LTGC.

## Approach

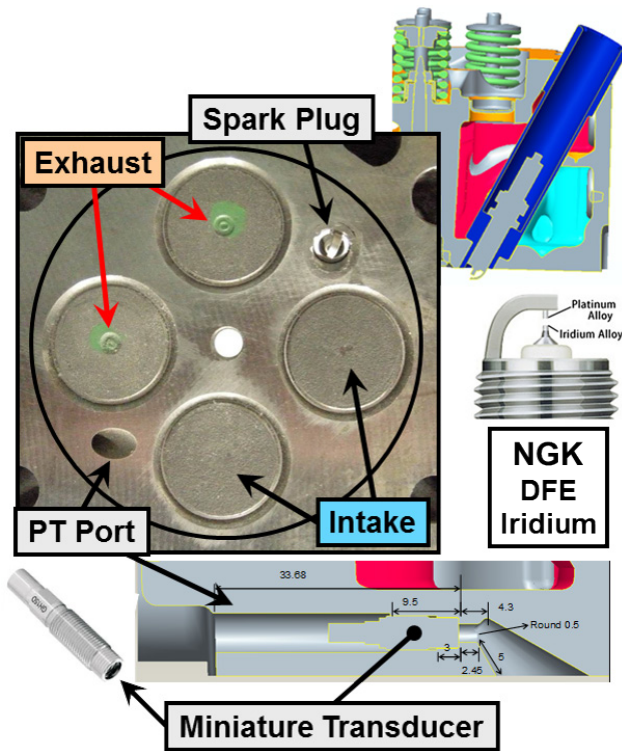
Studies were conducted in the Sandia LTGC Engine Laboratory using the all-metal single-cylinder LTGC research engine (displacement = 0.98 L). This facility allows operation over a wide range of conditions, and it has been designed to provide precise control of virtually all operating parameters for well-characterized experiments and high-quality data. This LTGC engine was derived from a Cummins B-Series diesel, so investigating SA-LTGC required equipping it with a new cylinder head modified to accommodate a spark plug. These modifications were designed in collaboration with Cummins who modified a new low-swirl cylinder head and supplied it to this project. Along with this new head, the engine was equipped with a new high-pressure capable gasoline-type direct injector and a high-energy spark-ignition system supplied by GM. The diesel piston was replaced with an LTGC piston having an open combustion chamber with a broad, shallow bowl, giving a CR = 16:1. For consistency between data points, the engine was typically operated with the combustion timing (as measured by the CA50) being as advanced as possible without inducing engine knock, which gives the highest thermal efficiency (TE) for a given operating condition. The knock onset point was taken to be a ringing intensity (RI) [1] of 5 MW/m<sup>2</sup> [2,3].

## Results

Modifying the diesel cylinder head to accommodate a spark plug presented some challenges. Most notably, the only place on the head with enough open space to

accommodate a spark plug was in the location previously used for the pressure transducer. Thus, in addition to working in a larger sleeve and hole in this location for the spark plug, a new approach was required to mount the pressure transducer. As shown in the photo and schematics in Figure 1, the spark plug was mounted between an intake and an exhaust valve using a custom tube to go through the water jacket. Mounting the spark plug at angle allowed the electrodes to be as far from the cylinder wall as possible. Since no other location existed where the transducer could be brought in from the top of the head, a very small (5 mm) transducer was inserted horizontally through the firedeck from the back end of the head, as shown in the schematic at the bottom of Figure 1. A conical opening (designed to minimize acoustic oscillations) allows the charge gases to reach the transducer. Subsequent analysis of the pressure transducer signal showed that this design works very well.

After additionally modifying the cylinder head to accommodate the gasoline direct injector and fitting it to our custom single-cylinder intake manifold, the engine performance with the new head (Head #2) was evaluated over a range of conditions. As shown in Figure 2, the



DFE – double fine electrode

Figure 1. Photo of the new spark plug capable cylinder head and schematics showing the method of mounting the spark plug and the installation of the miniature pressure transducer (PT) through the firedeck

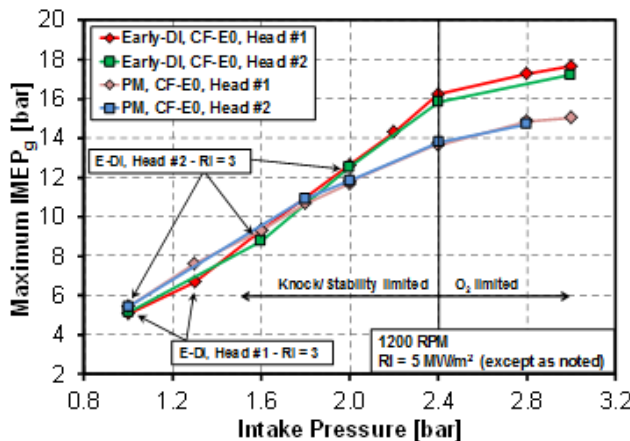


Figure 2. Comparison between Head #1 and Head #2 for the high-load limits as a function of  $P_{in}$  for both premixed and early DI fueling (single DI injection). RI = 5 MW/m<sup>2</sup> except as noted, 1,200 rpm, fuel = CF-E0.

maximum load is very close to that of Head #1 for  $P_{in}$ s from 1.0–3.0 bar absolute, i.e., naturally aspirated to high boost. For premixed fueling, the maximum loads are nearly identical, and for early DI fueling they are essentially the same except for  $P_{in} \geq 2.4$  bar where the load is about 2.5% lower with Head #2. For example, the maximum load for Head #1 with early DI fueling was 17.7 bar gross indicated mean effective pressure (IMEP<sub>g</sub>), compared to 17.2 bar IMEP<sub>g</sub> for Head #2. Similarly, the maximum TEs were also quite close between the two heads, with the largest differences being ~1%-unit and more typically ~0.2%-units for TEs that range from 44.5–49.8% over the operating map.

For a fuel whose autoignition timing varies with the local equivalence ratio ( $\phi$ ) in the cylinder ( $\phi$ -sensitive), as is often the case for regular gasoline, autoignition will occur sequentially from the richest regions to the leanest if the fuel distribution is partially stratified. This sequential autoignition reduces the heat release rate (HRR) compared to a premixed charge at the same CA50, allowing higher loads and/or a more advanced CA50 for higher efficiencies without knock [4]. However, if no other parameters are adjusted to control CA50 as PFS is applied, the faster autoignition of the richer regions will advance CA50 by an amount that depends on the degree of fuel stratification, offering the potential of using PFS to control combustion phasing in LTGC engines. PFS can be accomplished by various methods, but a recent study from our laboratory has shown advantages to using DDI-PFS, in which 60–90% of the fuel is directly injected early in the intake stroke (early DI), with the remainder being directly injected during the compression stroke (late DI) [5]. The amount of stratification can be varied

by adjusting either the timing or the amount of fuel in the late DI injection.

With this understanding, DDI-PFS was investigated as a method for controlling combustion phasing in an LTGC engine. The results in Figure 3a show that this technique is very effective for controlling CA50 over a wide range from near the stability limit to well beyond the knock limit. Starting from the left-hand side of the figure, with 70% of the fuel injected early and 30% late (70/30% split) and a relatively early second injection timing of 200° crank angle (CA) (0° CA = top dead center intake), the mixture is fairly well mixed, and CA50 is retarded to 376.6° CA (16.6° after top dead center-compression), which is near the stability limit with a coefficient of variation (COV) in IMEP<sub>g</sub> of 3%. Then, as the second DI timing is retarded further into the compression stroke, the charge becomes progressively more stratified, which advances CA50. This change in CA50 with later second DI timings is moderate at first, but as the late DI timing is retarded beyond 280° CA, fuel stratification increases more rapidly, causing a greater CA50 advancement

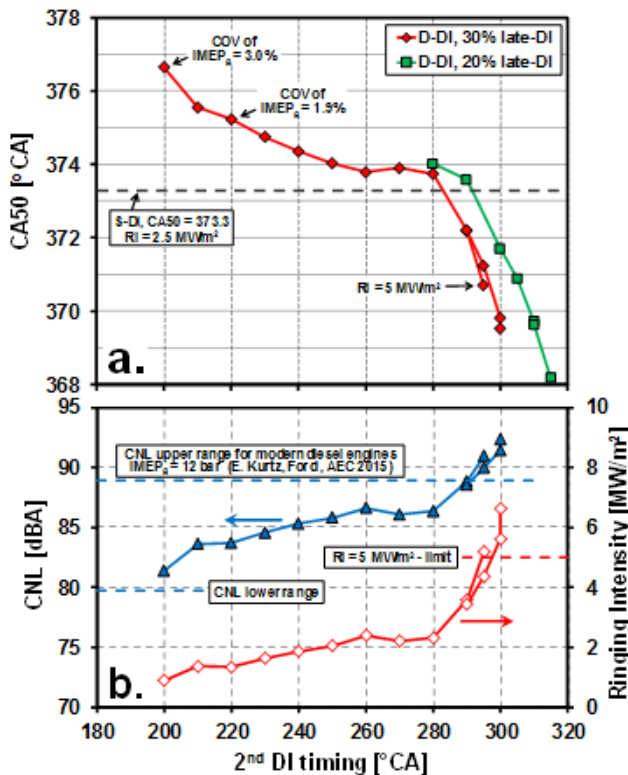


Figure 3. (a) Demonstration of CA50 control using DDI-PFS for 70/30% and 80/20% splits between the early DI and late DI fuel injections. (b) RI and CNL values for the 70/30% sweep in Figure 3a.  $T_{in} = 40^\circ\text{C}$ ,  $P_{in} = 2.0$  bar, 1,200 rpm,  $\phi_m = 0.4$ , fuel = RD5-87.

for a given change in late DI timing. As shown, CA50 can be advanced even beyond the  $RI = 5 \text{ MW/m}^2$  limit. Switching to an 80/20% fuel-fraction split allows CA50 to be advanced even further to  $368^\circ \text{ CA}$  for a total control authority range of  $8.6^\circ \text{ CA}$ .

Figure 3b shows the RI and combustion noise level (CNL) corresponding to the 70/30% sweep in Figure 3a. As can be seen, only the most advanced CA50s produce excessive ringing  $RI > 5 \text{ MW/m}^2$  (knock) or CNL values beyond the noise range of modern diesel engines [6]. Data points were acquired beyond these limits to demonstrate the full range of CA50 control with DDI-PFS, but in practice they could be easily avoided by adjusting the second DI timing. Finally,  $\text{NO}_x$  and soot emissions were very low over the entire sweep. The most retarded second DI timings produced the highest values of  $0.02 \text{ g/kWh}$  and  $0.001 \text{ g/kWh}$  for  $\text{NO}_x$  and soot, respectively.

Spark assist is another promising method for controlling combustion phasing in LTGC engines. With this technique, a spark plug is used to initiate a flame that burns a small portion of the charge. As the flame burns, the expansion of the hot gas behind the flame compresses the remaining charge, driving it into autoignition. This is illustrated in Figure 4, which shows pressure and HRR curves for pure compression ignition (CI) and for spark-assisted CI with four different spark timing. For these data,  $T_{in}$  was adjusted as shown in the legend to maintain the same CA50 for all five cases. Pure CI (no-spark) requires the hottest  $T_{in}$  of  $122^\circ \text{ C}$ , and as  $T_{in}$  is reduced, the spark must be progressively advanced, as shown, to allow the flame more time to burn and compress the remaining charge sufficiently to drive it into hot autoignition. The effect of this flame combustion is clearly evident as the increased early heat release (from about  $343\text{--}362^\circ \text{ CA}$ ) in the HRR curves in Figure 4b and in the pressure traces in Figure 4a.

Thus, with SA, the engine requires less intake charge heating, and it can tolerate a range of  $T_{in}$  by compensating with spark timing, as shown more thoroughly in Figure 5. The large triangle data point in the upper right shows the  $T_{in}$  required for CI (no spark) to obtain  $RI = 5 \text{ MW/m}^2$ , plotted at an artificial spark timing that is so close to the CI autoignition point that it would have no time to influence the autoignition (see Figure 4b). As  $T_{in}$  is reduced, the S-shaped curve shows how the spark timing must be advanced to maintain  $RI = 5 \text{ MW/m}^2$ . (The data in Figure 4 are from selected points on this curve.) For this condition,  $T_{in} = 99^\circ \text{ C}$  is the limit for SA-LTGC combustion because a sufficiently strong flame cannot be initiated at the low in-cylinder temperatures existing prior to  $\sim 312^\circ \text{ CA}$ . This shows that SA can maintain an appropriate CA50 timing for  $T_{in}$  ranging from  $99\text{--}122^\circ \text{ C}$ .

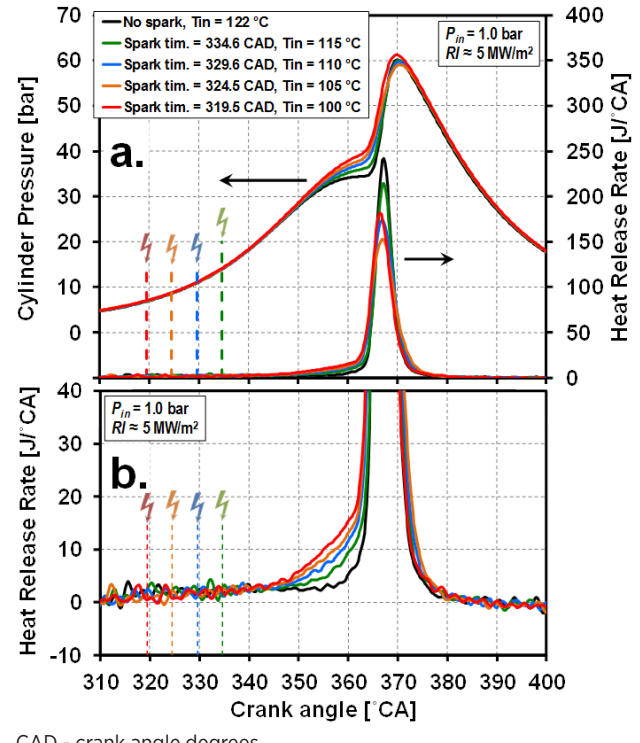


Figure 4. Comparisons of cylinder pressure and HRR traces for CI (no-spark) and spark-assisted LTGC at four spark timings.  $T_{in}$  varies with spark timing as shown in the legend. For all datasets,  $T_{in}$  and spark timing were adjusted to maintain  $RI = 5 \text{ MW/m}^2$ .  $P_{in} = 1.0 \text{ bar}$ , 1,200 rpm,  $\phi = 0.42$ , fuel = CF-E0.

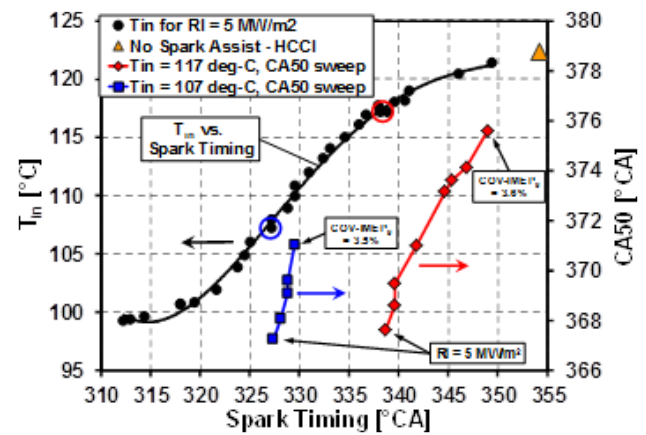


Figure 5. Change in spark timing to maintain  $RI = 5 \text{ MW/m}^2$  as  $T_{in}$  is reduced below the  $122^\circ \text{ C}$  value required for CI (no spark). Plotted against the right hand axis are the ranges over which CA50 can be controlled with SA at  $T_{in} = 107^\circ \text{ C}$  and  $117^\circ \text{ C}$ . For both curves, most advanced CA50 point was acquired at the same condition as the circled point on the  $T_{in}$  curve.

for this operating condition, making the engine operation much more robust than with CI alone.

Figure 5 also illustrates another important advantage of SA; it provides a means of controlling CA50. For the  $T_{in} = 107^{\circ}\text{C}$  and  $117^{\circ}\text{C}$  data points on the S-shaped curve (denoted by circles), the spark timing was retarded from the value required for  $\text{RI} = 5 \text{ MW/m}^2$  to see how far CA50 could be adjusted while maintaining acceptable operation with good stability. These results are plotted against the right-hand vertical axis. For both curves, the bottom-most point shows the CA50 for  $\text{RI} = 5 \text{ MW/m}^2$ , which is close to  $367.5^{\circ}$  CA for both  $T_{in}$ s. For  $T_{in} = 117^{\circ}\text{C}$ , CA50 can be retarded  $8^{\circ}$  CA before it becomes too unstable (COV of  $\text{IMEP}_g = 3.6\%$ ). However, with  $T_{in}$  reduced to  $107^{\circ}\text{C}$ , CA50 can only be retarded  $3.8^{\circ}$  CA at the stability limit (COV of  $\text{IMEP}_g = 3.5\%$ ). Taken together, these two spark timing sweeps indicate that SA can provide good CA50 control authority if  $T_{in}$  is relatively close to that required for CI alone (no spark), but the control authority diminishes significantly for  $T_{in}$ s well below those required for CI alone. Nevertheless, these data show that SA is a valuable tool for CA50 control and improved robustness of LTGC engines.

## Conclusions

- A new spark plug capable, low-swirl cylinder head has been installed, and its combustion performance characterized.
  - Overall performance is similar to our previous head except that TEs are slightly lower (0.2–1.0%-units) mainly due to increased heat transfer and a small reduction in combustion efficiency at low and high loads when early DI fueling is used.
  - High-load limits and CNLs are similar for both heads, for both premixed and early DI fueling for all intake pressures.
- DDI-PFS is a very effective technique for controlling combustion phasing in an LTGC engine. By varying the timing of the late DI injection to change the amount of PFS, CA50 was varied  $8.6^{\circ}$  CA from the stability/misfire limit to strong knocking, while maintaining very low  $\text{NO}_x$  and soot emissions.
- DDI-PFS can also substantially improve the robustness of LTGC combustion by increasing the allowable CA50 range from knock to near misfire, and it can increase stability for a significant extension of the load range at some conditions.

- Spark assist was found to be effective for CA50 control and increased  $T_{in}$  tolerance down to an equivalence ratio of 0.36 at  $P_{in} = 1 \text{ bar}$ .
- Both the RD5-87 (87 AKI, E10) regular gasoline and the high-octane, certification gasoline (CF-E0) were found to be  $\phi$ -sensitive from high boost down to  $P_{in} = 1.3 \text{ bar}$ , and they indicated some  $\phi$ -sensitivity at even lower  $P_{in}$ s, particularly the RD5-87.

## References

1. Eng, J.A., "Characterization of Pressure Waves in HCCI Combustion," SAE Technical Paper 2002-01-2859, 2002, doi:10.4271/2002-01-2859.
2. Dec, J.E., Yang, Y., and Dronniou, N., "Improving Efficiency and using E10 for Higher Loads in Boosted HCCI Engines," SAE Technical Paper 2012-01-1107, *SAE Int. J. Engines* 5(3):1009–1032, 2012, doi:10.4271/2012-01-1107.
3. Dernotte, J., Dec, J.E., and Ji, C., "Energy Distribution Analysis in Boosted HCCI-like / LTGC Engines – Understanding the Trade-offs to Maximize the Thermal Efficiency", SAE Technical Paper 2015-01-0824, and *SAE Int. J. Engines* 8(3): 956–980, 2015, doi:10.4271/2015-01-0824.
4. Dec, J.E., Yang, Y., and Dronniou, N., "Boosted HCCI – Controlling Pressure-Rise Rates for Performance Improvements using Partial Fuel Stratification with Conventional Gasoline," *SAE Int. J. Engines*, 4(1): 1169–1189, 2011, doi:10.4271/2011-01-0897.
5. Dernotte, J., Dec, J.E., and Ji, C. "Efficiency Improvement of Boosted Low-Temperature Gasoline Combustion Engines (LTGC) using a Double Direct-Injection Strategy," Submitted to the SAE 2017 International Congress, SAE paper offer number 17PFL-1110, October 2016.
6. Kurtz E., "Light-Duty Noise Guidelines for Advanced Combustion Research," USCAR Publications web page (<http://www.uscar.org/guest/tlc/1/Advanced-Powertrain>), 2015.

## FY 2016 Publications/Presentations

1. Ji, C., Dec, J.E., Dernotte, J. and Cannella, W.J., "Boosted Premixed-LTGC / HCCI Combustion of EHN-doped Gasoline for Engine Speeds Up to 2400 rpm," SAE Technical Paper 2016-01-2295, SAE 2016 Fall Powertrain, Fuels and Lubricants Meeting, October 2016.

2. Dec, J.E., Dernotte, J., and Ji, C., "Controlling LTGC Combustion Timing for Intake Pressures from 1.0 – 2.0 bar," DOE Advanced Engine Combustion Working Group Meeting, August 2016.
3. Dec, J.E., "Low-Temperature Gasoline Combustion (LTGC) Engine Research," DOE Annual Merit Review, Office of Vehicle Technologies, June 2016.
4. Dernotte, J., Dec, J.E., and Ji, C., "Evaluation of LTGC Engine Performance with a Low-Swirl Cylinder Head and the Potential of PFS for Timing Control," DOE Advanced Engine Combustion Working Group Meeting, February 2016.
5. Yang, Y., Dec, J.E., Sjöberg, M., and Ji, C., "Understanding Fuel Anti-Knock Performance in Modern SI Engines Using Fundamental HCCI Experiments," *Combustion and Flame*, **162**, pp. 4006–4013, 2015.
6. Dec, J.E., Yang, Y., Ji, C., and Dernotte, J., "Effects of Gasoline Reactivity and Ethanol Content on Boosted, Premixed and Partially Stratified Low-Temperature Gasoline Combustion (LTGC)," *SAE Int. J. Engines* 8(3): 935–955, 2015, doi:10.4271/2015-01-0813.
7. Dernotte, J., Dec, J.E., and Ji, C., "Energy Distribution Analysis in Boosted HCCI-like / LTGC Engines – Understanding the Trade-offs to Maximize the Thermal Efficiency," *SAE Int. J. Engines* 8(3): 956–980, 2015, doi:10.4271/2015-01-0824.

## Special Recognitions & Awards/ Patents Issued

1. U.S. Patent Application Filed, No. 14/855,809: Dec, J.E., and Renzi, R., September 2015.
2. DOE EERE Special Recognition Award: For research on diesel-engine and HCCI-like combustion. Presented by DOE at AMR, June 2016.
3. USCAR Team Award for work on the U.S. DRIVE ACEC Fuels Roadmap Sub-Team.

## II.5 Gasoline Combustion Fundamentals

### Overall Objectives

- Expand the fundamental knowledgebase of fluid flow, thermodynamics, and combustion processes needed to achieve clean and fuel-efficient gasoline engines
- Explore phenomenological characteristics of advanced ignition systems
- Acquire validation datasets needed to create predictive models for gasoline combustion

### Fiscal Year (FY) 2016 Objectives

- Measure important low-temperature plasma (LTP) generated radicals in an optically accessible spark calorimeter (OASC) with representative mixture conditions at ignition
- Perform spectroscopic imaging of LTP igniters
- Benchmark rebuilt engine performance

### FY 2016 Accomplishments

- Clarified how in-cylinder generated reformate addition accelerates main-period auto-ignition for low-load, low-temperature gasoline combustion (LTGC)
- Performed first quantitative measure of atomic oxygen (O) from LTP discharges in air at pressures above 1 atm via two-photon absorption laser-induced fluorescence (TALIF)
- Identified mechanisms responsible for arc transition when close-coupled LTP is used
- Tested rebuilt optically accessible gasoline engine ■

### Introduction

Advanced automotive gasoline engines needed to meet aggressive DOE Vehicle Technologies Office fuel economy and pollutant emission targets leverage a combination of reduced heat transfer, throttling, and mechanical losses; shorter combustion durations; and higher compression and mixture specific heat ratios. Central challenges include poor combustion stability at low-power conditions when large amounts of charge dilution are introduced and high sensitivity of conventional inductive coil ignition systems to elevated charge motion and density for boosted high-load operation. The primary project research objective is to investigate the fundamental aspects of enhanced

### Isaac W. Ekoto (Primary Contact), Benjamin M. Wolk

Sandia National Laboratories  
7011 East Ave.  
Livermore, CA 94551  
Phone: (925) 294-6586  
Email: iekoto@sandia.gov

DOE Technology Development Manager:  
Leo Breton

ignition. Novel ignition systems (e.g., LTP, pre-chamber, laser ignition) can improve dilution tolerances while maintaining good performance characteristics at elevated charge densities for conventional spark ignition operation. Strategies that improve the controllability compression induced auto-ignition LTGC are likewise explored. Objectives are accomplished through targeted experiments in a single-cylinder research engine and a custom OASC with in situ measurements by laser-based optical diagnostics and ex situ gas analysis from sampling measurements. Measurements are complemented by computational modeling results as needed. A primary audience for the project is the automotive original equipment manufacturers—close cooperation with these partners has resulted in project objectives that address crucial mid- to long-range research challenges.

### Approach

Performed research leverages experimental and numerical expertise from multiple partners to characterize different aspects of advanced gasoline engine combustion. In response to industry calls for low-cost, efficient, and onboard means of tailoring LTGC fuel properties a major research effort has been directed on negative valve overlap (NVO) strategies that facilitate auto-ignition control through retention and compression of exhaust gases and an auxiliary fuel injection. Detailed characterization of the resultant reformate composition at the end of the recompression stroke is performed using custom sampling valves, with speciation via gas chromatography (GC) or photoionization mass spectrometry (PIMS). Measurements are complemented by chemical kinetic analysis to clarify impact of the in-cylinder generated reformate on engine performance.

A parallel investigation seeks to explore the suitability of robust ignition systems that expand the operational envelope for high-efficiency dilute spark ignition combustion. A custom calorimeter has been developed that can replicate the mixture composition and density at the time of spark for representative engine environments. The calorimeter is used to measure the thermal energy deposition for both conventional and LTP discharges. Furthermore, optical access enables in situ measure of important LTP generated radicals through the use of optical emission spectroscopy or laser-induced fluorescence. There has been close coordination with relevant ignition system developers to evaluate optimal performance features for spark ignition systems and LTGC applications.

## Results

The influence in-cylinder reforming of a gasoline fuel injection during an auxiliary compression period created by NVO cam timing on main-period performance characteristics was investigated for low-load LTGC strategies where combustion stability is problematic. An unexpected result was that for a fixed reformate quantity, the lowest main-period fueling rates led to the fastest ignition. Detailed chemical modeling that leveraged the PIMS measurements of the sampled reformate (Figure 1) was performed to evaluate the impact of reformate addition on auto-ignition delays. Results plotted in Figure 2 demonstrate, that as expected, auto-ignition delays for a fixed reformate fraction (solid lines) and bulk gas temperature are slower for leaner charge mixtures (i.e., lower fueling rates). However, after accounting for higher compressed temperatures (due to increased charge mass specific heat ratios and decreased main injection charge cooling) and the enhanced reactivity from higher reformate fractions, the model indicates auto-ignition delays are actually 0.5 ms faster for the leaner mixture; these results are in good agreement with experiment data from the engine. A sensitivity study of the chemical model analysis indicates that the gasoline fuel reformate reactivity increases as compared to the unreacted parent fuel through production of more reactive species, namely acetylene, acetaldehyde, propene, and allene.

Igniter conversion efficiency of secondary electrical energy into deposited thermal energy into  $N_2$ ,  $O_2$ , and  $CO_2$  mixtures was measured using the OASC device for high-voltage (28 kV peak) pulsed nanosecond discharges with secondary streamer breakdown (SSB)—i.e., transition to thermal arc where electrode erosion becomes an issue—and similar LTP without. Initial pressures were varied between 1 bar and 9 bar absolute, with anode and cathode gap distances likewise varied between 1 mm and 8 mm.

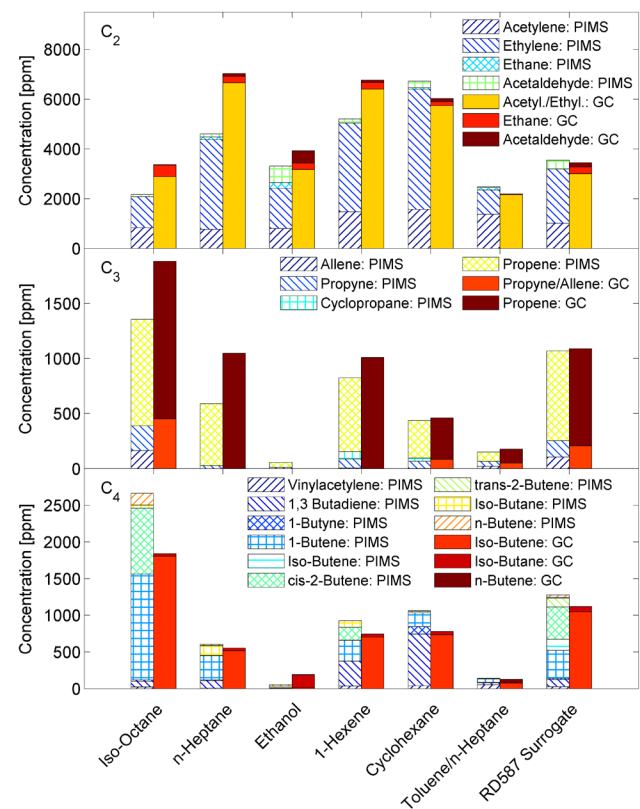


Figure 1. Comparison of GC and PIMS measured intermediate hydrocarbon concentrations ( $C_2$ – $C_4$ ) from the NVO-generated reformate samples for five neat fuels, a toluene/n-heptane blend, and a five-component gasoline (RD587) surrogate

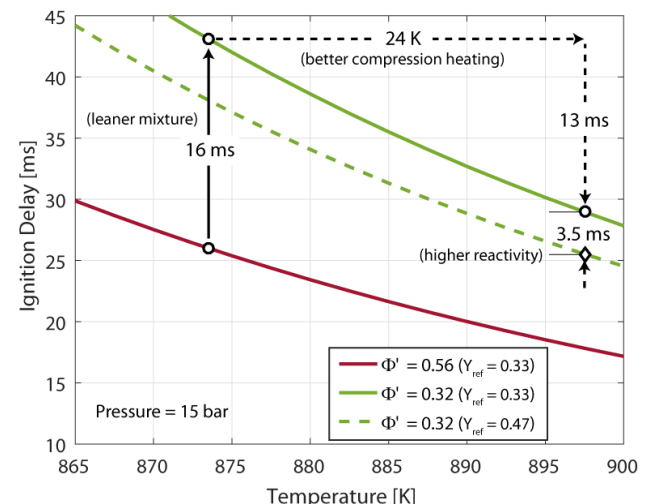


Figure 2. Calculated auto-ignition delays as a function of bulk gas temperature for different charge mass equivalence ratios

Secondary electrical energy was measured using an in-line attenuator with thermal energy deposition determined from pressure rise calorimetry measurements (Figure 3). Calorimetry measurements confirm that, similar to conventional inductive spark discharges, SSB discharges promote ignition through substantial increases to the local gas temperature. LTP discharges, on the other hand, result in very little local gas heating. Instead, the LTP was found to generate substantial O-atom populations, as measured by TALIF with results plotted in Figure 4, that persisted

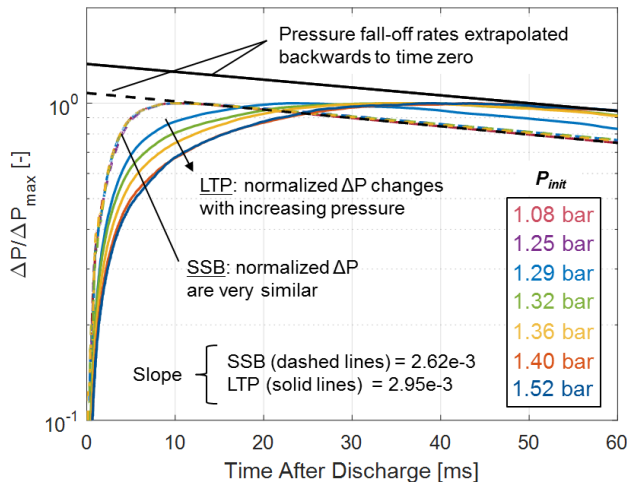


Figure 3. SSB (dashed) and LTP (solid) post-discharge pressure rise time histories from OASC normalized by the peak recorded pressure for a 5 mm gap in air for initial pressures between 1.08 bar and 1.52 bar. Pressure decay rates are also plotted for each discharge.

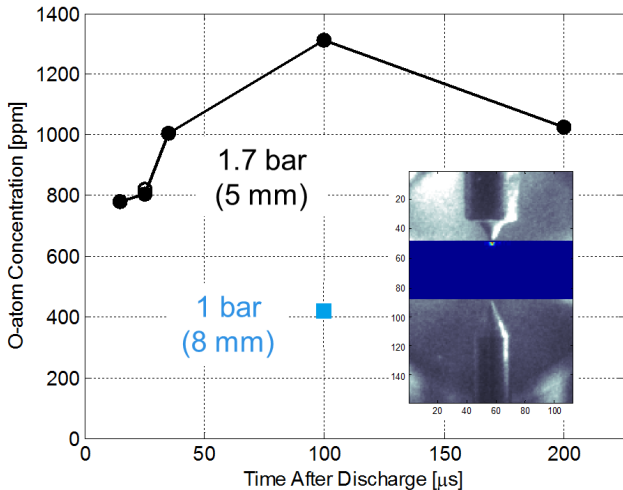


Figure 4. Concentrations of O-atom measured via TALIF as a function of time after the discharge for single 28 kV peak discharge at 1.7 bar initial pressure (black) and 1.0 bar initial pressure (blue). Inset in the figure is an image of the O-atom TALIF just below the high-voltage anode.

for hundreds of microseconds after the discharge. The influence of 10 repetitive pulses spaced 100  $\mu$ s apart was also evaluated for a fixed 5-mm electrode gap. In Figure 5, the conditional SSB probability for each pulse illustrates increased SSB occurrence for each successive pulse, which suggests some sort of chemical or thermal preconditioning by the preceding LTP pulse. Based on the output of a developed thermal deposition model (Figure 6), increased SSB occurrence for successive pulses is attributed mainly to mild gas heating that decreased number densities between the electrodes and hence the electrical resistance of the gas for subsequent pulses.

Finally, the rebuild of an optically accessible, single-cylinder research engine used to investigate the influence of advanced ignition systems on gasoline combustion is complete; a photo of the completed engine assembly is shown in Figure 7. The 0.55 L combustion chamber features central injection and spark, with a spray-guided piston and a 12.9:1 compression ratio. Quartz windows in the piston and the head side-wall enable viewing access. The side-mounted windows also serve as input/output beam access points from an available tunable laser source used for in situ spectroscopic measurements. A new bank of gas flow controllers along with a complementary water vaporizer allow for the use of realistic exhaust gas recirculation diluted intake flows (including trace amounts of H<sub>2</sub>, NO, and various hydrocarbons) when skip-fire operation is employed.

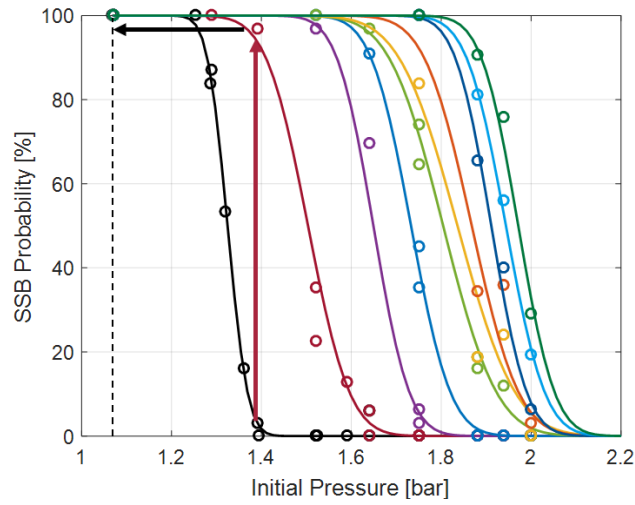


Figure 5. SSB probability for each pulse in a 10-pulse burst with a 100- $\mu$ s dwell between successive discharges is plotted as a function of initial pressure for a fixed 5-mm electrode gap

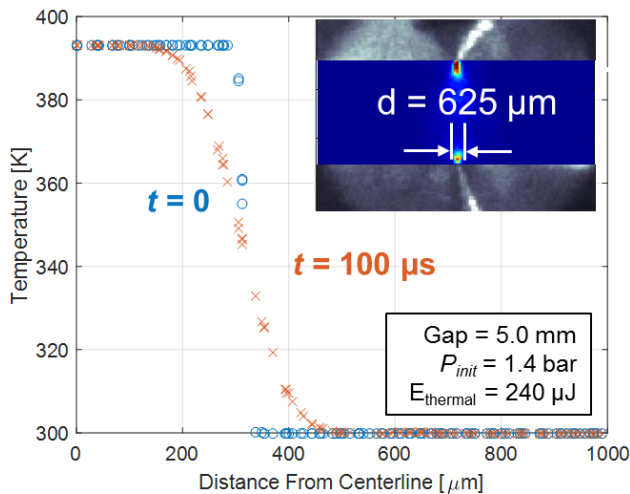


Figure 6. Estimated plasma channel temperature profiles for a single-pulse calorimetry experiment with a 1.4 bar initial pressure and a 5-mm electrode gap. From the calorimetry measurements, the discharge was assumed to uniformly heat a 625- $\mu\text{m}$  diameter cylinder (estimated from discharge imaging) by ~93 K, with the temperature profile 100  $\mu\text{s}$  later accounting for thermal diffusion.

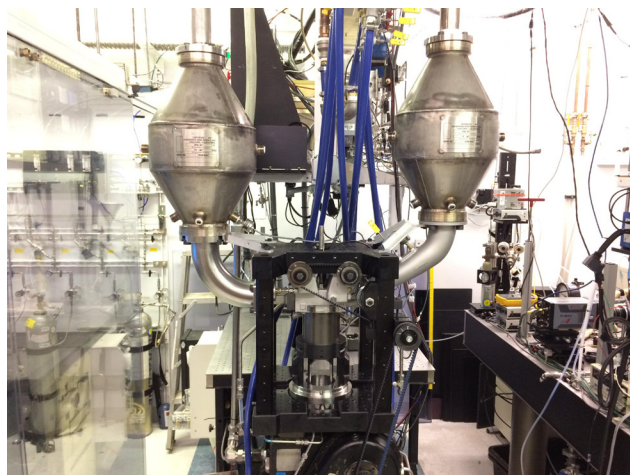


Figure 7. Image of the rebuilt optically accessible, direct-injection, single-cylinder, gasoline engine optimized for advanced ignition system research

## Conclusions

- A combination of improved charge reactivity and increased bulk gas heating from higher specific heat ratios was found to be responsible for improved main-period combustion stability when in-cylinder generated reformate is added for low-load LTGC strategies.

- TALIF has been used to perform the first quantitative O-atom measurements from LTP discharges at pressures above 1 atm. O-atom concentrations were found to persist for hundreds of microseconds after the discharge.
- The increased occurrence of arc transition for multi-pulse LTP operation has been attributed to reduced electrical resistance of the inter-electrode gas due to mild heating between the electrodes from previous pulses.
- A rebuild has been performed of an optically accessible, single-cylinder gasoline engine. The rebuilt engine has been optimized for advanced ignition experiments.

## FY 2016 Publications/Presentations

1. Wolk B., Ekoto I., Calorimetry and Atomic Oxygen Planar Laser-Induced Fluorescence of Low-Temperature Plasma Discharges and Nanosecond Pulsed Discharges at Above-Atmospheric Pressures. Proc. 3rd International Conference on Ignition Systems for Gasoline Engines, Berlin, Germany, November 3–4, 2016.
2. Ekoto I., Wolk B., Northrop W., Moshammer K., Hansen N., “Tailoring Charge Reactivity Using In-Cylinder Generated Reformate for Gasoline Compression Ignition Strategies,” International Combustion Engine Fall Technical Conference, Greenville, South Carolina, ASME ICEF2016-9458, 2016.
3. Wolk B., Ekoto I., Northrop W.F., Moshammer K., Hansen N., “Detailed speciation and reactivity characterization of fuel-specific in-cylinder reforming products and the associated impact on engine performance,” Fuel, 185:348–61, 2016.
4. Wolk B., Ekoto I., Northrop W., “Investigation of Fuel Effects in Negative Valve Overlap Reforming Chemistry Using Gas Chromatography,” SAE Int J Engines, 9 (2) 2016.
5. Ekoto I., “Tailoring charge reactivity using fuel reformate for gasoline compression ignition strategies,” 3rd International Flame Chemistry Workshop, Seoul, Korea, July 30, 2016.
6. Kane S., Northrop W., Wolk B., Ekoto I., “Stochastic reactor model for predicting engine exhaust composition using experimental in-cylinder pressure data,” Spring Technical Meeting, Central States Section of the Combustion Institute, Knoxville, TN, May 15–17, 2016.

## II.6 Advancements in Fuel Spray and Combustion Modeling with High Performance Computing Resources

### Overall Objectives

- Development of physics-based nozzle flow and spray models
  - Develop capability to perform coupled nozzle flow and spray simulations
- Development and validation of high-fidelity turbulence models for engine applications
- Development and validation of reduced chemical–kinetic models for realistic fuel surrogates
  - Develop robust turbulence chemistry interaction models for engine simulations
- High-performance computing (HPC) tool development for codes used by the industry for internal combustion engine (ICE) applications

### Fiscal Year (FY) 2016 Objectives

- Implement a robust approach to capture in-nozzle flow characteristics for both gasoline and diesel injectors in CONVERGE code [1] followed by validation against experimental data from the Advanced Photon Source at Argonne and the Engine Combustion Network (ECN) [2].
- Extend the one-way coupling approach (transition to Lagrangian parcels at the nozzle exit) previously developed for diesel sprays to gasoline sprays, and capture the influence of nozzle flow on fuel spray and combustion in a Lagrangian framework for use by industry
  - Extend this approach to capture plume merging phenomenon
- Develop an engineering approach to capture shot-to-shot variability during spray injection for large eddy simulation (LES) calculations of fuel sprays
- Develop and implement a robust turbulence–chemistry interaction (TCI) model based on the flamelet approach and apply for diesel engine simulations
- Using the Advanced Scientific Computing Research Leadership Computing Challenge core-hour allocation of 60,000,000 core-hours, integrate a workflow manager that will enable us to run thousands of

**Sibendu Som (Primary Contact),  
Janardhan Kodavasal, Kaushik Saha,  
Muhsin Ameen, Noah Van Dam,  
Prithwish Kundu**

Argonne National Laboratory  
9700 S. Cass Ave.  
Argonne, IL 60439  
Phone: (630) 252-9027  
Email: ssom@anl.gov

DOE Technology Development Manager:  
Leo Breton

engine simulations simultaneously, and thus get high throughput

### FY 2016 Accomplishments

- We developed a robust approach for predicting in-nozzle flow features for both diesel and gasoline injector applications. The approach is demonstrated to predict cavitation in diesel injectors, phase-change and flash-boiling in gasoline injectors.
- We developed an approach to couple the flow from inside the injector to the ensuing spray. This approach is called one-way coupling as it couples the Eulerian flow from an injector to a Lagrangian representation of the fuel spray. The computational cost with this approach is significantly lower compared to the previously developed approaches in literature.
- Plume merging is an important phenomenon for gasoline injection systems. We demonstrated that plume merging can be captured with LES turbulence model while Reynolds-average Navier–Stokes (RANS) turbulence model requires some tuning.
- We developed an engineering approach to capture shot-to-shot variation in nozzle flow and sprays using a random number seed perturbation. This is demonstrated to be critical for LES calculations.
- We developed a high-fidelity TCI model based on tabulating the flamelets. The model is shown to be more predictive than existing turbulent combustion models

in literature. The model is called Tabulated Flamelet Model (TFM).

- We developed an approach to perform capacity computing, i.e., high-throughput computing on the Mira supercomputer. This approach allows us to run thousands of simulations within a week, which would traditionally take more than a month. This high-throughput will help industry get results in a timely fashion. ■

## Introduction

ICE processes are multi-scale and highly coupled in nature and are characterized by turbulence, two-phase flows, and complicated spray physics. Furthermore, the complex combustion chemistry of fuel oxidation and emission formation makes engine simulations a computationally daunting task [3]. Given the cost for performing detailed experiments spanning a wide range of operating conditions and fuels, computational fluid dynamics (CFD) modeling aided by HPC has the potential to result in considerable cost savings. Development of physics-based CFD models for nozzle flow, spray, turbulence, and combustion are necessary for predictive simulations of the ICE. HPC can play an important role in ICE development by reducing the cost for design and optimization studies. This is largely accomplished by being able to conduct detailed simulations of complex geometries and moving boundaries with high-fidelity models describing the relevant physical and chemical interactions, and by resolving the relevant temporal and spatial scales. These simulations provide unprecedented physical insights into the complex processes taking place in these engines, thus aiding designers in making judicious choices. The major focus of our research in FY 2016 has been towards the development and validation of robust and predictive nozzle flow, spray, and turbulent combustion models for ICE applications aided by HPC tools.

## Approach

During the past year, we have focused on improving the fidelity of nozzle flow simulations within an Eulerian framework [4]. Our approach to improved modeling capability is highlighted here:

- In-nozzle flow simulations capability was extended to capture both gasoline and diesel fuel injection using a robust homogeneous relaxation model (HRM)-based two-phase flow model within a volume of fluid approach [5]. The boundary conditions for the simulations are obtained from X-ray phase-contrast

imaging at Argonne which includes the needle-lift and wobble profiles, including shot-to-shot variation in them for both diesel and gasoline injectors.

- A one-way coupling approach is developed that couples the flow from the injector to the ensuing spray. This is performed by transitioning at the orifice exit from an Eulerian to a Lagrangian framework. We then developed best practices for performing these one-way coupled simulations for both diesel and gasoline injectors using high-fidelity turbulence models. The approach can account for injection transients such as those detailed in our recent publication [6].
- The effects of strain rate history on turbulent flames have been recently shown to be important. We developed a tabulated equivalent strain flamelet model that accounts for the history effects with flamelets [7].
- Using a random number seed perturbation methodology, we developed an approach to capture shot-to-shot variation during an injection event with LES while performing multiple realizations using a grid-convergent approach [8]. Since the random number seed inherently perturbs the fuel spray through many submodels, we developed best practices to ensure that this approach provides reasonable levels of variability at run-times that are acceptable.
- Engine simulations on the Mira supercomputer were possible due to advancements in the writing of input/output (I/O) in FY 2015. We have extended the engine simulations capability to obtain high-throughput called capacity computing. This was performed through implementation of a Swift algorithm which is a workflow manager that automates job submission on Mira with optimum throughput, automated restarts, etc. We then obtained an Advanced Scientific Computing Research Leadership Computing Challenge allocation of 60,000,000 core-hours to run 10,000 simulations on the whole Mira.

## Results

Some critical findings associated with the different objectives for FY 2016 highlighted before are discussed here. Further details can be obtained from the authors' publications in FY 2016.

Figure 1 plots the fuel mass fraction contours for the gasoline injector from the ECN [2] for which the ambient conditions are plotted in Table 1. The cut-plane shows two of the eight holes for this injector. We first performed some thermodynamic analysis that showed that the G3 condition may be more susceptible to flash-boiling.

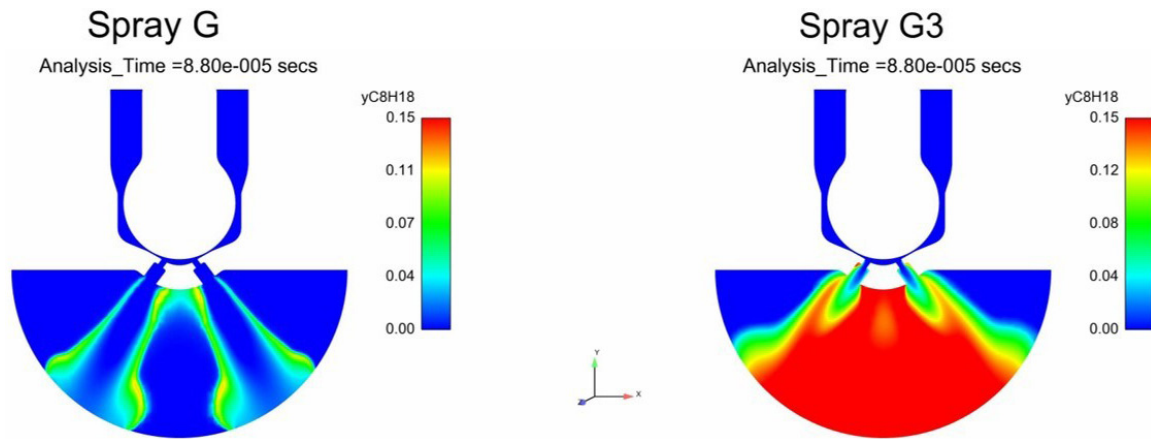


Figure 1. Fuel mass fraction contours are plotted under Spray G and Spray G3 condition at 0.88  $\mu$ s after start of injection for the Spray G injector from the ECN [2]. Flash-boiling is clearly observed under Spray G3 conditions which results in plume merging.

**Table 1. Injection and Ambient Conditions for a Gasoline Injector under Spray G and G3 of the ECN [2].**

Parameters	Spray G (non-Flashing)	Spray G3 (Flashing)
Injection pressure (Mpa)	20	20
Chamber pressure $\{P_{ch}\}$ (kPa)	600	100
Fuel injection temperature $\{T_{fuel}\}$ (K)	363	413
Fuel Saturation temperature at $P_{ch}$ (K)	451	372
Degree of superheat $\{\Delta T\}$ (K)	N/A	40.68
Pressure ratio ( $R_p$ )	0.13	2.83
Jacob number (Ja)	N/A	31.29

Three-dimensional CFD simulations demonstrated that indeed the Spray G3 condition flash-boils leading to higher vapor concentration at the nozzle exit, while the Spray G condition does not flash-boil, but undergoes classical evaporation. Flash-boiling results in increased spray cone angle and plume merging as can be seen clearly from Figure 1. These simulations are performed with the HRM approach discussed previously.

Figure 2 plots pictorially our approach to one-way coupling. First transient nozzle flow simulations are performed accounting for the in-nozzle geometrical details and needle transients. These simulations are performed with the HRM approach discussed previously. The liquid volume fraction at each of the orifice exits for all the cells are then tabulated as shown in the figure along with the velocity contours. This information along with the mass flow rate for every orifice is used to initiate the Lagrangian spray calculations.

Figure 3 plots the fuel vapor mass fraction contours for the Spray G conditions of the ECN [2] using RANS and LES turbulence models at 15 mm from the nozzle exit at

different time instants. It is interesting to note that while RANS does not capture plume merging phenomenon, the higher fidelity LES model does capture the plume merging phenomenon. This aspect of plume merging is being further explored for other operating conditions. Additionally, since LES is more expensive than RANS, we are exploring the possibility of the one-way coupling approach improving the fidelity of the RANS calculations.

Figure 4 plots the mean and standard deviation of projected mass density by different LES realizations based on the grid convergent approach presented by our group [10]. The LES results are perturbed using a random number seed that affects many spray submodels. The goal was to observe if the random number seed can mimic the variability observed in experiments. The figure clearly shows that the random number seed approach of perturbing the sprays can capture the mean and standard deviation as well. However, in the near nozzle region (i.e., within the first 2 mm), simulations show a higher level of standard deviation compared to experiments. There may be other methods to perturb LES calculations, but the random number seed is perhaps the easiest way and hence

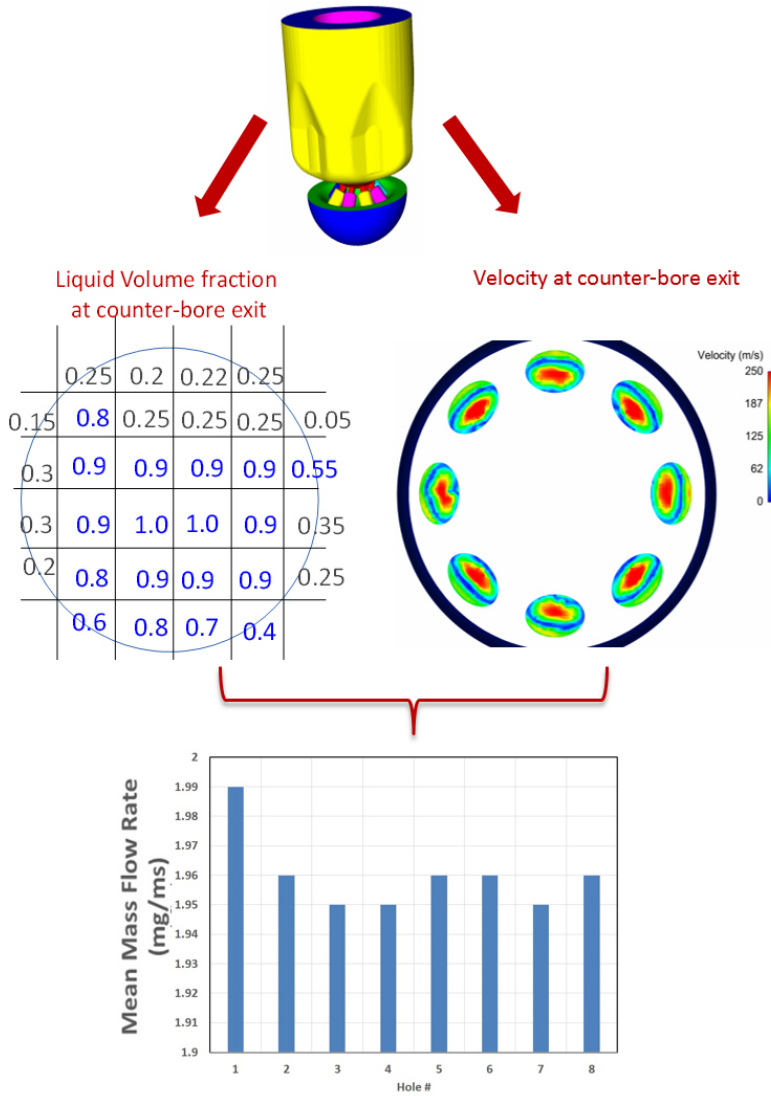


Figure 2. Depicts our approach to one-way coupling wherein, in-nozzle flow characteristics from multi-hole injector simulations in an Eulerian framework are tabulated at the nozzle exit to initiate Lagrangian spray simulations. The variations from plume-to-plume are clearly observed due to differences in the nozzle flow patterns originating from geometrical artifacts inside the nozzle.

is proposed as an engineering solution to capture spray variability with LES.

We implemented a new chemistry load balancing technique in CONVERGE code [11] which is based on equalizing the computational effort per processor rather than the number of cells per processors, as was the case with METIS [9]. This approach has enabled us to perform capability computing on 8,000 processors on Mira. This year we focused on capacity computing approach, wherein, we developed a capability to run 10,000 engine simulations on the whole of Mira. This approach has enabled us to reduce the time-to-science since a

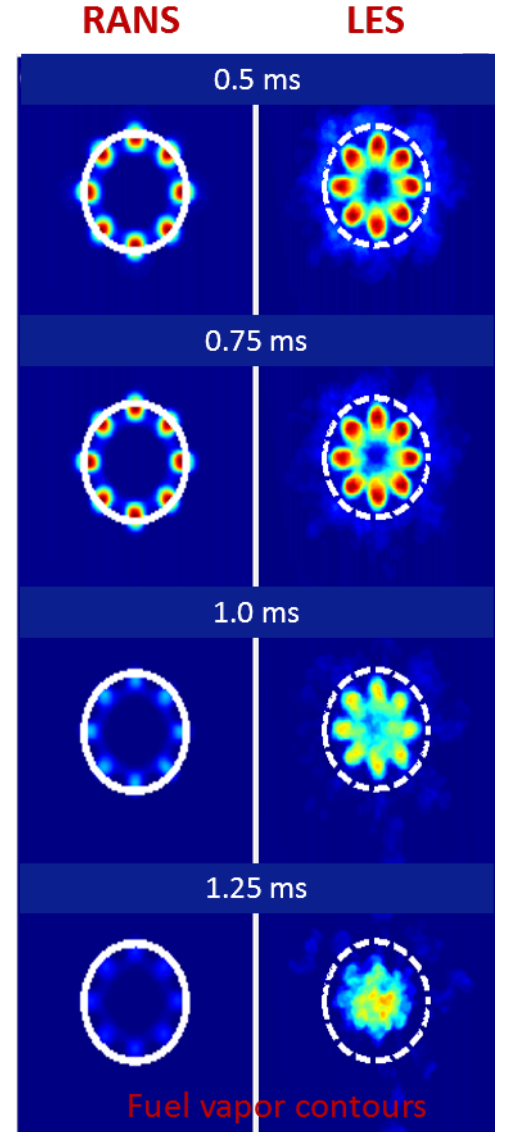


Figure 3. Fuel vapor mass fraction contours are plotted for Spray G calculations using RANS and LES turbulence models at a cut-plane 15 mm from the injector

simulation campaign of this scale would have otherwise taken in the order of months, whereas we were able to perform it in weeks on Mira. This tremendous capability was used to study the gasoline compression ignition engine concept by understanding the influence of different parameter sensitivities towards the final results.

We implemented and tested the TESF model in CONVERGE code and tested it against experimental data from the ECN [2] for ignition delay and flame lift-off length. The tabulated model is compared against the SAGE combustion model that does not account for TCI effects. Figure 5 plots the results and clearly shows that

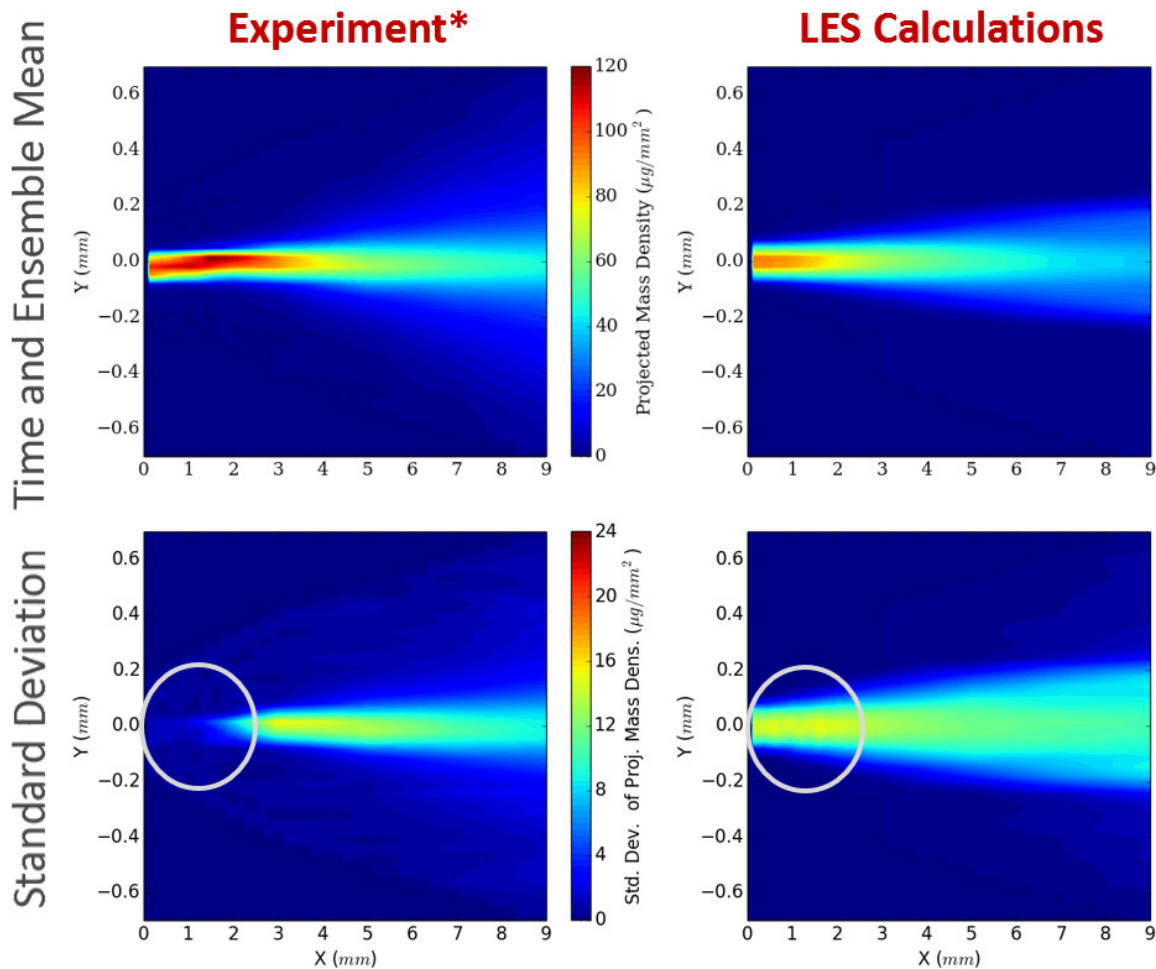


Figure 4. Projected mass density contours of mean and standard deviations compared between experiments and simulations using LES for a spray from a single-hole injector. Experimental data is from Advanced Photon Source at Argonne.

the TFM can better capture the lift-off and ignition delay trends compared to the SAGE model. Since the model is tabulated, it also is at least 50% faster than the SAGE combustion model, which is typically used for engine simulations. We are currently extending the tabulated model for engine simulations for multi-component diesel surrogates.

## Conclusions

- Our robust approach for predicting in-nozzle flow features for both diesel and gasoline injector applications can capture flash boiling in injectors. The simulations captured experimentally observed trends and is expected to predict the extent of flash boiling under different ambient and injection conditions.
- The one-way coupling approach can capture the influence of in-nozzle flow and spray dynamics. Under cavitation conditions or when there is flow recirculation

into the counterbore of a gasoline injector, the one-way coupling has been shown to be more predictive than the standard approach (simulations starting from a measured rate of injection).

- We demonstrated that higher fidelity LES turbulence model can capture plume merging for a gasoline injector under different ambient conditions.
- We demonstrated that shot-to-shot variation in nozzle flow and sprays can be captured using a random number seed perturbation.
- The TFM is shown to be more predictive than a standard SAGE model that does not account for TCI effects and is also a factor of two faster.
- With capacity computing we were able to run thousands of simulations within a week for gasoline compression ignition engine applications. This allowed us to understand the influence of different parameters on

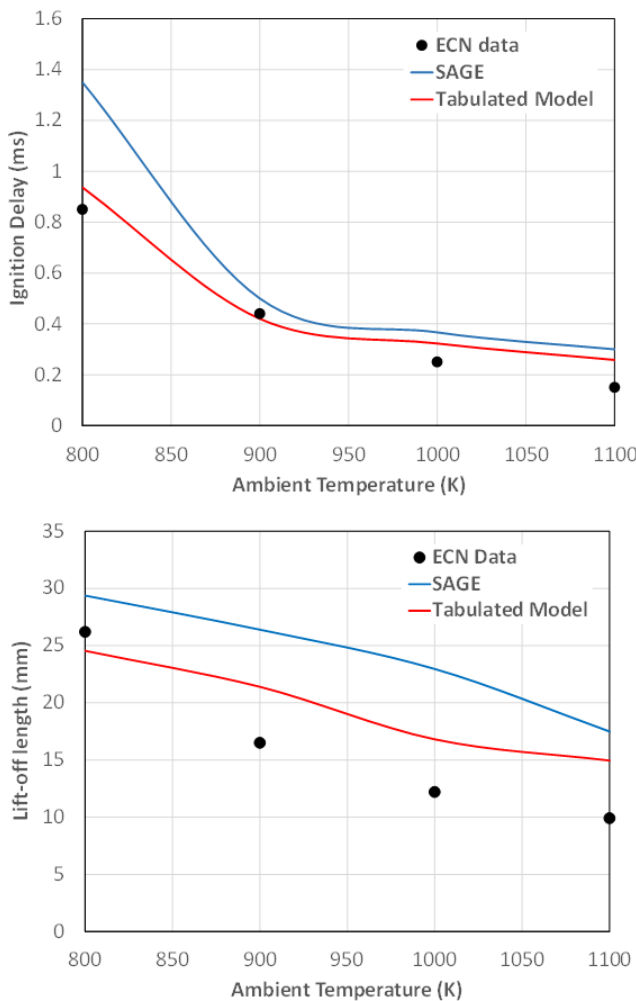


Figure 5. (top) Ignition delay and (bottom) flame lift-off length vs. ambient temperature compared between the SAGE combustion model, TESF (noted as tabulated model), and experimental data from ECN [2]. The simulations are performed using an LES approach developed by our group in previous years.

gasoline combustion, especially at idle and low-load conditions.

## References

1. Richards, K. J., Senecal, P. K., Pomraning, E., CONVERGE (Version 2.2.0) Manual, Convergent Science, Inc., Middleton, WI, 2014.
2. <http://www.sandia.gov/ecn/>
3. Som, S., Aggarwal, S.K., 2010, *Combustion and Flame*, Vol. 157, pp.1179–1193.
4. Q. Xue, M. Battistoni, S. Som, S. Quan, P.K. Senecal, E. Pomraning, D. Schmidt, “Eulerian CFD modeling of coupled nozzle flow and spray with validation against x-ray radiography data,” *SAE International Journal of Fuels and Lubricants*, 7(2):2014.
5. S. Quan, H. Zhao, M. Dai, E. Pomraning, P.K. Senecal, Q. Xue, M. Battistoni, S. Som, “Validation of a three-dimensional internal nozzle flow model including automatic mesh generation and cavitation effects,” *Journal of Engineering for Gas Turbine and Power* 136 (9), 092603: 1-10, 2014
6. M. Battistoni, Q. Xue, S. Som, “LES of Spray Transients: Start and End of Injection Phenomena,” *Oil and Gas Science Technology*, doi:10.2516/ogst/2015024, 2015.
7. P. Kundu, T. Echekki, Y. Pei, S. Som, “An equivalent dissipation rate model for capturing history effects in non-premixed flames,” accepted *Combustion and Flame*, 2016.
8. P.K. Senecal, E. Pomraning, K.J. Richards, S. Som, “Grid-Convergent Spray Models for Internal combustion engine CFD simulations,” *Journal of Energy Resource Technology* 136 (1), 12204, 2013.
9. S. Som, D.E. Longman, S.M. Aithal, R. Bair, M. Garcia, S.P. Quan, K.J. Richards, P.K. Senecal, *SAE Paper No. 2013-01-1095*, 2013.
10. Y. Pei, B. Hu, S. Som, “Flame structure analysis of Spray A under different ambient oxygen conditions,” *Proceedings of the ASME 2015 Internal Combustion Engine Division Fall Technical Conference*, ICEF2015-1034, Houston, TX, November 2015.
11. J. Kodavasal, K. Harms, P. Srivastava, S. Som, S. Quan, K.J. Richards, M. Garcia, “Development of stiffness-based chemistry load balancing scheme, and optimization of I/O and communication, to enable massively parallel high-fidelity internal combustion engine simulations,” *Proceedings of the ASME 2015 Internal Combustion Engine Division Fall Technical Conference*, ICEF2015-1035, Houston, TX, November 2015.

## Selected FY 2016 Publications

1. M. Ameen, P. Kundu, S. Som, “Novel Tabulated Combustion Model Approach for Lifted Spray Flames with Large Eddy Simulations,” accepted *SAE Journal of Engines*, 2016.
2. P. Kundu, T. Echekki, Y. Pei, S. Som, “An equivalent dissipation rate model for capturing history effects in non-premixed flames,” accepted *Combustion and Flame*, 2016.

3. K. Saha, S. Som, M. Battistoni, "Investigation of homogeneous relaxation model parameters and their implications on GDI spray formation," accepted *Atomization and Sprays*, 2016.
4. J. Kodavasal, C.P. Kolodziej, S.A. Ciatti, S. Som, "Effect of Injection Parameters, Boost, and Swirl Ratio on Gasoline Compression Ignition Operation at Idle and Low-Load Conditions," accepted *International Journal of Engine Research*, 2016.
5. A.A. Moiz, M.M. Ameen, S.Y. Lee, S. Som, "Study of soot production on double injections of n-dodecane in CI engine-like conditions," *Combustion and Flame*, 173:123–131, 2016.
6. M.M. Ameen, X. Yang, T.W. Kuo, S. Som, "Parallel Methodology to capture cyclic variability in Motored engines," *International Journal of Engine Research*, 2016. DOI: 10.1177/1468087416662544
7. Y. Pei, E.R. Hawkes, M.A. Chishty, M. Bolla, S. Kook, G.M. Goldin, Y. Yang, S.B. Pope, S. Som, "An Analysis of Structure of an n-dodecane spray flame using TPDF modelling," *Combustion and Flame*, 168: 420-435, 2016.
8. K. Saha, S. Som, M. Battistoni, Y. Li, E. Pomraning, P.K. Senecal, "Numerical investigation of two-phase flow evolution of in- and near-nozzle regions of a gasoline direct injection engine at different fixed needle lifts," SAE Paper No. 2016-01-0870, *SAE International Journal of Engines*; doi:10.4271/2016-01-0870, 2016.
9. S.A. Skeen, J. Manin, L.M. Pickett, E. Cenker, G. Bruneaux, T. Aizawa, F. Westlye, T. Tiexua, J.M. Garcia Oliver, S. Som, Y. Pei, T. Lucchini, G. D'Errico, S.S. Pandurangi, M. Bolla, E. Hawkes, "A progress review on Spray A soot experiments and modeling from the 4th Engine Combustion Network (ECN) workshop," SAE Paper No. 2016-01-0734, *SAE International Journal of Engines*; doi:10.4271/2016-01-0734, 2016.
10. K. Saha, Y. Li, S. Quan, P.K. Senecal, M. Battistoni, S. Som, "Modeling of internal and near-nozzle flow of a GDI Fuel injector," *Journal of Energy Resource Technology*; JERT-16-1023, doi: 10.1115/1.4032979, 2016.
11. Y. Pei, B. Hu, S. Som, "Flame structure analysis of Spray A under different ambient oxygen conditions," *Journal of Energy Resource Technology*; JERT-16-1021, doi: 10.1115/1.4032771, 2016.
12. J. Kodavasal, K. Harms, P. Srivastava, S. Som, S. Quan, K.J. Richards, M. Garcia, "Development of stiffness-based chemistry load balancing scheme, and optimization of I/O and communication, to enable massively parallel high-fidelity internal combustion engine simulations," *Journal of Energy Resource Technology*; JERT-16-1022, doi: 10.1115/1.4032623, 2016.
13. M. Battistoni, C. Poggiani, S. Som, "Prediction of nozzle flow and jet characteristics at start and end of injection: transient behaviors," *SAE International Journal of Engines* 9(1): doi:10.4271/2015-01-1850, 2016.
14. P. Kundu, R. Scarcelli, S. Som, A. Ickes, Y. Wang, J. Keidaisch, M. Rajkumar, "Modeling Heat Loss through Pistons and Effect on Thermal Boundary Coatings in Diesel Engine Simulations using Conjugate Heat Transfer Methods," SAE Paper No. 2016-01-2235, *SAE 2016 International Powertrain, Fuels & Lubricants Meeting*, Baltimore, MD, October 2016.
15. J. Kodavasal, S. Ciatti, S. Som, "Analysis of the impact of uncertainties in inputs on CFD predictions of gasoline compression ignition," *Proceedings of the ASME 2016 Internal Combustion Engine Division Fall Technical Conference*, ICEF2016-9328, Greenville, SC, October 2016.
16. N. Van Dam, S. Som, A. Swantek, C.F. Powell, "The effect of grid resolution on predicted spray variability using multiple large eddy spray simulations," *Proceedings of the ASME 2016 Internal Combustion Engine Division Fall Technical Conference*, ICEF2016-9384, Greenville, SC, October 2016.
17. S. Quan, P.K. Senecal, E. Pomraning, Q. Xue, B. Hu, D. Rajamohan, J.M. Deur, S. Som, "A one-way coupled volume of fluid and Eulerian-Lagrangian method for simulating sprays," *Proceedings of the ASME 2016 Internal Combustion Engine Division Fall Technical Conference*, ICEF2016-9390, Greenville, SC, October 2016.
18. K. Saha, A.M. Moiz, A.I. Ramirez, S. Som, M. Biruduganti, M. Bima, P. Powell, "Proof-of-concept numerical study for NOx reduction in diesel engines using enriched Nitrogen and enriched Oxygen," SAE Paper No. 2016-01-8082, *SAE 2016 Commercial Vehicle Conference*, Rosemont, IL, October 2016.
19. J. Kodavasal, N. Van Dam, Y. Pei, K. Harms, K. Maheshwari, A. Wagner, M. Garcia, S. Ciatti, P.K. Senecal, S. Som, "Sensitivity analysis on key CFD model inputs for gasoline compression ignition on IBM Blue Gene/Q supercomputer," *THIESEL 2016 Conference on Thermo- and Fluid Dynamic Processes in Direct Injection Engines*, Valencia, Spain, September 2016.

20. M. Ameen, Y. Pei, S. Som, "Computing Statistical Averaged from Large Eddy Simulations of Spray Flames," SAE Paper No. 2016-01-0585, *SAE 2016 World Congress*, Detroit, MI, April 2016.
21. J. Kodavasal, Y. Pei, A. Wagner, K. Harms, M. Garcia, S. Som, P.K. Senecal, "Global sensitivity analysis of a gasoline compression ignition engine simulation with multiple targets," SAE Paper No. 2016-01-0602, *SAE 2016 World Congress*, Detroit, MI, April 2016.
22. K. Saha, S. Som, M. Battistoni, Y. Li, S. Quan, P.K. Senecal, "Numerical simulation of internal and near-nozzle flow of a gasoline direct injection fuel injector," *9th International Symposium on Cavitation*, Lausanne, Switzerland, December 2015.
23. N. Van Dam, S. Som, A. Swantek, C.F. Powell, "The effect of parcel count on predictions of spray variability in large-eddy simulations of diesel fuel sprays," *ILASS Americas 28th Annual Conference on Liquid Atomization and Spray Systems*, Dearborn, MI, May 2016.
24. K. Saha, S. Som, M. Battistoni, "Parametric study of HRM for gasoline sprays," *ILASS Americas 28th Annual Conference on Liquid Atomization and Spray Systems*, Dearborn, MI, May 2016.
25. P. Kundu, M.M. Ameen, S. Som, "Implementation of a Tabulated Flamelet Model to Investigate Methyl Decanoate Combustion in an Optical Direct Injection Diesel Engine," 145IC-0074, *Spring Technical Meeting of the Central States Section of the Combustion Institute*, Knoxville, TN, May 2016.
26. M.M. Ameen, X. Yang, T.W. Kuo, S. Som, "Simulating cyclic variability with LES and HPC advancements," 145IC-0062, *Spring Technical Meeting of the Central States Section of the Combustion Institute*, Knoxville, TN, May 2016.
27. C. Xu, M.M. Ameen, S. Som, T. Lu, "Chemical explosive mode analysis for reacting spray flames under diesel engine conditions," *Spring Technical Meeting of the Eastern States Section of the Combustion Institute*, Princeton, NJ, March 2016.

## Special Recognitions & Awards/ Patents Issued

1. Sibendu Som: 2016 Outstanding Postdoctoral Supervisor Award, Argonne National Laboratory.
2. Sibendu Som: 2016 ASME Internal Combustion Engine Division "Outstanding Presenter" award.

## II.7 Fuel Injection and Spray Research Using X-Ray Diagnostics

### Overall Objectives

- Study the fuel injection process by performing detailed, quantitative measurements both inside and outside fuel injection nozzles
- Make the measurements under conditions as near as possible to those in modern engines
- Utilize the results of these unique measurements to advance the state of the art in spray modeling
- Provide industrial partners in the spray and engine community with access to a unique and powerful diagnostic of fuel injection and sprays

### Fiscal Year 2016 Objectives

- Develop the capability for high precision, nondestructive measurements of the flow passages inside fuel injectors
- Advance the state of the art in measurements of cavitation by developing the capability for quantitative measurements inside metal nozzles
- Perform measurements of nozzle geometry, needle motion, and spray density using the Spray C and Spray D diesel injectors from the Engine Combustion Network (ECN); share this data with computational modelers for validation and improvement of spray modeling

### Fiscal Year 2016 Accomplishments

- X-ray tomography of fuel injection nozzles can now achieve a spatial resolution  $<3 \mu\text{m}$ , and is being utilized by our academic and industry partners.
- ECN Spray C and Spray D injectors have been characterized, and the data has been shared with the simulations community.
- Simultaneous measurements of the fuel density inside a metal spray nozzle along with the fuel distribution outside that nozzle were completed. These measurements quantitatively link the effect of cavitation on fuel distribution and mixing. ■

**Christopher F. Powell (Primary Contact), Alan L. Kastengren**

Argonne National Laboratory

9700 S Cass Ave.

Argonne, IL 60439

Phone: (630) 252-9027

Email: powell@anl.gov

DOE Technology Development Manager:

Leo Breton

### Introduction

Fuel injection systems are one of the most important components in the design of combustion engines with high efficiency and low emissions. A detailed understanding of the fuel injection process and the mechanisms of spray atomization are needed to implement advanced combustion strategies with improved engine performance. The limitations of visible light diagnostics have spurred the development of X-ray diagnostics for the study of fuel sprays. X-rays are highly penetrative, and can generate quantitative, unambiguous measurements of useful spray properties, even in the optically opaque region very near the nozzle [1].

### Approach

The aim of this project is to develop and perform high precision measurements of fuel injection and sprays to further the development of accurate computational spray models. These measurements are primarily performed at the Advanced Photon Source at Argonne National Laboratory. This source provides a very high flux beam of X-rays, enabling quantitative, time-resolved measurements of sprays with very high spatial resolution. The X-rays are used for four different measurement techniques: radiography to measure spray density, phase contrast imaging to acquire high speed images, fluorescence to track atomic elements, and small-angle scattering to measure droplet size [2]. Each of these techniques complements other diagnostics by providing unique and useful information that cannot be obtained in other ways.

In the process of making these measurements, Argonne collaborates with industrial partners including engine and fuel injection system manufacturers so that they have access to these diagnostics for improvement of their products. The group also collaborates with spray modelers to incorporate this previously unknown information about the spray formation region into new models. This leads to an increased understanding of the mechanisms of spray atomization and facilitates the development of fuel injection systems designed to improve efficiency and reduce pollutants.

In addition to measurements of injectors and sprays, the group explores other applications of X-ray diagnostics for combustion research. Measurements of cavitating flows provide unique data to improve the fundamental understanding of internal fuel flow and its role in spray atomization, as well as the relationship between injector geometry, cavitation, and nozzle damage. Recent measurements have also evaluated the use of X-rays as a diagnostic for shock tubes, natural gas injectors, and spark ignition. These new applications broaden the impact of the work, and help to improve the fundamental understanding in other areas important to advanced combustion, including fundamental chemistry, gas jets, and ignition.

## Results

In FY 2016, a major upgrade to the Vehicle Technologies X-ray beamline at the Advanced Photon Source was completed. This upgrade allows high energy, broadband X-ray beams to be delivered into the dedicated spray research lab. This enables X-ray tomography measurements of the flow passages inside fuel injectors, a process that previously required us to use other facilities. A significant amount of effort has been spent to refine the capabilities, including development of specialized hardware for data acquisition and software for streamlined data analysis. After one year of work, the capability to measure nozzle geometry with spatial resolution  $<3\text{ }\mu\text{m}$  has been demonstrated (Figure 1). This represents a significant improvement over the resolution available from other providers. Three-dimensional models of the fuel injector nozzles are now being shared with computational modelers, providing them with the highly accurate geometries that ensure simulations are grounded on real boundary conditions.

A significant amount of effort over the last several years has been spent performing experiments in collaboration with the ECN [3]. This collaboration is led by Sandia National Laboratories, who have defined a specific set of operating conditions and procured a set of shared

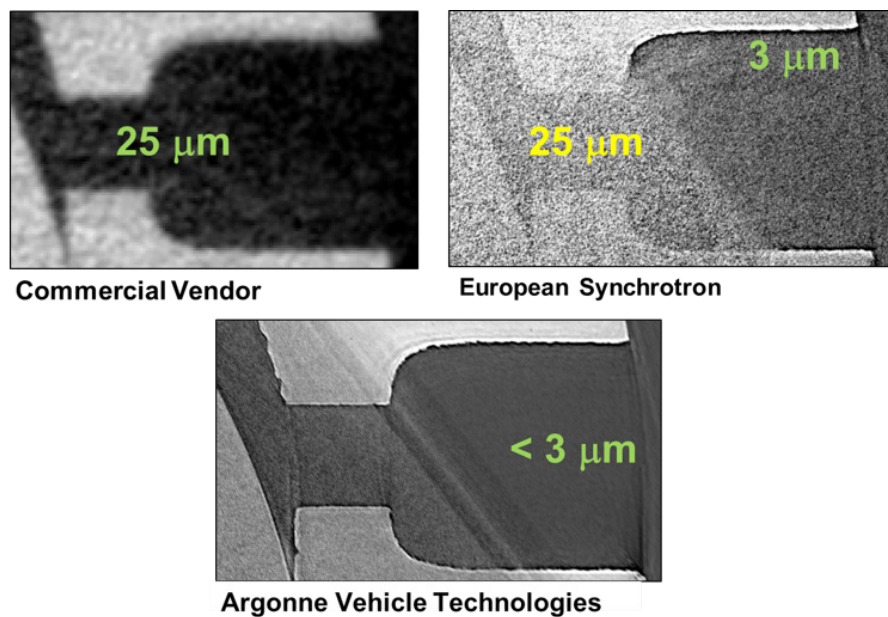


Figure 1. X-ray images showing the orifice and counterbore of a gasoline direct injection injector from three different institutions. By optimizing X-ray tomography techniques for steel fuel injectors, Argonne's Vehicle Technologies beamline has demonstrated superior spatial resolution.

identical hardware. Argonne uses its full suite of unique injector and spray diagnostics to contribute to the ECN community. This partnership puts Argonne's data in the hands of simulation groups worldwide, and maximizes the impact of the work on improving computational simulations of sprays, combustion, and engines. In FY 2016, measurements of using the ECN Spray C and Spray D diesel injectors were completed. These measurements included precise measurements of the nozzle geometry (Figure 2), valve motion, spray density, and near-nozzle droplet size. These data are now freely available, and provide modelers with a reference data set for model development and validation.

Cavitation is an important problem in high pressure fuel injection systems, such as those found in modern direct injection gasoline and diesel engines. Cavitation, where fuel in the injector vaporizes due to a drop in pressure,

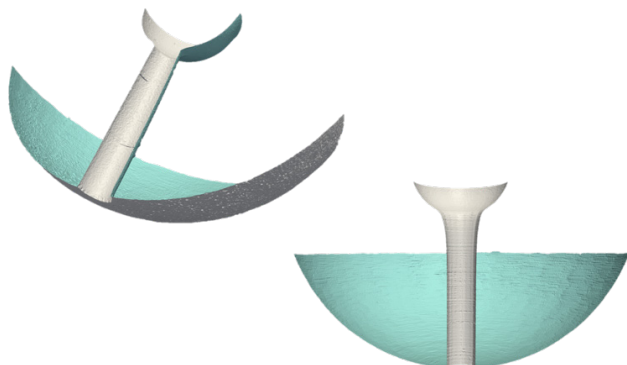


Figure 2. Cutaway views of the measured nozzle geometry of the ECN Spray C and Spray D injectors. These geometries enable CFD simulations using real-world nozzle geometries.

can cause mechanical damage to injector components and affect fuel-air mixing and thus efficiency and pollutant formation. State-of-the-art computer models for cavitation are now incorporated into engine models to account for cavitation, however, there is little information available on the accuracy of these models because cavitation is very difficult to measure experimentally. In FY 2016, a new X-ray transparent nozzle was procured that allows us to make measurements of fuel density inside the nozzle, and simultaneously measure the density of the spray emerging from the nozzle (Figure 3). For the first time, quantitative measurements can link the cavitation inside the nozzle with its effect on the resulting fuel spray.

One important discovery that emerged from these measurements of cavitation in FY 2016 is the confirmation of hydraulic flip in a cavitating nozzle. It has been observed that spray breakup is suppressed if cavitation extends all the way to the nozzle exit [4]. It has been postulated that gas from outside the nozzle may travel upstream, inside the nozzle in the cavitation film along the wall, stabilizing the flow and leading to a smooth, steady stream exiting the nozzle [5]. Using X-ray fluorescence and an ambient environment containing krypton gas, ambient gas moving upstream into the nozzle has been detected and quantified under hydraulically flipped conditions (Figure 4). These data are a powerful tool to enhance the understanding of cavitation, and the results are being used in collaboration with modelers from the University of Massachusetts Amherst to improve cavitation models. Improvements to those models will lead to a broader understanding of this complex physical phenomenon, as well as better and more accurate engine modeling software.

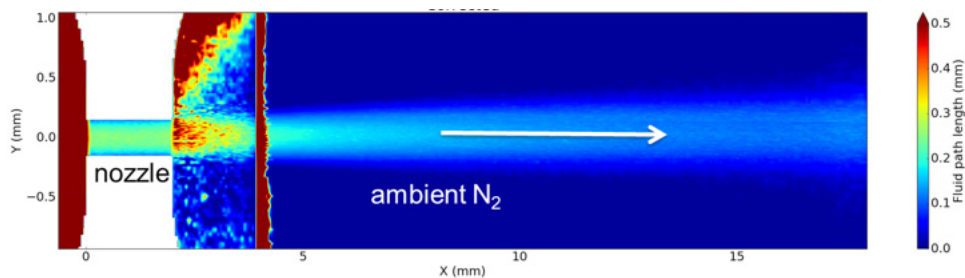


Figure 3. Density map showing the fluid density inside a metal nozzle (left) as well as the density of the fuel as it emerges from the nozzle and breaks up to form a spray. Measurements such as this one are being used to link the effect of cavitation inside the nozzle on the fuel and air mixing after injection.

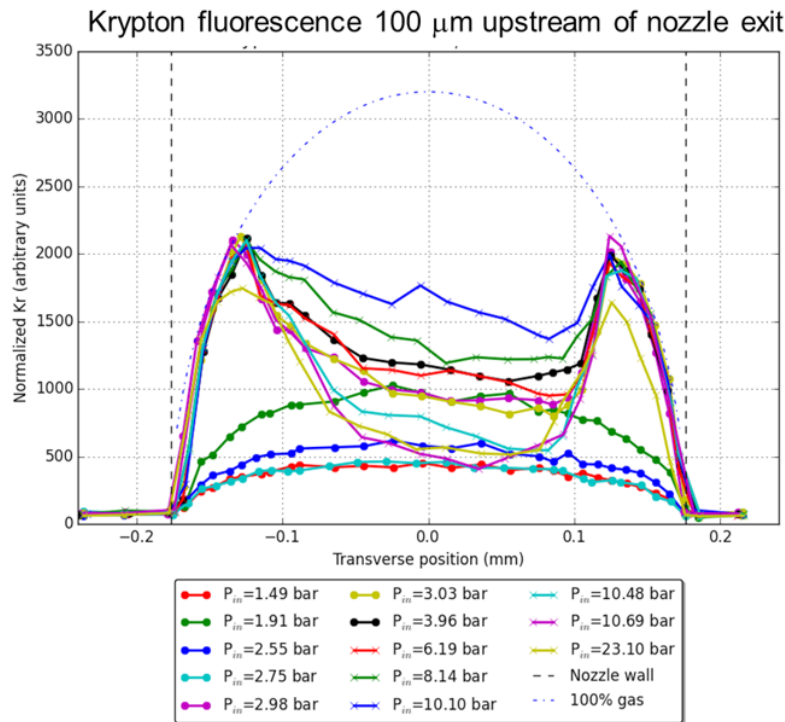


Figure 4. X-ray fluorescence measurements showing the location and quantity of krypton inside a metal fuel injection nozzle. Under hydraulic flip conditions, the krypton has moved upstream into the nozzle, stabilizing the flow. This leads to a drastic reduction in spray breakup and poor in-cylinder mixing.

## Conclusions

X-ray diagnostics can be used to help understand the flows inside the injector as well as the mixing of fuel and air in the engine. Such measurements are not possible using other imaging techniques, and represent a powerful data set for validating computational models of fuel flow. This data is crucial for the development of accurate spray models and for the detailed understanding of spray behavior. Improvements to these models will speed the development of cleaner, more efficient engines.

## References

1. “Time-Resolved Measurements of Supersonic Fuel Sprays using Synchrotron X-rays,” C.F. Powell, Y. Yue, R. Poola, and J. Wang, *J. Synchrotron Rad.* 7:356-360 (2000).
2. “Spray Density Measurements Using X-Ray Radiography,” A.L. Kastengren, C.F. Powell, *Journal of Automobile Engineering*, Volume 221, Number 6, 2007, pp 653–662.
3. “Engine Combustion Network (ECN): Measurements of Nozzle Geometry and Hydraulic Behavior,” A.L. Kastengren, F.Z. Tilocco, C.F. Powell, J. Manin, L.M. Pickett, R. Payri, T. Bazyn. *Atomization & Sprays* 22 (12), pp 1011–1052 (2012).
4. “Direct Injection Diesel Sprays and the Effect of Cavitation and Hydraulic Flip on Atomization,” Celia Soteriou, Richard Andrews, and Mark Smith, SAE Paper No. 950080, Detroit, Michigan, 1995.
5. “A Numerical Study of Cavitating Flow Through Various Nozzle Shapes,” David P. Schmidt, Christopher J. Rutland, M.L. Corradini, SAE Paper No. 971597, Detroit, Michigan, 1997.

## FY 2016 Publications/Presentations

1. “X-ray radiography of cavitation in a beryllium alloy nozzle,” Daniel J. Duke, Andrew B. Swantek, Katarzyna E. Matusik, Alan L. Kastengren, Juan P. Viera, Raul Payri, and Christopher .F Powell. THIESEL 2016 Conference on Thermo- and Fluid Dynamic Processes in Direct Injection Engines, Valencia, Spain, September 2016.
2. “Time-Resolved X-ray Radiography of Cavitation in a Metal Nozzle,” Daniel J. Duke, Alan L. Kastengren,

Andrew B. Swantek, Katarzyna E. Matusik, Raul Payri, Juan P. Viera, and Christopher F. Powell. ILASS – Europe 2016, 27th Annual Conference on Liquid Atomization and Spray Systems, Brighton, UK, September 2016.

3. “Numerical Investigation of Liquid Jet Breakup and Droplet Statistics with Comparison to X-ray Radiography”, L. Bravo, D. Kim, F. Ham, K.E. Matusik, D.J. Duke, A.L. Kastengren, A.B. Swantek, C.F. Powell. 52nd AIAA/SAE/ASEE Joint Propulsion Conference, Salt Lake City, UT, July 2016.
4. “The effects of parcel count on predictions of spray variability in large-eddy simulations of diesel fuel sprays,” N. Van Dam, S. Som, A. Swantek, C.F. Powell. ILASS Americas 28th Annual Conference on Liquid Atomization and Spray Systems, Dearborn, MI, May 2016.
5. “High Resolution X-Ray Tomography of Injection Nozzles,” K.E. Matusik, D.J. Duke, C.F. Powell, A.L. Kastengren. ILASS Americas 28th Annual Conference on Liquid Atomization and Spray Systems, Dearborn, MI, May 2016.
6. “High-Speed Radiography and Visible Light Extinction of a Pressure-Swirl Atomizer,” A.L. Kastengren, K.E. Matusik, D.J. Duke, C.F. Powell. ILASS Americas 28th Annual Conference on Liquid Atomization and Spray Systems, Dearborn, MI, May 2016.
7. “X-ray radiography measurements and numerical simulations of cavitation in a metal nozzle,” D.J. Duke, A.B. Swantek, K.E. Matusik, A.L. Kastengren, J.P. Viera, R. Payri, C.F. Powell and D.P. Schmidt. ILASS Americas 28th Annual Conference on Liquid Atomization and Spray Systems, Dearborn, MI, May 2016.
8. “Time-Resolved X-Ray Radiography of Spark Ignition Plasma,” A.L. Kastengren, D.J. Duke, A.B. Swantek, J.M. Sevik, T. Wallner, C.F. Powell. SAE Int. J. Engines 9(2):2016.
9. “X-Ray Radiography and CFD Studies of the ECN Spray G Injector,” P. Strek, D.J. Duke, A.L. Kastengren, C.F. Powell, D.P. Schmidt. SAE Paper No. 2016-01-0858, SAE 2016 World Congress, Detroit, MI, April 2016.
10. “CFD and X-ray Analysis of Gaseous Direct Injection from an Outward Opening Injector,” L. Bartolucci, R. Scarcelli, T. Wallner, A. Swantek, C.F. Powell. SAE Paper No. 2016-01-0850, SAE 2016 World Congress, Detroit, MI, April 2016.
11. “Linking instantaneous rate of injection to x-ray needle lift measurements for a direct-acting piezoelectric injector,” J.P. Viera, R. Payri, A. B. Swantek, D.J. Duke, N. Sovis, A.L. Kastengren, C.F. Powell. Energy Conversion & Management pp. 350–358, January 2016.
12. “Common Rail Diesel Sprays from Twin-hole Nozzle,” D. Nguyen, D. Duke, A. Kastengren, C. Powell and D. Honnery, Proc Australian Combustion Symposium, Melbourne, Australia, pp. 200–203, December 2015.
13. “A Review of Synchrotron Radiation Diagnostics for Fluid Mechanics,” D.J. Duke, Proc. 7th Australian Conference on Laser Diagnostics in Fluid Mechanics and Combustion, Melbourne, Australia, pp. 15–22, December 2015.
14. “X-ray Diagnostics for Cavitating Nozzle Flow,” D.J. Duke, A.B. Swantek, A.L. Kastengren and C.F. Powell, Journal of Physics: Conference Series 656 (2015) 012110.

## Special Recognitions and Awards/ Patents Issued

1. Pacesetter Award, Argonne National Laboratory. Awarded to Christopher Powell, Daniel Duke, Alan Kastengren, Katarzyna Matusik. “For excellence in achievement and performance which truly surpasses normal job expectations,” July 2016.
2. “Best Oral Presentation Award,” Awarded by ILASS Europe, Brighton, UK. For the Paper “Time-Resolved X-Ray Radiography of Cavitation in a Metal Nozzle,” D. Duke, A. Kastengren, A. Swantek, K. Matusik, R. Payri, J. P. Viera, C. F. Powell. September 2016.

## II.8 Large Eddy Simulation Applied to Advanced Engine Combustion Research

### Overall Objectives

- Combine unique state-of-the-art simulation capability based on the large eddy simulation (LES) technique with Advanced Combustion Engine R&D activities
- Perform companion simulations that directly complement optical engine and supporting experiments being conducted at the Combustion Research Facility and elsewhere
- Maximize benefits of high-performance massively parallel computing for advanced engine combustion research using DOE leadership class computer platforms
- Apply high-resolution LES and first principles models at conditions unattainable using direct numerical simulation (DNS) to complement key experiments and bridge gap between basic/applied research:
  - Perform detailed simulations that match operating conditions (e.g., high Reynolds number)
  - Retain full system coupling and incorporate detailed physics and geometry
  - Establish validated correspondence between available data and LES
  - Extract high-fidelity data from validated LES not available from experiments
  - Use these data to understand and develop affordable models for engineering

### Fiscal Year (FY) 2016 Objectives

- Perform a progressive set of simulations aimed at studying transient injection, mixing, and autoignition processes in the Sandia Spray A experiment
- Establish detailed database that complements available experimental data through analysis of the fully coupled broadband processes observed in the simulations

### FY 2016 Accomplishments

- Tested and demonstrated use of a coupled model framework for LES that simultaneously treats high-pressure thermodynamics, transport, and turbulence-chemistry interactions

**Joseph C. Oefelein (Primary Contact),  
Guilhem Lacaze, Layal Hakim**

Sandia National Laboratories  
7011 East Avenue, Mail Stop 9051  
Livermore, CA 94551-0969  
Phone: (925) 294-2648  
Email: oefelei@sandia.gov

DOE Technology Development Manager:  
Leo Breton

- Quantified the combined effects of broadband (small-scale) turbulence and transient mixing dynamics on the development of ignition kernels and combustion ■

### Introduction

Developing an improved understanding of transient injection, mixing, and combustion processes inherent in diesel injection continues to be an important element in the design of advanced engines. In FY 2016, a series of LES calculations were performed with the goal of illuminating the transient turbulent mixing and combustion phenomena that dominate at typical engine operating conditions. Conditions were selected that match those of the Sandia Spray A experiment (see [www.sandia.gov/ecn](http://www.sandia.gov/ecn)). Liquid n-dodecane at 363 K was injected through a 0.09-mm diameter injector nozzle into a gaseous ambient mixture at 900 K and 60 bar. The peak injection velocity was 620 m/s, which was selected to provide the same injected mass flow rate as the experiment.

Three-dimensional renderings of the instantaneous fields highlight the many intricate features of the flow that are not captured by current models. For example, the structure of turbulence, temperature, scalar dissipation, and ignition. Initial studies served to validate the models used to represent turbulent scalar mixing processes, which is an important first step toward detailed studies of autoignition. Relevant data was extracted and utilized to develop an optimized chemical scheme that was capable of reproducing key quantities such as the autoignition delay time over the full range of conditions encountered in the domain with quantified uncertainties. Design of the optimized chemical mechanism was

achieved using Bayesian inference, which quantifies the optimal values of the model parameters together with the associated uncertainties. It was demonstrated that the optimized mechanism provided predictions within the same variability as leading detailed mechanisms. The benchmark configuration was then used to study the effects of broadband transient dynamics by extracting data not available from the experiments. First, results were compared with available experimental data (e.g., penetration data, spreading angles, and shadowgraphs) to establish a validated correspondence with the experimental cases. The studies were then extended by coupling the full system of submodels to a first principles combustion closure with emphasis on accurately capturing the inherent autoignition processes observed in the experiment, as described below.

## Approach

LES calculations are performed using a single unified code framework called RAPTOR. Unlike conventional LES codes, RAPTOR is a DNS solver that has been optimized to meet the strict algorithmic requirements imposed by the LES formalism. The theoretical framework solves the fully-coupled conservation equations of mass, momentum, total energy, and species for a chemically reacting flow. It is designed to handle high Reynolds number, high-pressure, real gas, and/or liquid conditions over a wide Mach operating range. It also accounts for detailed thermodynamics and transport processes at the molecular level. A noteworthy aspect of RAPTOR is it was designed specifically for LES using nondissipative, discretely conservative, staggered, finite-volume differencing. This eliminates numerical contamination of the subfilter models due to artificial dissipation and provides discrete conservation of mass, momentum, energy, and species, which is an imperative requirement for high quality LES.

## Results

A major goal in the development of closure strategies for turbulent combustion is to use first principles models designed specifically for LES (i.e., using all the information available from the LES formalism in contrast to current closures derived from Reynolds-averaged Navier–Stokes that make use of relatively limited information). Recently, for example, a class of reconstruction models has been proposed that combines the purely mathematical approximate deconvolution procedure with physical information from an assumed scalar spectrum to match specific scalar moments. Using this method, a surrogate to the exact scalar field can be estimated such that filtered moments match to a

specified order. In principle, the surrogate field can be used to calculate the subfilter contribution of any related nonlinear function. In practice, however, the extent of the nonlinearity limits the accuracy of reconstruction methods and it has been shown that they cannot be used reliably to close the filtered chemical source terms directly. They can be used, however, to obtain highly accurate representations of polynomial nonlinearities such as the subfilter variances and covariances in the filtered equations for LES if appropriate levels of resolution are applied. These are precisely the input required to generate subfilter fluctuations stochastically.

Given these findings, an extension to the reconstruction approach has been derived by coupling it to a stochastic technique. The matrix of subfilter variances and covariances are obtained via reconstruction, then used as input to a Cholesky decomposition to obtain a correlated approximation of the subfilter velocity and scalar fluctuations in time. The modeled instantaneous fields (i.e., Favre averaged resolved-scale contribution plus the correlated subfilter fluctuations) are used to evaluate the filtered chemical source terms directly. The filtered source terms are closed using the optimized chemical mechanism described in previous work. The corresponding model coefficients are evaluated locally in a manner consistent with the dynamic modeling procedure. Thus, the only adjustable parameters are the filter size, time step, and boundary conditions. In the limit as the filter size and time step approach the smallest relevant scales, subfilter contributions approach zero and the solution converges to a DNS. A novel feature of this approach is that it naturally accounts for multiscalar mixing at subfilter timescales, which is an important requirement, both in general, and for modeling ignition transients.

To address the issue of variability in chemical kinetics mechanisms, an Arrhenius-based chemical model was developed using Bayesian inference to predict autoignition over the ranges of conditions (pressure, temperature, equivalence ratio) relevant to the Spray A case (see Hakim, et al. 2015 for details). The chemical model was coupled to the combustion closure outlined above along with models to treat real fluid (gas or liquid) thermodynamics and transport. The coupled system of models was then used to perform detailed LES of injection, mixing and the resultant autoignition processes in the Spray A case. Representative time traces of the modeled instantaneous subfilter fluctuations of temperature, mass fraction of n-dodecane, and mass fraction of carbon monoxide on the centerline 100 diameters downstream of injector are shown in Figure 1. Sensitizing the simulations to these subfilter

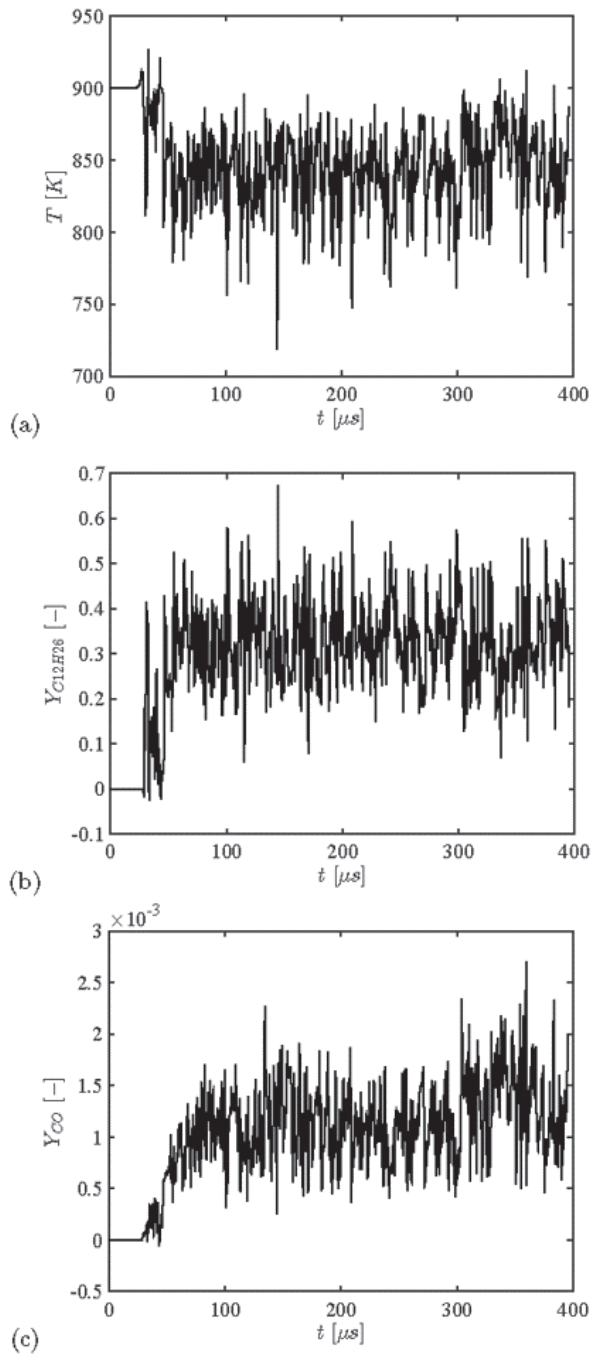


Figure 1. Modeled instantaneous fluctuations of (a) temperature, (b) n-dodecane, and (c) carbon monoxide on centerline 100 diameters downstream of injector nozzle exit

scales in time facilitates formation of ignition kernels in a manner consistent with the chemical timescales.

The transient ignition sequence predicted by LES at conditions identical to the experiment are shown in Figure 2. On the left is a three-dimensional rendering of the instantaneous liquid n-dodecane fuel jet injected at

a temperature of 363 K into the high-pressure chamber at 60 bar, 900 K, with 15% oxygen. Scalar mixing is represented by a blue volume rendering based on the fuel mixture fraction. The development of ignition kernels and resultant flame structure are tracked by a yellow volume rendering based on temperature. Corresponding shadowgraphs from the experiment highlight the flow structure as autoignition occurs at comparable points in time on the right. The locations of the first flame kernels are in good agreement with the shadowgraphs. The first kernels appear initially in the downstream region of the jet where large vortical structures carry fuel away from the high-speed jet. In those regions, turbulence and hot ambient conditions enhance the mixing of the fuel with the ambient. Subsequently, other locations reach a burning state by either autoignition or propagation mechanisms. The spatial and temporal fidelity provides access to the detailed broadband three-dimensional characteristics of injection, ignition, and combustion at conditions that (1) identically match the experiment, and (2) are directly relevant to practical systems. Further details are given in the FY 2016 publications section.

## Conclusions

The current high-resolution benchmark cases have revealed the instantaneous three-dimensional structure of injected fuel jets with a degree of fidelity that is not accessible by current experimental diagnostics or engineering computational fluid dynamics codes. Corresponding mixture fraction, temperature, density, Mach number, and speed of sound distributions (for example) were analyzed. Large density gradients associated with the compressed liquid core triggers a cascade of processes characteristic of supercritical flows, where high-pressure, non-linear mixing and diffusion profoundly modify turbulent mixing. These mixing processes happen concurrently to chemical runaway that is captured in the present work with the optimized chemical mechanism and companion turbulent combustion closure. Using this combined system of subfilter models, accurate prediction of the autoignition sequence has been obtained. The current work aims to find an optimal balance in requirements between the coupled system of turbulence and chemical models. Since the present approach is based on an Arrhenius formulation, its implementation in most research and design codes is greatly facilitated as well as its interface with any turbulent combustion closure. In future work, the uncertainties on the input parameters will be propagated through the LES to gain insights into the uncertainty on the simulation results.

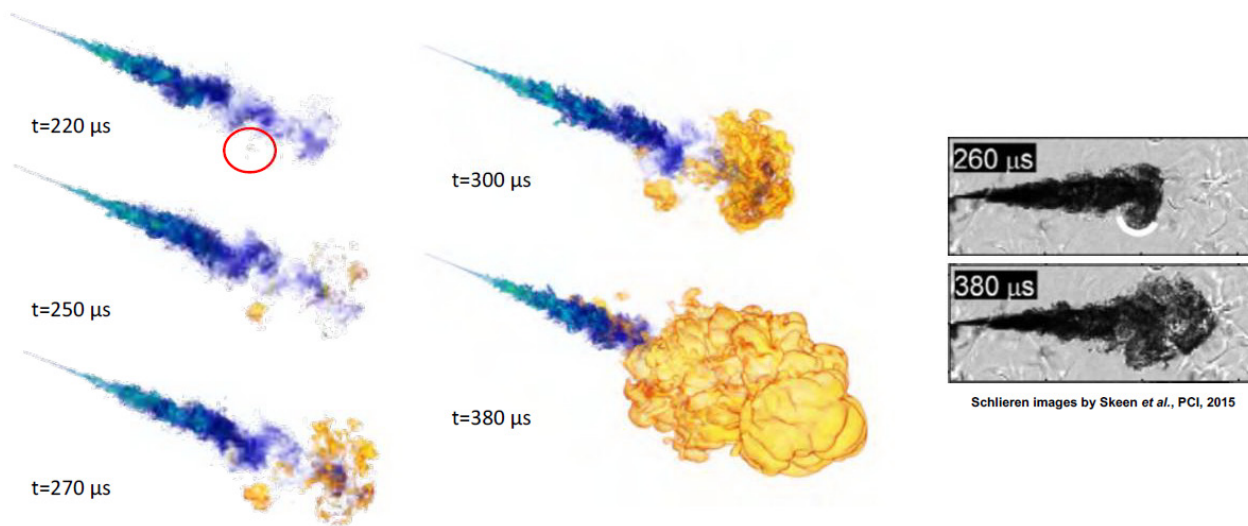


Figure 2. On the left is a representative result from LES showing the transient ignition sequence at conditions identical to the experiment. On the right are corresponding shadowgraphs that highlight the flow structure as autoignition occurs at comparable points in time.

## FY 2016 Publications/Presentations

1. L. Hakim, G. Lacaze, M. Khalil, K. Sargsyan, H. Najm, and J. Oefelein. Probabilistic parameter estimation of a 2-step chemical kinetics model for n-dodecane jet autoignition. *Combustion Theory and Modelling*, 2017. Submitted.
2. F. Doisneau, M. Arienti, and J.C. Oefelein. A semi-Lagrangian transport method for kinetic problems with application from dense to dilute polydisperse reacting spray flows. *Journal of Computational Physics*, 2017. In press.
3. F. Doisneau, M. Arienti, and J.C. Oefelein. On multi-fluid models for spray-resolved LES of reacting jets. *Proceedings of the Combustion Institute*, 36, 2017. In press.
4. J.C. Oefelein. Dynamics of gas-liquid interfaces in high-pressure systems. 24th International Congress of Theoretical and Applied Mechanics, Invited Topical Lecture and Paper, August 21–26, 2016. Montreal, Canada.
5. R.N. Dahms and J.C. Oefelein. The significance of drop non-sphericity in sprays. *International Journal of Multiphase Flow*, 86:67–85, 2016.
6. L. Hakim, G. Lacaze, M. Khalil, H.N. Najm, and J.C. Oefelein. Modeling auto-ignition transients in reacting diesel jets. *Journal of Engineering for Gas Turbines and Power*, 138:112806 1–8, 2016.
7. A.M. Ruiz, G. Lacaze, J.C. Oefelein, R. Mari, B. Cuenot, L. Selle, and T. Poinsot. A numerical benchmark for high-Reynolds number supercritical flows with large density gradients. *AIAA Journal*, 54(5):1445–1460, 2016.
8. L. Hakim, G. Lacaze, and J.C. Oefelein. Large eddy simulation of autoignition transients in a model diesel injector configuration. *SAE International Journal of Fuels and Lubricants*, 9(1): 165–176, 2016.
9. M. Arienti, F. Doisneau, and J.C. Oefelein. Computation of the break-up of a molten drop under sudden acceleration. *Proceedings of the 28th Annual Conference on Liquid Atomization and Spray Systems*, May 15–18, 2016. Dearborn, Michigan.
10. L. Hakim, G. Lacaze, and J.C. Oefelein. Large eddy simulation of autoignition transients in a model diesel injector configuration. *SAE World Congress*, Paper 2016-01-0872, April 12–14, 2016. Detroit, Michigan.
11. J.H. Frank, B. Coriton, A.M. Ruiz, and J.C. Oefelein. Evaluation of tomographic particle imaging velocimetry in turbulent flames using large eddy simulations. *Proceedings of the 2016 Spring Meeting of the Western States Section of the Combustion Institute*, March 21–22, 2016. Seattle, Washington.
12. L. Hakim, G. Lacaze, M. Khalil, H.N. Najm, and J.C. Oefelein. Modeling auto-ignition transients in reacting diesel jets. *Proceedings of the ASME 2015 Internal Combustion Engine Division Fall Technical Conference*, Paper 2015-1120, November 8–11, 2015. Houston, Texas.

## II.9 RCM Studies to Enable Gasoline-Relevant Low Temperature Combustion

### Overall Objectives

- Collaborate with combustion researchers within DOE's Offices of Vehicle Technologies and Basic Energy Science programs to develop and validate predictive chemical kinetic models for a range of transportation-relevant fuels
- Acquire ignition time delay, and other necessary combustion data using ANL's rapid compression machine (RCM) at conditions representative of today's and future internal combustion engines, including high pressure ( $P = 15\text{--}80$  bar) and low to intermediate temperatures ( $T = 650\text{--}1,100$  K)

### Fiscal Year (FY) 2016 Objectives

- Acquire ignition delay measurements for gasoline surrogates, surrogate blends, and a full-boiling-range gasoline, with these also blended with ethanol
- Assist in validating detailed chemical kinetic models for these fuels using metrics such as ignition delay times and the extents of low- and intermediate-temperature heat release, and with advanced tools such as uncertainty quantification and global sensitivity analysis

### FY 2016 Accomplishments

- Acquired additional measurements for research-grade gasoline, blends of this full-boiling-range fuel with ethanol from E0 to E30 (30% ethanol, 70% gasoline blend), and single-component surrogate candidates, including ignition delay times as well as extents of low- and intermediate-temperature heat release
- Continued development of new approaches to accurately quantify uncertainty in the Lawrence Livermore National Laboratory (LLNL) detailed chemical kinetic model for gasoline, and estimated extents of uncertainty at representative conditions ■

### Introduction

Accurate, predictive combustion models are necessary in order to reliably design and control next-generation fuels and future engines which can meet mandated fuel economy and emissions standards, while achieving reductions in development times and costs for new configurations [1]. The imprecision of available models prevents the adoption of detailed simulation techniques

### S. Scott Goldsborough

Argonne National Laboratory (ANL)

9700 S. Cass Avenue

Bldg. 362

Argonne, IL 60439

Phone: (630) 252-9375

Email: scott.goldsborough@anl.gov

DOE Technology Development Manager:

Leo Breton

within current design processes. Existing engineering-scale models can achieve satisfactory performance at some operating points. However, they are not sufficiently robust to cover complete ranges of conventional engine operation, or when novel or advanced combustion concepts are utilized. Towards this, there is a critical need to improve the understanding of the multiple physical and chemical processes that occur within combustion engines, some of which include chemical ignition, fluid–chemistry interactions, and pollutant formation and decomposition. To advance these understandings, collaborations are necessary across multiple disciplines, for example between combustion engineers within DOE's Vehicle Technologies Office and scientists who are supported through DOE's Basic Energy Science. Through these interactions, fundamental, engine-relevant data can be acquired with low experimental uncertainties, while predictive models can be developed and validated based on these datasets.

### Approach

RCMs are sophisticated experimental tools that can be employed to acquire fundamental insight into fuel ignition and pollutant formation chemistry, as well as fluid–chemistry interactions, especially at conditions that are relevant to advanced, low temperature combustion (LTC) concepts [2]. They are capable of creating and maintaining well-controlled, elevated temperature and pressure environments (e.g.,  $T = 600\text{--}1,100$  K,  $P = 5\text{--}80$  bar) where the chemically active period preceding autoignition can be monitored and probed via advanced *in situ* and *ex situ* diagnostics. The ability to utilize wide ranges of fuel and oxygen concentrations within RCMs, from ultra-lean to over-rich (e.g.,  $\phi = 0.2$  to

2.0+), and spanning dilute to oxy-rich regimes (e.g.,  $O_2 = 5\%$  to  $>21\%$ ), offers specific advantages relative to other laboratory apparatuses such as shock tubes and flow reactors, where complications can arise under such conditions. The understanding of interdependent, chemicophysical phenomena that can occur at some conditions within RCMs is a topic of ongoing investigation within the combustion community, while interpretation of facility influences on datasets is also being addressed [2]. Approaches to implement novel diagnostics which can provide more rigorous constraints for model validation compared to integrated metrics such as ignition delay times, e.g., quantification of important radical and stable intermediates such as  $H_2O_2$  and  $C_2H_4$  [3,4], are under development by many combustion researchers.

Argonne's existing twin-piston RCM is utilized in this project to acquire data necessary for chemical kinetic model development and validation, while improvements to the facility's hardware and data analysis protocol are performed to extend its capabilities and fidelity. Collaborations are undertaken with Basic Energy Science-funded scientists at ANL and other U.S. laboratories, as well as with researchers at national and international institutions, including complementary RCM facilities.

## Results

New hardware were integrated into the experimental setup in FY 2016. These included high resolution static transducers for the reaction chamber and mixing tank to reduce uncertainties in mixture composition, and initial pressure of the reacting gas, which can affect the assessment of the compressed conditions. A 1 MHz analog-to-digital card was also added to the data acquisition system in order to more accurately capture heat release characteristics of fuels during the high temperature oxidation period of the tests. A high-precision automated valve was acquired to meter the charge into the reaction chamber for each test shot. This has significantly increased throughput, where it is now possible to conduct more than 40 test shots per day. Additionally, new operational protocols were implemented to monitor the efficiency of the piston seals in the reaction chamber to minimize shot-to-shot and day-to-day variations in the measurements. Finally, linear displacement transducers acquired, and mounting brackets were designed and fabricated so that the piston position can be measured during the gas compression process. Additional safety features are being incorporated into the bracket, and these are expected to be added to the RCM in FY 2017.

Experiments were conducted to acquire additional data for three five-member ring napthenes including cyclopentane

(CP), methylcyclopentane (MCP) and ethylcyclopentane (ECP). Naphthenes can be a significant fraction gasoline, especially for fuels derived from non-conventional hydrocarbon feedstocks, e.g., oil shale. They are also present in large quantities in some research-grade gasolines formulated for the Coordinating Research Council's Fuels for Advanced Combustion Engine (FACE) Program [5]. Detailed hydrocarbon analysis of the FACE gasolines indicate that naphthenes with five and six carbons are generally more prevalent than molecules with six or greater member rings like methylcyclohexane. Three fuel structures were targeted to understand the influence of alkyl substitution and better quantify the ring processes that are critical at LTC conditions.

Figure 1 illustrates representative data acquired under stoichiometric conditions. Ignition delay times are plotted as a function of inverse temperature. Two different compressed pressures were used to quantify the influence of pressure on the autoignition behavior. It is clear from the RCM data that there are significant differences within the negative temperature coefficient (NTC) regime compared to higher temperatures. In the NTC regime,  $HO_2$  chemistry is important and there is significant competition between chemical kinetic pathways leading to peroxide formation and ensuing degenerate branching, and the production of more stable olefins. We have collaborated with LLNL and King Abdullah University of Science and Technology to develop and validate chemical kinetic models for CP and MCP, and the simulation results for these models are presented in Figure 1 as lines. The models generally exhibit good behavior overall in capturing the reactivity trends, although there

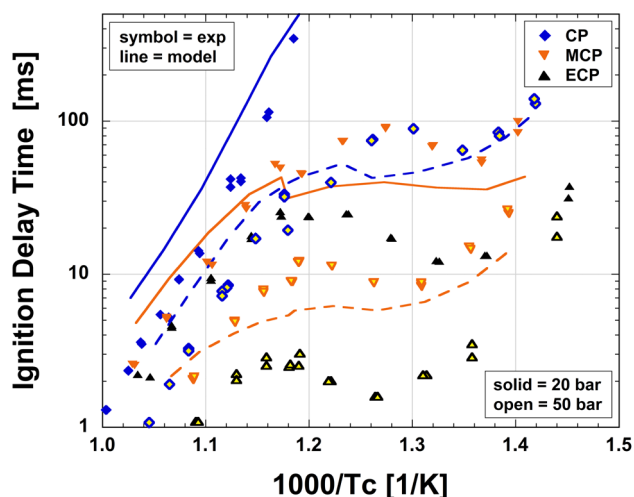


Figure 1. Ignition delay times as a function of inverse temperature for three five-member ring napthenes at two compressed pressure conditions

are discrepancies in the NTC regime that are still under investigation. The findings of these experimental and modeling efforts have been submitted for publication.

Experiments were also conducted using a research-grade, full-boiling-range gasoline, in this case FACE-F, along with blends of the fuel with ethanol. The autoignition characteristics of E0 (0% ethanol) were compared against E10, E20 (20% ethanol, 80% gasoline blend), E30 and E100 at conditions across the NTC regime, and at two pressures, including 20 bar and 40 bar. Additionally, in FY 2016 a campaign was conducted to facilitate direct comparisons between the RCM measurements and trends observed in internal combustion engines operating on LTC. Data for E0 are plotted in Figure 2 where a sweep of pressure ( $P_c = 15\text{--}80$  bar) and temperature ( $T_c = 800\text{--}1,000$  K) were pursued with the ignition delay times are presented as functions of these parameters. The ignition delay surface shown in this three-dimensional representation highlights the NTC behavior of this fuel, and how this feature changes with pressure. Overlaid on the surface for comparison are temperature–pressure trajectories for three HCCI engine test points (presented as thick black lines) where the intake pressure was adjusted from 0.9 bar to 1.6 bar. The start of combustion for the three trajectories are indicated on the plot by yellow stars. Apparent in this figure is that the RCM conditions and the autoignition chemistry that can be investigated in the tests are directly relevant to LTC in operating engines. The RCM measurements have inherently lower uncertainties associated with them, for instance the initial temperature and composition are known exactly, and thus can be compared in a more

straightforward manner against simulation results with chemical kinetic models. The data from these tests have been shared with LLNL and the findings of this work are being prepared for submission in FY 2017.

In FY 2016 further progress was made towards the implementation of novel mechanism analysis tools that are expected to improve the predictive capabilities of the LLNL gasoline surrogate model. Global sensitivity analysis [6,7] and other approaches [8] have recently been demonstrated as useful techniques to target specific reaction steps and reaction pathways that are critical in the decomposition and oxidation of fuels, thereby improving the overall robustness of a chemical kinetic model. However, this is difficult to implement for the LLNL gasoline surrogate model due to the integration of numerous kinetic sub-mechanisms and the extensive use of rate rule correlations for large hydrocarbon species. Furthermore, the naming convention in the model is based on historical approaches so that the molecular structure of each compound is not immediately identifiable. To overcome these challenges, an automated method was developed in FY 2015 to identify and classify all of the reactions in the gasoline surrogate model, and apply appropriate correlations between the reactions (e.g., when identical rate rules are used). To facilitate this, a collaboration was established with Northeastern University where software tools had been developed to identify the molecular structure of species contained within detailed chemical kinetic models such as the LLNL gasoline surrogate model [9–11].

Initial demonstrations of the methodology focused on first quantifying uncertainties associated with predictions of the kinetic model using constant-volume RCM conditions as well as variable-volume engine conditions, and on better understanding the influence of uncertainty factor assignment, as well as specification of correlations between reactions. Figure 3 illustrates representative results where iso-octane is used as the fuel. Here, ranges of predicted ignition delay times are presented to highlight the impact of branching ratio uncertainty on the calculations. Two sets of  $\text{RO}_2 \leftrightarrow \text{QOOH}$  reactions are investigated, namely the isomerization of  $\text{aC}_8\text{H}_{17}\text{O}_2$  (Case 6) and  $\text{dC}_8\text{H}_{17}\text{O}_2$  (Case 7), which are two important iso-octyl radicals that result from H-abstraction of the iso-octane fuel molecule (Case 5). Uncertainty levels of  $\pm 10$ ,  $\pm 50$ , and  $\pm 90\%$  are considered. Significant changes in the ignition delay time predictions are observed for some of the tests, e.g., Case 5, while not for all, e.g., Case 6. These results, which have been published in Fridlyand et al. [12], highlight the importance of properly incorporating uncertainties into model predictions. These activities

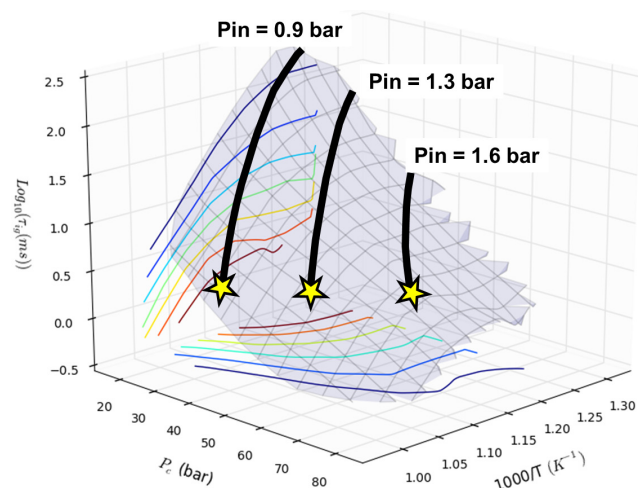


Figure 2. Ignition delay times as a function of inverse temperature and pressure for FACE-F where the temperature–pressure trajectories from three engine cycles are overlaid on the surface

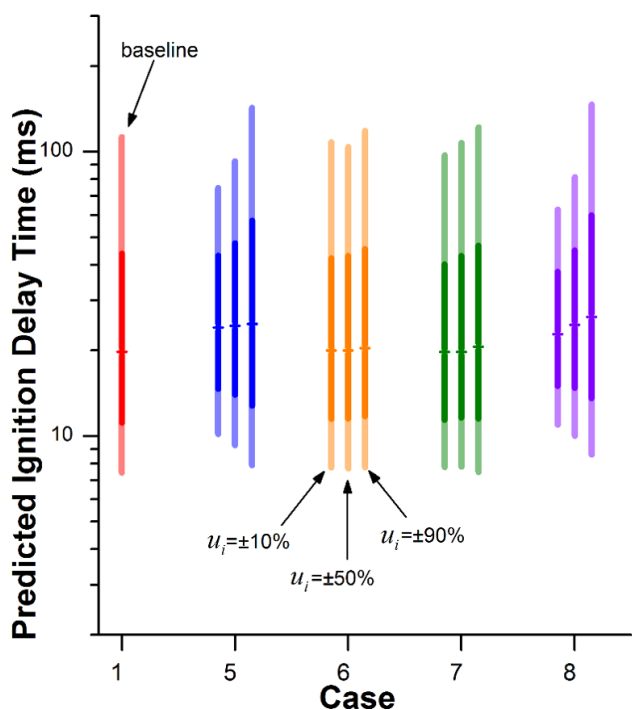


Figure 3. Range of predicted ignition delay times presented for various levels of uncertainty of important multi-channel reactions.

will be continued in FY 2017 towards reducing overall uncertainties in the chemical kinetic model.

Finally, a collaboration was initiated with the Combustion Chemistry Department at Sandia's Combustion Research Facility to acquire RCM data that will support efforts to investigate LTC chemistry, quantifying important chemical intermediates such as QOOH. Tests were conducted using various fuel blends over a range of temperature and pressure, and the findings of this work will be described in future publications.

## Conclusions

- ANL's RCM has been used to acquire autoignition data for needed gasoline surrogate components and blends of a full-boiling-range gasoline with ethanol at various blending ratios.
- Ignition delay times are combined with quantifications of pre-ignition heat release, i.e., low- and intermediate-temperature heat release, for model comparison.
- Work is ongoing to refine uncertainty predictions for the LLNL gasoline surrogate model covering a range of conditions, and to facilitate improvements to this model via implementation of novel tools like global sensitivity analysis.

## References

1. Basic Research Needs for Clean and Efficient Combustion of 21st Century Transportation Fuels. ([http://science.energy.gov/~/media/bes/pdf/reports/files/ctf\\_rpt.pdf](http://science.energy.gov/~/media/bes/pdf/reports/files/ctf_rpt.pdf))
2. S.S. Goldsborough, D. Longman, M.S. Wooldridge, R.S. Tranter and S. Pratt, "1st International RCM Workshop Meeting Report," August 28–29, 2012. (<http://www.transportation.anl.gov/rcmworkshop>)
3. C. Bahrini, O. Herbinet, P.-A. Glaude, C. Schoemaecker, C. Fittschen and F. Battin-Leclerc, *J. Am. Chem. Soc.* (139) 11944–11947, 2012.
4. I. Stranic, S.H. Pyun, D.F. Davidson, R.K. Hanson, *Combust. Flame* (159) 3242–3250, 2012.
5. CRC Report No. AVFL-24, 2014.
6. M.J. Davis, R.T. Skodje, A.S. Tomlin, *J. Phys. Chem. A* 115:1556–1578, 2011.
7. D.D.Y. Zhou, M.J. Davis, R.T. Skodje, *J. Phys. Chem. A* 117:3569–3584, 2013.
8. S. Bai, M.J. Davis, R.T. Skodje, *J. Phys. Chem. A* (in press).
9. M. Mehl, W.J. Pitz, C.K. Westbrook, H.J. Curran, *Proc. Comb. Inst.* 33:193–200, 2011.
10. G. Kukkadapu, K. Kumar, C.-J. Sung, M. Mehl, W.J. Pitz, *Combust. Flame* 159:3066–3078, 2012.
11. G. Kukkadapu, K. Kumar, C.-J. Sung, M. Mehl, W.J. Pitz, *Proc. Comb. Inst.* 34:345–352, 2013.
12. A. Fridlyand, S.S. Goldsborough, R.H. West, M.J. McEnally, M. Mehl, W.J. Pitz, accepted to *Combustion & Flame*, 2016.

## FY 2016 Publications/Presentations

1. A. Fridlyand, S.S. Goldsborough, "Progress using RCM experiments to elucidate fundamental gasoline LTC behavior and develop predictive kinetic models," AEC Winter Meeting, 2016.
2. N. Bourgeois, S.S. Goldsborough, G. Vanhove, M. Duponcheel, H. Jeanmart, F. Contino, "CFD simulations of rapid compression machines using detailed chemistry: impact of multi-dimensional effects on the auto-ignition of iso-octane," accepted to Proceedings Combustion Institute, 2016.
3. A. Fridlyand, S.S. Goldsborough, R.H. West, M.J. McEnally, M. Mehl, W.J. Pitz, "The role of correlations in uncertainty quantification of

transportation relevant fuel models,” accepted to Combustion & Flame, 2016.

4. S.S. Goldsborough, G. Vanhove, M.S. Wooldridge, H.J. Curran, C.J. Sung, S. Hochgreb, “Rapid compression machines: reducing the uncertainties in the low temperature combustion regime,” in revision for Progress in Energy and Combustion Science, 2016.
5. J. Santner, S.S. Goldsborough, “A numerical study of hot spot ignition at rapid compression machine conditions,” Central States Section of the Combustion Institute Spring Technical Meeting, Knoxville, TN, May 2016.
6. A. Fridlyand, S.S. Goldsborough, M. Al Rachidi, M. Sarathy, M. Mehl, W.J. Pitz, “Experimental and modeling investigation of autoignition characteristics of substituted cyclopentanes at engine-relevant conditions,” Central States Section of the Combustion Institute Spring Technical Meeting, Knoxville, TN, May 2016.
7. S.S. Goldsborough and J. Santner, “Iso-octane characterization initiative – new data, new insights,” presented at the 3rd International RCM Workshop, Seoul, Korea, July 2016.

## II.10 Chemical Kinetic Models for Advanced Engine Combustion

### Overall Objectives

- Develop detailed chemical kinetic models for fuel components used in surrogate fuels for compression ignition, homogeneous charge compression ignition, and reactivity controlled compression ignition engines
- Combine component models into surrogate fuel models to represent real transportation fuels; use them to model low-temperature combustion strategies in homogeneous charge compression ignition, reactivity controlled compression ignition, and compression ignition engines that lead to low emissions and high efficiency

### Fiscal Year (FY) 2016 Objectives

- Develop remaining component for inclusion in the Coordinating Research Council Advanced Vehicle/Fuel/Lubricants (AVFL)-18 nine-component diesel surrogate palette kinetic model [1]
- Develop and improve surrogate mechanisms for high-octane gasoline fuels and ethanol–gasoline mixtures
- Improve 2,2,4,4,6,8,8-heptamethylnonane (HMN) mechanism using fundamentally-based rate constants

### FY 2016 Accomplishments

- Developed an improved HMN kinetic model
- Finished development of a complete mechanism for diesel component decalin including low and high temperature chemistry
- Validated and improved chemical kinetic models for Fuels for Advanced Combustion Engines (FACE) gasoline Fuels F and G using University of Connecticut (UConn) rapid compression machine (RCM) experimental data
- Updated toluene mechanism and improved its behavior in fuel blends ■

### Introduction

Predictive engine simulation models are needed to make rapid progress towards DOE's goals of increasing combustion engine efficiency and reducing pollutant emissions. In order to assess the effect of fuel composition on engine performance and emissions,

**William J. Pitz (Primary Contact),  
Marco Mehl, Scott W. Wagnon,  
Kuiwen Zhang, Charles K. Westbrook,  
Goutham Kukkadapu**

Lawrence Livermore National Laboratory  
P.O. Box 808, L-372  
Livermore, CA 94551  
Phone: (925) 422-7730  
Email: pitz1@llnl.gov

DOE Technology Development Manager:  
Leo Breton

these engine simulations need to couple fluid dynamic and fuel chemistry submodels. Reliable chemical kinetic submodels representative of conventional and next-generation transportation fuels need to be developed to fulfill these requirements.

### Approach

Gasoline and diesel fuels consist of complex mixtures of hundreds of different components. These components can be grouped into chemical classes including n-alkanes, iso-alkanes, cyclo-alkanes, alkenes, oxygenates, and aromatics. Since it is not practicable to develop chemical kinetic models for hundreds of components, specific components need to be identified to represent each of these chemical classes. Then detailed chemical kinetic models can be developed for these selected components. These component models are subsequently merged together to produce a “surrogate” fuel model for gasoline, diesel, and next-generation transportation fuels. This approach creates realistic surrogates for gasoline or diesel fuels that can reproduce experimental behavior of the practical real fuels that they represent. Detailed kinetic models for surrogate fuels can then be simplified as needed for inclusion in multidimensional computational fluid dynamics models of engine combustion.

### Results

Mueller et al. [1] have proposed a nine-component surrogate to represent the ignition behavior of representative diesel fuels in terms of distillation

characteristics, density, and chemical composition. In FY 2016, the development of a chemical model for the final component in the nine-component diesel surrogate (decalin) was completed so that kinetic models for all nine components are now available. This kinetic model was challenging to develop due to decalin's two-ring cyclic structure that allows more complex reactions than in non-cyclic alkanes. These reactions control its low temperature chemistry important for ignition in diesel engines. Model simulations for decalin were compared to RCM experimental data from UConn and shock tube data from Rensselaer Polytechnic Institute [3]. The comparison between the simulated and measured ignition delay times in the RCM was reasonable. Also in FY 2017, the chemical kinetic mechanism for one of the components (HMN) was improved using updated thermodynamic properties of species, fundamentally-based reaction rate constants, added reaction pathways and new validation data from the UConn RCM. The updated model improved the agreement between simulations and the new RCM data for HMN (Figure 1) compared to the previous model. This increased the fidelity of the HMN model which will help to increase the accuracy of the nine-component gasoline surrogate model to be assembled in FY 2017.

FACE fuels for gasoline have been developed to provide researchers with controlled compositions that can be used to assess fuel effects on advanced engine combustion [4]. We have developed a 10-component gasoline surrogate palette to represent FACE fuels. In FY 2016, we improved the chemical kinetic models for the components in the surrogate palette. In collaboration with National

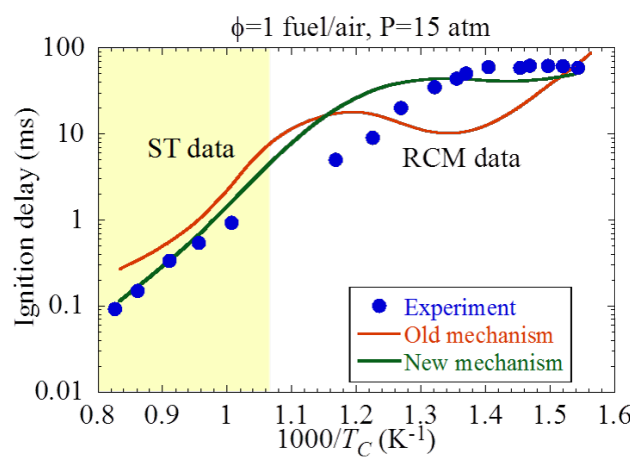


Figure 1. A comparison of ignition behavior computed from the chemical kinetic model (curves) and measured in the experiments (symbols) for HMN in an RCM from UConn (unpublished) and shock tube (ST) from Rensselaer Polytechnic Institute [7]

University of Ireland Galway, we improved the toluene model and how it behaves in binary fuel blends [5] by including pressure-dependent rate constants for the reaction of benzyl radical with HO<sub>2</sub> and by using new experimental data in a shock tube and an RCM from the National University of Ireland Galway (Figure 2). It is important to simulate the complex kinetic interactions in binary fuel blends for accurate simulation of multi-component fuel mixtures. We developed surrogate mixtures to represent FACE Fuels F and G using auto-ignition knock index and octane-sensitivity correlations developed at Lawrence Livermore National Laboratory. The surrogate model was compared against experimental data for these high-octane gasoline fuels taken in the UConn RCM [6] (Figures 3 and 4). The agreement is quite good considering that the surrogate mixture was matched to the target fuel just using the auto-ignition knock index, octane sensitivity, and relative amount of each chemical class of the target FACE fuel.

## Conclusions

- The chemical kinetic model for the last component needed (decalin) in the nine-component diesel surrogate [1] was completed.
- The diesel component model for HMN was improved and validated with new experimental RCM data from UConn.
- The model for the gasoline component toluene was updated and its behavior in binary blends improved.

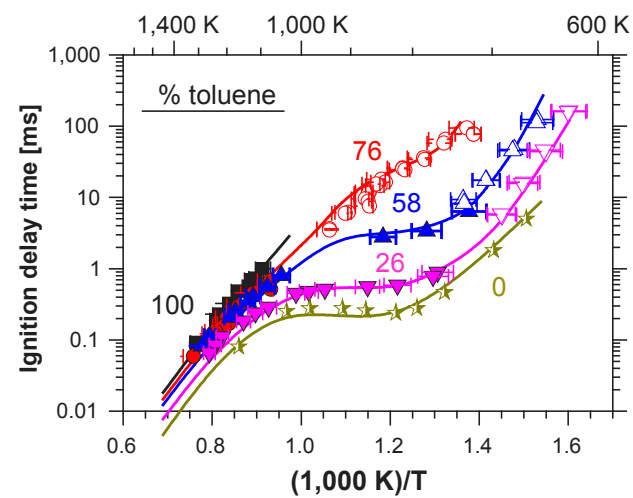


Figure 2. A comparison of ignition behavior computed from the chemical kinetic model (curves) and measured in the experiments [5] (symbols) for stoichiometric fuel-air mixtures of toluene and dimethylether in a shock tube and RCM at a pressure of 40 atm

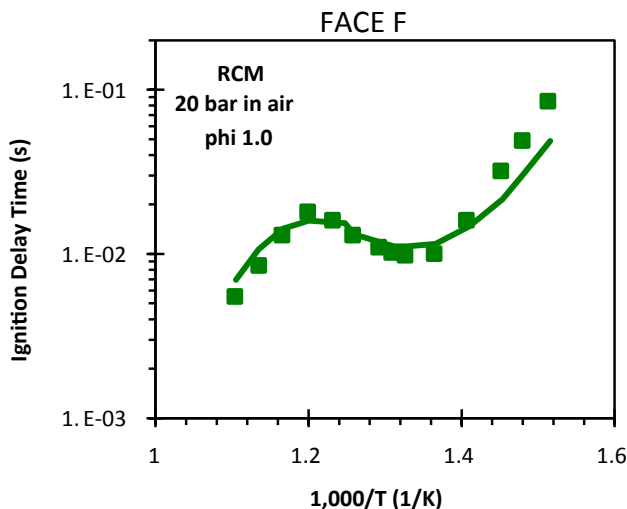


Figure 3. A comparison of ignition behavior computed from the chemical kinetic model (curves) and measured in the experiments [6] (symbols) for stoichiometric fuel-air mixtures in an RCM at pressure of 20 atm for FACE F

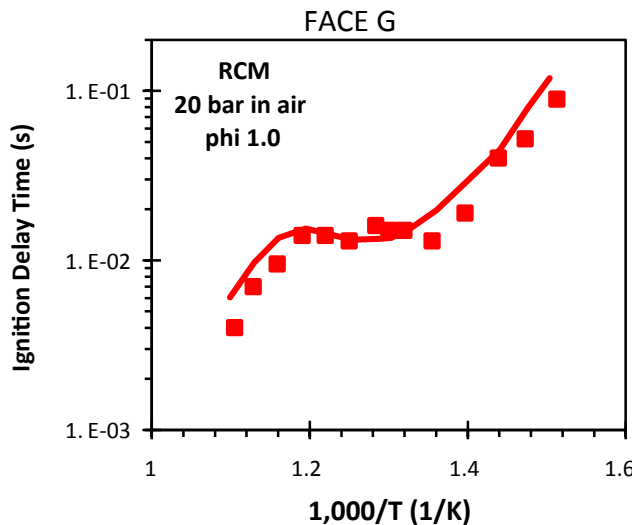


Figure 4. A comparison of ignition behavior computed from the chemical kinetic model (curves) and measured in the experiments [6] (symbols) for stoichiometric fuel-air mixtures in an RCM at pressure of 20 atm for FACE G

- Detailed chemical kinetic models to represent FACE F and G were validated using new experimental RCM data from UConn.
- This work was performed under the auspices of the U.S. Department of Energy by Lawrence Livermore National Laboratory under Contract DE-AC52-07NA27344.

## References

1. C.J. Mueller, W.J. Cannella, T.J. Bruno, B. Bunting, H.D. Dettman, J.A. Franz, M.L. Huber, M. Natarajan, W.J. Pitz, M.A. Ratcliff and K. Wright, "Methodology for Formulating Diesel Surrogate Fuels with Accurate Compositional, Ignition-Quality, and Volatility Characteristics," *Energy & Fuels* 26 (6) (2012) 3284–3303.
2. C.J. Mueller, W.J. Cannella, J.T. Bays, T.J. Bruno, K. DeFabio, H.D. Dettman, R.M. Gieleciak, M.L. Huber, C.-B. Kweon, S.S. McConnell, W.J. Pitz and M.A. Ratcliff, "Diesel Surrogate Fuels for Engine Testing and Chemical-Kinetic Modeling: Compositions and Properties," *Energy & Fuels* 30 (2) (2016) 1445-1461.
3. M.A. Oehlschlaeger, H.-P. S. Shen, A. Frassoldati, S. Pierucci and E. Ranzi, "Experimental and Kinetic Modeling Study of the Pyrolysis and Oxidation of Decalin," *Energy & Fuels* 23 (3) (2009) 1464–1472.
4. W. Cannella, M. Foster, G. Gunter and W. Leppard, "Face Gasolines and Blends with Ethanol: Detailed Characterization of Physical and Chemical Properties," Coordinating Research Council, Inc., CRC Report No. AVFL-24, (2014) <http://www.crcap.org/Publications/advancedVehiclesFuelsLubricants/index.html>.
5. Y. Zhang, K.P. Somers, M. Mehl, W.J. Pitz, R.F. Cracknell and H.J. Curran, "Probing the antagonistic effect of toluene as a component in surrogate fuel models at low temperatures and high pressures. A case study of toluene/dimethyl ether mixtures," *Proc. Combust. Inst.* (2017).
6. S.M. Sarathy, G. Kukkadapu, M. Mehl, T. Javed, A. Ahmed, N. Naser, A. Tekawade, G. Kosiba, M. AlAbbad, E. Singh, S. Park, M.A. Rashidi, S.H. Chung, W.L. Roberts, M.A. Oehlschlaeger, C.-J. Sung and A. Farooq, "Compositional effects on the ignition of FACE gasolines," *Combust. Flame* 169 (2016) 171–193.
7. M.A. Oehlschlaeger, J. Steinberg, C.K. Westbrook and W.J. Pitz, "The autoignition of iso-cetane at high to moderate temperatures and elevated pressures: Shock tube experiments and kinetic modeling," *Combust. Flame* 156 (11) (2009) 2165–2172.

## FY 2016 Publications/Presentations

1. Sarathy, S.M., Kukkadapu, G., Mehl, M., Javed, T., Ahmed, A., Naser, N., Tekawade, A., Kosiba, G., AlAbbad, M., Singh, E., Park, S., Rashidi, M.A., Chung, S.H., Roberts, W.L., Oehlschlaeger, M.A.,

Sung, C.-J. and Farooq, A., "Compositional Effects on the Ignition of Face Gasolines," *Combustion and Flame* 169 (2016) 171–193.

2. Mueller, C.J., Cannella, W.J., Bays, J.T., Bruno, T.J., DeFabio, K., Dettman, H.D., Gieleciak, R.M., Huber, M.L., Kweon, C.-B., McConnell, S.S., Pitz, W.J. and Ratcliff, M.A., "Diesel Surrogate Fuels for Engine Testing and Chemical-Kinetic Modeling: Compositions and Properties," *Energy & Fuels* 30 (2) (2016) 1445–1461.

3. Zhang, Y., Somers, K.P., Mehl, M., Pitz, W.J., Cracknell, R.F. and Curran, H.J., "Probing the Antagonistic Effect of Toluene as a Component in Surrogate Fuel Models at Low Temperatures and High Pressures. A Case Study of Toluene/Dimethyl Ether Mixtures," *Proceedings of the Combustion Institute* (2017).

4. Al Rashid, M.J.A., Thion, S., Togbé, C., Dayma, G., Mehl, M., Dagaut, P., Pitz, W.J., Zádor, J. and Sarathy, S.M., "Elucidating Reactivity Regimes in Cyclopentane Oxidation: Jet Stirred Reactor Experiments, Computational Chemistry, and Kinetic Modeling," *Proceedings of The Combustion Institute* (2017).

5. Fridlyand, A., Johnson, M.S., Goldsborough, S.S., West, R.H., McNenly, M.J., Mehl, M. and Pitz, W.J., "The Role of Correlations in Uncertainty Quantification of Transportation Relevant Fuel Models Combustion and Flame," *Combustion and Flame* (2016).

## II.11 Model Development and Analysis of Clean and Efficient Engine Combustion

### Overall Objectives

- Gain fundamental and practical insight into high efficiency clean combustion (HECC) regimes through numerical simulations
- Develop and apply numerical tools to improve simulations of HECC by combining multidimensional fluid mechanics with chemical kinetics
- Reduce computational expense for HECC simulations while maintaining fidelity
- Create predictive computational tools that can be used by industry for HECC research and development

### Fiscal Year (FY) 2016 Objectives

- Evaluate uncertainty in homogeneous charge compression ignition (HCCI) engine experiments
- Broaden graphical processing unit (GPU) chemical kinetics applicability by developing robust parallel work-sharing algorithms
- Deploy GPU chemistry capability in collaboration with industry partners

### FY 2016 Accomplishments

- Performed first “bottom up” uncertainty analysis of HCCI engine experimental measurements and analysis input quantities
- Developed detailed uncertainty propagation method for experimental HCCI engine performance measurements for comparison with simulations
- Improved robustness of work-sharing methods for GPU chemistry calculations in parallel computational fluid dynamics (CFD)
- Collaborated with Oak Ridge National Laboratory (ORNL) and General Motors (GM) to deploy GPU chemistry solver on Titan supercomputer for 8,000,000 core-hour Advanced Scientific Computing Research Leadership Computing Challenge award for virtual engine design and calibration ■

**Russell Whitesides (Primary Contact),  
Nick Killingsworth, Guillaume Petitpas,  
Matthew McNenly**

Lawrence Livermore National Laboratory (LLNL)  
P.O. Box 808, L-792  
Livermore, CA 94551  
Phone: (925) 423-2500  
Email: whitesides1@llnl.gov

DOE Technology Development Manager:  
Leo Breton

### Introduction

Numerical simulation has become a vital design tool for engine manufacturers. Computational models also allow researchers to probe fundamental aspects of combustion phenomena that are inaccessible via experiments. However, simulations that have sufficient spatial, temporal, and physical detail to capture relevant combustion characteristics are often computationally intractable. In these cases, modelers must simplify their analyses with the understanding that results may be compromised by lack of fidelity. The combustion model development and analysis effort at LLNL is focused on reducing the number of simplifications engine researchers and designers must make in their simulations and analyses. More efficient detailed combustion simulations allow engine designers to test more configurations in the same amount of time at a given level of fidelity, or to pursue more physically accurate simulations capable of revealing key chemical kinetic processes affecting engine performance.

### Approach

The main thrust of this work is the development of efficient and accurate chemical kinetic models for CFD simulations of advanced engine combustion. Secondarily, the work exercises the models to generate new understanding of fundamentals of engine combustion in HECC regimes. This project is an ongoing research effort under Advanced Combustion Engine R&D subprogram with annual feedback and direction from program managers and memorandum of understanding partners. Work in the current performance period has focused on

two thrusts: (1) rigorous accounting of experimental and model uncertainty in analysis of HCCI engine performance, and (2) continuing development of GPU enabled detailed chemistry for CFD. The project is closely linked with related LLNL projects headed by Matthew McNenly [1] and William Pitz [2].

## Results

### Quantifying Measurement Uncertainties and Uncertainty Propagation in HCCI Engine Experiments

The experimental measurement uncertainties for a HCCI engine testing facility were estimated and then propagated using a Monte Carlo simulation method to calculate derived uncertainties in mass-average temperatures, composition, and engine performance metrics. Detailed uncertainty quantification was first carried out for the measurement of the in-cylinder pressure, whose variations during the cycle provide most of the information for performance evaluation. It was shown that relative overall uncertainties, given with a 95% confidence interval assuming a uniform distribution, vary between 3% (at top dead center) and 25% (at intake valve closure, or IVC). The rather large relative uncertainty at IVC is attributed to the large span of pressures measured by the piezo-electric pressure transducer. Standard uncertainties of other measured quantities, such as the engine geometry and speed, the air and fuel flow rate and the intake and exhaust dry molar fractions were also estimated. Propagating those uncertainties using a Monte Carlo simulation and Bayesian inference methods then allowed for estimation of uncertainties of the mass-average temperature and composition at IVC and throughout the cycle, and also of the engine performance metrics such as indicated mean effective pressure, heat release, and ringing intensity. An uncertainty of 32 K was found on the IVC temperature estimate, mainly attributed to the uncertainty of the pressure measurement at IVC. It was also found that the uncertainty in the amount of water removal in the exhaust gas recirculation loop induces large uncertainties in the residuals mass fraction (up to 36%). The uncertainty of the indicated mean effective pressure appears fairly small (3%), and it is shown that the large uncertainty on the ringing intensity (25%) is due to the large error in the peak mass-average temperature estimate, which stems from the large uncertainty of the pressure measurement at IVC.

### Continued Development and Deployment of Accelerated Chemistry in Engine Simulations Using GPUs

Building on previous years efforts under this program, LLNL engineers have improved the robustness of

the Zero-RK software, designed to accelerate engine simulations. The current work addressed proper batching of chemical reactors for solution on GPUs, which was an issue identified in the previous year's report for this project [3]. The chemical reactor solution refers to the time evolution of the chemical system at a given thermodynamic state. Each reactor can represent the combustion process at an individual point in the engine, or entire regions in the engine at similar thermodynamic conditions. Consequently, the number of simultaneous chemical reactor calculations needed for an engine design simulation can range from hundreds to tens of millions, which motivates the need for a computational efficient parallel solution, or "batch processing." By taking into account the expected solution cost per reactor, reactor batches can be formed by grouping together reactors with similar timescales into "smart batches." This effort required implementation of sophisticated memory management subroutines to coordinate information exchange among many central processing unit (CPU) cores and associated GPU devices employed in modern distributed memory computing systems. The work-sharing method was implemented in the Zero-RK package using the standard Message Passing Interface, which allows the package to be seamlessly incorporated into many parallel CFD software packages. A typical spark ignited engine configuration was chosen to test the performance of the improved work-sharing technique. Figure 1 shows a cut-plane of the cylinder volume shortly after ignition with temperature and oxygen mass fractions plotted showing the flame propagation. For the test, simulation times and chemistry subcycles were evaluated with and without the GPU enabled. Performance of the new work-sharing method is shown in Figures 2 and 3, where one can see the reduction in chemistry subcycles due to the new "smart batching" method and overall run time being decreased dramatically with the GPU from 13 h down to less than 8 h.

After verifying the expected performance gains in sample test cases, the Zero-RK GPU technology was deployed in collaboration with ORNL and GM. The first broad application was in acceleration of simulations aimed at virtual engine design and calibration. The effort included hundreds of engine simulations running on a world-class supercomputer and accelerated by the software work developed under this program. In addition to using simulations to confirm engine performance trends including power and emissions, the work has pushed the boundaries of what is possible in enabling highly detailed chemistry in an engine simulation. In the most detailed case a chemical mechanism including over 5,000 species was included, which is the largest mechanism reported to be used in a CFD calculation. This is only possible due

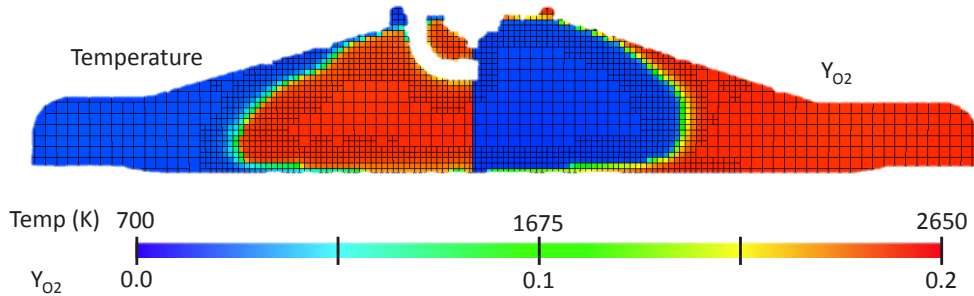


Figure 1. Cut-plane of in-cylinder volume for the spark ignited engine simulation used to benchmark Zero-RK GPU chemistry solver with the improved work-sharing algorithm

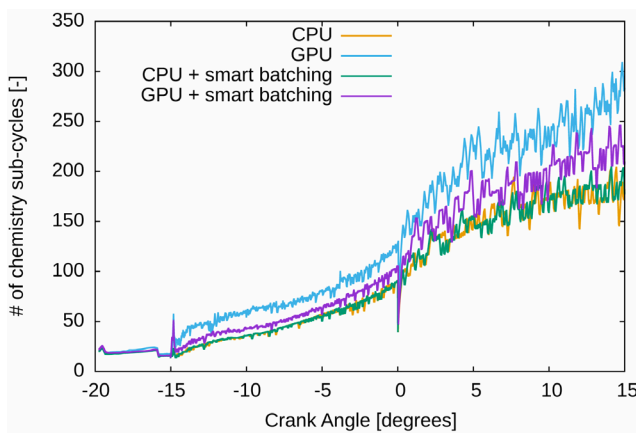


Figure 2. Performance comparison of different solution methods for chemistry in terms of subcycles per CFD time step. Fewer subcycles are better.

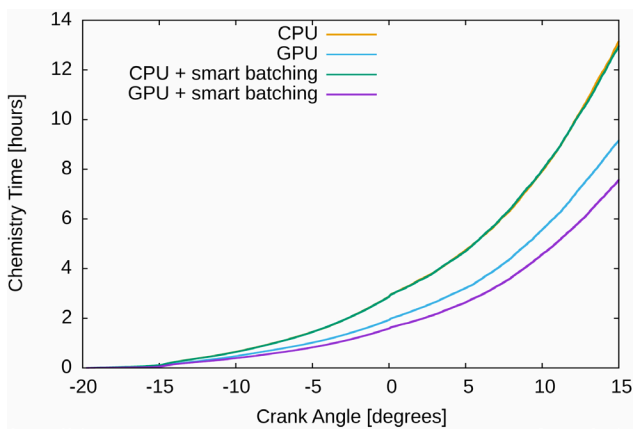


Figure 3. Performance comparison of different solution methods for chemistry in terms of wall-clock time as a function of simulation time. Lower wall-clock time is better.

the greater than 20 times reduction in simulation time provided by Zero-RK GPU.

## Conclusions

- Uncertainty quantification is vital to create and validate predictive simulations of engine performance. The first reported full accounting of uncertainties of a well-characterized engine experiment yields low uncertainties on most quantities, but rather high values for the intake mass averaged temperatures.
- Hardware and software enabled improvements to simulation run times for detailed engine models are allowing researchers to develop new understanding of tradeoffs in engine design parameters.

## References

1. McMenly, M.J., “Improved solvers for advanced engine combustion simulation,” in Advanced Combustion Engine Research and Development 2016 Annual Progress Report, U.S. Department of Energy, 2016.
2. Pitz, W.J., “Chemical Kinetics Models for Advanced Engine Combustion,” in Advanced Combustion Engine Research and Development 2016 Annual Progress Report, U.S. Department of Energy, 2016.
3. Whitesides, R.A., “Model Development and Analysis of Clean & Efficient Engine Combustion,” in Advanced Combustion Engine Research and Development 2015 Annual Progress Report, U.S. Department of Energy, 2015.

## FY 2016 Publications/Presentations

1. R.A. Whitesides, “Burning on the GPU: Fast and Accurate Chemical Kinetics,” GPU Technology Conference, San Jose, CA, April 7, 2016.

2. G. Petitpas, M.J. McNenly, and R.A. Whitesides, "Measurement Uncertainty Quantification in HCCI engine experiments," AEC Working Group Meeting, Livermore, CA, February 8–11, 2016.
3. R.A. Whitesides and M.J. McNenly, "Continued effort to accelerate chemistry in engine combustion CFD at LLNL," AEC Working Group Meeting, Southfield, MI, August 15–19, 2016.

## Special Recognitions and Awards/ Patents Issued

1. 2016 R&D 100 Award Winner for Zero-RK in Software/ Services Category.
2. OLCF User Conference Best Poster Award (with ORNL and GM).

## II.12 Improved Solvers for Advanced Combustion Engine Simulation

### Overall Objectives

- Accelerate development and deployment of high-efficiency clean combustion (HECC) engine concepts through deeper understanding of complex fluid and chemistry interactions
- Improve physical accuracy of combustion simulations by enabling the use of large chemistry mechanisms representing real transportation fuels
- Reduce the time and resource cost for combustion simulations by designing efficient algorithms guided by applied mathematics and physics
- Develop truly predictive combustion models and software that are fast enough to impact the engine design cycle

### Fiscal Year (FY) 2016 Objectives

- Improve the mechanism development tools to better identify potential errors and provide automatic correction whenever possible
- Extend LLNL's accelerated combustion solvers to include more reaction classes that are needed for accurate multi-component fuel surrogates and soot formation
- Verify and validate the generalized framework for LLNL's adaptive preconditioner approach for fully coupled fluid dynamics and chemistry models using canonical steady and unsteady flame experiments.

### FY 2016 Accomplishments

- Guided the correction of several new mechanisms developed for use in the Advanced Combustion Engine (ACE) and Co-Optima programs resulting in faster, more accurate combustion simulations
- Created several mechanism debugging tools to uncover new errors leading to more robust fuel chemistry models for engine simulation
- Deployed the first version of the mechanism debugging website for further testing on the internal LLNL network

**Matthew McNenly (Primary Contact),  
Salvador Aceves, Nick Killingsworth,  
Guillaume Petitpas, and  
Russell Whitesides**

Lawrence Livermore National Laboratory (LLNL)  
7000 East Ave. (L-140)  
Livermore, CA 94550  
Phone: (925) 424-6418  
Email: mcnenly1@llnl.gov

DOE Technology Development Manager:  
Leo Breton

- Created the unit test framework for code verification and validation of the new flame solver using the adaptive preconditioner approach ■

### Introduction

This project fills the present knowledge gap through substantial improvements in the performance and accuracy of combustion models and software. The project focuses on the applied mathematics underpinning efficient algorithms and the development of combustion software on new computing architectures. It is a natural complement to the other LLNL projects in the quest to gain fundamental understanding of the new engine modes investigated under the ACE subprogram. Other LLNL projects include the multidimensional engine simulation project led by Whitesides (see II.11) and the high-fidelity chemistry mechanisms developed for real transportation fuels by Pitz (see II.10). The long-term goal of this project is to develop predictive combustion software that is computationally fast enough to impact the design cycle and reduce the deployment time for new high-efficiency, low-emissions engine concepts. Toward this goal, the project developed a new thermochemistry library and chemistry solver [1–3] that achieves multiple orders of magnitude speedup over the traditional approaches found in CFD (e.g., OpenFOAM) without any loss of accuracy. Further, the LLNL library and solver are 5–15 times faster than sophisticated commercial solvers like Chemkin-Pro. This performance has led to the LLNL library, named Zero-RK, to win a 2015 R&D 100 award in the Software and Services category. As a consequence of this project,

it is now possible to model high fidelity fuel mechanisms (on the order of a thousand species) in multidimensional engine simulations that run in a day on industry-scale computational resources.

## Approach

The project is focused on creating combustion software capable of producing accurate solutions in a short time relative to the engineering design cycle on commodity computing architectures. The approach advances engine simulations along several fronts simultaneously. Major bottlenecks in the software are found through detailed code profiling, while bottlenecks in the general computational-aided analysis are identified through engagements with the original equipment manufacturers, universities, and national laboratories. New algorithms are created for the slowest code sections and existing algorithms are adapted to new applications that can accelerate the overall analysis workflow for HECC design. The new algorithms seek performance gains by implementing new theories from applied mathematics and/or by exploiting the new low-cost, massively parallel computing architectures like the general purpose GPU.

## Results

The project completed Tasks 1 and 2 in FY 2016 in support of the overall goals of the ACE subprogram, with the Task 3 on track to be completed in the first quarter of FY 2017:

- Task 1. Improve the identification and correction procedures for detailed kinetic mechanisms
- Task 2. Extend Zero-RK to efficiently solve additional reaction classes needed for more accurate multi-component fuel mixture ignition and soot formation
- Task 3. Verify and validate the generalized framework for LLNL's adaptive preconditioner approach for fully coupled fluid dynamics and chemistry models with multi-species transport

### Task 1

New methods to identify errors in fuel models were developed for LLNL's suite of mechanism debugging tools. Updating and debugging the thermodynamic and chemical data contained in a realistic fuel mechanism is similar to searching a 1,000-page book, or larger, for typos. This is an example of the project removing a key bottleneck in the overall workflow for HECC design. Mechanisms at the leading edge of development can still show numerical evidence of errors despite passing all the tests in the FY 2015 version of the debugging suite

(e.g., an updated version of the methyldecanoate model in Sarathy et al. [4]). A key indicator of a likely mechanism error is when the ordinary differential equation integrator for the chemical system needs artificially small time steps at thermodynamic states far from ignition. Further evidence is present when excessive chemical integration errors are reported by CFD software, which if left uncorrected, can lead to simulation failures.

A number of new methods were created to isolate and identify the sources of the remaining mechanism errors. These include: (1) calculating the eigenstructure of the chemical system, (2) tracking the species and the associated reactions that are at the integrator error limit (i.e., slowest to converge), and (3) tracking the number of times a species is generated and then extinguished relative to the integrator error limit. These methods identify species with pathological behavior despite having reaction rates that still satisfy the known physical limits used to check mechanisms in the FY 2015 version. The methods, however, do not pinpoint exact datum in the input files responsible for the potential error.

To accelerate the correction process, new statistical methods were developed to find the species or reaction datum that is most likely erroneous. These methods are based on similar techniques used in machine learning and automatic error detection, and rely on the fact that molecules with similar structures often have similar thermochemical properties. One method checks the likelihood the specific heat of a species is correct based solely on its atomic composition. The likelihood is estimated using a model created using Bayesian parameter estimation for a simple linear weighting of the number of hydrogen, carbon, and oxygen atoms. Using the well-tested LLNL gasoline surrogate mechanism [5] to "train" the model, the distributions of the weight parameters (or atomic count multipliers) are shown in Figure 1. The model parameters have a relatively narrow range, and the standard deviation of the non-dimensional specific heat is less than 0.75 (see Figure 2). As a consequence, the resulting model provides rapid feedback to the developer, and can automatically be updated as new mechanism data is validated.

The improved debugging tools were applied to several new fuel mechanisms under development for the ACE and Co-Optima programs, which saved countless computer and human hours. These included updated diesel and gasoline surrogates, methyldecanoate, and propane. To improve the usability of the debugging suite, an online version is being developed for the larger ACE community and is currently available within LLNL for beta testing by the chemical kineticists.

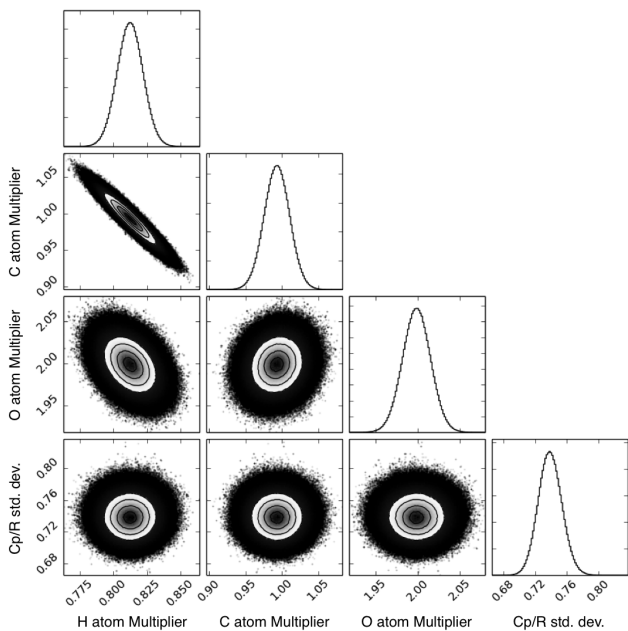


Figure 1. Bayesian parameter estimation is used to determine an error detection model for the specific heat at 298 K using the species of the gasoline surrogate mechanism [5] as a training set. The joint and cumulative probability distributions have a narrow range of parameter values and a sufficiently small standard deviation (std. dev.) that indicate the model will be effective for error screening.

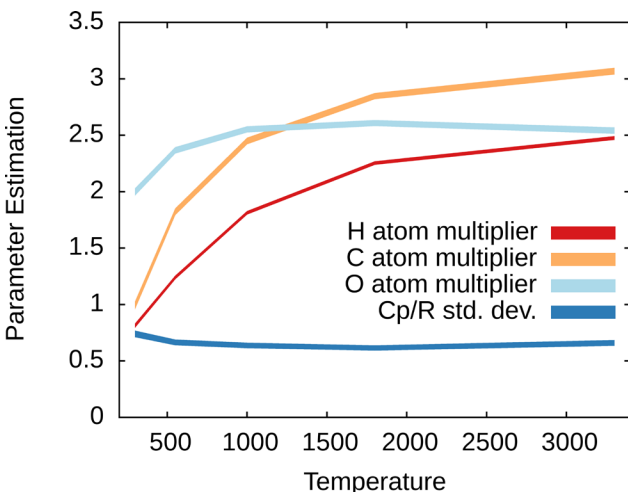


Figure 2. Parameter ranges (95% confidence interval) for the specific heat model over the full range of combustion temperatures using  $10^5$  Markov Chain Monte Carlo samples at each temperature in the Bayesian analysis

## Task 2

LLNL's advanced chemistry solver library Zero-RK was extended to include more reaction classes needed for accurate multi-component fuel mixtures and soot

formation. The computational performance of Zero-RK is due in large part to the efficiency of computing the sparse reaction network. Adding any new reaction class requires careful rewriting of key algorithms so that the speed and accuracy are maintained. To improve the modeling of multi-component mixtures, the tabulated pressure dependent reactions with logarithmic interpolation were redesigned. The reaction class can now more accurately resolve competing product channels that are calculated using quantum or transition state theory. These are crucial for the complex interactions between aromatics (and cycloalkanes) and the rest of the gasoline mechanism. The change in computational cost updating the original five-component gasoline surrogate [5] to the new 12-component model is shown by blue line in Figure 3. The larger surrogate has nearly 200 reactions using the more detailed pressure dependent formulation, yet it is shown to have the same computational scaling as the original version of Zero-RK used for several single component alkane mechanisms (red line). Similarly, new features were added to handle the reactions found in detailed soot models. These include the ability to handle non-integer stoichiometry, arbitrary reaction orders, and very large molecules (more than two billion atoms). To verify that the original performance of Zero-RK is maintained, a detailed soot model with over 11,000 reactions is simulated with the 12-component gasoline surrogate. In Figure 3, the resulting ignition delay calculations for the gasoline surrogates (blue line) are shown to have the same computational scaling as the original version of Zero-RK.

## Task 3

A more general software framework was created for the LLNL adaptive preconditioner method in Zero-RK to accelerate fully coupled fluid chemistry models in FY 2015. The fluid dynamic transport of species using detailed fuel chemistry mechanisms was identified in FY 2014 as an increasingly important code bottleneck to address for the ACE program. A new framework was proposed that would combine the block preconditioner technique developed initially in this project [6] with the adaptive preconditioner technique in Zero-RK applied to each sub-block. In this performance period, the new framework was applied to the development of steady and unsteady flame models using detailed chemistry with fully coupled multi-species transport. The new simulations are projected to achieve a similar speedup on a single processor as reported for the homogenous reactor calculations in McLeny et al. [1] (i.e., one order of magnitude faster than commercial codes and several orders of magnitude faster than open source codes). However, the parallel version will deliver even faster

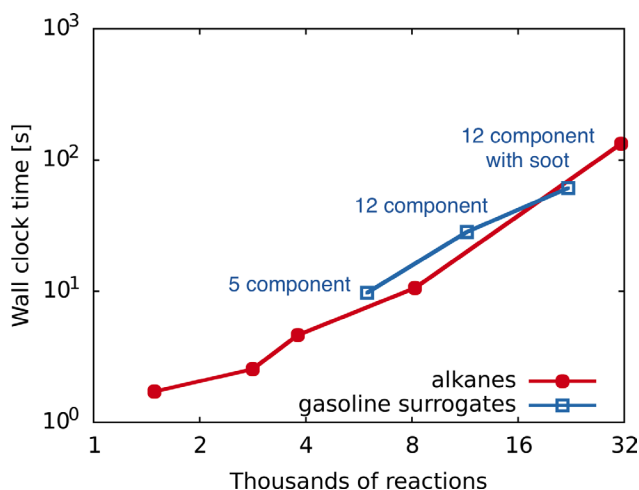


Figure 3. The enhanced reaction models added to Zero-RK achieve the same central processing unit cost scaling for a constant pressure, homogeneous reactor: (red) the original tabulated pressure dependent reactions with logarithmic interpolation (excludes soot), and (blue) the new reaction classes

turnaround time given the highly scalable nature of the detailed chemistry solver. The unit test framework for the new algorithms was completed in this performance period, and the verification and validation effort is on schedule to be completed at the end of the first quarter in FY 2017.

## Conclusions

In FY 2016, this project progressed toward the goal of bringing truly predictive combustion software to the computational level needed to impact the engine design cycle for new HECC operating modes. Key achievements included:

- Improved mechanism development tools to better identify potential errors and provide automatic correction whenever possible
- Extended Zero-RK to include more reaction classes needed for accurate multi-component fuel ignition and soot formation
- Created the unit test framework for code verification and validation of the new flame solver using the adaptive preconditioner approach

In FY 2017, the project will continue its efforts to distribute the high performance solvers and libraries developed here to industrial and academic partners, and explore new algorithms to further accelerate the software

and new applications to accelerate the workflow of the advanced combustion engine community.

## References

1. M.J. McMenly, R.A. Whitesides and D.L. Flowers, “Faster solvers for large kinetic mechanisms using adaptive preconditioners,” *Proc. Combust. Inst.*, 35:581–587, 2015.
2. M.J. McMenly, R.A. Whitesides and D.L. Flowers, “Adaptive preconditioning strategies for integrating large kinetic mechanisms,” The 8th U.S. National Combustion Meeting, Park City, UT, May 19–22, 2013.
3. R.A. Whitesides, M.J. McMenly and D.L. Flowers, “Optimizing time integration of chemical-kinetic networks for speed and accuracy,” The 8th U.S. National Combustion Meeting, Park City, UT, May 19–22, 2013.
4. S.M. Sarathy, M.J. Thomson, W.J. Pitz, and T. Lu, “An experimental and kinetic modeling study of methyldecanoate combustion,” *Proc. Combust. Inst.*, 33:399–405, 2011.
5. M. Mehl, W.J. Pitz, C.K. Westbrook, and H.J. Curran, “Kinetic modeling of gasoline surrogate components under engine conditions,” *Proc. Combust. Inst.*, 33:193–200, 2011.
6. M.J. McMenly, M.A. Havstad, S.M. Aceves and W.J. Pitz, “Integration strategies for efficient multizone chemical kinetics models,” *SAE Int. J. Fuels Lubr.*, 3(1):241–255, 2010.

## FY 2016 Publications/Presentations

1. R.A. Whitesides, “Burning on the GPU: fast and accurate chemical kinetics,” GPU Technology Conference, San Jose, CA, April 2016.
2. G. Petitpas, M.J. McMenly, and R.A. Whitesides, “Measurement uncertainty quantification in HCCI engine experiments,” AEC Working Group Meeting, Livermore, CA, February 2016.
3. R.A. Whitesides and M.J. McMenly, “Continued effort to accelerate chemistry in engine combustion CFD at LLNL,” AEC Working Group Meeting, Southfield, MI, August 15–19, 2016.
4. A. Fridlyand, et al., “The role of correlations in uncertainty quantification of transportation relevant fuel models,” *Combust. Flame*, 2016. (Accepted for publication)

5. G. Petitpas, M.J. McNenly, and R.A. Whitesides, "Quantifying Measurement Uncertainties and Uncertainty Propagation in HCCI Engine Experiments," SAE World Congress, Detroit, 2017. (Paper offer 17PFL-1126)

## Special Recognitions and Awards/ Patents Issued

1. M.J. McNenly and R.A. Whitesides, "Zero-RK," R&D 100 Winner – Software & Services, R&D Magazine, November 2015.

## II.13 2016 KIVA-hpFE Development: a Robust and Accurate Engine Modeling Software

### Objectives

- Develop algorithms and software for the advancement of speed, accuracy, robustness, and range of applicability of the KIVA internal engine combustion modeling to be more predictive; this is to be accomplished by employing higher-order spatially accurate methods for reactive turbulent flow, and spray injection, combined with robust and accurate actuated parts simulation and more appropriate turbulence modeling
- To provide engine modeling software that is easier to maintain and is easier to add models to than the current KIVA; to reduce code development costs into the future via more modern code architecture

### Fiscal Year (FY) 2016 Objectives

- Continue developing code and algorithms for the advancement of speed, accuracy, robustness, and range of applicability of combustion modeling software to higher-order spatial accuracy with a minimal computational effort
- Finish developing a large eddy simulation (LES) turbulence model that is capable of spanning transition to turbulence and hence fluid boundary layers without the law-of-the-wall
- Finish developing the KIVA-hpFE to be parallel using Message Passing Interface (MPI) to facilitate speed of solution of more fully resolved domains including moving parts, chemistry, and sprays
- Continue developing the three dimensional (3D) overset grid system, to quickly utilize the “stl” file type from the grid generator for quick and automatic over-set parts surface generation.
- Start developing parallel implementation of 3D *hp*-adaptive finite element method (FEM) system
- Start developing a predictive initial spray break-up model that transitions to atomized droplets by directly modeling and evaluating the forces involved of any injected fluid
- Start implementing higher fidelity reactive chemistry packages, such as ChemKin-Pro and Lawrence Livermore National Laboratory’s ZeroRK2

**David B. Carrington (Primary Contact),  
Jiajia Waters**

Los Alamos National Laboratory

P.O. Box 1663

Los Alamos, NM 87545

Phone: (505) 667-3569

Email: dcarrin@lanl.gov

DOE Technology Development Manager:

Leo Breton

Staff and Subcontractors:

- Brad Philipbar, Los Alamos National Laboratory, Los Alamos, NM
- Dr. Juan Heinrich, University of New Mexico, Albuquerque, NM
- Dr. Xiuling Wang, Purdue University Northwest, Hammond, IN

### FY 2016 Accomplishments

- Finished developing an LES turbulence model that is capable of spanning transition to turbulence and hence fluid boundary layers
- Finished developing the KIVA-hpFE to be parallel using MPI to facilitate speed of solution of more fully resolved domains and parallel solution method for the moving parts, reactive chemistry, and sprays, showing  $\sim 30\times$  speed-up over serial version
- Developed implicit solution system for diffusive and stress forces for an extra  $10\times$  speed-up per processor in some cases, giving a  $300\times$  speed-up over our original serial version
- Started parallelization of the *hp*-adaptive FEM methods; serial version completed
- Continued development of the 3D overset grid system, to quickly utilize the “stl” file type from the grid generator for quick and automatic overset parts surface generation and much easier creation of quality grids.
- Developing a volume of fluid (VOF) method for use in spray modeling to have a more predictive capability,

particularly the initial break-up. The VOF system includes fluid surface curvatures and interacting stress on the fluid–gas interface. Implementing higher fidelity reactive chemistry packages, such as Chemkin-Pro and Lawrence Livermore National Laboratory's ZeroRK

- Continued validation and verification adding capabilities for many benchmark problems ■

## Introduction

Los Alamos National Laboratory and its collaborators are facilitating engine modeling by improving accuracy and robustness of the modeling, and improving the robustness of software. We also continue to improve the physical modeling methods. We are developing and implementing new mathematical algorithms, those that represent the physics within an engine. We provide software that others may use directly or that they may alter with various models, e.g., sophisticated chemical kinetics, different turbulent closure methods, or other fuel injection and spray systems.

## Approach

Our approach is founded in design and to invent new modeling methods and code. The new design is a change of discretization to FEM; essentially every other beneficial and salient attribute of the software stems from this foundation. We invented and developed the following systems to date.

- Invented the Petrov–Galerkin FEM predictor-corrector scheme projection method for all flow regimes
- Developed the *hp*-adaptive system for higher order accuracy and resolution when and where needed as a function of measured error
- Invented the local Arbitrary Lagrangian–Eulerian (ALE) method for moving bodies, allowing for accurate moving boundaries and easy grid generation keeping the flow solution Eulerian
- Developed new dynamic LES turbulence model especially designed for wall bounded, unsteady, laminar, transitional to turbulent flow
- Invented an efficient (superlinear) parallel FEM method using MPI for today's and future platforms

We are building models and code in order to meet all the objectives in a clean, easy to maintain software which easily handles addition of submodels. Careful verification and validation is required. The development of this technology utilizes many areas of expertise in the areas

of multi-species turbulent reactive flow modeling with liquid sprays, modeling of immersed moving bodies, and numerical methods for the solution of the model and governing equations.

## Results

When considering the development of algorithms and the significant effort involved producing reliable software, it is often best to create algorithms that are more accurate at a given resolution and then resolve the system more accurately only where and when it is required. We began developing a new KIVA engine/combustion code with this idea in mind [1]. This new construction is a Galerkin FEM approach that utilizes conservative momentum, species, and energy transport. The FEM system is Petrov–Galerkin and pressure stabilized [2].

A projection method is combined with higher-order polynomial approximation for model dependent physical variables (*p*-adaptive) along with grid enrichment (locally higher grid resolution, *h*-adaptive). Overset grids are used for actuated and immersed moving parts to provide more accurate and robust solutions in the next generation of KIVA. The scheme is particularly effective for complex domains, such as engines.

The *hp*-adaptive FEM becomes higher-order, more accurate, where required as prescribed by the adaptive procedures that is determined by the mathematical analysis of solution's error as the solution proceeds [2]. The *hp*-adaptive method employs hierarchical basis functions, constructed on the fly as determined by a stress-error measure [3]. In the following, we discuss the progress made during the last year on grid generation, dynamic LES, parallelization, comparison to the older KIVA system, and spray modeling.

## Grid Generation and Los Alamos National Laboratory's Local ALE FEM

The overset parts of the ALE system adjust the grid locally as the parts move through the fluid grid. The fluid grid is formed as a continuous grid without having to form the grid around the complex parts. This system maintains second order spatial accuracy while never allowing the grid to tangle [4]. Since the fluid is represented continuously, fluxing of material through the grid as it moves is not required. This need to flux through the grid is just one portion of the error when the usual ALE method is employed with finite volumes. Here the fluid solver remains Eulerian and the moving grid portions are no longer entwined with fluid solution. The local ALE method is robust; the grid will never tangle and the parts can move in any way desired through the cylinder's grid.

We are using GridPro tools for robust and automatic grid generation and collaborating with the GridPro team on the use for engine modeling for all KIVA versions. Figure 1 shows the use of GridPro for the FEM code using Los Alamos National Laboratory's local ALE method (the overset parts system). Figure 1a shows a simple cylinder with one port and the valve overlaid. Figure 1b shows the grid for Sandia's direct injection, spark ignition engine with spark plug, injection ports, and valve guides, waiting for the valves to be overlaid.

### **Dynamic LES**

A dynamic LES method has been completed for the predictor-corrector FEM scheme system that spans flow regimes from the laminar to highly turbulent flow

without needed special damping such wall functions. This dynamic LES is based on a scheme developed by Vreman [5]. The model removes assumptions about the laminar sublayer and allows modeling non-equilibrium turbulent flows. The method allows backscatter, a natural process that is inherent turbulent flow. The results for flow over a 3D cylinder are shown in Figure 2 at Reynolds numbers of 120,000 solved in parallel with KIVA-hpFE. Figure 2a shows the domain decomposition (number of processors or "# of PEs") and Figure 2b the vortex street downstream of the cylinder. In Figure 3 a snapshot in time of the unsteady solution is shown for  $Re = 120,000$  and the resulting average coefficient of pressure as compared data from Merrick and Bitsuamlak [6].

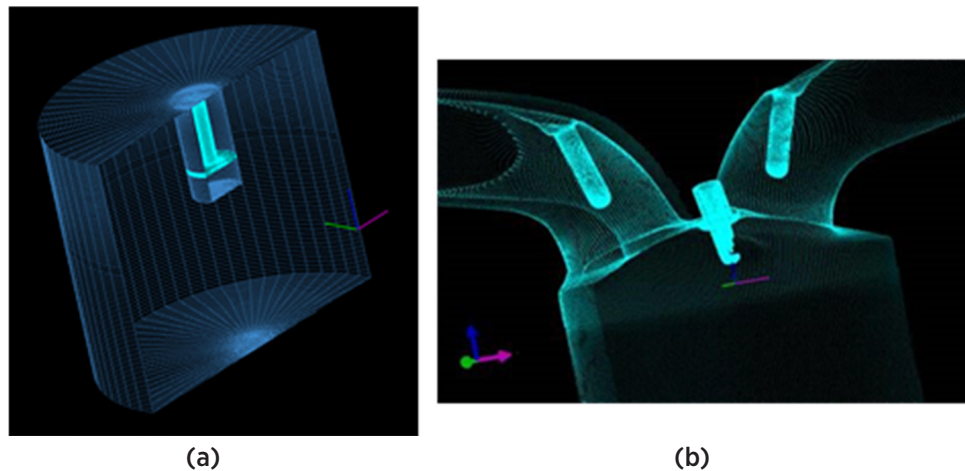


Figure 1. Engine parts to be overlaid onto the grid. (a) Valve overlaying the grid as constructed in GridPro and (b) Sandia's direct injection, spark ignition four-valve engine with spark and injection ports ready for overlaid parts.

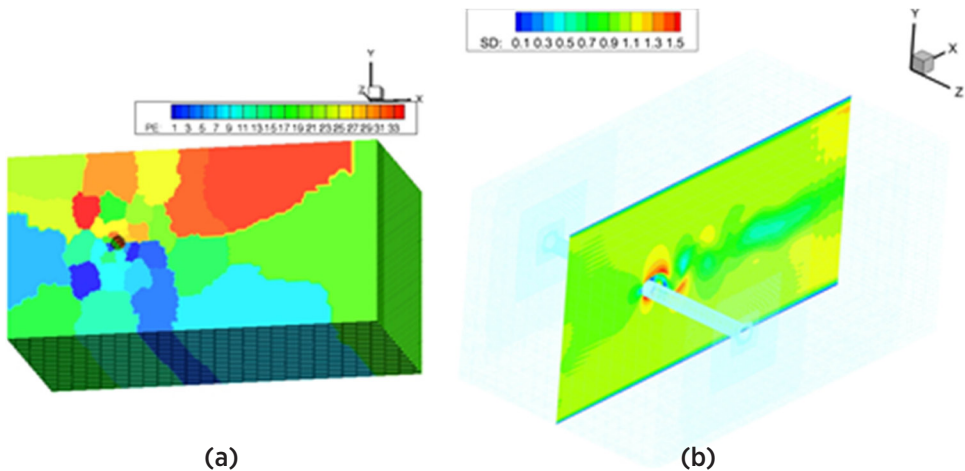


Figure 2. Subsonic flow over a cylinder at  $Re = 1,000$ . (a) 450,000 cells decomposed onto 36 processors and (b) vortex street of the fully developed flow.

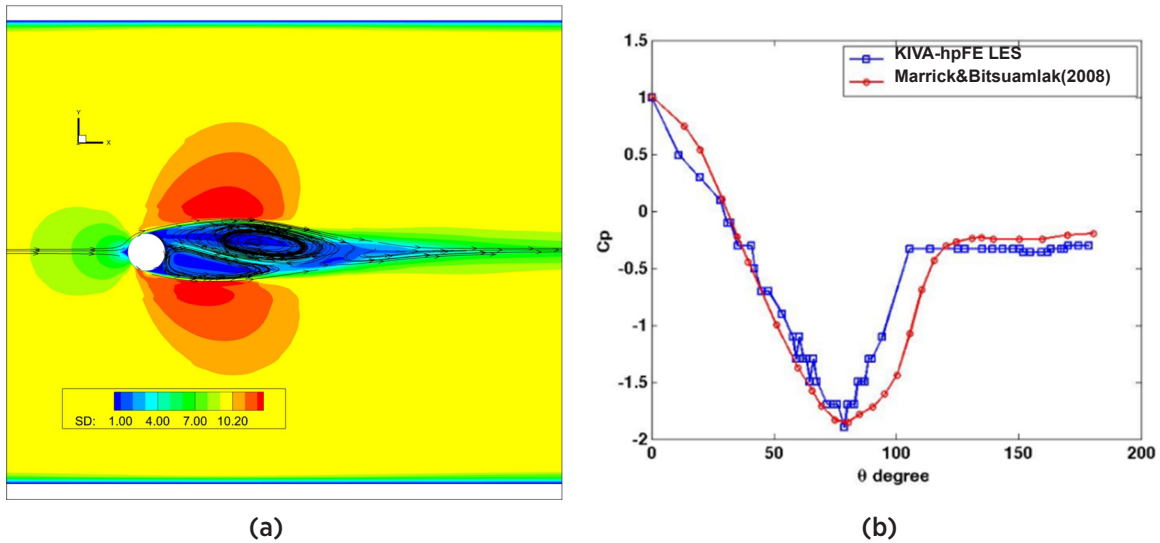


Figure 3. Subsonic flow over a cylinder at  $Re = 120,000$ . (a) Vortex street developing at and (b) average coefficient of pressure compared to data.

### Parallelization and New KIVA-hpFE Versus Older KIVA-4mpi

Determining how much headway we've made to date over our previous software called KIVA-4mpi we investigate a problem of flow over a cylinder. This test case uses the same grid resolution (the same grid), the same size time step, and solving in the same manner. Shown in Figure 4a is the simulation fluid motion elapsed time versus wall-clock. KIVA-hpFE is faster at every time step, shown by the diverging curves. For example, at 10 min of computational time, the new code is  $1.5 \times$  faster than the old KIVA-4mpi code. KIVA-hpFE is not only faster, but is more accurate given the same number of cells, and often requires far fewer cells for the same

accuracy as older KIVA codes (showed this behavior on numerous benchmark cases), without using the higher order approximations. Second order accuracy states little about the actual accuracy of a method, just revealing the convergence is with a slope of 2. A method can have error and be second order accurate; our new system is more accurate than previous versions when using the same number or fewer cells.

We have finished developing KIVA-hpFE parallel version using MPI to facilitate speed of solution of more fully resolved domains showing a  $30 \times$  speed-up over the serial system, as shown in Figure 4b. The speed-up is super-linear, meaning the speed-up for any particular problem

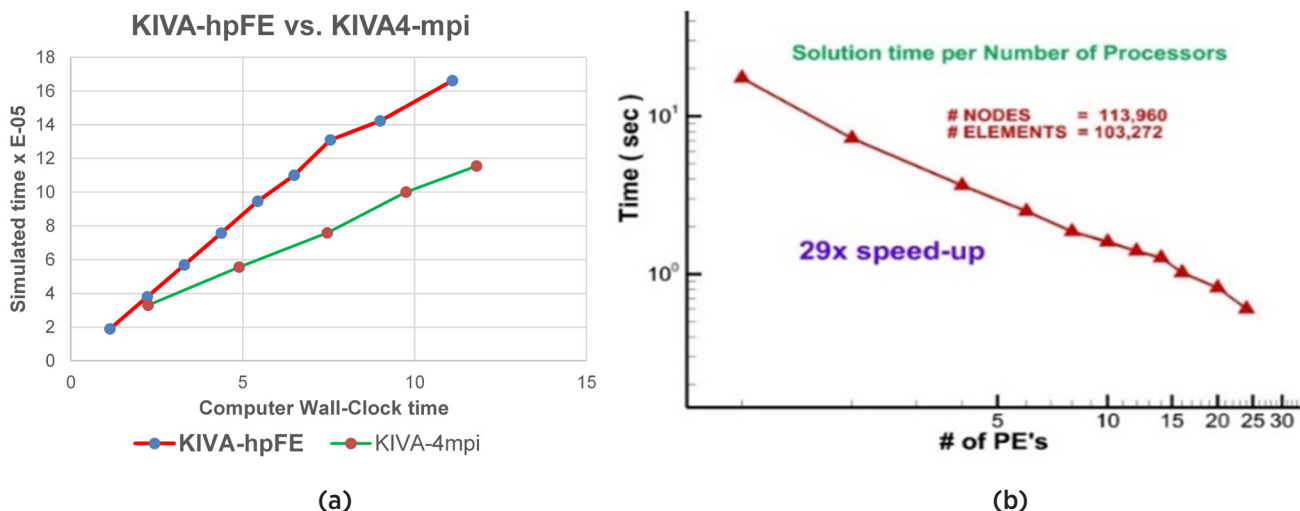


Figure 4. Solution speed for flow over cylinder benchmark problem, KIVA-hpFE vs. KIVA4-mpi

will continue to increase linearly provided the problem size (number degrees of freedom) increases. In addition, we developed an implicit solution system for diffusive and stress forces for an extra  $10\times$  speed-up per processor for an overall  $300\times$  speed-up over the serial version on some problems.

### Spray Modeling

Sprays can be described by a cloud of diffuse particles; tens of thousands of droplets of various sizes streaming through what is usually a gaseous media. These particle clouds proceed through numerous processes of agglomeration and break-up as they move through the conveying fluid (often air). The droplets experience interactions with this conveying media where stresses on the droplets force breakup and agglomeration. Droplet sizes changes occur when they breakup, agglomerate, and evaporate. Newton's Third Law allows for the evaluation of opposing forces acting on the conveying fluid.

Solution of the dispersed spray equation requires initial conditions for the droplets after it transforms from a continuously connected fluid. In jet atomization, liquid fuel is injected through a nozzle and forms a jet which breaks into very fine droplets. Understanding the effect of the geometry of the injector nozzle, the initial jet conditions, the fluid properties in the liquid film the break-up, and the resulting droplet sizes and distribution are of primary importance to improve fuel efficiency and lower gas emissions.

Supplying predictive initial conditions for the phase-space represented in the spray equation at the time the model spray equation is applicable would go a long way to having a predictive capability for sprays in combustion modeling. In addition, properly applying any dispersed droplet solution method requires determining the point in time where the jet breakup occurs. Phase-space information that is vital to solving the spray equation needs to include spatial position, velocities, sizes, and temperatures. To accomplish the task of predictively initiating the Lagrangian particle transport method we are developing a VOF method to track the evolving interface of fluid stream immersing from the injector, providing needed initial phase-space information and time of applicability for the spray equation to be employed. In the VOF method a single velocity field with a single pressure field formulation is used for solving the mass and momentum conservation equations on a fixed computational mesh. The interface is capture through a “color” function,  $C$ , and its kinematics is represented by the following evolution equation:

$$\frac{\partial C}{\partial t} + \nabla \cdot (C \bar{u}) = 0$$

The color function is the volume fraction (amount) of each fluid in a computational cell, and is intrinsically mass conserving and can automatically handle change in topology (break-up and coalescence) because of the nature of the evolution equation at the interface.

Coupling of a Lagrangian particle transport method with a volume tracking method or VOF concurrently in a single domain is not straightforward and requires new research. The first task is to derive transition criteria to identify if the fluids are “separated” or “dispersed.” An obvious criterion is based on the interface length scale relative to the mesh resolution. Can the mesh spacing resolve the interface structure? Is the interface characteristic length scale, such as droplet diameter, greater or smaller than the mesh spacing? To answer these questions, we propose to use interface curvature,  $\kappa$ , which is an interface characteristic length scale as our first criterion. The equation is as follows:

$$\kappa = -\nabla \cdot \bar{n} = -\nabla \cdot \left( \frac{\nabla C}{\|\nabla C\|} \right)$$

In Figure 5, we show the current progress of our initial break-up model of an injected jet of gasoline at 100 m/s. The liquid core is showing ligaments more clearly seen in Figure 5b by the density variations. Both curvature and stresses between the liquid and gas fluids are incorporated into the solution of the governing equations. The solution currently is being performed on a very coarse grid to expedite development purposes, reducing the accuracy of the VOF method. The h-adaptive mesh refinement scheme will be used in conjunction with VOF to precisely capture the liquid-air interface without requiring a priori information about the jet's behavior, thereby reducing the need for a highly refined grid everywhere to precisely capture the interface. Simulations of an engine injector are now being developed using this method. Once the initial break-up shows the liquid ligaments smaller than the cell size, we intend to transfer those small ligaments (large droplets), to the secondary break-up model and transport the drops with our standard Lagrangian particle transport model.

### Conclusions

In FY 2016, we continued advancing the accuracy, robustness, and range of applicability of internal combustion engine modeling algorithms and coding for engine simulation. We have performed the following to advance the state of the art.

- Finished developing an LES turbulence model that is capable of spanning transition to turbulence and hence fluid boundary layers

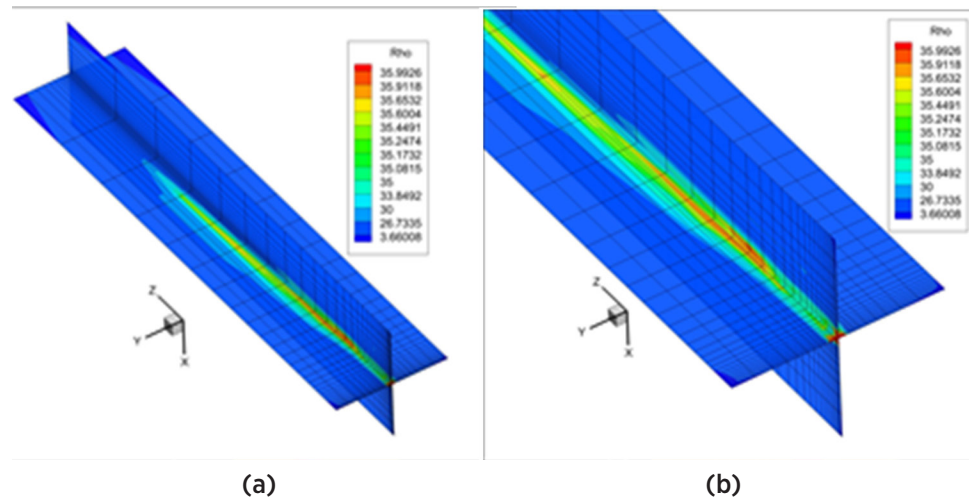


Figure 5. Multi-phase flow modeling of initial jet break-up. VOF system with stresses and curvature of liquid interface is calculated on a jet of density  $35 \text{ g/cm}^3$  into air at 1 atm. Inlet velocity is 100 m/s.

- Finished developing the KIVA-hpFE to be parallel using MPI to facilitate speed of solution of more fully resolved domains and parallel solution method for the moving parts, reactive chemistry, and sprays, showing a  $30\times$  speed-up over the serial system
- Developed implicit solution system for diffusive and stress forces for an extra  $10\times$  speed-up per processor for an overall  $300\times$  speed-up over the serial version
- Continued development of the 3D overset grid system, to quickly utilize the “stl” file type from the grid generator for quick and automatic overset parts surface generation and much easier creation of quality grids.
- Continued development of the *hp*-adaptive FEM methods; serial version completed
- Incorporating the VOF method in spray modeling for more predictive modeling capability on initial break-up
- Continued validation and verification adding capabilities for many benchmark problems

## References

1. Carrington, D.B., Wang, X. and Pepper, D.W. (2013), A predictor-corrector split projection method for turbulent reactive flow, *Journal of Computational Thermal Sciences*, Begell House Inc., vol 5, no. 4, pp. 333–352.
2. Carrington, D.B., (2011), A Fractional step *hp*-adaptive finite element method for turbulent reactive flow, Los Alamos National Laboratory Report, LA-UR-11-00466.

3. Wang, X., Carrington, D.B., Pepper, D.W. (2009), An adaptive FEM model for unsteady turbulent convective flow over a backward-facing step, *Journal of Computational Thermal Sciences*, vol 1, no. 2, Begell House Inc., pp. 121–135.
4. Carrington, D.B., Munzo, D.A., Heinrich, J.C. (2014), “A local ALE for flow calculations in physical domains containing moving interfaces,” *Progress in Computational Fluid Dynamics, an Int. Jour.* vol 14, no, 3, pp. 139–150.
5. Waters, J., Carrington, D.B., (2016), “A parallel Large Eddy Simulation in a finite element projection method for all flow regimes,” *Numerical Heat Transfer Part A-Applications*, vol.70 (2), pp.117–131.
6. Merrick, R., and Bitsuamlak, G., (2008), “Control of flow around a circular cylinder by the use of surface roughness: A computational and experimental approach.” Internet publication at [http://www.ihrc.fiu.edu/wpcontent/uploads/2014/03/MerrickandBitsuamlak\\_FlowAroundCircularCylinders.pdf](http://www.ihrc.fiu.edu/wpcontent/uploads/2014/03/MerrickandBitsuamlak_FlowAroundCircularCylinders.pdf)

## FY 2016 Publications/Presentations

1. Waters J., Carrington, D.B., Pepper, D.W. (2016), “An Adaptive Finite Element Method with Dynamic LES for Turbulent Reactive Flows,” *Journal of Computational Thermal Sciences*, Begell House Inc., vol. 8, no. 1, pp. 57–71.
2. V.D. Hatamipour, David B. Carrington, Juan C. Heinrich (to appear), “Accuracy and Convergence of Arbitrary Lagrangian-Eulerian Finite Element

Simulations based on a Fixed Mesh," Progress in Computational Fluid Dynamics, An International Journal.

3. Carrington. D.B., Mazumder, M., Heinrich, J.C., (to appear), "Three-Dimensional Local ALE-FEM Method for Fluid Flow in Domains Containing Moving Boundaries/Objects Interfaces," Progress in Computational Fluid Dynamics, An International Journal.
4. Waters, J., Carrington, D.B., (2016), "A parallel Large Eddy Simulation in a finite element projection method for all flow regimes," Numerical Heat Transfer Part A-Applications, vol.70 (2), pp.117–131.
5. J. Waters, D.B. Carrington (2016), "Modeling Turbulent Reactive Flow in Internal Combustion Engines with an LES in a semi-implicit/explicit Finite Element Projection Method," Procs. of the ASME 2016 Internal Combustion Engine Fall Tech. Conf., ICEF2016, October 9–12, 2016, Greenville, SC, USA.
6. J. Waters, D.B. Carrington, D.W. Pepper (2015), "Application of a dynamic LES model with an H-adaptive FEM for fluid and thermal processes," Procs. of 1st Thermal and Fluid Engineering Summer Conference - TFESC, 2015-08-09/2015-08-12, NY, United States.
7. J. Waters, D.B. Carrington, D.W. Pepper (2015), "Parallel Large Eddy Simulation for Turbulent Reactive Flow Modeling," Procs. of the Int. Conf. Computational & Experimental Engr. & Sci. (ICCES'15), Reno, NV.
8. J. Waters, D.B. Carrington, D.W. Pepper (2015), "An Adaptive Finite Element Technique with Dynamic LES for Incompressible and Compressible Flows," Procs. of the 15th Computational Heat Transfer Conference, CHT-15, Piscataway, New Jersey.

## II.14 Accelerating Predictive Simulation of Internal Combustion Engines with High Performance Computing

### Overall Objectives

- Develop and apply innovative strategies that maximize the benefit of high performance computing (HPC) resources and predictive simulation to support accelerated design and development of advanced engines to meet future fuel economy and emissions goals

### Fiscal Year (FY) 2016 Objectives

- Transition cyclic variability efforts to simulation of a light-duty, gasoline direct injection (GDI) engine for better synergy with experimental efforts at ORNL
- Evaluate impact of increased chemistry detail on accuracy of emissions predictions and computational time of engine simulations across the full speed-load range

### FY 2016 Accomplishments

- Developed and validated computational fluid dynamics (CFD) model of light-duty GDI engine
- Studied the impact of increasingly detailed chemistry on emissions predictions ■

### Introduction

This project supports rapid advancements in engine design, optimization, and control required to meet increasingly stringent fuel economy and emissions regulations through the development of advanced simulation tools and novel techniques to best utilize HPC resources such as ORNL's Titan. This effort couples ORNL's experimental and modeling expertise for engine and emissions control technologies with DOE's ASCR leadership HPC resources and fundamental research tools. Specific efforts evolve to support the needs of industry and DOE. Efforts during FY 2016 focused on two subtasks.

- Subtask 1: Use of highly parallelized engine simulations to understand the stochastic and deterministic processes which drive cyclic variability in highly dilute combustion systems.
- Subtask 2: Evaluate the potential of detailed chemical kinetic mechanisms to improve accuracy of emissions predictions across the full speed-load range of an

**K. Dean Edwards (Primary Contact),  
Charles E.A. Finney, Wael R. Elwasif,  
Robert M. Wagner**

Oak Ridge National Laboratory (ORNL)

National Transportation Research Center

2360 Cherahala Blvd.

Knoxville, TN 37932

Phone: (865) 946-1213

Email: edwardskd@ornl.gov

DOE Technology Development Manager:

Leo Breton

engine. Collaborative effort with General Motors (GM), Lawrence Livermore National Laboratory (LLNL), and Convergent Science. Supported by an ALCC award for 8,000,000 h on Titan.

### Approach

The aim of this project is to develop and apply innovative approaches which use HPC resources for high fidelity simulation of engine systems to address specific issues of interest to industry and DOE. The specific approaches applied for the current efforts are described below.

#### Subtask 1

Dilute combustion provides a potential pathway to simultaneous improvement of engine efficiency and emissions. However, at sufficiently high dilution levels, flame propagation becomes unstable, and small changes in initial cylinder conditions can produce complex cycle-to-cycle combustion variability, forcing the adoption of wide safety margins and failure to achieve the full potential benefits of charge dilution. The use of computational simulations to understand the physics and chemistry behind the combustion stability limit has the potential to facilitate control of the instabilities allowing operation at the "edge of stability." A major challenge is that many of the associated dynamical features are very subtle and/or infrequent, requiring simulation of hundreds or thousands of sequential engine cycles in order to observe the important unstable events with any statistical significance. Complex CFD simulations can require days of computational time for a single engine cycle making

serial simulation of thousands of cycles time-prohibitive. Our approach to address these computational challenges uses uncertainty quantification and sparse-grid sampling of the parameter space to replace simulation of many successive engine cycles with parallel ensembles of single-cycle simulations which exhibit statistically similar behavior. Results from these simulations are then used to generate lower order metamodels which retain the key dynamic features of the complex model but computationally are simple enough to allow simulation of serial combustion events and detailed studies of the parameters that promote combustion instability.

### Subtask 2

Virtual design and calibration has the potential to significantly accelerate development of advanced engine designs by using results from engine simulations to focus the scope of physical experiments. This approach has the potential to both accelerate and expand evaluation of concept engines across the design and operational space. Among the barriers to widespread application of virtual design are the accuracy and speed of CFD and chemical reaction simulations. GM, ORNL, and LLNL are partnering to evaluate the potential to improve the accuracy of emissions predictions by increasing the level of chemistry detail included in CFD simulations through inclusion of additional surrogate species in the fuel mixture and additional species and reactions in the kinetic mechanism. Because simulation accuracy can vary across the operating range as shown in Figure 1, parallel ensembles of simulations on Titan are used to cover the full speed–load range of the engine. The graphics processing unit-enabled Zero-RK chemistry solvers developed by LLNL are used to reduce the impact of the larger chemistry sets on computational time.

### Results

For Subtask 1, efforts focused on transitioning simulation tasks to a light-duty GDI engine to provide better coordination of simulation and experimental studies of cyclic variability at ORNL. The eventual goal will be to evaluate the use of metamodels developed by the simulation task in model-based control strategies on the experimental setup to reduce cyclic variability and extend dilute operating conditions. During this FY, an X-ray computed tomography scan of the engine head and laser scans of the piston and valves were used to generate a geometry model for CFD simulations in CONVERGE (see Figure 2). Experimental data for motored and fired operation with varying levels of exhaust gas recirculation (EGR) were used to tune the CFD model (Figure 3). With validation complete, ongoing simulation efforts with the model are evaluating the impact of EGR on combustion

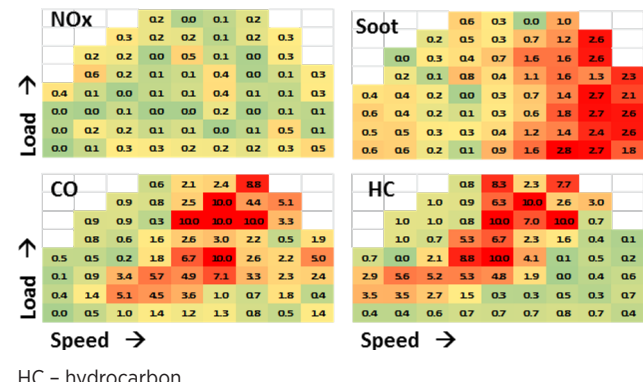


Figure 1. Variation across the speed-load range in error between steady-state experimental emissions measurements and simulation predictions using multi-zone chemistry with skeletal n-heptane mechanism

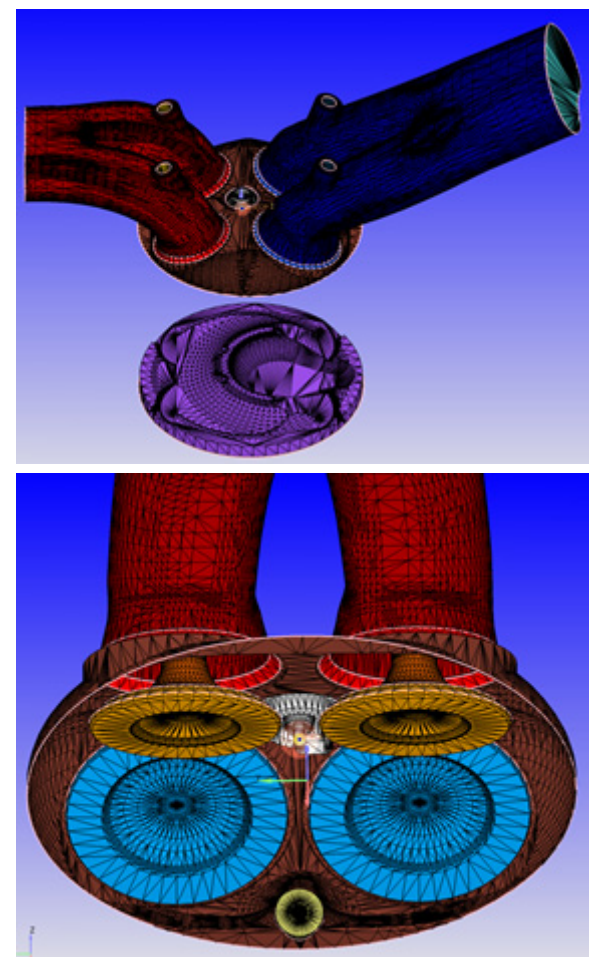
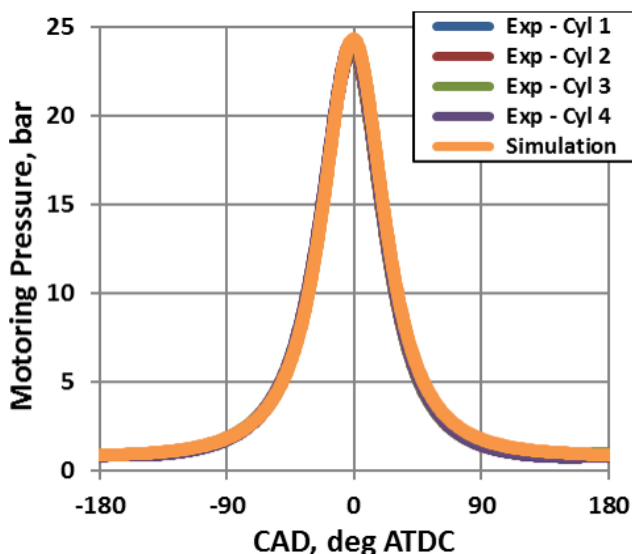


Figure 2. CONVERGE geometry model for the light-duty GDI engine



CAD - crank angle degrees; ATDC - after top dead center

Figure 3. Comparison of simulated and experimental motoring traces for the light-duty GDI engine

performance and investigating how short- and long-term perturbations in EGR contribute to cyclic variability.

For Subtask 2, efforts were focused on performing a series of ensemble diesel engine simulations covering the full engine speed-load range with increasing chemistry detail and mesh refinement. These simulations are being performed on Titan with CONVERGE using a closed-cycle, diesel sector model provided by GM with

approximately 50,000 cells. Experimental data provided by GM are being used to evaluate the accuracy of the emissions predictions from the simulations.

Table 1 provides a summary of the chemistry and solver details for the simulation cases. Three simulation sets using n-heptane as a single-component diesel surrogate and a multi-zone solver with skeletal and reduced n-heptane kinetic mechanisms have been completed. Initial results from these cases have shown only a marginal improvement in emissions accuracy with the reduced mechanism and a refined mesh over the baseline case using the skeletal n-heptane mechanism. The remaining simulation sets using a multi-component diesel surrogate and every-cell chemistry solvers with reduced and fully detailed kinetic mechanisms are underway on Titan with efforts continuing into FY 2017.

## Conclusions

Increasingly stringent fuel economy and emissions regulations are driving interest in utilizing HPC resources to accelerate advancements in engine design leading to collaborative efforts with industry stakeholders in several important areas. Transitioning the cyclic variability effort to simulate the light-duty GDI engine platform is expected to strengthen coordination between simulation and experimental cyclic variability studies at ORNL leading to increased progress toward understanding the key contributors to cyclic variability and development of model-based control strategies to extend dilute operation. The simulations with multi-component fuel surrogates

**Table 1. Summary of Chemistry Details and Mesh Refinement Used in the Six Study Cases Exploring Impact on Accuracy of Emissions Predictions**

Kinetic Mechanism		Chemistry Solver	Mesh	Status
Skeletal n-heptane	47 species 74 reactions	Multi-zone SAGE	Base	Complete
Reduced n-heptane	144 species 900 reactions	Multi-zone ZeroRK+GPU	Base	Complete
Reduced n-heptane	144 species 900 reactions	Multi-zone ZeroRK+GPU	Refined	Complete
Reduced n-heptane with detailed soot	144 species 900 reactions	Every Cell SAGE	Refined	In Progress
Reduced multi-component	766 species 6787 reactions	Every Cell ZeroRK+GPU	Refined	In Progress
Detailed multi-component	5155 species 31,058 reactions	Every Cell ZeroRK+GPU	Refined	In Progress

and fully detailed chemistry across the full speed-load range of the engine are some of the largest-scale engine simulations ever performed. The results of this study will help to assess whether highly detailed chemistry is needed to produce accurate emissions predictions or whether other factors are contributing to the errors.

## FY 2016 Publications/Presentations

1. C.E.A. Finney, K.D. Edwards, M.K. Stoyanov, R.M. Wagner (2015). *Application of high performance computing for studying cyclic variability in dilute internal combustion engines*. **ASME ICEF2015-1172**.
2. R.S. Jupudi, C.E.A. Finney, R.J. Primus, S.D. Wijeyakulasuriya, A.E. Klingbeil, B. Tamma, M.K. Stoyanov (2015). *Application of High Performance Computing for Simulating Cycle-to-Cycle Variation in Dual-Fuel Combustion Engines*. **SAE 2016-01-0798**.
3. K.D. Edwards, C.E.A. Finney, W.R. Elwasif, M.K. Stoyanov, R.M. Wagner (2016). *Accelerating predictive simulation of IC engines with high-performance computing (ACE017)*. **2016 DOE Vehicle Technologies Office Annual Merit Review**.
4. R.O. Grover Jr., R. Diwakar, J. Gao, V. Gopalakrishnan, W.R. Elwasif, C.E.A. Finney, K.D. Edwards, R. Whitesides (2016). *Steady state calibration for diesel engines using general purpose GPU-enabled CFD tools*. **2016 OLCF Users Meeting**.
5. C.E.A. Finney, K.D. Edwards, W.R. Elwasif, M.K. Stoyanov, S. Simunovic, G. Muralidharan, J.A. Haynes (2016). *A review of CONVERGE-based simulations at ORNL & Conjugate Heat Transfer simulations of a heavy-duty engine*. **2016 CONVERGE User Conference**.

## Special Recognitions and Awards/ Patents Issued

1. GM, ORNL, and LLNL received an ALCC award for 16,000,000 h on Titan to support simulation of partial fuel stratification strategies in FY 2017.
2. General Electric, Argonne National Laboratory, and ORNL received an ALCC award of 25,000,000 h on Mira to support simulation of cyclic variability in dual-fuel engines in FY 2017.
3. GM and ORNL received Best Poster award at the 2016 Oak Ridge Leadership Computing Facility (OLCF) Users Meeting.

## II.15 Use of Low Cetane Fuel to Enable Low Temperature Combustion

### Overall Objectives

- Optimize the operating conditions with low cetane fuel to achieve clean, high-efficiency engine operation
- Demonstrate the use of low temperature combustion (LTC) as an enabling technology for high-efficiency vehicles

### Fiscal Year (FY) 2016 Objectives

- Evaluate effect of low pressure exhaust gas recirculation (LP-EGR) upon autoignition and engine performance characteristics
- Quantitatively study effect of injection strategy upon autoignition to develop approach for transient operation and reduced fuel sensitivity
- Perform factorial experiments to quantify the effect of important input parameters upon engine performance, noise, and emissions

### FY 2016 Accomplishments

- Determine nozzle inclusion angle effects upon high load combustion noise, particulate matter (PM), and NO<sub>x</sub> (120° works well at high load)
- Determine injection strategy requirements to enable transient operation (time-based injections work well)
- Quantify boost sensitivity of E10 (10% ethanol, 90% gasoline mixture) (less than E0 but only marginally less sensitive)
- Continue to develop strategy for gasoline compression ignition (GCI) operation for entire speed and load range on E10 (integrate LP-EGR, boost, and injection strategy); parametric study has been done for low and intermediate loads ■

### Introduction

Current diesel engines already take advantage of the most important factors for efficiency: no throttling, high compression ratio, and low heat rejection. However, diesel combustion creates a significant emissions problem. Mixing or diffusion combustion results in very steep pressure gradients in the combustion chamber because the ignition delay of diesel fuel is extremely short. High

### Stephen A. Ciatti

Argonne National Laboratory  
9700 S. Cass Ave.  
Bldg. 362  
Argonne, IL 60439  
Phone: (630) 252-5635  
Email: sciatti@anl.gov

DOE Technology Development Manager:  
Leo Breton

PM and NO<sub>x</sub> are the results of this type of combustion, requiring expensive aftertreatment solutions to meet Environmental Protection Agency emissions regulations.

The current work seeks to overcome the mixing controlled combustion dilemma by taking advantage of the long ignition delay of gasoline to provide much more premixing of fuel and air before ignition occurs. This premixing allows for the gradients of fuel and air to be much less steep, drastically reducing the PM–NO<sub>x</sub> tradeoff relationship of typical mixing controlled combustion.

### Approach

The intent of this project is to utilize the long ignition delays of low cetane fuels to create an advanced combustion system that generates premixed (but not homogeneous) mixtures of fuel and air in the combustion chamber. As reported in several articles, if the local equivalence ratio is below 2 (meaning at most, twice as much fuel as oxidizer) and the peak combustion temperature is below 2,000 K (using EGR to drop the oxygen concentration below ambient 21%, thereby slowing the peak reaction rates and dropping the peak combustion temperature), a combustion regime that is very clean and yet retains reasonably high power density is achieved.

The challenge to this type of combustion system is the metering of fuel into the combustion chamber needs to be precise, both in timing and amount. If too much fuel is added too early, a very loud, ringing type of combustion occurs, which creates unacceptably high combustion noise or worse. If not enough fuel is added,

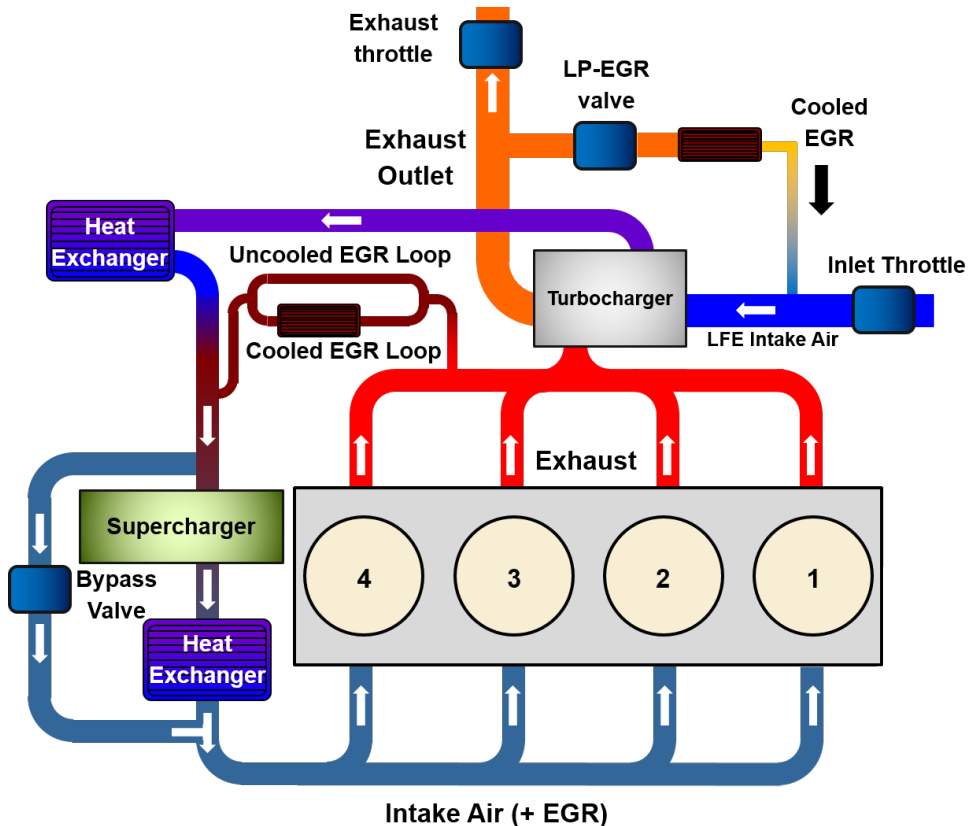
ignition may not occur at all and high raw hydrocarbon (HC) appears in the exhaust gas. Controlling over the relevant operating parameters is very important – fuel properties, injection strategy, dilution level, compression ratio, and intake temperature all have large influence upon ignition propensity, combustion phasing and the emission (i.e., soot and  $\text{NO}_x$ ). Design of experiments tests were performed to determine the most influential factors that influence GCI performance, efficiency, and emissions.

LP-EGR capability was recently installed in the test cell (see Figure 1) to minimize the volumetric efficiency losses associated with high-pressure EGR. LP-EGR allows for the simultaneous increase of boost pressure and EGR levels instead of a tradeoff between them. In this manner, boost and EGR could be studied as independent variables rather than dependent because both could be increased and decreased independently of one another. Combining with proper injection strategy, initial results have shown low emission and soot production with approximately 30% EGR to achieve low and intermediate loads.

## Results

An investigation into the effect of injection timing, boost pressure, injection pressure, and lambda ( $\lambda$ ) on LTC was done in this study using a light-duty 1.9 L diesel engine. A design of experiment was set up to investigate these effects at low and high engine speed. A double injection strategy was used at 2,000 rpm in order to operate the engine within the tolerable limits of noise level and combustion stability. Example of results is shown in Figure 2.

The design of experiment analysis showed that boost and lambda have the strongest impact on ignition, combustion phasing, combustion stability, and emissions. The fuel injection pressure (400 bar vs. 600 bar) was found to be less significant at both engine speeds. Early SOI or shorter dwell time (“quasi homogeneous charge compression ignition”) results in shorter start of combustion (CA10) but delayed end of combustion (CA90) when compared to late start of injection or longer dwell time (GCI operation). Specific fuel consumption and combustion stability were negatively impacted by increasing lambda.



LFE – Laminar Flow Element

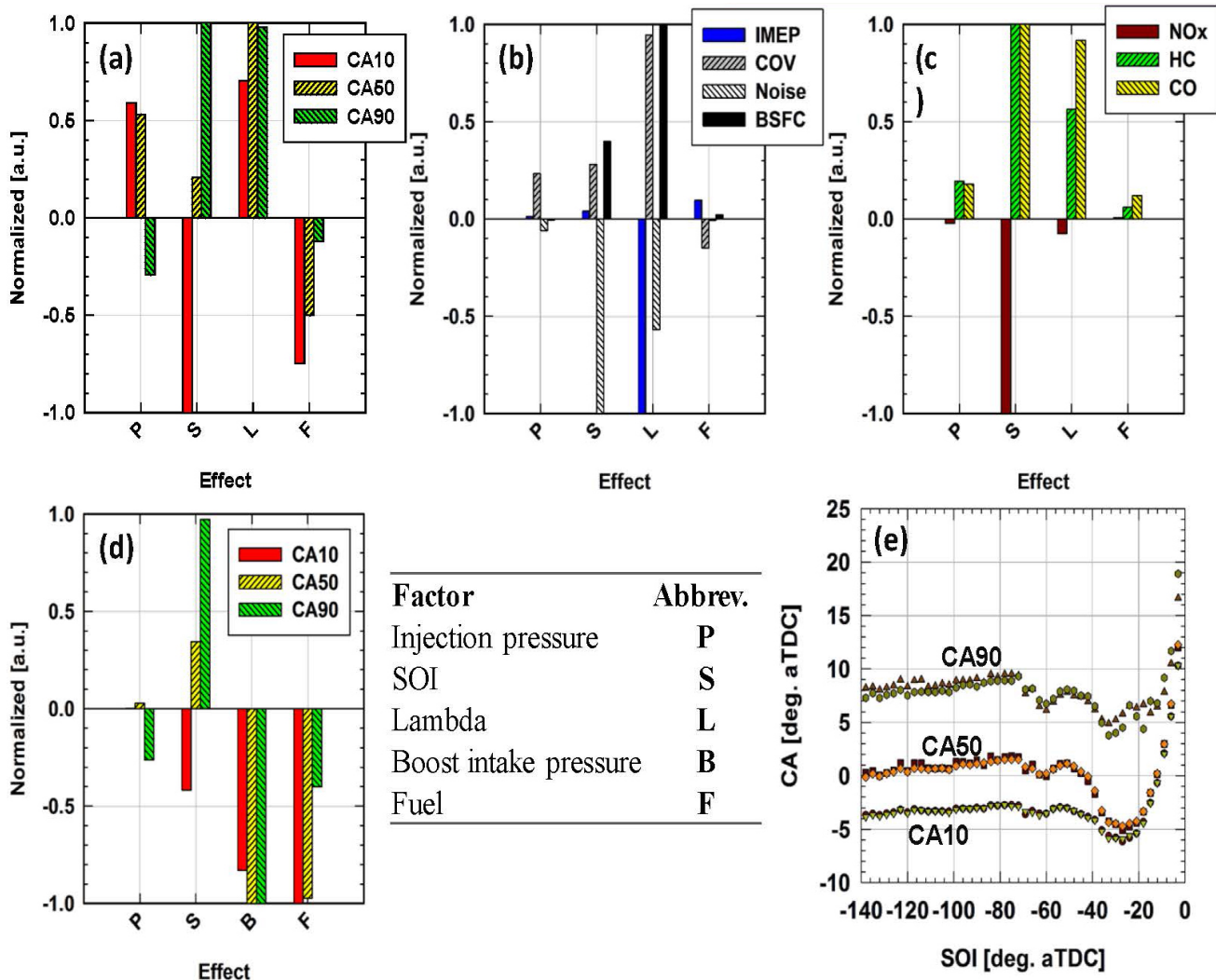
Figure 1. Schematic of engine setup

HC and CO were highest in homogeneous charge compression ignition mode while  $\text{NO}_x$  was lowest. This trend was switched when operating in GCI mode.

An SOI sweep was done for both fuels (different reactivity) under constant lambda. The start of combustion (CA10) at each SOI was matched effectively by adjusting the intake pressure. Smoke number was less than 0.1 for all the testing conditions as mixture was maintained relatively lean.

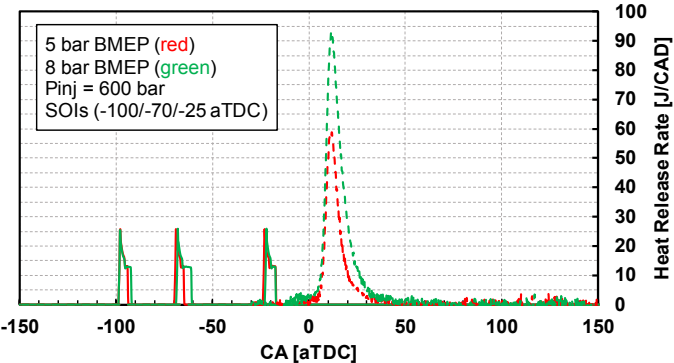
Some preliminary results using LP-EGR has shown very low emission and soot production using up to 30% EGR.

The injection strategy, engine performance, and emissions are shown in Figure 3. Low and intermediate load were achieved with emission target. The remaining challenge is to reduce noise and improve fuel consumption. Noise problem can be solved by adjusting the injection timing (late SOI tends to retard combustion phasing) with benefits of high injection system (avoid fuel rich condition that favors smoke generation). Detailed efficiency (combustion, gas exchange, thermodynamic, mechanical) will be performed to identify energy loss that results in high fuel consumption.



SOI – start of injection; aTDC – after top dead center; CA – crank angle; IMEP – indicated mean effective pressure; COV – cooefficnt of variance; BSFC – brake specific fuel consumption

Figure 2. Effects of injection pressure, fuel stratification, boost and fuel reactivity upon engine performance. (a, b, c) Outputs with constant boost study; (d) effect of boost during constant lambda study; (e) effectiveness of boost to control fuel reactivity during SOI sweep at constant lambda.



EGR	Intake T	T_exh	BMEP	BSFC	Noise	NO <sub>x</sub>	HC	CO	FSN
[%]	[deg. C]	[deg C]	[bar]	[g/kw-hr]	[dB]	[g/kW-hr]	[g/kW-hr]	[g/kW-hr]	[a.u.]
29.41	53.64	309.5	4.32	346.13	90.13	0.45	0.91	2.10	0.030
29.84	45.56	316.9	4.91	312.04	93.90	0.42	1.16	3.20	0.017
29.43	47.11	327.5	5.16	317.10	91.58	0.33	0.57	1.34	0.020
30.50	47.58	419.9	8.27	280.25	93.88	0.04	0.37	1.27	0.027
30.48	47.91	412.2	8.33	278.78	91.01	0.05	0.37	1.44	0.024

BMEP – brake mean effective pressure;  $P_{inj}$  – injection pressure; CAD – crank angle degree; FSN – Filter Smoke Number

Figure 3. (top) Injection strategy and heat release rate for 5 bar and 8 bar BMEP; (bottom) summary of engine performance and emission with influence of LP-EGR

## Conclusions

- Boost has the most substantial influence upon start of combustion and combustion phasing, even more than injection pressure or injection strategy, for E10 fuel (Figure 2).
- However, injection strategy and injection pressure have significant influence over efficiency, emissions production, and combustion noise (Figure 2).
- Based upon the FY 2015 results, EGR and boost needed to be investigated independently. An LP-EGR system was installed to provide this opportunity (Figure 1).
- LP-EGR provides a significant influence in reducing NO<sub>x</sub> emissions and retaining high combustion stability by retaining boost (Figure 3).
- LP-EGR causes a slight efficiency penalty due to reduced volumetric efficiency.

## FY 2016 Publications/Presentations

1. Cung, K., Rockstroh, T., Ciatti, S.A., Goldsborough, S., Cannella, W., (October 2016) ASME ICEF 2016-9395, "Parametric study of Ignition and Combustion Characteristics from a Gasoline Compression Ignition Engine Using Two Different Reactivity Fuels," ASME Fall Technical Conference, Greenville, SC.
2. Kodavasal, J., Pei, Y., Harms, K., Ciatti, S.A., Wagner, A., Sencal, P.K., Garcia, M., Som, S., (April 2016) SAE 2016-01-0602, "Global Sensitivity Analysis of a Gasoline Compression Ignition Engine Simulation with Multiple Targets on an IBM Blue Gene/Q Supercomputer," SAE World Congress, Detroit, MI.
3. Invited speaker for THIESEL 2016, Valencia, Spain (September 2016).
4. Invited speaker for IEA Task Leaders Meeting on Advanced Combustion, Ruka, Finland (June 2016).

## II.16 High Efficiency GDI Engine Research

### Overall Objectives

- Quantify efficiency potential and combustion stability limitations of advanced gasoline direct injection (GDI) engines operating under lean and exhaust gas recirculation (EGR) dilute conditions
- Extend lean and EGR dilution tolerance of light-duty GDI engines through the implementation of advanced ignition systems
- Develop a three-dimensional computational fluid dynamics (3D-CFD) methodology to analyze and predict cyclic variability in GDI engines using conventional as well as advanced ignition systems

### Fiscal Year (FY) 2016 Objectives

- Use advanced diagnostics to characterize ignition systems and provide experimental data for ignition model validation
- Evaluate impact of pulse characteristics and plug geometry of transient plasma ignition on dilution tolerance and benchmark compared to conventional and advanced ignition systems
- Develop and validate state-of-the-art ignition models against experimental data
- Evaluate dilution tolerance improvements for laser ignition systems by optimizing the location of the ignition point(s)

### FY 2016 Accomplishments

- X-ray diagnostics was successfully used to visualize the spark event and characterize the thermal properties of the ignition plasma quantitatively.
- Dilution tolerance was extended with nano-pulse delivery system from Transient Plasma Systems, Inc. (TPS) with increased pulse repetition rate with respect to conventional ignition and opportunities for future improvement were identified.
- Characteristics of the ignition discharge have been implemented in the ignition model and numerical results demonstrated that the expanded model is capable of describing the ignition behavior for conventional spark systems and capture the plasma thermal properties.

**Riccardo Scarcelli (Primary Contact),  
Thomas Wallner, Anqi Zhang,  
James Sevik, Michael Pamminger**

Argonne National Laboratory

9700 S. Cass Avenue

Lemont, IL 60439

Phone: (630) 252-6940

Email: rscarcelli@anl.gov

DOE Technology Development Manager:  
Leo Breton

- Numerical simulations showed stability and efficiency improvements by adjusting the laser focal length and protruding the ignition point further in the combustion chamber. ■

### Introduction

Due to the United States' heavy reliance on gasoline engines for automotive transportation, efficiency improvements of advanced gasoline combustion concepts have the potential to dramatically reduce foreign oil consumption. However, combustion strategies such as stratified, lean-burn, high EGR, and boosted operation present challenging conditions for conventional ignition systems thereby limiting the attainable benefits of these advanced combustion concepts. Compared to stoichiometric operation, dilute combustion exhibits increased cyclic variability which negatively affects combustion stability and thermal efficiency. This project is designed to identify and overcome the fundamental limitations of lean, boosted, and EGR dilute combustion through experimental research and development combined with advanced 3D-CFD simulation. The main goal is to extend the lean and dilute limits by combining fundamental analysis of cyclic variability and combustion stability with benefits offered by advanced ignition systems.

### Approach

The main thrust areas of this project are (1) expanding the fundamental understanding of characteristics and limitations of lean, boosted and EGR-dilute combustion; (2) performing a technology evaluation of advanced, non-coil-based ignition systems on a consistent state-of-the-art

automotive engine platform; and (3) developing robust modeling tools for the analysis of dilute combustion and development of advanced ignition systems. The project includes experimental, as well as simulation-focused components. Engine testing is carried out to highlight current performance and potential for future development of the next generation of ignition systems for automotive applications. 3D-CFD simulation is used to (1) investigate the fundamental interaction between the ignition source and the in-cylinder flow to reduce cyclic variability under dilute operation, and (2) develop ignition models to deliver realistic simulations of advanced non-coil-based ignition systems in internal combustion engine applications. Advanced X-ray based diagnostics were integrated with modeling and engine experiments to provide a more comprehensive understanding of the ignition process and experimental data for model validation.

## Results

### X-Ray Diagnostics Used to Characterize Thermal Properties of Ignition Plasmas

X-ray diagnostics have been performed for many years at the Advanced Photon Source facility at Argonne to investigate the properties of fuel sprays, and provide local quantitative measurements of the spray mass distribution that can be used for spray modeling validation. Expanding on those capabilities, X-ray radiography was applied to capture density changes in the spark plug gap region during conventional ignition processes. In Figure 1, a typical result provided by X-ray diagnostics, i.e. the two-dimensional distribution of the gas path-length (which can be related to the gas density) in the near-spark region is shown together with the spatial resolution of the X-ray measurement points.

This was defined as a stretch goal for FY 2016 and represented a tremendous achievement in the ignition diagnostics field. X-ray diagnostics have benefits compared to other diagnostics such as the capability of delivering precise quantitative measurements of the mass (or density) distribution within the fluid system of interest. Based on these promising proof-of-concept results, X-ray ignition characterization will be expanded to support model development for conventional and non-conventional ignition systems of interest.

### Dilution Tolerance Further Extended with Optimized Transient Plasma Ignition System

In FY 2015 it was shown that transient plasma ignition systems have the capability to extend both lean and EGR dilution tolerance with respect to conventional ignition, with benefits in terms of thermal efficiency. However the

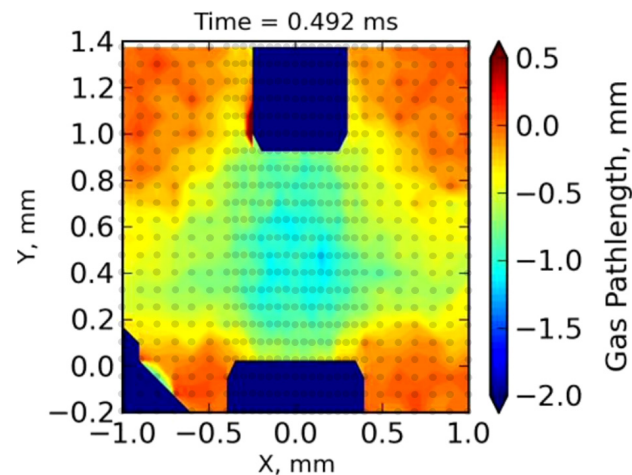


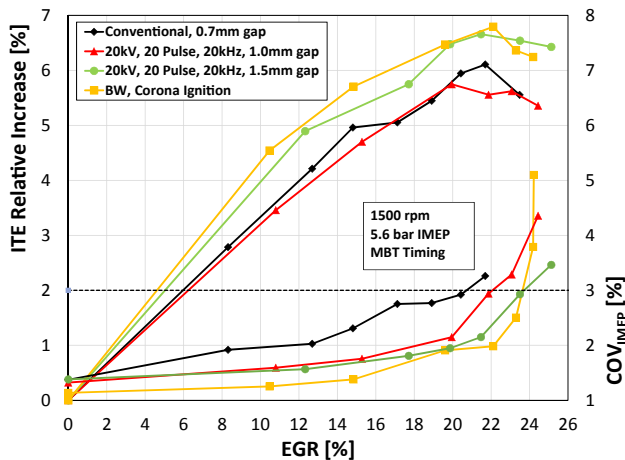
Figure 1. Quantitative evaluation of plasma thermal properties during the ignition process by using X-ray radiography

pulse generator had limited capabilities and only one plug geometry had been evaluated. Furthermore, feedback from industry indicated that benchmarking of alternative ignition systems should include conventional production systems as well as competing advanced technologies. An updated nano-pulse delivery system from TPS and a Corona ignition system from BorgWarner were tested under dilute operation and compared to conventional ignition technology. The TPS system was updated to increase the pulse repetition rate and several plug gap options were evaluated. However, the delivery voltage had to be limited to meet requirements for system compactness.

Figure 2 shows that both, the 20-pulse TPS system as well as the BorgWarner Corona system (labeled as BW) were able to surpass conventional ignition in terms of EGR dilution tolerance and thermal efficiency. The results also suggest further potential for improvement by optimizing the gap size of TPS plugs, which can be achieved by increasing the delivery voltage. Pulse repetition rate is another parameter of interest as it has shown the potential to further extend the EGR dilution tolerance. Results for lean operation were qualitatively similar to those for EGR dilution.

### Ignition model developed to capture physical trends and match experimental data quantitatively

A detailed energy deposition model was developed to take all the energy losses from the secondary circuit to the electrodes into account. This model relies on accurate rate of energy release, realistic shape of the spark channel, and conjugate heat transfer calculations. The ignition



IMEP – indicated mean effective pressure; MBT – maximum brake torque;  $COV_{IMEP}$  – coefficient of variation in indicated mean effective pressure; ITE – indicated thermal efficiency

Figure 2. TPS multi-pulse transient plasma ignition and BorgWarner Corona ignition surpassing conventional ignition in terms of dilution tolerance and thermal efficiency

model was tested against experimental data from an optical vessel at Michigan Technological University and was capable of capturing the experimental trend between successful and failed ignition (see Figure 3), where failed ignition is defined as an event where the flame kernel is formed but does not propagate due to the vessel conditions. In FY 2016 it was shown that the choice of the ignition model inputs is critical, indicating that inaccurate assumptions and non-realistic inputs lead to false prediction from the model with respect to the trends observed experimentally.

In FY 2016 the model development work continued by leveraging the experimental data provided by X-ray diagnostics. Refined assumptions were tested such as removing the assumption of uniform energy deposition and considering electrode voltage drops, and numerical results more closely resembled experimental data (see Figure 4). It is worth mentioning that the main goal of this ongoing effort is to capture the thermal properties of the plasma from a quantitative standpoint, and results shown in Figure 4 are encouraging. Future improvements are expected by adding additional physics to the chemistry of plasma in the numerical simulations.

### Effect of Ignition Location on Laser Performance Investigated Using CFD Simulations

In FY 2015 it was shown that merely replacing a conventional spark plug with laser ignition without optimization resulted in lower performance, especially

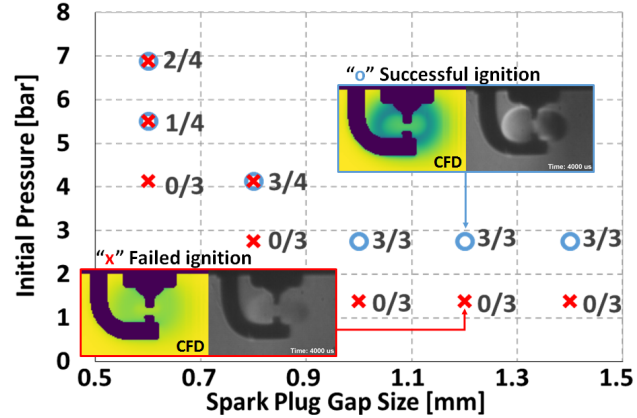


Figure 3. Detailed energy deposition model capturing experimentally observed trends (data from Michigan Technological University) of ignition success or failure

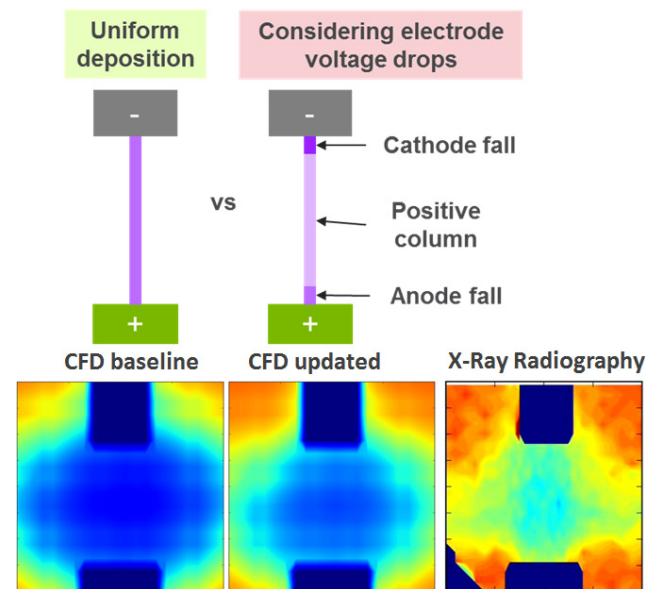
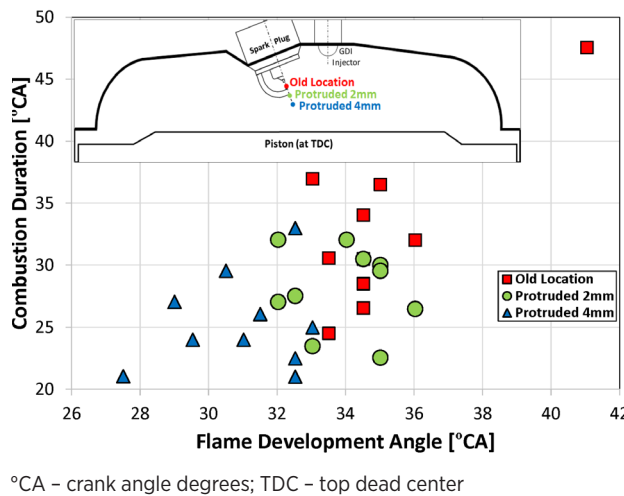


Figure 4. X-ray diagnostics used for ignition model refinement and validation

at part load and EGR dilute operation. While the ignition location of the baseline laser configuration was in close proximity to the center gap of the conventional spark system, it was also shown that the laser ignition location had significant impact on combustion.

Numerical simulations were performed in FY 2016 to show the effect of adjusting the focal length and protruding the location of the laser ignition in the combustion chamber. Figure 5 shows the effect of the laser ignition location on combustion metrics for 21% EGR dilute operation at 2,000 rpm and 6 bar IMEP. The maximum protrusion of the ignition point is limited



°CA – crank angle degrees; TDC – top dead center

Figure 5. Effect of laser focal length on combustion stability for highly dilute (EGR = 21%) operation

to approximately 4 mm to avoid piston local melting issues during the ignition process. Cyclic variability was assessed by simulating 10 consecutive cycles suggesting that combustion stability can be significantly improved by protruding the focal length about 4 mm in the combustion chamber.

## Conclusions

- X-ray diagnostics were successfully integrated with multi-dimensional modeling and engine experiments to broaden the basic understanding of the ignition process and deliver data for model development and validation.
- Non-conventional ignition systems including a near-production Corona as well as a transient plasma system showed improved performance compared to conventional ignition. Plug geometry and discharge mode were identified as areas for further improvement for transient plasma systems.
- Ignition modeling work continued to improve the model assumptions and the numerical results were successfully validated against experimental data generated using advanced diagnostics.
- Numerical simulations showed that it is possible to improve the performance of laser ignition technology by adjusting the focal length and optimizing the location of the ignition point.
- Future work will focus on improving the basic understanding of non-conventional ignition systems by leveraging advanced diagnostics and developing comprehensive modeling tools.

## FY 2015 Publications/Presentations

1. Scarcelli, R., Sevik, J., Wallner, T., Richards, K., Pomraning, E., Senecal, P.K., "Capturing Cyclic Variability in Exhaust Gas Recirculation Dilute Spark-Ignition Combustion Using Multicycle RANS," ASME. J. Eng. Gas Turbines Power. 2016; 138(11):112803-112803-8. doi:10.1115/1.4033184.
2. Sevik, J., Wallner, T., Pamminger, M., Scarcelli, R., Singleton, D., Sanders, J., "Extending Lean and Exhaust Gas Recirculation-Dilute Operating Limits of a Modern Gasoline Direct-Injection Engine Using a Low-Energy Transient Plasma Ignition System," ASME. J. Eng. Gas Turbines Power. 2016; 138(11):112807-112807-8. doi:10.1115/1.4033470.
3. Scarcelli, R., Wallner, T., Richards, K., Pomraning, E., Senecal, P.K., "A Detailed Analysis of the Cycle-To-Cycle Variations featured by RANS Engine Modeling," International Multidimensional Engine Modeling User's Group Meeting, Detroit, MI, USA, April 2016.
4. Scarcelli, R., Richards, K., Pomraning, E., Senecal, P. et al., "Cycle-to-Cycle Variations in Multi-Cycle Engine RANS Simulations," SAE Technical Paper 2016-01-0593, 2016, doi:10.4271/2016-01-0593.
5. Zhang, A., Scarcelli, R., Lee, S., Wallner, T. et al., "Numerical Investigation of Spark Ignition Events in Lean and Dilute Methane/Air Mixtures Using a Detailed Energy Deposition Model," SAE Technical Paper 2016-01-0609, 2016, doi:10.4271/2016-01-0609.
6. Scarcelli, R., "High Efficiency GDI Engine Research with Emphasis on Ignition Systems," DOE Annual Merit Review, ACE084, Washington D.C., June 8, 2016.
7. Zhang, A., "Numerical Investigation of Spark Ignition for Dilute Combustion through Detailed Characterization of the Energy Deposition Process," AEC Program Review Meeting, Southfield, MI, August 16, 2016.
8. Zhang, A., "Towards Predictive Ignition Simulation under Dilute/Lean Conditions through Detailed Understanding of the Energy Deposition Process," 2016 CONVERGE User Conference, Madison, WI, September 28, 2016.

## II.17 High Dilution Stoichiometric Gasoline Direct-Injection (GDI) Combustion Control Development

### Overall Objectives

- Address barriers to the Vehicle Technologies Office goal of improving light-duty vehicle fuel economy by developing control strategies that enable high-efficiency, high-dilution, gasoline direct-injection (GDI) engine operation
- Extend dilution limit to enable greater efficiency gains in modern GDI engines, leading to increased vehicle fuel economy

### Fiscal Year (FY) 2016 Objectives

- Develop control-oriented models that capture the dynamics of long-timescale combustion variations caused by exhaust gas recirculation as well as short-timescale variations from internal residuals
- Integrate models with symbol sequence analysis techniques to enhance predictive capabilities
- Further refine next-cycle control methodologies to mitigate long- and short-timescale combustion variations from charge dilution

### FY 2016 Accomplishments

- Developed low-order model that effectively simulates the dynamics of cyclic combustion variations for dilute engine operation
- Implemented model in online engine control system and evaluated differences in model performance between offline simulations and online next-cycle predictions
- Quantified sensitivity of engine operation to fueling changes at dilute conditions ■

### Introduction

Operation of spark ignition engines with high levels of charge dilution through exhaust gas recirculation (EGR) achieves significant efficiency gains while maintaining stoichiometric operation for compatibility with three-way catalysts. At high engine loads, efficiency gains of 10–15% are achievable with current technology. Dilution levels, however, are limited by cyclic variability—including significant numbers of misfires—that increases in frequency with dilution, especially at low engine loads typical of operation on standard light-duty drive cycles. The cyclic variability encountered at the dilution limit is

**Brian C. Kaul (Primary Contact),  
Gurneesh S. Jatana, Robert M. Wagner**

Fuels, Engines, and Emissions Research Center  
Oak Ridge National Laboratory (ORNL)  
2360 Cherahala Boulevard  
Knoxville, TN 37932  
Phone: (865) 946-1299  
Email: kaulbc@ornl.gov

DOE Technology Development Manager:  
Leo Breton

not random, but has been shown to be influenced by the events of prior engine cycles. This determinism offers an opportunity for dilution limit extension through active engine control, thus enabling significant efficiency gains by extending practically achievable dilution levels to the edge of combustion stability.

This project is focused on gaining and utilizing knowledge of the recurring patterns that occur in cyclic variability, in order to improve the fundamental understanding of causes of cyclic variability, which will enable prediction and control of cyclic variations that reduce engine efficiency at the dilution limit. In particular, the dynamics of systems using cooled EGR loops have been elucidated for the first time, and are somewhat different from those of lean combustion systems for which similar background work has been carried out in the past. This knowledge will be utilized to develop and implement next-cycle active control strategies for extending the dilution limit.

### Approach

The cyclic variability that limits dilution levels in spark-ignition engines is evaluated using data analysis tools that have been developed at ORNL based on nonlinear dynamics and chaos theory. These tools give insight into the deterministic features of cycle-to-cycle variations and improve fundamental understanding of the causes of cyclic dispersion. This will inform the development of models to better explain and predict next-cycle behavior, and enable control strategies to stabilize engine operation at the dilution limit. Low-order models based on nonlinear dynamics are presently being evaluated

for their suitability in online prediction and control, and more advanced models developed in an ORNL high-performance computing simulations project [1] will be applied once they become available.

A modern, turbocharged 2.0 L GDI engine, modified with a higher than stock compression ratio and an external cooled EGR loop, as illustrated in Figure 1, has been installed in an engine test facility at ORNL. An open, LabVIEW-based engine controller with next-cycle control capabilities is used to operate the engine and evaluate model prediction and control strategies. Experimental data from this platform is also used to aid the validation and development of the high-performance computing models that will inform future efforts.

## Results

Prior efforts at predicting next-cycle engine events have primarily focused on an approach based on symbol sequence analysis. This approach was shown to be robust in the presence of noisy, imperfect data, but provided only low-fidelity predictions, such that it's difficult to determine the appropriate control action to stabilize the system. A model-based approach that can provide more detailed information in addition to the directional trends indicated by symbol sequence analysis was determined to be warranted. To this end, an existing low-order model

previously developed by Daw, et al. [2] that simulates the dynamics of cyclic variability for lean combustion was adapted to account for EGR dilution as well. This model determines a combustion efficiency dependent on the composition of each cycle, and carries residual gas composition forward to impact the starting condition of the next cycle. Gaussian noise on the input parameters simulates the stochastic effects of mixing, turbulence, etc. As can be seen in the similarity of the shape of the return maps in Figure 2, the dynamics of this model are very similar to those observed in experimental engine data. In order to evaluate its effectiveness at predicting next-cycle variations, this model was implemented online in the engine control system, with measured data instead of simulated inputs, including use of the cumulative heat release results from the prior cycle to determine the combustion efficiency and thus the estimated residual gas composition for the upcoming cycle.

As shown in Figure 3, while the level of variability is similar, the shape of the return map is not the same, indicating that the model does not exhibit the same cycle-to-cycle dynamics when measured engine data is used instead of simulated inputs. This implies that not all relevant effects are being effectively captured. Additional work in the upcoming fiscal year will be directed towards identifying the causes of these differences and developing

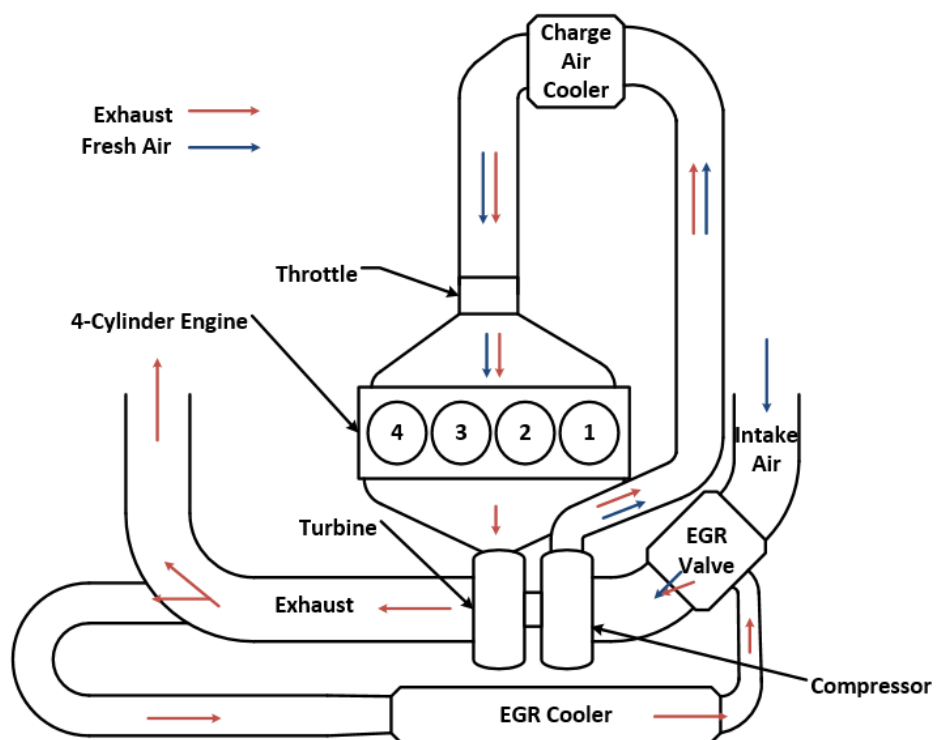


Figure 1. EGR system diagram

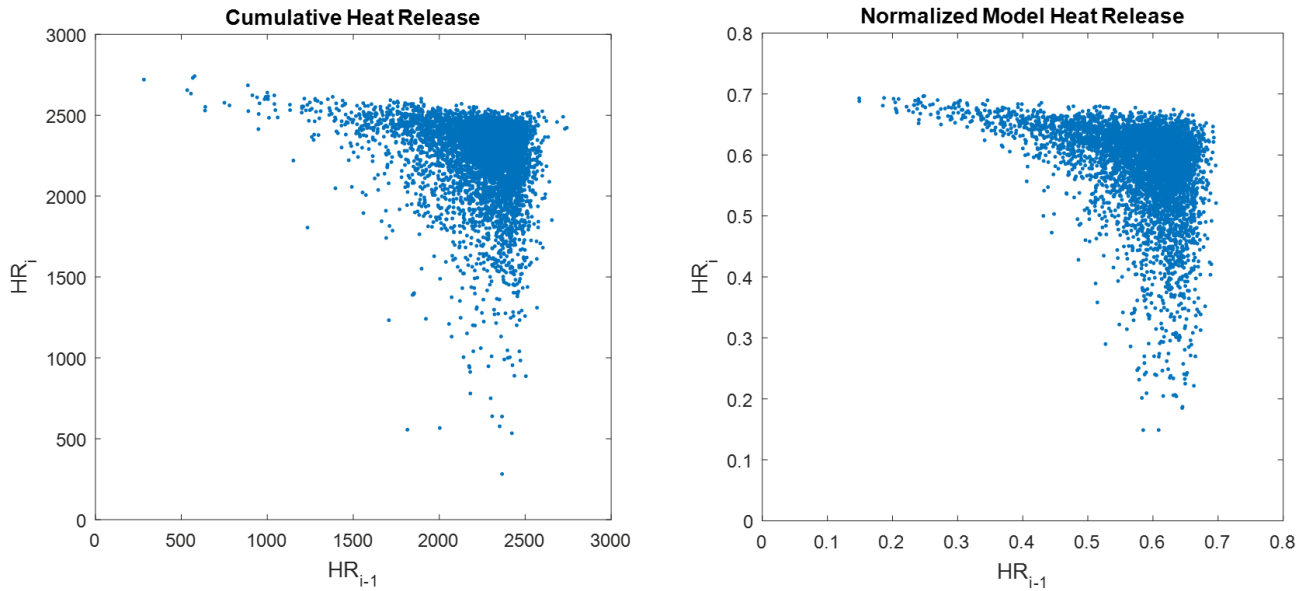


Figure 2. Return maps of cumulative heat release (HR) for engine operation at 20% EGR and model-simulated normalized heat release

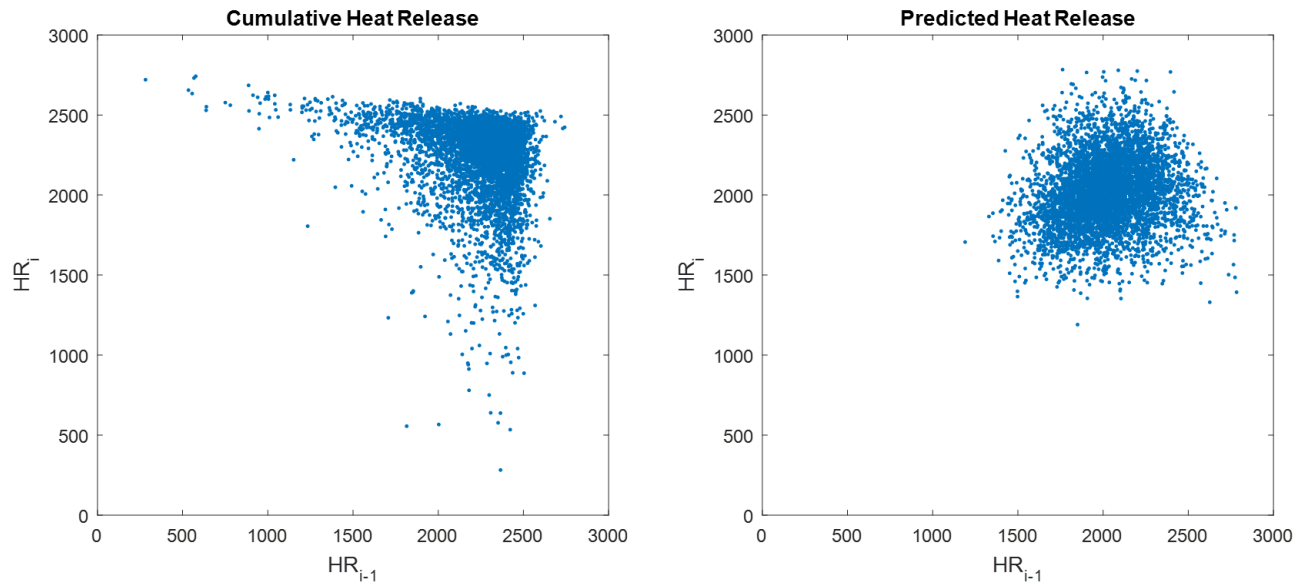


Figure 3. Return maps of actual and model-predicted heat release for engine operation with 20% EGR

revised low-order models that can predict the cyclic variations in real engine operation with better fidelity.

In addition to work aimed at predicting next-cycle behavior, additional efforts have been directed towards improving the understanding of what control actions are needed to stabilize engine operation, given an effective prediction. Experiments conducted in the previous fiscal year and published this fiscal year [3] elucidated the effects of spark restrike delays on the dynamics

encountered in cycle-to-cycle variability, and earlier efforts in collaboration with Argonne National Laboratory examined some effects of alternating cycle control perturbations [4]. Further experiments this fiscal year aimed at improving the understanding of the sensitivity of combustion to changes in fueling for dilute operation. Sinusoidal variations in fuel mass were imposed with a period of 50 engine cycles for both lean and EGR dilution, and the resulting changes in cumulative cycle heat release were evaluated through a fast Fourier

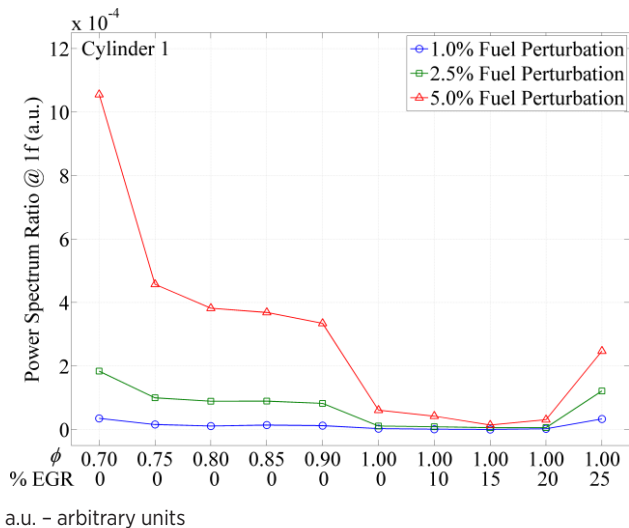


Figure 4. Ratio of FFT power content at the perturbation frequency (1f) to total FFT power content

transform (FFT). Results indicate that the nonlinear effect of composition on flame speed result in not only increased cyclic variability with increasing dilution, but also increased sensitivity to changes in fueling, as shown in Figure 4, where the power spectrum ratio is indicative of the effects of perturbations relative to the overall cyclic variations. For lean operation, the sensitivity increases linearly until the dilution limit is approached and then exponentially once cyclic variability becomes a concern. For EGR operation, the sensitivity is somewhat suppressed for low dilution levels, but at the dilution limit also increases nonlinearly for cases with higher cyclic variability. This implies that small changes in fueling will be able to effect the desired result on an engine cycle, provided sufficiently accurate next-cycle predictions. Results from this study will be published in the upcoming fiscal year at the 2017 SAE World Congress.

## Conclusions

- The initial low order model works well with simulated inputs, but does not capture all relevant features with measured engine data inputs.
- An improved understanding of the underlying causes of cyclic variability and additional model development efforts are needed to capture the dynamics of cycle-to-cycle variations in real time based on measured engine data.

- The nonlinear dependence of flame speed on composition that drives cyclic variability at dilute operating conditions also makes the engine cycle results highly sensitive to intentional changes in fuel input in conditions where cyclic variability is a concern.

## References

- Edwards K.D., Daw C.S., Finney C.E.A., Pannala S., Stoyanov M.K., Wagner R.M., et al. "Accelerating predictive simulation of IC engines with high performance computing (ACE017)," In DOE Vehicle Technologies Office Annual Merit Review; 2016; Washington, D.C.
- Daw C.S., Finney C.E.A., Green J.B.J., Kennel M.B., Thomas J.F., Connolly F.T. "A simple model for cyclic variations in a spark-ignition engine," SAE Technical Paper 962086. 1996, doi:10.4271/962086.
- Jatana G., Kaul B., Wagner R. "Impact of delayed spark restrike on the dynamics of cyclic variability in dilute SI Combustion," SAE Technical Paper 2016-01-0691. 2016, doi:10.4271/2016-01-0691.
- Wallner, T., Sevik J.M., Scarcelli R., Kaul B.C., Wagner R.M., "Effects of Ignition and Injection Perturbation under Lean and Dilute GDI Engine Operation," SAE Technical Paper 2015-01-1871. 2015, doi:10.4271/2015-01-1871.

## FY 2016 Publications/Presentations

- Jatana G.S., Kaul B.C., and Wagner R.M., "Impact of delayed spark restrike on the dynamics of cyclic variability in dilute SI combustion," SAE Technical Paper 2016-01-0691, 2016, doi:10.4271/2016-01-0691.
- Wissink M.L., Splitter D.A., Dempsey A.B., Curran S.J., Kaul B.C., and Szybist J.P., "An assessment of thermodynamic merits for current and potential future engine operating strategies," Proceedings of THIESEL 2016, Valencia, Spain.

## II.18 High-Efficiency Clean Combustion in Light-Duty Multi-Cylinder Diesel Engines

### Overall Objectives

- Develop and evaluate the potential of High Efficiency Clean Combustion (HECC) strategies with production viable hardware and aftertreatment on multi-cylinder engines
- Expand the HECC operational range for conditions consistent with real-world drive cycles in a variety of driveline configurations including down-sized, and hybrid electric and plug-in hybrid electric vehicles
- Improve the fundamental thermodynamic understanding of HECC concepts in order to better identify the associated opportunities, barriers, and tradeoffs
- Characterize the controls challenges including transient operation and fundamental instability mechanisms which may limit the operational range of potential of HECC
- Understand the interdependent emissions and efficiency challenges including integration of exhaust aftertreatments for HECC and multi-mode operation
- Support demonstration of DOE and U.S. DRIVE efficiency and emissions milestones for light-duty diesel and advanced combustion engines

### Fiscal Year (FY) 2016 Objectives

- Demonstrate 25% increase in dynamometer fuel economy with reactively controlled compression ignition (RCCI) over light-duty drive cycle on transient experiments
- Develop experimental multi-mode RCCI map suitable for drive cycle simulations
- Explore the concept of low-delta RCCI in which the difference in reactivity between the high-reactivity fuel and the low-reactivity fuel is narrowed
- Characterize the challenge of emissions control at low temperatures associated with high efficiency combustion concepts including particulate matter (PM)
- Utilize cycle simulation models for evaluating air handling system effects on advanced combustion regimes
- Develop thermodynamic models for comparing advanced combustion regimes

**Scott J. Curran (Primary Contact),  
Vitaly Y. Prikhodko, Martin L. Wissink,  
John M. Storey, James E. Parks, and  
Robert M. Wagner**

Oak Ridge National Laboratory (ORNL)

2360 Cherahala Blvd.

Knoxville, TN 37830

Phone: (865) 946-1522

Email: curransj@ornl.gov

DOE Technology Development Manager:

Leo Breton

Subcontractors:

- The University of Wisconsin, Madison, WI,
- Oak Ridge Associated Universities, Oak Ridge, TN

### FY 2016 Accomplishments

- Attained the 2016 technical target of demonstrating greater than 25% improvement dynamometer fuel economy with RCCI over light-duty drive cycle on transient experiments in fuel economy with multi-mode RCCI operation as compared to a 2009 port fuel injection (PFI) gasoline baseline
- Developed a RCCI combustion map on a multi-cylinder engine suitable for light-duty drive cycle simulations to explore the concept of low-delta RCCI
- Published comprehensive paper summarizing ORNL RCCI PM research
- Developed new thermodynamic model to perform comparative analysis between measured and modelled efficiencies to examine the fundamental sources of efficiency reductions or opportunities inherent to various combustion regimes ■

### Introduction

Advanced combustion concepts have shown promise in achieving high thermal efficiencies with ultra-low  $\text{NO}_x$  and PM emissions. RCCI makes use of in-cylinder blending of two fuels with differing reactivity for improved

control of the combustion process. Previous research and development at ORNL has demonstrated successful implementation of RCCI on a light-duty multi-cylinder engine over a wide range of operating conditions with a focus on identifying the translational effects of going from a combustion concept to a multi-cylinder engine with production viable hardware. The scope of the project focuses on the challenges of implementing advanced combustion concepts on production-viable multi-cylinder engines and includes addressing emissions with advanced emission control technologies (aftertreatment). More specifically, this effort includes investigating high-efficiency concepts developed on single-cylinder engines and addressing challenges related to dilution levels, heat rejection, boosting, thermal management, adaptive controls, and aftertreatment requirements. This activity helps to characterize the interdependency of fuel economy and emissions performance, including the performance of exhaust aftertreatments, and focuses on understanding the synergies between aftertreatment and combustion modes with the expectation that engines may operate in both conventional and advanced combustion modes (“multi-mode”).

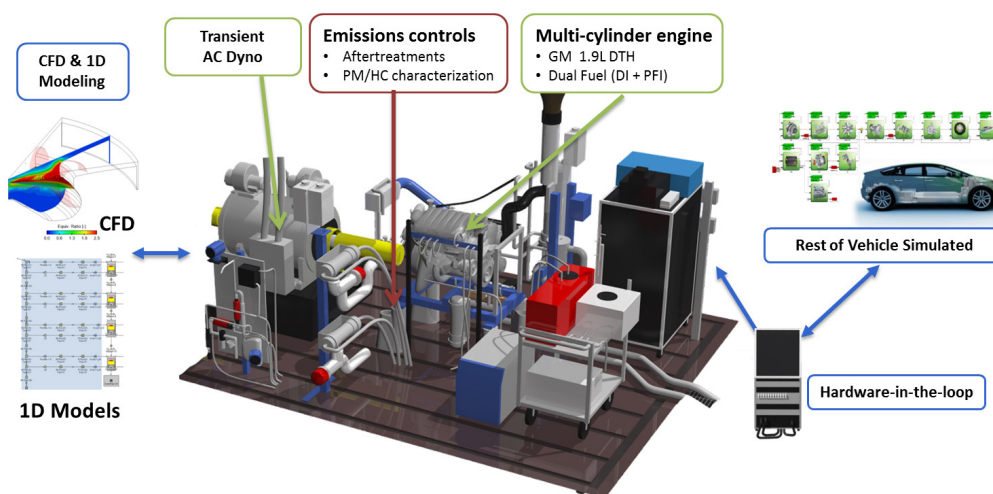
## Approach

A light-duty engine laboratory is in operation based on a 2007 model year General Motors 1.9-L common rail turbocharged diesel in both the stock configuration and with pistons modified for RCCI operation. This research platform has advanced and flexible control systems that enable nonstandard fuel delivery approaches, permit the override of all engine control parameters, and enable new

control schemes to be evaluated on-engine. Integration of the engine and emissions control activities at ORNL provide an avenue for detailed study of the aftertreatment integration issues for advanced combustion approaches. A new capability at ORNL is a transient-capable engine dynamometer configured with a hardware-in-the-loop (HIL) platform. Technical challenges associated with transient operation of advanced combustion, as well as transient emissions, can also be addressed using this facility. The use of computational fluid dynamics modeling and cycle simulations are integrated to accelerate the development of advanced combustion modes and enhance analytical capabilities on understanding the opportunities and challenges of achieving high engine efficiency and minimizing engine out emissions. The combination of these research capabilities, as illustrated in Figure 1, permits a thorough and detailed study of the critical technical issues associated with the implementation of advanced combustion approaches. Collaborations with industry, university, and national laboratory partners leverage expertise at ORNL to meet the project objectives.

## Results

ORNL demonstrated greater than 25% fuel economy improvement with multi-mode RCCI combustion compared to representative PFI gasoline vehicle baseline on a transient light-duty drive cycle using a HIL transient enabled engine laboratory. The ORNL dual-fuel advanced combustion engine was integrated in a HIL system which simulates the remainder of the vehicle and controls dyno/engine speed and engine controller pedal position as shown in Figure 2. RCCI multi-mode operation took place



1D – one-dimensional; CFD – computational fluid dynamics; AC – alternating current; Dyno – dynamometer; DI – direct injection

Figure 1. Comprehensive approach to advanced combustion research centered on multi-cylinder engine experiments

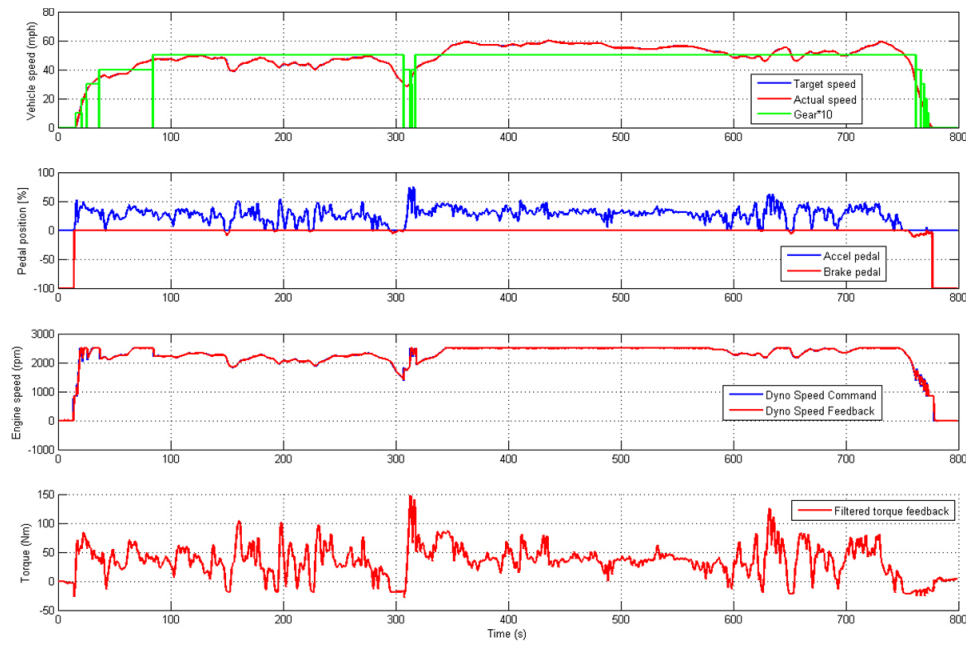


Figure 2. HIL transient experiment showing commanded and actual dyno speed along with gear changes over the Highway Fuel Economy Test

automatically using previously generated RCCI maps as part of previous Advanced Combustion Engine R&D milestones. The HIL experiments showed greater than 25% fuel economy over the federal Highway Fuel Economy Test compared to previous PFI vehicle system simulations.

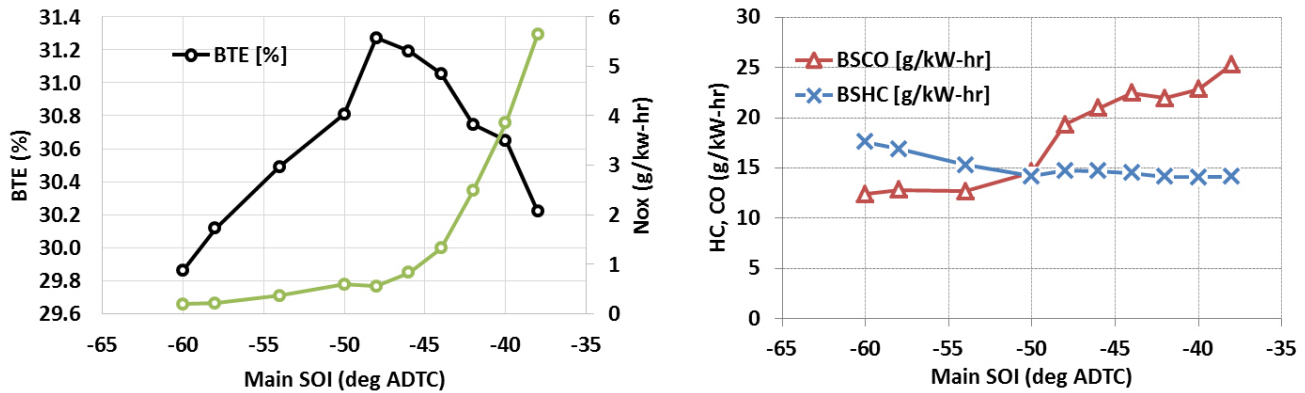
The concept of low-delta RCCI in which the difference in reactivity between the high-reactivity fuel (i.e., direct injection diesel fuel) and the low-reactivity fuel (i.e., port fuel injected gasoline) is narrowed was investigated through engine mapping. The low-delta RCCI map was developed using jointly developed guidelines between ORNL and Argonne National Laboratory which reference the Advanced Combustion and Emissions Control Tech Team combustion noise guidelines and the efficiency goal setting guidelines. Previous maps have focused on high-delta RCCI in which the difference in reactivities was made as large as possible. For this map, a 70 Research Octane Number gasoline range fuel was used for the port fuel injected low-reactivity fuel and a certification grade diesel fuel was used for the direct injected high-reactivity fuel. Initial mapping shows expected lowering of peak load with a conventional RCCI injection strategy but further development is underway. Results from this mapping are shown in Figure 3.

A one-dimensional engine modeling approach which was used to analyze the behavior of a production light-duty diesel engine equipped with a variable geometry turbocharger and a high pressure loop exhaust gas

recirculation (EGR) system under LTC conditions. The results of the simulations show that at light loads, large amounts of EGR can be used while maintaining globally lean operation. However, as the engine load increases, a globally stoichiometric condition is reached relatively quickly and high engine loads with greater than 30% EGR and overall lean conditions were not possible to achieve. These results reinforce the importance of air handling on LTC concepts, and that care should be taken with single-cylinder engines to utilize realistic air handling boundary conditions Figure 4 shows the contour plot of global equivalence ratio over a map of brake mean effective pressure (BMEP) vs. engine speed at 16% EGR.

Experiments were run to better understand the soot/PM- $\text{NO}_x$  tradeoff as diesel SOI is advanced from just before dead center (BTDC) to RCCI-like timings of 40° BTDC or earlier, as shown in Figure 5, allowing for substantial dwell between end of diesel injection and start of combustion allowing for sufficient time for premixing fuel and avoiding locally rich in-cylinder conditions which could lead to soot formation.

A new thermodynamic analysis of the RCCI and conventional diesel combustion (CDC) were completed as part of a comparative analysis between measured and modelled efficiency to illustrate fundamental sources of efficiency reductions or opportunities inherent to various advanced combustion modes. Comparative analysis between measured and modeled efficiencies, as shown



BSCO – brake specific carbon monoxide; BSHC – brake specific hydrocarbons; ATDC – after top dead center

Figure 3. Brake thermal efficiency (BTE) and  $\text{NO}_x$  results (left) and CO and HC emissions (right) over a main diesel start of injection (SOI) sweep low-delta RCCI with 70 Research Octane Number PFI and ultra-low sulfur diesel DI @ 2,000 rpm, 3.0 bar BMEP, 75% premixed ratio (rP)

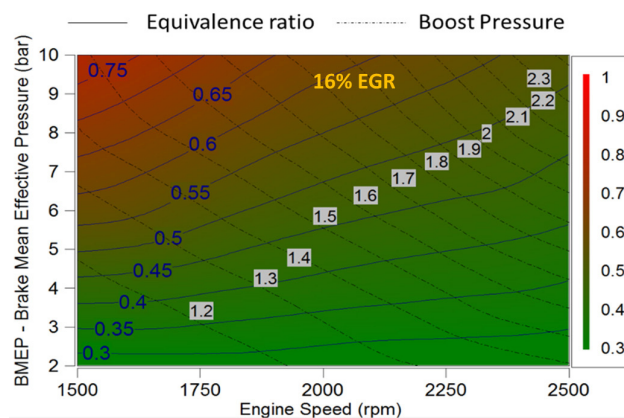
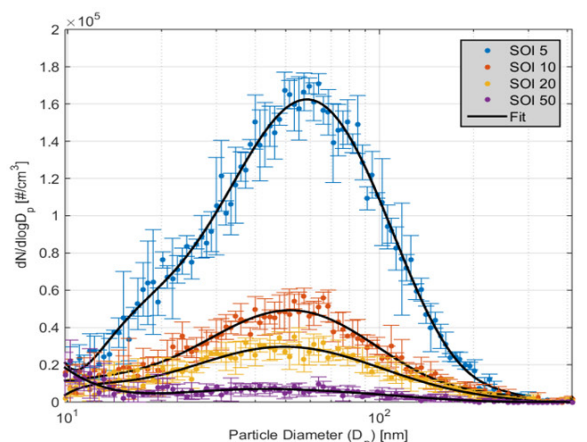


Figure 4. Contour plot of global equivalence ratio over a map of BMEP vs. engine speed at 16% EGR. Lines of constant boost pressure and constant equivalence ratio are also shown.

in Figure 6, illustrates fundamental sources of efficiency reductions or opportunities. The findings highlight the importance of examining the measured efficiency in context of what is thermodynamically possible with the working fluid and boundary conditions prescribed by a strategy.

## Conclusions

Advanced combustion techniques such as RCCI can increase engine efficiency and lower  $\text{NO}_x$  and soot emissions over the engine map. Furthermore, a RCCI–CDC multi-mode approach has been shown to allow greater than 25% fuel economy improvement over a 2009 PFI gasoline baseline in a mid-size passenger vehicle using transient multi-mode experiments. This activity has shown the importance of taking a comprehensive engine



FSN – Filter Smoke Number; CAD – crank angle degrees

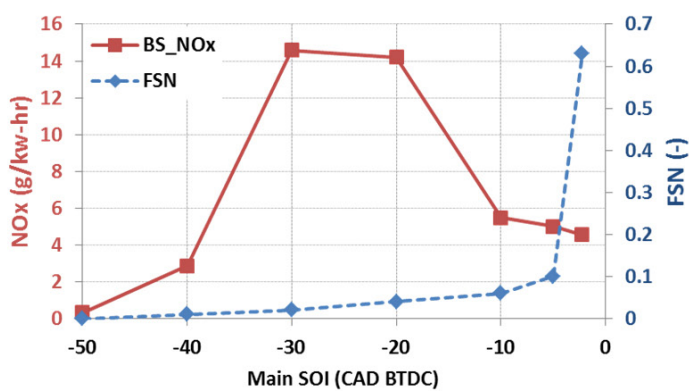
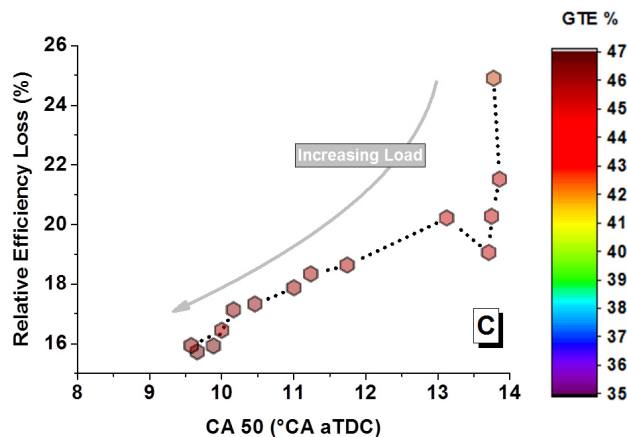


Figure 5. Particulate size distribution (left) and  $\text{NO}_x$ /soot tradeoff (right) for advancing main SOI with 75% gasoline dual-fuel combustion transitioning to RCCI (SOI = -50)



CA50 – crank angle at which 50% of the heat has been released; °CA – degrees crank angle; aTDC – after top dead center

Figure 6. CDC efficiency loss compared to model showing incomplete combustion losses and heat transfer losses both go down as load increases

systems approach to help meet Vehicle Technologies Office goals and milestones.

## FY 2016 Publications/Presentations

1. Wissink, M., Splitter, D., Dempsey, A., Curran, S., Kaul, B., Szybist, J., "An Assessment of Thermodynamic Merits for Current and Potential Future Engine Operating Strategies," THIESEL 2016 Conference on Thermo-and Fluid Dynamic Processes in Direct Injection Engines, Valencia, Spain, September 13–16, 2016.
2. Curran S.J., "Evolution and current understanding of physicochemical characterization of particulate matter from RCCI," AEC Program Review, Southfield, MI., August 2016.
3. Wissink, M., Splitter, D., Dempsey, A., Curran, S., Kaul, B., Szybist, J., "An Assessment of Thermodynamic Merits for Current and Potential Future Engine Operating Strategies," Advanced Engine Combustion Program Review, Southfield, Michigan, August 16–19, 2016.
4. Storey, S.J., Curran, S., Lewis, S., et al., "Evolution and current understanding of physicochemical characterization of particulate matter from reactivity controlled compression ignition combustion on a multi-cylinder light-duty engine," International Journal of Engine Research, 2016. doi:10.1177/1468087416661637
5. Gowda Kodebyle Raju, N., Dempsey, A., and Curran, S., "Analysis of Engine Air Handling Systems for Light-Duty Compression Ignition Engines Using 1-D Cycle Simulation: Achieving High Dilution Levels for Advanced Combustion," ICEF2016-9459, 2016.
6. Curran, S., Project ID ACE016, 2016 VTO Merit Review, June 2015, Washington D.C.
7. Lucachick, G., Curran, S., Storey, J., Prikhodko, V., and Northrop, W., "Volatility characterization of nanoparticles from single and dual-fuel low temperature combustion in compression ignition engines," Aerosol Science and Technology, Vol. 50, Iss. 5, 2016.
8. Curran, S., Wagner, R., "Reactivity Stratified Combustion Development for Light-Duty Multi-Cylinder Engines" IEA Technology Collaboration Programmes (TCP) for Clean and Efficient Combustion, 38th Task Leaders Meeting in Ruka, Finland, June 26–30, 2016.
9. Parks, J.E, "Emission Challenges for Advanced Combustion Engines," 2016 SAE High Efficiency Engine Symposium, April 2016.
10. Curran, S., "Update on Single-/Dual-Fuel Low Temperature Combustion Light-Duty Multi-Cylinder Research at ORNL," AEC Program Review, Livermore, CA, February 2016.
11. Wagner, R.M., "Engines of the Future," Mechanical Engineering: The Magazine of ASME, No 12. 137, December 2015.

## II.19 Stretch Efficiency—Exploiting New Combustion Regimes

### Overall Objectives

- Define and analyze specific advanced pathways to improve the energy conversion efficiency of internal combustion engines with emphasis on thermodynamic opportunities afforded by new approaches to combustion
- Implement critical measurements and proof of principle experiments for the identified pathways to stretch efficiency

### Fiscal Year (FY) 2016 Objectives

- Investigate methods to increase the fuel conversion during the in-cylinder reforming process in an effort to achieve thermochemical recuperation (TCR)
- Determine the operating conditions under which TCR can be achieved in the exhaust gas recirculation (EGR) loop catalytic reforming process
- Compare the brake thermal efficiency of the in-cylinder reforming process relative to the catalytic reforming process on the same engine platform
- Investigate reformer catalyst stability and sulfur tolerance

### FY 2016 Accomplishments

- Demonstrated TCR under fuel-rich conditions with the catalytic reforming process in the bench-flow reactor with a mix of partial oxidation and steam reforming
- Determined that while sulfur tolerance does impact the H<sub>2</sub>/CO ratio during catalytic reforming, the performance of the reforming process is recovered when sulfur is removed from the feed gas
- Demonstrated a fuel consumption benefit of over 10% using the catalytic reforming process on the engine at the U.S. DRIVE Advanced Combustion and Emissions Control Tech Team part-load efficiency point ■

### Introduction

The overarching goal of this project is to use a thermodynamics-based approach to identify and pursue opportunities for improved efficiency in internal combustion engines. The project is guided by combined

**James P. Szybist (Primary Contact),  
Josh A. Pihl, Daniel W. Brookshear,  
and Yan Chang**

Oak Ridge National Laboratory

NTRC Site

2360 Cherahala Blvd.

Knoxville, TN 37932

Phone: (865) 946-1514

Email: szybistjp@ornl.gov

DOE Technology Development Manager:

Leo Breton

Subcontractor:

Galen Fisher, University of Michigan, Ann Arbor, MI

input from industry, academia, and national labs, such as that summarized in the report from the Colloquium on Transportation Engine Efficiency held in March 2010 at the United States Council for Automotive Research [1]. Since 2011, the project has been on a multi-year path to pursue what was identified as the most promising approach to improving light-duty engine efficiency: high EGR dilution spark ignition combustion enabled by fuel reforming through TCR.

The overall efficiency advantages for high EGR conditions are summarized in a thermodynamic modeling study by Caton [2]. First, the EGR increases the manifold pressure at a given load, decreasing pumping work at part-load conditions. Second, the peak cylinder temperature decreases with EGR, causing the heat transfer to decrease. Finally, due to a combined thermal and composition effect, the ratio of specific heat ( $\gamma$ ) increases with EGR. The amount of EGR that can be used is limited due to combustion instabilities, but the dilution limit can be extended for additional efficiency improvements with the use of high flame speed components, namely H<sub>2</sub>. This project is pursuing fuel reforming to generate H<sub>2</sub> in an effort to extend the EGR dilution limits for spark ignition combustion in the most thermodynamically favorable way possible. Ideally, this involves using exhaust heat to drive endothermic reforming reactions to increase the chemical fuel energy to achieve TCR, a form of waste heat recovery.

## Approach

In 2016, there were two pathways to TCR to support high EGR dilution that were investigated: (1) a non-catalytic in-cylinder reforming approach that thermally reforms the fuel in a hot, oxygen-deficient negative valve overlap portion of an engine cycle and (2) a strategy that relies on a catalyst to reform the fuel in an oxygen-deficient EGR stream. Both approaches aim to use waste exhaust heat to drive endothermic reforming reactions to produce a mixed reformate and EGR stream that is rich in H<sub>2</sub> and CO. The reformate can then be used to extend the EGR dilution limit of spark-ignited combustion for a more thermodynamically favorable engine cycle.

A flexible engine platform was constructed in 2014 to pursue the in-cylinder reforming approach. It involved modifying the valvetrain so that one cylinder of a multi-cylinder engine operated in reverse: breathing in hot, oxygen-deficient exhaust with fuel, and then compressing to further increase the temperature and drive endothermic reforming reactions. The reformate from this cylinder was then fed into the intake manifold for the other three cylinders. Results from experiments in FY 2015 showed a lack of fuel conversion in the reforming cylinder, so FY 2016 efforts focused on three strategies to increase the fuel conversion.

The catalytic EGR loop reforming strategy included both synthetic exhaust gas flow reactor and engine experiments in 2016. The flow reactor experiments involved using a core sample of a catalyst to investigate the catalyst performance and guide engine experiments. Efforts included investigating thermochemical recuperation over the equivalence ratio/temperature range expected on the engine, durability experiments, sulfur tolerance, and compatibility with different fuel types. The second path focused on applying the catalytic EGR loop reforming strategy to the engine. For this, full-sized precommercial catalyst samples were obtained from Umicore and installed at Oak Ridge National Laboratory.

## Results

### In-Cylinder Reforming

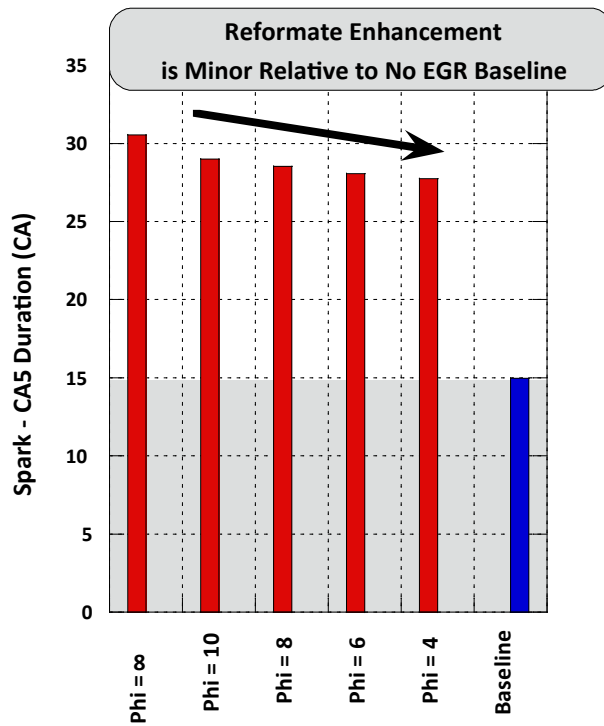
Three strategies aimed at increasing fuel conversion during the in-cylinder reforming process were investigated: (1) increased compression ratio, (2) introduction of modest levels of oxygen, and (3) a reconfigured exhaust manifold to minimize heat losses. Of these, only the strategy using modest levels of oxygen injection proved to provide a substantial difference in fuel conversion during the in-cylinder reforming process. The reformate mixture that was produced by this method produced a mixture of unburned and partially oxidized

hydrocarbons along with the desirable products of reforming, H<sub>2</sub> and CO.

The effectiveness of this mixture to increase EGR dilution tolerance, presented as the ability of the reformate to reduce the combustion duration, is presented in Figure 1. Adding oxygen to the mixture increases fuel conversion and reformate, and it does decrease the combustion duration. However, relative to the baseline case without EGR, the reductions to the combustion duration are small and ultimately have a minimal impact. Thus, a decision was made to put additional investigations of the in-cylinder reforming strategy on-hold and instead direct resources to the catalytic EGR loop reforming strategy for the foreseeable future.

### EGR Loop Reforming: Bench Flow Reactor Experiments

Synthetic exhaust gas flow reactor experiments using a Rh/Al<sub>2</sub>O<sub>3</sub> catalyst core sample continued in an effort to guide engine experiments. Investigations in 2015 on the



CA5 – crank angle at which 5% of the fuel energy has been released

Figure 1. Spark-to-CA5 combustion duration for the in-cylinder reforming strategy with various equivalence ratios (Phi) relative to the combustion duration for the baseline efficiency. As the equivalence ratio is reduced, the combustion duration decreases by a small amount. This decrease in combustion duration, however, does not provide a substantial enough change to increase the EGR dilution tolerance.

flow reactor indicated that steam reforming alone lacked sufficient enthalpy to drive the endothermic reactions at the conditions of interest. However, a small amount of oxygen in the feed gas to produce a combination of partial oxidation and steam reforming was significantly more robust, and that under sufficiently fuel-rich conditions with oxygen present, thermochemical recuperation with good fuel conversion was possible. In 2016, parametric investigations continued to investigate fuel effects, comparing iso-octane to a low sulfur gasoline as well as ethanol. Results showed that the fuel composition is important to the refueling process, both in terms of the products of the reforming process and the products generated.

Flow reactor investigations in FY 2016 also included testing catalyst stability and sulfur tolerance. To evaluate the stability of the reforming process and determine if coking or other deactivation mechanisms could pose a problem during engine application, a subset of the gasoline reforming experiments was repeated, but for extended durations (3–6 hours). Figure 2A shows a representative data set from one of these extended runs. For all of the operating conditions that generate significant quantities of reformate, the H<sub>2</sub> and CO concentrations are quite stable, indicating that there are no significant deactivation mechanisms that would compromise catalyst performance over extended run times or require periodic regeneration strategies. Sulfur tolerance was tested by establishing stable reformer operation for 1 h, adding 2 ppm SO<sub>2</sub> to the feed gas for 1 h, and then

removing the SO<sub>2</sub> from the feed gas and observing the catalyst performance recovery for 1 h. Figure 2B shows results from one of the sulfur tolerance experiments. The addition of SO<sub>2</sub> to the gas stream decreases the H<sub>2</sub> and CO concentrations, indicating that SO<sub>2</sub> does poison the catalyst. The degree of deactivation depends on the reformer operating conditions (inlet gas temperature, fuel feed rate, and equivalence ratio). However, in no instance does SO<sub>2</sub> completely shut down all reforming activity as it did under pure steam reforming conditions tested in prior years of this project. Furthermore, the SO<sub>2</sub> impact is completely reversible; removal of SO<sub>2</sub> from the gas stream leads to rapid recovery of H<sub>2</sub> and CO production to their initial levels. Overall, the catalytic partial oxidation reforming strategy is quite stable and tolerant to exposure to sulfur at levels anticipated in engine exhaust.

### EGR Loop Reforming: Engine Experiment

A schematic and photograph of the EGR loop reforming strategy used on the engine is shown in Figure 3. In this strategy, one of the cylinders has an isolated intake and exhaust manifold. The entirety of the exhaust from this cylinder (Cylinder 4) is fed directly to the reforming catalyst, which then feeds into the intake for Cylinders 1–3. In the synthetic exhaust gas flow reactor experiments significant reformate production requires a small amount of oxygen in the reformer feed. In the engine experiment, this is accomplished by operating the main combustion event in Cylinder 4 fuel-lean, but then using a post-injection when the exhaust valve opens to feed the

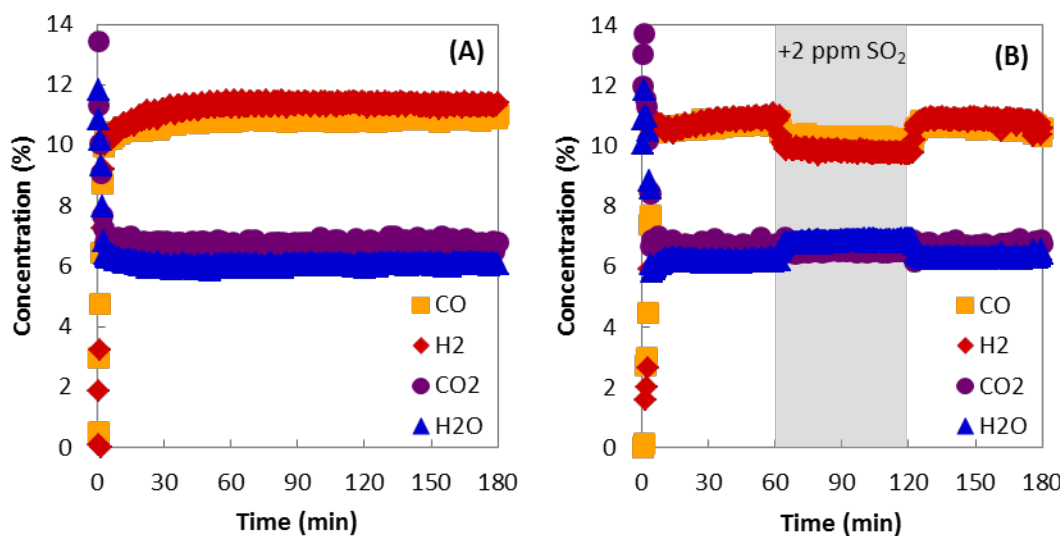


Figure 2. Reformer catalyst outlet concentrations as a function of time during synthetic exhaust gas flow reactor experiments run with a 2 wt% Rh/Al<sub>2</sub>O<sub>3</sub> catalyst at an inlet temperature of 500°C using a low sulfur gasoline fuel fed into a simulated EGR mixture with sufficient excess air to create a catalyst inlet equivalence ratio of 3.3 (A) under a constant inlet composition and (B) before, during (shaded), and after exposure to 2 ppm SO<sub>2</sub>.

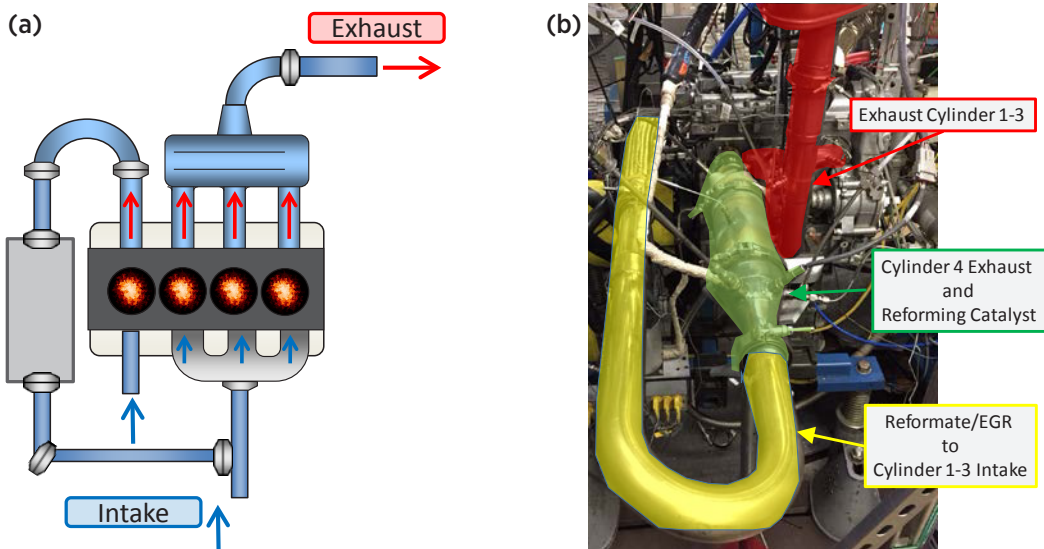


Figure 3. (a) Schematic of the in-cylinder reforming process where one cylinder has an isolated intake and exhaust, feeds the reforming catalyst, and is incorporated into the intake for the other three cylinders, and (b) a photograph of the experimental catalytic reforming setup on the engine.

catalyst the appropriate mixture. The fuel-lean strategy with a post-injection to produce the appropriate catalyst feed is shown in Figure 4.

Parametric investigations were conducted at an operating point of 2,000 rpm and 4 bar brake mean effective pressure (20% load), a part-load condition identified by the U.S. DRIVE Advanced Combustion and Emissions Control Tech Team. Parametric investigations focused on changing the catalyst equivalence ratio (by changing the amount of fuel in the post-injection) and on varying the oxygen flow rate over the catalyst (by changing the air-to-fuel ratio of the main combustion event). Engine experiments were conducted in two phases using both iso-octane and a low sulfur gasoline (3 ppm sulfur). In the first phase, the catalyst reformate was exhausted without recirculation so that the catalyst performance could be mapped. The production of  $H_2$  and CO from the catalyst, shown in Figure 5, illustrates that there is a maximum in  $H_2$  production that approaches 15% at equivalence ratios between 5 and 7 and with high oxygen flow rate. At leaner equivalence ratios, the  $H_2$  is oxidized to water, and at equivalence ratios richer than this the steam reforming process is enthalpy-limited, decreasing the total hydrogen production. The iso-lines on the contour plots indicate the approximate fraction of fuel energy that is supplied to the catalyst that is required by the remaining three cylinders. The operating conditions investigated span a range of about 10% of the fuel energy to over 100% of the fuel energy.

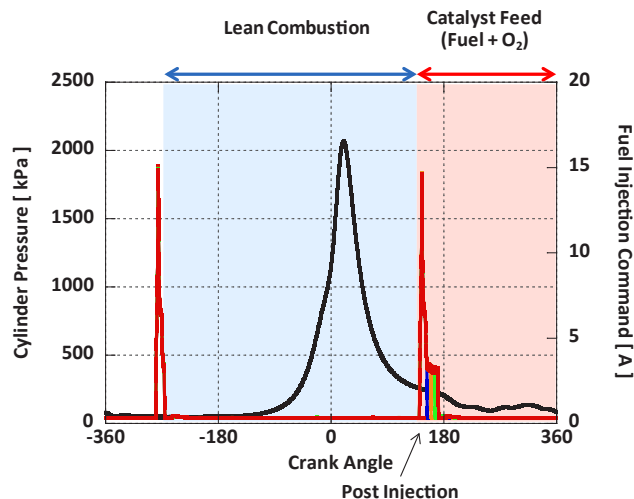


Figure 4. Operational strategy of the cylinder that feeds the catalytic reformer. The main combustion event is operated fuel-lean, followed by a post-injection near exhaust valve opening. The result is a fuel-rich catalyst feed that contains oxygen and is appropriate for catalytic reforming.

The second phase of experiments involved routing the reformate and EGR mixture to the remaining cylinders to increase the brake efficiency of the engine. This was done at a stoichiometric exhaust equivalence ratio, and with a CA50 (crank angle at which 50% of the fuel energy has been released) combustion phasing of between 4° and 8° crank angle after firing top dead center. The brake efficiency of this reforming strategy, and how it compares

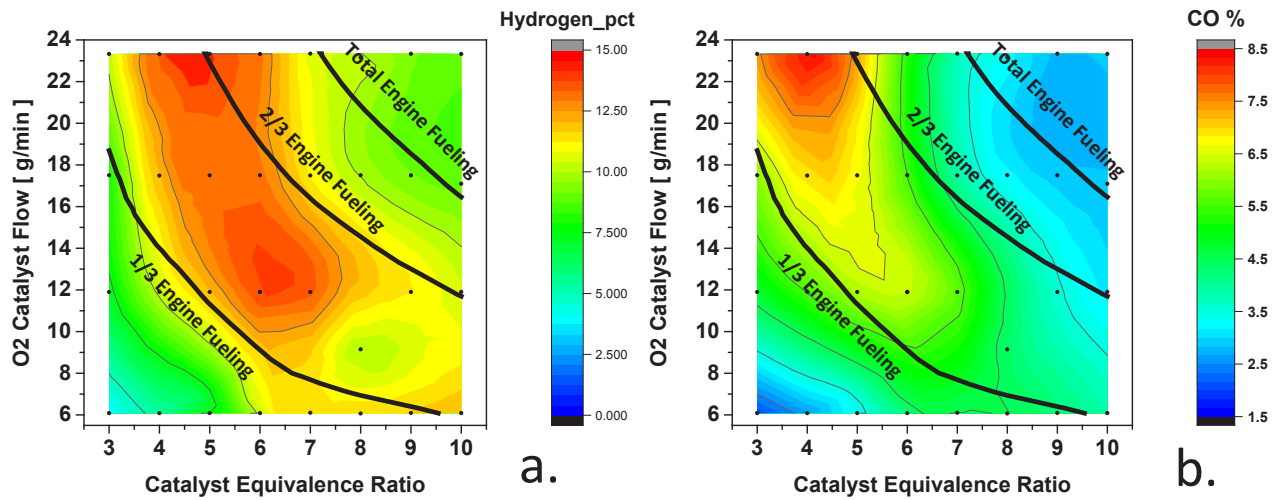


Figure 5. Catalyst reforming production of (a) hydrogen, and (b) carbon monoxide over the range of oxygen flow rates and equivalence ratios investigated.

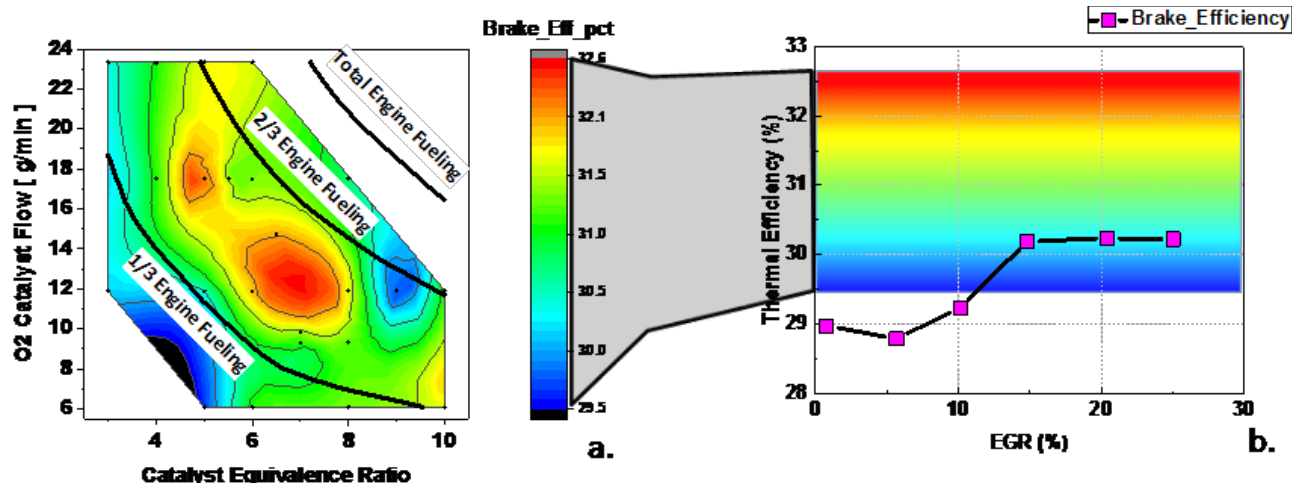


Figure 6. (a) Brake efficiency of the catalytic reforming strategy as functions of the  $O_2$  flow rate and the catalyst equivalence ratio, and (b) a comparison of how the brake efficiency of the catalytic reforming strategy compares to conventional EGR with the same fuel in the same engine.

to the brake efficiency of conventional EGR dilution, is shown in Figure 6. The catalytic reforming strategy provided a brake efficiency that was 32.5%, or about 3.5 efficiency points higher than the baseline condition without EGR. This efficiency increase is significant and correlates to a fuel consumption decrease of more than 10%.

## Conclusions

- Three approaches were investigated to increase fuel conversion during the in-cylinder reforming activities. Only one of these, the introduction of small amounts of oxygen, proved to be effective at increasing the

conversion. However, even the highest fuel conversion rates achieved were ineffective at increasing the EGR dilution tolerance in the remaining cylinders. Thus, this approach was placed on-hold while resources are focused on the catalytic reforming approach.

- Synthetic exhaust gas flow reactor experiments have verified that TCR can be accomplished under conditions that combine partial oxidation reforming with steam reforming with both iso-octane and gasoline at sufficiently fuel-rich conditions.
- Durability experiments with the catalyst show that the catalyst can achieve continuous reforming for durations of over an hour without a need to regenerate.

- Experiments show that the catalyst H<sub>2</sub> production decreases in the presence of sulfur, but that the catalyst quickly recovers performance when the sulfur in the feed gas is removed.
- The catalytic reforming process was successfully applied on the engine. Experiments on the engine closely match the results from the flow reactor in terms of H<sub>2</sub> and CO production over a wide range of reforming conditions.
- A significant increase in engine efficiency was achieved with the catalytic reforming process. Over the baseline case, brake thermal efficiency was increased from 29% to 32.5%, which amounts to more than a 10% reduction in fuel consumption.

## References

1. C.S. Daw, R.L. Graves, R.M. Wagner, and J.A. Caton, "Report on the Transportation Combustion Engine Efficiency Colloquium Held at USCAR, March 3–4, 2010," ORNL/TM-2010/265, October 2010.
2. Caton, J., "A Comparison of Lean Operation and Exhaust Gas Recirculation: Thermodynamic Reasons for the Increases of Efficiency," SAE Technical Paper 2013-01-0266, 2013, doi:10.4271/2013-01-0266.

## FY 2016 Publications/Presentations

1. Szybist, J.P., "Opportunities for Improved Efficiency in Spark Ignited Engines," Invited Plenary Talk at the 2016 Central States Section Meeting of the Combustion Institute, Knoxville, TN, May 17, 2016.
2. Chang, Y., and Szybist, J., "Fuel Effects on Combustion with EGR Dilution in Spark Ignited Engines," Proceedings of the 2016 Central States Meeting of the Combustion Institute.
3. Szybist, J., Pihl, J., Daw, S., Chang, Y., and Fisher, G., "Stretch Efficiency for Combustion Engines: Exploiting New Combustion Regimes," 2016 DOE Vehicle Technologies Annual Merit Review, Project ID ACE015, presented June 7, 2016.

## II.20 Cummins-ORNL Combustion CRADA: Characterization and Reduction of Combustion Variations

### Overall Objectives

- Improve engine efficiency through better combustion uniformity
- Develop and apply diagnostics to resolve combustion uniformity drivers
- Understand origins of combustion nonuniformity and develop mitigation strategies
- Address critical barriers to engine efficiency and market penetration

### Fiscal Year (FY) 2016 Objectives

- Develop diagnostic for measuring exhaust O<sub>2</sub> variations
- Demonstrate exhaust transient measurement sufficient for resolving cylinder-specific variations
- Expand species measurement capabilities of the EGR Probe

### FY 2016 Accomplishments

- New Exhaust Measurement Apparatus developed for fast (5 kHz) simultaneous measurement of O<sub>2</sub>, H<sub>2</sub>O, temperature, and pressure
- Intra-valve-event exhaust transients measured in engine applications provide for quantifying cylinder-to-cylinder and cycle-to-cycle combustion variations
- Specified methodology for integrating CO measurement capability into the EGR Probe
- Two archival publications, two conference papers, and four oral presentations ■

### Introduction

A combination of improved engine and aftertreatment technologies are required to meet increased efficiency and emissions goals. This cooperative research and development agreement (CRADA) section focuses on engine and combustion uniformity technologies. Improved efficiency, durability and cost can be realized via combustion uniformity improvements which enable reduction of engineering margins required by nonuniformities; these margins limit efficiency. Specific needs exist in terms of reducing cylinder-to-cylinder and cycle-to-cycle combustion variations. Advanced

**Bill Partridge<sup>1</sup> (Primary Contact),  
Sam Geckler<sup>2</sup>, Gurneesh Jatana<sup>1</sup>,  
Anthony Perfetto<sup>2</sup>**

<sup>1</sup>Oak Ridge National Laboratory (ORNL)  
2360 Cherahala Blvd.  
Knoxville, TN 37932  
Phone: (865) 946-1234  
Email: partridgewp@ornl.gov

<sup>2</sup>Cummins Inc.  
Columbus, IN 47201

DOE Technology Development Manager:  
Leo Breton

efficiency engine systems require understanding and reducing combustion variations. Development and application of advanced diagnostic tools are required to realize these technology improvements, and is a major focus of this CRADA.

### Approach

The CRADA applies the historically successful approach of developing and applying minimally invasive advanced diagnostic tools to resolve spatial and temporal variations within operating engines. Diagnostics are developed and demonstrated in the lab and on engines at ORNL prior to field application at Cummins; e.g., for cylinder-to-cylinder CO<sub>2</sub> variations due to nonuniform fueling, exhaust gas recirculation (EGR), combustion, component tolerance stacking, etc. Detailed measurements are used to assess the performance of specific hardware designs and numerical design tools, and identify nonuniformity origins and mitigation strategies, e.g., hardware and control changes.

### Results

#### Exhaust Measurement Apparatus Development and Application for Resolving Exhaust Transients Sufficient to Quantify Cylinder-to-Cylinder and Cycle-to-Cycle Combustion Variations

A new instrument for measuring fast exhaust O<sub>2</sub>, H<sub>2</sub>O, temperature, and pressure transients was developed with

the goal of achieving sufficient intra-cycle temporal resolution to assess combustion uniformity and air-to-fuel ratio variations in multi-cylinder engines. Figure 1 shows the resulting Exhaust Measurement Apparatus for fast, 5 kHz (200  $\mu$ s, 1.2° crank angle at 1,000 rpm), measurement of O<sub>2</sub> and H<sub>2</sub>O concentration, temperature, and pressure for characterizing exhaust transients to detect and quantify cylinder-to-cylinder and cycle-to-cycle combustion variations. The instrumented exhaust section is based on a 3-in inside diameter by 10-in long duct, mounted to an optical breadboard which supports the associated components and an inert-purged 6-in  $\times$  6-in  $\times$  18-in enclosure (not shown). The multi-pass Herriott cell optics along with the collimation and detection hardware for the O<sub>2</sub> measurements are mounted directly on the breadboard; these provide ca. 3-m absorption pathlength, and function in a line-of-sight mode. The collimation optics and detector for H<sub>2</sub>O measurements are mounted directly to the instrumented exhaust duct, and function in a line-of-sight mode normal to the breadboard. Additional lines for water cooling, inert purge, and window guard flow are shown in the Figure 1 picture. Via laboratory calibration, the O<sub>2</sub> detection limit was determined to be 0.4%; for reference, the EGR Probe CO<sub>2</sub> detection limit was also 0.4%. Not only is this O<sub>2</sub> detection limit sufficient to study combustion uniformity, it is also relevant to studying residual exhaust O<sub>2</sub>, which can impact catalyst performance and which cannot be measured by standard universal exhaust gas oxygen or lambda sensors (which measure net stoichiometry).

The diagnostic's performance was evaluated via single- and multi-cylinder engine applications. The diagnostic is robust to engine vibrations, which do not impact measurements or Herriott cell mode (number of passes). The instrument was able to resolve very fast exhaust transients on the crank angle order, which is more than sufficient to resolved cylinder- and cycle-specific fluctuations, and indeed sufficient to resolve intra-valve-event transients. Specifically, cylinder-specific

transients were resolved downstream of the turbocharger in the multi-cylinder engine experiments. While the Herriott cell provides unique sensitivity to the weak O<sub>2</sub> absorption transitions, it also provides great sensitivity to window deposits; these are most significant during cold startup (less significant for hot engine startup). An isopropanol window guard flow proved effective for mitigating window deposits during startup. Nevertheless, in gasoline engine applications, measurement times could be limited to 20 min before window cleaning was required, and applications with significant oil utilization could significantly limit practical measurement times. However, using E85 (85% ethanol, 15% gasoline mixture) in the single-cylinder experiments allowed for over 3 h of continuous exhaust measurements without window cleaning. Insights from the campaign will be used to further refine the diagnostic, and guide analytical strategies for advancing engine efficiency. Specifically, the next generation Exhaust Measurement Apparatus may include mechanical shutters to guard windows when not making measurements, an integrated wiper for in-operando cleaning, integrated purge/containment box, and improved control and integration of purge and coolant flows.

### Methodology for Integrating CO Measurement into the EGR Probe

A methodology for integrating CO measurements into the EGR Probe capabilities, provides insights for resolving combustion variations, and is consistent with advancing the CRADA goals. A specific CO absorption transition at 2325.2 nm (4300.75  $\text{cm}^{-1}$ ) was selected for spectroscopic-based measurements. In an H<sub>2</sub>O–CO EGR Probe application, standard silica optical fibers would be used to guide the 2,325 nm light between the probe and instrument box. For an H<sub>2</sub>O–CO<sub>2</sub>–CO EGR Probe the light for CO<sub>2</sub> (2.7  $\mu\text{m}$ ) and CO spectroscopy would be multiplexed on ZrF<sub>4</sub> optical fibers; modification of the CO<sub>2</sub> measurement to use ca. 2  $\mu\text{m}$  light would allow the

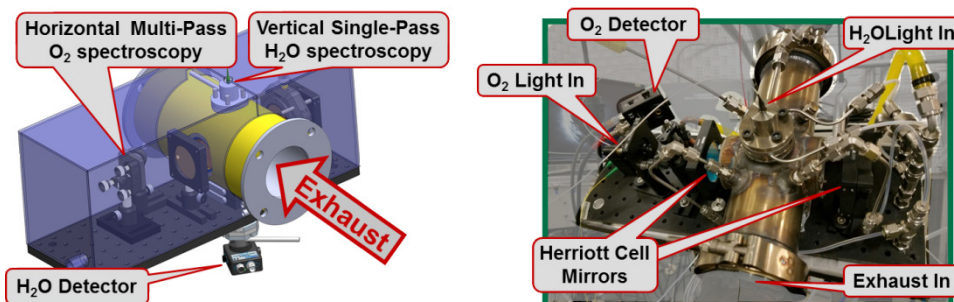


Figure 1. Schematic and picture detailing components of the instrumented exhaust section for cycle-resolved O<sub>2</sub> and H<sub>2</sub>O concentration, temperature, and pressure measurements

$\text{CO}_2$  and CO measurements to be multiplexed on more conventional and less expensive optical fibers. While the 2325.2 nm CO transition has minimal impact from  $\text{NH}_3$  and  $\text{CH}_4$  interferences as shown in Figure 2, these are not practical limitations in most automotive applications where the concentrations of these interfering species are less than that of CO. We investigated the impact of such interferences on quantification of 1% CO concentration at 300 K, 600 K, and 1,000 K for interfering-species concentrations up to 1%, and found the impact of  $\text{NH}_3$  to be negligible and that of  $\text{CH}_4$  to be suitably accounted for by the standard iterative baseline correction procedure currently incorporated in the EGR Probe measurements, as shown in Figure 3. This procedure is enabled by the spectrally indistinct nature of the  $\text{CH}_4$  spectra in this region, and reduces the interfering impact of  $\text{CH}_4$  on CO measurements by an order of magnitude to ca. 2–4% error as long as the  $\text{CH}_4$  concentration is less than that of CO, which is typically the case except for  $\text{CH}_4$ -fueled engines. In cases where  $\text{CH}_4$  concentrations are significant, separate absorption-based  $\text{CH}_4$  measurements can be made and applied to correct for its interfering impact and enable quantitative CO measurements; in this case the 1,645 nm light for  $\text{CH}_4$  spectroscopy would be multiplexed on the same optical fibers used for  $\text{H}_2\text{O}$  measurements, i.e., this would produce an  $\text{H}_2\text{O}-\text{CO}_2-\text{CO}-\text{CH}_4$  EGR Probe.

## Conclusions

- Exhaust Measurement Apparatus developed and applied for resolving intra-cycle transients sufficient to quantify cylinder-to-cylinder and cycle-to-cycle combustion variations
  - Direct measurement of exhaust parameters and uniformity
  - Improved characterization of air-to-fuel ratio and combustion variations
  - Enables more comprehensive system characterization by correlating input (intake) and response (exhaust) variations
- Applications provided insights for improving exhaust  $\text{O}_2$  and other measurements
  - Improved capabilities for exhaust  $\text{O}_2$  characterization for longer measurement times and improved signal-to-noise ratio
- Pathway defined for incorporating CO into the EGR Probe measurement capabilities

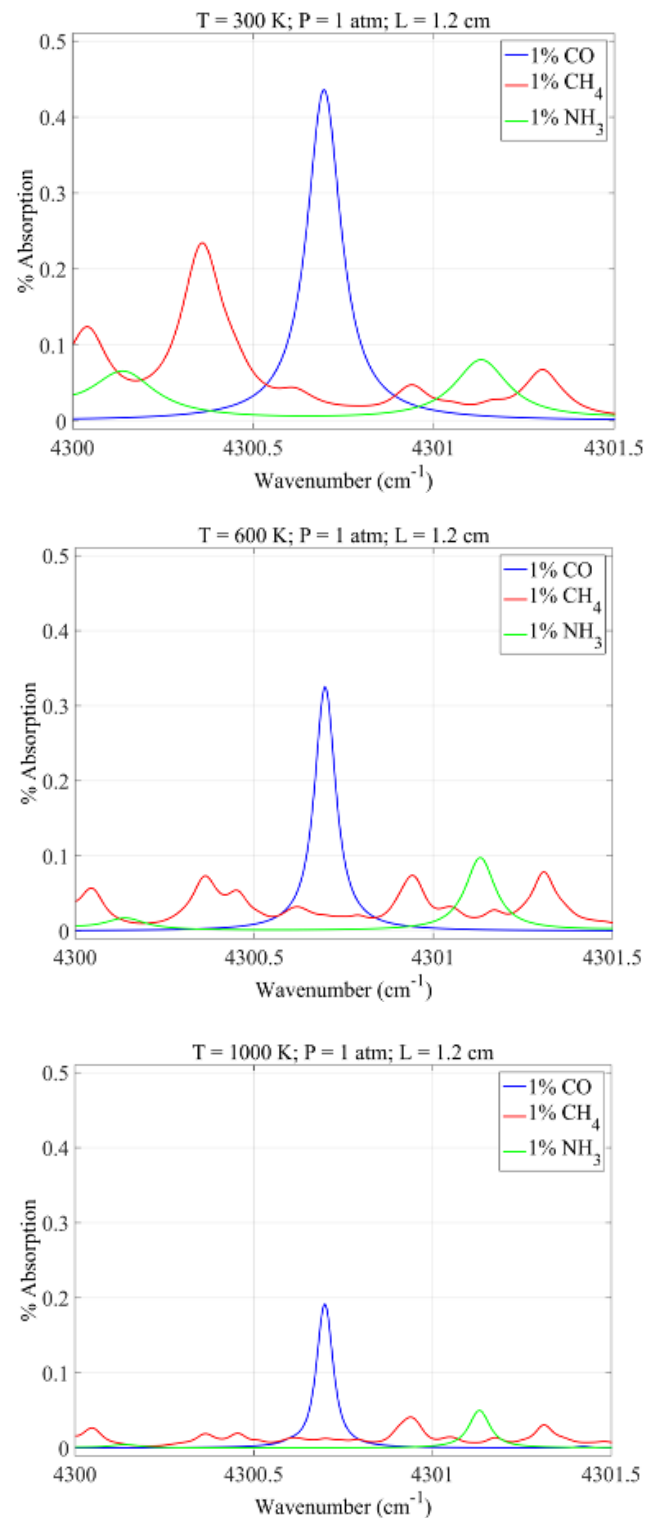


Figure 2. Absorption spectra in the 2,325-nm region for 1% volume/volume concentration each of CO,  $\text{CH}_4$ , and  $\text{NH}_3$  at 300 K, 600 K, and 1,000 K

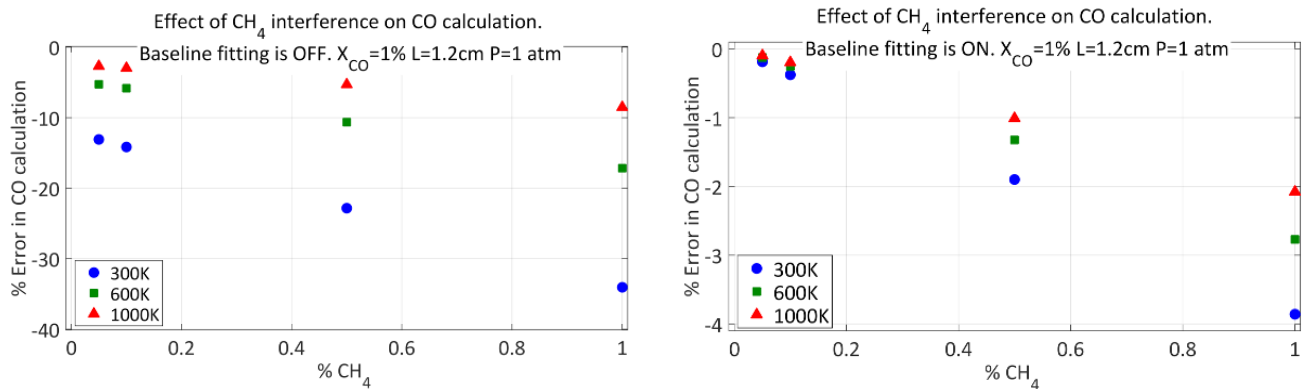


Figure 3. Effectiveness of the iterative baseline fitting procedure for correcting CH<sub>4</sub> interference impacts on the CO measurements. Graphs are error in the calculated CO concentration for a range of temperatures and CH<sub>4</sub> concentrations with the baseline procedure turned off (left) and on (right).

- More complete characterization of combustion and engine system uniformity

## FY 2016 Publications/Presentations

Two archival publications (AP), two conference papers (CP), four oral presentations (OP)

1. J. Yoo, V. Prikhodko, J.E. Parks, A. Perfetto, S. Geckler, W.P. Partridge (2016). "High-speed multiplexed spatiotemporally resolved measurements of EGR dynamics in a multi-cylinder engine using laser absorption spectroscopy," *Applied Spectroscopy* 70, No. 4, 572–584. DOI: 10.1177/0003702816636802. (AP)
2. Kyle Thurmond, Zachary Loparo William Partridge, Subith Vasu (2015). "An LED Based Absorption Sensor for Simultaneous Detection of CO & CO<sub>2</sub>," *Applied Spectroscopy* 70, No. 6, 962–971. DOI: 10.1177/0003702816641261. (AP)
3. W.P. Partridge, G. Jatana, S. Geckler, A. Perfetto. "Cummins-ORNL Combustion CRADA: Characterization & Reduction of Combustion Variations," 2016 DOE Vehicle Technologies Program Annual Merit Review, Washington, DC, June 7, 2016. [http://energy.gov/sites/prod/files/2016/06/f32/ace032\\_partridge\\_2016\\_o.pdf](http://energy.gov/sites/prod/files/2016/06/f32/ace032_partridge_2016_o.pdf). (OP)
4. Gurneesh Jatana, Anthony Perfetto, Sam Geckler, and William Partridge. "Development of an Absorption Spectroscopy Sensor for High-Speed Oxygen Concentration Measurements in the Exhaust of I.C. Engines," 2016 Spring Technical Meeting, Central States Section of the Combustion Institute, Knoxville, TN, May 15–17, 2016. (CP, OP)
5. Kyle Thurmond, et al. "A Light-Emitting-Diode (LED) Non-Dispersive Absorption Sensor for Early Fire and Hazardous Gases Detection," Paper # 138DI-0087, Topic: Diagnostics, 2016 Spring Technical Meeting of the Eastern States Section of the Combustion Institute, Princeton, NJ, March 13–16, 2016. (CP, OP)
6. Michael Villar, Justin Urso, Kyle Thurmond, Akshita Parupalli, Dr. Subith Vasu, Dr. Jayanta Kapat, Dr. Bill Partridge Jr. "Progress in Development and Testing of a LED-Based Fire and Hazard Detection Sensor for Space Vehicles," Commercial and Government Responsive Access to Space Technology Exchange (CRASTE) 2016, Westminster, Colorado, July 21, 2016. (OP)

## II.21 Neutron Radiography of Advanced Transportation Technologies

### Overall Objectives

- Implement high-fidelity neutron imaging capabilities using the High Flux Isotope Reactor (HFIR) for advanced transportation research
  - Once fully developed, this advanced capability will allow the imaging of a range of processes that occur in advanced vehicle systems
- Employ technique to aid improved design and control of complex advanced combustion systems and help to guide model validation and input
- Report findings to research community and work with industrial partners to ensure research is focused on the most critical topics

### Fiscal Year (FY) 2016 Objectives

- Obtain time-stamped neutron radiographs of injection to study internal fluid dynamics using high-frame rate microchannel plate detector
- Compare dynamic injection images of two conditions using gasoline direct injection (GDI)-based injectors; one when cavitation events are likely and one when they are not
- Demonstrate chamber and dynamic neutron radiography can occur using Engine Combustion Network (ECN)-relevant fuel (iso-octane) and temperatures

### FY 2016 Accomplishments

- Dynamic imaging of fluid dynamics inside GDI-based injectors
  - Analyzed flow inside injector using cyclopentane under two conditions
  - Identified fuel in sac long after pintle closed in both cases
- Recorded fuel injection dynamic neutron images using ECN conditions
  - Iso-octane at Spray G2 and G3 conditions
  - Obtained series of images showing deep penetration of liquid into chamber, fluid in sac after closing, prolonged fluid on tip

**Todd J. Toops (Primary Contact),  
Charles E.A. Finney, Eric J. Nafziger,  
Derek Splitter, Hassina Bilheux**

Oak Ridge National Laboratory (ORNL)

1 Bethel Valley Road

Oak Ridge, TN 37763

Phone: (865) 946-1207

Email: [toopstj@ornl.gov](mailto:toopstj@ornl.gov)

DOE Technology Development Manager:

Leo Breton

Subcontractor:

- Professor Jens Gregor, University of Tennessee, Knoxville, TN

- Recorded computed tomography (CT) scan of Spray G-type injector in collaboration with Argonne National Laboratory (ANL)
  - To be combined with their high definition tip CT scan (X-ray)
- GDI-generated particulate study in gasoline particulate filters (GPFs)
  - Demonstrated that the particulate characteristics have markedly different behavior compared to diesel-based particulate ■

### Introduction

Unlike X-rays, neutrons are very sensitive to light elements such as hydrogen (H) atoms and can penetrate through thick layers of metals (Figure 1a) [1]. These two properties suggest neutrons are well suited to probe engine parts such as diesel particulate filters, exhaust gas recirculation coolers, fuel injectors, oil in engines, oil residues in filters, batteries, advanced materials, etc. Neutron imaging is based on the interactions of a sample with a neutron beam. The interactions are dependent on sample thickness/density and elemental make-up and result in absorption and scattering of neutrons within the sample. A two-dimensional position-sensitive detector placed behind the sample can measure the transmitted neutron flux, as illustrated in Figure 1b. When combined

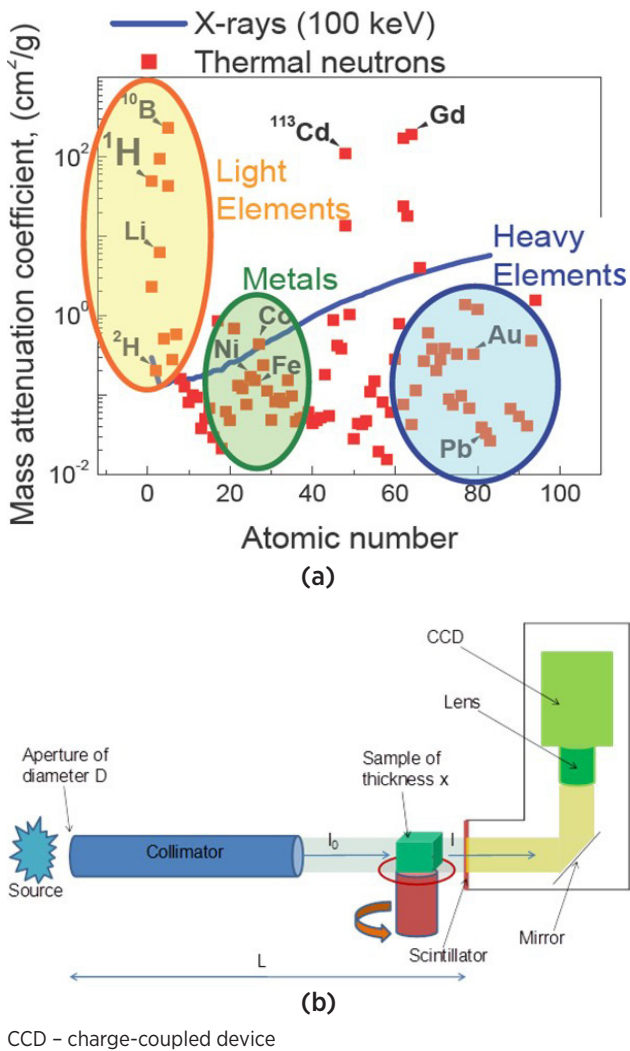


Figure 1. (a) Mass attenuation coefficients of a range of elements as a function of atomic number. Comparison given between neutron (squares) and X-rays (line). (b) Schematic of a neutron imaging facility at ORNL.

with a high-precision ( $\sim 1/100$ th of a degree) rotational stage it is possible to perform CT scans and thus generate three-dimensional images of working fluids inside real devices. Samples can be analyzed at one position or a complete reconstruction can provide a cross-section of the entire sample at a resolution of the detector; the detector resolution is currently at  $\sim 50 \mu\text{m}$  (at the detector).

## Approach

This project is focused on using this unique neutron imaging capability to advance the understanding of two components being employed in modern vehicles: the particulate filter and the in-cylinder fuel injector. Recent efforts are aimed at investigating intra-nozzle fuel injector fluid dynamics while spraying. A specialized fuel delivery

system and spray chamber are employed in this study that mesh well with the neutron beamline and GDI-based injectors (Figure 2). These efforts are designed to improve understanding of how injector design, external conditions, and fuel properties influence internal dynamics, especially as it relates to advanced combustion regimes and injector durability. Particulate filters are a key component of the emissions control system for modern diesel engines, and possibly gasoline engines in the future, yet there remain significant questions about the basic behavior of the filters. In particular, understanding how ash, or non-regenerable metal oxide-based particulate, fills the particulate filter and interacts with the wall is a focus of this effort. The results of these measurements will provide important data to the aftertreatment modeling community on the soot and ash profiles, which change over the course of the vehicle's lifetime. In carrying out these studies, we work closely with industrial partners to obtain relevant systems and devices. The proximity of our research facility to the neutron beam allows for iterative studies when appropriate.

## Results

For the dynamic imaging efforts this year, the project was refocused to facilitate coordination with the ECN. This global community has set guidelines as to which baseline experimental conditions should be employed, and even goes as far as supplying injectors and other hardware. The experimental results can then be shared with the modeling community to help accelerate findings. For the GDI-based injectors that this project is targeting, the specific injection and chamber conditions are listed in Table 1. We are able to approximate the early injection conditions G2 and G3 in our current chamber, and with our new fuel flow meter we can verify the amount of fuel that is being injected. Although we were not able to procure the specific eight-hole injector from the ECN, General Motors provided a single-hole injector that has the same internal geometries and injector hole sizes and angles.

Using the ECN-preferred fuel, iso-octane, a neutron imaging campaign was performed for the G2 and G3 condition. Figure 3a shows a 20  $\mu\text{s}$  composite image for the G2 flash-boiling condition. As in the results discussed last year [2], it is possible to observe the fuel fill the injector sac before being emitted from the injector and into the chamber. The iso-octane spray penetrates into the chamber significantly more than was the case when employing cyclopentane last year. This increased visibility allows for further analysis, as it is possible to quantify the non-uniformity of the spray pattern. The details are not sufficient here to provide detailed analysis, but allows us to compare to other studies to ensure we

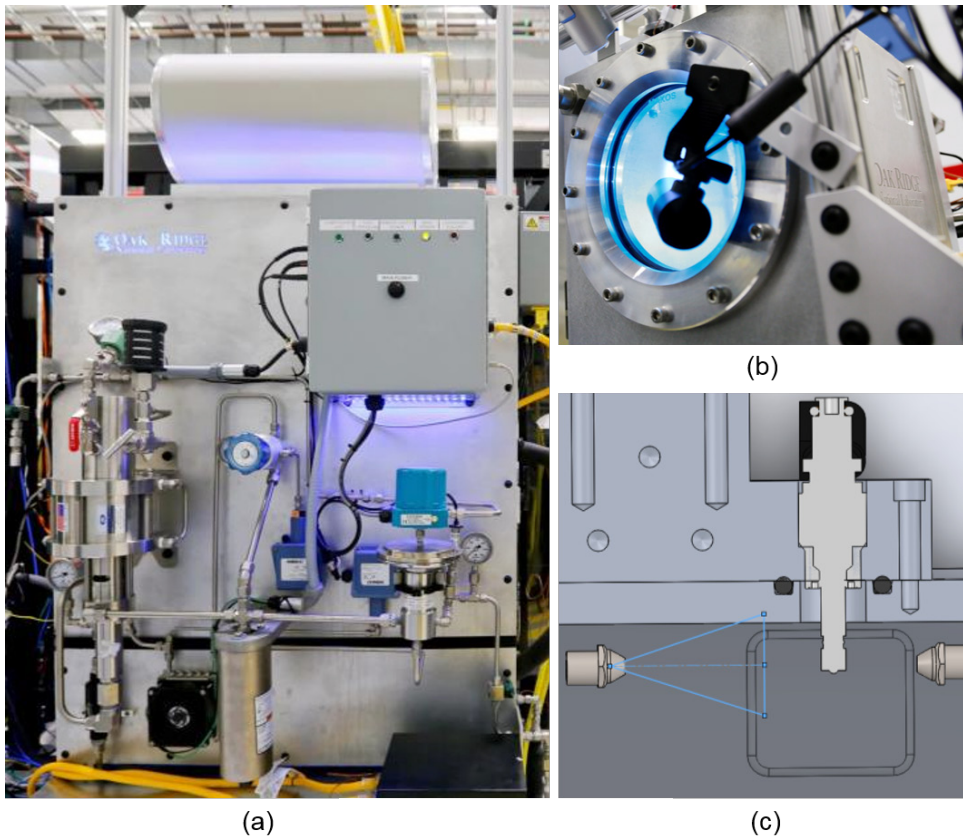


Figure 2. System used to study intra-nozzle fluid dynamics of fuel injection include the (a) high pressure fuel delivery system and (b) the aluminum spray chamber with optical viewport. The spray chamber is designed with (c) directed fans to minimize fuel buildup on the chamber walls and the injector.

**Table 1. ECN Spray G Conditions for GDI-Based Fuel Injectors**

<u>Parameter</u>	<u>Spray G</u> Late injection	<u>Spray G2</u> Early injection	<u>Spray G3</u> Early injection
• Fuel	Iso-octane	Iso-octane	Iso-octane
• Fuel pressure	20 Mpa	20 Mpa	20 MPa
• Fuel temperature	90° C	90° C	90° C
• Injector temperature	90° C	90° C	90° C
• Ambient temperature	300° C	60° C	60° C
• Ambient density (Pressure - Nitrogen)	3.5 kg/m <sup>3</sup> (600 kPa)	0.5 kg/m <sup>3</sup> (50 kPa)	1.0 kg/m <sup>3</sup> (100 kPa)
• Injected quantity	10 mg	10 mg	10 mg
• Number of injections	1	1	1

are achieving similar spray patterns. In this data we can approximate the cone angle and the uniformity of the spray pattern. Figures 3b and 3c show that there are significant gradients in the spray pattern, and this can be used to ensure the results produced here are in line with those produced in other studies. Future analysis will seek to quantify the fluid in the sac by estimating how much of the fuel entering the sac is in the liquid phase versus the

vaporization in the sac. The low density of the vapor fuel will essentially render it invisible to neutrons, especially when compared to the liquid phase.

Additional ECN-relevant efforts this year focused on providing the best possible CT scan of the Spray G GDI injector. In collaboration with ANL, a two-part CT scan was completed employing X-rays for the very tip of the

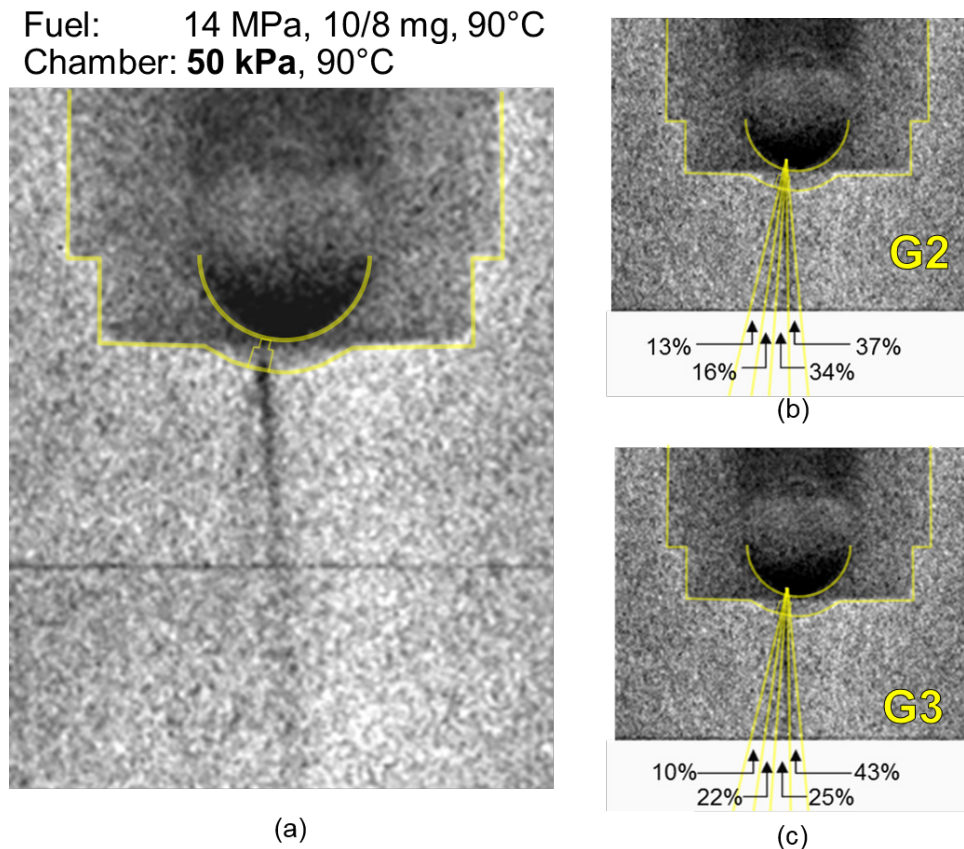


Figure 3. (a) Composite neutron image of iso-octane injection from single-hole GDI-based injector. Penetration of vapor into the chamber is significant and the general uniformity of the spray is analyzed based on chamber condition. Results shown for (b) G2 and (c) G3 which are described in Table 1.

injector and neutrons in the thick metal section that is difficult to fully penetrate with X-rays. The initial results are shown in Figure 4. The results will be co-registered using sophisticated registration software and will be published next FY in an SAE International paper.

Another area of focus continues to be particulate layers that are observed in GPF-studies. GPFs that were filled with particulate from a GDI-based engine using either E0 or E30 (30% ethanol, 70% gasoline mixture) were imaged at HFIR using CT techniques (Figure 5a). The GPFs were originally filled to 4 g/L and then sequentially regenerated followed by imaging (Figure 5b). In contrast to diesel particulate filter-based particulate layers [3], there is minimal decrease in thickness until 40% of the particulate is regenerated. This is observed for both E0 (Figure 5c) and E30 (Figure 5d).

## Conclusions

- Identified and quantified fuel inside injector sac after pintle closed with multiple fuels and conditions

- Applied ECN conditions/fuel in dynamic imaging study (iso-octane at Spray G2 and G3 conditions)
  - Images show deep penetration of liquid into chamber, fluid in sac after closing, prolonged fluid on tip
- Recorded CT scan of Spray G-type injector in collaboration with Argonne National Laboratory
  - To be combined with their high definition tip CT scan
- GPF characteristics continue to demonstrate different behavior compared to diesel-based particulate

## References

- N. Kardjilov, "Absorption and phase contrast neutron imaging," Imaging and Neutrons 2006, Oak Ridge, TN, October 23–25, 2006. [http://neutrons.ornl.gov/workshops/ian2006/MO1/IAN2006oct\\_Kardjilov\\_02.pdf](http://neutrons.ornl.gov/workshops/ian2006/MO1/IAN2006oct_Kardjilov_02.pdf).

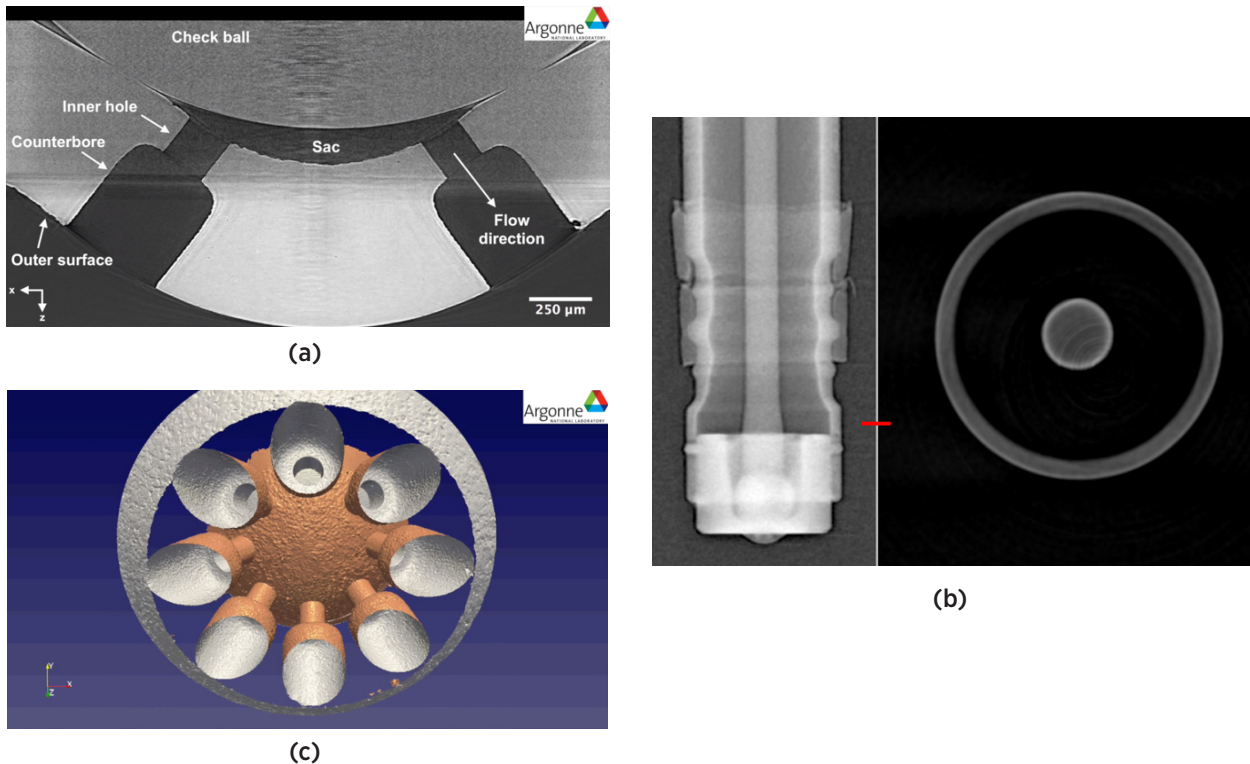


Figure 4. ANL and ORNL are combining (a) X-ray and (b) neutron tomographic image sequences in an effort to compile a composite (c) three-dimensional rendering of the entire GDI-based injector.

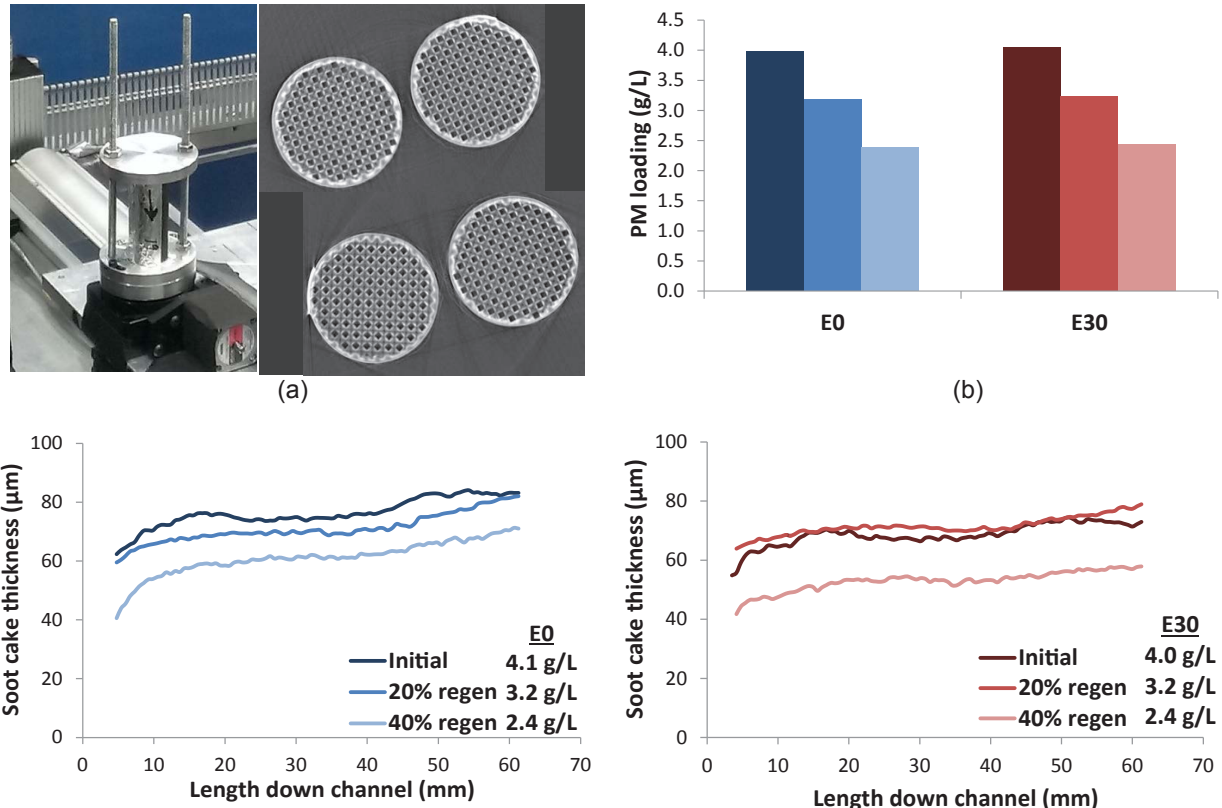


Figure 5. (a) GPFs being imaged at HFIR using CT techniques. (b) GPFs were originally filled to 4 g/L and then sequentially regenerated followed by imaging. Change in soot cake thickness during sequential regeneration for (c) EO and (d) E30.

2. Todd J. Toops, Charles E.A. Finney, Eric J. Nafziger, Hassina Bilheux, "Neutron Imaging of Advanced Transportation Technologies," DOE 2015 Annual Progress Report, March 2016, <http://energy.gov/sites/prod/files/2016/03/f30/FY2015%20Advanced%20Combustion%20Engine%20R%26D%20Annual%20Report.pdf>.
3. Todd J. Toops, Josh A. Pihl, Charles E.A. Finney, Jens Gregor, Hassina Bilheux, "Progression of soot cake layer properties during the systematic regeneration of diesel particulate filters measured with neutron tomography," Emission Control Science and Technology 1:1 (2015) 24-31; DOI: 10.1007/s40825-014-0008-1.

## FY 2016 Publications/Presentations

1. Todd J. Toops, Charles E.A. Finney, Eric J. Nafziger, Hassina Bilheux, "Neutron Imaging of Advanced Transportation Technologies," DOE 2015 Annual Progress Report, March 2016, <http://energy.gov/sites/prod/files/2016/03/f30/FY2015%20Advanced%20Combustion%20Engine%20R%26D%20Annual%20Report.pdf>.
2. (INVITED) Todd J. Toops, Charles E.A. Finney, Eric J. Nafziger, Derek Splitter, Melanie DeBusk, Alex Pawlowski, "Neutron Imaging of Advanced Transportation Technologies," University of New South Wales, Sydney, Australia, July 15, 2016.
3. (INVITED) Todd J. Toops, Charles E.A. Finney, Eric J. Nafziger, Derek Splitter, Melanie DeBusk, Alex Pawlowski, "Neutron Imaging of Advanced Transportation Technologies," U.S. DOE Vehicle Technologies Office 2016 Annual Merit Review and Peer Evaluation Meeting, Washington D.C., June 6–9, 2016.
4. Todd J. Toops, Charles E.A. Finney, Eric J. Nafziger, Derek Splitter, Alex Pawlowski, Hassina Bilheux, Louis Santodonato, Anton Tremsin, "NEUTRON IMAGING OF INTRA-NOZZLE FLUID DYNAMICS IN FUEL INJECTORS," 2016 SAE World Congress, Detroit, Michigan, Detroit, MI, April 12, 2016.
5. (INVITED) Todd J. Toops, Charles E.A. Finney, Eric J. Nafziger, Derek A. Splitter, Hassina Z. Bilheux, Louis J. Santodonato, Jens Gregor, Alex E. Pawlowski, and Anton S. Tremsin, "Neutron radiography of automotive fuel injectors and particulate filters," presentation at the 2015 American Society of Nondestructive Testing Annual Meeting, Salt Lake City, Utah, October 27, 2015.
6. Todd J. Toops, Charles E.A. Finney, Eric J. Nafziger, Derek Splitter, Melanie DeBusk, Alex Pawlowski, "Neutron Imaging of Advanced Transportation Technologies," THIESEL 2016 - Conference on Thermo- and Fluid-Dynamic Processes in Direct Injection Engines, Valencia, Spain, September 13–16, 2016.

## II.22 Ignition and Combustion Characteristics of Transportation Fuels under Lean-Burn Conditions for Advanced Engine Concepts

### Overall Objectives

The primary objective of the proposed research is to characterize low-temperature combustion (LTC) of dimethyl ether (DME) through experiment under conditions of (1) high injection pressure, (2) highly dilute ambient condition, and through numerical work including (3) development of computational fluid dynamics (CFD) predictive tools for emissions, and (4) optimization of a high injection pressure to achieve low emissions formation and high combustion efficiency. The results of this project provide a fundamental study of spray and combustion processes over a wide range of pressures and temperatures through experimentation with support of high-fidelity CFD simulation.

### Fiscal Year (FY) 2016 Objectives

- Perform DME and diesel engine bench test with various exhaust gas recirculation (EGR) levels
- Explore DME spray and combustion characteristics with multi-hole injector under nonvaporizing, vaporizing, and combusting conditions
- Provide a fundamental understanding of DME LTC via combustion vessel (CV) experiment
- Demonstrate engine performance of DME
- Build and validate CFD simulations for both CV tests and engine tests

### FY 2016 Accomplishments

- Manufactured a new generation hydraulically actuated, electronically controlled, unit injector (HEUI) and tested in CV and engine for stated condition above
- Performed multi-hole injector tests for nonvaporizing, vaporizing, and combusting spray high-speed visualization, for a wide range of injection pressures including diesel like pressures, in CV
- Demonstrated LTC of DME spray in CV
- Developed a mechanical injection system with electronic throttle for engine bench test

### Seong-Young Lee

Michigan Technological University  
815 R.L. Smith Bldg.  
1400 Townsend Drive  
Houghton, MI 49931  
Phone: (906) 487-2559  
Email: sylee@mtu.edu

DOE Technology Development Manager:  
Leo Breton

#### Subcontractors:

- Sreenath Gupta, Argonne National Laboratory, Chicago, IL
- James Cigler, Navistar, Chicago, IL
- William de Ojeda, WMI, Chicago, IL (main fuel injection system vendor)

- Performed DME and diesel engine bench test with various EGR rates
- Updated injector modeling for multi-hole DME and diesel injectors
- Completed Reynolds-averaged Navier-Stokes (RANS) CFD of DME sprays (including multi-hole nozzle) with validated experimental combustion data
- Developed large eddy simulation (LES) CFD of DME sprays with validated experimental combustion data
- One doctoral student (full support, Khanh Cung) completed Ph.D. defense in 2015 and is currently working at Argonne National Laboratory as a postdoctoral scholar
- One doctoral student (partial support, Ahmed Abdul Moiz) completed Ph.D. defense in 2016 and he is currently working at Argonne National Laboratory as a postdoctoral scholar ■

## Introduction

This project consists of an extensive numerical and experimental characterization of spray and combustion of DME, which is an attractive alternative to conventional diesel fuel for compression ignition engines. DME produces no soot and has a higher combustion quality due to its higher cetane number relative to diesel fuel. Additionally, fast evaporation and good atomization are superior characteristics of DME relative to diesel, resulting in improved combustion performance. The third year of this project mainly focused on multi-hole injector CV tests, LTC CV tests, engine bench tests, and engine simulations using RANS models. We have moved on into the engine bench testing phase and established a correlation between results from the CV test and engine experiment. The significance of performance of various DME tests and their CFD models is to achieve the LTC for higher engine combustion efficiency and reduction of harmful emissions.

## Approach

This project is a collaborative work between Michigan Technological University, Navistar, Argonne National Laboratory, and WMI. The DME injection system was integrated to the Michigan Technological University CV system. This system is designed to enable various experiments (nonvaporizing, vaporizing, and combusting) and nonintrusive visualization diagnostics (hybrid of Mie scattering and schlieren,  $\text{CH}_2\text{O}$ -planar laser-induced

fluorescence [PLIF], photodiode, spectroscopy, and direct flame luminosity). Rate of injection (ROI) was also tested using a Bosch tube method. Two-stage Lagrangian, three-dimensional RANS and LES CFD simulations were performed and validated against experimental data. Engine bench tests and engine simulations were performed and validated.

## Results

The injector model was updated to accurately predict ROI of DME and diesel with multi-hole ( $8 \mu\text{m} \times 155 \mu\text{m}$ ) and single-hole ( $180 \mu\text{m}$ ) at injection pressures of 750 bar, 1,000 bar, 1,250 bar, and 1,500 bar. Results indicated that higher injection pressure leads to longer injection duration and shorter injection delay. Single-hole injector ROI profiles at different injection pressure show a two-stage shape with the first stage ending at the same time, but the second stage ending later at a higher injection pressure. This study provides the basis for future work to optimize a DME injection system in compression ignition engines.

An eight-hole injector with  $145^\circ$  inclined angle was tested with both diesel and DME spray combustion in a CV. Ambient temperature ranged from 750 K to 1,100 K, and ambient density was  $14.8 \text{ kg/m}^3$ . Fuel energy content for both fuels was matched by varying (1) injection pressure, and (2) injection duration. Photodiode, flame luminosity, and  $\text{OH}^*$  chemiluminescence were used in this test. Figure 1 shows the sample images from all

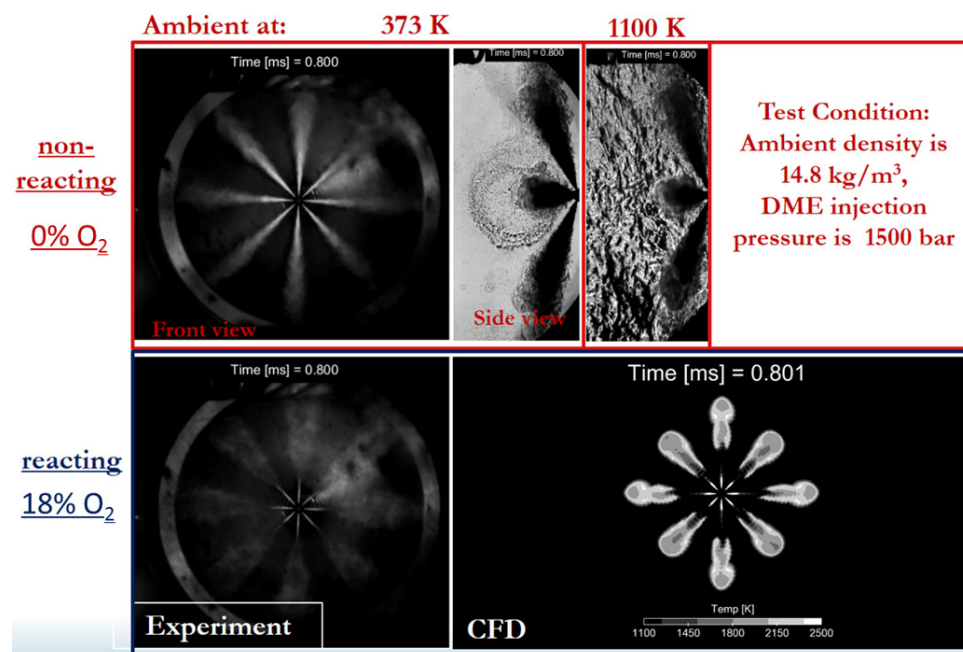


Figure 1. High-speed images of DME eight-hole sprays in nonreacting and reacting conditions with comparison of CFD results (after start of injection [ASOI] = 0.8 ms)

techniques. From the luminosity images, we can see clearly that DME produces lower soot compared to diesel. In-cylinder pressure was interpreted into pressure-based ignition delay and apparent heat release rate (AHRR). Injection pressure of 1,000 bar cases shows overall comparable ignition delay with 1,500 bar cases, and displays a similar trend that ignition delay decreases while ambient temperature increases. Compared to diesel, DME has a shorter ignition delay. Based on fractions (10% and 90%) of cumulative heat release, the burn duration was determined. Figure 2 shows the AHRRs and burn durations for DME and diesel. The amount of energy injected in the chamber is the same for both DME and diesel injections. Energy adjustment by injection pressure (Figure 2, bottom plot) causes low injection pressure diesel to combust inefficiently, which may be caused by the poor mixing. Energy adjustment by injection duration (Figure 2, top plot) does not show this trend. Burn duration of diesel is longer than DME. End gas combusts near the chamber walls for a longer time for diesel at 900 K and 1,100 K ambient temperatures.

Pressure fluctuations were observed between 850–1,050 K tested ranges, which was also observed in DME spray combustion with an equivalent diesel energy content. This is mostly caused by the ignition of top plumes before the bottom plumes ignite (temperature inhomogeneity in CV preburn). A CFD RANS model was validated against the experimental data.

The 180- $\mu\text{m}$  nozzle was tested for nonvaporizing ( $\text{N}_2$ ), vaporizing (0%  $\text{O}_2$ ), and LTC (15–21%  $\text{O}_2$ ) conditions, with ambient temperatures ranging from 700–800 K, injection pressures of 500–1,500 bar, and ambient density of 14.8  $\text{kg/m}^3$ . Optical diagnostics used were a hybrid of Mie and schlieren, formaldehyde-PLIF, and direct flame luminosity. Injection pressure and injection duration effects were studied in LTC conditions, as shown in Figure 3. At 1,500 bar injection condition, injection starts earlier with longer injection duration, and slightly longer ignition delay due to the charge cooling effect. Earlier injection in AHRR shows premixed and a significant flame recession takes place after maximum AHRR. The small platform in AHRR (red circle) is from the initial

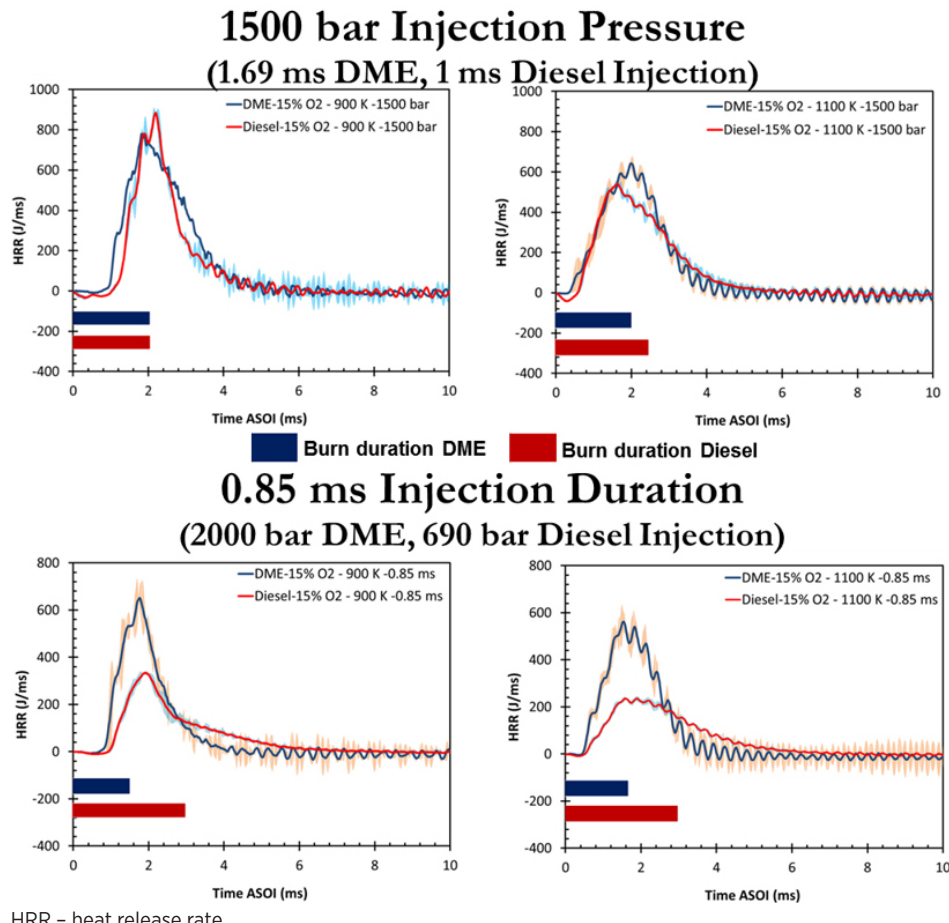


Figure 2. Impact of injection pressure and injection duration on AHRR for equivalent DME and diesel energy (eight-hole injector)

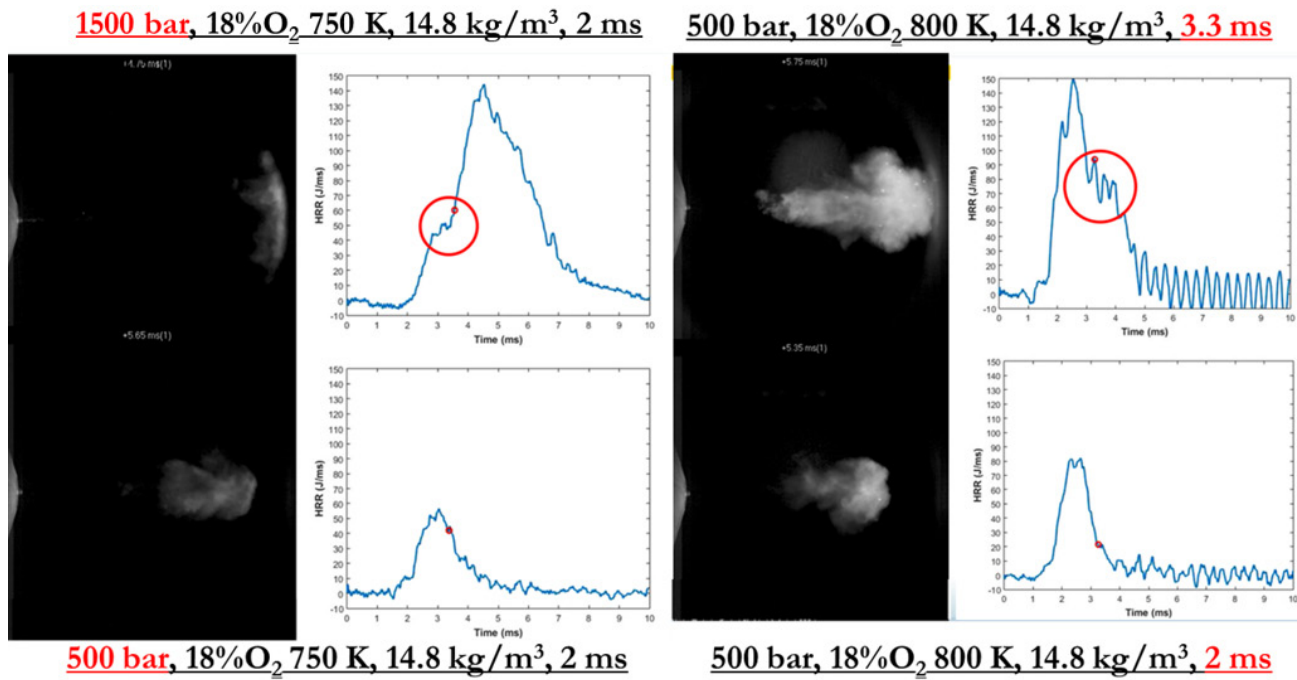


Figure 3. Flame luminosity with heat release rate: injection pressure effect and injection duration effect

contact with the cold wall. Pressure rise is slightly faster than the visible luminosity possibly due to cool flames. In the 1,500 bar injection pressure case, injection starts later and has a shorter injection duration. Similar liquid penetration is observed for two cases (1,000 bar and 1,500 bar), but shorter lift-off length and less flame recession are seen in low injection pressure condition. In the long duration case, strong unstable flame takes place on auto-ignition where flame propagates upstream and downstream. Pressure oscillation starts where intensive flame takes place near the wall. The platform (red circle) in AHRR is from the initial contact with the cold wall, and triggers strong pressure oscillation. Long injection keeps providing the reaction source to sustain the pressure oscillation and helps to reach a high peak in AHRR. With the short injection duration, the flame initiates at the end of the injection and does not reach the opposite wall which is a geometrical bound for the flame oscillation. Injection duration and the location of intense reaction are a major source of flame instability.

In a prior report, simulations were run with RANS turbulence modeling approach for DME. The LES approach has been adopted for an LTC condition in this work and the results are encouraging. RANS simulations predict longer ignition delays due to the poor mixing prediction, leading to the slow flame penetration (flame takes longer time to reach wall). Mixture distribution is wider and homogenous at first-stage ignition spots in the LES simulation compared to that in the RANS simulation.

LES is critical in studying ignition processes which are highly dependent on mixture formation impacted from turbulent fuel-air mixing. Figure 4 shows the ignition and flame stabilization processes in LES simulations. Subtle changes in temperature is seen all throughout the ignition process starting from the first-stage ignition until the fuel-air mixture temperature reaches the high-temperature, second-stage ignition conditions. This process lasts for about 0.3–0.4 ms. Ignition occurs in the far downstream region which usually has lower turbulence than upstream. Flame stabilization occurs via creation of ignition kernels near the lift-off zone as seen in diesel cases.

Engine tests and simulations in this work were performed with a 0.44 L single-cylinder compression ignition engine. The bore diameter and stroke are 86 mm and 75 mm, respectively, with a compression ratio of 21.2. A five-hole injector with diameter of 180  $\mu$ m was used and located in the top center of the chamber head. Engine tests were done at varying speeds, loads, and combustion phasing for both diesel and DME to compare the combustion performance and emissions characteristics. The engine fuel supply system was put in place to provide the capability to switch between diesel and DME during its operation and evacuate the DME upon shutdown. The engine mechanical fuel system was modified to have electronic control over the throttle. Engine results in Figure 5 showed that in-cylinder pressure curves from both DME and diesel cases are similar but DME has a shorter ignition delay than diesel. Besides, the emissions

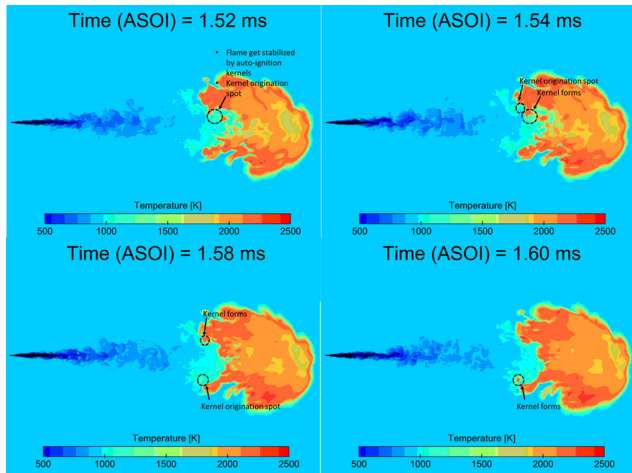


Figure 4. LES ignition and flame stabilization processes

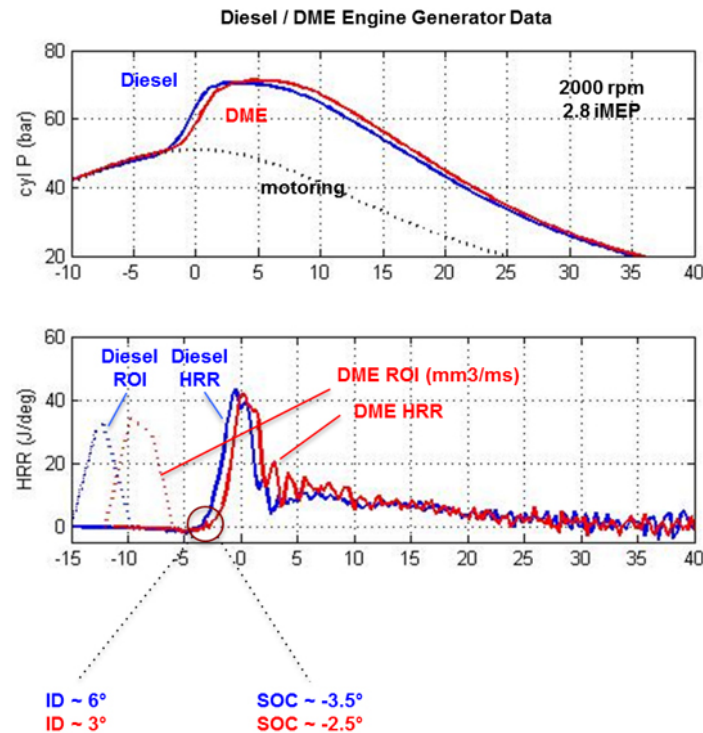
of  $\text{NO}_x$  from DME (142 ppm) is less than diesel (281 ppm) at the same operating condition (8% EGR). Engine simulations were done only for DME and were for the closed portion of the cycle going from intake valve closing at  $-180^\circ$  crank angle (CA) before top dead center, through exhaust valve opening at  $101^\circ$  CA after top dead center (ATDC) at 2,000 rpm. The in-cylinder pressure and

heat release rate are illustrated in Figure 6. The dash line indicates the experimental results while solid lines are simulation results of mean pressure and heat release rate. The overall pressure trends showed a good agreement with the experimental results. Ignition delay in the current study is predicted from CA 10 in both experiment and simulation. Ignition delay from simulation matches well with the experimental result. Furthermore, until exhaust valve open (end of the combustion cycle), the emission of  $\text{NO}_x$  ( $\text{NO} + \text{NO}_2$ ) from the simulation (174 ppm) shows good agreement with the experimental measurement (175 ppm) at the same operating condition (10% EGR).

## Conclusions

### Multi-Hole Spray

The eight-hole HEUI injector was tested at the CV for both DME and diesel fuels. Comparisons were done on the effects of ambient temperature and injection pressure on DME and diesel combustion characteristics for the same fuel energy content. Fuel energy content for both fuels was matched by varying injection pressure and injection duration. Overall, DME has stronger reactivity than diesel. Diesel has longer burn durations which resulted in energy losses through flame-wall interactions.



ID – ignition delay; SOC – start of combustion; iMEP – indicated mean effective pressure; SOI – start of injection; EOI – end of injection; HC – hydrocarbon; PM – particulate matter; NOx – oxides of nitrogen; deg – degree; dur – duration; Ign – ignition; dBTD – degrees before top dead center

Figure 5. Engine test data: combustion of DME vs. diesel

**Ignition characteristics exhibit differences between Diesel and DME**

	Diesel	DME
iMEP, bar	2.7	2.8
Mf, mm <sup>3</sup>	8.5	11.6
Mf DGE	-	~7
SOI, dBTD	15	12
Dur, deg	5.3	5.6
EOI, dBTD	9.7	6.4
SOC, dBTD	3.5	2.5
Ign delay, deg	6.2	2.9
HRR, J	260	250
NOx, ppm	281	142
HC, ppm	10	30
PM, g/kWhr	0.12	0.005

**DME shorter ignition delay is compensated by more rapid mixing process reflected too in better NOx emissions**

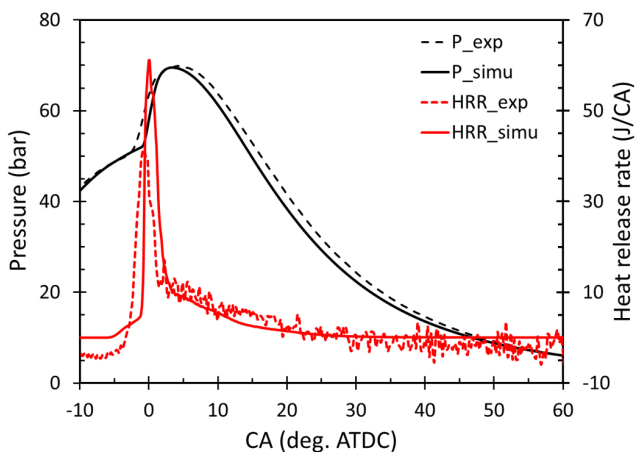


Figure 6. In-cylinder pressure and apparent heat release rate comparison between experiment and simulation for DME

### LES vs. RANS Model Comparison

LES simulation is critical in providing the detail ignition and flame stabilization processes due to better mixing predictions.

### Spray Tests under LTC

Flame recession which diesel does not show was detected happening near end of ignition in LTC of DME spray, which reduces the unburned hydrocarbon emissions. It is observed unstable flame behavior and combustion instability under LTC. High-pressure injection has a shorter injection delay, longer duration, longer lift-off length, and slightly longer ignition delay at 750 K due to the charge cooling effect, but different injection pressures have similar liquid penetrations.

### Engine Test and Engine Simulation

Engine testing showed that the fuel system could switch between diesel and DME within a few seconds. The supply system is capable to retain the fuel supply under liquid phase by means of direct control over the fuel pumps. Tests showed that the fuels impact the heat release process while the gas exchange process is nearly the same. The injection system allows approximately 10% high volumetric flow rates of DME, but the required longer injection duration of DME retains the same energy

for a given load. Engine test results also showed that DME has a shorter ignition delay than diesel. Engine simulations were done only for DME and simulation results of in-cylinder pressure and heat release rate showed good agreement with the test results. Engine simulations also predicted a reasonable emissions formation which matches with experimental data.

### FY 2016 Publications/Presentations

1. Khanh Cung, Ahmed Abdul Moiz, Xiucheng Zhu, Seong-Young Lee. Ignition and Formaldehyde Formation in Dimethyl Ether (DME) Reaction Spray under Various EGR Levels. Proceedings of the Combustion Institute 36, 2016.
2. Xiucheng Zhu, Sanjeet Limbu, Khanh Cung, William De Ojeda, and Seong-Young Lee. HEUI Injector Modeling and ROI Experiment for High Injection Pressure of Diesel and Dimethyl Ether (DME). No. 2016-01-0855. SAE Technical Paper, 2016.
3. Khanh Cung, Xiucheng Zhu, Ahmed Abdul Moiz, Seong-Young Lee, and William De Ojeda. Characteristics of Formaldehyde (CH<sub>2</sub>O) Formation in Dimethyl Ether (DME) Spray Combustion using PLIF Imaging. *SAE Int. J. Fuels Lubr.* 9(1):138–148, 2016, doi:10.4271/2016-01-0864, April 2016.
4. Seong-Young Lee, “NSF/DOE AEC Program: High Injection Pressure Dimethyl Ether (DME) Spray and Combustion Characteristics under Engine-Relative Conditions,” Ulsan University, South Korea, April 8, 2016.
5. Seong-Young Lee, “NSF/DOE Partnership on Advanced Engine Combustion: DME Spray CV Testing, Modeling and Application of High Pressure DME Fuel System to Engine,” 2016 Advanced Engine Combustion Program Review Meeting at Sandia National Laboratories (Livermore), February 2016.
6. Seong-Young Lee, “DME Spray Combustion and Engine Performance,” 2016 Advanced Engine Combustion Program Review Meeting at USCAR – Southfields, August 2016.

# II.23 A Comprehensive Investigation of Unsteady Reciprocating Effects on Near-Wall Heat Transfer in Engines

## Overall Objectives

- Use collaborative experiments and numerical simulations to investigate unsteady reciprocating effects on heat transfer in piston engines
- Develop a two-wavelength infrared (IR) temperature diagnostic capable of acquiring surface temperature measurements and wall heat flux in piston engines at high frequency
- Formulate the foundations for the modeling of heat transfer in piston engines that account for the effects of rapid transients and non-equilibrium boundary layer behaviors

## Fiscal Year (FY) 2016 Objectives

- Conduct optical engine experiments to study and quantify near-wall transport of momentum and heat in a piston engine under reversing flow motored conditions
- Conduct pulsatile boundary layer flow experiments to study and quantify near-wall transport of momentum and heat in a periodically forced boundary layer flow
- Study the mechanism of transition to turbulence in reciprocating flow

## FY 2016 Accomplishments

- Acquired near-wall profiles of velocity (using micro-scale particle image velocimetry [PIV]) and temperature (using planar laser-induced fluorescence [PLIF]) in a motored engine near top dead center (TDC)
- Acquired planar fields of velocity (using PIV) in pulsatile boundary layer flow for various forcing parameters
- Identified that an internal shear layer, which emerges just prior to flow deceleration, is the key mechanistic trigger for transition to turbulence in reciprocating flow ■

## Introduction

This project investigates the effects of rapid transients on heat transfer in reciprocating piston engines. The capacity to understand and predict heat transfer is critically important for optimizing fuel efficiency, reducing harmful engine-out emissions, and furthering advanced combustion strategies. This research project

**Christopher White<sup>1</sup> (Primary Contact),  
Marcis Jansons<sup>2</sup>, Yves Dubief<sup>3</sup>**

<sup>1</sup>University of New Hampshire,  
Kingsbury Hall Room W101  
33 Academic Way  
Durham, NH 03824  
Phone: (603) 862-1495  
Email: chris.white@unh.edu

<sup>2</sup>Wayne State University  
Detroit, MI 48202

<sup>3</sup>University of Vermont  
Burlington, VT 05405

DOE Technology Development Manager:  
Leo Breton

is motivated by the fact that engine computational fluid dynamics simulations almost exclusively use heat transfer models that cannot accurately capture the effects of rapid transients, and in turn cannot accurately predict heat transfer over a typical drive cycle.

The modeling difficulty is owed to nonlinear interactions between in-cylinder turbulence, fuel injection, combustion, piston geometry, and piston motion that produce complex fluid transport behaviors adjacent to the cylinder wall. The project work combines analytical, numerical simulations, and experiments to study how these complex transport behaviors affect heat transfer. The overarching goal is to use the results from these scientific investigations to improve upon the robustness of engine heat transfer models so that they can be used for engineering design of low-emission, high-efficiency engines. Increasing the efficiency of internal combustion engines while reducing their emissions is one strategic goal of the DOE Vehicle Technologies Office [1].

## Approach

Complementary laboratory and numerical experiments of increasing complexity are being conducted to study and quantify the fundamental thermal transport processes found in reciprocating piston engines. The approach is to conduct experiments in an optical piston engine as well as in a simpler flow configuration, namely boundary

layer flow over a constant temperature wall. The engine experiments will provide data necessary to evaluate and develop engine heat transfer models. The experiments will also further develop the fundamental knowledge base of heat transfer in internal combustion engines. The boundary layer studies are designed to simulate and isolate certain boundary layer behaviors found in piston engines. For example, to understand the effects of unsteady pressure forcing, flow reversal, or the effects of flow separation on heat transfer. Isolating these effects are not possible in an engine flow but important to develop robust heat transfer models that capture the dominant physics.

Informed by experimental and numerical results, a first-principles modeling approach is being used to develop new heat transfer models that better capture the transport mechanisms in non-equilibrium boundary layers and piston engines. The modeling approach exploits scale separation associated with either coherent turbulent flow structures or distinct turbulence regimes identified through existing but newly emerging data analysis techniques.

## Results

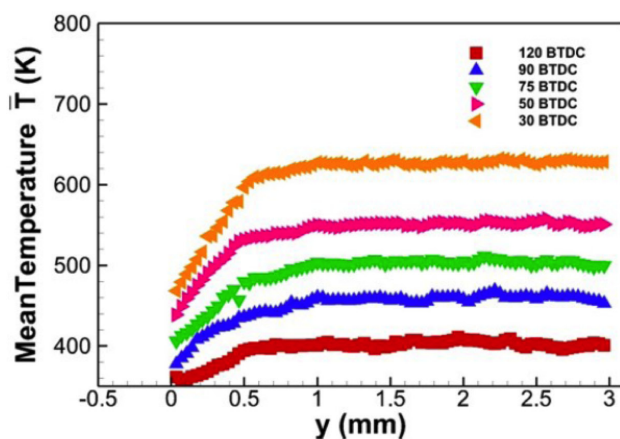
FY 2016 (third year of the project) results primarily relate to (1) near-wall measurements of the boundary layer velocity and temperature fields in a piston engine near TDC, (2) fundamental studies of pulsatile boundary layer flow, and (3) understanding the mechanism of transition to turbulence in reciprocating flow.

### Optical Engine Experiments

Simultaneous measurements of surface temperature (IR diagnostic) and thermal boundary layer temperature fields

(toluene PLIF) performed in FY 2015 were repeated and extended to include measurements near TDC. In the optical engine under motored conditions and with an oxygen-free charge of pure nitrogen, a pulsed 266-nm laser sheet was directed through the thermal boundary layer perpendicular to the firing deck. A spectrometer and micro lens system measured the resulting temperature-dependent fluorescence spectrum while the IR diagnostic was used to measure the surface temperature. The measured temperature profiles followed equilibrium flow scaling laws during compression, but deviated significantly from these scaling laws during expansion (see Figure 1). This suggests that heat transfer models based on equilibrium flow scaling laws will not accurately predict the wall heat flux during the early portion of the expansion stroke. The likely reason being that flow reversal near TDC generates large-scale vortical motions that strongly influence the boundary layer dynamics.

The flow field near TDC was investigated using micro-PIV. The experiments were conducted for the same engine operating conditions as for the toluene PLIF experiments. Diesel fuel droplets, injected towards the end of the intake stroke (250° BTDC), were used as flow tracers. Planar fields of velocity were acquired in a  $4.2 \text{ mm}^2 \times 4.6 \text{ mm}^2$  area perpendicular to the firing deck and 3.5 mm from the cylinder axis. Wall-normal profiles of the velocity component parallel to the wall (denoted by U) and normal to the wall (denoted by V) normalized by piston velocity ( $V_p$ ) are plotted in Figure 2 and Figure 3, respectively. It is evident that the flow near TDC is complex. In particular, the flow is not symmetric about TDC, and the velocity magnitude is smaller during the expansion stroke compared to the compression stroke.



BTDC – before top dead center; ATDC – after top dead center

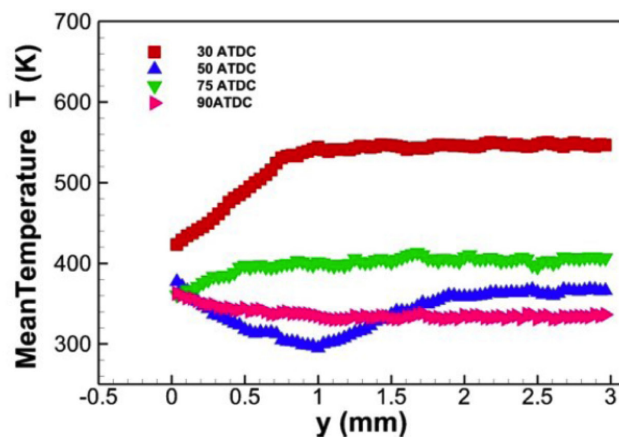


Figure 1. Mean temperature profiles during compression stroke (left) and expansion stroke (right)

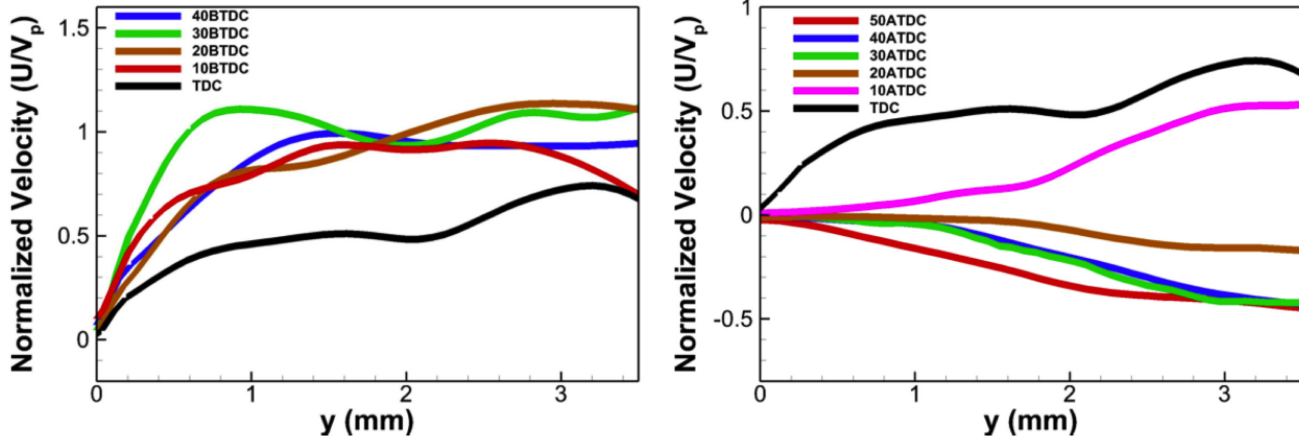


Figure 2. Mean U-velocity profiles during compression stroke (left) and expansion stroke (right)

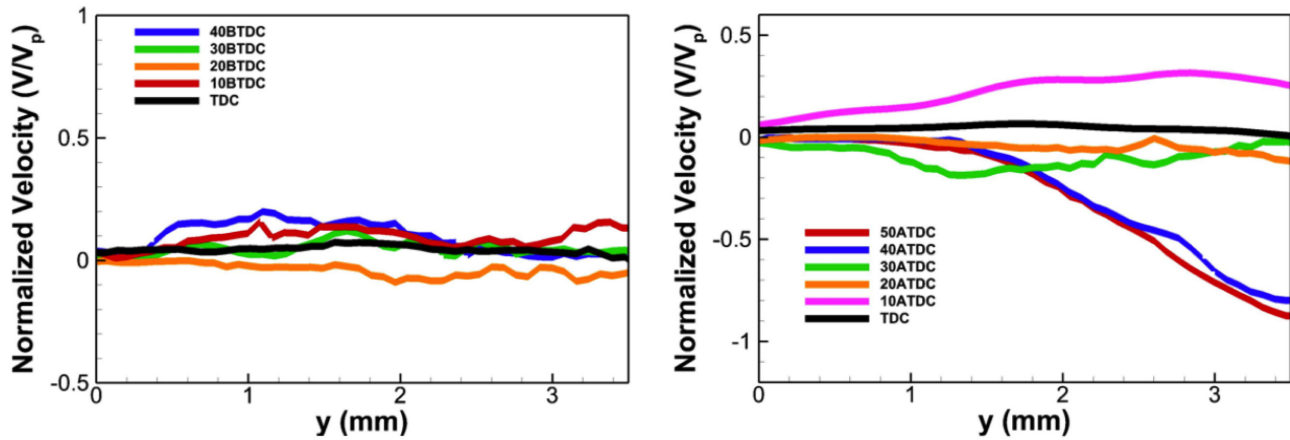


Figure 3. Mean V-velocity profiles during compression stroke (left) and expansion stroke (right)

Additionally, the U component in the measurement plane reverses direction between 10–20° ATDC (i.e., later than TDC). The V component also reverses direction but is very small in magnitude at the crank angle degree when the U component reverses direction. In summary, both temperature and velocity fields in the boundary layer show complex behaviors (different than equilibrium boundary layer behaviors) near TDC.

### Boundary Layer Experiments

Pulsatile boundary layer flow is a wall-bounded, unidirectional flow driven by a periodic pressure gradient. The transport of momentum in pulsatile boundary layer flow was studied using PIV. The objective was to isolate and study the effects of unsteady pressure forcing (which occurs in an engine as induced by the piston motion) on the transport of momentum in the boundary layer.

Experiments were conducted at three forcing frequencies:  $\omega^+ = 0.007; 0.014; 0.020$  where + denotes normalization

by viscous units. Analysis of the PIV vector fields showed that the oscillating component of the wall shear stress for the highest forcing frequency case phase-leads the free-stream velocity. Consequently, owing to this phase difference, eddy viscosity models (i.e., the typical turbulence model type used in computational fluid dynamics simulation) are not expected to predict the oscillating field correctly, as these models assume the stress and strain are in phase.

### Fundamental Studies Investigating Transition to Turbulence in Reciprocating Flow

The mean dynamics in reciprocating channel flow was studied to better understand transition to turbulence in reciprocating flows. The balance of the leading order terms in the phase-averaged mean momentum equation confirmed that fully developed turbulence first emerges at the early phases in the decelerating portion of the cycle. The underlying mechanism of this transition is the

emergence of an internal shear layer that first develops during the late phases of the accelerating portion of the cycle. In the absence of this internal shear layer, the flow remains transitional over the entire cycle.

In fully-developed channel flow with a periodic pressure gradient, the phase-averaged momentum equation is

$$\underbrace{-\frac{\partial U}{\partial t}}_{\text{i}} + \underbrace{\frac{1}{\rho} \cos(\omega t)}_{\text{ii}} + \underbrace{\nu \frac{\partial^2 U}{\partial y^2}}_{\text{iii}} + \underbrace{\frac{\partial(-\bar{u}'v')}{\partial y}}_{\text{iv}} = 0, \quad (1)$$

where  $t$  is time,  $\omega$  is the angular frequency,  $x$  and  $y$  are streamwise and wall-normal directions,  $U$  is the phase-averaged velocity in the  $x$  direction,  $u'$  and  $v'$  are fluctuating velocities in  $x$  and  $y$  directions, and  $\rho$  and  $\nu$  are the density and viscosity of the fluid, respectively. The ratio of term iii and term iv as a function of wall-normal position is shown in Figures 4a and 4d for  $Re_s = 648$  and 1019, respectively, where  $Re_s$  is the Reynolds number based on the Stokes length (which depends here only on the forcing frequency,  $\omega$ ). A four-layer structure similar to that first described by Luo et al. [2] for canonical

wall-bounded flow emerges at  $9\pi/16 \leq \phi \leq 11\pi/16$  for  $Re_s = 1019$ , where  $\phi$  denotes the phase angle. Similarly, the phase-averaged velocity and temperature profiles shown in Figure 4e at the same phase angles agree reasonably well with the expected scaling laws for equilibrium wall-bounded turbulent flow. Conversely, the profiles for  $Re_s = 648$  do not exhibit behaviors similar to canonical wall-bounded flow at any phase. In summary, fully-developed turbulent flow behaviors are observed for  $Re_s = 1019$  (during the early phases in the decelerating portion of the cycle) but not for  $Re_s = 648$ .

To investigate the mechanisms of transition to turbulence, the temporal acceleration (term i in Equation 1) for each phase angle in a half-cycle is shown Figures 4c and 4f for  $Re_s = 648$  and 1019, respectively. For  $Re_s = 1019$ , inspection of the phases prior to and after  $\phi = \pi/2$ , when the bulk flow transitions from an accelerating flow to a decelerating flow, reveals the emergence of an internal shear layer that decelerates at a phase-lead compared to the near-wall and core regions. With increasing phase

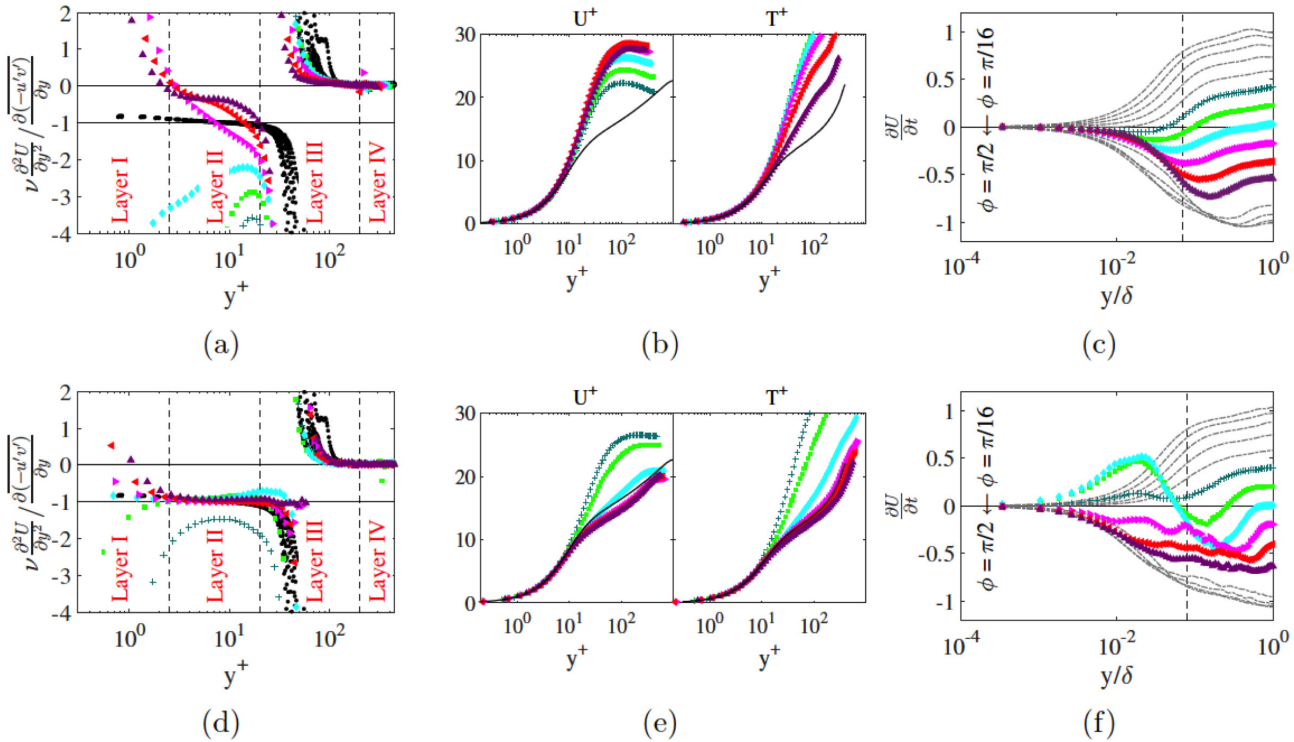


Figure 4. The ratio of term iii and term iv in Equation 1 as a function of wall-normal position for  $Re_s = 648$ . Black circles represent equilibrium turbulent boundary layer behaviors at different Reynolds numbers. Vertical dashed lines mark the approximate boundary between the four layers introduced by Luo et al. [2]. Dark green ( $\oplus$ ), light green ( $\blacksquare$ ), and cyan ( $\blacklozenge$ ) are  $\phi = 6\pi/16, 7\pi/16, 8\pi/16$ , respectively. Magna ( $\blacktriangleright$ ), red ( $\blacktriangleleft$ ) and purple ( $\blacktriangleup$ ) are  $\phi = 9\pi/16, 10\pi/16, 11\pi/16$ , respectively. (b) Phase-averaged profiles of velocity and temperature in wall-units for  $Re_s = 648$ . Black lines represent ensemble-averaged profiles of fully-developed turbulent channel flow. (c) Phase-averaged profiles of term i in Equation 1 for  $Re_s = 648$ . Grey lines are the rest of the phases with phase increasing from top to bottom. Vertical dashed line marks the laminar Stokes layer. (d), (e) and (f) are the same profiles as (a), (b) and (c) for  $Re_s = 1019$ . Colored line identifiers and symbols are the same in all six figures.

(i.e., bulk flow deceleration), the internal shear layer likely rolls-up triggering further flow instabilities that transition the flow to a fully-developed turbulent channel. The eventual acceleration of the flow suppresses the turbulence and the flow transitions back to a transitional flow. The cycle is then repeated indefinitely. For  $Re_s = 648$ , an internal shear layer does not emerge and the flow never transitions to a fully developed turbulent channel. It follows that the key mechanism of transition to turbulence in periodic flow is the emergence of an internal shear layer that first emerges during the late stage of the accelerating portion of the cycle.

## Conclusions

- The results from the engine and boundary layer experiments show that strong flow perturbations (e.g., flow reversal and/or strong pressure forcing) significantly modify the distribution of temperature and velocity in the boundary layer compared to equilibrium boundary layer behaviors.
- The observed flow complexities (see bullet above) strongly suggest that existing heat transfer models (based on equilibrium flow behaviors) will fail in an engine near TDC during flow reversal or for other strong boundary layer perturbations.
- The specific work related to the engine experiments, fundamental boundary layer studies, and numerical simulations is converging. The objective is to utilize the knowledge gained from these converged studies to develop robust engine heat transfer models.

## References

1. United States Department of Energy. Office of Energy Efficiency and Renewable Energy. U.S. DRIVE, Advanced Combustion and Emission Control Technical Team Roadmap 2013. [http://energy.gov/sites/prod/files/2014/02/f8/acec\\_roadmap\\_june2013.pdf](http://energy.gov/sites/prod/files/2014/02/f8/acec_roadmap_june2013.pdf)
2. Wei T., Fife P., Klewicki J., McMurtry P., "Properties of the mean momentum balance in turbulent boundary layer, pipe and channel flows," *J. Fluid Mech.*, 552 (2005) 303–327.
3. Yu, X., Liu, X., Jansons, M., Kim, D., Martz, J., Violi, A., "A Fuel Surrogate Validation Approach Using a JP-8 Fueled Optically Accessible Compression Ignition Engine," *SAE Int. J. Fuels Lubr.* 8(1) 2015, doi:10.4271/2015-01-0906.
4. Luo, X., Yu, X., Jansons, M., "Simultaneous In-Cylinder Surface Temperature Measurements with Thermocouple, Laser-induced Phosphorescence, and Dual Wavelength Infrared Diagnostic Techniques in an Optical Engine," *SAE Technical Publication* 2015-01-1658.
5. Ebadi A., White C.M., Pond I., Dubief Y., "Mechanism of transition to turbulence in reciprocating channel flow," *24th Int. Conf. Theor. Mech.*, Montreal, Canada (2016).
6. C.M. White, M. Jansons and Y. Dubief. "NSF/DOE Partnership On Advanced Combustion Engines: Unsteady Reciprocating Effects On Near-Wall Heat Transfer In Engines," Advanced Engine Combustion Program Review Meeting, Southfield, Michigan (2016).
7. C.M. White, M. Jansons and Y. Dubief. "NSF/DOE Partnership On Advanced Combustion Engines: Unsteady Reciprocating Effects On Near-Wall Heat Transfer In Engines," Advanced Engine Combustion Program Review Meeting, Livermore, CA (2016).
8. I. Pond., Ebadi A., White C.M., Dubief Y., "Integral Method for the Assessment of U-RANS Effectiveness in Non-Equilibrium Flows and Heat Transfer," *APS DFD Meeting*, 2015, Boston, MA, abstract R7.00003.
9. Ebadi A., Biles D., White C.M., Pond I., Dubief Y., "Transport of heat and momentum in oscillatory wall-bounded flow," *APS DFD Meeting*, 2015, Boston, MA, abstract R20.00008.
10. Biles D., Ebadi A., Ma A., White C., "Construction of a Non-Equilibrium Thermal Boundary Layer Facility," *APS DFD Meeting*, Boston, MA, abstract A20.00007.

## FY 2016 Publications/Presentations

## II.24 Development of a Dynamic Wall Layer Model for LES of Internal Combustion Engines

### Overall Objectives

The overall objectives of this research are to conduct detailed measurements and develop advanced modeling capabilities to improve current understanding about heat transfer, thermal stratification, and non-equilibrium coupling processes in the near-wall region of internal combustion (IC) engines that are operated under low-temperature combustion conditions. Specific objectives include:

- Extend non-equilibrium boundary layer model to fired operating conditions; compare modeling results against measurements of wall heat flux and wall shear stress
- Compare performance of wall-layer models against particle image velocimetry (PIV) and heat flux measurements in IC engines at motored and fired operating conditions
- Perform high-speed, high-resolution PIV measurements in boundary layer of an engine at multiple operating conditions and speeds

### Fiscal Year (FY) 2016 Objectives

- Develop non-equilibrium boundary layer model for representation of thermal near-wall region and wall heat flux
- Conduct measurements for heat flux at motored and fired engine conditions
- Compare heat flux measurement against predictions from non-equilibrium wall model

### FY 2016 Accomplishments

- Derived and applied non-equilibrium wall model for thermal boundary layer
- Performed high-quality heat flux measurements at motored and fired engine conditions
- Comparison of model predictions against measurements for wall heat flux
- Assess performance of algebraic models and correlations for heat flux predictions, showing significant discrepancies in capturing peak heat flux ■

### Matthias Ihme

Stanford University  
488 Escondido Mall  
Building 500, Room 500A  
Stanford, CA 94304  
Phone: (650) 724-3730  
Email: mihme@stanford.edu

DOE Technology Development Manager:  
Leo Breton

Subcontractors:

- Volker Sick, University of Michigan, Ann Arbor, MI
- Claudia Fajardo, Western Michigan University, Kalamazoo, MI

### Introduction

This project supports advancements of in-cylinder LES wall layer models to improve engine simulation accuracy, thereby facilitating computational engine design from high-accuracy predictive simulations. Convective heat transfer plays an important role in the performance of IC engines, and significant progress has been made towards the quantitative prediction of heat transfer. However, most of the proposed correlations that have been developed provide spatially averaged heat transfer coefficients, and as such lack a detailed description of local convective heat transfer. By addressing this issue, the objectives of this research are to conduct simultaneous high-speed, high-resolution PIV and wall heat flux measurements at the cylinder head to study the near-wall region of IC engines. The performance of different wall models and heat flux correlations for the prediction of the viscous and thermal boundary layers in IC engines is examined through comparisons with experimental measurements. The non-equilibrium wall model developed by Ma et al. [1] is extended to include the heat release term for the modeling of chemical reactions under fired conditions. The focus of this study is to evaluate the capabilities of different models, including heat transfer correlations, equilibrium wall function models, and the non-equilibrium wall model, in predicting the wall heat transfer at the cylinder head for both motored and fired operating conditions.

## Approach

The aim of the project is to develop wall layer models with predictive accuracy to facilitate high-fidelity engine simulations for computational design leading to faster and less costly development of high-efficiency, low-emission engines. The specific approaches used for each task are described in the following.

- Task 1: Measurements of surface temperature, heat flux, and velocity fields were conducted at the engine head in the Transparent Combustion Chamber (TCC-III) engine. The TCC-III engine contains a flat piston surface and a flat head, two symmetrical valves, a centrally located spark plug, simplified port and runner geometries, and features a 92-mm bore full quartz cylinder liner and a piston window to allow optical access to the pancake-shaped combustion chamber. The engine contains a Bowditch-style piston extension that provides for optical access into the engine cylinder through a window in the center of the piston. Surface temperature and heat flux measurements were conducted under motored and fired engine operation at 500 rpm and 1,300 rpm. For the fired experiments, the engine was operated with homogeneous stoichiometric propane/air mixtures with a spark timing of 342 crank angle degrees (CAD). Surface temperature and heat flux were measured with a microsecond response Medtherm TCS-244-JU(JU-.156)-72-11340 heat transfer probe. The surface and in-depth temperatures were recorded every 0.5 CAD throughout the cycle.
- Task 2: Models for predicting the thermoviscous boundary layers in IC engines with different levels of fidelity are assessed. Empirical correlations due to Woschni and Annand for the prediction of instantaneous convective heat transfer in IC engines have been developed in literature, and are usually derived based on steady-state boundary-layer flow assumptions.

The main outcome of this work was the development of a non-equilibrium wall model that solves a one-dimensional partial differential equation for momentum and energy conservation along wall-normal direction. Effects of heat release, variable transport properties, and pressure variations in the boundary layer are considered by coupling the model to the solution of a zero-dimensional GT-POWER equation. Turbulence is modeled using a two-equation wall model. Experimental data from PIV measurements and heat flux probes are used to examine to performance of the model.

## Results

The different wall models are applied to the engine under motored and fired conditions at 500 rpm. In Figure 1, the relative error between the model predictions and measurements are plotted as a function of matching locations and crank angles. It can be seen that the behavior of the non-equilibrium wall model is insensitive to the matching location, and the relative error is mostly below 10% except for a small region around 340 CAD where the wall-parallel velocity changes sign and the shear velocity from experiment is close to zero. The wall function model shows significant difficulties in the prediction of the shear velocity before and after top dead center if the matching location is outside the viscous sublayer resulting in an error that can exceed 80% of the measurements. The performance improves when the matching location is moved closer to the wall.

Figure 2 shows the wall heat flux predictions from different wall models in comparison with measurements. It can be seen that the equilibrium wall-function model significantly underpredicts the heat flux under fired conditions by almost an order of magnitude. This deficiency can be attributed to the fact that the heat

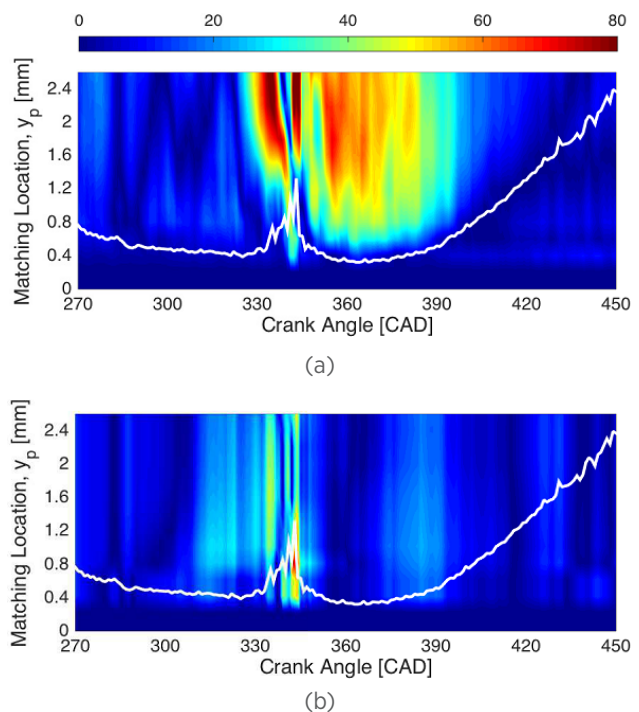


Figure 1. Relative error (in percentage) in shear velocity between PIV measurements and (a) equilibrium and (b) non-equilibrium models under motored conditions for engine speed at 500 rpm. The solid curve shows the buffer layer location, where  $y+ = 11$ .

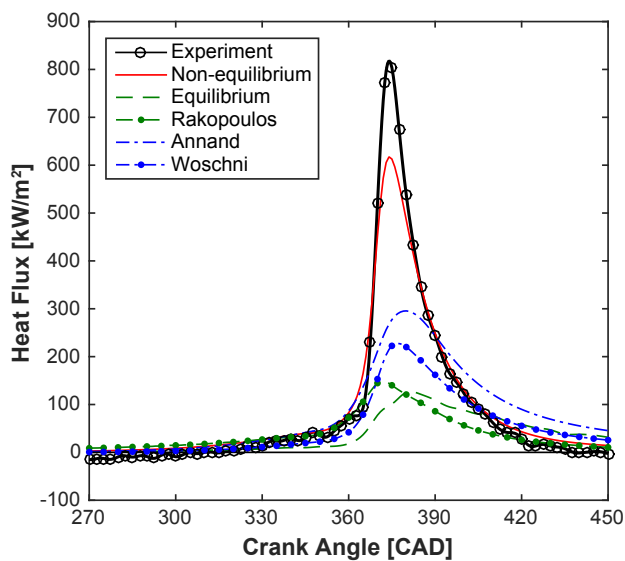


Figure 2. Heat flux predicted by different models in comparison with measurements under fired conditions for engine speed at 500 rpm

release and pressure work terms are neglected in the wall-function model. The modified wall-function model by Rakopoulos et al. [2], originally formulated for motored conditions, is shown to provide a better performance compared to the equilibrium wall-function model. The two correlation-type models show better behavior right after top dead center with larger heat flux predictions compared to the wall-function models. The non-equilibrium wall model provides the best performance and accurately captures the combustion phase though still with underprediction of the heat flux. The improved performance of the non-equilibrium wall model over the other models is due to the inclusion of the heat release term which takes into account the heat release from combustion.

Figure 3 shows results for the cumulative heat flux under fired conditions for different models in comparison with experimental data. The results are consistent with the results shown in Figure 2. Wall-function models and correlations yield underpredictions of the heat flux at different levels. The model due to Annand predicts similar amount of heat flux at the end due to the significant overprediction of the heat flux after the combustion processes, as can be seen in Figure 2. The non-equilibrium wall model gives the best results.

## Conclusions

High-speed, high-resolution PIV measurements and wall heat flux measurements were conducted at the cylinder head in an optically accessible IC engine under

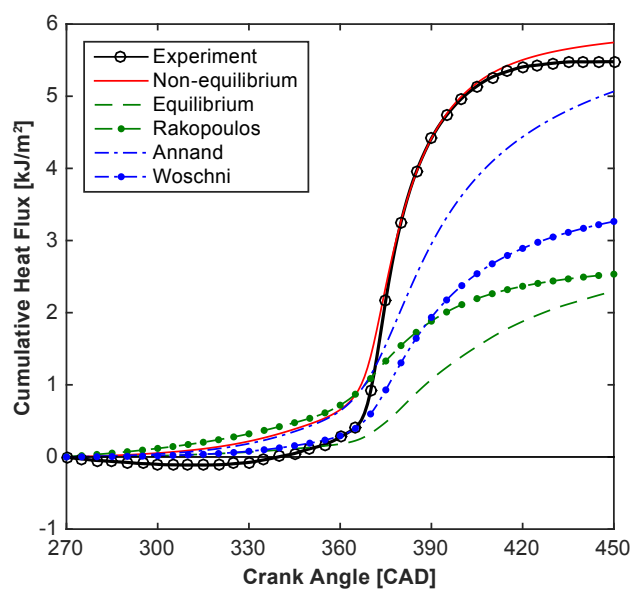


Figure 3. Cumulative heat flux predicted by different models in comparison with measurements under fired conditions for engine speed at 500 rpm

both motored and fired conditions. Experimental data was utilized to assess the performance of a series of correlation-based and algebraic wall models and a newly developed non-equilibrium wall model. The following conclusions can be drawn from this study.

- The non-equilibrium wall model was found to provide improved performance in predicting the velocity profiles and shear velocities compared to the equilibrium wall function model. The relative error in the shear velocity with respect to measurements is below 10% for most of the engine cycle.
- The non-equilibrium wall model is able to predict the reversal of the heat flux during the expansion due to the pressure gradient term, whereas this feature is completely missed by correlation-type models and the equilibrium wall function model.
- The equilibrium wall function model shows substantial underpredictions of heat flux under fired conditions by almost an order of magnitude compared to measurements.
- By taking into account the combustion processes, pressure work, and variable thermo-transport properties in the boundary layer, the non-equilibrium wall model is able to capture the peak heat flux under fired conditions.

## FY 2016 Publications/Presentations

1. P.C. Ma, M.L. Greene, V. Sick, and M. Ihme, "Non-equilibrium wall-modeling for internal combustion engine simulations with wall heat transfer." *International Journal of Engine Research*, 2016, Special Issue of THIESEL Conference, accepted.
2. P.C. Ma, T. Ewan, C. Jainski, L. Lu, A. Dreizler, V. Sick, and M. Ihme, "Development and Analysis of Wall Models for Internal Combustion Engine Simulations Using High-speed Micro-PIV Measurements." *Flow Turb. Combust.* 2016, in press.
3. Annual Report: NSF/DOE Advanced Combustion Engines: Development of a Dynamic Wall Layer Model for LES of Internal Combustion Engines, NSF, 2016.
4. M. Ihme, P.C. Ma, M. Greene, V. Sick, C. Jainski, A. Dreizler, "Non-equilibrium Wall-Modeling for Simulations of Internal Combustion Engines." THIESEL 2016 Conference on Thermo- and Fluid Dynamic Processes in Direct Injection Engines.
5. V. Sick, invited talk at International Combustion Institute Summer School on Flame-Wall Interactions, held in Bensheim, Germany, June 2016.
6. M. Greene, D. Reuss, V. Sick, Poster "Near-wall flow measurements in a canonical internal combustion engine", International Combustion Institute Summer School on Flame-Wall Interactions, held in Bensheim, Germany, June 2016.

## References

1. P.C. Ma, T. Ewan, C. Jainski, L. Lu, A. Dreizler, V. Sick, and M. Ihme, "Development and Analysis of Wall Models for Internal Combustion Engine Simulations Using High-speed Micro-PIV Measurements." *Flow Turb. Combust.* 2016, in press.
2. C. Rakopoulos, G. Kosmadakis, and E. Pariotis, "Critical evaluation of current heat transfer models used in CFD in-cylinder engine simulations and establishment of a comprehensive wall-function formulation." *Appl. Energy*, 2010; 87(5): 1612–1630.

## II.25 Collaborative Research: NSF/DOE Partnership on Advanced Combustion Engines: Advancing Low Temperature Combustion and Lean Burning Engines for Light- and Heavy-Duty Vehicles with Advanced Ignition Systems and Fuel Stratification

### Overall Objectives

- Demonstrate extension of engine load and speed limits using partial fuel stratification (PFS) compared to homogeneous charge compression ignition (HCCI), understand fuel chemistry and improve fuel mechanisms, and develop validated models of PFS
- Demonstrate extension of ignition limits to high pressure and exhaust gas recirculation (EGR) using advanced ignition systems and PFS, optimize ignition strategies, and optimize injection strategies
- Develop an improved understanding of the fundamental physics governing advanced ignition and flame propagation in stratified charges

### Fiscal Year (FY) 2016 Objectives

- Computationally examine the effects of varying PFS strategies in overall engine system efficiency and emissions
- Experimentally demonstrate extension of ignition limits using advanced ignitions systems for a range of pressures, air and EGR dilution, and PFS
- Improve the state-of-the-art chemical mechanism reduction approaches and develop reduced chemistry models targeted for different gasoline surrogates for simulations of HCCI/PFS engine operation conditions
- Understand the physics of flame propagation in a stratified charge of different hydrocarbon fuels

### FY 2016 Accomplishments

- Computationally estimated that PFS strategies can result in multiple high-efficiency (>43%) operating points with different combinations of intake pressure, intake temperature, EGR, and injection timing
- Experimentally demonstrated an extension of the EGR dilute limits (16% to 25% at low loads of 8 bar brake mean effective pressure [BMEP]; 10% to 15% at high loads of 20 bar BMEP) using a radio frequency corona

#### Robert W. Dibble (Primary Contact), Jyh-Yuan Chen

University of California, Berkeley  
6159 Etcheverry Hall, Mailstop 1740  
Berkeley, CA 94720-1740  
Phone: (510) 642-4901  
Email: rdibble@berkeley.edu

#### Wai Cheng

Massachusetts Institute of Technology  
77 Massachusetts Avenue  
Cambridge, MA 02139  
Phone: (617) 253-4531  
Email: wkcheng@mit.edu

DOE Technology Development Manager:  
Leo Breton

Subcontractor:

Ricardo North America, Burr Ridge, IL

discharge ignition (RFCDI) system in a gasoline direct injection single-cylinder research engine, resulting in a maximum reduction in brake specific  $\text{NO}_x$  of 73% and a maximum reduction in brake specific fuel consumption of 4%

- Developed a small reduced mechanism for multiple gasoline surrogates containing ethanol under HCCI/PFS engine operating conditions using the newly developed reduction approaches with high accuracy (10% relative error)
- Successfully performed the stratified flame simulation studies for methane, propane, and n-heptane, concluding that flame speed enhancement in stratified mixtures is due to preferential diffusion of hydrogen molecules and radicals from the burned gas into the fresh gas; enhancement is greater for fuels with a higher hydrogen-to-carbon ratio, such as methane (up to

~25% enhancement), while heavier fuels like n-heptane display a more complicated behavior (up to ~7% enhancement or ~10% penalty) ■

## Introduction

This project set out to help achieve the 54 mpg target (year 2025) for vehicle mileage by providing experimental data, simulation tools, and understanding of fundamental phenomena to develop the next generation of high-efficiency engines for vehicles. The main objective is the extension of clean and efficient low temperature combustion (LTC) technology to operate over the full load and speed range required of an engine. Two main technology paths were proposed: (1) PFS in LTC compression ignition engines, and (2) enhance ignition systems combined with PFS in spark ignition engines.

On a fundamental level, this program set out to provide detailed understanding of the chemical kinetics that cause pressure-sensitive intermediate temperature heat release and equivalence ratio sensitivity in gasoline, phenomena that enable high load boosted LTC with PFS. For the advanced ignition system technology, this program set out to provide understanding of the interactions between the spark discharge, the electric field, and the stratified mixture in the flame kernel formation process. Additionally, the fundamental physics behind flame propagation through a stratified charge are studied to obtain a comprehensive description of the PFS ignition process. These scientific insights are applied, through fundamentally-based phenomenological models, to engines for improving engine efficiency and lowering emissions.

## Approach

The approach used to conduct the research under this project involves close collaboration between experimental and numerical efforts. The experimental approach is to collect high-quality data at a wide range of relevant conditions to understand the response of the system to a range of external inputs. The computational approach is to use multiple levels of numerical tools, from simplified to detailed models, to complement the experimental results and elucidate the physical processes governing observed trends. In short, experiments are used to guide simulations and simulations are used to guide experiments.

## Results

### Extend Engine Load and Speed Limits of HCCI with PFS

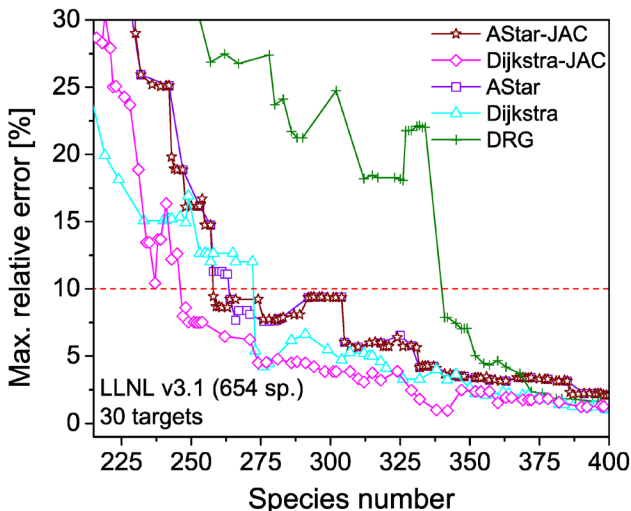
To assess the feasibility of using a PFS operating strategy on a multi-cylinder engine, a multilevel computational

study using 3D CFD combustion simulations with reduced gasoline chemistry and one-dimensional full-engine simulations with a turbocharger model were conducted [1]. This study used an experimentally validated PFS operating point, which was then optimized with the 3D model. Once the optimized operating point was selected, the heat release rate profile and required intake conditions were used in a cycle simulation model built in the AVL software BOOST™ [2]. The effects of the turbocharger and heat exchangers on cycle efficiency were evaluated, as well as the required engine and turbocharger sizing for effective operation across the load-speed range. Investigations into the operability of a mid-load (10.5 bar indicated mean effective pressure) PFS engine operating point on a multi-cylinder engine suggest that the 10.5 bar indicated mean effective pressure PFS operating point is achievable in practical engines using a turbocharger. Additionally, PFS is most useful for controlling combustion phasing. Therefore, to reduce NO<sub>x</sub> emissions, early direct injections (60–100° before top dead center) with small fractions of the total fuel (6–12%, with the balance being supplied with port fuel injection) provide better efficiency/emissions results (up to >43% indicated efficiency) than late direct injections with higher fractions of the total fuel.

### Understand Fuel Chemistry and Improve Mechanisms

To improve the skeletal and reduced mechanisms for engine CFD simulations, directed relation graph with error propagation-based (DRGEP-based) chemical mechanism reduction methods were first investigated [3] and then employed to develop a reduced chemical mechanism for multiple gasoline–ethanol surrogates. An example of the chemical species reduction using the different methods for n-heptane is shown in Figure 1, and resulting comparisons in calculated flame speeds are shown in Figure 2.

Once confidence in the DRGEP-based methods was established, the ignition of heavy fuels and multiple fuel surrogates were investigated to validate the applicability of a formulated Jacobian pairwise relation for a pair of species for the mechanism reduction. Simultaneously, the newly developed reduced mechanisms were validated by the HCCI engine experiments for the five target fuel surrogates (California Air Resources Board Low Emissions Vehicle III Certification regular gasoline, Anti-Knock Index (AKI) = 87.8; Fuels for Advanced Combustion Engines (FACE) C with 7% ethanol by volume, AKI = 88.0; FACE C with 14% ethanol by volume, AKI = 91.5; FACE J with 23% ethanol by volume, AKI = 88.4; and FACE J with 36% ethanol by volume, AKI = 90.2). With HCCI engine experimental



LLNL – Lawrence Livermore National Laboratory

Figure 1. Maximum relative error against species number of skeletal mechanism developed by various graph search methods in negative temperature coefficient regions

data validation for the five target fuel surrogates, the skeletal and reduced mechanisms can both accurately predict the boundary conditions affected by the low temperature heat release.

#### Advanced Ignition and PFS Enabled Spark Ignition for High Efficiency and Low Emissions

The gasoline direct injection single-cylinder engine tests at Ricardo North America with the RFCDI system from Federal Mogul evaluated the dilute EGR limits for acceptable engine operation under conditions associated with both naturally aspirated and boosted loads at moderate and high engine speeds for stoichiometric and slightly fuel-rich charges [8].

For low loads, the RFCDI system reduced cycle-to-cycle variability and decreased both the flame development angles and burning angles for a given EGR rate, seen in Figure 3. This allowed for higher EGR that drove down brake specific  $\text{NO}_x$  emissions (73% reduction compared to the baseline spark ignition). For boosted loads, the RFCDI system extended the knock limit, allowing for advanced combustion phasing (Figure 4). Flame development angles decreased for a given EGR rate, while burning angles remained unchanged or increased, suggesting higher pressures reduce the benefits of the ignition system. Definitive decreases in brake specific fuel consumption (4%) and emissions (29% reduction in  $\text{NO}_x$ ) were observed.

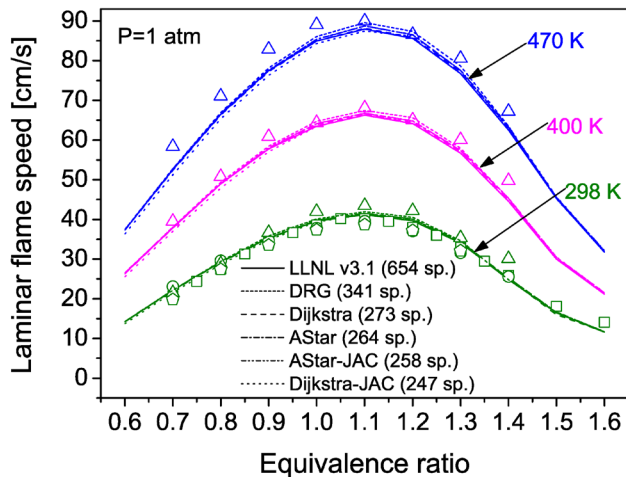
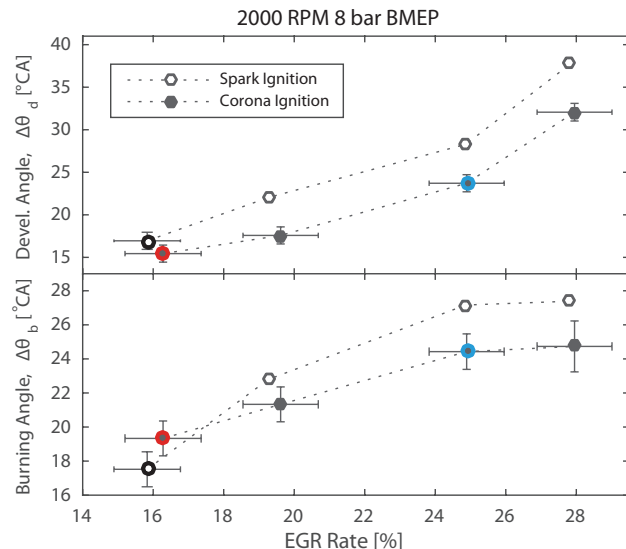
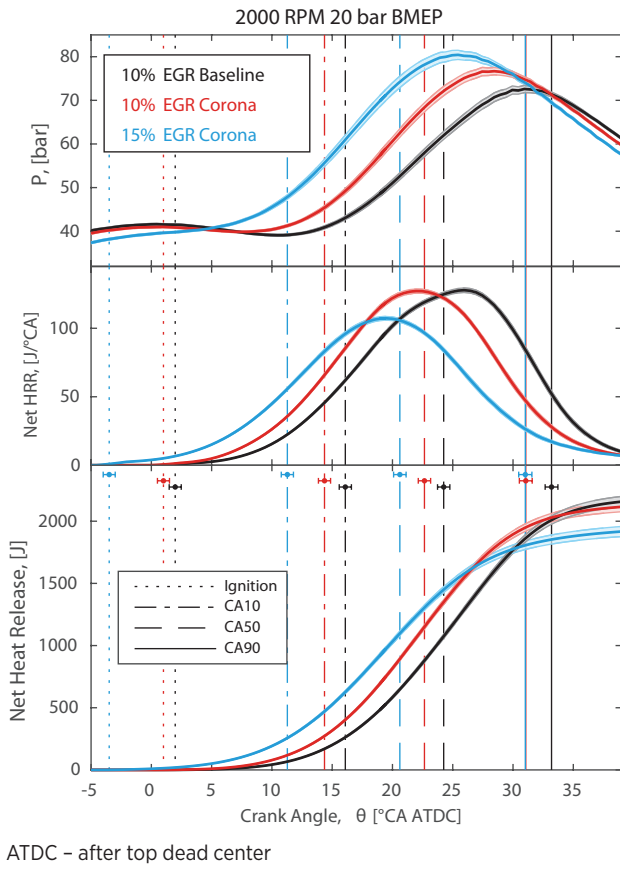


Figure 2. Comparison of laminar flame speed between the detailed mechanism and skeletal mechanisms generated by DRGEP-based methods for unburned gas temperatures of 298 K, 400 K, and 470 K under the pressure of 1 atm. Symbols are experimental data: triangle: Kumar et al. [4]; square: Davis and Law [5]; circle: Huang et al. [6]; pentagon: Sileghem et al. [7].



°CA – degrees crank angle

Figure 3. Plots of burn duration for the 2,000 rpm/8 bar BMEP tests. Baseline spark ignition operation is shown with open markers and RFCDI operation is shown with filled markers.  $\lambda = 1 \pm 0.05$  for all operating points shown. Flame development angle  $\Delta\theta_d$  (top) and burning angle  $\Delta\theta_b$  (bottom). EGR conditions shown are 16% EGR inductive spark ignition (black), 16% EGR RFCDI (red), and 25% EGR RFCDI (blue).



ATDC – after top dead center

Figure 4. Combustion phasing plots shown for selected EGR conditions for the 2,000 rpm/20 bar BMEP tests as a function of crank angle degree: Pressure (top), net heat release rate (HRR) (middle), and total cumulative net heat release (bottom).  $\lambda = 1 \pm 0.05$  for all operating points shown. The shaded regions depict the uncertainty in the values plotted. EGR conditions shown are: 10% EGR with traditional inductive spark ignition (black), 10% EGR with RFCDI (red), and 15% EGR with RFCDI (blue). Crank angle locations of both ignition and fractional charge burn are shown as vertical lines throughout the figure, with uncertainties shown as horizontal error bars.

The RFCDI ignition system tested with Ricardo required between 265 mJ and 670 mJ per cycle, about an order of magnitude larger than traditional spark ignition as well as a nanosecond pulsed discharge system tested in Year 2 of the project [9].

### Understand Fundamental Physics of Advanced Ignition and Flame Propagation in a Stratified Charge

Simulations of a one-dimensional planar stratified propagating flames of three hydrocarbon fuels, i.e., methane, propane and n-heptane in Adaptive Simulation of Unsteady Reacting Flow have been performed and studied [10]. For each fuel, fuel consumption speeds

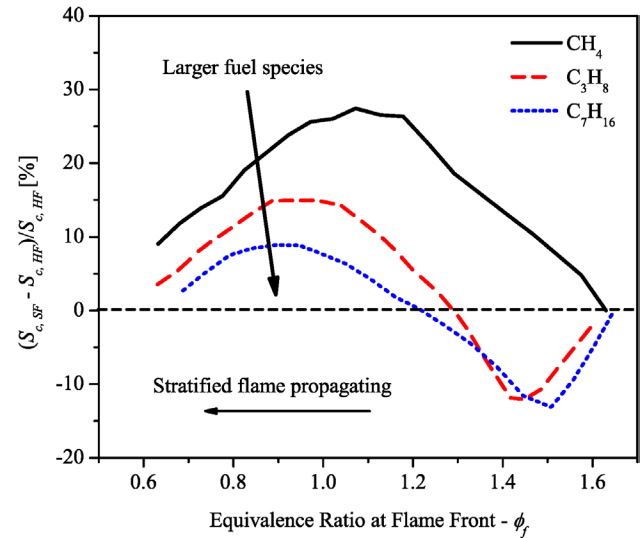


Figure 5. Percentage change between fuel consumption speeds of rich-to-lean stratified flame and the corresponding homogeneous flames

of a rich-to-lean stratified flame are compared to those of their corresponding homogeneous flames, and their relative changes are plotted in Figure 5. For methane–air flames, fuel consumption speeds of the stratified flame are generally faster than those of homogeneous flames due to hydrogen molecule and radical diffusion from the burned gas. In contrast, stratified flames of both propane–air and n-heptane–air mixtures have lower fuel consumption speeds than their homogeneous flames on the rich side. In these two flames, fuel is consumed on the unburned side of the peak heat release location due to higher reactivity. Additionally, as more intermediate species and hydrocarbon fragments are formed in the richer burned gas of stratified flames, these species consume more key radicals on the burned side of the flame, leading to lower fuel consumption rates. In comparison to homogeneous flames, chemical activities are suppressed in rich stratified flames of larger hydrocarbon fuels.

### Conclusions

- PFS in conjunction with the use of a turbocharger is possible in practical HCCI engines, and PFS is most useful for controlling combustion phasing in these environments.
- New reduced mechanisms have been developed and have been validated for several surrogate fuels and against HCCI experimental data.
- A significant advantage of advanced ignition systems for downsized and boosted spark ignition engine operation is the extension of EGR limits, enabling

advanced ignition timing and greater work output per cycle.

- The differences associated with stratified flame speed enhancement vary on the order of 10%, which for many researchers may be an acceptable level of error for engine simulation development.

## References

- Vuilleumier, D., Taritas, I., Wolk, B., Kozarac, D., Saxena, S., Dibble, R.W., "Multi-level computational exploration of advanced combustion engine operating strategies," *Appl. Energy*, In Press, 2016.
- AVL BOOST v2013.2 – Theory, AVL LIST GmbH; 2013.
- Chen, Y., Chen, J.-Y., "Application of Jacobian defined direct interaction coefficient in DRGEP-based chemical mechanism reduction methods using different graph search algorithms," *Combust. Flame*. 174 (2016) 77–84. doi:10.1016/j.combustflame.2016.09.006.
- Kumar, K., Freeh, J.E., Sung, C.J., Huang, Y., "Laminar Flame Speeds of Preheated iso-Octane/O<sub>2</sub>/N<sub>2</sub> and n-Heptane/O<sub>2</sub>/N<sub>2</sub> Mixtures," *J. Propuls. Power*. 23 (2007) 428–436. doi:10.2514/1.24391.
- Davis, S.G., Law, C.K., "Determination of and Fuel Structure Effects on Laminar Flame Speeds of C1 to C8 Hydrocarbons," *Combust. Sci. Technol.* 140 (1998) 427–449. doi:10.1080/00102209808915781.
- Huang, Y., Sung, C.J., Eng, J.A., "Laminar flame speeds of primary reference fuels and reformer gas mixtures," *Combust. Flame*. 139 (2004) 239–251. doi:10.1016/j.combustflame.2004.08.011.
- Sileghem, L., Alekseev, V.A., Vancoillie, J., Van Geem, K.M., Nilsson, E.J.K., Verhelst, S., Konnov, A.A., "Laminar burning velocity of gasoline and the gasoline surrogate components iso-octane, n-heptane and toluene," *Fuel*. 112 (2013) 355–365. doi:10.1016/j.fuel.2013.05.049.
- Pineda, D.I., Wolk, B., Chen, J.-Y., and Dibble, R., "Application of Corona Discharge Ignition in a Boosted Direct-Injection Single Cylinder Gasoline Engine: Effects on Combustion Phasing, Fuel Consumption, and Emissions," *SAE Int. J. Engines* 9(3):1970–1988, 2016, doi:10.4271/2016-01-9045.
- Pineda, D.I., Wolk, B., Sennott, T., Chen, J.-Y., Dibble, R.W., and Singleton, D., "Nanosecond Pulsed Discharge in a Lean Methane-Air Mixture," in *Laser Ignition Conference*, OSA Technical Digest (online) (Optical Society of America, 2015), paper T5A.2. doi:10.1364/LIC.2015.T5A.2.
- Shi, X., Chen, J.-Y., Chen, Y., "Laminar Flame Speeds of Stratified Methane, Propane, and n-Heptane Flames," *Combust. Flame*, In Press, 2016.

## FY 2016 Publications/Presentations

- Chen, Y., Chen, J.-Y., "Application of Jacobian defined direct interaction coefficient in DRGEP-based chemical mechanism reduction methods using different graph search algorithms," *Combust. Flame*. 174 (2016) 77–84. doi:10.1016/j.combustflame.2016.09.006.
- Pineda, D.I., Wolk, B., Chen, J.-Y., and Dibble, R., "Application of Corona Discharge Ignition in a Boosted Direct-Injection Single Cylinder Gasoline Engine: Effects on Combustion Phasing, Fuel Consumption, and Emissions," *SAE Int. J. Engines* 9(3):1970–1988, 2016, doi:10.4271/2016-01-9045.
- Pineda, D.I., Shi, X., Wolk, B., Vuilleumier, D., Saxena, S., Chen, J.-Y., Dibble, R.W., "Berkeley-MIT Research Program: Advancing Low Temperature Combustion and Lean Burning Engines for Light- and Heavy-Duty Vehicles with Advanced Spark Ignition and Fuel Stratification," Advanced Engine Consortium Review Meeting, U.S. Council of Automotive Research, Southfield, MI, August 2016.
- Shi, X., Chen, J.-Y., Chen, Z., "Numerical study of laminar flame speed of fuel-stratified hydrogen/air flames," *Combust. Flame* 163:394–405, 2016, doi:10.1016/j.combustflame.2015.10.014.
- Shi, X., Chen, J.-Y., Chen, Y., "Laminar Flame Speeds of Stratified Methane, Propane, and n-Heptane Flames," *Combust. Flame*, In Press, 2016.
- Shi, X., Chen, Y., Vuilleumier, D., Wolk, B., Saxena, S., Dibble, R.W., Sorensen, C., Chen, Y., Cheng, W.K., "Update on Berkeley-MIT Research Program: Numerical Study of Laminar Flame Speeds of Methane, Propane, and n-Heptane/Air Stratified Flames," Advanced Engine Consortium Review Meeting, Sandia National Laboratories, Livermore, CA, February 2016.
- Vuilleumier, D., Taritas, I., Wolk, B., Kozarac, D., Saxena, S., Dibble, R.W., "Multi-level computational exploration of advanced combustion engine operating strategies," *Appl. Energy*, In Press, 2016.

# II.26 Progress Report: NSF/DOE Partnership on Advanced Combustion Engines – Modeling and Experiments of a Novel Controllable Cavity Turbulent Jet Ignition System

## Overall Objectives

- Examine the active radicals generated in the turbulent jet ignition (TJI) process through both rapid compression machine (RCM) and optically accessible engine experiments
- Develop a new large eddy simulation (LES) modeling technique to model the TJI system, as both turbulence and active species from the pre-chamber play a role in TJI combustion
- Demonstrate the controllable cavity TJI system's performance in engine tests

## Fiscal Year (FY) 2016 Objectives

- Experimental testing of the DM-TJI (dual-mode TJI) system with liquid pre-chamber and main chamber fuel in the RCM and single-cylinder engine
- Implement the TJI control system in the single-cylinder liquid-fueled engine
- Develop, validate, and test a hybrid LES/filtered mass density function (FMDF) model and a Reynolds-averaged Navier–Stokes (RANS) model of the TJI process

## FY 2016 Accomplishments

- Tested the DM-TJI system in the RCM with iso-octane and demonstrated the effects of pre-chamber main/ chamber fueling ratio on combustion under ultra-lean conditions
- Tested the DM-TJI system with liquid gasoline in the single-cylinder engine at a range of lean and dilute conditions with a thermal efficiency greater than 46% achieved
- Developed and tested a model-based closed-loop combustion control system for the single-cylinder liquid-fueled DM-TJI engine
- Conducted LES/FMDF and RANS modeling of TJI in a coupled pre-chamber RCM for a series of TJI configurations to study the effects of various flow/flame parameters ■

**Elisa Toulson (Primary Contact),  
Harold Schock, George Zhu,  
Farhad Jaber, Indrek Wichman,  
Giles Brereton**

Michigan State University (MSU)  
1497 Engineering Research Ct.  
East Lansing, MI 48824  
Phone: (517) 884-1549  
Email: toulson@msu.edu

DOE Technology Development Manager:  
Leo Breton

## Introduction

TJI is an advanced pre-chamber initiated combustion system that enables very fast burn rates due to the ignition system producing multiple, distributed ignition sites, which consume the main charge rapidly and with minimal combustion variability. The fast burn rates allow for increased levels of dilution (lean burn and/or exhaust gas recirculation) when compared to conventional spark ignition combustion. The purpose of this research project is to conduct a thorough study of the TJI process. To fulfill this purpose, a novel DM-TJI system with variable pressure control of the pre-chamber is studied numerically and experimentally in MSU's RCM, and single-cylinder optical engine. The major goals of the project are (1) to experimentally examining the active radicals generated in the TJI process through both RCM and optically accessible engine experiments, and (2) to develop a new LES modeling technique to model the TJI system, as both turbulence and active species from the pre-chamber play a role in TJI combustion. The main project tasks that were supported during FY 2016 include:

- **Task 1:** Testing of the RCM and single-cylinder engine DM-TJI system with liquid pre-chamber and main chamber fuel and development and implementation of a control system for pressure and mixture control of the pre-chamber
- **Task 2:** LES/FMDF and RANS modeling of TJI in a coupled prechamber RCM

## Approach

The aim of this project is to gain a better understanding of the contributions of thermal, turbulence, and active radical influences on ignition enhancement through both experimental testing and modeling of the TJI process.

### Task 1

The TJI method is used to achieve overall very lean and dilute combustion control by providing properly timed, distributed ignition sites in the main combustion chamber via turbulent mixing. The unique features of the system designed and fabricated for this project include the ability to maintain the pressure in the pre-chamber at nearly that of the main combustion chamber during the compression stroke thereby inhibiting residual main chamber gases from entering the TJI assembly. Secondly, independent control of the stoichiometry of the pre-chamber for each cycle is possible, depending on engine operating conditions, important for operating over a range of power outputs

### Task 2

The high fidelity computational model used in this project was developed by the computational team at MSU and is based on the hybrid LES/FMDF methodology [1]. The LES/FMDF is used for TJI and flows/combustion in three configurations: (1) three-dimensional planar jet, (2) round hot product jet injected into a closed square chamber, and (3) a prechamber coupled with an RCM.

## Results

Our progress during FY 2016 on the experimental RCM and optical engine testing and the LES/FMDS modeling is described in each of the tasks below.

### Task 1

**TJI RCM Experimental Testing:** During FY 2016 testing of the DM-TJI system was carried out in the RCM with a single and dual orifice nozzle and a variety of injection timings, spark timings, and main chamber/pre-chamber fueling ratios (global  $\lambda = 3$ ) with liquid fuel (iso-octane). Additionally, a new borescope configuration was used to gain optical access into the RCM pre-chamber to visualize the fuel and air injection and their interaction (Figure 1). With the iso-octane pre-chamber and main chamber fueling strategy that was used for the testing it was found that increased pre-chamber fueling (up to 9% of the total fuel mass) decreased ignition delay and improved repeatability (Figure 2). In addition, with the lean iso-octane fueling conditions studied an autoignition event was observed following the initial turbulent jet ignition event as can be seen in the images and pressure traces shown in Figure 2. A second objective of the RCM experiments was to gain a better understanding of the fundamental properties of the turbulent jet. To accomplish this a set of experiments were completed with varying orifice diameter and equivalence ratios and the hot jet velocity at the orifice outlet, together with other parameters such as the Mach and Reynolds number were calculated; see Gholamisheri et al. [1].

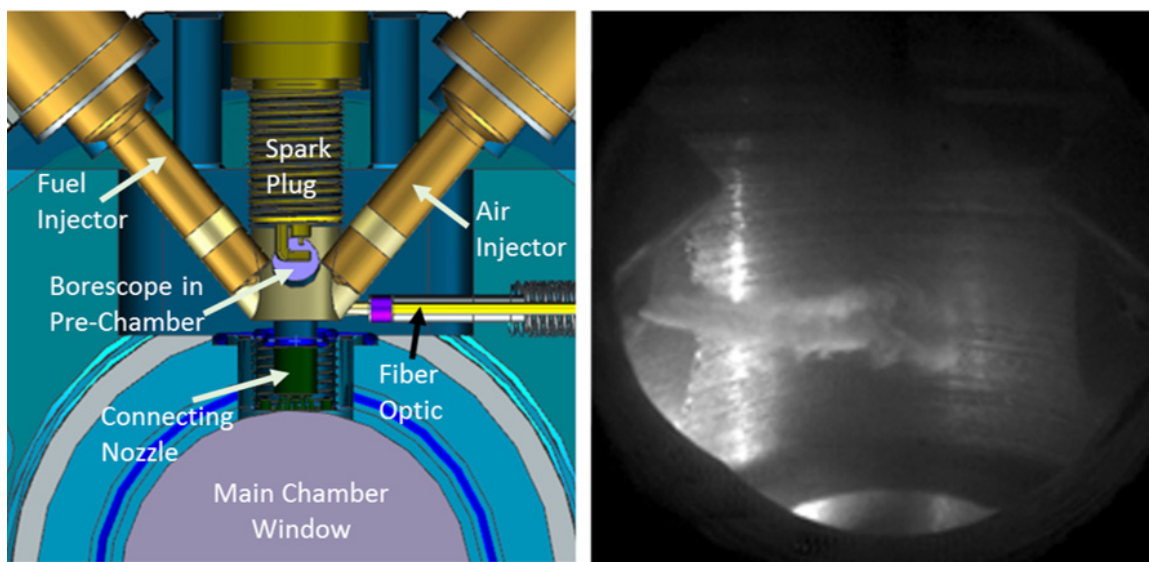


Figure 1. (left) RCM boroscope setup in RCM DM-TJI pre-chamber and (right) high speed image of iso-octane fuel spray in the pre-chamber with auxiliary air injection

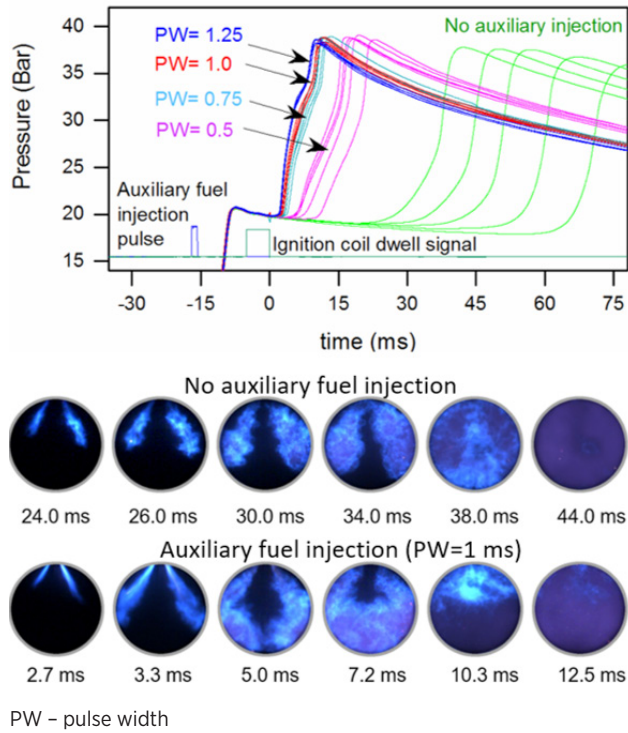


Figure 2. (top) RCM pressure traces for DM-TJI combustion of iso-octane air mixtures (global  $\lambda = 3$ ) with various pre-chamber injection pulse widths. (bottom) Optical images of DM-TJI combustion with and without pre-chamber auxiliary fueling.

**TJI Optical Engine Experimental Testing:** The single-cylinder DM-TJI engine (compression ratio = 12) was tested at wide open throttle with liquid gasoline with and without intake charge dilution with good combustion stability (coefficient of variation in indicated mean effective pressure [IMEP] <2%) achieved. The DM-TJI engine delivered a part-load indicated efficiency of 46.8% at 1,500 rpm and 6.0 bar IMEP at a global  $\lambda \approx 1.85$ . With 30% nitrogen dilution and near stoichiometric operation an indicated efficiency greater than 46% was achieved. It should be noted that this efficiency includes work required to supply high-pressure air to the pre-chamber. With this operating condition, a conventional three-way catalytic converter could be employed to manage criteria emissions, making this technology viable with the current state-of-the-art aftertreatment technology. The net thermal efficiency obtained after subtracting the non-optimized pumping work and not subtracting friction losses was noted to be  $45.5\% \pm 0.5\%$  for both lean and near stoichiometric operation. Figure 3 shows the non-optimized net thermal efficiency maps for various engine speeds and loads without intake charge dilution, the highest net thermal efficiency was obtained at 2,000 rpm, 6.5 bar net mean effective pressure (NMEP), and a global

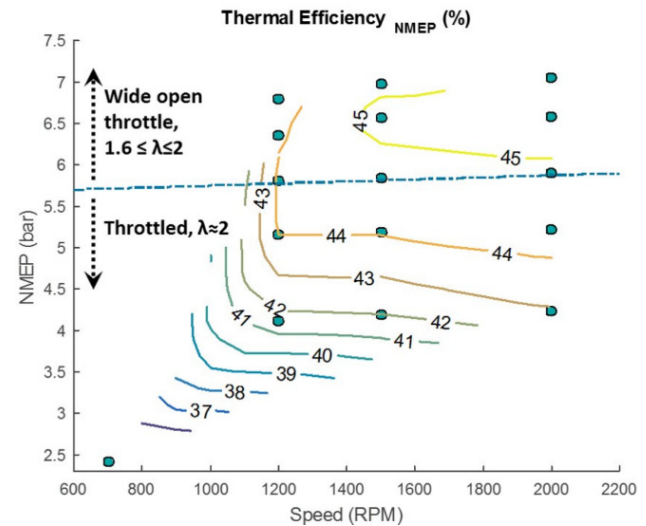
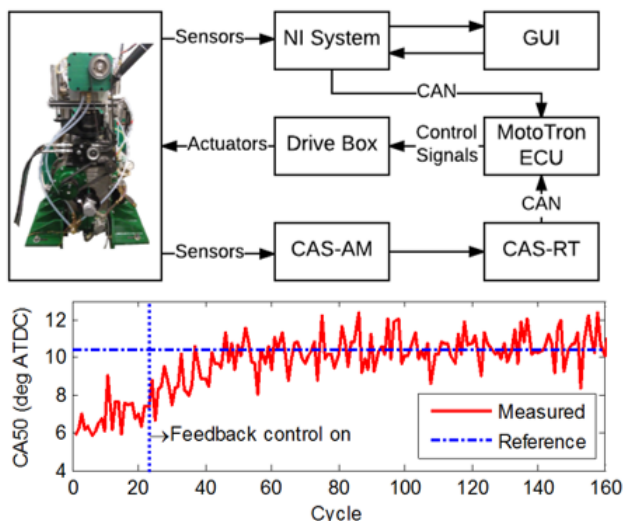


Figure 3. Net thermal efficiency maps of the DM-TJI engine without intake dilution

$\lambda = 1.7$ . A preliminary estimate showed that the DM-TJI engine could reduce the fuel consumption by 12.5% compared to the conventional spark ignition engines at the current speed/load conditions.

**TJI Control:** In FY 2016 the control-oriented gaseous fuel TJI combustion model was extended to incorporate liquid gasoline fuel. The liquid fuel model considers the pre-chamber fuel wall-wetting dynamics and the main chamber combustion rate is calculated based on the mass flow rate of the turbulent jet from the pre-chamber. The simulation results match the experiment very well; see Song et al. [2]. The new control system (Figure 4) is able to conduct a sequence of tests with different experimental parameters automatically. It mainly consists of three parts, the National Instruments (NI) system, MotoTron ECU (engine control unit) and Phoenix CAS (combustion analysis system). All the test parameters are preloaded through the GUI (graphical user interface) into the NI system. Now, up to 10 different sets of experimental parameters can be preloaded for one test run. The NI system communicates with the MotoTron ECU through a controller area network (CAN), and the MotoTron ECU controls the engine through an MSU engine control drive box. The Phoenix CAS-AM is used for data acquisition, such as the in-cylinder pressure traces; and the Phoenix CAS-RT system is able to calculate the combustion related parameters, such as IMEP and CA50 (crank position of 50% mass fraction burned) in real-time. These parameters are sent to MotoTron ECU for feedback control. The experimental results of the closed-loop CA50 position control to maintain the CA50 at the desired location by adjusting the spark timing in the pre-chamber for the best thermal efficiency can be seen in Figure 4.



ATDC – after top dead center; GUI – graphical user interface

Figure 4. TJI control system architecture and CA50 with feedback control

## Task 2

During this project, the turbulent flow and combustion in an RCM and a single round turbulent jet igniter have been computed with an LES/FMDF model. The simulated RCM-TJI system is similar to that experimentally studied in this project. The flow and combustion in the RCM-TJI system are simulated for various thermochemical and hydrodynamic conditions by the LES/FMDF with an immersed boundary method for handling complex geometrical features. The simulation results are found to be in good overall agreement with the experimental data. Figure 5 shows a comparison between experimental and LES/FMDF results for the turbulent jet injected from the pre-chamber to the main chamber at different times. The overall jet features such as the tip jet velocity are well predicted by the LES/FMDF. The LES/FMDF results shown in Figure 6 reveal three main combustion phases in the RCM-TJI system: (I) cold fuel jet, (II) turbulent hot product/fuel jet, and (III) reverse fuel-air/product jet. The main chamber ignition and other combustion features are dependent on the pre-chamber and main chamber initial thermochemical and gas dynamics conditions, as well as the amount of heat loss through walls. For example, a higher turbulence level inside the pre-chamber leads to faster hot jet and shorter main chamber combustion duration. Or in the process of pre-chamber ignition, a jet of unburned fuel exits out to the main chamber, which is an undesirable effect of locating the igniter far away from the nozzle. A remedy is to put the spark closer to the nozzle in the pre-chamber. This allows for faster combustion and decreases the lower flammability limit

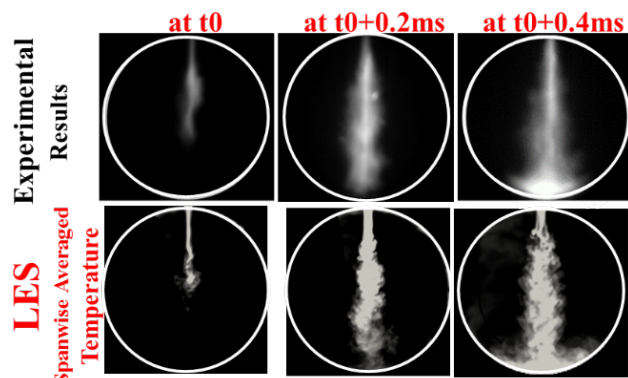


Figure 5. Experimental and LES/FMDF turbulent jet images taken at different times in the MSU RCM

of the ultra-lean premixed mixture. Numerical study conducted with LES/FMDF was proven to be very useful in identifying the primary factors affecting the performance of RCM-TJI system.

## Conclusions

During FY 2016, a third generation DM-TJI system was tested with liquid fuel in both the RCM and single-cylinder engine. Experiments showed that a thermal efficiency  $>46\%$  could be achieved in the engine under lean and dilute conditions with a coefficient of variation of IMEP  $<2\%$ . In addition, a model-based closed-loop combustion control system was developed and tested with the engine. LES/FMDF and RANS simulations of TJI in a coupled pre-chamber RCM were conducted.

## References

1. M. Gholamisheri, B.C. Thelen, G. Gentz, I.S. Wichman, E. Toulson, Rapid Compression Machine Study of a Premixed, Variable Inlet Density and Flow Rate, Confined Turbulent Jet, Combustion and Flame. 2016. 169:321-332.
2. R. Song, G. Gentz, G. Zhu, E. Toulson, and H. Schock and G. Zhu, "A two-stage combustion model for turbulence-jet ignition engines with RCM validation," to be submitted to IMechE Journal of Automobile Engineering.

## FY 2016 Publications/Presentations

1. H. Schock, E. Toulson, F. Jaber, G. Zhu, G. Brereton, I. Wichman, AEC Program Review Meeting, February 2016.

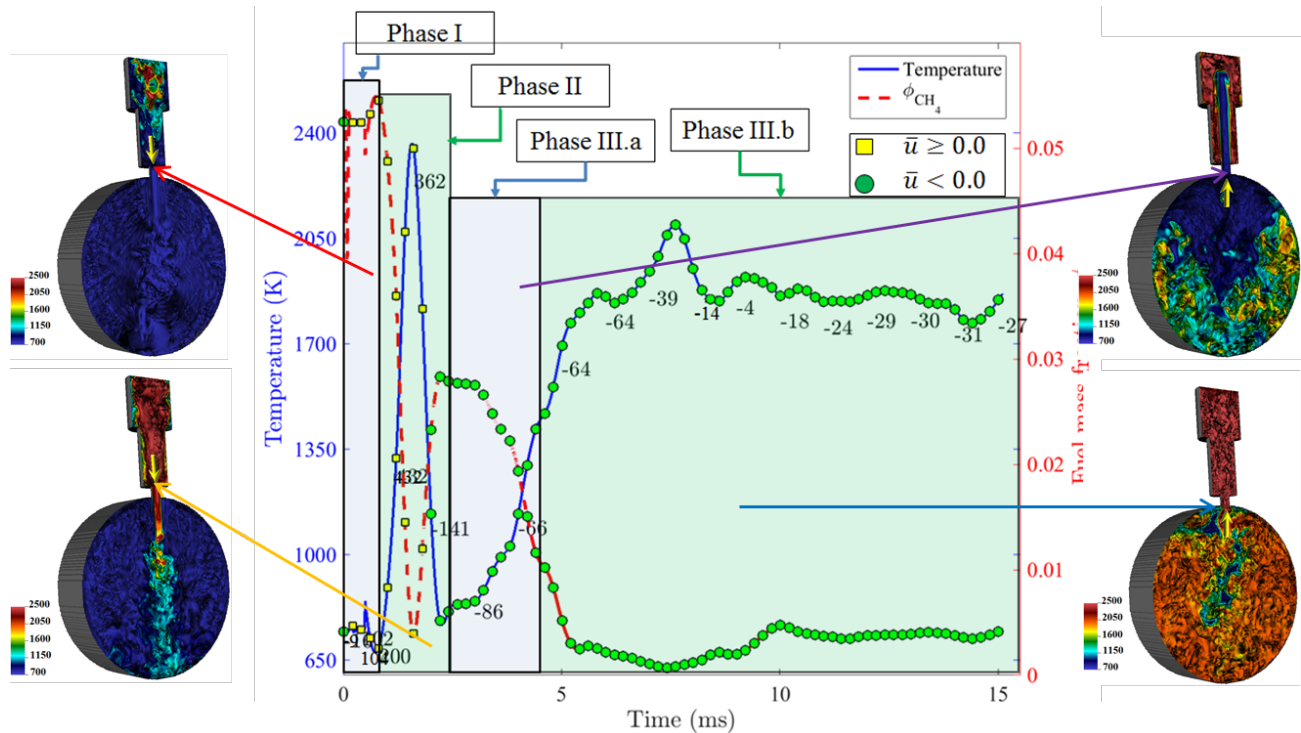


Figure 6. TJI-RCM combustion phases based on the composition and direction of the flow at the nozzle

2. H. Schock, E. Toulson, F. Jaber, G. Zhu, G. Brereton, I. Wichman, AEC Program Review Meeting, August 2016.
3. M. Gholamisheri, B.C. Thelen, G. Gentz, I.S. Wichman, E. Toulson, *Rapid Compression Machine Study of a Premixed, Variable Inlet Density and Flow Rate, Confined Turbulent Jet, Combustion and Flame*. 2016. 169:321-332.
4. G. Gentz, E. Toulson, *Experimental Studies of a Liquid Propane Auxiliary Fueled Turbulent Jet Igniter in a Rapid Compression Machine*, SAE Int. J. Engines 9(2), 2016. Presented at SAE World Congress, Detroit, MI, April 2016.
5. M. Gholamisheri, B.C. Thelen, G. Gentz, E. Toulson, *CFD Modeling of an Auxiliary Fueled Turbulent Jet Ignition System In A Rapid Compression Machine*, SAE Paper 2016-01-0599, Presented at SAE World Congress, Detroit, MI, April 2016.
6. R. Song, G. Gentz, G. Zhu, E. Toulson, and H. Schock and G. Zhu, "A control-oriented jet ignition combustion model for an SI engine," 2015 ASME Dynamic Systems and Control Conference, DSCC2015-9687, Columbus, Ohio, October 2015.
7. R. Song, G. Gentz, G. Zhu, E. Toulson, and H. Schock and G. Zhu, "A two-stage combustion model for turbulence-jet ignition engines with RCM validation," IMechE Journal of Automobile Engineering, Accepted in August 2016.
8. A. Validi, F. Jaber, *Numerical Study of Turbulent Jet Ignition Assisted Combustion in a Lean Premixed Configuration*, Submitted to Journal of Fluid Mechanics, JFM-16-S-0919.
9. G.R. Gentz, M. Gholamisheri, and E. Toulson, *A Study of a Turbulent Jet Ignition System Fueled with Iso-octane: Pressure Trace Analysis and Combustion Visualization* Submitted to Applied Energy Ms. Ref. No.: APEN-D-16-05131.
10. R. Vedula, R. Song, T. Stuecken, G. Zhu, H. Schock, *Thermal Efficiency of a Dual-Mode Turbulent Jet Ignition Engine under Lean and Near Stoichiometric Operation*. Submitted to International Journal of Engine Research, Manuscript ID: IJER 16-0156.
11. R. Vedula, G. Gentz, T. Stuecken, E. Toulson, H. Schock, *Combustion Characteristics of Lean Burn Iso-octane in a Rapid Compression Machine Equipped With Dual Mode Turbulent Jet Ignition System*. Submitted to Applied Energy, Ms. Ref. No.: APEN-D-16-06579.

## II.27 Collaborative Research: NSF/DOE Partnership on Advanced Combustion Engines: A Universal Combustion Model to Predict Premixed and Non-Premixed Turbulent Flames in Compression Ignition Engines

### Overall Objectives

The primary objective of the proposed research is to develop a predictive turbulent combustion model that is universally applicable to mixed regimes of combustion including elements of both premixed and non-premixed flames in the presence of local limit phenomena, such as extinction and auto-ignition.

### Fiscal Year (FY) 2016 Objectives

- Develop turbulent combustion models based on chemical explosive mode analysis (CEMA) for large eddy simulation (LES) and Reynolds-averaged Navier–Stokes (RANS) simulations of compression ignition engines
- Perform direct numerical simulation (DNS) and LES of diesel fuel flames at engine-relevant conditions involving negative temperature coefficient (NTC) behaviors for model development and validation

### FY 2016 Accomplishments

- Developed a dynamic adaptive combustion modeling framework based on CEMA
- Developed an explicit CEMA approximation to enable efficient on-the-fly CEMA in three-dimensional (3D) simulations
- Implemented the dynamic adaptive model into the CONVERGE software for engine combustion simulations
- Developed a tabulated flamelet model (TFM) for LES of engine combustion, which can be potentially integrated into the universal modeling framework
- Developed a statistical averaging method for LES of spray flames
- Performed 3D DNS of a turbulent n-dodecane temporal jet in counterflowing air and a turbulent lifted dimethyl ether (DME) jet flame, both cases involve with NTC effect ■

### Tianfeng Lu (Primary Contact), Zhuoyin Ren

University of Connecticut  
191 Auditorium Rd., U-3139  
Storrs, CT 06269-3139  
Phone: (860) 486-3942  
Email: tianfeng.lu@uconn.edu

DOE Technology Development Manager:  
Leo Breton

#### Subcontractors:

- Sibendu Som, Argonne National Laboratory, Argonne, IL
- Jacqueline H. Chen, Sandia National Laboratories, Livermore, CA

### Introduction

Predictive simulation of turbulent combustion is critical to enable computer-aided design and optimization of advanced combustion engines. However, there is a lack of a turbulent combustion model that is simultaneously valid for different flame features. The primary objective of the proposed research is to develop a predictive turbulent combustion model that is universally applicable to mixed regimes of combustion including elements of both premixed and non-premixed flames in the presence of different local limit phenomena, such as extinction/re-ignition, auto-ignition, and premixed fronts propagating in different modes. LES and RANS of engine combustion with the new combustion model can then be used to address many long-standing questions on fuel efficiency, combustion control, and emissions reduction.

### Approach

This objective of the proposed research is achieved through a collaborative effort between the University of Connecticut, Sandia, and Argonne based on state-of-the-art DNS with systematically reduced non-stiff

chemistry for practical engine fuels at diesel engine conditions. The model development is based on CEMA that can rigorously detect critical flame features, e.g., local ignition, extinction, and premixed and non-premixed flamelets, from highly complex turbulent flames. Existing and new models specifically applicable to specific flame features are then applied on-the-fly based on the CEMA-based flame segmentation, such that each model is only used within its applicable range. The model development further exploits the low-dimensional manifold and thin spatial structures induced by exhausted fast chemistry in turbulent flames. The new model has been implemented into LES and RANS and will be validated against DNS results and experimental data at engine conditions.

## Results

### DNS of NTC-Affected Turbulent Flames

DNS of a 3D turbulent, auto-igniting temporal jet between partially premixed n-dodecane and diluted air was performed at 25 bar and at a jet Reynolds number of 7,000 with a newly developed 35-species reduced chemical kinetic model including both low-temperature chemistry [1]. It is found in Figure 1 that turbulence induced scalar dissipation rate in the jet redistributes heat generated in earlier ignited lean mixtures toward richer regions, resulting in significant low-temperature reactions occurring at all mixture compositions. DNS of a turbulent lifted DME slot jet flame was performed at a moderate pressure of 5 bar to study interactions between chemical reactions with low temperature heat release and shear-generated turbulence in a DME jet into heated coflow [2].

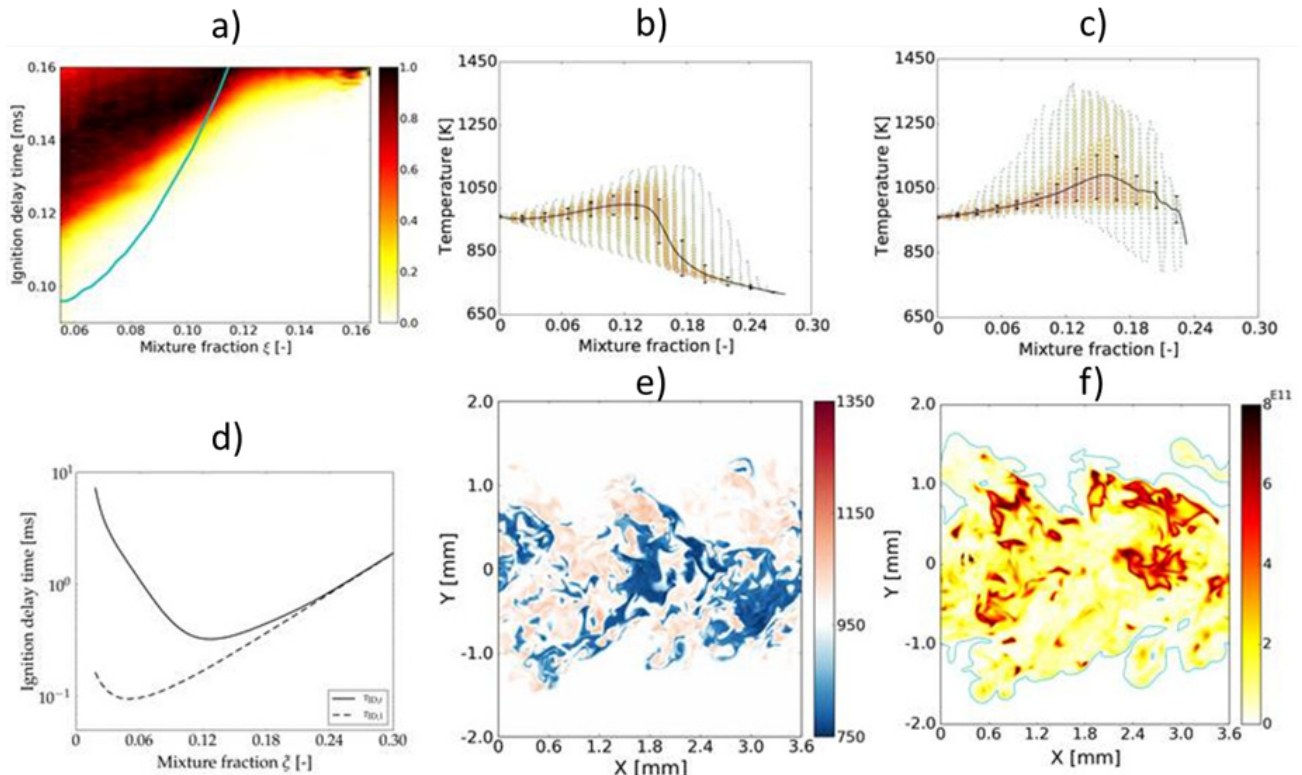


Figure 1. Turbulent cool flame auto-ignition of n-dodecane at 25 bar: (a) normalized conditional distribution of the cool flame ignition delay time of reacted fluid elements, conditioned on mixture fraction. The cyan line corresponds to the corresponding homogeneous ignition temperature (HIT); (b) and (c) conditional temperature evolution at 0.62 HIT and 0.98 HIT, respectively, where the condition mean (solid line) and standard deviation (bars) are superposed; colored symbols represent fraction of data in a given temperature/mixture fraction bin; second stage ignition occurs for  $T > 1,300$  K; d) first and second ignition delay times for homogeneous mixtures of diluted air (15%  $O_2$ ) and n-dodecane as a function of mixture fraction at  $p = 25$  bar,  $T_{amb} = 960$  K, and  $T_{fuel} = 450$  K; (e) spanwise slice of temperature isocontours at 0.67 HIT showing simultaneous first stage (blue) and second stage (red) ignition occurring; and (f) spanwise slice of heat release rate isocontours at 0.98 HIT showing spontaneous ignition propagation from rich conditions towards the stoichiometric mixture fraction (cyan line) following ignition.

The results suggest that the low temperature heat release and radicals affect the triple point propagation speed through enhancement of the laminar flame speed, and thus stabilize the flame further upstream. The DNS results verified that different flame features, including premixed reaction fronts, may coexist in non-premixed flames and need to be captured in modeling. The DNS data are being employed for the model development and validation.

### Development of a Dynamic Adaptive Combustion Modeling Framework Based on CEMA

A new dynamic adaptive combustion model is developed for LES and RANS of diesel spray flames to accurately capture both premixed and non-premixed flame features and to reduce the overall computational cost based on systematic computational flame diagnostics using CEMA. Critical flame features, such as the pre-ignition zone, non-premixed flame core, that is the post-ignition zone, and premixed flame fronts, are rigorously identified by CEMA-based criteria as shown in Figure 2a. To avoid the time-consuming eigenanalysis in CEMA, an explicit scheme for CEMA approximation is developed to accelerate on-the-fly flame zone segmentation in 3D turbulent flames with negligible computational overhead. The dynamic adaptive modeling framework was then constructed by assigning different combustion models to different CEMA-identified flame zones. As shown in Figures 2a and 2b, the ambient flow is treated as chemically frozen, the flamelet progress variable model together with a CEMA-assisted flamelet timescale model is applied in the post-ignition zone, and the SAGE combustion model in CONVERGE is applied in the pre-ignition mixtures to capture the fully transient two-stage ignition process. CEMA-based adaptive mesh refinement (AMR) is further applied near the premixed fronts, corresponding to the eigenvalue zero-crossing in CEMA, to improve the flame speed prediction, which is important for stabilization of lifted flames. The dynamic adaptive modeling framework is implemented into the CONVERGE software as user defined functions.

CEMA-based dynamic adaptive chemistry is developed and applied in LES of spray flames to demonstrate the effectiveness of the dynamic flame segmentation. Applying different chemical models in different flame zones, little error is induced to the prediction of such global behaviors as ignition delay and lift-off length as shown in Figure 3a. Scatter of temperature and OH mass fraction against mixture fraction in Figure 3b further shows that CEMA-based dynamic adaptive chemistry can effectively capture flame behaviors in different flame zones.

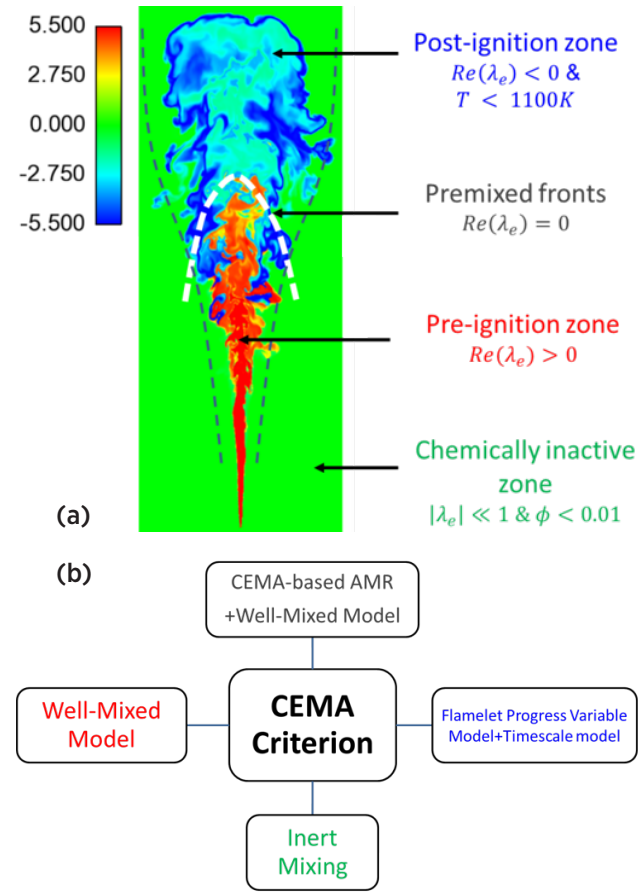


Figure 2. (a) Flame zone segmentation in the eigenvalue contour in a two-dimensional center cut of a 3D LES of a turbulent n-dodecane spray flame. (b) The framework of the CEMA-based dynamic adaptive combustion model.

Significant speedup can be achieved by using the dynamic adaptive modeling strategy with appropriate load balancing scheme. This point is demonstrated in Figure 4 showing the per-cell per-step central processing unit (CPU) time for I-Zone (SAGE only) and III-Zone (SAGE, flamelet, and inert mixing) models at two different time instances. It is seen that for I-Zone model, the CPU cost is  $\sim O(1 \text{ ms})$  for the entire flame zone. In contrast, with the III-Zone model, the high-cost SAGE model is only activated in a thin layer before the rich premixed fronts and near the flame edge, while the CPU cost of the flamelet model used in the post-ignition zone is lower than that of SAGE by three orders of magnitude, leading to significant overall time savings.

The dynamic adaptive modeling framework is then applied to LES of Spray A flames. Figure 5 shows the comparison of I-Zone (SAGE only) and II-Zone (SAGE and flamelet) models for temperature, OH mass fraction and the eigenvalue fields at two time instances before

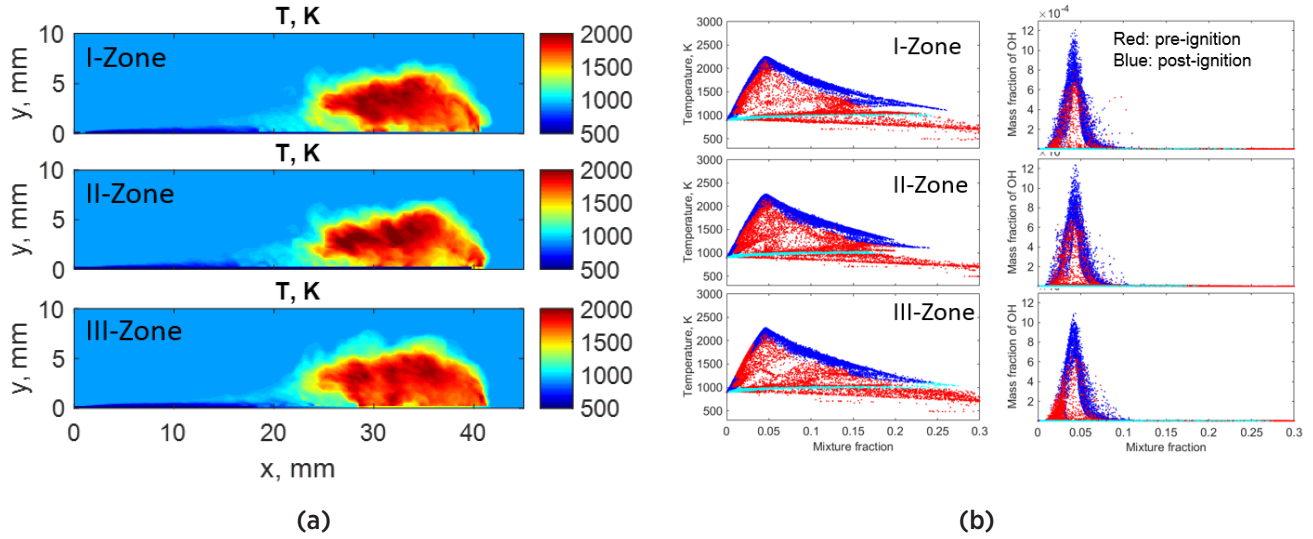


Figure 3. Comparison of (a) azimuthal averaged temperature, and (b) scattering of temperature and OH mass fraction in mixture fraction space, for three different chemistry sets at  $t = 0.6$  ms. In I-Zone chemistry, full chemistry with 54 species is applied for the whole domain, in II-Zone chemistry, a 42-species reduced chemistry is used for the post-ignition zone, while in the III-Zone chemistry, a 26-species reduced chemistry is further applied for the chemically inactive zone.

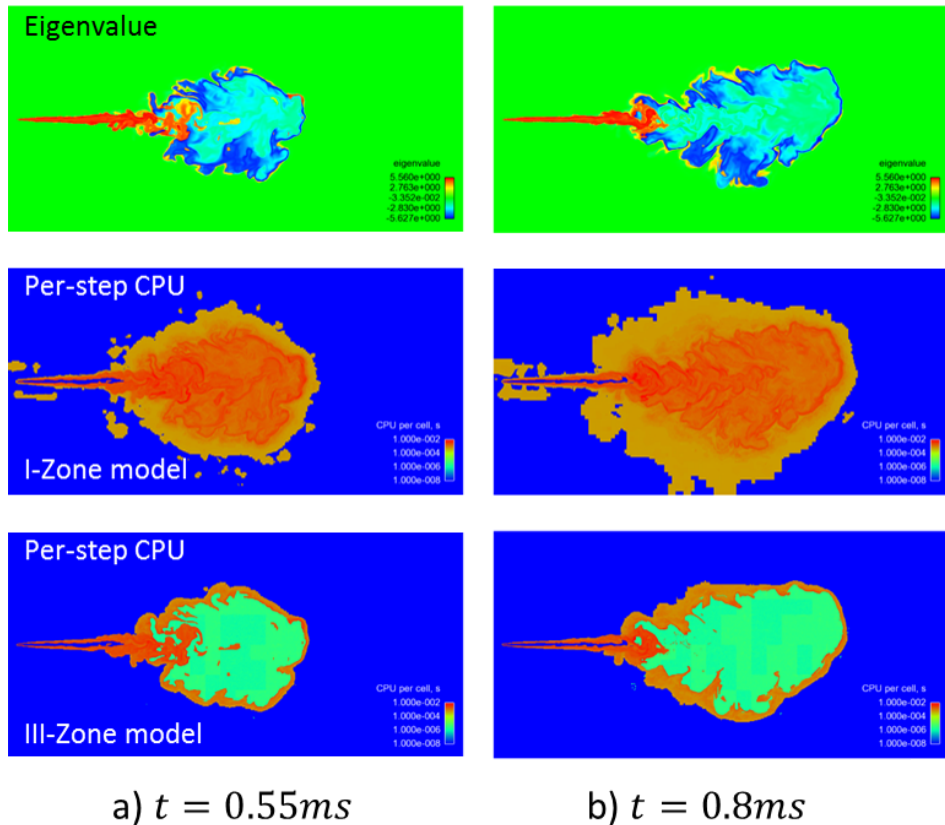


Figure 4. Per-cell computational cost for I-Zone model and III-Zone model at (a)  $t = 0.55$  ms and (b)  $t = 0.8$  ms. The first row represents the eigenvalue contours showing the overall flame structures.

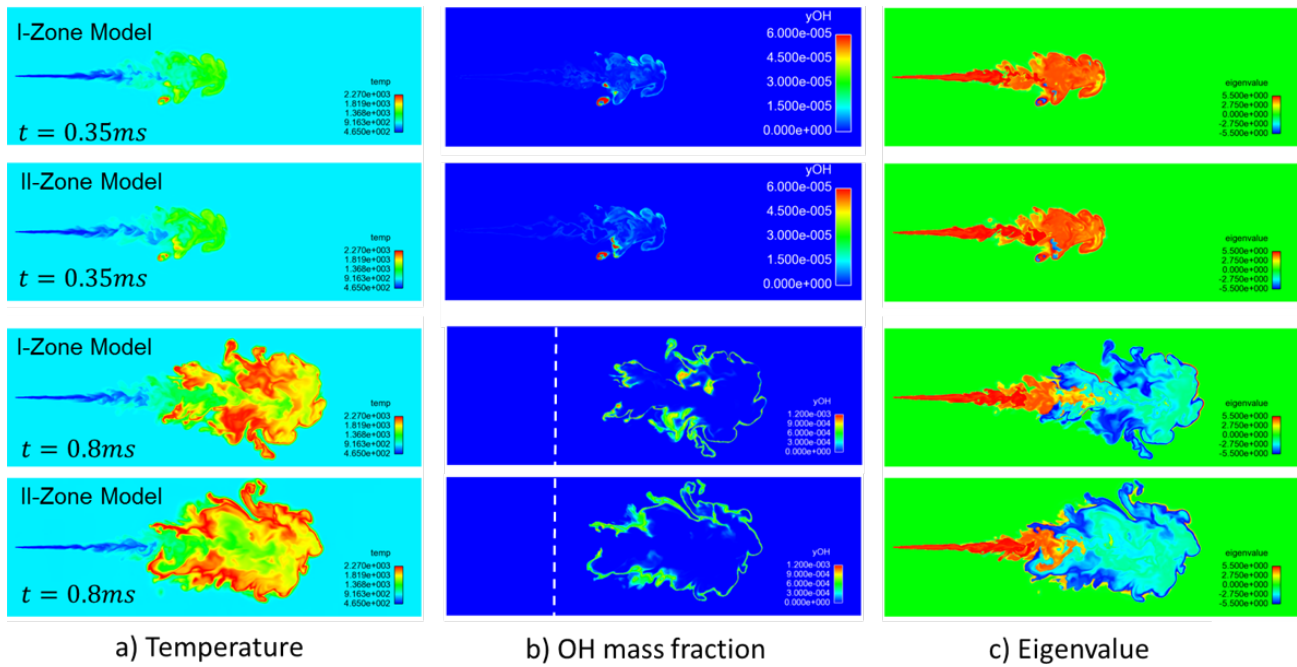


Figure 5. Comparison of (a) temperature, (b) OH mass fraction, and (c) eigenvalue for I-Zone model and II-Zone model at different times. White dash line indicates the experiment lift-off length of 16.5 mm.

and after ignition, respectively. Scalar fields before ignition are identical for the cases with and without using the adaptive modeling in that the flamelet model is not activated yet at this stage. After ignition occurred at  $t = 0.35$  ms, the use of adaptive modeling induces slight changes on the shape and locations of the ignition spots, while the effect on the ignition delay time is minimal. As a quasi-steady flame is being established near the flame base at  $t = 0.8$  ms, the II-Zone model predicts a shorter lift-off length and shows better agreement with the experimental lift-off length of 16.5 mm than the I-Zone model, while the overall flame length is not affected. Similar observations are made for the III-Zone model (SAGE, flamelet, and chemically frozen). The III-Zone model is also combined with the CEMA-based AMR and predicts shorter lift-off length and overall longer flame penetration compared with I-Zone model due to combined effect of dynamic adaptive modeling and CEMA-based AMR. Therefore, flamelet-type models are suitable for the post-ignition zone, and the adaptive modeling strategy can well capture the global flame behaviors of the diesel spray flame. The above results demonstrate the high fidelity and low computation cost of CEMA-based dynamic adaptive modeling.

### Development of a TFM Model and a Statistical Averaging Method for LES of Spray Flames

A TFM model is developed for LES based on the framework of the multi-flamelet representative

interactive flamelet model, using a novel technique of implementing four-dimensional unsteady flamelet libraries based on scalar dissipation rate, residence time, mixture fraction variance, and filtered mixture fraction. Figures 6a and 6b compare the ignition delay and lift-off length predictions by the TFM and SAGE models with experiment for igniting n-dodecane sprays under diesel engine conditions. It is seen that the TFM model shows excellent agreement with the experimental results at all the ambient temperatures. Figure 6c further shows that the TFM model leads to at least  $1.5\times$  speedup over the SAGE model for all the ambient temperatures, while higher speedups are expected for larger chemistry mechanisms.

To take advantage of LES in directly resolving the instantaneous large-scale flow features while reducing the number of LES realizations for validation of LES results with experimental or DNS datasets, a new statistical averaging method was developed by combining of azimuthal and ensemble averages to estimate statistical averages. It is concluded by applying magnitude similarity index defined by Hu et al. [3] that five LES realizations are sufficient to obtain convergence in the statistical means for the combined method. To obtain a more physical basis, multiple LES realizations by varying the initial ambient turbulent kinetic energy in the chamber were also performed. Similar results are observed using five realizations for different turbulent kinetic energy values.

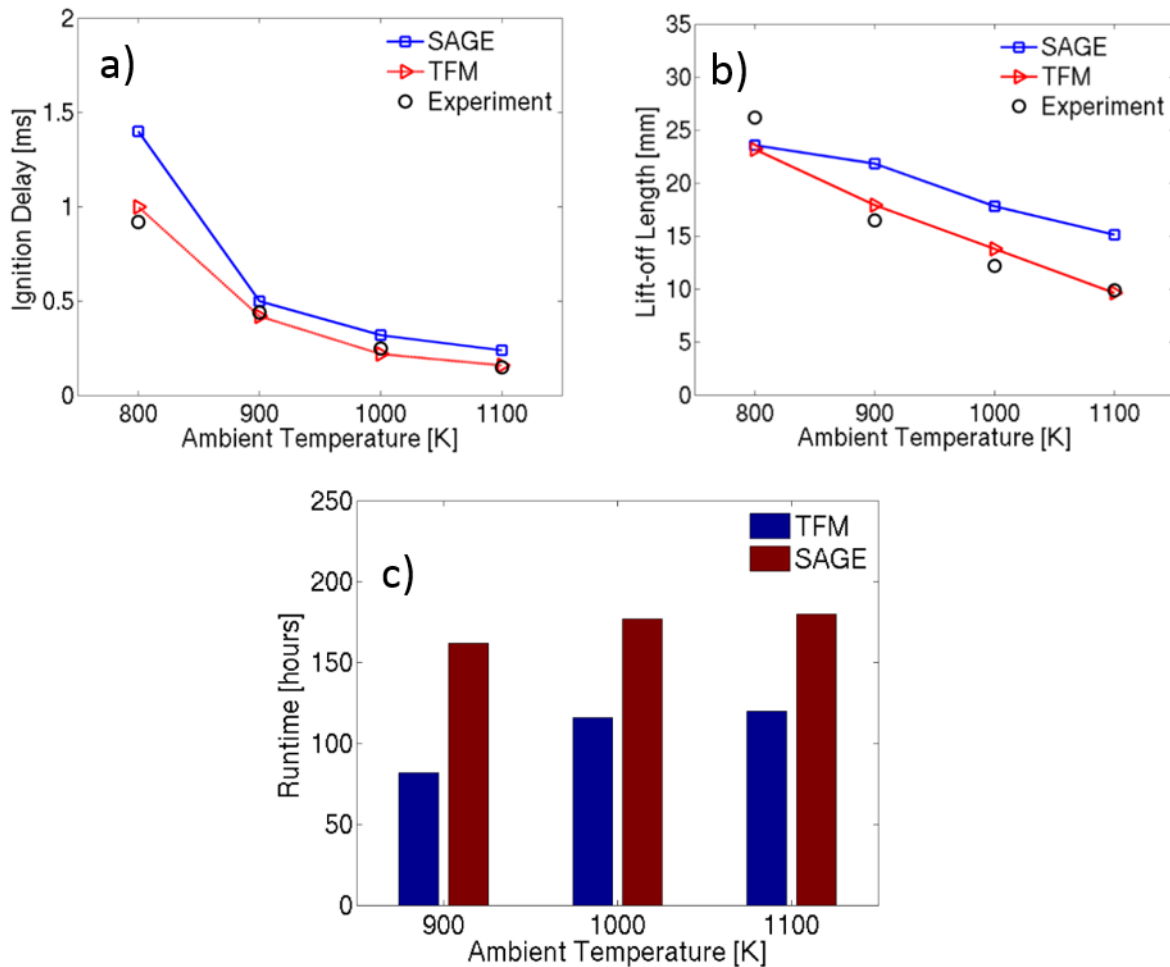


Figure 6. Comparison of (a) ignition delay, and (b) lift-off length between SAGE, TFM, and experimental data from the Engine Combustion Network across a range of ambient temperatures. (c) Comparison of speedup between the TFM and SAGE for various ambient temperature conditions.

## Conclusions

- A dynamic adaptive combustion modeling framework based on CEMA was developed and implemented into the CONVERGE commercial software for engine combustion simulations.
- An explicit CEMA approximation is developed to efficiently evaluate the eigenvalue of the chemical explosive mode.
- Different flame zones are identified by CEMA, such that appropriate models can be applied on-the-fly in different zones. The dynamic adaptive model is shown to be accurate and efficient.
- A TFM model was developed for LES of engine combustion, and can be potentially integrated into the universal modeling framework.

- A statistical averaging method for LES of spray flames was developed.
- DNS of a turbulent n-dodecane-air temporal jet into counter-flowing air and a turbulent lifted DME jet flame were performed including low-temperature chemistry to understand the underlying fluid dynamic and chemical kinetic processes in turbulent flames relevant to engine combustion conditions. The DNS data are employed for model development and validation.

## References

1. Borghesi, G. and Chen, J.H., A DNS investigation of turbulent n-dodecane/air jet autoignition, Western States Section of the Combustion Institute Spring 2016 Meeting, Seattle, WA, 2016.
2. Minamoto, Y. and Chen, J.H., DNS of a turbulent lifted DME jet flame, Combust. Flame 169 (2016) 38–50.

3. Hu, B., Banerjee, S., Liu, K., Rajamohan, D. et al., Large eddy simulation of a turbulent non-reacting spray jet (Spray H), ASME 2015 Internal Combustion Engine Division Fall Technical Conference, USA, November 8–11, 2015.
6. Pei Y., Mehl M., Liu W., Lu T.F., Pitz W.J., Som S., A multi-component blend as a diesel fuel surrogate for compression ignition engine applications, ASME J. Eng. Gas Turbines Power, 137.11 (2015) 111502.

## FY 2016 Publications/Presentations

1. C.M. Bolla, Y. Pei, E.R. Hawkes, S. Kook, T. Lu, Soot Formation Modelling of Spray-A Using a Transported PDF Approach, No. 2015-01-1849, SAE Technical Paper, 2015.
2. Zhou, L., Lu, Z., Ren, Z., Lu, T. et al., Large Eddy Simulation of an n-Heptane Spray Flame with Dynamic Adaptive Chemistry under Different Oxygen Concentrations, SAE Int. J. Engines, doi:10.4271/2015-01-0400, 8.2 2015.
3. Zhou L., Lu Z., Ren Z., Lu T.F., Luo K.H., Numerical analysis of ignition and flame stabilization in an n-heptane spray flame, Int. J. Heat Mass Transfer, Int. J. Heat Mass Transfer, 88 565–571, 2015.
4. M. Kuron, E.R. Hawkes, Z. Ren, J.C.K. Tang, H. Zhou, J.H. Chen, T. Lu, Performance of transported PDF mixing models in a turbulent premixed flame, Proceedings of the Combustion Institute, 2016.
5. Pei Y., Hawkes E.R., Kook S., Goldin G.M., Lu T.F., Modelling n-dodecane spray and combustion with the transported probability density function method, Combust. Flame, 162.5 (2015) 2006–2019.
7. Yao T., Pei Y., Zhong B.J., Som S., Lu T.F., A Hybrid Mechanism for n-Dodecane Combustion with Optimized Low-Temperature Chemistry, 9th U.S. National Combustion Meeting, Cincinnati, OH, May 17–20, 2015.
8. M. Kuron, Z. Ren, H. Kolla, E.R. Hawkes, J.H. Chen, T. Lu, An Investigation of the Scalar Dissipation Rate Behavior in a Premixed Hydrogen Flame, 10th Asia Pacific Conference on Combustion. Beijing, China, 2015.
9. Kuron M., Ren Z., Kolla H.N., Hawkes E., Chen J.H., Lu T.F., An Investigation of the Scalar Dissipation Rate Behavior in a Premixed Hydrogen Flame, 9th U.S. National Combustion Meeting, Cincinnati, OH, May 17–20, 2015.
10. C. Xu, T.F. Lu, Z. Ren, M.M. Ameen, S. Som, J.H. Chen, Chemical explosive mode analysis for adaptive modeling of diesel spray flames, Spring Technical Meeting of the Eastern States Section of the Combustion Institute, Princeton, NJ, 2016.

## II.28 NSF/DOE Partnership on Advanced Combustion Engines: Thermal Barrier Coatings for the LTC Engine – Heat Loss, Combustion, Thermal vs. Catalytic Effects, Emissions, and Exhaust Heat

### Overall Objectives

- Elucidate the impact of thermal barrier coatings on low temperature combustion (LTC) engines, and design engineered coatings that will produce the most desirable effects on combustion, efficiency, LTC operating range, and emissions of CO and unburned hydrocarbons
- Perform experimental heat transfer investigations with thermal barrier coatings (TBCs) which manipulate the wall temperature of a homogenous charge compression ignition (HCCI) engine to reduce heat losses and characterize their ability to improve performance, efficiency (thermal, combustion), and emissions; generate guidance for developing new coating formulations
- Develop new piston coatings (materials, properties, and application processes) that maximize benefits
- Develop simulation tools capable of predicting the temperature swing on the coating surface in order to correlate the coating properties and their impact on combustion; leverage experiments and three-dimensional finite element analysis simulation to enhance the heat transfer prediction capability of the one-dimensional cycle simulation; quantify the benefits of the preferred TBC over a range of operating conditions expected in a practical engine

### Fiscal Year (FY) 2016 Objectives

- Develop the third generation yttria-stabilized zirconia with structured porosity (YSZ-SP) coating with the optimized level of structured porosity
- Use ex situ testing to characterize thermal characteristics of yttria-stabilized zirconia (YSZ) and YSZ-SP coatings
- Carry out engine tests with YSZ and YSZ-SP coatings to correlate coating properties with reductions in combustion, heat transfer, emissions, and efficiency
- Utilize the sequential function specification method (SFSM) inverse conduction tool to predict coating surface temperatures and heat flux

**Zoran Filipi<sup>1</sup> (Primary Contact),  
Mark Hoffman<sup>1</sup>, Eric Jordan<sup>2</sup>,  
Nick Killingsworth<sup>3</sup>**

<sup>1</sup>Clemson University

Department of Automotive Engineering

4 Research Drive

Greenville, SC 29607

Phone: (864) 283-7222

Email: zfilipi@clemson.edu

DOE Technology Development Manager:

Leo Breton

Subcontractors:

• <sup>2</sup>University of Connecticut, Storrs, CT

• <sup>3</sup>Lawrence Livermore National Laboratory,  
Livermore, CA

- Research catalytic materials and propose a material suitable for application on the piston top
- Perform a sensitivity study using the finite element analysis model of the probe to understand the impacts of individual coating thermal and morphological properties on temperature to guide future coating design
- Utilize the guidance to develop the final formulation(s) with enhanced thermal properties tailored for LTC engine application

### FY 2016 Accomplishments

- Developed and refined the “Fuel Match/Phase Match” operational procedure. This process attempts to isolate the strictly thermal impact(s) of TBCs from those of combustion phasing
- Assessed candidate materials for in-cylinder catalytic coatings based on literature review and communication with Oak Ridge National Laboratory (ORNL)

- Refined YSZ-SP spray parameters including utilization of a dense top coat
- Assessed YSZ-SP impact on LTC emissions, heat transfer, and efficiency, including lessons learned regarding coating morphology and durability
- Assessed impact of the YSZ TBCs on surface temperature and heat flux via the inverse heat conduction SFSM solver
- Completed simulation analysis of surface temperature sensitivity to coating thermal and physical properties; conductivity and low-thickness were identified as the best path towards ideal TBC; lessons learned from work on three generations of the YSZ-SP coating led to a decision to focus on a new material, rather than manipulation of porosity
- Developed a novel low-conductivity coating based on gadolinium zirconate (GdZr) material ■

## Introduction

This research examines the impact of TBCs on LTC engines, and the design of the engineered coatings capable of maximizing the beneficial effects on combustion, efficiency, and emissions. The combined efforts on coating development, characterization of thermal properties, and in-depth LTC engine experimental investigations advances the understanding of the underlying mechanisms, thus making coating design less empirical. Achieving the goals required a multi-disciplinary team. We bring together expertise in (1) LTC engine combustion, heat transfer, emissions; (2) ceramic and metallic coatings; and (3) modeling of heat transfer in thin coatings.

## Approach

The investigation focuses on achieving the desired swing of instantaneous temperature on the coated piston surface to reduce heat losses during combustion while having minimal impact on the rest of the cycle. Achieving an increased surface temperature swing during combustion reduces the temperature difference between the charge and the wall, thus reducing compression and combustion heat loss and improving both cycle thermal efficiency and the LTC combustion efficiency. The reduced heat transfer also enables more robust engine operation at low loads. This is fundamentally different than the old idea of “low heat rejection engines,” that relied on complete insulation of the combustion chamber, which elevated the mean surface temperature and caused adverse effects on the volumetric efficiency and control of combustion.

Systematic experimentation with coatings in LTC engines is designed to correlate coating properties with their impacts on the kinetics-drive combustion. In parallel, coating application methods are being developed which allow for rapid screening of materials and systematic manipulation of material formulation, thermal properties, and porosity. In particular, a spray technique developed to create inter-pass boundaries enables a reduction of coating conductivity without changing material density.

Insights and measurements are used to develop and validate a physics-based model capable of predicting temperature gradients in the coating, and the instantaneous temperature swing in the surface during combustion. This tool can subsequently be utilized to carry out systematic studies, characterize the impact of key parameters, and guide final decisions regarding coating formulations.

## Results

### Design of a Low Conductivity Yttria-Stabilized Zirconia Coating with Structured Porosity

The first generation of SPPS applied YSZ-SP and was successful in providing additional improvements in emissions and efficiency (over traditional YSZ), but was subject to erosion. The second generation YSZ-SP coating was covered with a dense topcoat to address the erosion problems. The goal was to enable further reduction of coating’s conductivity by increasing porosity fraction. Unfortunately, the attempt to increase porosity led to a rougher surface as well, and a variable coverage thermal with the sealing coat sprayed on top (see Figure 1). The roughness and open porosity of the underlying TBC increased heat transfer and limited emissions and efficiency gains. Subsequent redesign for the third generation YSZ-SP coating addressed the cause of the topcoat separation. In this iteration, the thermal barrier layer had a lower overall porosity fraction to increase adhesion with a dense topcoat layer (see Figure 2). However, the secondary effect of the plasma spray adjustments was increased thickness. While intuition might suggest that increased thickness can be beneficial, detailed insights from engine experiments and simulation work proved it to be a detriment. More discussion on the impact of the third generation YSZ-SP coating, comparison of all three structured porosity coatings and synthesis of findings is presented in the section on Engine Experimentation.

### Engine Experimentation

Experimental testing was completed for two TBCs, a standard YSZ coating and a third generation YSZ coating

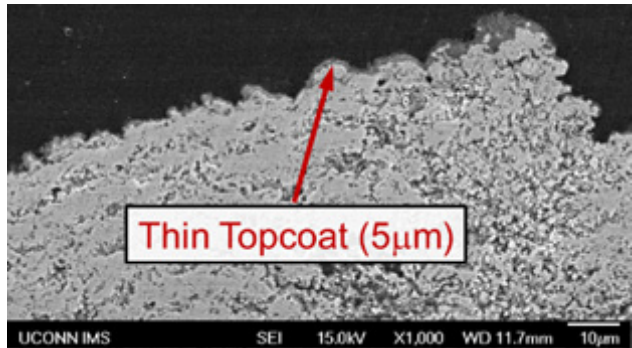


Figure 1. Second generation YSZ-SP coating covered with a dense topcoat

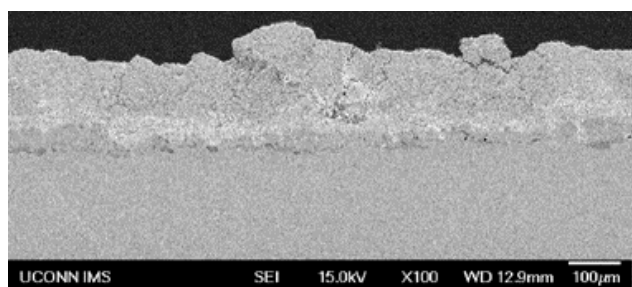
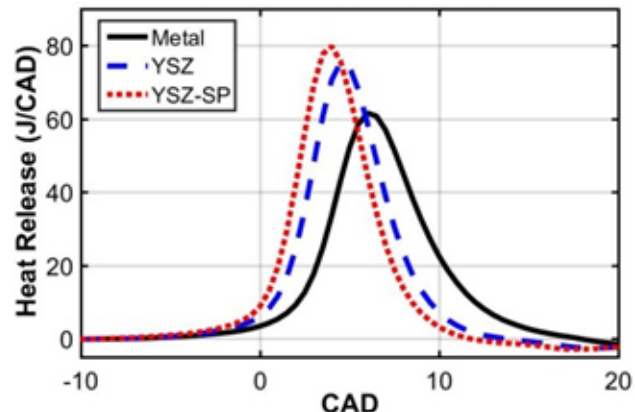


Figure 2. Third generation YSZ-SP coating with optimized porosity and higher thickness

with structured porosity (YSZ-SP). The first round of testing was performed under constant conditions between the baseline and coated engine cases to observe the real-world impacts of the coating. Combustion advanced when coatings were employed due to a reduction of heat transfer during compression, and combustion duration was reduced as well. This, in turn, led to higher rates of heat release and higher cylinder pressures (Figure 3). Substantial reduction in both hydrocarbon and CO emissions was observed, coupled with gains in both combustion (Figure 4a) and gross indicated thermal efficiencies (Figure 4b). Overall, there was a positive correlation between reduced TBC conductivity with structured porosity and increases in both combustion and thermal efficiencies. On average, the third generation YSZ-SP coating led to  $\sim 0.7\%$  improvement of the combustion efficiency, and more than 2% increases of thermal efficiency. Magnitude of the incremental improvements achieved with structured porosity was not as high as expected. The application of the inverse heat conduction analysis provided and explanation and guidance for the next steps, see the section on Inverse Heat Transfer Analysis.

A second set of tests was performed with combustion phasing controlled at  $7^\circ$  after top dead center through



CAD – crank angle degrees

Figure 3. Heat release rates for fuel-matched HCCI operation: baseline, YSZ, and YSZ-SP coated piston

the addition of recirculated cooled exhaust gas, to address a question from the audience during a 2015 Automotive Electronics Council review at the United States Council for Automotive Research. As illustrated in Figure 5, it was possible to maintain the same peak pressure location. The magnitudes of the improvements in emissions and combustion efficiency are reduced, but gross indicated efficiency is not only preserved, but even increased, as seen in Figure 6. Therefore, the fundamental mechanisms of improving the thermal efficiency due to a high-amplitude temperature swing on the coating surface is confirmed. Overall, in both real-world and phasing matched testing, coatings offered significant improvements in emissions, combustion, and indicated efficiency.

### Inverse Heat Transfer Analysis

An inverse heat transfer (IHT) solution algorithm was developed to correlate sub-TBC temperature measurements with corresponding surface temperature and heat flux profiles at the in-cylinder gas–wall interface [3]. The modified solution methodology is applied to ex situ sub-TBC temperature measurements, validating SFSM-derived results against well-established forward techniques [6]. Subsequently, the validated analysis tool is extended to evaluate experimentally measured sub-TBC temperature profiles from an HCCI engine.

The motivation for employing the IHT tool is two-fold: (1) SFSM-derived surface temperature profiles can be correlated with material properties (thermal conductivity, diffusivity, porosity fraction, etc.) to assess the impact of critical design parameters, and (2) SFSM surface heat flux profiles may be used to construct global heat transfer metrics, enabling quantitative analysis of coatings with respect to instantaneous/cumulative heat loss trends.

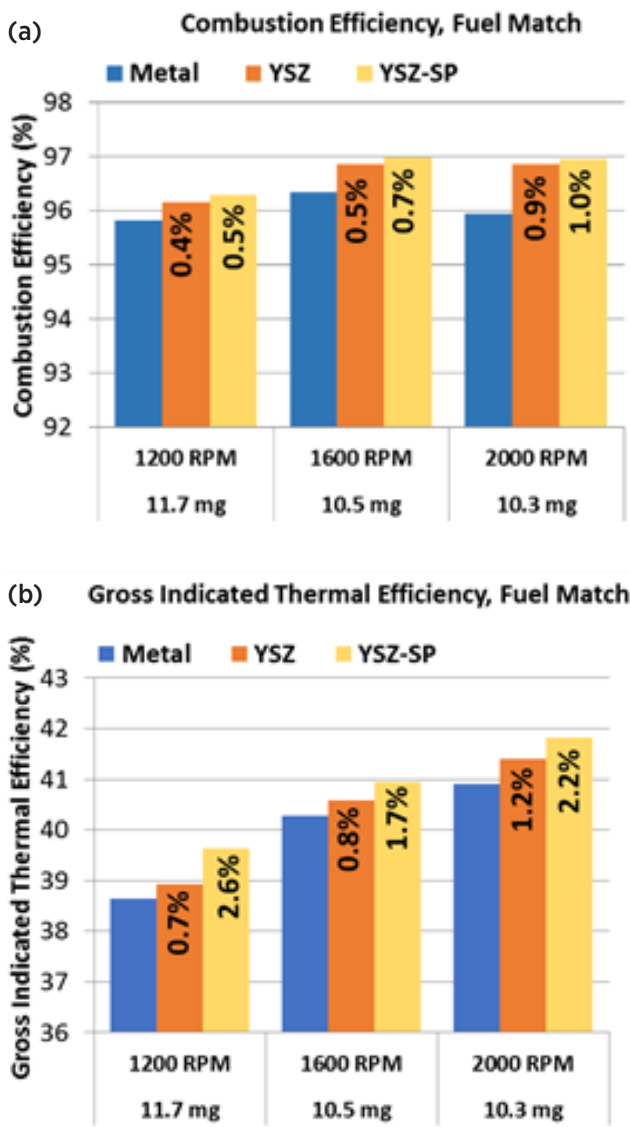
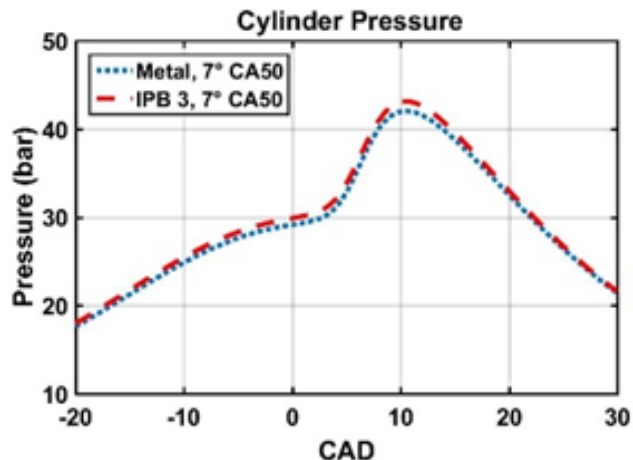


Figure 4. Combustion and gross indicated efficiencies obtained for fuel-matched operation with baseline, YSZ, and YSZ-SP coated piston

In short, IHT generated critical insights regarding the underlying mechanism and systematic development of guidance for subsequent iterations in coating development.

Ex situ validation of the inverse solution technique against a traditional, direct solution methodology through simultaneous exposure of metal and TBC-coated probes to a known heat flux pulse is demonstrated in Figure 7 for both the YSZ-SP and YSZ coatings. The inverse solver is unable to fully resolve the highest frequency component(s) of the YSZ-SP surface heat flux (i.e., the rising/falling edge of the experimental pulse). Despite this slight distortion, the overall magnitude and phasing



CA50 – crank angle at which 50% of the heat has been released

Figure 5. Cylinder pressures for baseline and TBC phase-matched operation, achieved with cooled exhaust gas recirculation

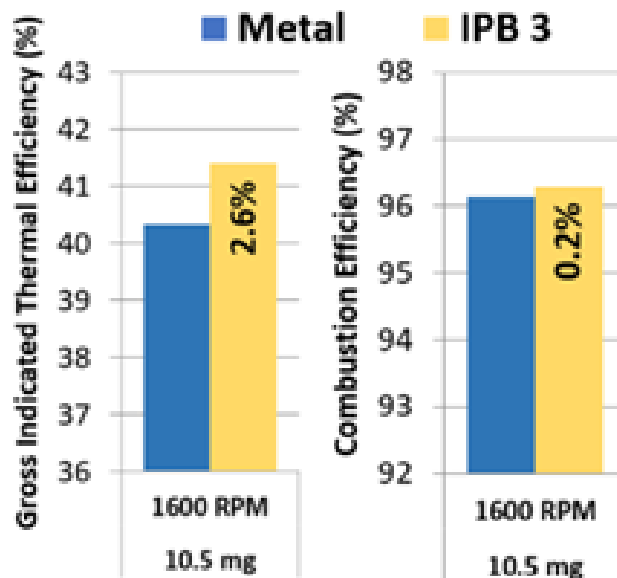


Figure 6. Combustion and gross indicated efficiencies obtained for phase-matched operation, 1,600 rpm

of the heat flux estimate remains intact. Increased TBC layer thickness referred to in sections on coating development and engine experiment is responsible for YSZ-SP's increased level of temperature profile, rather than amplitude. The additional coating material retains more heat over the time scale associated with the ex situ heating event.

Analysis is extended in situ to evaluate surface conditions at the gas–wall interface during fired operation of the LTC engine. The inverse solver again utilizes sub-TBC

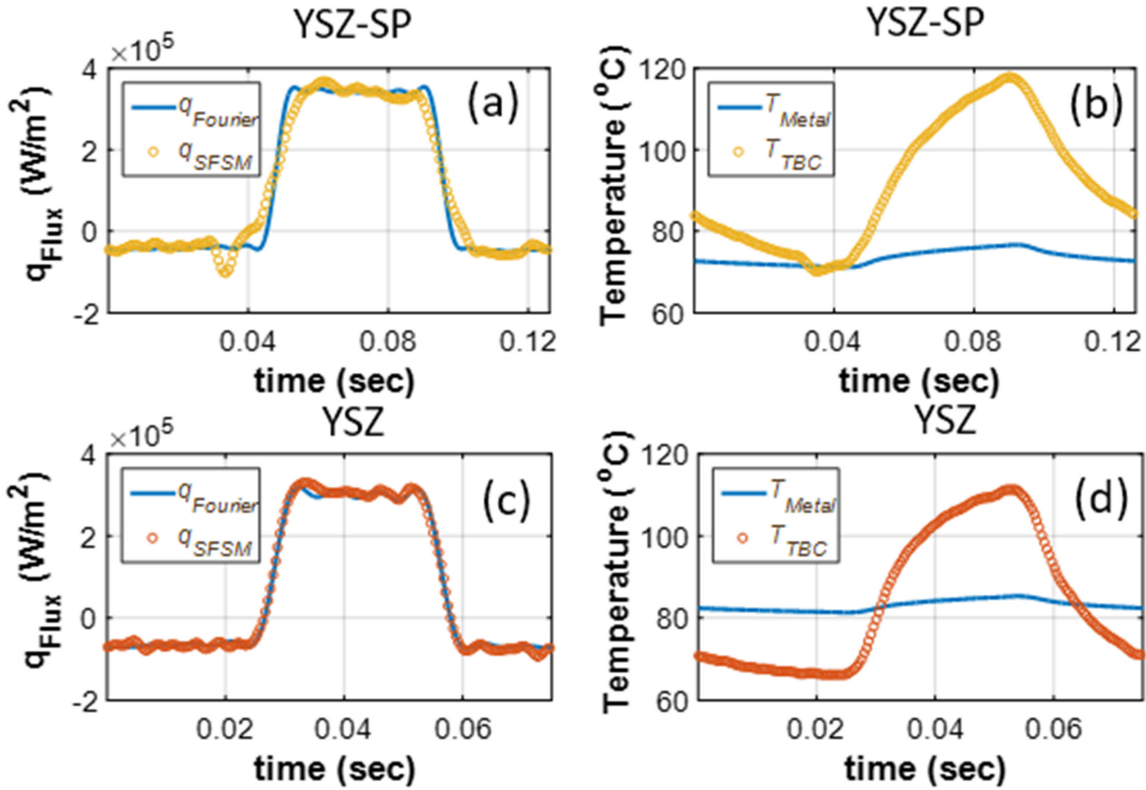


Figure 7. Ex situ (radiation chamber) results comparing inverse vs. forward solution methodologies for both YSZ-SP (a, b) and YSZ (c, d) materials

temperature measurements to resolve the corresponding surface heat flux and temperature profiles. The outcome for 1,600 rpm is summarized in Figure 8. Even though the conductivity of the YSZ-SP coating is reduced due to the layered porosity, the amplitude of the temperature swing compared to the baseline YSZ did not increase. Rather, the instantaneous temperature trace shifted upwards, leading to the increased cycle-average temperature.

This explains the modest magnitude of incremental improvements achieved with third generation structured porosity, and reinforces the strategic focus of our project on achieving a high-amplitude surface temperature swing rather than high degree of insulation. The synthesis of previous findings [4,5] and results in FY 2016 generates clear guidance for the final stage of the thermal barrier coating development. Both low-conductivity and

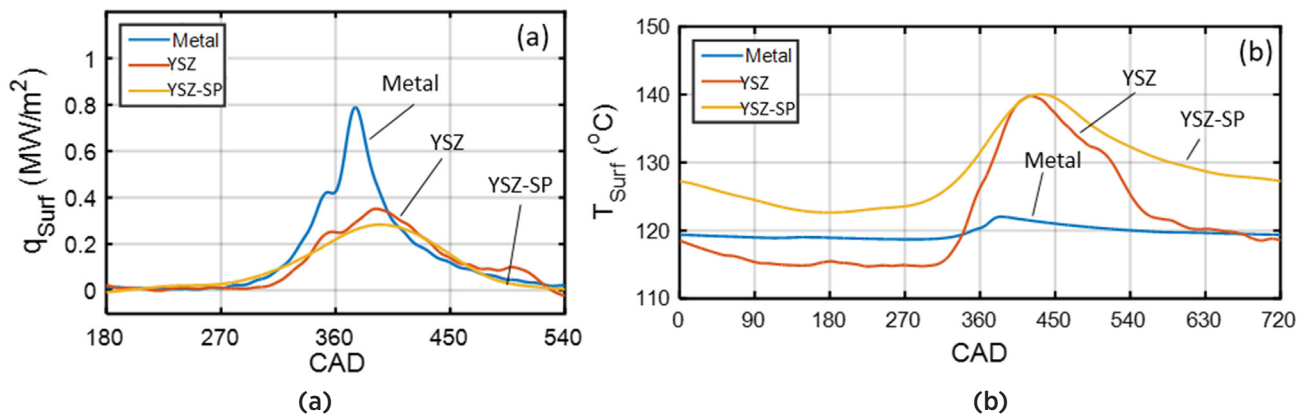


Figure 8. In situ surface heat flux (a) and resultant temperature estimates (b) for 1,600 rpm during Fuel Match/Phase Match operation

relatively low thickness (and thus low heat capacity) are desirable. In addition, achieving low-capacity through reduced thickness is much preferred compared to porosity, as indicated by challenges incurred working on the three generations of YSZ-SP. Consequently, future work will focus on searching for materials that can provide low-conductivity of a dense coating.

### Inclusion of Catalytic Materials in TBC Design

Recent studies of aftertreatment systems for LTC engines have focused on developing catalysts with low light-off temperatures. This provides encouragement for a hypothesis that in-cylinder catalysts can be achieved in LTC with the goal of improving oxidation in near-wall zones. In particular, ORNL's team has developed a catalyst that successfully achieves light-off at temperatures as low as 150°C [1,2]. The catalyst is comprised of three metal oxides, cobalt oxide, copper oxide, and cerium oxide (CCC). The low temperature activity makes the CCC catalyst an excellent choice for an in-cylinder catalysts. Discussions with ORNL have revealed that a solution precursor plasma spray process is ideally suited for applying a CCC top coat on the surface of the thermal barrier.

### Conclusions

- A YSZ-SP coating was successfully applied to an LTC piston.
- LTC engine experimentation with a YSZ coated piston revealed significant improvements in hydrocarbon/CO emissions and both combustion and indicated efficiencies. The YSZ-SP coating offers additional gains.
- With matched combustion phasing, both YSZ TBCs retained their gross thermal efficiency benefits.
- Inverse heat conduction analysis of TBC surface conditions revealed a dynamic surface temperature profile which mimics the bulk gas behavior during fired operation.
- The temperature swing effectively reduced the  $T_{\text{Gas}}/T_{\text{Surf}}$  temperature differential during combustion-relevant CADs, preserving thermal energy in-cylinder while fostering more complete oxidation of the cylinder's fuel content. Higher thickness of the coating elevates the temperature level, rather than amplitude of the swing. Therefore, low conductivity material and low thickness (<150 mm) are favored.
- Gadolinium zirconate, a coating that has half the native thermal conductivity of YSZ, has been identified as the

next TBC. Spray parameters have been developed for application on LTC pistons.

- A CCC catalyst developed by ORNL is a promising option for in-cylinder application in the LTC engine.
- The SPPS process is ideally suited for spraying the catalyst as a coating. Work is underway to develop the plasma spray parameters for the low-conductivity materials, e.g. GdZr and low-cost proprietary.

### References

1. Binder, A.J., Toops, T.J., Unocic, R.R., Parks, J.E., & Dai, S. (2015). Low-Temperature CO Oxidation over a Ternary Oxide Catalyst with High Resistance to Hydrocarbon Inhibition. *Angewandte Chemie International Edition*, 54(45), 13263–13267.
2. Parks, J. (2016, April). *Emissions Challenges for Advanced Combustion Engines*. Presented at the SAE High Efficiency Engine Symposium, Detroit, MI.
3. O'Donnell, R., Powell, Filipi, Z., Hoffman, M., "Estimation of Thermal Barrier Coating Surface Temperature and Heat Flux Profiles in a Low Temperature Combustion Engine using a Modified Sequential Function Specification Approach," *ASME Journal of Heat Transfer*, HT-16-1101. In print.
4. O'Donnell, R., Powell, Hoffman, M., Filipi, Z., "Inverse Analysis of In-cylinder Gas-Wall Boundary Conditions: Investigation of a Yttria Stabilized Zirconia Thermal Barrier Coating for Homogeneous Charge Compression Ignition," Proceedings of the Internal Combustion Fall Technical Conference (ASME), ICEF2016-9401.
5. Powell, T., O'Donnell, R., Hoffman, M., Filipi, Z. (2016) "Impact of a Yttria-Stabilized Zirconia Thermal Barrier Coating on HCCI Engine Combustion, Emissions, and Efficiency," Proceedings of the Internal Combustion Fall Technical Conference (ASME).
6. Powell, T., Killingsworth, N., Hoffman, M., Prucka, R., Filipi, Z. "Simulating the Gas-Wall Boundary Conditions on a Thermal Barrier Coated Low Temperature Combustion Engine," *International Journal of Powertrains*, IJPT-105629. In print

### FY 2016 Publications/Presentations

1. O'Donnell, R., Powell, Filipi, Z., Hoffman, M., "Estimation of Thermal Barrier Coating Surface Temperature and Heat Flux Profiles in a Low Temperature Combustion Engine using a Modified Sequential Function Specification Approach," *ASME Journal of Heat Transfer*, HT-16-1101, *in print*.

2. O'Donnell, R., Powell, Hoffman, M., Filipi, Z., "Inverse Analysis of In-cylinder Gas-Wall Boundary Conditions: Investigation of a Yttria Stabilized Zirconia Thermal Barrier Coating for Homogeneous Charge Compression Ignition," *Proceedings of the 2016 Internal Combustion Fall Technical Conference (ASME)*, ICEF2016-9401.
3. Powell, T., O'Donnell, R., Hoffman, M., Filipi, Z. "Impact of a Yttria-Stabilized Zirconia Thermal Barrier Coating on HCCI Engine Combustion, Emissions, and Efficiency." *Proceedings of the 2016 Internal Combustion Fall Technical Conference (ASME)*.
4. Filipi, Z., "Interplay Between Heat Transfer and Kinetics-driven Combustion: Lessons Learned and Directions for Future," *Keynote Address, ASME ICEF Conference*, Greenville, SC, October 2016.

## II.29 Radiation Heat Transfer and Turbulent Fluctuations in IC Engines – Toward Predictive Models to Enable High Efficiency

### Overall Objectives

- Quantify effects of radiative heat transfer and turbulent fluctuations in composition and temperature on combustion, emissions, and heat losses in internal combustion (IC) engines
- Develop computational fluid dynamics (CFD)-based models to capture these effects in simulations of in-cylinder processes in IC engines
- Exercise the models to explore advanced combustion concepts for IC engines and to develop next-generation high-efficiency engines

### Fiscal Year (FY) 2016 Objectives

- Perform coupled engine simulations (where the radiative source term feeds back into the CFD simulation through the energy equation) using various spectral models and radiative transfer equation (RTE) solvers to isolate and quantify the relative importance of different aspects of the radiation modeling on computed heat release, heat losses, and pollutant emissions
- Account for the influences of unresolved turbulent fluctuations in composition and temperature on soot and radiation using a transported probability density function (PDF) method
- Exercise an advanced radiation model (photon Monte Carlo [PMC]/line-by-line [LBL]/PDF) to develop new insight into radiative transfer under engine-relevant conditions

### FY 2016 Accomplishments

- Continued coupled engine simulations using different spectral models and RTE solvers
- Coupled soot and radiation models with a transported PDF method to account for effects of unresolved turbulent fluctuations in engines
- Performed PMC/LBL/PDF simulations of a high-pressure turbulent spray flame where experimental measurements are available, which provided new insight into earlier radiation measurements for this flame ■

**Daniel C. Haworth<sup>1</sup> (Primary Contact),  
Michael F. Modest<sup>2</sup>**

<sup>1</sup>The Pennsylvania State University  
233 Research East Building  
University Park, PA 16802  
Phone: (814) 863-6269  
Email: dch12@psu.edu

<sup>2</sup>University of California, Merced  
Science & Engineering Building, Room 392  
Merced, CA 95343  
Phone: (209) 228-4113  
Email: MModest@ucmerced.edu

DOE Technology Development Manager:  
Leo Breton

### Introduction

While radiation in IC engines has received relatively little attention up until now, advanced high-efficiency engines are expected to function close to the limits of stable operation, where even small perturbations to the energy balance can have a large influence on system behavior. The premise of this research is that radiative heat transfer and complex turbulence–chemistry–soot–radiation interactions (TCSRI) may be particularly important in the “non-robust” combustion environments that will characterize advanced high-efficiency IC engines. These effects warrant thorough investigation under engine-relevant conditions, and predictive models that account for them will be required to realize the ambitious efficiency targets that have been established for next-generation engines and vehicles.

### Approach

CFD tools for radiative heat transfer and TCSRI are being developed using the open-source CFD toolkit, OpenFOAM®. The research is organized into four tasks: (1) extend multiphase radiation models to engine-relevant conditions; (2) explore radiation and TCSRIs in engine-relevant environments; (3) perform quantitative comparisons with experiment for constant-volume

combustion chambers; and (4) perform quantitative comparisons with experiment for compression ignition engines. Through collaboration with the Combustion Research Facility at Sandia National Laboratories (Joseph C. Oefelein), the models and tools also will be implemented in a high-fidelity large eddy simulation code. Ongoing active participation in the Engine Combustion Network (ECN) provides access to experimental data for high-pressure, constant-volume turbulent spray combustion under engine-relevant conditions. And through collaboration with Volvo (Samuel L. McLaughlin), engine data for model validation are available for heavy-duty compression ignition engines operating in conventional diesel combustion modes and in advanced combustion modes.

## Results

CFD simulations with coupled radiation models continued for a production heavy-duty diesel engine and for a single-cylinder, optical heavy-duty engine. Computed engine-out soot emissions show the largest sensitivity to the details of the radiation model. Depending on the specific combination of spectral radiative properties model, RTE solver, and whether or not the effects of unresolved TCSRI are considered, computed soot levels can vary by 50% or more. The most sophisticated radiation model considers LBL spectral radiation properties, a stochastic PMC method to solve the RTE, and a transported PDF method to account for TCSRI.

To sort out the relative importance of molecular gas radiation versus soot radiation, quantitatively accurate soot predictions are needed. An important finding pertains to the differences in the relative importance of different physical processes in soot formation between atmospheric-pressure versus high-pressure turbulent combustion. Compared to atmospheric pressure flames (where most soot modeling and experimental studies have been done), it has been found that at engine-relevant pressures, computed soot volume fractions are relatively less sensitive to the kinetic rates in the soot models (because the rates are so fast) and are relatively more sensitive to the details of the turbulent combustion modeling (accurate accounting for unresolved turbulent fluctuations in composition and temperature) and turbulent mixing. This does not mean that soot kinetics are unimportant at high pressures. Rather, it means that transport and mixing become relatively more important as rate-controlling processes. One must exercise caution to avoid tuning rate coefficients to account for deficiencies in the turbulent combustion modeling. The PDF method provides a framework that allows these different physical processes to be separated cleanly.

Examples are shown in Figures 1 and 2. In Figure 1, the computed and measured total soot mass are plotted as functions of time after start of injection for ECN Spray A [1]: a transient high-pressure n-dodecane turbulent spray flame. Results from a well-stirred reactor (WSR) model that neglects unresolved turbulent fluctuations in composition and temperature are compared with those from a PDF model that accounts for unresolved turbulent fluctuations, both using the same chemical mechanism and soot model (here a semi-empirical two-equation model). The PDF model shows better agreement with experiment, especially in capturing the rapid initial transient rise and drop off in soot before a quasi-stationary state is reached. Computed spatial distributions of soot volume fraction are also in much better agreement with experiment for the PDF model (not shown). This suggests that it is important to account for unresolved turbulent fluctuations, but that the specific spatial/temporal coherence of the fluctuations is not as important (these are unsteady Reynolds-averaged Navier-Stokes results, not large eddy simulation).

Computed power spectra of emitted radiation and radiation reaching the wall are shown at one instant in time during the quasi-stationary flame in Figure 2. There the individual contributions from three molecular gases ( $\text{CO}$ ,  $\text{CO}_2$ , and  $\text{H}_2\text{O}$ ) and from soot particles are shown, in addition to the total radiation. Approximately 94% of the radiation that is emitted is reabsorbed before reaching the wall. Radiative emission is dominated by  $\text{CO}_2$  (~87% of total emission). However, the system is

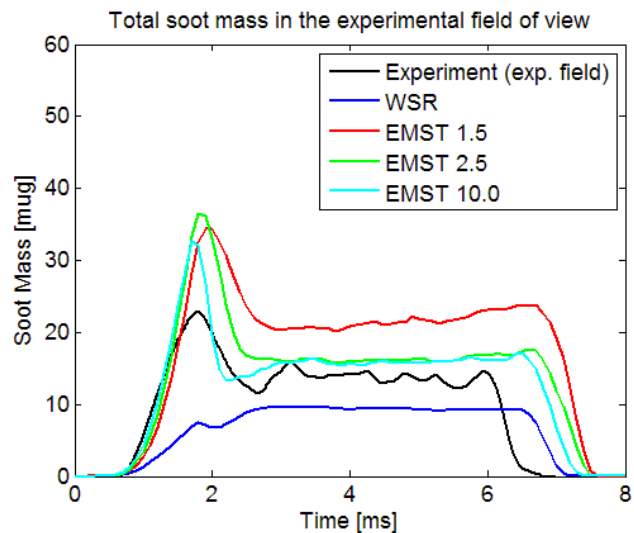
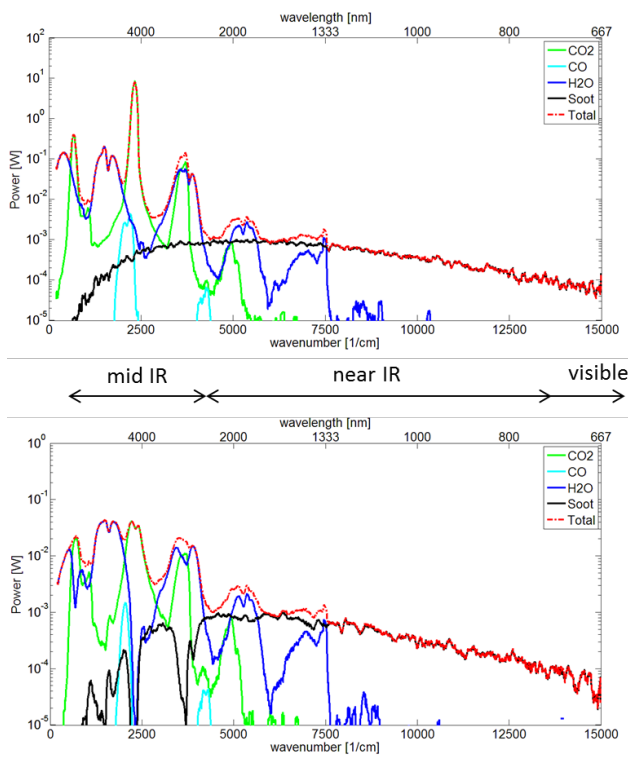


Figure 1. Computed and measured total soot mass as a function of time for ECN Spray A. Computed results are shown for a WSR model and a PDF method using the Euclidean Minimum Spanning Tree (EMST) mixing model, for three different values of the mixing model coefficient.



IR – infrared

Figure 2. Computed power spectra of radiative emission (top) and radiation reaching the wall (bottom) for ECN Spray A at one instant in time during the quasi-stationary flame ( $t = 3$  ms after start of injection).

optically very thick at wavenumbers corresponding to  $\text{CO}_2$  emission (especially in the 4  $\mu\text{m}$  band), such that the radiation reaching the wall is dominated by  $\text{H}_2\text{O}$  radiation (~58% of radiation reaching the wall). The contribution of soot radiation to the total radiation reaching the wall is approximately 7%. Experimental measurements of radiation for this flame have been reported in Skeen et al. [2]. There the measurements were limited to visible wavelengths of 400–700 nm. As can be seen in Figure 2, this corresponds to a small fraction of the radiation that reaches the wall. The experimentally reported radiant fraction for this flame (percentage of fuel energy reaching the wall as thermal radiation) was 0.068% [2]. The computed total radiant fraction is approximately 1%, but the computed radiant fraction considering soot radiation alone is 0.07%, very close to the measured value. This provides some confidence that the model can be used to extrapolate to wavenumbers for which experimental measurements are not available.

## Conclusions

- At engine-relevant pressures, turbulent transport and mixing become relatively more important compared to kinetics in determining the amount of soot that is formed.
- Global radiation effects in heavy-duty compression ignition engines (influences of radiation on heat release rate, wall heat transfer, and emissions) are in the 5–50% range.
- Molecular gas radiation is more important than soot radiation for conditions that are of interest for next-generation compression ignition engines (higher pressures and higher levels of exhaust gas recirculation compared to current state-of-the-art engines).
- There are complex spectral interactions that would be difficult, if not impossible, to unravel without the PMC/LBL radiation model.
- PMC/LBL provides insight that can be used to interpret experimental measurements.

## References

1. Engine Combustion Network (ECN), <https://ecn.sandia.gov/>. 2016.
2. S. Skeen, J. Manin, L. Pickett, C. Dalen, A. Ivarsson (2014). Quantitative Spatially Resolved Measurements of Total Radiation in High-Pressure Spray Flames, SAE Technical Paper No. 2014-01-1252.

## FY 2016 Publications/Presentations

1. M.F. Modest and D.C. Haworth, Radiative Heat Transfer in Turbulent Combustion Systems: Theory and Applications, SpringerBriefs in Applied Sciences and Technology, 2016. ISBN 978-3-319-27289-4.
2. C. Paul, A. Sircar, A. Imren, S. Ferreyro-Fernandez, S.P. Roy, W. Ge, D.C. Haworth, M.F. Modest, Radiative Heat Transfer and Turbulence-Radiation Interactions in a Heavy-Duty Diesel Engine, 2016 Spring Technical Meeting of the U.S. Eastern States Section of the Combustion Institute, Princeton, NJ (13–16 March 2016).
3. D.C. Haworth, Radiative heat transfer in engine-relevant environments, Advanced Engine Combustion Review Meeting, Livermore, CA (8–11 February 2016).
4. D.C. Haworth, Radiative heat transfer in engine-relevant environments, Advanced Engine Combustion Review Meeting, Southfield, MI (16–19 August 2016).

## II.30 Sooting Behavior of Conventional and Renewable Diesel Fuel Compounds and Mixtures

### Overall Objectives

- Develop a knowledge base that allows surrogate mixtures to be formulated that match the sooting behavior of any given real diesel fuel

### Fiscal Year (FY) 2016 Objectives

- Measure quantitative sooting tendencies of the components of the Coordinating Research Council (CRC) diesel surrogates
- Determine whether the CRC surrogates reproduce the sooting behavior of real diesel fuels
- Develop procedures that can predict sooting tendencies of any likely surrogate mixture without further measurements

### FY 2016 Accomplishments

- Measured sooting tendencies of 25 components of proposed diesel surrogates, including all nine components of the first generation CRC surrogates
- Measured sooting tendencies for all of the CRC surrogate mixtures and several reference diesel fuels
- Developed two procedures for predicting the sooting tendencies of surrogate mixtures
- Posted the measured two-dimensional soot and temperature data to the internet to maximize its availability to the research community
- Involved two high school students and two undergraduates in scanning transmission electron microscopy research ■

### Introduction

Emissions of soot particles are one of the most objectionable aspects of internal combustion engines. Exposure to soot and other fine particulates suspended in ambient air is estimated to cause over 3 million deaths each year worldwide [1]. Moreover, soot contributes directly to global warming by absorbing sunlight and heating the atmosphere; recent studies indicate that it is the second most important source of climate change and has a radiative forcing only one-third less than CO<sub>2</sub> [2]. Unfortunately, engine strategies that improve efficiency,

**Lisa Pfefferle (Primary Contact),  
Charles McEnally**

Yale University  
9 Hillhouse Avenue  
New Haven, CT 06520-8286  
Phone: (203) 432-4377  
Email: lisa.pfefferle@yale.edu

DOE Technology Development Manager:  
Leo Breton

such as gasoline direct injection and compression ignition, tend to increase soot emissions. Thus, keeping soot emissions to acceptable levels is a major challenge of advanced engine combustion.

A critical part of meeting this challenge is using computational fluid dynamic simulations to optimize engine design without building costly prototypes [3]. However, real fuels, especially diesel fuels, are chemically complex and must be replaced in computation fluid dynamic simulations by simplified mixtures that act as surrogates to the real fuel [4]. A number of diesel surrogates have been proposed, most prominently the four CRC surrogate mixtures of Mueller et al. [5,6]. The CRC surrogates have been shown to reproduce the density, ignitability, volatility, and some compositional aspects of real diesel fuels, but little is known about how accurately they reproduce sooting behavior. The goal of this project was to answer this question and develop knowledge that would allow surrogates to be formulated that accurately mimic the sooting behavior of any given diesel fuel.

### Approach

In this project the sooting tendency of a fuel was characterized by a novel method based on the yield of soot when 0.5% by mass of the test fuel was added to the fuel of a methane-air coflow nonpremixed flame [7]. Compared to other techniques such as smoke point, this method is well-suited to diesel fuels, which have very low volatilities, since only about 600 ppm of the fuel has to be vaporized. Soot concentrations in the resulting flame were measured by color ratio pyrometry or by line-of-sight spectral radiance. The maximum soot concentrations for each test fuel were rescaled, in a manner analogous to an

octane rating, to produce a Yield Sooting Index (YSI) for that fuel. In particular, YSI is defined by

$$YSI = A * f_{v,max} + B$$

where  $f_{v,max}$  is the maximum soot concentration for the test fuel, and  $A$  and  $B$  are constants determined by the conditions that  $YSI = 0$  for n-hexane and 100 for benzene. Figure 1 shows that the YSIs measured for a number of diesel fuels, jet fuels, and their surrogates correlate well with smoke point, i.e., YSI is more convenient to measure than smoke point but it characterizes the same underlying fuel property. (Jet fuels were included to increase the number of data points and range of sooting tendencies.)

## Results

The YSIs and underlying temperature and soot data generated during this study have been posted to a flame data website [8] and to a Dataverse [9] to make them widely available to the research community.

The first generation CRC surrogates are mixtures of nine compounds representative of various chemical classes found in real diesel fuels. Figure 2 shows the YSIs determined for each of these nine compounds. The YSIs are strongly correlated with the number of aromatic rings; thus 1-methylnaphthalene (1MN), with two rings, has the largest YSI, tetralin (TET) and 1,2,4-trimethylbenzene (TMB), with one ring, have intermediate YSIs, and the remaining nonaromatic hydrocarbons have low sooting tendencies.

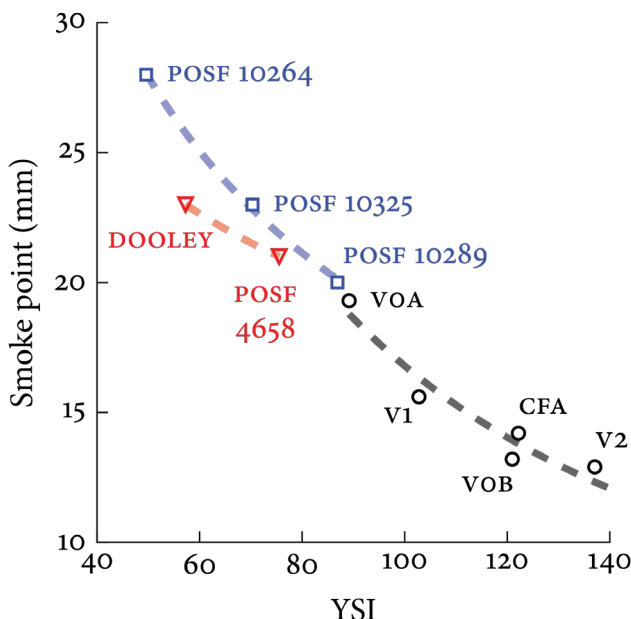
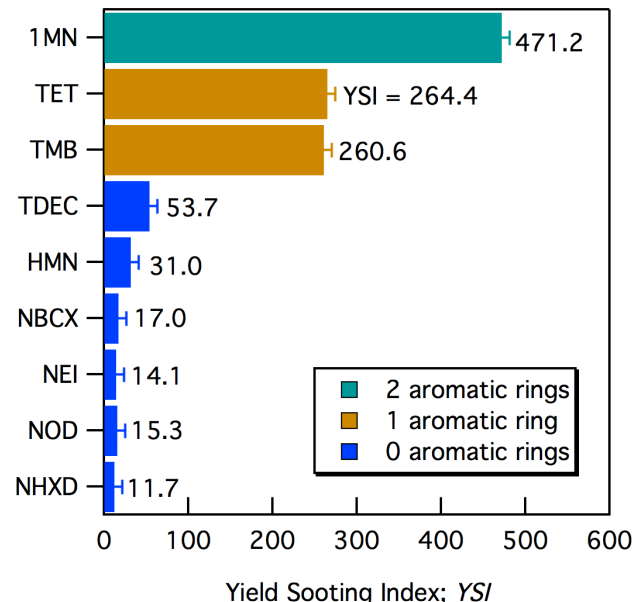


Figure 1. Comparison of YSIs and smoke points measured for diesel fuels, jet fuels, and their surrogates.

To determine how the YSIs of surrogate mixtures relate to the YSIs of their components, 32 mixtures of the nine first generation compounds were prepared and tested. Figure 3 compares the measured mixture YSIs to predicted YSIs based on the mixture YSI being the mass fraction-weighted average of the component YSIs; the excellent agreement demonstrates that this linear mixing rule is accurate enough to be used for predicting surrogate YSIs and that there are no significant nonlinear interactions between the components.

Figure 4 compares two-dimensional soot volume fraction fields measured in flames doped with two reference diesel fuels and the four CRC surrogates. Samples of these fuels were provided by this project's collaborators at Sandia National Laboratories and Chevron Energy Technologies. The results show that surrogate V0B (4th panel) closely matches the Certification Fuel, Batch A (CFA) target fuel (2nd panel), while V2 (6th panel) overpredicts soot, and V1 and especially V0A (5th and 3rd panels) underpredict it.

YSIs were measured for a number of other compounds that are components of proposed diesel surrogates. Figure 5 shows that the YSIs of these components can be accurately predicted from their carbon atom types (e.g., primary alkyl, secondary alkyl, etc.). This further implies that if surrogates are formulated to match the carbon atom types of the target fuels, as is the case with the CRC



TDEC - *trans*-decalin; HMN - 2,2,4,4,6,8,8-heptamethylnonane; NBCX - *n*-butylcyclohexane; NEI - *n*-eicosane; NOD - *n*-octadecane; NHXD - *n*-hexadecane

Figure 2. Measured values of YSIs for the first generation CRC surrogate components

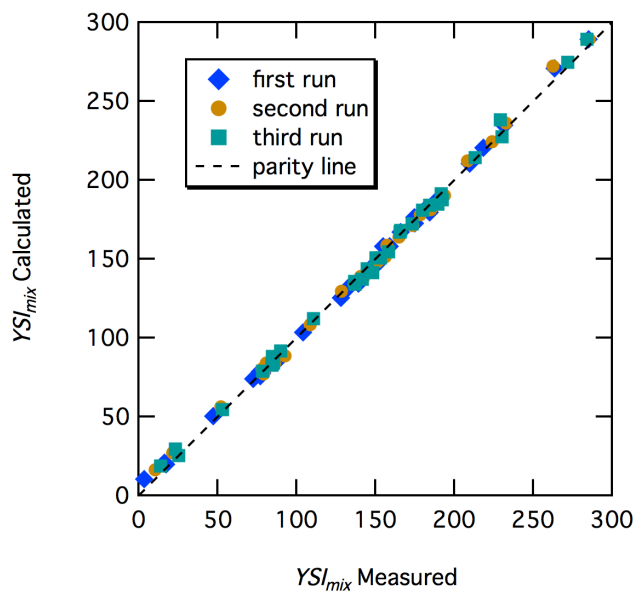


Figure 3. Comparison of measured and linear fit YSIs for 32 mixtures of the first generation CRC surrogate components

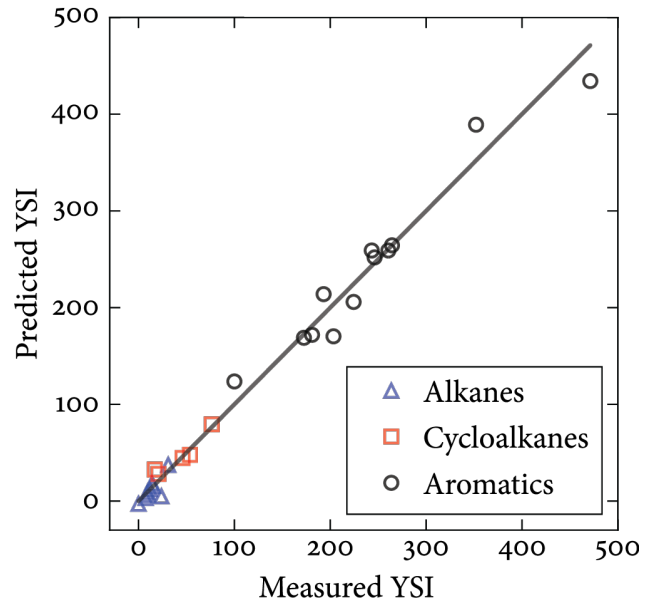
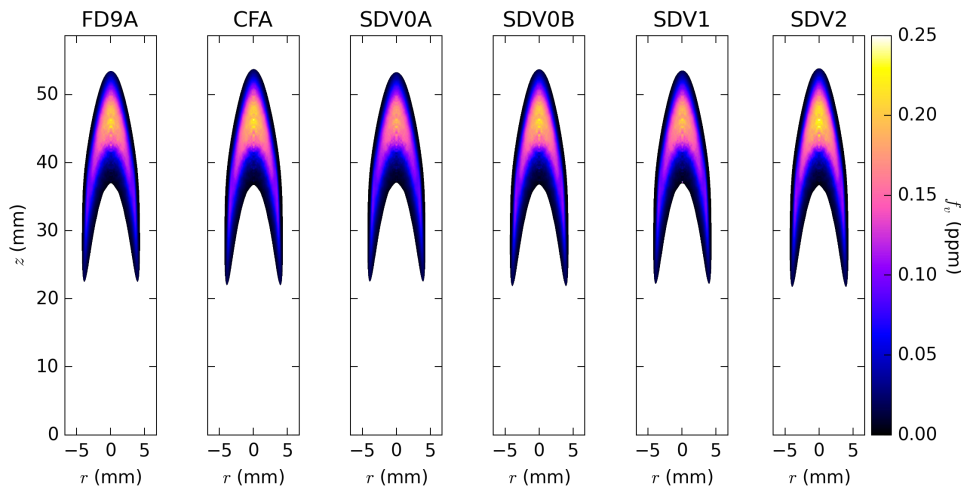


Figure 5. Comparison of measured and predicted YSIs for surrogate components



FD9A - Fuels for Advanced Combustion Engines Diesel #9, Batch A

Figure 4. Soot volume fractions measured in flames doped with two reference diesel fuels and the four CRC surrogate mixtures

surrogate approach, they will match its sooting behavior fairly well, even if sooting behavior is not explicitly matched.

Finally, Figure 6 compares the YSIs measured for the CRC surrogates with values predicted by two procedures: (A) the linear mixing rule and the YSIs of the components, and (B) from the carbon atom type correlation in Figure 5. The results show that both of

these procedures are able to predict the sooting tendency of surrogates to within experimental error. Significantly, method (A) could not be applied to surrogate V2 since one of that surrogate's components was not available for testing; however method (B) could still be applied and predicted the YSI very accurately.

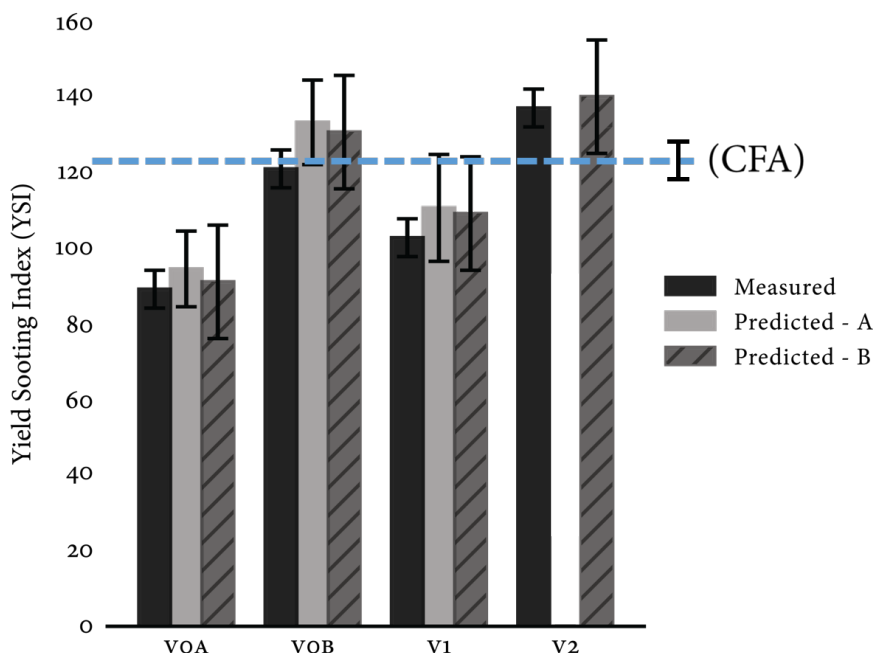


Figure 6. Comparison of measured and predicted YSIs for the CRC surrogate mixtures

## Conclusions

- Demonstrated that the YSI method can be used to quantify sooting tendencies of diesel fuels and their surrogates
- Determined that the CRC surrogates match the sooting behavior of CFA diesel fuel in the order V0B > V2 ~ V1 > V0A
- Demonstrated that the two procedures developed in this study for predicting the sooting tendencies of surrogates are accurate to within experimental error for the CRC surrogates

## References

1. S.S. Lim, et al., “A comparative risk assessment of burden of disease and injury attributable to 67 risk factors and risk factor clusters in 21 regions, 1990–2010: a systematic analysis for the Global Burden of Disease Study 2010,” *Lancet* 380:2224–2260 (2012).
2. T.C. Bond, et al., “Bounding the role of black carbon in the climate system: a scientific assessment,” *J Geophysical Res: Atm* 118:5380–5552 (2013).
3. C.K. Westbrook, et al., “Computational Combustion,” *Proc Combust Inst* 30:125–127 (2005).
4. W.J. Pitz, C.J. Mueller, “Recent progress in the development of diesel surrogate fuels,” *Prog Energy Combust Sci* 37:330–350 (2011).
5. C.J. Mueller, et al., “Methodology for formulating diesel surrogate fuels with accurate compositional, ignition-quality, and volatility characteristics,” *Energy Fuels* 26:3284–3303 (2012).
6. C.J. Mueller, et al., “Diesel surrogate fuels for engine testing and chemical-kinetic modeling: compositions and properties,” *Energy Fuels* 30:1445–1461 (2016).
7. C.S. McEnally, L.D. Pfefferle, “Sooting tendencies of oxygenated hydrocarbons in laboratory-scale flames,” *Env Sci Technol* 45:2498–2503 (2011).
8. [http://guilford.eng.yale.edu/yalecoflowflames/doped\\_home.html](http://guilford.eng.yale.edu/yalecoflowflames/doped_home.html)
9. <https://dataverse.harvard.edu/dataverse/pfefferle>

## FY 2016 Publications/Presentations

1. D.D. Das, W.J. Cannella, C.S. McEnally, C.J. Mueller, L.D. Pfefferle, “Two-dimensional soot volume fraction measurements in flames doped with large hydrocarbons,” *Proc Combust Inst* <http://dx.doi.org/10.1016/j.proci.2016.06.047> (2016).
2. C.S. McEnally, L.D. Pfefferle, “Sooting tendencies of diesel fuel surrogate compounds and mixtures,”

AEC Program Review Meeting, February 8–11, 2016, Livermore, CA.

3. M.L. Lichtenberg, C.S. McEnally, D.D. Das, L.D. Pfefferle, “Sooting tendencies of biodiesel fuels,” presented at 2016 ESSCI Spring Technical Meeting, March 13–16, 2016, Princeton, NJ.
4. D.D. Das, C.S. McEnally, L.D. Pfefferle, “Sooting tendencies of diesel and jet fuel surrogate components,” presented at 2016 ESSCI Spring Technical Meeting, March 13–16, 2016, Princeton, NJ.
5. D.D. Das, D. Giassi, N.J. Kempema, M.B. long, C.S. McEnally, L.D. Pfefferle, “The Yale coflow burner: a tool for studying soot formation,” presented at 2016 International Sooting Flame (ISF) Workshop, July 30–31, Seoul, Korea.
6. D.D. Das, W.J. Cannella, C.S. McEnally, C.J. Mueller, L.D. Pfefferle, “Two-dimensional soot volume fraction measurements in flames doped with large hydrocarbons,” presented at 36th International Symposium on Combustion, August 1–5, 2016, Seoul, Korea.
7. C.S. McEnally, L.D. Pfefferle, “Measurements and predictions of sooting tendencies of diesel fuels and their surrogates,” AEC Program Review Meeting, August 16–19, 2016, Southfield, MI.

## II.31 Micro-Jet Enhanced Ignition with a Variable Orifice Fuel Injector for High Efficiency Lean-Burn Combustion

### Overall Objectives

- Design and configure an alpha version of the micro-jet enhanced ignition components with embedded micro-chamber (MJEI-EMC) which only needs one direct injection fuel injector without modifying cylinder head structure and spark plug
- Prototype and test alpha version of the MJEI-EMC with a single injector which provides targeted spray pattern for ignition and also be capable of producing stratified-charged mixture for lean burn
- Conduct engine combustion simulation to evaluate fuel economy and emission benefits
- Conduct engine combustion testing to evaluate fuel economy and emission benefits

### Fiscal Year (FY) 2016 Objectives

- Finalize numerical optimization of the injector design and control parameters
- Modify engine for the injection system and micro chamber
- Install the optimized injection system
- Perform basic tests ensuring the whole system including the in-cylinder laser diagnostics is ready

### FY 2016 Accomplishments

- Purchased and installed optical engine components: optical mirror, piston rings, and optical piston head
- Installed ignition coil and spark energy booster
- Modified the LabVIEW code for injection and spark control parameters
- Fully assembled the optical engine
- Finalized the injector design
- Performed preliminary metal engine combustion analysis
- Obtained combustion traces ■

### Chia-Fon F. Lee

University of Illinois at Urbana-Champaign

1206 West Green Street

Urbana, IL 61801

Phone: (217) 333-5879

Email: cflee@illinois.edu

DOE Technology Development Manager:

Leo Breton

NETL Project Manager:

Ralph D. Nine

Subcontractor:

Deyang Hou, QuantLogic, Sugar Land, TX

### Introduction

This project investigates the technical merits and potential commercial feasibility of micro-jet enhanced ignition with a variable orifice fuel injector and a novel embedded micro-chamber for high efficiency combustion. The overall aim is to improve the performance of the gasoline direct injection engine in stratified charge mode with MJEI-EMC. The scope of this project includes design, prototyping, and engine combustion simulation.

The numerical simulation is compared with experiments and used to provide insight understandings of the engine processes and optimize the engine operations. The subcontractor, QuantLogic, creates prototypes of micro-jet fuel injectors with variable orifice for enhancing lean burn combustion based on the optimized design. The design is customized for the testing optical engine configurations at the University of Illinois at Urbana-Champaign. The spray characteristics study is performed to optimize the micro-jet enhanced injection system design both experimentally and numerically. The combustion and emission characteristics are also investigated by integrating the micro-jet enhanced ignition components into the embedded micro-chamber engine. By performing extensive numerical simulations, deeper fundamental understandings for the key component configurations, engine operation parameters, combustion performance and emissions of the MJEI-EMC system are gained. In this project, a fully functional MJEI-EMC system will be built and tested; a fundamental numerical model for

engine simulation will be developed. With an advanced injector to provide the targeted micro-jet spray pattern for ignition at lean fuel condition, only minor modification will be needed for the conventional gasoline engine and the reduced production expense can promote the high efficiency gasoline direct injection engine to replace the conventional port fuel injection engine.

## Approach

The experiments and computations are working in tandem with one another, beginning with numerical optimizations performed to guide the designs of the injector and the embedded chamber. Then, the design prototype is manufactured, assembled, and tested using laser diagnostics to generate data for model calibration. Finally, control parameters are further optimized numerically and assessed against additional experiments. Spray features of interest for design consideration include: penetration, droplets size, and velocity distribution. Other effects of operation parameters such as injection pressure, injection cone angle, and so on are also tested, and numerical simulation is conducted to build a deeper understanding and help optimize the injection system design. The injection system is integrated into the embedded micro chamber optically accessible engine. The combustion characteristics and the emissions are investigated under the stratified-charged engine operation conditions.

## Results

### Numerical Optimization

The final injector design has two groups of nozzles. Two injections are applied in each cycle of the engine operation with the final injector. In the first injection, nozzles in both Group 1 and Group 2 are opened; only nozzles in the Group 2 are opened in the second injection. The control optimization is repeated for all the eight tested operation conditions for the updated injector configuration. Sample pressure traces of the optimal operation at each of the operation conditions are plotted in Figure 1. In order to study the mixture preparation, the distribution of fuel vapor is processed and visualized. Sample fuel vapor distribution is visualized in Figure 2. It can be seen that the two-chamber design of the piston geometry keeps a considerable portion of the fuel within a set distance from the center.

In the sector optimization, the location of the spark plug is assumed to be at the center of the combustion chamber. However, in the experimental setup, the spark plug is offset to a location near the edge of the inner piston bowl. It is expected that the sector simulation will underestimate the distance that the flame needs to travel, hence the

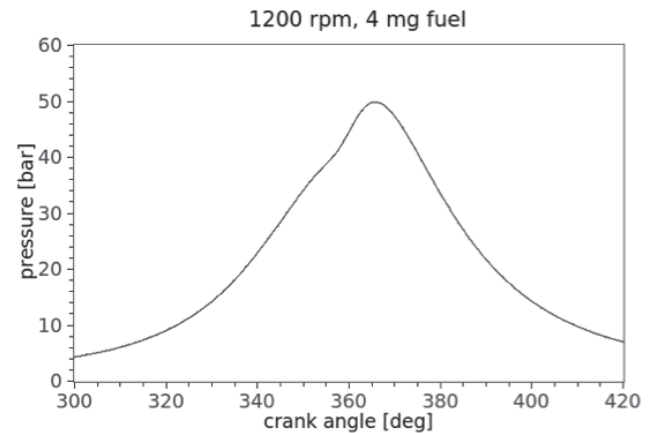


Figure 1. Pressure trace of optimal operation at 1,200 rpm, 4 mg fuel, with the final injector design

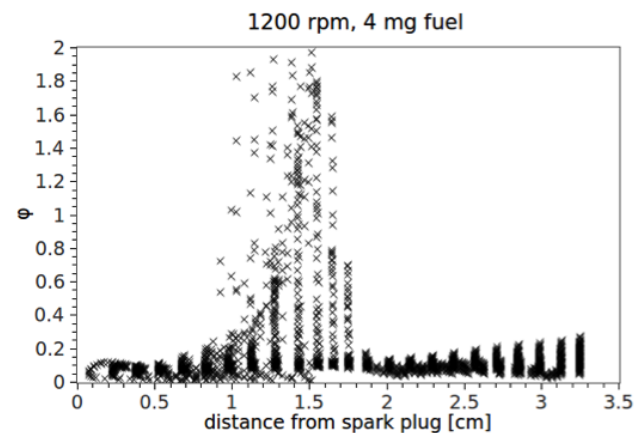


Figure 2. Stratified mixture distributions before spark discharge in optimal operation at 1,200 rpm, 4 mg fuel, with the final injector design

combustion duration. In order to improve the credibility of the optimization results, the optimization is repeated with a full-chamber geometry and an offset spark plug placement. Due to the longer distance that the flame needs to travel and the subsequent longer duration of heat release, the pressure rise in the computation with full chamber geometry and offset spark plug is slower than that in the sector computation; the peak pressure is also lower. The distance between the multi-hole injector and the spark plug poses additional challenge in generating near stoichiometric mixture near the spark plug. In the cases where the fuel quantity is small, the optimal engine operation relies on a late second injection, which is either briefly before the spark discharge or after the spark discharge, to enrich the mixture near the ignition kernel, generating additional turbulent, and enhance the flame propagation. The price of such strategy is increased soot emission.

## Optical Engine Setup

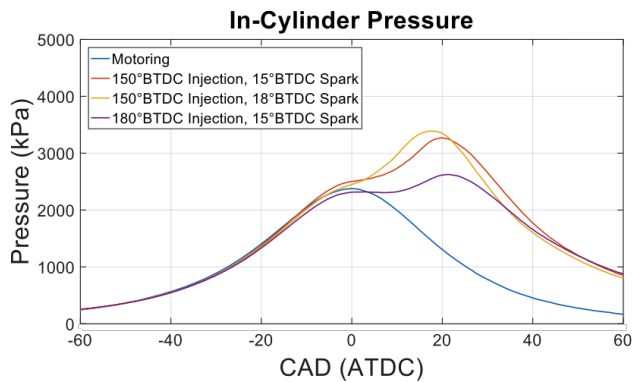
By working with the LabVIEW code to produce sparks with sufficient energy, and using a high-octane blend, the engine successfully fired smoothly and consistently. Figure 3 shows combustion pressure traces for three different injection/spark timing combinations in gasoline direct injection mode alongside a motoring trace.

## Conclusions

- The MJEI-EMC design can successfully create stratified charge fuel distribution within the piston chamber.
- Off-center spark plug and injector configuration require non-trivial considerations for the optimization process.

## FY 2016 Publications/Presentations

1. Lee, C.F., et. al., "Numerical Study and Validation of Lean-Burn Combustion and Multi-Component Droplet Vaporization," Advanced Engine Consortium Review Meeting, USCAR, Southfield, Michigan, August 2016.



BTDC – before top dead center; ATDC – after top dead center

Figure 3. Combustion pressure traces for three different injection and spark timing combinations in gasoline direct injection mode alongside a motoring trace at 1,200 rpm, with an intake pressure of 12.5 psi, and an injection duration of 1.54 ms

## II.32 Development and Validation of Predictive Models for In-Cylinder Radiation and Wall Heat Transfer

### Overall Objectives

- Quantify the relative importance of turbulent boundary layer wall heat transfer, radiative transfer, and boundary layer/radiation couplings in engines
- Provide new experimental datasets that can be used to provide physical insight into heat transfer processes in engines, and to validate models
- Augment the experimental measurements with data from high-resolution numerical simulations
- Develop, implement and validate a hierarchy of computational fluid dynamics (CFD)-based models that can be used as part of predictive engine simulations to develop high-efficiency, low-emissions engines

### Fiscal Year (FY) 2016 Objectives

- Implement and exercise multiple Reynolds-averaged Navier–Stokes (RANS)-based turbulent boundary layer wall heat transfer models and radiative heat transfer models in OpenFOAM
- Implement wall heat transfer and radiation models in RAPTOR for high-resolution large eddy simulation (LES)
- Procure an infrared (IR) camera to measure spectral radiative intensities in an optical engine at the University of Michigan
- Develop a plan for metal engine experiments to be performed at Oak Ridge National Laboratory

### FY 2016 Accomplishments

- Implemented multiple wall heat transfer and radiation models in OpenFOAM, and exercised models to guide the design of the engine experiments
- Implemented a baseline wall heat transfer model in RAPTOR
- Procured the IR camera for the University of Michigan engine laboratory
- Planned the FY 2017 metal engine experiments ■

**Daniel C. Haworth<sup>1</sup> (Primary Contact),  
Volker Sick<sup>2</sup>, Joseph C. Oefelein<sup>3</sup>,  
James P. Szybist<sup>4</sup>**

<sup>1</sup>The Pennsylvania State University

233 Research East Building

University Park, PA 16802

Phone: (814) 863-6269

Email: dch12@psu.edu

DOE Technology Development Manager:

Leo Breton

NETL Project Manager:

Nick D'Amico

Subcontractors:

• <sup>2</sup>University of Michigan, Ann Arbor, MI

• <sup>3</sup>Sandia National Laboratories, Livermore, CA

• <sup>4</sup>Oak Ridge National Laboratory, Knoxville, TN

### Introduction

The lack of accurate submodels for in-cylinder radiation and heat transfer has been identified as a key shortcoming in developing truly predictive, physics-based CFD models that can be used to develop and design combustion systems for advanced high-efficiency, low-emissions engines. Recent measurements of wall layers in engines show discrepancies of up to 100% with respect to standard CFD boundary layer models. And recent analysis of in-cylinder radiation based on the most recent spectral property databases and high-fidelity radiative transfer equation solvers has shown that at operating pressures and exhaust gas recirculation levels typical of modern compression ignition truck engines, radiative emission can be as high as 40% of the wall heat losses, that molecular gas radiation (mainly CO<sub>2</sub> and H<sub>2</sub>O) can be more important than soot radiation, and that a significant fraction of the emitted radiation (50% or more) can be reabsorbed before reaching the walls.

A hierarchical modeling approach is adopted that ranges from high-resolution “scientific” LES to medium-resolution “engineering” LES to low-resolution time-dependent RANS. The submodels are being implemented

in a code-neutral manner to facilitate implementation into CFD codes other than the ones that are used to carry out the research. Experimental data for model validation are being generated in single-cylinder research engines, and additional data for model development and validation are being derived using high-resolution LES. The overarching goal of this project is to develop, implement and provide to the community open submodels for radiation and boundary layer wall heat transfer in medium-resolution LES and unsteady RANS that (when coupled with models of equal fidelity for other key physical processes, such as liquid fuel sprays) provide truly predictive capability for CFD of in-cylinder processes in engines, including couplings between different modes of heat transfer.

## Approach

Four different engine configurations are being explored experimentally and/or computationally: a canonical engine configuration that is an idealized version of a two-valve, single-cylinder optical research engine; the two-valve, single-cylinder optical research engine itself; a four-valve, single-cylinder optical research engine; and a four-valve metal engine. The program builds on the efforts of projects that have been funded through the National Science Foundation/DOE Advanced Combustion Engine R&D Program, and on other ongoing projects and collaborations among the investigators.

The research program has three novel elements that together, will enable significant advances in predictive CFD submodels for in-cylinder heat transfer: explicit accounting for couplings between radiation and wall heat transfer modeling; tight collaboration between modeling and experiment, including new experimental measurements and high-resolution LES data for model validation; and a hierarchical modeling approach that includes high-fidelity modeling for physics discovery (high-resolution LES) to augment the experimental measurements, and predictive models that can be used for medium-resolution LES and unsteady RANS for engine combustion system development and design.

## Results

Several variants of turbulent wall boundary layer heat transfer models have been proposed for in-cylinder CFD in piston engines. These include different underlying turbulence models, different forms of wall functions in the momentum equation, and different formulations for the wall heat flux in the energy equation. In this first year of the project, several engine wall heat transfer models from the literature and from various CFD codes have been implemented in OpenFOAM, and the models have

been exercised for simplified engine configurations. An example illustrating the range of results obtained using different models from the literature is shown in Figure 1. There the cumulative wall heat loss as a function of crank angle degrees of rotation is plotted from unsteady RANS simulations of a two-valve, spark ignition, single-cylinder optical research engine at a part-load operating condition (stoichiometric propane-air reactants, 40 kPa intake manifold pressure, 1,300 rpm). Here a simple ignition model and turbulent flame propagation model have been used. The computed wall heat loss varies by more than a factor of two, depending on the wall heat transfer model used.

In parallel with the boundary layer wall heat transfer model work, radiative heat transfer model development and implementation continued. The most detailed radiation model features line-by-line spectral resolution for participating molecular gases and soot particles, and a stochastic photon Monte Carlo method to solve the radiative transfer equation and to account for reabsorption. An example of the detailed information that can be extracted using photon Monte Carlo/line-by-line is shown in Figure 2. There an instantaneous snapshot (at 75° crank angle degrees after piston top dead center) from the engine simulation shown in Figure 1 has been processed to compute the spectral distributions of radiation. The figure shows power spectra of the emitted radiation (top) and of the radiation reaching the walls (bottom), with the individual contributions from  $\text{CO}_2$  and  $\text{H}_2\text{O}$  separated out (there is no soot). Approximately 67% of the emitted

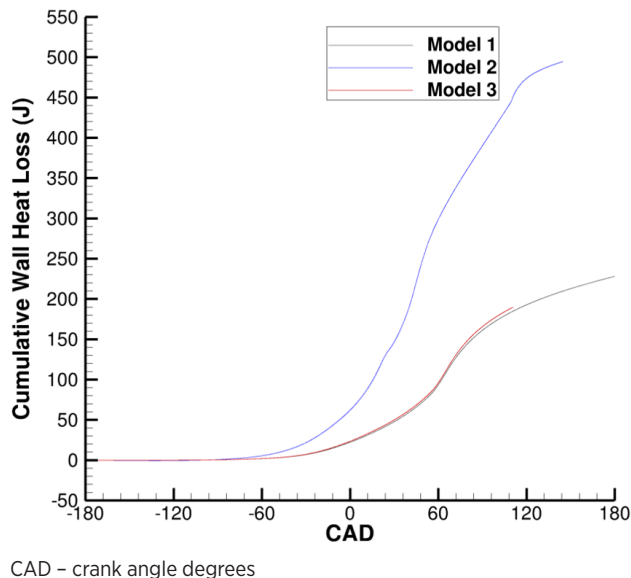


Figure 1. Computed cumulative wall heat loss versus crank angle for a two-valve research engine using three different wall heat transfer models

radiation is reabsorbed before reaching a wall, and the radiative power reaching the walls corresponds to approximately 20% of the turbulent boundary layer wall heat loss. This detailed spectral information is being used to guide the setup of the optical engine measurements, where direct measurements of IR radiation will be made.

On the experimental side, an IR camera has been procured that is capable of measuring radiative intensities over wavelengths of 1–5.5  $\mu\text{m}$ . This spans much of the near-to-mid IR range that is of primary interest for radiative heat transfer in combustion systems (Figure 2). Most earlier measurements have been limited to visible wavelengths. That allowed a fraction of the soot radiation to be measured, but not the  $\text{CO}_2$  and  $\text{H}_2\text{O}$  bands that dominate the radiative transfer in engines. The camera is being installed in the engine laboratory at the University of Michigan, and will be used to make direct measurements

of spectral radiation in the same two-valve engine for which initial simulation results are shown in Figures 1 and 2. An example of preliminary IR imaging results is provided in Figure 3.

Planning was initiated for the metal engine experiments that are to be performed at Oak Ridge National Laboratory in year two of the project. This involves further exercising of the combustion and radiation models that were used to generate the results shown in Figures 1 and 2. Specifically, the models are being used to determine what combinations of temperature, molecular gas concentrations, and/or particles could be used to significantly alter the radiation environment in the engine.

At Sandia National Laboratories, development and implementation of first-principles-based models for high-resolution LES (with near-direct numerical

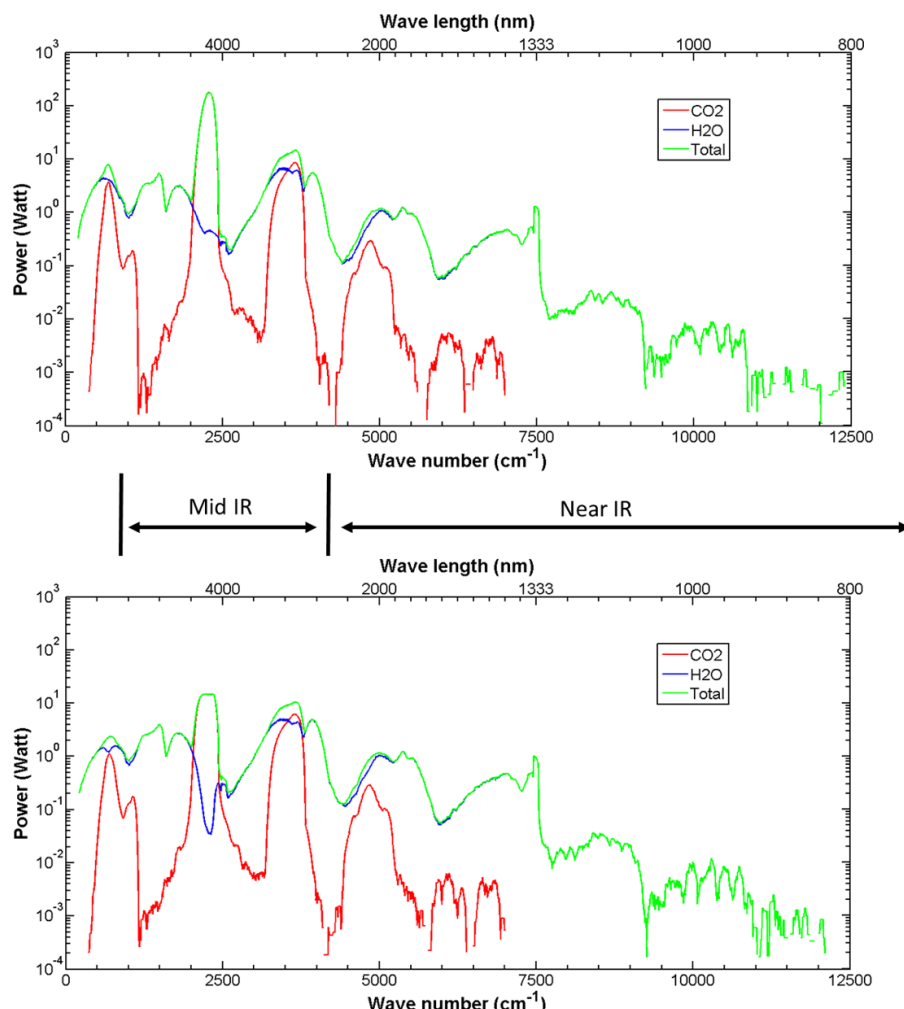


Figure 2. Computed power spectra of radiative emission (top) and radiation reaching the wall (bottom) for a two-valve research engine at one instant in time. Emission from and reabsorption by  $\text{CO}_2$  and  $\text{H}_2\text{O}$  are considered.

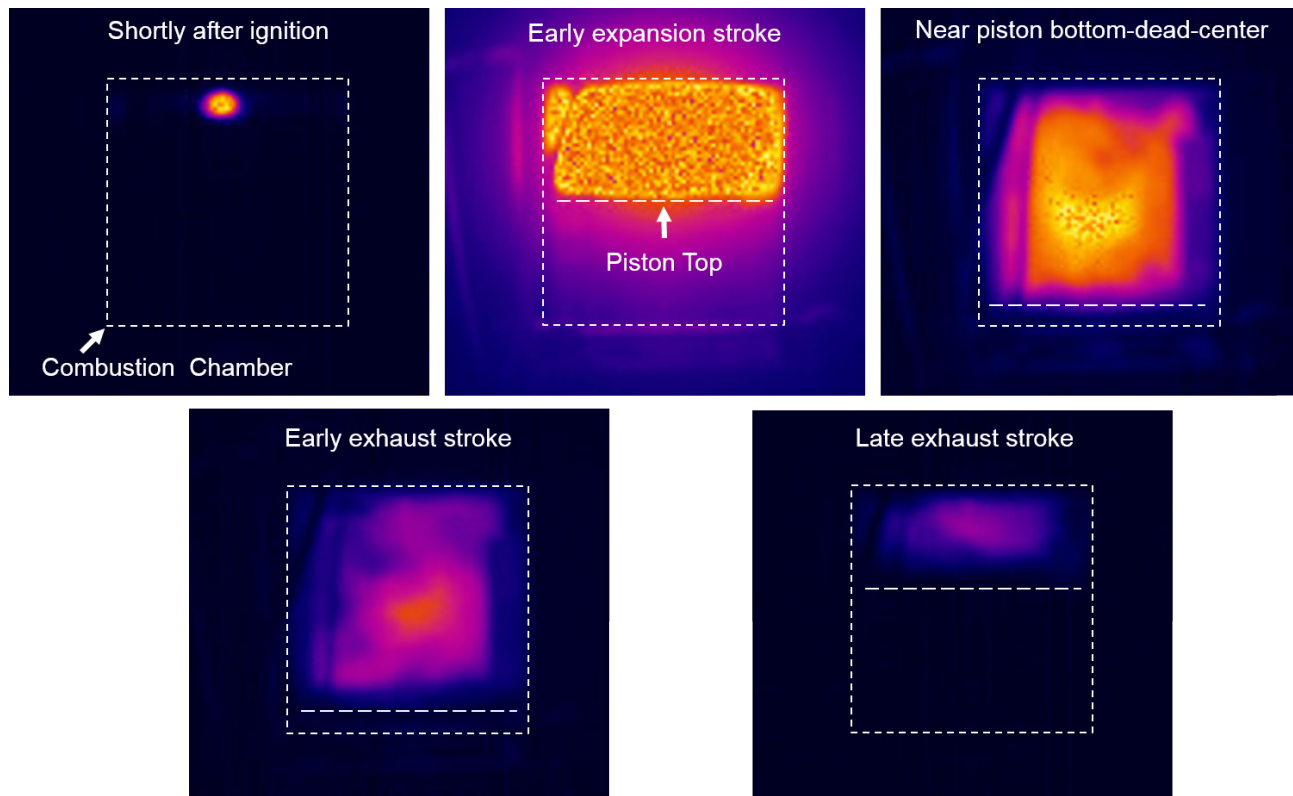


Figure 3. A sequence of images taken using an IR camera in an optically accessible single-cylinder research engine

simulation resolution) continued. This leverages and complements ongoing work funded through DOE's Vehicle Technologies Office. Under the current project, advanced wall heat transfer and radiation models are being implemented in RAPTOR.

## Conclusions

In this first year of the project, the focus has been on establishing the basic simulation and experimental tools that will be used to generate physical insight and to develop new predictive models in subsequent years.

- Large variations (greater than a factor of two) in computed wall heat losses are found among the wall heat transfer models that have been proposed in the literature.

- In an initial look at radiative heat transfer in a single-cylinder research engine, the radiative energy reaching the wall corresponds to approximately 20% of the boundary layer wall heat loss.
- Direct comparisons between computed and measured spectral radiative intensities in near-to-mid IR wavenumbers in an engine are expected to provide new insight into in-cylinder heat transfer processes.

## II.33 Model Development for Multi-Component Fuel Vaporization and Flash Boiling

### Overall Objectives

- Design and develop a multi-component fuel droplet and wall film vaporization model using both discrete and continuous thermodynamics methods
- Design and develop an analytical model for multi-component flash boiling
- Integrate the multi-component droplet and film model into multi-dimensional engine calculations to predict the fuel vaporization process under engine operation condition
- Conduct multi-component droplet and fuel film vaporization experiments in a non-combusting chamber to verify the proposed vaporization models
- Characterize flash boiling phenomena of multi-component fuel sprays by various optical and laser diagnostic techniques

### Fiscal Year (FY) 2016 Objectives

- Perform sample spray calculations using the current multi-component vaporization model
- Expand the single-component flash boiling model to accommodate for multi-component fuel with appropriate mixing rules and saturation properties
- Design and implement the droplet generator for multi-component, complex droplets
- Design and construct the spray vaporization chamber (for both flash boiling and non-flash boiling sprays)
- Design a novel setup to study wall film vaporization

### FY 2016 Accomplishments

- Obtained promising results performing one-way coupling validation of single-component, gasoline-type fuel in gasoline direct injection systems for the multi-component flash boiling model
- Performed preliminary set of flash boiling simulations for different fuels: iso-octane, ethanol, and binary blends of iso-octane and ethanol
- Established the workflow for KIVA sprays simulations and tested the capability of the current models

#### Chia-Fon F. Lee

University of Illinois at Urbana-Champaign  
1206 West Green Street  
Urbana, IL 61801  
Phone: (217) 333-5879  
Email: cflee@illinois.edu

#### Sibendu Som

Argonne National Laboratory Energy Systems Division  
9700 S. Cass Avenue  
Argonne, IL 60439  
Phone: (630) 252-5273  
Email: ssom@anl.gov

DOE Technology Development Manager:  
Leo Breton

NETL Project Manager:  
Carl Maronde

- Developed the modular droplet evaporation model
- Designed and built prototype of dynamic droplet generator
- Designed and constructed the setup for fuel spray experiments
- Designed the fuel system, nitrogen flow system, and measurement system for the wall film vaporization experiments ■

### Introduction

The performance of currently available sub-models for fuel atomization is limited by the lack of proper physical representation that is both computationally efficient and quantitatively accurate for both fuel injection and the subsequent fuel-air mixing process. Thus, this project aims to improve the multi-component fuel vaporization sub-models used in internal combustion engine simulations. In addition, a unified model to predict the occurrence of flash boiling and micro-explosion will be developed by modifying the present single component model. These phenomena are important for improving engine design through fuel vaporization enhancement.

The sub-models will be integrated into a high-fidelity framework for testing. The appropriate methodology for evaluating mixing rules and saturation properties of the multi-component fuel will be examined. The outcome of this project will lead to designs process of greater efficiency and accuracy for internal combustion engines.

## Approach

Experiments will be performed to verify the proposed sub-model, where a comprehensive dataset will be created for model validation to bridge the gap between single-component droplet and multi-component spray combustion. These experiments will employ both optical and laser diagnostic techniques. These validated sub-models will be implemented into engine simulations models for final testing and validation.

## Results

### Flash Boiling Modeling

Sector geometry is used for testing the effect of pure and blended fuels, and iso-octane; ethanol and its blend have been chosen for preliminary analysis. Before moving to the blended fuel results it would be vital to demonstrate the predictive capability for single-component fuels. The predicted mass flow rates are only over-predicting by 4%. Therefore, the Eulerian simulation tends to provide reliable predictions. At Argonne, in collaboration with Convergent Science, a one-way coupling methodology to incorporate in-nozzle flow effects on Lagrangian spray simulations for gasoline direct injection applications has been developed. The predicted liquid penetrations for eight different plumes of Spray G injector have been compared with Engine Combustion Network data for iso-octane. The predicted penetrations tend to match reasonably well with experimental data and provide some

aspects of plume-to-plume differences, which were not apparent in pure Lagrangian simulations (rate of injection based). This clearly proves the current simulation setups in CONVERGE are capable of capturing essence of single-component spray characteristics. Next, other single-component fuels (e.g., ethanol) and blended fuels (iso-octane and ethanol) in terms of Eulerian flash boiling simulations (in-nozzle and near-nozzle) were examined. Iso-octane is typically a lower density fuel than ethanol and the blended fuel will have density in between these two fuels. The mass flow rates will primarily depend on density and also on the viscosity of the fuels. The mass flow rates (single-hole) for the iso-octane case are in accordance with previous full three-dimensional simulations and experimental data (less than 16 mg/ms). Therefore, the mass flow rate predictions for a blended fuel are reasonable. The density of ethanol is higher than that of iso-octane, and the density of the blended fuel should lie between these two single-component fuels. The resultant density of the blended fuel should have a value in between the two other cases and the predicted results abide by the expectations, as shown in Figure 1.

### Hollow Cone Spray Simulation

Hollow cone sprays in a cylindrical constant volume chamber are simulated to test the capability of the current models and understand the two-phase flow behaviors in hollow cone spray processes. The model is tested using axial-symmetric, two-dimensional computational fluid dynamics hollow cone spray simulations. The predicted result is compared with the high speed images obtained from spray measurements [1]. In the simulation, both atmospheric ambient pressure and an elevated ambient pressure of 15 bar are tested. The injector configurations, injection parameters, fuel selection, and the state of the ambient gas follow the experimental information. The

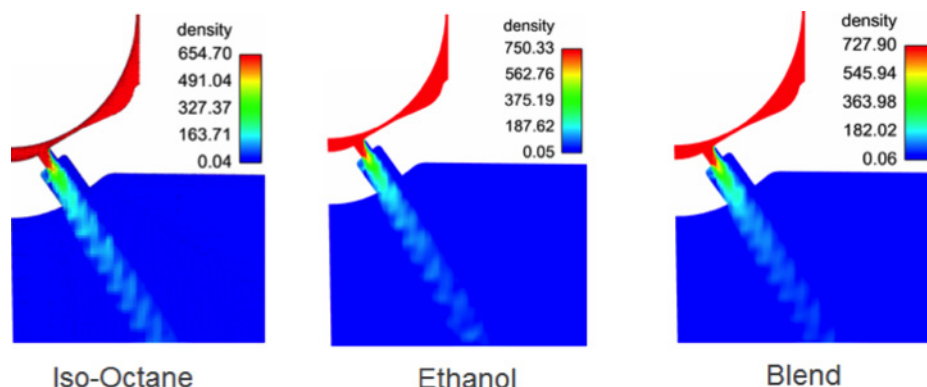


Figure 1. Preliminary mixture density predictions for iso-octane, ethanol, and blended fuel (ethanol: 0.2 mass fraction and iso-octane: 0.8 mass fraction) from a sector (1/8th) Eulerian simulation

computational and real-life snapshot at 1 ms after the start of injection are compared in Figure 2. The comparison shows reasonable agreement between simulation and experiment, demonstrating the basic capability of the existing models. The three-dimensional simulation of the hollow cone spray shows that with the ambient pressures at 6 bar and 10 bar, the hollow cone structure of the spray is maintained for longer time relative to cases with both higher and lower ambient pressure. With higher ambient pressure, the hollow cone spray collapses and forms a solid cone-like spray. This is due to the enhanced droplet breakup, which is a consequence of the increased gas density. The rapid droplet breakup process generates small droplets that are effective in exchanging momentum with the gas phase and enhances the momentum transport between the spray region and the core recirculation region. As a consequence, the recirculation in the core region is stalled and the gas in the core region starts to move downward with the spray. With the ambient pressure equal to 2 bar, the evaporation of the liquid is rapid. The evaporation reduces the droplet

size effectively, enhances momentum exchange, and the fuel vapor directly carries momentum from the liquid phase to the gas phase. Such effects result in the solid cone spray structure. Other noticeable effects of elevating the ambient pressure from 2 bar to 30 bar include higher drag force, slower liquid motion, more nitrogen mass, and lower equilibrium gasoline concentration.

### Droplet Evaporation Model

The developed droplet evaporation model consists of three parts: liquid phase model, gas phase model, and the interface model. The liquid phase model and gas phase model resolve the mass and energy transport in the liquid phase and the gas phase, respectively. The preliminary results show that the quasi-one-dimensional model precisely recovers the surface state predicted by the fully resolved one-dimensional finite volume method model at both high and low Péclet number. The evaporation rate is validated against multiple suspended droplet experiments and a floating droplet experiment. The comparisons show reasonable agreement between the model and the

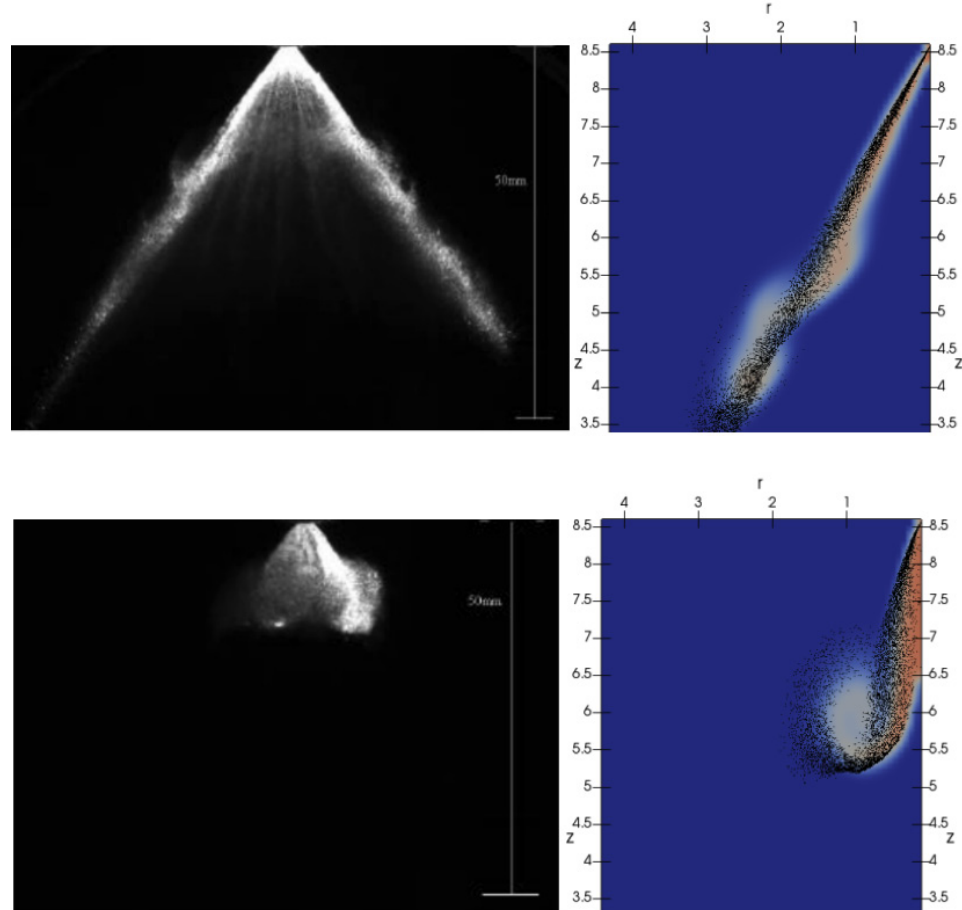


Figure 2. Comparison between measured spray [1] (left) and predicted spray (right) at 1 ms after the start of injection into ambient gas at pressure of 1 bar (top) and 15 bar (bottom)

experiments under the condition without relative motion between the droplet and the ambient gas. The multi-component droplet evaporation experiments [2] are used to validate the multi-component droplet evaporation computation. In the experiments, n-decane, n-dodecan, and n-tetradecan were blended with n-hexadecane. The molar fraction of the more volatile species in the droplets was recorded at different stages of the evaporation process. The computational and experimental results are compared in Figure 3. The results show the capability of the evaporation model in predicting the evaporation of multi-component droplets.

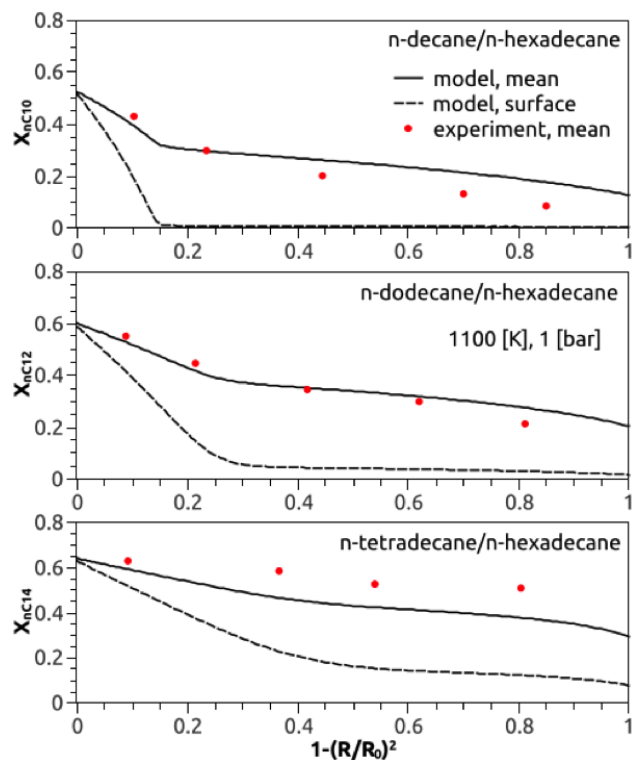


Figure 3. The molar fraction of the more volatile species in the droplet at different stages of the evaporation process observed experimentally (red dots) and predicted by the model (lines)

## Conclusions

- Flash boiling model: the simulations with different needle lifts indicated that at low needle lift, the spray radially diverges and more chances for phase change occur in the near-nozzle region for flashing conditions.
- Spray model using KIVA: the effects of evaporation on the hollow cone spray structure have been preliminarily studied. It is found that the spray structure, liquid motion speed, and the equilibrium gasoline concentration are changed by varying the ambient pressure.
- Droplet evaporation model: the predictions of multi-component droplet evaporation characteristics are consistent with experimental observations.

## References

1. Xu, M., and L.E. Markle. "CFD-aided development of spray for an outwardly opening direct injection gasoline injector." No. 980493. SAE Technical Paper, 1998.
2. Randolph, A., A. Makino, and C. Law, "Twenty-first symposium (international on combustion) liquid-phase diffusional resistance in multicomponent droplet gasification," Symposium (International) on Combustion, vol. 21, no. 1, pp. 601–608, 1988.

## FY 2016 Publications/Presentations

1. Saha, K. et al., "Numerical Investigation of Two-phase Flow Evolution of In-and Near-Nozzle Regions of a Gasoline Direct Injection Engine During Needle Transients," *SAE Int. J. Engines* 9(2):1230–1240, 2016, doi:10.4271/2016-01-0870.
2. Saha, K. et. al., "Modeling of Gasoline Direct Injection Nozzle Flow and Spray Formation," Advanced Engine Consortium Review Meeting, USCAR, Southfield, Michigan, August 2016.
3. Lee, C.F., et. al., "Numerical Study and Validation of Lean-Burn Combustion and Multi-Component Droplet Vaporization," Advanced Engine Consortium Review Meeting, USCAR, Southfield, Michigan, August 2016.

## II.34 Evaporation Submodel Development for Volume of Fluid (eVOF) Method Applicable to Spray-Wall Interaction Including Film Characteristics with Validation

### Overall Objectives

The primary objective of the proposed research is to develop, implement, and validate a volume of fluid (VOF) modeling approach including vaporization integrated into computational fluid dynamics (CFD) codes to provide accurate and predictive simulation of spray-wall interactions without extensive need of parameters tuning. This will be accomplished by development and inclusion of an evaporation submodel in existing VOF modeling framework. This model will be validated through extensive experimentation of the spray-wall interaction and film formation, spread and vaporization dynamics.

### Fiscal Year (FY) 2016 Objectives

- Complete design and fabrication of heated metal impinging plate, metal injector window, transparent impinging plate, and injector nozzle
- Perform Spray A conditions in Engine Combustion Network (ECN): Nonvaporizing data for penetration of single- and multi-component fuels
- Review of advanced optical diagnostics and wall impingement characteristics
- Develop optical diagnostics of Mie and schlieren for individual and simultaneous measurement
- Perform preliminary spray-wall interaction test and data analysis of key parameters
- Validate Lagrangian–Eulerian (LE) spray model by means of CFD simulations of ECN Spray A conditions consistent with nominal initial and boundary conditions of MTU experiments and generate boundary conditions for subsequent direct numerical simulation (DNS) studies

### FY 2016 Accomplishments

- Completed finite element analysis (FEA) of metal impinging window for heat, displacement and load capabilities, and finalized locations of heaters and thermocouples
- Finished two different drawings of metal impinging windows (with and without heaters); heated window contains six heaters, seven thermocouples, and three

**Seong-Young Lee (Primary Contact),  
Jeffery Naber, Riccardo Scarcelli,  
Sibendu Som, Mehdi Raessi**

Michigan Technological University (MTU)  
815 R.L. Smith Bldg.  
1400 Townsend Drive  
Houghton, MI 49931  
Phone: (906) 487-2559  
Email: sylee@mtu.edu

DOE Technology Development Manager:  
Leo Breton

Subcontractors:

- Argonne National Laboratory, Lemont, IL
- University of Massachusetts Dartmouth, Dartmouth, MA

heat flux transducers, which can maintain varied constant surface temperature, using closed-loop control

- Finished the design and drawing of injector window with an off-axis (1 in) injector mount
- Designed single-hole injector nozzles with 120° full-included angle with two different fuel injector nominal nozzle outlet diameters: 100  $\mu\text{m}$  and 200  $\mu\text{m}$
- Established collaboration work of impingement research with Istituto Motori in Italy
- Developed and implemented automated tools for extraction of liquid droplet information and physical properties at location of interest within the simulated sprays
- Completed data acquisition layout for temperature and heat flux measurement
- Conducted the first spray-wall interaction test with seven-hole diesel injector
- Validated the state-of-the-art spray models in the CONVERGE framework; completed LE CFD

simulations of ECN Spray A cases and MTU experiments in terms of boundary and initial conditions

- Developed capabilities to extract the required pre-impingement droplet characteristics from LE CFD simulations ■

## Introduction

The unique and innovative approach of this project is the development of a physics-based improved accuracy CFD modeling approach with fewer parameter tuning requirements for predicting spray-wall interactions including wall film characteristics. It is anticipated these new submodels will yield considerably higher accuracy and predictive capability than those employed in current CFD codes.

## Approach

Firstly, targeted experimentation of the spray-wall interactions and liquid wall film under conditions matching the thermodynamic charge state and surface temperatures to those of engines will be performed. Second, the experimental data will be used to support development and validation of an advanced spray-wall interaction and associated film formation and vaporization modeling approach via application of a VOF method with an integrated evaporation submodel (eVOF). With the

inclusion of a vaporization submodel for the film and the results of the DNS analysis of spray-wall impingement, accurate predictive simulations of sprays and their impingement can be eventually performed without need of extensive parameter tuning.

## Results

### FEA Analysis

The FEA analysis has been carried out using Abaqus/CAE 6.14-3 tool and the best-suited design has been chosen based upon stress and temperature distributions on the window plate surface (Figure 1). The window design consists of six heaters, seven thermocouples, and three heat flux transducers. From the FEA simulation results based on Figure 1a, the window plate temperature is estimated as 800 K and the von Mises stresses are around 10 MPa (see Figure 1b and 1c). It can be concluded that the window design/configuration can withstand the given pressure and thermal conditions of combustion vessel (CV) and can be achieved desired uniform temperature of plate. Further, all six heaters should be positioned 10 mm below the window plate (top surface), in order to maintain the uniform desired temperature. The analysis for 350 bar load conditions is made to study the material elastic limitations. In this analysis, the only external load is applied in terms of pressure and omitted the thermal loads. From the analysis, the von Mises stresses that are

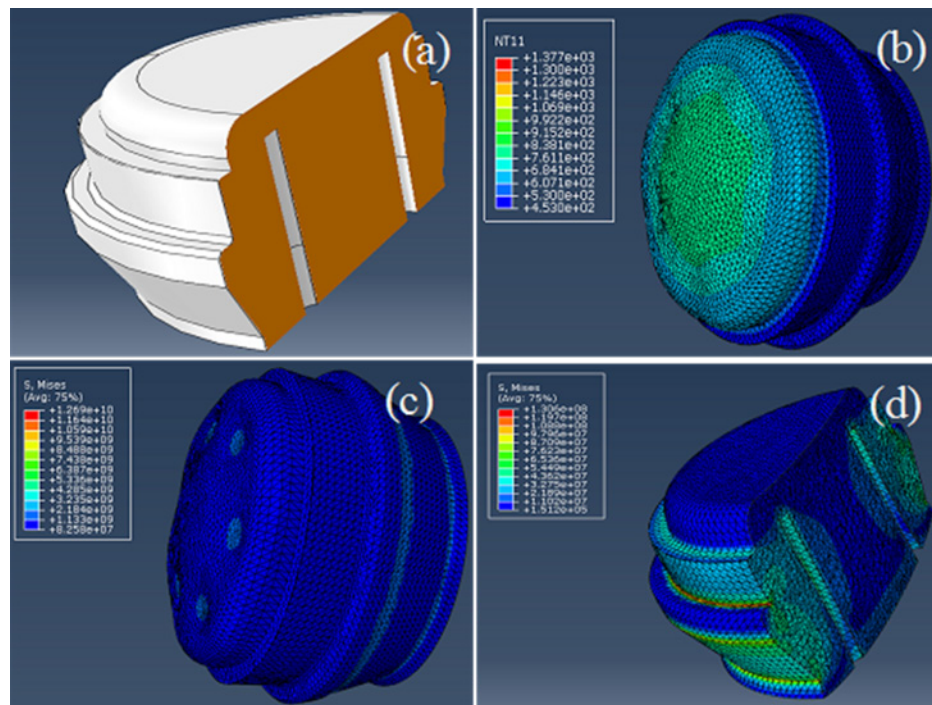


Figure 1. (a) Impingement window final design/configuration; (b) temperature distribution; (c) von Mises stress distribution; (d) von Mises stress distribution with 350 bar load

well below the yield strength of the window material is shown in Figure 1d. Therefore, the current window design/configuration can be used for spray impingement experiments in CV.

### Impingement Window Hardware

After finishing the window design from FEA analysis, drawings were made using the Creo Parametric 2.0 modeling tool. The window can maintain varied constant surface temperature, using closed-loop control. An injector window with an off-axis (1 in) injector mount was also designed. Figure 2 shows the photos of impingement and injector windows including the diesel injector mounted in CV. The injector window has been mounted in CV and the seven-hole diesel injector has been tested for the preliminary spray-wall interaction validation.

### Rate of Injection (ROI) Measurement

Bosch rate of injection meter is adopted to measure the injection rate shape by measuring the pressure wave generated when the injector injects diesel fuel. The ROI profiles for an injection pressure of 1,500 bar and injection durations of 1 ms, 2 ms, and 4 ms are shown in Figure 3. ROI profile at the injection duration of 2 ms is selected as the baseline condition applied in both experiment and simulation and the total injected mass is 45.8 mg. It is also seen from Figure 3 that the ROI profile is repeatable under different injection durations.

### Optical Diagnostics and Experimental Results

For this preliminary test, simultaneous Mie scattering of liquid spray and schlieren of liquid and vapor spray were carried out. Due to the current in-progress of single-hole diesel nozzle building, we tested the seven-hole diesel

nozzle instead. The nozzle is 139  $\mu\text{m}$  in diameter, has a K factor of 1.5, and inclined angle of 148°. The test conditions are an injection pressure of 150 MPa, and an ambient density and temperature of 22.8  $\text{kg/m}^3$  and 423 K, respectively.

The proposed, detailed schematic of spray-wall impingement and two different spray views in the test are shown in Figure 4. Droplets induced by spray injection are distributed near the plate where these droplets show high velocity and momentum than those on the outside plate. As a result, the less momentum droplets are lifted higher from the plate surface and their height parallel to the plate becomes thicker. The spray layer away from the plate stays quiescent while the spray near the

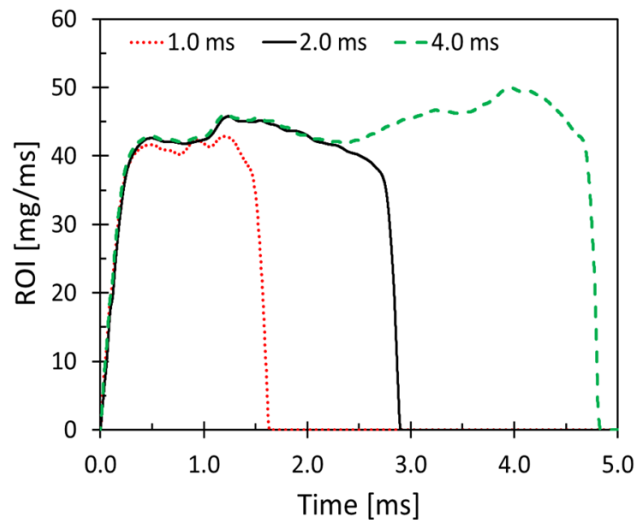


Figure 3. ROI profiles for injection pressure of 1,500 bar and 1 ms, 2 ms, and 4 ms energizing injection durations

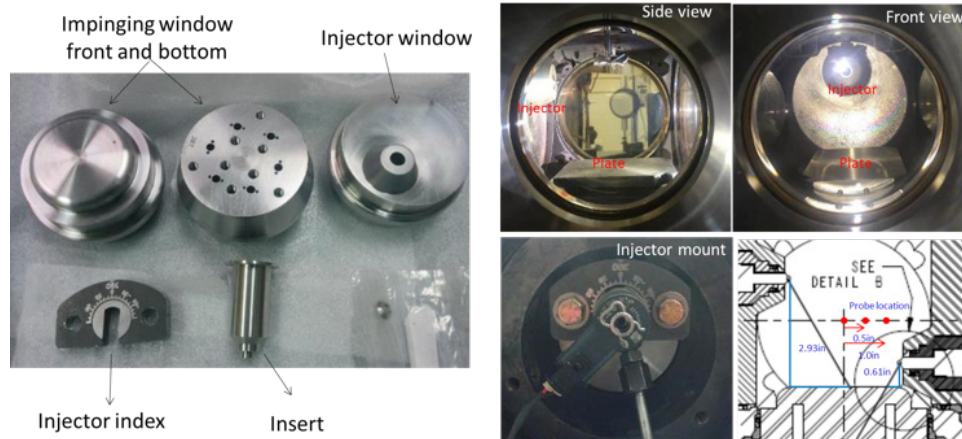


Figure 2. Impingement and injector windows (left) and the view of injector window mount in the combustion vessel (right)

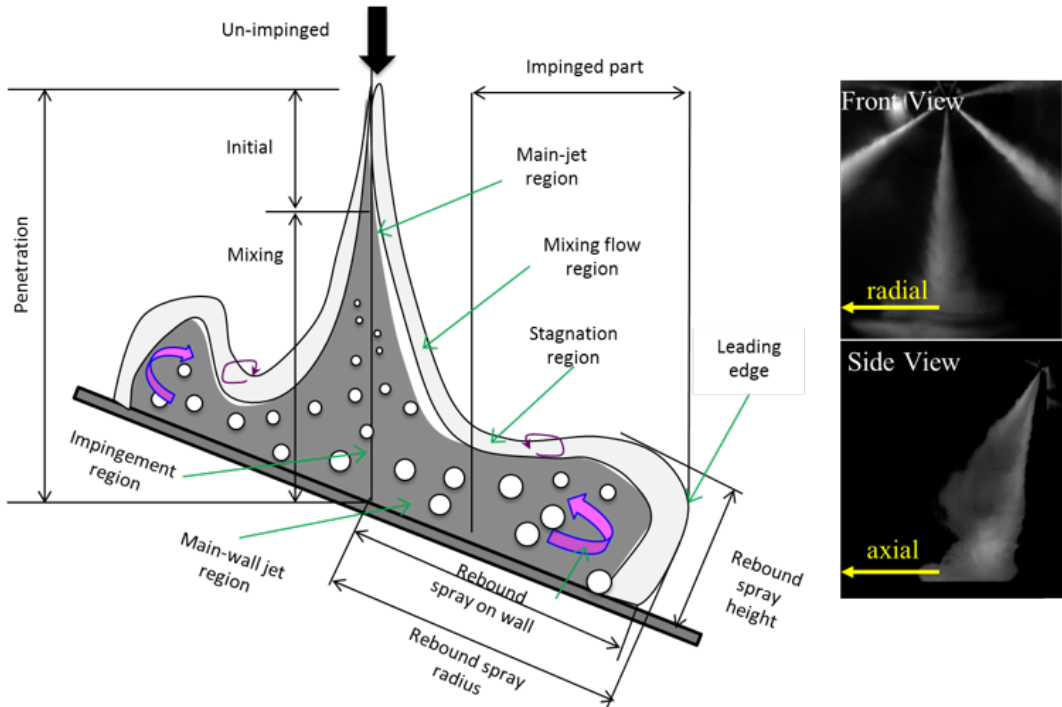
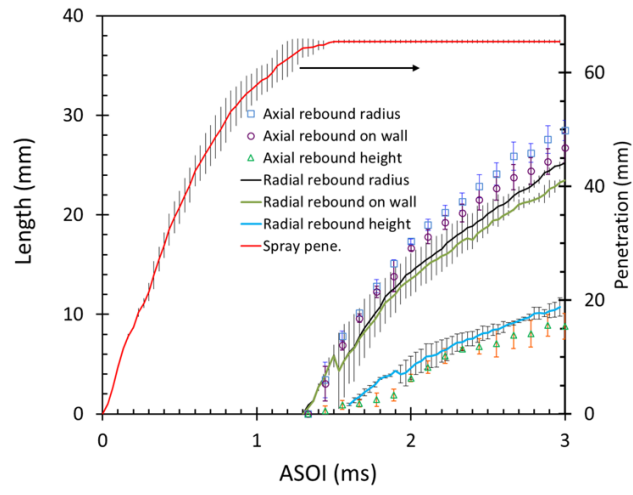


Figure 4. Schematic of spray-wall interaction with nomenclature (left) and front/side views for spray test images (right)

plate is preceded by the larger size droplets. Due to this phenomenon, the leading edge parallel to the plate generates wake (called wall jet vortex) and increases surrounding air entrainment. The main jet region resides inside the unimpinged part and their velocities, momentum, and densities are quite large. The mixing flow region stays outside of the spray surrounding the main flow region where turbulence is highly generated between the spray and surrounding gas such that these droplets rebound above due to the loss of momentum between the surrounding and droplets. A wall jet vortex is observed near the area for impinging jet. Droplet distribution around the region is complicated by the mixing of oncoming, less-momentum droplets and relatively high-momentum droplets. Therefore, there exists a secondary region for a high probability of collisions between the large and small droplets. Figure 5 shows the results of the spray and rebound spray properties. The rebound radii have larger penetrations than the spray expanding distance on the wall. However, the rebound height in the axial direction is slightly higher than the radial direction rebound height. See the directions in Figure 4.

### CFD Simulations

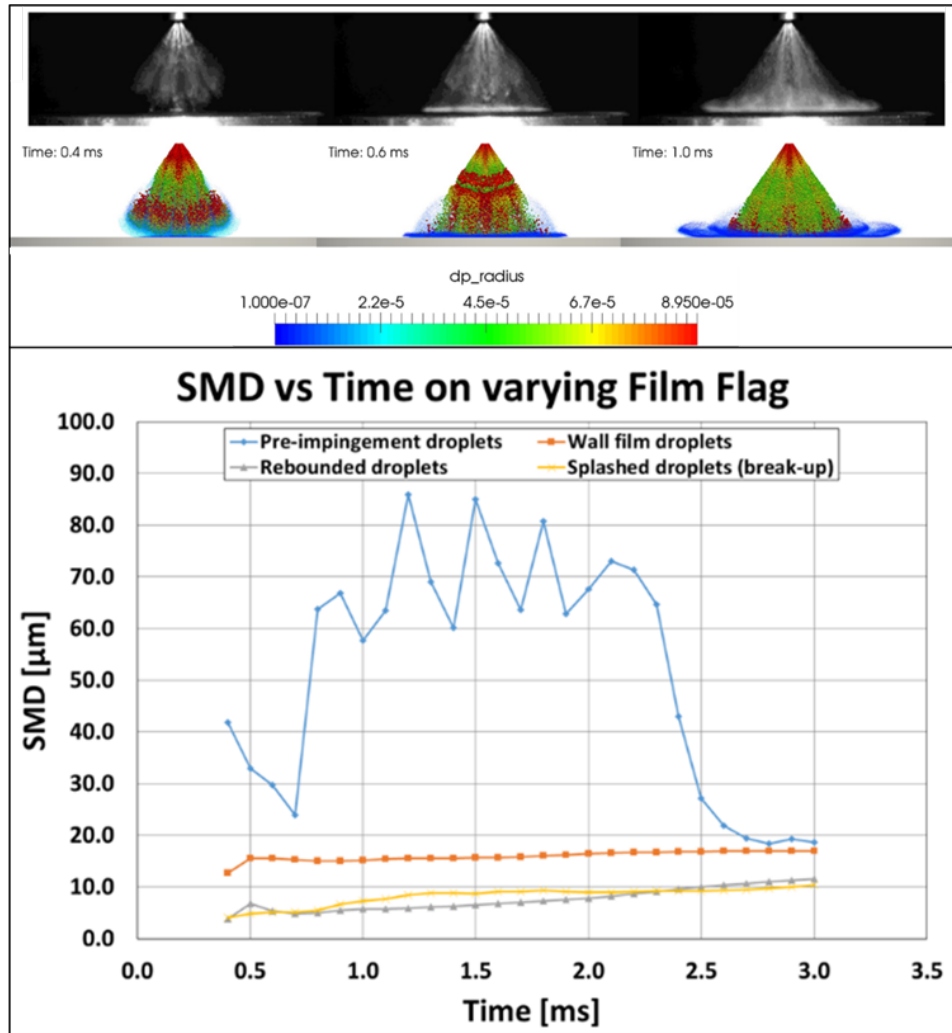
A screening of the available literature on both experimental and numerical studies of spray-wall interaction was initially performed. This allowed selecting some test cases for which boundary and initial conditions,



ASOI – after start of injection

Figure 5. Spray penetration and rebound spray properties

and experimental results for validation were properly documented. Several simulations were performed using the CONVERGE commercial CFD code [1] and the available spray models. CFD preliminary results were compared against experimental data, showing good qualitative agreement on penetration and radial spreading on the plate (see Figure 6a, for gasoline direct injection multi-hole sprays [2]). Initial validation was



SMD – Sauter mean diameter

Figure 6. (a) Comparison between CFD results and schlieren images for gasoline direct injection multi-hole sprays. (b) Data processing to extract droplet characteristics for future DNS spray impingement studies

followed by the implementation of automated tools for data analysis and extraction of predefined information related to physical properties of the liquid droplets as a function of the type of interaction that those droplets established with the impinged wall (see Figure 6b). The tools were developed with the goal of feeding future DNS simulations of spray impingement.

A more in-depth quantitative validation of the available spray models and submodels was subsequently carried out. Two Spray A datasets were selected from the ECN online database [3] to match as close as possible the nominal conditions of the future MTU experiments. The first case, which served as validation of the spray model,

was characterized by a low ambient temperature (440 K) which is comparable to one of the MTU cases (423 K) and named “Low-T.” The second case, named “High-T,” had a higher ambient temperature (900 K), same as the planned MTU experiments. For the “Low-T” case, the validation of the spray model setup was made against the only available experimental measurement, i.e., vapor penetration. A sensitivity analysis on minimum mesh size was performed considering 0.25 mm as the reference size. The plots in Figure 7a present liquid and vapor penetration for the “Low-T” case. Both show a satisfying grid convergence at 0.25 mm and the latter shows also good agreement with experimental data. To test the robustness of the numerical setup, the “High-T” condition

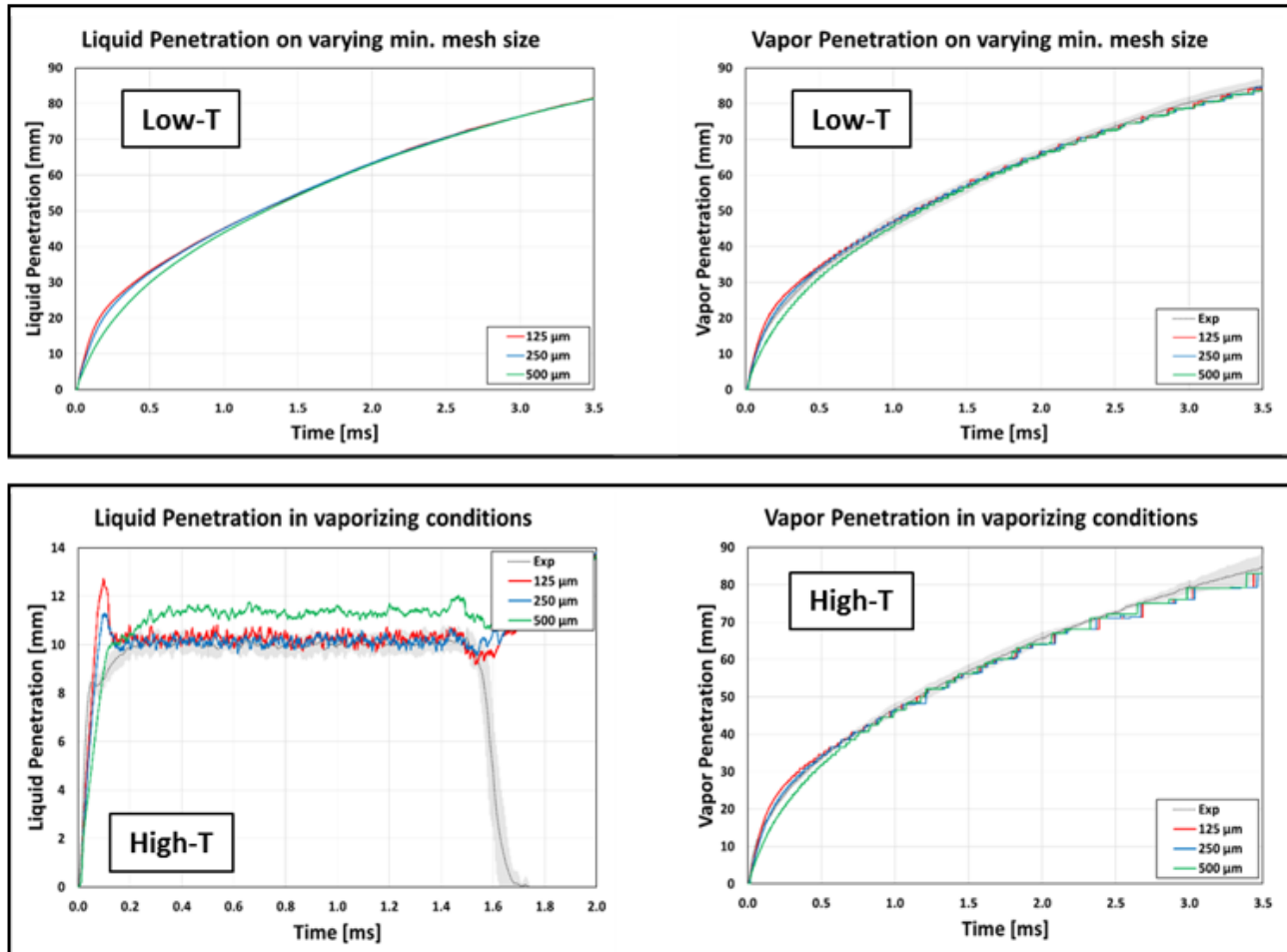


Figure 7. (a) Liquid and vapor penetration – Spray A “Low-T” case; (b) liquid and vapor penetration – Spray A “High-T” case

was subsequently tested using the same submodel setup. The comparison with experimental data (see Figure 7b) shows not only that grid convergence was again obtained with a minimum mesh size of 0.25 mm, but also that the spray model setup properly addressed the change of ambient conditions by delivering a correct estimate of liquid and vapor penetration.

Current CFD activities are aimed at matching the experiments performed at MTU on the seven-hole diesel injector. Preliminary calculations showed that even though the overall trends are correctly predicted in terms of profile shapes, the quantitative agreement between experimental and numerical measurement values is not satisfactory. Some possible causes for these discrepancies have been identified and are under current investigation.

## Conclusions

- Completed and fabricated the hardware including the impingement and injector windows, all necessary items for assembly

- At the time of preparing this annual report, discovered that there are several minor modifications necessary for the final assembly
- Vendor that manufactured the hardware has experienced difficulty to meet the on-time delivery and lack of worker
- Completed the data acquisition system for temperature and heat flux measurement
- Conducted the preliminary spray-wall test with the seven-hole nozzle
- Validated LE CFD simulations of ECN Spray A cases and performed preliminary CFD analysis of MTU experiments
- Developed automated tools to extract droplet information from LE calculations for future DNS calculations of spray-wall impingement

- No progress on nonevaporating DNS initiation and exploration complete due to the lack of foreign national restriction

## References

1. Richards, K. J., Senecal, P. K., and Pomraning, E., "CONVERGE Manual (Version 2.3)," Convergent Science Inc., Madison, WI, USA, 2016.
2. Montanaro, A., Malaguti, S., and Alfuso, S., "Wall Impingement Process of a Multi-Hole GDI Spray: Experimental and Numerical Investigation," SAE Technical Paper 2012-01-1266, 2012, doi:10.4271/2012-01-1266.
3. Sandia National Laboratory ECN website  
<http://www.sandia.gov/ecn>.

## FY 2016 Publications/Presentations

1. Le Zhao, Roberto Torelli, Xiucheng Zhu, Riccardo Scarcelli, Sibendu Som, Jeffrey Naber, Seong-Young Lee. An Experimental and Modeling Study of Diesel Spray Impingement on a Flat Plate. under preparation, SAE Technical Paper, 2017.

## II.35 Development and Validation of a Lagrangian Soot Model Considering Detailed Gas Phase Kinetics and Surface Chemistry

### Overall Objectives

- Improve soot modeling capabilities in government sponsored and commercial computational fluid dynamics (CFD) codes to enable the engine industry to design high efficiency, clean engines for transportation applications
- Identify, develop, and validate a semi-detailed reaction mechanism capable of predicting polycyclic aromatic hydrocarbon (PAH) chemistry up to at least benzo[a]pyrene
- Perform high fidelity optical and metal engine experiments to measure in-cylinder PAH formation and engine out soot mass and particle size distribution to improve the combustion community's fundamental understanding of soot formation

### Fiscal Year (FY) 2016 Objectives

- Validate reaction mechanism containing PAH chemistry up to benzo[a]pyrene
- Develop framework for Lagrangian soot particle simulations in government sponsored CFD code (ERC-KIVA)
- Perform high-speed imaging of conventional and low temperature diesel combustion

### FY 2016 Accomplishments

- Identified detailed reaction mechanism containing PAH chemistry up to benzo[a]pyrene
- Implemented benzo[a]pyrene and ethanol chemistry into an existing toluene reference fuel mechanism to enable simulation of fuels ranging from ethanol containing gasoline to high aromatic content diesel fuel
- Compared mechanism predictions to data from the literature; reduced reaction mechanism was found to agree well with ignition delays from shock tubes, species profiles from burner stabilized premixed flames, and cylinder pressure and heat release from both conventional, high temperature combustion, and advanced low temperature combustion modes.

### Sage Kokjohn

Engine Research Center (ERC)  
University of Wisconsin-Madison  
111 Engineering Research Building  
1500 Engineering Dr.  
Madison, WI 53706  
Phone: (608) 263-1610  
Email: kokjohn@wisc.edu

DOE Technology Development Manager:  
Leo Breton

NETL Project Manager:  
Nick D'Amico

#### Subcontractors:

- Sandia National Laboratories, Livermore, CA
- Convergent Science Inc., Madison, WI

- Developed framework to model soot using a Lagrangian approach
- Performed high-speed imaging of conventional and low temperature diesel combustion at several injection pressures and a range of start of injection timings ■

### Introduction

The objective of this project is to improve soot modeling capabilities to enable the engine industry to design advanced combustion engines. A focus of the project is developing and validating a detailed reaction mechanism including PAH chemistry up to benzo[a]pyrene. The advanced soot model will consider surface chemistry, collision, condensation, and wall interactions. The model will be rigorously validated through comparisons with existing constant volume vessel experiments and engine experiments.

The model will be developed in a Lagrangian framework that will use a statistical representation of the soot aggregates to allow detailed tracking of soot makeup without the need to assume a fractal dimension. Optical and metal engine experiments necessary to validate PAH

growth and soot formation and soot number density will be conducted. Additionally, the overall CFD codes ability to predict spray, mixing, and combustion processes to ensure the inputs to the soot model are as accurate as possible will be validated. The final outcome of the project will be a new soot model that is validated under conditions ranging from conventional diesel to advanced, low temperature combustion.

## Approach

An advanced soot modeling framework is being developed in the government sponsored CFD code (KIVA) and commercial CFD code (CONVERGE) and a targeted validation effort is being undertaken to ensure the computational tools are able to adequately capture all of the upstream processes influencing soot formation (spray, mixing, ignition, and combustion). Simultaneously, optical and metal engine experiments are being performed to enable detailed characterization of PAH formation and soot production. The final effort will combine the validation experiments and simulation framework development to test the soot model and make comparisons to existing models.

## Results

### Reaction Mechanism Validation: Ignition Delay and Species Profiles

The PAH mechanism of Slavinskaya et al. [1] was selected to describe reaction pathways up to five ring aromatics (i.e., benzo[a]pyrene). The PAH pathways up to benzo[a]pyrene were incorporated into the toluene reference fuel mechanism of Wang et al. [2]. Reaction mechanism validation was performed by comparing to shock tube pressure measurements for blends of iso-octane, n-heptane, and air gathered by K. Fieweger et al. [3]. Figure 1 shows the measured and predicted ignition delay. It can be seen that the combined mechanism is able to capture the ignition characteristics accurately.

The PAH mechanism was compared to premixed burner stabilized flame experiments from the literature [4–7] and validation was performed by comparing the measured and predicted species profiles. Figure 2 shows comparisons between the measured and predicted species profiles. The model shows excellent quantitative agreement with the species in high concentrations for each flame (e.g., CO). Although some differences exist in the prediction of the smaller species profiles (e.g., the shape of A4 for Flame 4), the overall prediction of the species profiles is very good. The mechanism appears to be able to capture the general PAH trends up to at least pyrene.

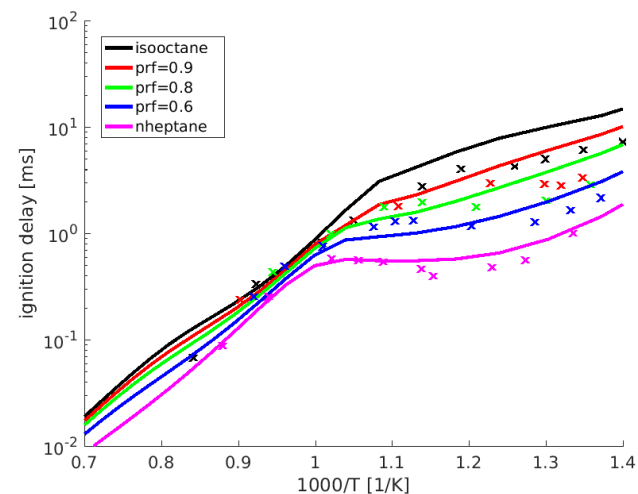
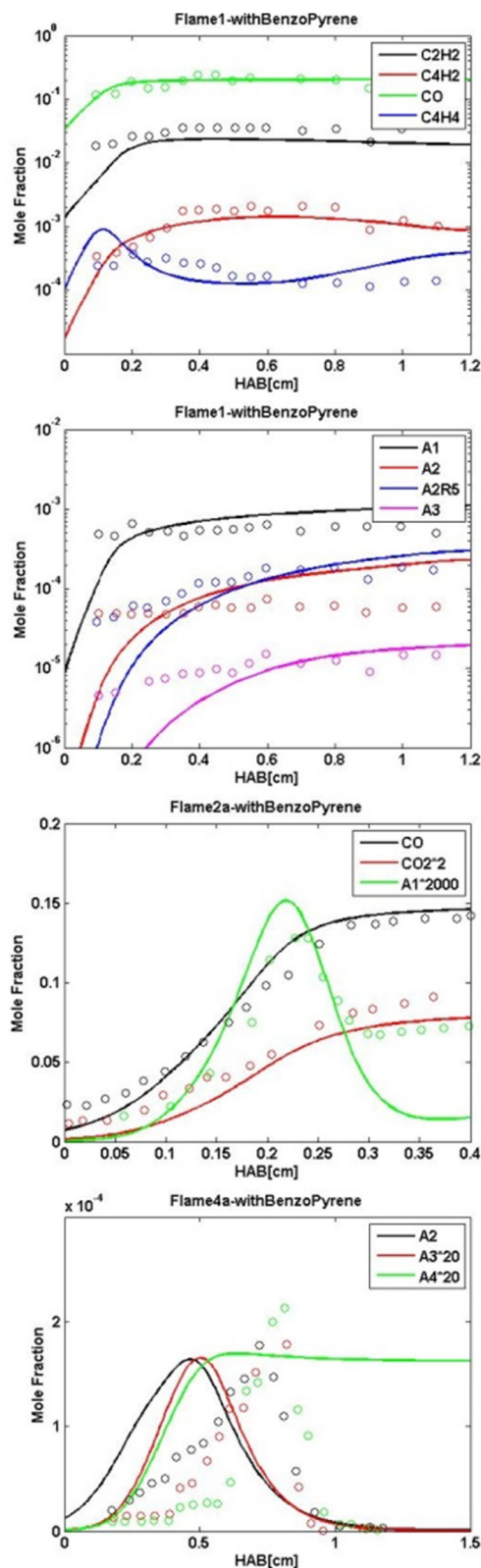


Figure 1. Measured and predicted ignition delay for primary reference fuel (PRF) mixtures

### Reaction Mechanism Validation: Engine Experiments

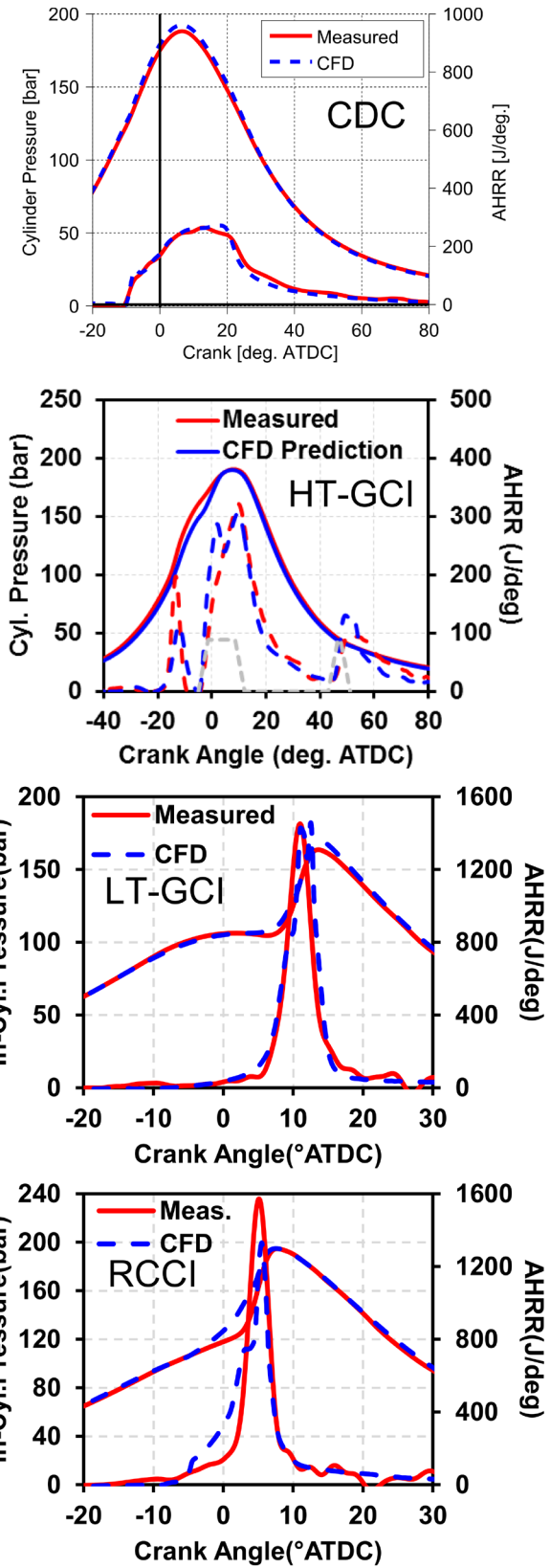
To ensure the reaction mechanism is suitable for use for both conventional and low temperature combustion, comparisons were made to measurements from a heavy-duty diesel engine operating in four different combustion modes: conventional diesel combustion (CDC), high temperature gasoline compression ignition combustion (HT-GCI), low temperature gasoline compression ignition combustion (LT-GCI), and reactivity controlled compression ignition combustion (RCCI). For each combustion mode, the engine was operated near 20 bar gross indicated mean effective pressure. The CDC mode used 25% exhaust gas recirculation (EGR) and a single injection of diesel fuel at an injection pressure of 1,600 bar. The HT-GCI mode operated without EGR and used a triple injection of 91 Anti-Knock Index (AKI) gasoline with an injection pressure of 1,500 bar. The LT-GCI mode used 55% EGR and a triple injection of 91 AKI gasoline with a pressure of 741 bar. The RCCI mode used 55% EGR, a double injection of gasoline, and a single diesel injection. Both the gasoline and diesel used an injection pressure of 741 bar. To model the ethanol containing gasoline used in the GCI and RCCI experiments, the mechanism was further extended to include ethanol oxidation.

Figure 3 shows comparisons of measured and predicted cylinder pressure and heat release rate for each combustion mode. It can be seen that the reaction mechanism captures the combustion phasing and heat release accurately. The soot modeling approach used the two-step soot model based on the approach of Hiroyasu [8]. In the typical soot model formulation, acetylene is



HAB – height above burner

Figure 2. Comparison of measured and predicted species profiles using the base reaction mechanism from Wang et al. [2] with the addition of PAH chemistry from pyrene (A4) up to benzo[a]pyrene



ATDC – after top dead center

Figure 3. Comparison of measured and predicted cylinder pressure and apparent heat release rate (AHRR) using the reduced reaction mechanism validated in the present study

used as the soot inception species. The present work extended this approach to consider soot inception through PAH. This was found to better capture soot trends over a wider range of conditions than considering inception through acetylene [9]. Using this approach, it was found that the soot model could be tuned to capture the soot magnitudes at each condition; however, different soot constants were required for each combustion mode. For example, the pre-exponential on the soot formation reaction differed by an order of magnitude between conventional diesel and high temperature, gasoline compression ignition combustion. For the low temperature combustion cases (LT-GCI and RCCI), the activation energy on the soot formation reaction had to be changed by an order of magnitude.

### Soot Parcel Model

The structure for the Lagrangian soot parcel framework was developed and implemented into the ERC KIVA code. To test the model prior to completion of the statistical soot modeling tool, it was coupled with the two-step soot model based on Hiroyasu [8]. The conventional diesel combustion cases shown in Figure 2 were simulated. When soot was predicted to form, it was transferred out of the gas phase and tracked in a Lagrangian parcel. Figure 4 shows an example of soot parcels during the conventional diesel combustion process, illustrating functionality of the approach.

### Optical Engine Experiments

High-speed imaging of conventional diesel and diesel low temperature combustion (D-LTC) were completed. For all cases, the engine was operated at 1,200 rpm and a load near 6 bar gross indicated mean effective pressure.

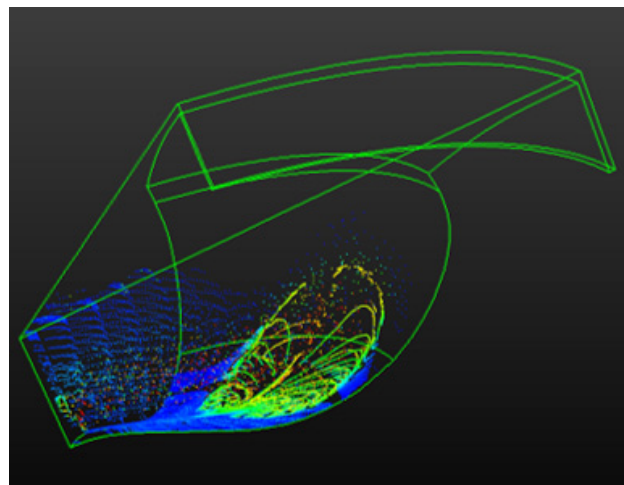


Figure 4. Soot parcels colored by soot mass for conventional diesel combustion

The CDC cases operated without inlet dilution and experiments were performed at injection pressures of 500 bar and 1,500 bar over a range of start of injection (SOI) timings. The D-LTC cases used an inlet oxygen concentration of 12.7% and an injection pressure of 500 bar. The injection timing range for the D-LTC cases spanned from early injection D-LTC (SOI = -30° ATDC) to late injection D-LTC (SOI = +10° ATDC) to enable validation over a wide range of conditions. For each SOI condition 30 cycles of cylinder pressure data at  $\frac{1}{4}$  crank angle degree resolution is used for AHRR analysis. Corresponding imaging data are acquired at 1 crank angle degree resolution from SOI for a duration of 100° crank angle. For explicit computation of experimental uncertainty, the SOI command is changed between experiments in a random order until each SOI condition is repeated twice. Image processing algorithms were written to compute sector average spatially integrated natural luminosity signal and this was compared with both AVL Smoke Meter exhaust-out engine emissions and AHRR. Image saturation is avoided through the use of 0.7 neutral density filter and lens arrangement with f/11. Figure 5 shows an example set of natural luminosity images at several different SOI timings for the CDC cases. In all cases, it was found that the influence of bulk charge motion (swirl) and the natural luminosity increased as the injection timing was delayed.

### Conclusions

- A PAH mechanism was defined and implemented into a multi-fuel chemical kinetics mechanism to simulate gasoline, ethanol, and diesel fueled combustion. The combined reaction mechanism shows good agreement with ignition delays from shock tubes, species profiles from burner stabilized premixed flames, and cylinder pressure and heat release from both conventional, high temperature combustion, and advanced low temperature combustion modes.
- When using PAH (A4 or benzo[a]pyrene) as the soot inception species, simplified soot models could be tuned to capture soot magnitudes and trends from a range of conditions. However, the model constants required for different combustion modes differed by an order of magnitude.
- The coding is complete for the Lagrangian soot framework in KIVA.
- High-speed imaging studies are complete for conventional and diesel low temperature combustion conditions.

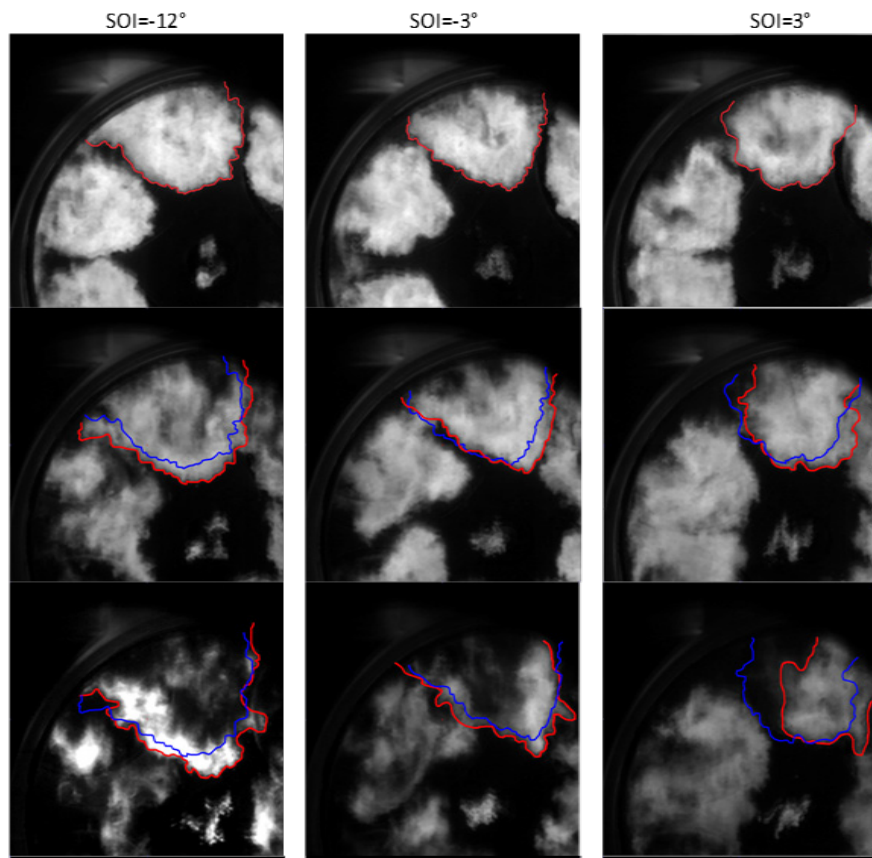


Figure 5. Example high speed imaging under conventional diesel combustion conditions. Red outlines show current image's soot cloud and blue outline shows previous image's soot cloud. Images shown are 17°, 20°, 23°, and 26° after SOI. The gain of some later images in increased for better viewing.

## References

1. N.A. Slavinskaya, P. Frank, Combust. Flame 156 (2009) 1705–1722.
2. Wang, Hu, Yao, Mingfa, Yue, Zongyu, Jia, Ming, and Reitz, Rolf D, Combust. Flame 162 (2015) 2390–2404.
3. K. Fieweger, R. Blumenthal, G. Adomeit, Combust. Flame 109 (4) (1997) 599–619.
4. M.J. Castaldi, N.M. Marinov, C.F. Melius, J. Huang, S.M. Senkan, W.J. Pit, C.K. Westbrook, Symp. (Int.) Combust. 26 (1) (1996) 693–702.
5. C. Marchal, J.-L. Delfau, C. Vovelle, G. Moréac, C. Mounaïm-Rousselle, F. Mauss, Proc. Combust. Inst. 32 (1) (2009) 753–759.
6. A.E. Bakali, J.-L. Delfau, C. Vovelle, Combust. Sci. Technol. 140 (1–6) (1998) 69–91.
7. F. Defoex, V. Dias, C. Renard, P.J. Van Tiggelen, J. Vandooren, Proc. Combust. Inst. 30 (1) (2005) 1407–1415.

8. Hiroyasu, H. and Kadota, T., “Models for Combustion and Formation of Nitric Oxide and Soot in Direct Injection Diesel Engines,” SAE Technical Paper 760129, 1976, doi:10.4271/760129.
9. Kavuri, C., Tiriy, M., Paz, J., and Kokjohn, S.L., Int. J. Engine Research, 2016.

## FY 2016 Publications/Presentations

1. Kavuri, C., Strickland, T., and Kokjohn, S.L., “An evaluation of the impact of soot inception species on conventional and low temperature combustion,” In Preparation, Int. J. Engine Research.
2. Kavuri, C., Paz, J., and Kokjohn, S.L., “A comparison of Reactivity Controlled Compression Ignition (RCCI) and Gasoline Compression Ignition (GCI) strategies at high load, low speed conditions,” Energy Conv. Management, 127:324–341, 2016.

## II.36 Development and Validation of Physics-Based Sub-Models of High Pressure Supercritical Fuel Injection at Diesel Conditions

### Overall Objectives

- Produce a validated real-fluid property code which can be integrated with computational fluid dynamics (CFD) solvers to improve their accuracy in simulating high-pressure diesel sprays
- Provide documentation containing information associated with CFD code modifications needed for supercritical fluid spray simulations using the Eulerian-Eulerian (EE) approach
- Establish the accuracy assessment of the EE approach to simulate fuel spray at high-pressure diesel engine operating conditions
- Produce an extensive experimental data set to validate CFD models simulating high-pressure diesel fuel spray

### Fiscal Year (FY) 2016 Objectives

- Design and construct a constant pressure flow rig (CFR) for non-reacting experiments
- Optimize high-speed rainbow schlieren deflectometry (RSD) optical setup for the present study
- Modify existing schlieren analysis codes to account for window effects and other optical distortions introduced in this experiment.
- Evaluate various existing equations of state and methodologies to assess their appropriateness and accuracy in describing correlations between the thermal properties and their corresponding transport properties at the high-pressure conditions
- Develop a stand-alone numerical module to calculate thermo-physical properties based on the selected real-fluid model, or to interpolate the database of real-fluid thermal properties available
- Validate the developed real-fluid property with the available property data
- Develop interface to facilitate the code integration

**Professor Ajay K. Agrawal  
(Primary Contact), Joshua Bittle, and  
Chih-Hsiung Cheng**

The University of Alabama  
359 H.M. Comer Hall  
Tuscaloosa, AL 35487  
Phone: (205) 348-4964  
Email: aagrawal@eng.ua.edu

**Sibendu Som**

Argonne National Laboratory  
9700 Cass Avenue  
Argonne, IL 60540  
DOE Technology Development Manager:  
Leo Breton  
NETL Manager:  
Carl P. Maronde

### FY 2016 Accomplishments

- Designed and commissioned for construction a CFR for non-reacting experiments
- Optimized high-speed RSD optical setup for diagnostics in a CFR facility
- Modified and developed schlieren analysis codes to obtain equivalence ratio and liquid penetration depth
- Evaluated various existing equations of state and methodologies to assess their appropriateness and accuracy in describing correlations between the thermal properties and their corresponding transport properties at the high-pressure conditions
- Developed a stand-alone numerical module to calculate thermo-physical properties based on the selected real-fluid model, or to interpolate the database of real-fluid thermal properties available
- Validated the developed real-fluid property with the available property data ■

## Introduction

This proposed research seeks to develop and validate accurate, physics-based, numerical sub-models and framework, which can be implemented in CFD software to enable it to accurately predict high-pressure diesel spray. The combined experimental-computational effort has four major objectives: (1) acquire spatially and temporally resolved scalar measurements of fuel oxidizer mixing in the near field of the jet for a range of supercritical or nearly supercritical test conditions relevant to diesel engines; (2) develop real-fluid model and code to calculate thermo-physical properties of diesel surrogates and their mixtures with oxidizer of interest at a wide range of operating conditions, especially at pressures near and above the critical conditions; (3) integrate the real-fluid model into a commercial and an open-source CFD codes to demonstrate the use of the model to accurately simulating high-pressure diesel spray; and (4) assess the robustness, accuracy, and uncertainty of the integrated CFD solvers in computing injection spray.

## Approach

Experiments will be conducted in a CFR whereby a low-speed flow of heated, pressurized air is supplied to the test chamber, and the fuel is injected against this flow. High-speed RSD, a novel optical diagnostics technique pioneered in our lab to acquire quantitative scalar measurements in jets and flames, and supersonic flows is utilized to resolve the highly dynamic features of the mixing process. Experiments will be conducted initially at conditions approximating the Engine Combustion Network Spray A, and then at different chamber and fuel injection conditions, and fuel-types, i.e., pure or mixtures of surrogate species, and eventually the real diesel fuel.

A real-fluid model, which can account for the compressibility effects in diesel fuels, will be developed and validated using the available database. The property models will be integrated with an open source CFD code, which will be validated using experimental data. The models will also be integrated into a commercial CFD code by our partner team at the Argonne National Laboratory.

## Results

### Rainbow Schlieren Imaging of Heptane Injection

Design of the CFR and associated flow systems has been completed, the flow systems upstream of the CFR have been installed in the lab, and in order to design and construct the optical windows has been placed. The optical setup for the RSD technique was optimized and multiple experiments were conducted to acquire and analyze color schlieren images for a range of operating conditions. Images provide vivid illustration of the dynamic nature of the injected jet as it undergoes transient evolution to evolve into a quasi-steady jet. Multiple injection events (say 50 or more in any experiment) thus allow us to obtain ensemble-averaged images during the jet evolution and an average image depicting steady state. Sample results are shown for fuel n-heptane injected into the chamber with air at pressure of 1.36 MPa and temperature of 180°C. Figure 1 shows instantaneous schlieren images after steady state is attained. Figure 2a shows a time-average schlieren image based on 2,000 images, 40 steady images from each of the 50 jet injections. Turbulent structures observed in instantaneous images can no longer be detected in the average images, as expected. Moreover, the average image shows excellent symmetry, and thus, Abel inversion technique can be used to obtain the local profiles of average density and equivalence ratio; these calculations are currently in progress. Figure 2b shows a Mie scattering image acquired at the same time as schlieren images to identify the liquid core. Currently, we are exploring various approaches to detect the liquid core boundary directly from color schlieren images, thereby eliminating the need for Mie scattering.

### Evaluate Various Existing Equations of State and Methodologies to Assess Their Appropriateness and Accuracy in Describing Correlations Between the Thermal Properties and Their Corresponding Transport Properties at the High-Pressure Conditions

The literature review of various equations of state available for modeling thermal properties and transport property models of pure substances of interest was

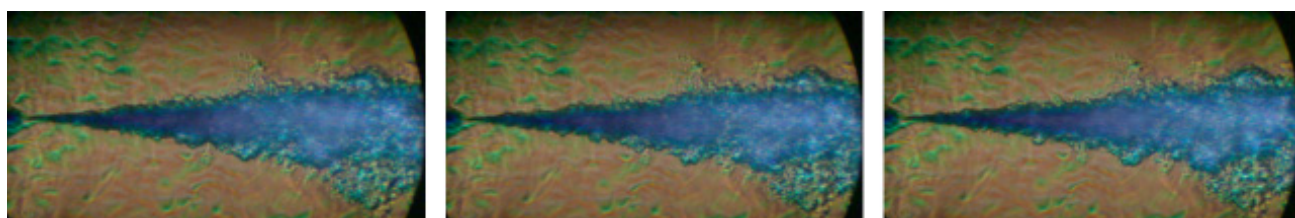


Figure 1. Instantaneous RSD images during fuel injection

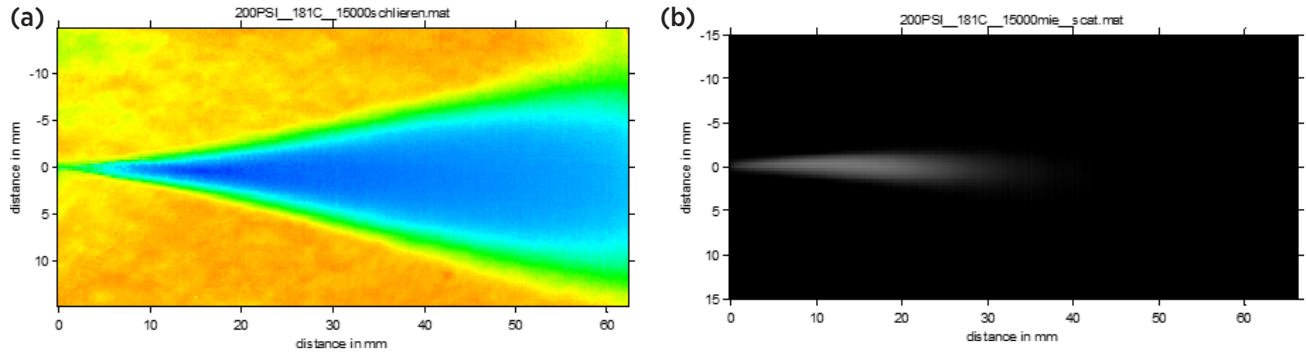


Figure 2. (a) Time-averaged schlieren image (based on 40 steady images from each of the 50 injections) depicting the steady spray (left), and (b) Mie scattering image (right) depicting the liquid boundary

completed. Preliminary evaluations of equations of state for the thermal properties were performed, while the evaluation of transport properties is in progress. The selected equations of state and their associated property models are described in the quarterly report submitted in July 2016. For example, Pitzer correlation (Reid, et al. [2]) provides successful fit for a variety of species,

$$\ln p_{v,r} = \psi + \omega \xi; \text{ or } p_{v,r} = e^{\psi + \omega \xi} \quad (1a)$$

where

$$\begin{aligned} p_{v,r} &= p_v / p_c; \text{ and} \\ \psi &= \psi_1 + \psi_2 T_r^{-1} + \psi_3 \ln T_r + \psi_4 T_r^6; \\ \xi &= \xi_1 + \xi_2 T_r^{-1} + \xi_3 \ln T_r + \xi_4 T_r^6 \end{aligned} \quad (1b)$$

Using the Pitzer correlation, the vapor pressure as a function of temperature for *n*-dodecane is plotted and compared to the National Institute of Standards and Technology (NIST) database [1] as shown in Figure 3. It can be seen the agreement between the Pitzer correlation and NIST database is very good.

In Figure 4, the pressure–enthalpy and temperature–enthalpy curves at the saturation conditions calculated from the present model are compared to the NIST database. It can be seen that the agreement is very good. The largest discrepancy occurs around the critical point, but is within the margin of error (1%). It should be noted that the specific enthalpy calculated from the selected model is shifted with a fixed value so that the saturated vapor enthalpies of the selected model and NIST database are the same at the temperature of 300 K because the NIST database and the model have different reference states for zero enthalpy.

The development of a stand-alone numerical module has been initiated. Some of the numerical results reported here

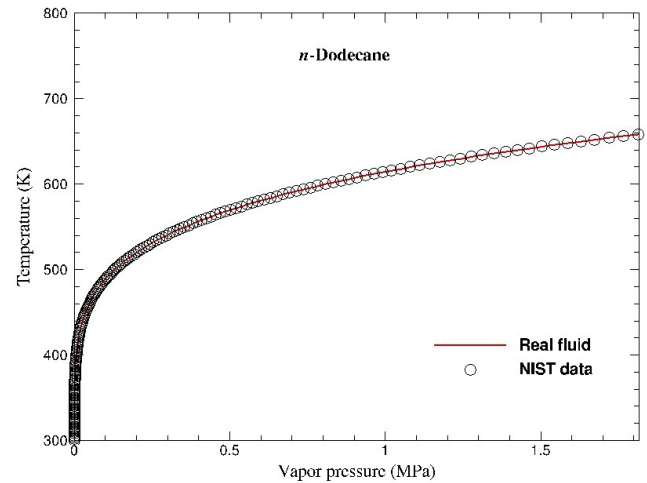


Figure 3. Comparison of vapor pressure–temperature relation (NIST [1])

were generated from the code. Further debugging, model implementations and evaluations will continue in the next quarter.

## Conclusions

- Rainbow schlieren deflectometry technique has been applied to observe fuel spray in CFR for the first time.
- RSD technique provides detailed dynamic features of the spray, and allow quantification of the vapor and liquid regions.
- Real-fluid property models accurately replicate NIST database for dodecane.

## References

1. NIST Thermophysical Properties of Fluid Systems, [www.webbook.nist.gov](http://www.webbook.nist.gov).

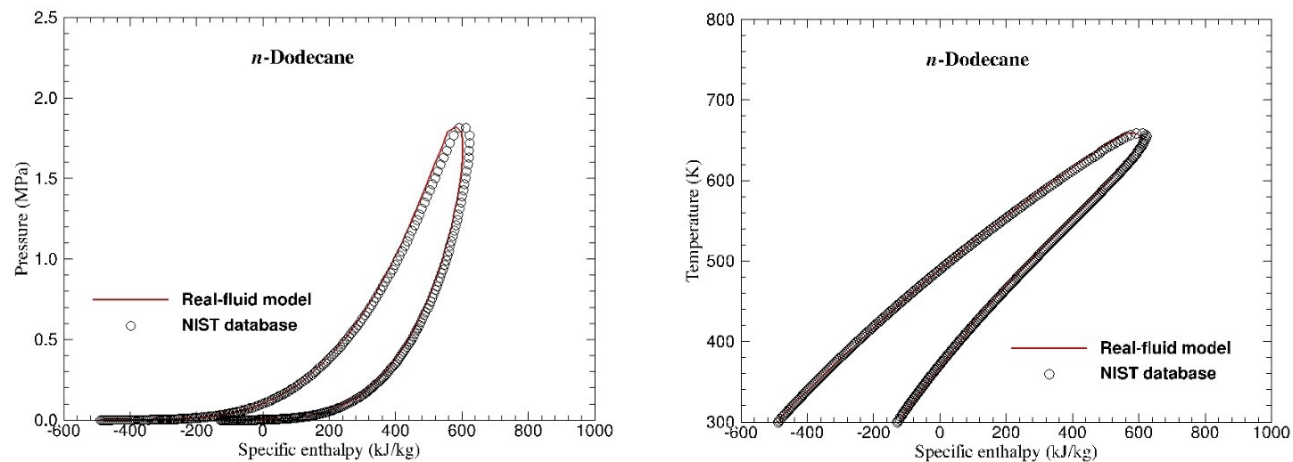


Figure 4. Comparisons of pressure-enthalpy and temperature-enthalpy relations at the saturation condition (NIST [1])

- Reid, R.C., Prausnitz, J.M., and Sherwood, T.K., *The Properties of Gases and Liquids*, McGraw-Hill Co., 3rd Ed., 1977.

## FY 2016 Publications/Presentations

- Wanstall, C., Bittle, J., and Agrawal, A.K., 2016, "Quantifying Liquid Core of a Fuel Spray by Rainbow Schlieren Deflection," in preparation, *Applied Optics*.

## II.37 Development of a Physics-Based Combustion Model for Engine Knock Prediction

### Overall Objectives

- Develop a predictive combustion model for engine knock, which can capture turbulence–chemistry interactions in a physics-based way and incorporate detailed chemistry into large eddy simulation (LES) of in-cylinder turbulent reacting flows
- Advance a fundamental understanding of turbulence–chemistry interactions during end-gas ignition through engine LES, high-fidelity direct numerical simulation (DNS), and engine experiments

### Fiscal Year (FY) 2016 Objectives

- Develop a base computational code for the combustion model
- Generate DNS database to guide the combustion model development
- Generate experimental data for in-cylinder pressure and species evolution under knocking and knock-free operation of a single-cylinder engine

### FY 2016 Accomplishments

- Developed a base computational code for the combustion model
- Generated and analyzed DNS data for turbulent premixed flame propagation
- Generated detailed chemistry DNS data for end-gas ignition
- Experimental in-cylinder sampling hardware and operating conditions are acquired and fully defined ■

### Introduction

The U.S. DOE has set the goals to improve the fuel economy of passenger vehicles by 35%–50% and commercial vehicles by 30% by 2020, with the reference of 2010 baseline vehicles. Efforts to increase fuel economy through techniques such as increasing the compression ratio or downsizing are constrained by the increased tendency for engine knock—an undesired ignition of the end-gas containing unburned fuel–air mixture ahead of the spark-ignited premixed flame resulting in rapid in-cylinder pressure rise and potential engine damage. The ability to accurately simulate and

### Seung Hyun Kim

The Ohio State University  
201 W. 19th Avenue  
Columbus, OH 43210  
Phone: (614) 688-2116  
Email: kim.5061@osu.edu

Derek Splitter, K. Dean Edwards  
Oak Ridge National Laboratory (ORNL)  
2360 Cherahala Blvd.  
Knoxville, TN 37932  
Phone: (865) 946-1347  
Email: splitterda@ornl.gov, edwardskd@ornl.gov  
DOE Technology Development Manager:  
Leo Breton  
NETL Project Manager:  
Nicholas D'Amico

predict knock events is crucial to the development of advanced engines capable of meeting the fuel economy goals.

This project seeks to develop a new combustion model for end-gas knock prediction, where turbulence–chemistry interactions during end-gas ignition and spark-ignited flame propagation are modeled in a physics-based, consistent way. The proposed model is targeted to directly incorporate a detailed (reduced) chemical mechanism developed for ignition and combustion reactions under engine relevant conditions. With such features, the developed model will advance the predictive capability for engine knock simulations and enable reliable use of engine simulation tools in knock prediction and engine development.

### Approach

The overall approach includes joint computational and experimental efforts focusing on the model development and validation with high-fidelity numerical and experimental data. The physics-based and mathematically consistent modeling framework consists of separate models for spark-ignited premixed flame propagation and end-gas ignition processes to consider fundamentally different turbulence–chemistry interactions during the

two processes. The model is developed in the context of LES to consider the stochastic nature of the knocking phenomena. For thorough validation, DNS and engine knock and knock-free experiments coupled with measurements of in-cylinder pressure and gas species temporal evolutions will be performed to provide high-fidelity data sets. DNS data will guide the model development by providing detailed statistical information.

## Results

The end-gas ignition process is modeled in the framework of conditional moment closure (CMC) [1]. The developed solver is based on CVODE (and DVODE) and CHEMKIN, and adopts adaptive mesh refinement to resolve the ignition front. Figure 1 shows the results for simple hypothetical cases that are used to test the base CMC solver. The cases correspond to ignition of fuel-air mixtures with prescribed in-cylinder pressure evolution due to piston motion and premixed flame propagation. The stoichiometric iso-octane-air mixture is considered. A reduced mechanism for primary reference fuel (PRF), which consists of 116 species [2], is used. The initial temperature of the fuel-air mixture and the spark timing in the prescribed pressure profile are changed. The mean mixture temperature at 30° of crank angle before top dead center (TDC) is set to be 650 K, 700 K, or 725 K for each spark timing. Temperature inhomogeneity is also imposed. The engine speed is set to be 1,200 rpm. The simulation results reproduce qualitative behaviors, verifying the implementation of the model. As the spark timing is retarded, autoignition of end-gas tends to be delayed. For given spark timing, a fuel-air mixture with

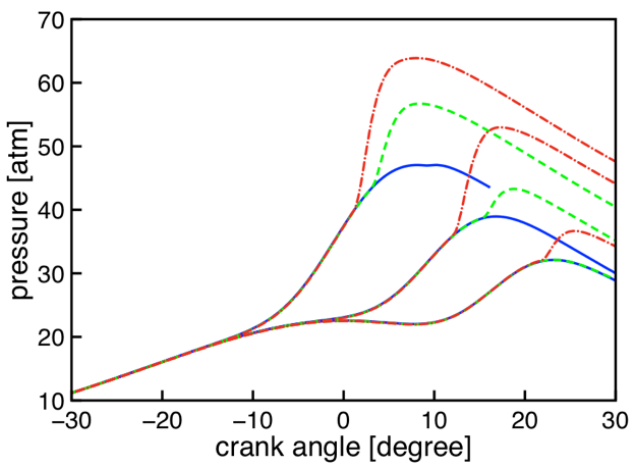


Figure 1. Pressure evolution for various spark timing and intake mixture temperature (red dashed-dotted lines:  $T_0 = 725$  K, green dashed lines:  $T_0 = 700$  K, blue solid line:  $T_0 = 650$  K;  $T_0$  is the temperature of a fuel-air mixture at the crank angle of 30° before TDC).

higher intake temperature is more prone to knock in Figure 1.

DNS of end-gas ignition has been performed to provide detailed statistical data to guide the development of end-gas ignition CMC. Three types of DNS have been performed: autoignition in two-dimensional homogeneous isotropic turbulence, premixed flame propagation and end-gas ignition in homogeneous isotropic turbulence, and mixing in three-dimensional homogeneous isotropic turbulence. Figure 2 shows the temperature field at the onset of end-gas ignition in two-dimensional homogeneous isotropic turbulence. The computational domain size is 5 mm  $\times$  5 mm, which is discretized into 1,024  $\times$  1,024 grid points. The fuel is PRF80 and the equivalence ratio is set to be 0.7. A reduced PRF mechanism consisting of 116 species is used [2]. The initial pressure is 30 bar. Initial mean temperature of the end gas is 970 K. The temperature and pressure values belong to the range of the pressure and temperature at the time of spark ignition. The temperature inhomogeneity level is maintained at about 40 K. DNSs are being performed to generate the database for various operating conditions by changing temperature, pressure, PRF composition, and equivalence ratio. In Figure 3, the temperature and velocity fields in turbulent mixing DNS. This DNS will be used to extract the statistics of the scalar dissipation rate, which is a key quantity to capture turbulence-chemistry interactions in high scalar dissipation layers. The domain size is 3.2 mm  $\times$  3.2 mm  $\times$  3.2 mm, which is discretized into 256  $\times$  256  $\times$  256 grid points. Larger-scale DNS is planned.

Spark-ignited premixed flame propagation is modeled in the framework of front propagation formulation [3].

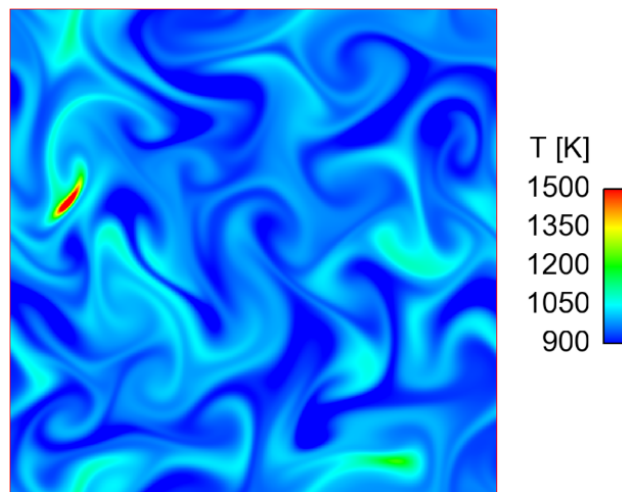


Figure 2. Temperature field in DNS of end-gas ignition in homogeneous isotropic turbulence

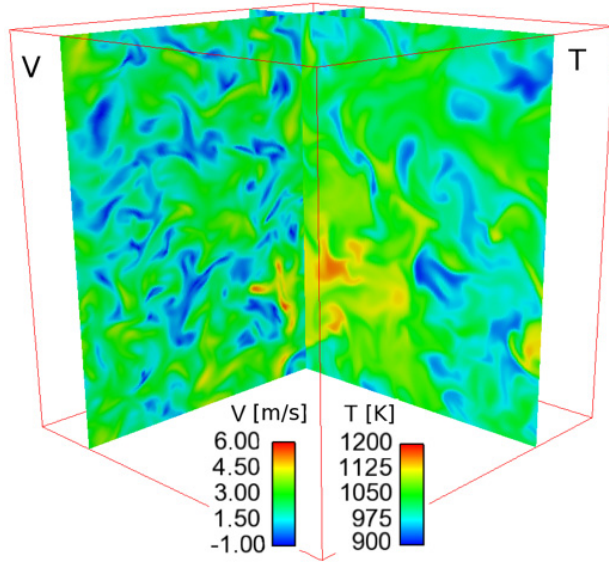


Figure 3. Temperature and velocity fields in DNS of turbulent mixing

In FY 2016, DNS of premixed flame propagation in homogeneous isotropic turbulence is firstly conducted to analyze the submodels in front propagation formulation. Figure 4 shows the comparison of existing models for the wrinkling factor [4–7]. The wrinkling factor represents the effects of small-scale turbulence on the increase in flame surface area and is one of the key quantities for accurate prediction of burning rates due to premixed flame propagation. The model parameters in each model are adjusted to minimize the error. The Damkohler model [4] performs very well and reproduces the DNS results for all the filter sizes that are tested. The fractal or power law model [5] also works well except for the small filter sizes that are close to or below the inner cut-off scale.

Currently an experimental campaign to support the simulation effort is underway. The campaign is conducted at ORNL and utilizes a single-cylinder version of the General Motors LNF 2.0 L four-cylinder design turbocharged gasoline direct injected engine from the 2007 Pontiac Solstice. The multi-cylinder engine has been converted to single-cylinder operation by deactivating Cylinders 1–3, and has been a mainstay of research at ORNL since its installation. The engine and laboratory has full control over all pertinent systems and subsystems including port and/or direct fuel injection, external cooled exhaust gas recirculation, full cam phasing authority, and full authority over intake pressure, exhaust pressure, external exhaust gas recirculation rate, spark timing, fuel pressure, fuel injection timing, and number of fuel injections. The engine is controlled and data is acquired by a purpose built National Instruments' LabVIEW

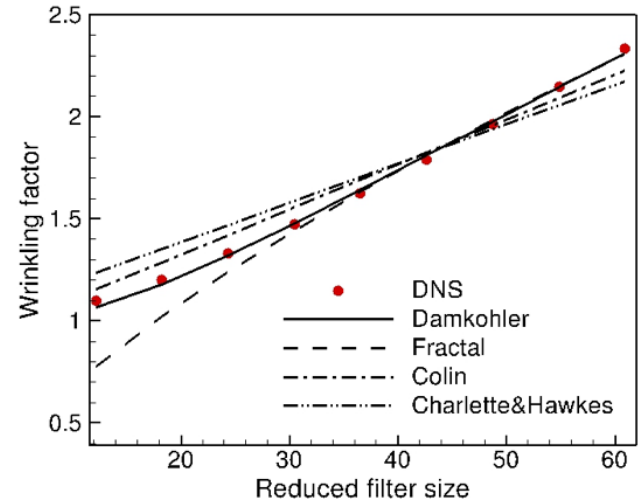


Figure 4. Comparison of the wrinkling factor models to estimate the increase of flame surface area due to subfilter-scale turbulence

code that operates through a Drivven controller. To date the experimental effort has encompassed acquisition of custom hardware and capabilities that will be used for in-cylinder sampling of gas species. An upcoming campaign to be completed by the end of Month 12 of the project (January 2017) will encompass pressure-based data that probes ignition delay contours of iso-octane as a function of in-cylinder TDC pressure and temperature. Follow on work in the project will augment these measurements with select conditions where direct in-cylinder gas sample acquisition from the end gas region (i.e., knocking region) at determined and finite crank angle window(s) using a purpose build gas sampling valve by SMEtech (valve is capable of 0–720° crank angle duration at  $\pm 1^\circ$  crank angle resolution). Both the measured gas pressure and species will be used to validate the simulations. These measurements will be focused mostly in Year 2 of the project. The measurements in year one of the project will focus on the TDC conditions and subsequent end gas conditions that are required to achieve knock. Measurements and analysis of phenomena such as pre-spark heat release will be conducted to probe the conditions at which knock onset are relevant.

## Conclusions

In FY 2016, the base computational code for the knock combustion model has been developed. The code is capable of describing turbulence–chemistry interactions during end-gas ignition processes, based on detailed chemistry, in a computationally efficient way. DNSs of end-gas ignition and premixed flame propagation in homogeneous isotropic turbulence have been

performed to guide the model development and advance a fundamental understanding of turbulence–chemistry interactions. In FY 2017, larger-scale DNS will be performed, the submodels in the modeling framework will be validated and refined using the DNS data, the experimental data will be acquired, and LES of in-cylinder reacting flows under knock-free operation will be performed.

## References

1. A.Y. Klimenko and R.W. Bilger, *Prog. Energy Combust. Sci.*, 25:595–687 (1999).
2. M.B. Luong, Z. Luo, T.F. Lu, S.H. Chung, C.S. Yoo, *Combust. Flame*, 160:2038–2047 (2013).
3. S.H. Kim, *J. Comput. Phys.* 285:193–207 (2015).
4. T. Poinsot, D. Veynante, *Theoretical and Numerical Combustion*, 3rd ed., 2011.
5. O. Colin, F. Ducros, D. Veynante, T. Poinsot, *Phys. Fluids A* 12:1843–1863 (2000).
6. F. Charlette, C. Meneveau, D. Veynante, *Combust. Flame* 131:181–197 (2002).
7. D. Veynante, V. Moureau, *Combust. Flame*, 162:4622–4642 (2015).

## FY 2016 Publications/Presentations

1. S.H. Kim et al. Development of a Physics-Based Combustion Model for Engine Knock Prediction, Research Performance Progress Report, April 30, 2016.
2. S.H. Kim et al. Development of a Physics-Based Combustion Model for Engine Knock Prediction, Research Performance Progress Report, July 30, 2016.

## II.38 Development and Multiscale Validation of Euler–Lagrange-Based Computational Methods for Modeling Cavitation Within Fuel Injectors

### Overall Objectives

- Develop and validate physics-based, mathematical submodels for use in standard multiphase computational fluid dynamics (CFD) software to enable better prediction of cavitation within fuel injectors

### Fiscal Year (FY) 2016 Objectives

- Select appropriate open source Lagrangian code for cavitation simulations
- Construct small-scale experimental setup of cavitation in a canonical nozzle
- Image cavitation in real fuel injector using the High Flux Isotope Reactor (HFIR) at ORNL

### FY 2016 Accomplishments

- Selected and validated an appropriate open source Lagrangian code modeling cavitation
- Implemented and partially validated necessary physics to model air/water bubble dynamics.
- Developed controlled cavitation experiments for flow ranges of Reynolds number = 15,000–25,000 to test inside acrylic orifices of varying dimensions and geometry
- Demonstrated two viable methods of detecting and characterizing cavitation
- Imagined fuel flow and cavitation in real fuel injector ORNL using the HFIR ■

### Introduction

The main objective of this research project is to develop and validate more accurate, physics-based, mathematical submodels for use in CFD software to enable better prediction of cavitation within fuel injectors. The outcome of the research will be two new submodels for cavitation that can be used in conjunction with CFD, one for preliminary design and the second for final design analysis.

Controlled cavitation in fuel injectors can improve the atomization of the spray which improves combustion

**Emily Ryan (Primary Contact),  
Sheryl Grace, Glynn Holt, James Bird**

Boston University

25 Buick Street

Boston, MA 02215-1301

Phone: (617) 353-7767

Email: ryanem@bu.edu

DOE Technology Development Manager:

Leo Breton

Subcontractor:

Oak Ridge National Laboratory (ORNL), Oak Ridge, TN

and reduces emissions. However, excess cavitation can be detrimental to efficiency and can damage the injector. Therefore the global motivation for research into cavitation in fuel injectors stems from the fact that improvements in fuel injection systems will increase fuel efficiency, reduce the emission of harmful pollutants and improve the lifetime and reliability of nozzles.

### Approach

The project will develop methods for simulating cavitation dynamics in a fuel injector that can be used in preliminary design and for final design analysis, and will perform experiments for validation of the models. Research focuses on three specific thrusts: computational model development, small-scale cavitation experiments, and HFIR imaging of a real fuel injector.

### Computational Model Development

The computational sub-models that are being developed rely on cavitation analysis performed with a Lagrangian frame solver in the form of the smoothed particle hydrodynamics (SPH) method. One submodel will create constitutive relations for inclusion in a CFD solver using an upscaling process based on the results from detailed computational studies of canonical injectors. Detailed simulations of cavitation in nozzles using SPH will form a database from which an upscaling method will be used to define a new submodel that can be integrated into a Reynolds-averaged Navier–Stokes-based multiphase CFD

code (much like turbulence models are used in CFD). The second submodel will consist of the SPH model itself by defining the two-way coupling interface equations for use with unsteady Reynolds-averaged Navier–Stokes CFD. Using a two-way coupled SPH and CFD approach will create a more detailed and accurate model but will be much more computationally expensive than upscaling and as such is proposed for final design analysis.

### Small-Scale Experiments

Development and validation of the SPH tool and the subsequent full simulation capabilities based on the new sub-models relies on outcomes from experimental studies of detailed flow characteristics for canonical and real geometry injectors performed at Boston University and Oak Ridge National Laboratory. A small-scale canonical nozzles setup is being designed and created at Boston University to investigate the effects of flow rate and nozzle size/shape on the onset of cavitation.

### HFIR Imaging

In performing dynamic studies of fuel injector operation a heated and pressure controlled spray chamber is employed. A closed loop fuel injection system (Figure 1a) with heated spray chamber (Figure 1b) is installed at the neutron imaging beamline at ORNL's HFIR. The sophisticated system is designed to operate with commercial and prototype injectors and deliver fuel to the injectors at rail pressures up to 150 bar.

The spray chamber can be operated at absolute pressures as low as 0.2 bar, and currently has a maximum pressure of approximately 4 bar and can be heated over 100°C while also flowing 10–40 L/min of directed sweep gas to further eliminate condensation build-up (Figure 1c). These conditions are necessary to avoid condensation of the fuel in the chamber, because it will block neutron flux.

### Results

During FY 2016 research for this project focused on the three complimentary tasks discussed in the Approach section. A brief description of the results for each of these areas is given in the following.

### Computational Model Development

An SPH computational model is being developed to model cavitation in a fuel injector. Initial work focuses on the development and validation of the SPH code to model bubble dynamics. Critical extensions and applications of the

existing SPH framework were tested and validated. In particular, validation cases were setup to investigate the ability to model large density differences (1/1000) and the implementation of surface tension. As seen in Figure 2, the simulation is able to accurately model the relaxation of a square bubble to a circular bubble. These results test the implementations of the surface tension, pressure, and viscosity in SPH. Simulations were run for both a liquid droplet in air and an air bubble in water. Both cases show good results when compared to analytical solutions.

### Small-Scale Detailed Cavitation Experiments

A working apparatus for creating and studying flow-induced cavitation was assembled and tested. The apparatus is now ready for parameter studies, with parameters to be tested for Year 2 to be selected in conjunction with the computational team members, and the ORNL team members. Our prototype setup is shown in Figure 3. It has undergone two iterations to address a variety of issues. The final version consists of a variable frequency drive vane pump for precise flow control, coupled to a modular nozzle which can accommodate a range of nozzle types (orifice shape, taper) and sizes. Both volume flow and head pressure sensors are available in the section upstream of the nozzle. Optical imaging to date has used a stroboscopic backlight and a complementary metal-oxide-semiconductor camera. A

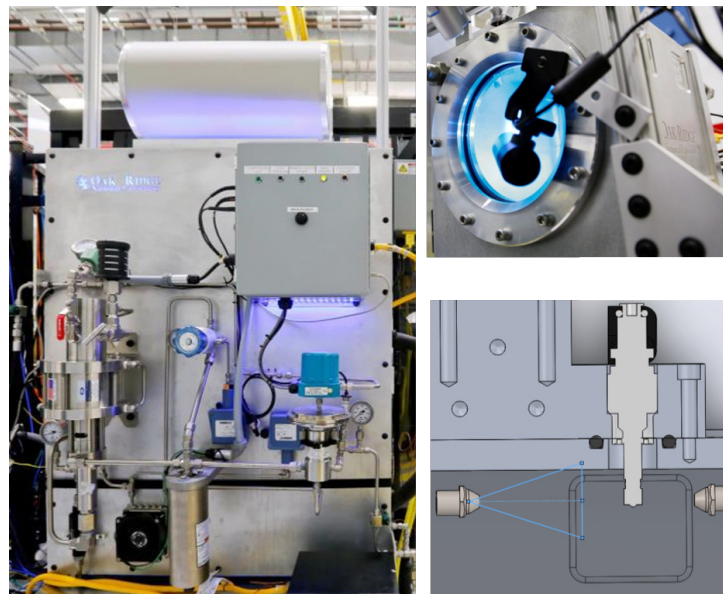


Figure 1. (a) High pressure fuel delivery system and (b) spray chamber installed at HFIR. (c) computer-aided design drawing of injector holder and the necessary sweep gases to minimize fuel buildup on the chamber walls and injector.

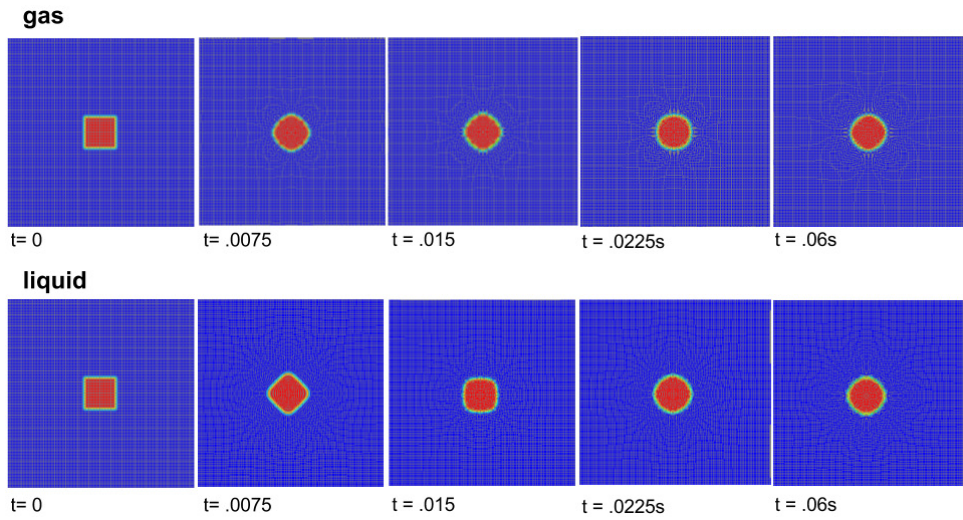
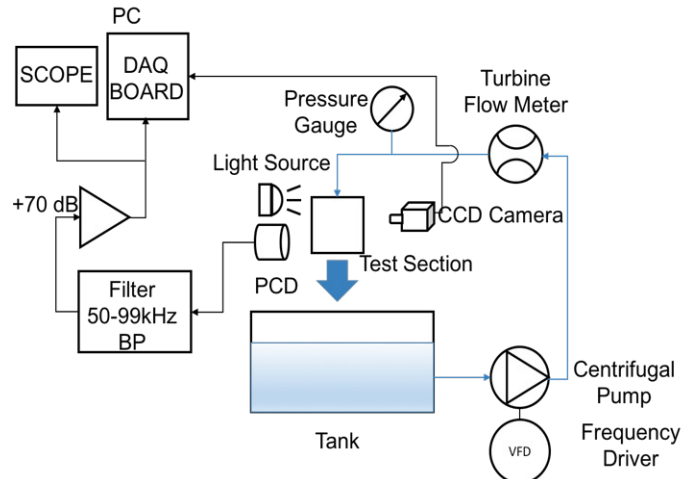
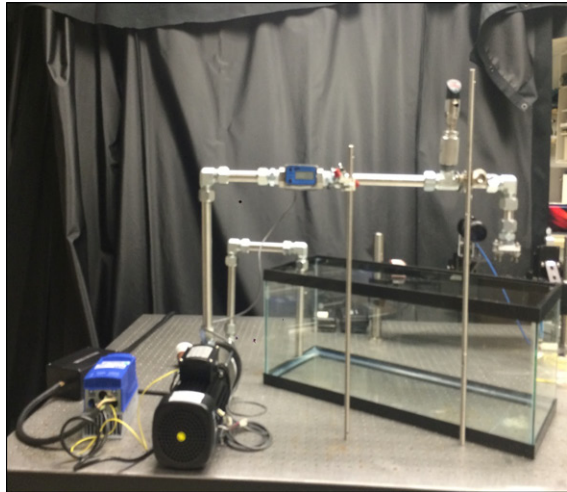


Figure 2. SPH simulations of bubble shape oscillation due to relaxation from an initial square. Top figure shows a liquid droplet in air and bottom figure shows a gas bubble in water.



DAQ – data acquisition; CCD – charge-coupled device; PCD – passive cavitation detector; VFD – variable-frequency drive; PC – personal computer

Figure 3. Schematic of the experimental setup including diagnostic systems

high-speed camera is available for incorporation in Year 2. Passive acoustic sensing is achieved using piezoceramic single-element transducers, with characteristics chosen to enhance sensitivity to transient events.

Figure 4 displays sample images for a nozzle with a  $2.5\text{ mm} \times 2.5\text{ mm}$  square orifice. The flow was driven continuously at varying flow rates and untreated tap water was the working fluid. The sample images highlight the different flow regimes (from left to right): noncavitating, cavitating, and hydraulic flip flows. These images are processed in MATLAB (MathWorks, Massachusetts) where they are converted to grey scale and the mean brightness are compared for detection of cavitation.

Similarly, cavitation activity is determined acoustically by recording time series of conditions identical for optical analysis. Impulse excitation response is considered the result of inertial cavitation and is used as an indicator of cavitation activity. Figure 5 summarizes the two techniques employed to observe cavitation activity. There exists an agreement between the methods that onset of cavitation can be detected at approximately 65 mL/s. These results tell us that vaporous inertial cavitation dominates the onset and post-onset regime.

### HFIR Imaging Campaign

In September, a Boston University student travelled to ORNL to help complete a neutron imaging campaign at

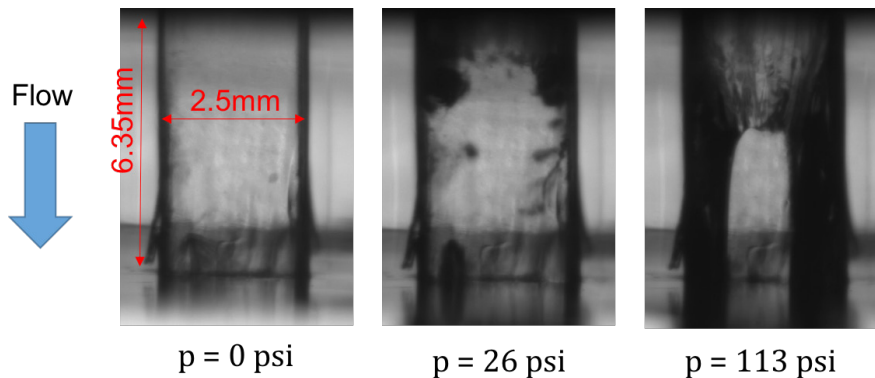


Figure 4. Transition from no cavitation event to cavitating flow to hydraulic flip activity. Camera settings are digitally set at 12 fps with 41 ms exposure time.

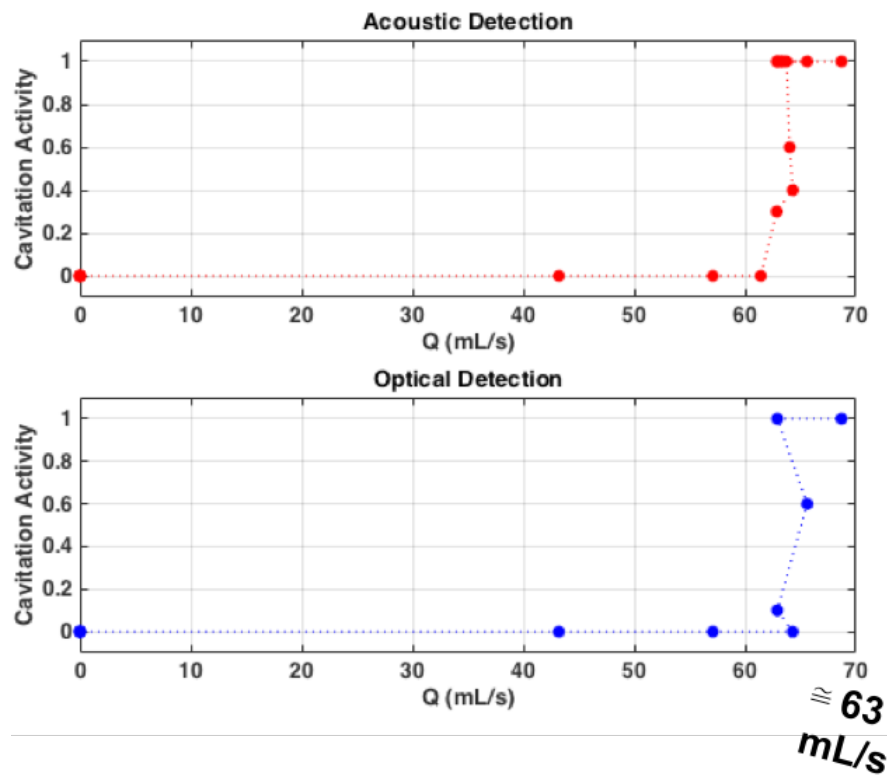


Figure 5. Comparison of acoustic and optical sensing for cavitation activity varying flowrate

the HFIR. Stroboscopic imaging using a gasoline direct injection injector was employed to record a fuel injection event with 20  $\mu$ s temporal resolution at 25 Hz. This technique required observing  $\sim 1$  M periodic injection events and integrating sparse neutron counts in each snapshot to produce a high-contrast injection moving image record. Two conditions were imaged, both with 0.367 ms injection duration of pressurized cyclopentane: (1) a higher-temperature, lower ambient pressure

condition to induce flashing (70°C and 30 kPa), and (2) a lower-temperature, higher ambient pressure condition to inhibit flashing (40°C and 110 kPa). Figure 6 shows the injection sequence that was recorded during Condition 1. Figure 7 shows comparative emptying rates at the two conditions; lower intensity values indicate the visibility of injected fluid.

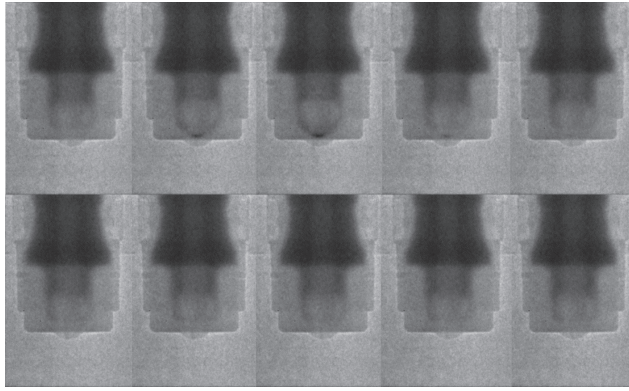


Figure 6. Image sequence shows 20  $\mu$ s composite frames of one-hole injection at flash conditions with cyclopentane (Condition 1); injection starts before second frame.

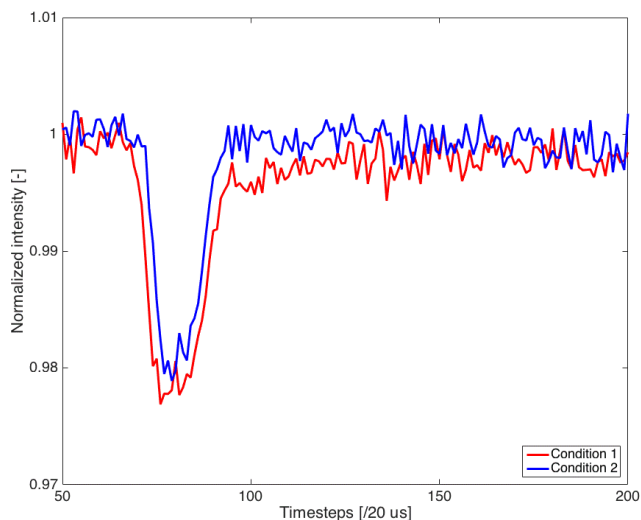


Figure 7. Neutron-attenuation profiles of the two injection conditions imaged at the HFIR in September (lower intensity denotes more fluid). Intensities were averaged over a small region encompassing the sac and nozzles. A distinct difference in conditions was observed using the dynamic imaging technique.

## Conclusions

- Initial SPH model development included the addition of multiphase physics to an existing free surface flow SPH code and initial validation of bubble dynamics
- Baseline experimental system developed which demonstrates capability of providing canonical data for comparison with computational results
- Successful imaging campaign of a real fuel injector using the HFIR at ORNL

## References

1. N. Kardjilov, “Absorption and phase contrast neutron imaging,” Imaging and Neutrons 2006, Oak Ridge, TN, October 23–25, 2006; [http://neutrons.ornl.gov/workshops/ian2006/MO1/IAN2006oct\\_Kardjilov\\_02.pdf](http://neutrons.ornl.gov/workshops/ian2006/MO1/IAN2006oct_Kardjilov_02.pdf)

## II.39 Development and Validation of a Turbulent Liquid Spray Atomization Submodel for Diesel Engine Simulations

### Overall Objectives

- Demonstrate a new spray atomization submodel for engine computational fluid dynamics (CFD) codes with improved capability to accurately predict local spray morphology and global spray characteristics over a wide range of engine operating conditions, including conditions relevant for advanced combustion engines
- Develop an improved understanding of the fundamental physics governing atomization in diesel fuel sprays
- Demonstrate a new measurement technique that quantifies diesel spray morphology, including spatially resolved distributions of Sauter mean diameter (SMD) and liquid volume fraction, from the near-nozzle region to the far-field fully atomized spray, over a wide range of engine-relevant operating conditions

### Fiscal Year (FY) 2016 Objectives

- Identify a comprehensive set of non-vaporizing spray experiment testing conditions that can be achieved jointly at Argonne and Georgia Tech (leveraging a shared Engine Combustion Network [ECN] Spray D injector), which suppress aerodynamic breakup forces and favor turbulent liquid atomization
- Measure two-dimensional (2D) liquid mass distributions of ECN Spray D at the Argonne Advanced Photon Source under target experimental conditions
- Measure 2D distributions of optical thickness in ECN Spray D at Georgia Tech under target experimental conditions
- Demonstrate new measurement technique, ultra-small angle X-ray scattering (USAXS), to measure SMD in high optical thickness regions of Spray D at target experimental conditions
- Benchmark predictive capabilities of existing diesel spray atomization submodels within the open-source CFD code OpenFOAM

### FY 2016 Accomplishments

- Demonstrated that measured nozzle area-contraction coefficient of ECN Spray D is not highly sensitive to backpressure, indicating that nozzle cavitation should not confound atomization physics under target experimental conditions

#### Caroline L. Genzale

Georgia Institute of Technology (Georgia Tech)  
 GW Woodruff School of Mechanical Engineering  
 771 Ferst Drive  
 Atlanta, GA 30332  
 Phone: (404) 894-5099  
 Email: caroline.genzale@me.gatech.edu

#### Christopher Powell

Argonne National Laboratory  
 9700 South Cass Avenue  
 Lemont, IL 60439  
 Phone: (630) 252-9027  
 Email: powell@anl.gov

DOE Technology Development Manager:  
 Leo Breton

NETL Project Manager:  
 Carl Maronde

- Demonstrated axi-symmetry of spray produced by target ECN Spray D injector
- Measured 2D distributions of liquid mass within ECN Spray D at target experimental conditions
- Demonstrated consistency between visible laser extinction (VLE) and diffuse back illumination (DBI) measurement techniques for quantifying optical thickness distribution
- Measured 2D distributions of optical thickness within ECN Spray D at target experimental conditions
- Completed USAXS measurements of SMD in Spray D at target experimental conditions
- Demonstrated predictive capabilities and inaccuracies of literature spray atomization submodels implemented within a consistent open-source CFD framework ■

### Introduction

This project is working towards the improvement of spray submodels for use in engine CFD codes. The objective is to produce a new spray atomization submodel that

appropriately captures the role of liquid turbulence on diesel jet breakup, challenging the widespread adoption of submodels that treat atomization as primarily limited by aerodynamic inertial forces. Our objective is motivated by: (1) a significant body of literature that demonstrates the importance of injector flow conditions on atomization, (2) experimental data indicating that liquid turbulence plays a fundamental role in spray atomization when gas inertial forces are low, and (3) a systematic lack of predictive capabilities for current spray submodels. Even when global spray characteristics are well predicted, current spray submodels can vary widely in predictions of local spray morphology (e.g., local drop sizes). These inaccuracies suggest a fundamental mismatch of the modeled atomization physics and the actual physics governing the atomization process.

Modeling inaccuracies are largely due to a lack of quantitative measurements to guide fundamental understanding and atomization submodel development. Measurements of local spray morphology are needed within practical diesel sprays, and especially and under engine-relevant operating conditions. This project aims to fill this measurement gap. An innovative experimental approach is under development, which leverages the joint capabilities of Georgia Tech's high-pressure continuous flow spray chamber and Argonne National Laboratory's near-nozzle X-ray diagnostics. Joint measurements at the two institutions will yield a 2D quantitative description of liquid volume fraction and drop size distribution within a diesel spray, from the near-nozzle region to the far-field fully atomized spray.

## Approach

A new 2D measurement technique is developed to quantify the spatial and temporal scales of diesel spray atomization under engine-relevant conditions. These new measurements then provide the necessary insight to guide and validate the formulation of a new, more predictive, spray atomization submodel for engine CFD codes. The 2D spray atomization measurements accomplished in this project result from the coupling of two measurement techniques at two institutions, liquid-scattering extinction performed at Georgia Tech and X-ray radiography at Argonne, and yield a spatially resolved measurement of SMD. The X-ray radiography measurements quantify radially integrated liquid volume fraction, while the liquid-scattering extinction measurements are a joint function of the radially integrated liquid volume fraction and SMD. Execution of these measurements in overlapping measurement regions, under matched experimental conditions, enables deconvolution of the liquid-scattering extinction signal

to yield SMD. Diesel spray experiments are replicated at the two institutions using shared ECN Spray D and Spray A injectors. Several existing spray atomization submodels are then benchmarked against this data to identify model formulation inaccuracies, leading to the formulation of a new modeling approach that better replicates the measured data and incorporates the improved fundamental understanding resulting from these measurement campaigns.

## Results

### Spatially Resolved Diesel Spray Morphology Measurement

Replicated diesel spray experiments were executed at Georgia Tech and Argonne National Laboratory using shared ECN Spray A ( $d_{nozz} = 90 \mu\text{m}$ ) and Spray D ( $d_{nozz} = 180 \mu\text{m}$ ) injectors. Dodecane sprays ( $\rho_{liq} = 750 \text{ kg/m}^3$ ) were injected into near-quiescent gas environments under non-vaporizing ambient temperature (300 K) environments. Purely turbulent liquid breakup conditions are targeted in the first project year, generating a reduced order atomization problem where quantitative measurements have been accomplished in the literature. Ambient gas densities of  $1.2 \text{ kg/m}^3$  and  $1.6 \text{ kg/m}^3$  were selected for study to provide liquid-to-gas density ratios of 625 and 469, respectively. Under these liquid-to-gas density ratios, aerodynamic forces are low and breakup is dominated by liquid turbulence characteristics [1]. The target experiments further aim to suppress nozzle flow cavitation to avoid confounding turbulent breakup mechanisms. Figure 1 shows nozzle coefficient measurements for Spray D at Georgia Tech, which indicates a lack of flow cavitation in this injector. Flow cavitation is typically observed by a significant degradation of the nozzle area coefficient,  $C_a$ , as back pressure is reduced.

Coordinated spray measurements were accomplished at Georgia Tech and Argonne National Laboratory using visible light and X-ray diagnostic techniques, respectively. Figure 2 shows an example of X-ray radiography measurements (Argonne), which yield a line-of-sight path-integrated measurement of liquid mass (projected mass). Measurements taken from two viewing angles and at two axial locations downstream of the injector nozzle show that the spray is largely symmetric. Thus, a single viewing angle is adopted for all spray measurements at Argonne and Georgia Tech. At Georgia Tech, two different visible light liquid-scattering extinction measurement techniques were evaluated to quantify the path-integrated optical thickness of the spray. The two methods, visible laser extinction (VLE) and diffuse back-illumination imaging (DBI), are compared in Figure 3

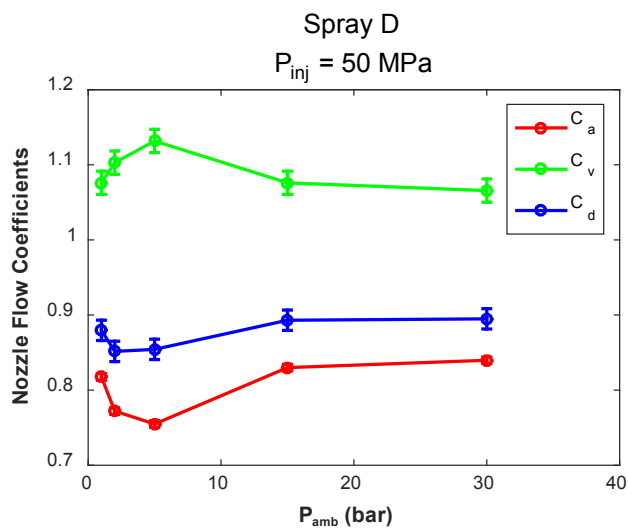


Figure 1. Nozzle flow coefficient measurements for Spray D,  $P_{\text{inj}} = 50 \text{ MPa}$ , demonstrating no significant degradation of  $C_a$  (cavitation) under reduced backpressure, low ambient density conditions

and demonstrate consistent measurements throughout most of the spray. Differences in measured optical thickness within the central region of the spray are due to unavoidable multiple scattering effects from high droplet number densities near the spray centerline and should not be quantitatively interpreted. Select DBI measurements for Spray A and Spray D are demonstrated in Figure 4. The measurements show that higher optical thicknesses are measured for Spray D, consistent with higher injected mass flow rates for this larger nozzle diameter. These optical thickness measurements, which are a joint function of the path-integrated SMD and liquid volume fraction, will be deconvolved to yield 2D distributions of SMD using the Argonne X-ray radiography measurements of projected liquid mass.

### Spray Atomization Submodel Development

Researchers at Georgia Tech are benchmarking the predictive capabilities and inaccuracies of existing literature spray atomization submodels against the new spray morphology measurements accomplished in this project. Two widely employed literature submodels (i.e., Kelvin–Helmholtz Rayleigh–Taylor [KH-RT] and Huh–Gosman) were implemented into the open-source CFD code OpenFOAM. As shown in Figure 5 the two models predict vastly different SMD distributions even though their predictions of the global spray penetration rate are equivalent (not shown). Also shown in Figure 5 are SMD measurements accomplished using the USAXS technique at Argonne, which enables quantification of SMD along the optically-thick centerline region of the

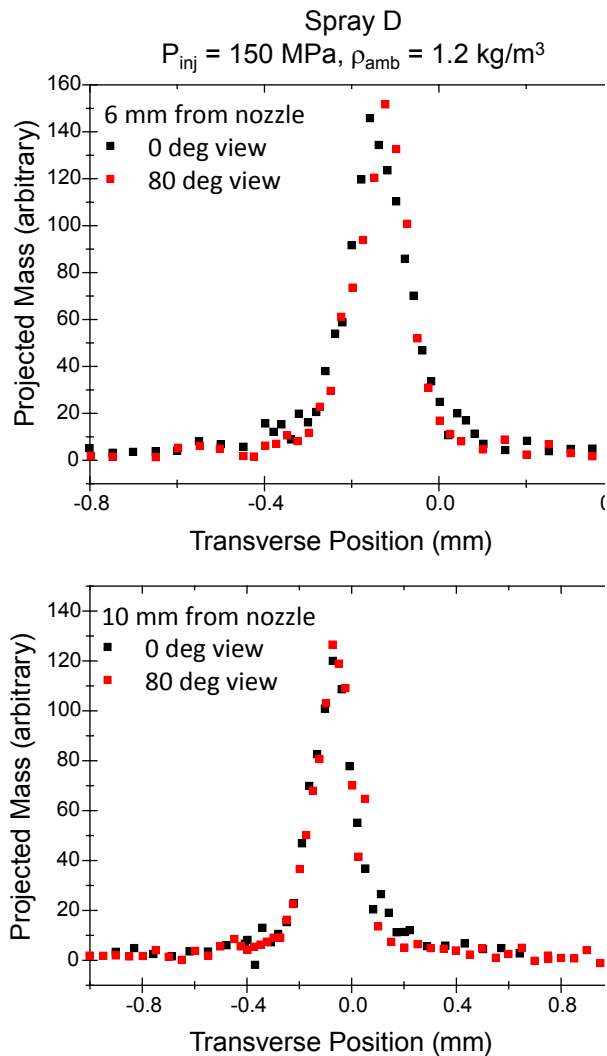


Figure 2. Measurements demonstrating axi-symmetry of liquid mass distribution in Spray D, at 6 mm and 10 mm from the injector nozzle exit, and from two viewing angles separated by  $80^\circ$

spray. At the high ambient density conditions of Spray A, the KH-RT model well replicates trends in measured axial SMD while the Huh–Gosman model predicts overly rapid breakup and SMD values approximately one order of magnitude smaller than the measurements. A detailed analysis of these models against the spray morphology data set accomplished this year will lead to an improved model formulation for low-density turbulent breakup conditions in year two of the project.

### Conclusions

- The axially drilled single-orifice ECN Spray D injector ( $d_{\text{nozz}} = 180 \mu\text{m}$ ) selected for this project injects a predominantly symmetric liquid mass distribution. 2D

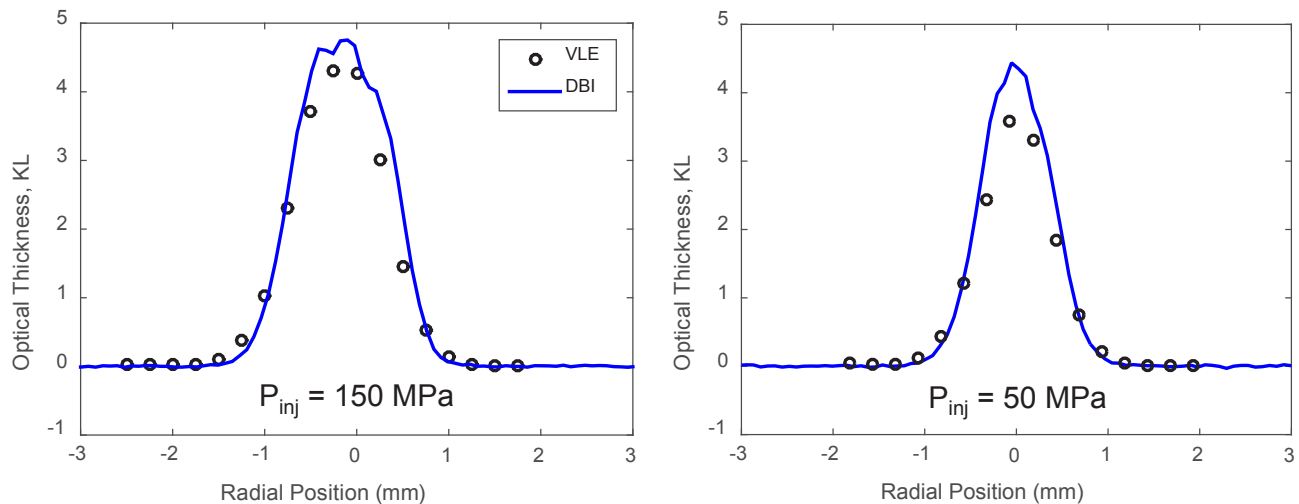


Figure 3. Measured optical thickness of Spray A at  $1.2 \text{ kg/m}^3$  using two different liquid-scattering extinction measurement techniques. Close agreement is seen between the two measurements in regions where multiple scattering errors are low ( $KL < \sim 2.0$ ).

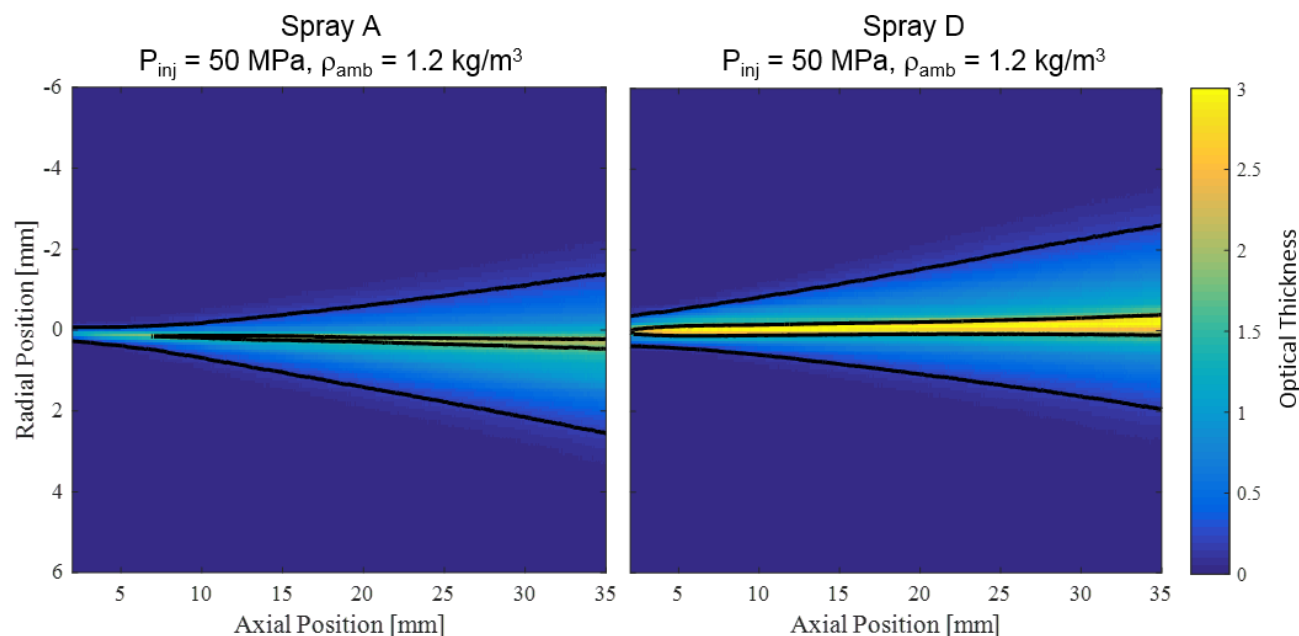


Figure 4. 2D measurements of optical thickness in Spray A and Spray D at  $1.2 \text{ kg/m}^3$  and  $50 \text{ MPa}$  injection pressure. Line boundaries are drawn at  $KL = 2.0$  and  $KL = 0.2$  to indicate most viable measurement interpretation regions.

path-integrated measurements will faithfully represent the three dimensional mass distribution.

- Diffuse back-illumination and laser liquid scattering techniques yield consistent measurements of optical thickness under the target non-vaporizing spray operating conditions.

- KH-RT and Huh-Gosman spray atomization submodels predict axial SMD distributions that vary by up to one order of magnitude for simulations of Spray A even when the predicted global spray penetration rates are the same. 2D SMD distribution measurements to be accomplished in this project will lead to improved validation and assessment of specific model formulation inaccuracies.

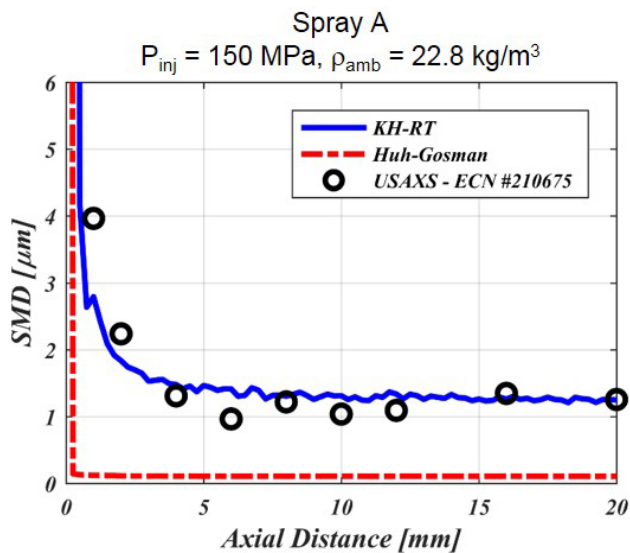


Figure 5. CFD model predictions of SMD in Spray A using the KH-RT and Huh-Gosman spray atomization submodels in OpenFOAM

## References

1. Wu, P.-K. and Faeth, G.M. (1993). Aerodynamic Effects on Primary Breakup of Turbulent Liquids. *Atomization and Sprays*, 3:265–289.

## FY 2016 Publications/Presentations

1. Magnotti, G.M. and Genzale, C.L., “Exploration of Turbulent Atomization Mechanisms for Diesel Spray Simulations,” submitted for SAE World Congress 2017.

### III. Emission Control R&D

The Vehicle Technologies Office (VTO) supports research and development of aftertreatment technologies to control advanced combustion engine exhaust emissions. All engines that enter the vehicle market must comply with the Environmental Protection Agency's emissions regulations. The energy required for emission control often reduces vehicle fuel economy and increases vehicle cost. VTO's Emission Control R&D focuses on developing efficient, durable, low-cost emission control systems that complement new combustion strategies while minimizing efficiency losses. VTO leverages the national laboratories' unique capabilities and facilities to conduct this research. To enable further developments in these areas, VTO also supports research into materials for controlling exhaust gases and materials by design for exhaust aftertreatment.

# III.1 Joint Development and Coordination of Emission Control Data and Models: Cross-Cut Lean Exhaust Emissions Reduction Simulations (CLEERS) Analysis and Coordination

## Overall Objectives

This project supports industry in the development of accurate simulation tools for the design of catalytic emissions control systems that will enable advanced high efficiency combustion engines to meet emissions regulations while maximizing fuel efficiency through the following activities:

- Coordinate the CLEERS activity for the DOE Advanced Engine Crosscut Team
- Support precompetitive collaborative interactions and provide a consistent framework for sharing information among the emissions control research and development community
- Identify emissions control research and development needs and priorities
- Collaborate with Pacific Northwest National Laboratory (PNNL) to develop mechanistic insights, modeling strategies, benchmark data sets, and representative device parameters for catalytic emissions control devices
- Utilize the CLEERS framework to share the resulting insights, strategies, data sets, and parameters with the emissions control community

## Fiscal Year (FY) 2016 Objectives

- Facilitate CLEERS Focus Group teleconferences
- Organize and conduct the 2016 DOE Crosscut Workshop on Lean Emissions Reduction Simulation (CLEERS Workshop)
- Maintain CLEERS website
- Develop measurement and modeling strategies that accurately capture the effects of catalyst formulation, hydrothermal aging, and operating environment on the NH<sub>3</sub> storage capacity of commercial selective catalytic reduction (SCR) catalysts (collaboration with PNNL)
- Investigate reaction mechanisms for NO SCR by NH<sub>3</sub> over small pore copper zeolite catalysts (collaboration with Politecnico di Milano)

**Josh Pihl (Primary Contact),  
Jae-Soon Choi, Vitaly Prikhodko,  
Charles Finney, Bill Partridge,  
Todd Toops, William Brookshear,  
Stuart Daw**

Oak Ridge National Laboratory (ORNL)  
2360 Cherahala Blvd.  
Knoxville, TN 37932  
Phone: (865) 946-1524  
Email: pihlja@ornl.gov

DOE Technology Development Manager:  
Ken Howden

Subcontractor:  
Richard Blint, N2Kinetics Research, Shelby Township,  
MI

- Begin investigations into hydrocarbon and NO<sub>x</sub> adsorbers for low temperature exhaust applications

## FY 2016 Accomplishments

- Facilitated CLEERS Focus Group teleconferences, which continue to have strong domestic and international participation (typically over 50 participants, a majority of which are from industry)
- Provided regular update reports to DOE Advanced Combustion Engine Crosscut Team
- Organized the 2016 DOE Crosscut Workshop on Lean Emissions Reduction Simulation (CLEERS Workshop) in Ann Arbor, Michigan, on April 6–8, 2016
- Maintained the CLEERS website ([www.cleers.org](http://www.cleers.org))
- Supported the Advanced Combustion and Emissions Control (ACEC) Low Temperature Aftertreatment Team in developing evaluation protocols for low temperature catalysts
- Developed measurement and modeling strategies that accurately capture the effects of operating temperature, NH<sub>3</sub> concentration, H<sub>2</sub>O concentration,

and hydrothermal aging on the  $\text{NH}_3$  storage capacity of a commercial small pore copper zeolite SCR catalyst

- Demonstrated that the  $\text{NH}_3$  isotherm measurement and modeling strategies work for a second, very different, commercial small pore copper zeolite SCR catalyst formulation
- Hosted a visiting graduate student from Politecnico di Milano, who conducted detailed surface spectroscopy experiments aimed at elucidating key mechanistic steps in the SCR of NO by  $\text{NH}_3$  at low temperatures and at measuring the reactivity of  $\text{NH}_3$  adsorbed at different sites in the SCR catalyst ■

## Introduction

Catalytic emissions control devices will play a critical role in deployment of advanced high efficiency engine systems by enabling compliance with increasingly stringent emissions regulations. High efficiency diesel and lean gasoline engines, for example, will require  $\text{NO}_x$  reduction catalysts with very high conversion efficiencies to meet the Environmental Protection Agency Tier 3  $\text{NO}_x$  emissions standard. Low temperature combustion strategies, on the other hand, significantly reduce engine-out  $\text{NO}_x$ , but they generate a challenging combination of high hydrocarbon and carbon monoxide concentrations at low exhaust temperatures that will likely demand novel approaches to emissions control. Design of progressively more complex engine and aftertreatment systems will increasingly rely on advanced simulation tools to ensure that next generation vehicles maximize efficiency while still meeting emissions standards. These simulation tools will, in turn, require accurate, robust, and computationally efficient component models for emissions control devices. Recognizing this need, the DOE Advanced Engine Cross-cut Team initiated the CLEERS activity to support the development of improved computational tools and data for simulating realistic full-system performance of high-efficiency engines and associated emissions control systems. DOE provides funding to ORNL to perform two complementary roles that support this goal: (1) coordination of CLEERS activities that provide a consistent framework for sharing information and supporting precompetitive collaborative interactions among the emissions control community, and (2) focused measurement, analysis, and modeling activities aimed at developing the strategies, data sets, and device parameters needed for better models of catalytic emissions control devices through collaborations with other national labs and partners in academia and industry.

## Approach

In its administrative role, ORNL coordinates the CLEERS Planning Committee, the CLEERS Focus Group teleconferences, CLEERS public workshops, the biannual CLEERS industry survey, and the CLEERS website (<http://www.cleers.org>). ORNL acts as a communication hub and scheduling coordinator among these groups and as the spokesperson and documentation source for CLEERS information and reports. The latter includes preparation and presentation of status reports to the Advanced Engine Crosscut Team, responses to requests and inquiries about CLEERS from the public, and summary reports from the biannual industry surveys.

Measurement, analysis, and modeling activities are conducted in close collaboration with Pacific Northwest National Laboratory and include: identification of reaction mechanisms occurring over catalytic devices under relevant operating conditions; development of modeling strategies that represent key catalyst processes in a computationally efficient manner; generation of benchmark data sets for model calibration and validation; and measurement of critical device parameters needed for model development. The results of these activities are disseminated through the CLEERS information sharing apparatuses, and through publications and presentations. Research directions are guided by the DOE Advanced Engine Crosscut Team, which collectively oversees CLEERS, and by regular CLEERS industry participant priority surveys. ORNL's CLEERS research activities have historically focused on approaches to  $\text{NO}_x$  reduction in lean exhaust such as lean  $\text{NO}_x$  traps and urea SCR, but have recently shifted to include low temperature aftertreatment technologies such as passive adsorbers for  $\text{NO}_x$  and hydrocarbons.

## Results

ORNL's CLEERS coordination work during FY 2016 continued to focus on activities that have been identified as high priorities by industrial participants in CLEERS. In partnership with PNNL, ORNL continued hosting CLEERS Focus Group technical teleconferences. The presentations covered a wide range of research results in emissions control experimentation, modeling, and simulation by members of the CLEERS Focus Group as well as outside experts, including: Prof. Mark Crocker (University of Kentucky), Todd Toops (ORNL), Manish Sharma (Ford Motor Co.), and Krishna Kamasamudram and Saurabh Joshi (Cummins Inc.). Teleconference attendance typically exceeded 50 participants, with well over half of the participants from industry. There were a

significant number of international participants, mostly from Europe.

The 2016 (19th) CLEERS Workshop was held April 6–8, 2016, in Ann Arbor, Michigan. The workshop was open to participants from any organization or institution. Attendance reached full capacity at 140 individuals. The workshop program included five invited speakers, 34 contributed talks, 24 posters (more than any prior workshop), and five industry panelists that discussed “meeting Tier 3 and the potential future impact of on-board emissions measurements and real-world/on-road emissions standards.” The presentations covered a wide range of emissions control topics, including: engine emissions, low temperature traps, oxidation catalysts, particulate filters, SCR/filters, urea/NH<sub>3</sub> SCR, and non-urea NO<sub>x</sub> control. Additional details can be found on the CLEERS website ([www.cleers.org](http://www.cleers.org)) under the 2016 Workshop heading.

As in FY 2014 and FY 2015, ORNL has worked closely over the past year with PNNL and the industry members of the ACEC Tech Team Low Temperature Aftertreatment Working Group to support the development of new low temperature catalyst laboratory evaluation protocols. The oxidation catalyst protocol is available for download from the CLEERS website. The second protocol for passive adsorber materials has been completed and will also be posted to the CLEERS website after final approval by United States Council for Automotive Research (USCAR) managers. A third protocol for low temperature three way catalysts is under development.

ORNL's CLEERS analysis activities focused on a combination of experiments and simulations aimed at understanding and controlling processes critical to the design and operation of emissions control systems for high efficiency engines, with a particular emphasis on modeling adsorption and desorption processes in catalytic devices. While small pore copper zeolites are already being applied in commercial urea SCR systems, there is still room for improvement in real-world system performance. Respondents to the 2015 CLEERS Industry Priority Survey from the heavy-duty diesel market segment ranked both SCR aging and NH<sub>3</sub> storage/release in the top 10 of all technical topics surveyed. ORNL has been working with partners at PNNL to determine how urea SCR model parameters can be adjusted to reflect changes in catalyst properties over the vehicle lifetime, with a particular emphasis on the impact of aging on NH<sub>3</sub> storage. These efforts revealed that the standard experimental methods for characterizing NH<sub>3</sub> storage over zeolite SCR catalysts generate data sets in which the thermodynamics of the NH<sub>3</sub> adsorption/

desorption processes are intertwined with reaction rates and mass transport. Calibrating models to these data sets results in non-unique parameter estimates that are not robust to changes in operating conditions. To avoid these complications, ORNL developed a new strategy for measuring the energetics of the NH<sub>3</sub> adsorption process that relies on equilibrium isotherm measurements, thereby eliminating kinetic and mass transport effects. Through straightforward thermodynamic analysis, these isotherms can be used to calculate the NH<sub>3</sub> adsorption enthalpy as a function of NH<sub>3</sub> coverage, which can then be used to determine the appropriate structure for the NH<sub>3</sub> storage model.

During FY 2015, it was determined that catalyst hydration and oxidation state both significantly impact equilibrium NH<sub>3</sub> inventories. The experimental methods for collecting NH<sub>3</sub> isotherms were subsequently updated to control catalyst oxidation state and to quantify the effects of H<sub>2</sub>O concentration. The experiments were also modified to improve catalyst temperature control and to reduce measurement times. All of these changes resulted in more reproducible and predictable NH<sub>3</sub> isotherms, which in turn significantly reduced the uncertainties associated with the adsorption enthalpy estimates. During FY 2016, the updated experimental protocols were used to measure NH<sub>3</sub> isotherms over a commercial copper ion-exchanged aluminosilicate zeolite (Cu- SSZ-13) sample after sequential hydrothermal aging steps that capture the full useful life of the catalyst in a light-duty vehicle. The results of these experiments are shown in Figure 1.

Careful analysis of the NH<sub>3</sub> inventories and calculation of adsorption enthalpies revealed that there appear to be two distinct NH<sub>3</sub> storage sites throughout the aging process, and that H<sub>2</sub>O only inhibits NH<sub>3</sub> storage at one of the two sites. An equilibrium NH<sub>3</sub> storage model with two adsorption sites, both having constant adsorption enthalpies as a function of coverage, and one having competitive adsorption from H<sub>2</sub>O, was fit to the experimentally measured NH<sub>3</sub> inventories. During the fitting process, only the two site densities were allowed to change with hydrothermal aging; all other parameters were constant across all aged states. The simulated NH<sub>3</sub> inventories based on the resulting model parameters are shown as dashed lines in Figure 1. This relatively simple storage model does a reasonably good job of capturing the effects of temperature, NH<sub>3</sub> concentration, H<sub>2</sub>O concentration, and aging on equilibrium NH<sub>3</sub> storage capacity. This model can now be incorporated into SCR device models to provide better predictions of local NH<sub>3</sub> inventories under transient conditions, which will increase the fidelity of estimated NO<sub>x</sub> conversion performance and NH<sub>3</sub> slip. Higher fidelity device models should enable

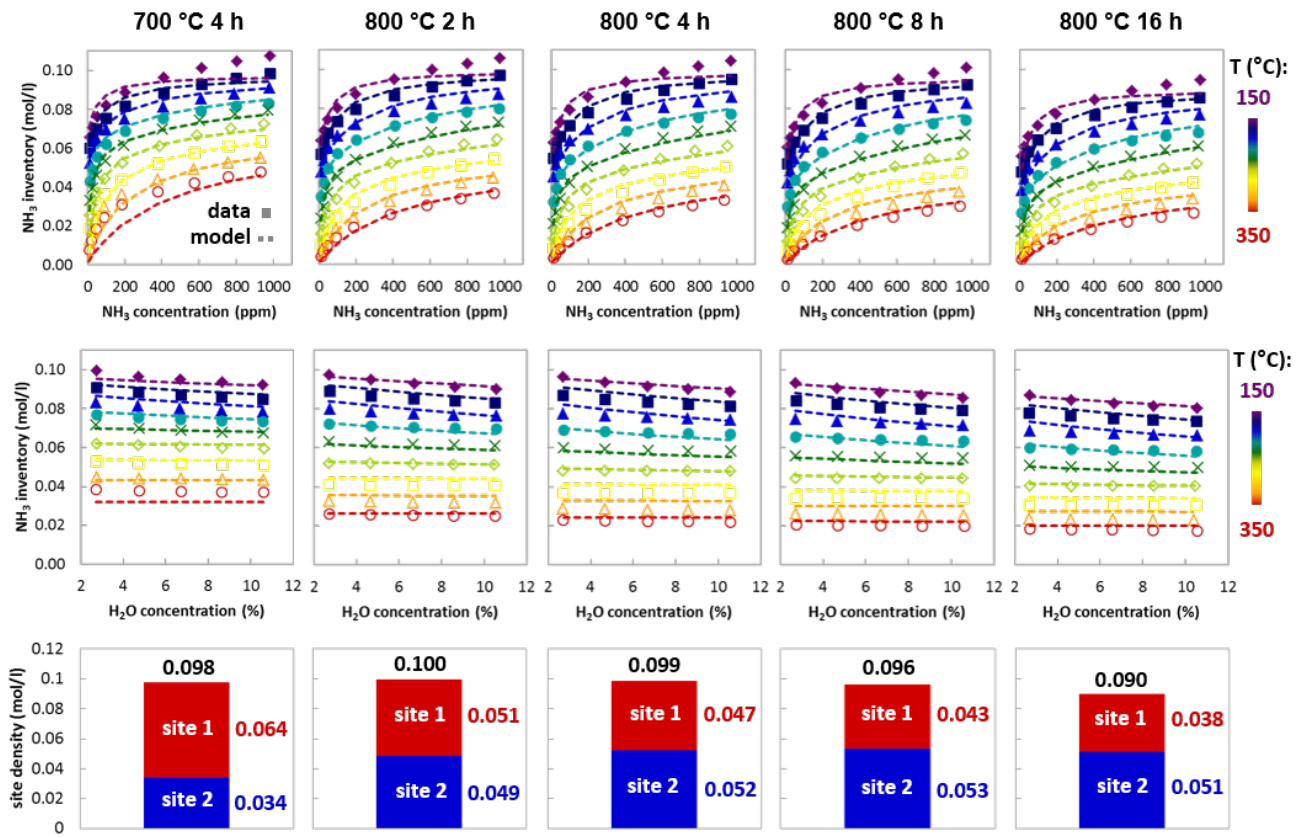


Figure 1.  $\text{NH}_3$  storage properties of a commercial Cu-SSZ-13 urea SCR catalyst hydrothermally aged under 10%  $\text{O}_2$ , 5%  $\text{H}_2\text{O}$ , balance  $\text{N}_2$  for: 4 h at 700°C, 2 h at 800°C, 4 h at 800°C, 8 h at 800°C, or 16 h at 800°C. Top and middle panels show measured (points) and modeled (dashed lines) steady state  $\text{NH}_3$  inventories as a function of temperature and (top)  $\text{NH}_3$  concentration under 0.2%  $\text{O}_2$ , 5%  $\text{H}_2\text{O}$ , balance  $\text{N}_2$  or (middle)  $\text{H}_2\text{O}$  concentration under 0.2%  $\text{O}_2$ , 400 ppm  $\text{NH}_3$ , balance  $\text{N}_2$ . Bottom panels show estimated storage site densities for Site 1 and Site 2 based on the model fits shown in the other plots. All measurements were conducted on an automated flow reactor at a gas hourly space velocity of 30,000  $\text{h}^{-1}$ .

development of better urea dosing strategies, which will improve  $\text{NO}_x$  conversion performance and minimize urea consumption.

The  $\text{NH}_3$  storage measurement and modeling strategies were also applied to a second commercial small pore copper zeolite SCR catalyst formulation (Cu/SAPO-34) with a very different zeolite composition during FY 2016. The measured  $\text{NH}_3$  isotherms (Figure 2) and calculated adsorption enthalpy as a function of  $\text{NH}_3$  coverage look qualitatively very similar to those obtained with the Cu-SSZ-13 catalyst, indicating that the same two site equilibrium storage model structure could be applied to predict  $\text{NH}_3$  inventories on both catalysts. The dashed lines in Figure 2 show that recalibrating the two site equilibrium  $\text{NH}_3$  storage model to the Cu/SAPO-34  $\text{NH}_3$  isotherm data results in simulated  $\text{NH}_3$  inventories that agree well with the measured values over a wide range of compositions and temperatures. Future work will focus on model Cu-exchanged zeolite materials with varying

acid site densities and copper loadings to correlate storage model parameters with physical sites on the catalyst.

Efforts on low temperature adsorber materials were also initiated during FY 2016. Most of this work focused on procuring laboratory equipment and instruments for delivery and measurement of liquid hydrocarbons on ORNL's automated flow reactor systems. A non-disclosure agreement was set up with a major catalyst supplier, and the supplier provided core samples of relevant low temperature adsorber materials for use in future experiments, which will likely begin in the first quarter of FY 2017.

## Conclusions

- Based on the high level of participation in the CLEERS Workshop and Focus Group teleconferences, CLEERS continues to be a valuable resource for the aftertreatment development community.

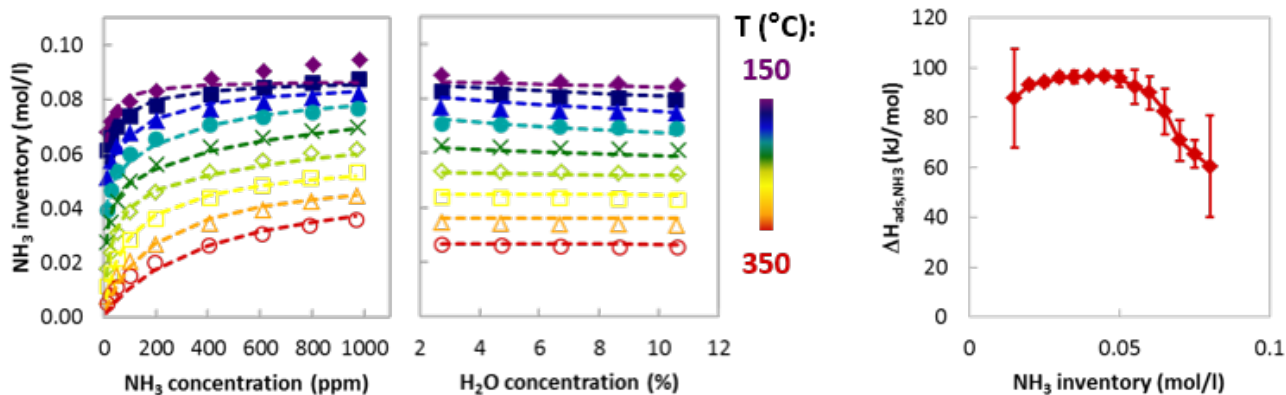


Figure 2.  $\text{NH}_3$  storage properties of a commercial Cu/SAPO-34 urea SCR catalyst hydrothermally aged under 10%  $\text{O}_2$ , 5%  $\text{H}_2\text{O}$ , balance  $\text{N}_2$  for 4 h at 700°C. Left and center panels show measured (points) and modeled (dashed lines) steady state  $\text{NH}_3$  inventories as a function of temperature and (left)  $\text{NH}_3$  concentration under 0.2%  $\text{O}_2$ , 5%  $\text{H}_2\text{O}$ , balance  $\text{N}_2$  or (center)  $\text{H}_2\text{O}$  concentration under 0.2%  $\text{O}_2$ , 400 ppm  $\text{NH}_3$ , balance  $\text{N}_2$ . Right panel shows calculated  $\text{NH}_3$  adsorption enthalpy as a function of  $\text{NH}_3$  inventory; error bars indicate 95% confidence intervals. All measurements were conducted on an automated flow reactor at a gas hourly space velocity of 30,000  $\text{h}^{-1}$ .

- $\text{NH}_3$  isotherms measured under carefully controlled conditions can be used to develop and calibrate accurate models of  $\text{NH}_3$  storage on SCR catalysts.
- A relatively simple model based on two  $\text{NH}_3$  storage sites with constant adsorption enthalpies and competitive adsorption of  $\text{H}_2\text{O}$  at one of the sites can accurately capture how the  $\text{NH}_3$  storage over a commercial Cu-SSZ-13 catalyst varies with temperature,  $\text{NH}_3$  concentration, and  $\text{H}_2\text{O}$  concentration. The impacts of hydrothermal aging on  $\text{NH}_3$  inventories can be represented by changing the densities of the two storage sites while holding all other storage model parameters constant.
- The same two site equilibrium model structure accurately captures  $\text{NH}_3$  inventories over a second commercial urea SCR catalyst formulation with a very different composition (Cu/SAPO-34).
- Low temperature adsorber material samples have been obtained from a major catalyst supplier, and experimental measurements of hydrocarbon and  $\text{NO}_x$  adsorption/desorption will begin in early FY 2017.

## FY 2016 Publications/Presentations

1. M.P. Ruggeri, T. Selleri, I. Nova, E. Tronconi, J.A. Pihl, T.J. Toops, W.P. Partridge, "New Mechanistic Insights in the  $\text{NH}_3$ -SCR Reactions at Low Temperature," *Topics in Catalysis* 59 (2016) 907–912.
2. M.P. Ruggeri, I. Nova, E. Tronconi, J.A. Pihl, T.J. Toops, W.P. Partridge, "In-situ DRIFTS Measurements for the Mechanistic Study of  $\text{NO}$

Oxidation over a Commercial Cu-CHA Catalyst," *Applied Catalysis B: Environmental* 166 (2015) 181–192.

3. K. Morgan, J. Touitou, J.-S. Choi, C. Coney, C. Hardacre, J.A. Pihl, C.E. Stere, M.Y. Kim, C. Stewart, A. Goguet, W.P. Partridge, "Evolution and Enabling Capabilities of Spatially Resolved Techniques for the Characterization of Heterogeneously Catalyzed Reactions," *ACS Catalysis*, 6 (2016) 1356–1381.
4. J.-S. Choi, P. Kočí, "Automotive Emission Control Catalyst," *Catalysts*, 6 (2016) 155.
5. J.A. Pihl, C.S. Daw, "Energetics of  $\text{NH}_3$  Storage on Zeolite SCR Catalysts," poster presented to the 2016 Crosscut Lean/Low-temperature Exhaust Emissions Reduction Simulations Workshop, Ann Arbor, MI, April 7, 2016.
6. J.A. Pihl, C.S. Daw, "CLEERS – Measurement and Modeling of Aging Impacts on Ammonia Storage in a Commercial Urea SCR Catalyst," presentation to the Advanced Engine Crosscut Team, Southfield, MI, May 12, 2016.
7. C.S. Daw, J.A. Pihl, J.-S. Choi, W.P. Partridge, T.J. Toops, V.Y. Prikhodko, C.E.A. Finney, D.W. Brookshear, "Joint Development and Coordination of Emissions Control Data and Models (CLEERS Analysis and Coordination), presentation to the DOE Vehicle Technologies Office, Annual Merit Review & Peer Evaluation Meeting, Washington, D.C., June 8, 2016.

8. J.A. Pihl, "CLEERS Update: Overview of 2016 CLEERS Workshop," presentation to the Advanced Engine Crosscut Team, Southfield, MI, July 21, 2016.

## **Special Recognitions and Awards/ Patents Issued**

1. The ACEC Low-Temp Aftertreatment Team, in which Josh Pihl is a participant, received a USCAR Team Award at the USCAR Annual Recognition Luncheon on May 26, 2016.

## III.2 CLEERS Aftertreatment Modeling and Analysis

### Overall Objectives

- Promote the development of improved computational tools for simulating realistic full-system performance of lean burn engines and the associated emissions control systems
- Provide the practical and scientific understanding and analytical base required to enable the development of efficient, commercially viable emissions control solutions for ultra-high efficiency vehicles

### Fiscal Year (FY) 2016 Objectives

- Lead and contribute to the Cross-Cut Lean Exhaust Emissions Reduction Simulations (CLEERS) activities, e.g., lead technical discussions, invite distinguished speakers, and maintain an open dialogue on modeling issues
- Continue research on model selective catalytic reduction (SCR) catalysts developed in the previous FY for fundamental studies, including iron ion-exchanged aluminosilicate zeolite (Fe/SSZ-13), copper-containing silicoaluminophosphate (Cu/SAPO-34), and copper ion-exchanged aluminosilicate zeolite (Cu-SSZ-13) with varying particle size, Si/Al ratios and Cu loadings
- Develop ammonia storage and oxidation reaction kinetics using bench reactor data from Oak Ridge National Laboratory (ORNL) obtained for a state-of-the-art Cu-SSZ-13 catalyst at various aging states
- Develop a parallel optimization framework that can be used to generate transient reaction kinetics
- Investigate novel passive  $\text{NO}_x$  adsorber (PNA) formulations
- With the Advanced Combustion and Emission Control (ACEC) Low Temperature Aftertreatment (LTAT) team, complete round-robin testing for validation of the low temperature oxidation catalyst testing protocol
- With the ACEC LTAT team, complete development of a low temperature trap testing protocol
- Procure a commercial SCR-coated diesel particulate filter (DPF) and obtain high resolution X-ray computed tomography (CT) images

**Yong Wang (Primary Contact),  
Mark Stewart, Feng Gao, Janos Szanyi,  
Ken Rappe, Chaitanya Sampara**

Institute for Integrated Catalysis  
Pacific Northwest National Laboratory (PNNL)  
P.O. Box 999, MS K2-12  
Richland, WA 99354  
Phone: (509) 371-6273  
Email: yong.wang@pnnl.gov

DOE Technology Development Manager:  
Ken Howden

### FY 2016 Accomplishments

- Three journal publications and five presentations (four invited)
- Studied Fe-ion positioning in Fe/SSZ-13 with chemical titration and density functional theory (DFT) calculation
- Characterized fresh, low-temperature and high-temperature hydrothermally aged Cu/SAPO-34 catalysts with two-dimensional electron paramagnetic resonance spectroscopy
- Studied active site and framework Al migration during Cu-SSZ-13 hydrothermal aging with kinetics and  $\text{Co}^{2+}$  titration
- Initiated research on effects of extra framework Al species to SCR kinetics
- Developed ammonia storage and oxidation kinetics models for a commercial Cu-SSZ-13 catalyst and correlated the same for different catalyst aging conditions that represent its lifecycle
- A generalized optimization algorithm was written and implemented on PNNL's parallel computing workspace; process was shown to accelerate the kinetics development timeline by a factor of 5 while simultaneously improving accuracy of final kinetics
- Studied nature of Pd in zeolite supported Pd PNAs with X-ray photoelectron spectroscopy and chemical titrations

- Completed round-robin testing for validation of low temperature oxidation catalyst test protocol with ACEC LTAT team
- Completed low temperature trap protocol with ACEC LTAT team
- Specimens from three different locations within a commercial SCR-coated DPF were scanned and reconstructed in three dimensions with a resolution of 1.7  $\mu\text{m}$  ■

## Introduction

CLEERS is a research and development focus project of the Diesel Cross-Cut Team. The overall objective is to promote the development of improved computational tools for simulating realistic full-system performance of lean-burn engines and the associated emissions control systems. Three fundamental research projects have historically been supported at PNNL through CLEERS: DPF, SCR, and  $\text{NO}_x$  storage/reduction. PNNL has recently also been active in a new thrust centered around development of technologies for low temperature aftertreatment. Resources are shared among these efforts in order to actively respond to current industrial needs.

## Approach

### SCR

Considerable progress has been made in updating SCR kinetics models to accurately describe the performance of state-of-the-art Cu-CHA catalysts. However, a need still exists for accurate yet relatively simple kinetics models for the design of aftertreatment systems. Moreover, systems designers need a simple method to account for changes in performance due to aging over the life of an SCR unit. Investigations of SCR catalysts involve the coordinated efforts of modeling, testing, and research. In FY 2013 PNNL bolstered its test capability with the development of an automated protocol reactor system. In FY 2016, this capability became available for round robin testing of a new low temperature oxidation protocol developed by the U.S. DRIVE/ACEC Tech Team. To develop SCR catalysts that can potentially address The 150°C Challenge, we also provide mechanistic studies by synthesizing and utilizing model powder catalysts, via the application of micro-kinetics studies and in situ/in operando spectroscopic investigations, to address  $\text{NH}_3$  adsorption/storage, NO adsorption/activation, surface nitrite formation/conversion, surface nitrate inhibition, as well as lowering redox barriers of the cationic centers.

### PNA Fundamentals Research

Currently commercialized  $\text{NO}_x$  storage reduction catalysts that include barium oxide for storage functionality require the formation of  $\text{NO}_2$  via oxidation of NO, limiting the low temperature performance of such systems due to the low activity of NO oxidation. Recent work by Johnson Matthey has shown that noble metals (Pt and Pd) supported on zeolites (ZSM-5, beta and chabazite) can directly store NO without oxidation, as well as unburnt hydrocarbons. Our efforts focus on the nature of Pd and Pt species supported on the various zeolites (positioning, degree of agglomeration, oxidation states, etc). These studies lay out foundation to aid our practical PNA research in the form of cooperative research and development agreement with industrial partners.

### Protocol Development with the ACEC LTAT Tech Team

A widely recognized challenge is the anticipated decrease in average exhaust temperatures as new technologies are employed to improve engine efficiency, which will likely preclude the continued use of many current aftertreatment catalysts. In response, the United States Council for Automotive Research ACEC Tech Team has formed a LTAT sub-team made up of representatives from national laboratories and major automobile manufacturers. The LTAT sub-team convenes at the bimonthly ACEC Tech Team meetings in Detroit, as well as in regular teleconferences, which are generally held on a biweekly basis. Current technologies and testing methods are discussed. Reports and testing protocols are developed iteratively by consensus.

### Multi-Functional Exhaust Filters

Ceramic exhaust particulate filters have become ubiquitous on diesel vehicles and are beginning to appear on advanced gasoline vehicles as well. With onboard “real estate” at a premium, manufacturers are motivated to combine multiple exhaust aftertreatment functionalities into fewer components where possible. An obvious solution is to incorporate new catalytic functions into exhaust filter units. Catalyst coating techniques must be carefully developed in order to achieve required loadings without having unacceptable impacts on backpressure or filtration performance. A first-of-its kind system in the U.S. market employs an SCR coating on a particulate filter in passenger diesel vehicles. One of these systems was procured, and the coated filter monolith was sectioned. Specimens from three locations in the monolith were scanned at a resolution of 1.7  $\mu\text{m}$  in a micro X-ray CT system. Previous analysis of micro X-ray CT data for a number of cordierite and aluminum titanate filter substrates showed a common feature: relatively low

porosity layers at the filter wall surfaces. Experiments were conducted in cooperation with the University of Wisconsin–Madison to look for potential differences in filtration behavior as affected by such low porosity layers using the Exhaust Filtration Analysis apparatus. Filter specimens were loaded with soot using exhaust from a spark ignition direct injection test engine, regenerated, and then reloaded, flipping the wafer samples around between trials.

## Results

### SCR Fundamentals

During FY 2016, PNNL researchers focused on: (1) nature and positioning of Fe-ions in Fe/SSZ-13 as probed with chemical titration, spectroscopy, and DFT calculations; (2) changes to the Cu active centers and the chabazite framework during hydrothermal aging as probed with spectroscopy and  $\text{Co}^{2+}$  titration; and (3) continuing research on alternative SCR materials with a potential to replace the current state-of-the-art Cu-CHA catalysts.

From researches on a series of Fe/SSZ-13 catalysts with various Fe loadings, we discovered that the key active sites in this material are isolated monomeric and dimeric Fe(III) centers, i.e.,  $[\text{Fe}(\text{OH})_2]^+$ , and  $[\text{HO-Fe-O-Fe-OH}]^{2+}$  species. From NO/CO titration Fourier transform infrared spectroscopy, it can be further confirmed that the former species are located at faces of six-membered rings (6MR) of the chabazite structure, while the latter are located at faces of eight-membered rings. This notion is fully supported from DFT simulations. The optimized structures of the two active species are presented in Figure 1.

For Cu-SSZ-13 catalysts (Si/Al = 12, Cu loading 2.09%), it was found that hydrothermal aging at mild conditions (600°C, in the presence of 10%  $\text{H}_2\text{O}$ ) causes

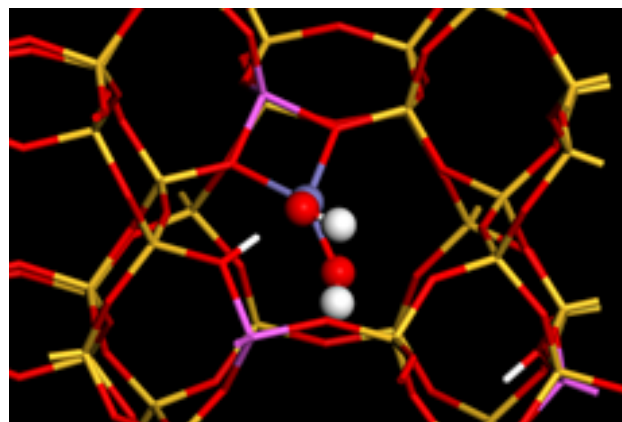
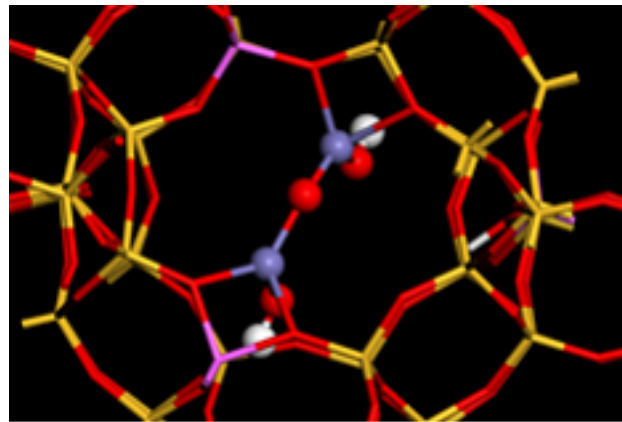


Figure 1. Optimized structures of  $[\text{Fe}(\text{OH})_2]^+$  and  $[\text{HO-Fe-O-Fe-OH}]^{2+}$  active centers in Fe/SSZ-13

gradual changes to the chabazite unit cell parameters (Figure 2a). Such changes indicate Cu-ion migration from eight-membered rings to 6MR. Based also on the fact that the catalyst experiences little dealumination during hydrothermal aging as shown in Figure 2b while the full width at half maximum of framework Al signal decrease from ~10 ppm for the fresh catalyst to ~6 ppm for the catalyst hydrothermally aged at 600°C for 12 h, it can be concluded that Al also migrates during hydrothermal aging, most likely towards generation of paired Al sites in 6MR, sites that are energetically most favorable for  $\text{Cu}^{2+}$  ions.

Besides the work described above, work has been continued on the search for alternative SCR catalysts with performance comparable to or even better than Cu-CHA. Extensive studies have been carried out on the synthesis and performance testing on SSZ-16, SSZ-17, and SSZ-39 materials.

A one-dimensional reactor model that incorporates global/micro reaction kinetics, heat and mass transfer was developed in MATLAB Simulink® environment. A generalized optimization algorithm that can be used for transient reaction kinetics development was written in MATLAB and integrated with the reactor model. The reactor model plus optimization system utilized parallel computing infrastructure to accelerate the kinetics development process. Mathematical models that describe reaction kinetics of  $\text{NH}_3$  adsorption, desorption and oxidation were developed for five different aging conditions of a commercial Cu-SSZ-13 SCR catalyst. Our parallel computing architecture demonstrated that the kinetics development timeline was reduced at least by a factor of 5 (for the most complex reactions set). Activation energies of the kinetics developed correlated well with the characterization information described previously.



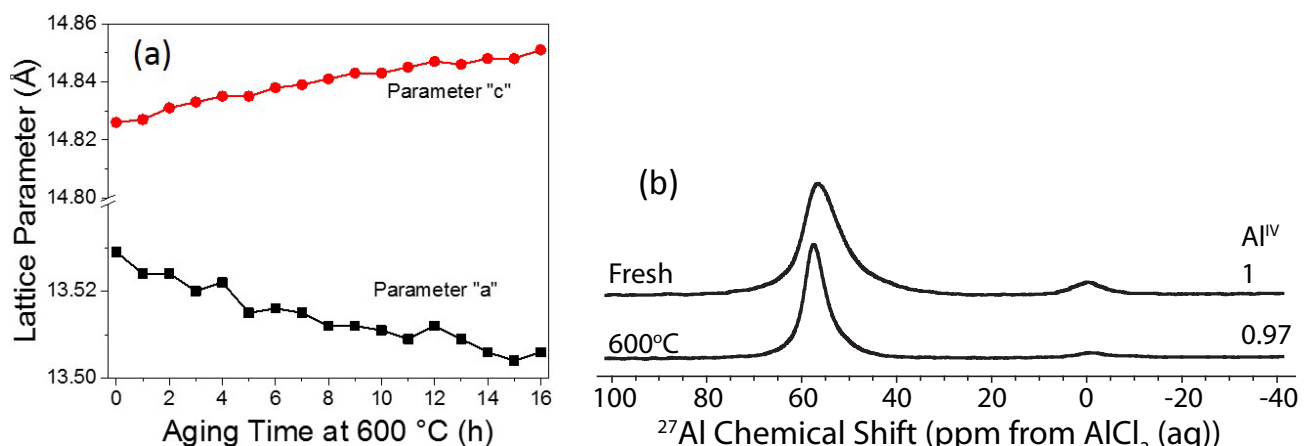


Figure 2. (a) Hexagonal unit cell parameter change as a function of hydrothermal aging at 600°C. (b)  $^{27}\text{Al}$  solid-state nuclear magnetic resonance for the fresh and hydrothermally aged sample.

### Low-Temperature Protocol Development

Protocol development activities in support of the ACEC LTAT Tech Team were two-fold: (1) round-robin testing for validation of the Low-Temperature Oxidation Catalyst Test Protocol, and (2) completion and release of the Low-Temperature Storage Catalyst Test Protocol.

Four LTAT sub-team members participated in a round-robin study to demonstrate the Low-Temperature Oxidation Catalyst Test Protocol's reproducibility: Ford, General Motors, ORNL, and PNNL. The purpose of the study was to verify the Low-Temperature Oxidation Catalyst Test Protocol as capable of providing consistent and reproducible results, with the challenge that comparison of catalyst test results across multiple institutions has historically been difficult. The goal of the study was to demonstrate <10% standard deviation across the results from the various members. To have confidence in the protocol's utility, no additional steps were taken amongst the participants to harmonize equipment or testing strategies aside from accurately following the protocol guidelines. A production diesel oxidation catalyst was selected for the study, and each organization tested unique mini-core samples removed from a single aftertreatment part. Figure 3 below shows the compiled results for the degreened catalysts, represented as T50 and T90 values (temperature at which 50% and 90% is removed, respectively). The results show that a maximum standard deviation of 6.5% and 4.9% are demonstrated for T50 and T90 values for the degreened catalyst, respectively. This validates the capability of the protocol to yield consistent and reproducible results.

The Low Temperature Storage Catalyst Test Protocol was completed this year. Similar to the Low Temperature

Oxidation Catalyst Test Protocol, it identifies a minimum set of hardware requirements and specifications for:

- The concentrations of important species to be used during testing (i.e., hydrocarbon, CO, CO<sub>2</sub>, H<sub>2</sub>, NO<sub>x</sub>, O<sub>2</sub>, H<sub>2</sub>O) that simulate the exhaust composition from different engines and combustion modes.
- The procedures for degreening, aging, and poisoning of the catalyst.
- The evaluation methods (e.g., temperature, ramp rates) for reproducibly measuring the oxidation activity of the catalyst.

The focus of the storage protocol is to provide the detailed steps necessary to adequately characterize performance of hydrocarbon and NO<sub>x</sub> storage and release/react catalysts in a manner that is simple to execute, yet comprehensive enough to encompass many scenarios. Figure 4 below shows the general strategy and structure of the protocol. The differences in comparison to the oxidation catalyst protocol are primarily driven by the transient nature of the storage/release events (versus steady-state conversion), and the steps necessary to adequately measure them.

### Multi-Functional Exhaust Filters

The dark grey color of the base substrate in the commercial SCR filter examined is consistent with silicon carbide, as is the granular texture. The brick geometry is asymmetric, with larger inlet channels, presumably for enhanced ash storage. It was not readily apparent by visual examination whether the filter brick had been coated from the inlet, outlet, or both. No surface coating accumulation was apparent over most of the filter area examined, but there were a few exceptions. One such

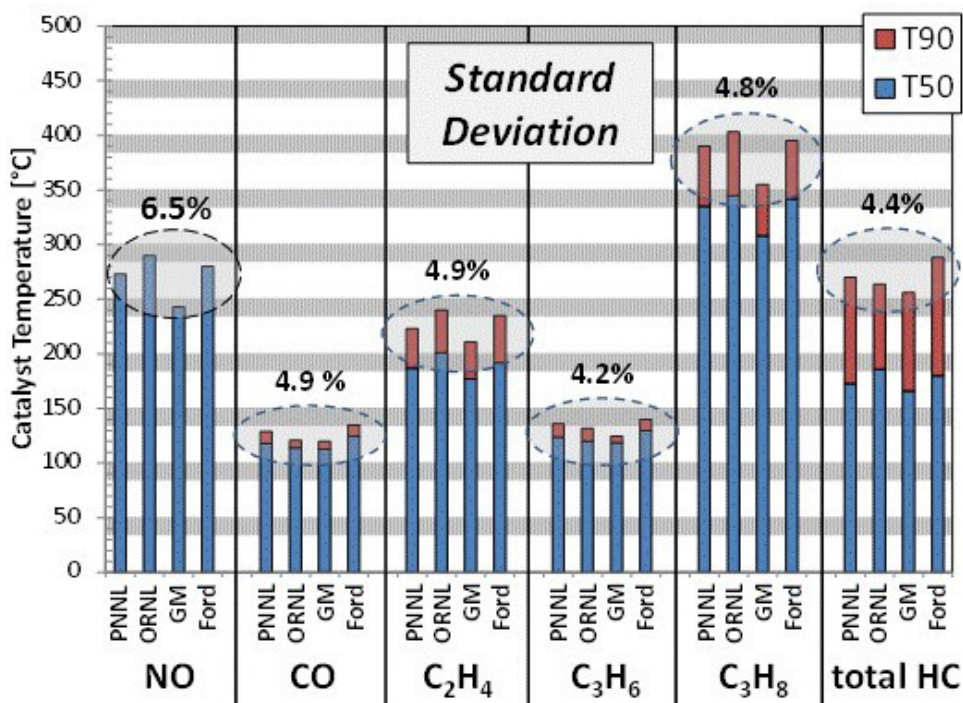


Figure 3. Compiled results of round-robin study on degreened catalysts, represented as T50 and T90 values

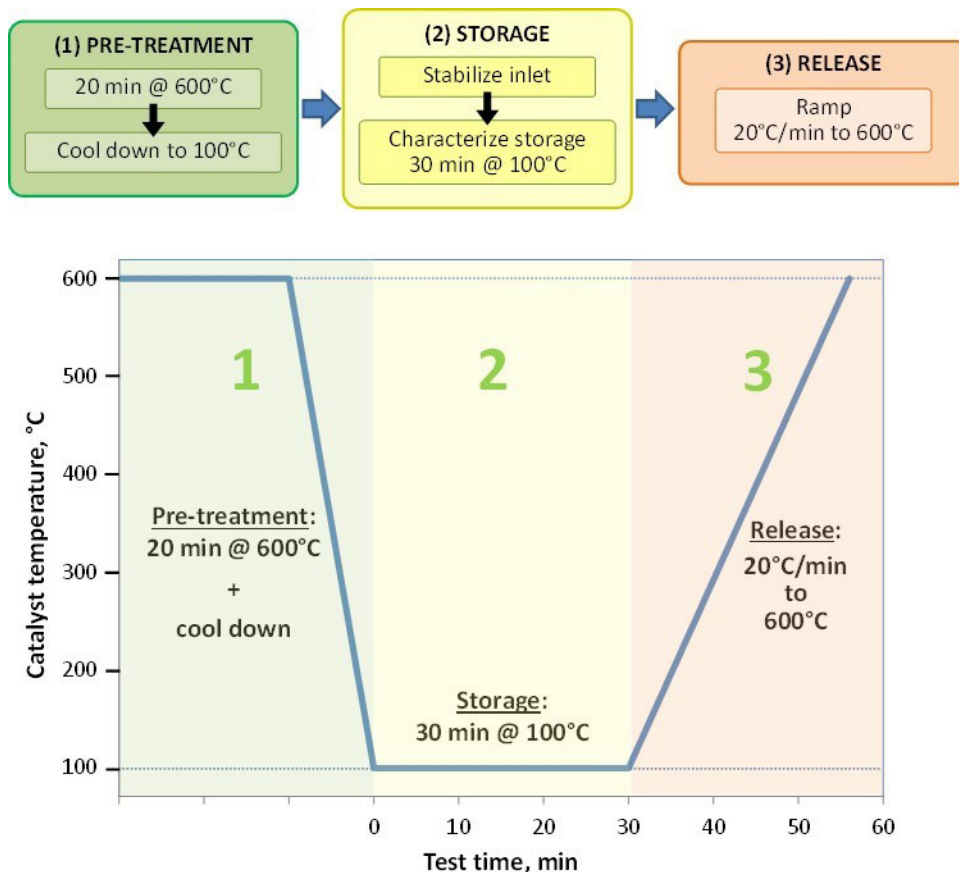


Figure 4. General structure and temperature control strategy of the Low Temperature Storage Catalyst Test Protocol

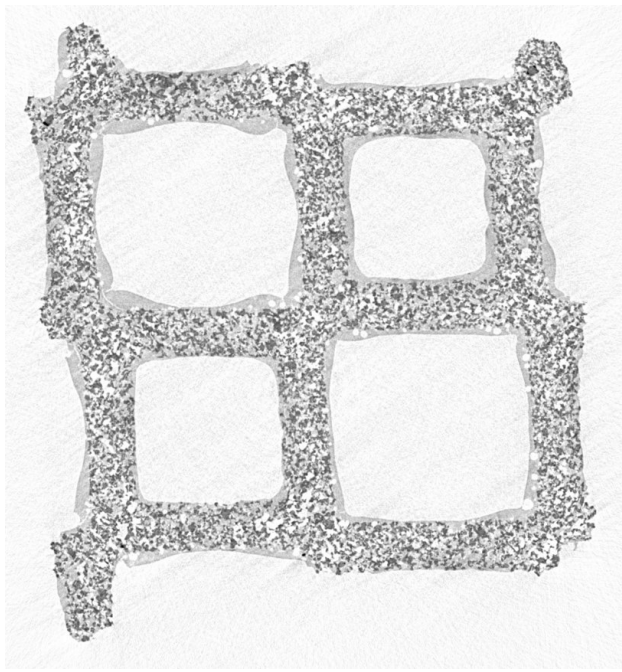


Figure 5. Micro X-ray CT image of commercial SCR-coated DPF filter wall cross-section

example is shown in Figure 5, where thick surface coatings are apparent in both inlet and outlet channels. Subsequent analysis of the micro X-ray CT data will seek to better define catalyst locations and effects on flow paths through the filter walls.

Experiments with the Exhaust Filtration Analysis system did not show a conclusive difference in either particulate removal efficiency or backpressure during filter loading between the original low-porosity filter surface and the surface from which the low-porosity layer had been removed. Interpretation of results was complicated by the fact that even very small quantities of soot left from a single soot loading appeared to have a comparable or greater impact on the filter behavior than the presence of the low-porosity surface layer. Additional experiments could be designed using more filter specimens in order to isolate these effects, but understanding the role of ash within the filter wall in changing performance over time may be the higher priority.

## Conclusions

- The combination of spectroscopy, microscopy, chemical titration, and DFT calculations allows for the precise determination of the nature and location of Fe active species in Fe/SSZ-13.

- For the first time, it is determined that during hydrothermal aging, both Cu-ions and Al tetrahedral sites are mobile, generating hydrothermally most stable  $\text{Cu}^{2+}\text{-}2\text{Al}$  sites.
- Several SCR catalysts with performance and stability comparable to Cu-CHA were identified. Thus far a catalyst that apparently outperforms Cu-CHA has not yet to be identified.
- Very small amounts of ash accumulation in a ceramic filter wall can have measureable effects on backpressure and filtration efficiency.

## FY 2016 Publications/Presentations

### Publications

1. Zelenyuk, Alla; Wilson, J.; Imre, D.; Stewart, M.L.; Muntean, G.; Storey, J.; Prikhodko, V.; Lewis, S.; Eibl, M.; Parks, J.. 2016 “Detailed Characterization of Particulate Matter Emitted by Lean-Burn Gasoline Direct Injection Engine.” *International Journal of Engine Research*.
2. Gao, F., Y. Zheng, R.K. Kukkadapu, Y. Wang, E.D. Walter, B. Schwenzer, J. Szanyi, and C.H.F. Peden. 2016. “Iron loading effects in Fe/SSZ-13 NH<sub>3</sub>-SCR catalysts: nature of the Fe-ions and structure-function relationships.” *ACS Catalysis* 6(5):2939–2954. doi:10.1021/acscatal.6b00647
3. Szanyi, J., F. Gao, J.H. Kwak, M. Kollar, Y. Wang, and C.H.F. Peden. 2016. “Characterization of Fe<sup>2+</sup> Ions in Fe<sub>x</sub>H/SSZ-13 Zeolites: FTIR Spectroscopy of CO and NO Probe Molecules.” *Physical Chemistry Chemical Physics. PCCP* 18(15):10473-10485. doi:10.1039/c6cp00136j

### Invited Presentations

1. Gao, F., Y.L. Wang, J. Szanyi, and C.H.F. Peden, CAPOCX, 10/28/2015, Brussels, Belgium. Title: Hydrothermal aging effects on Fe/SSZ-13 and Fe/beta NH<sub>3</sub>-SCR catalysts. Presented by Feng Gao. (invited presentation)
2. Gao, F., Y.L. Wang, J. Szanyi, and C.H.F. Peden, Pacifichem, 12/15/2015, Honolulu, Hawaii. Title: Approaching rational design of Cu- and Fe/CHA SCR catalysts. Presented by Feng Gao. (keynote presentation)
3. Gao, F., Y.L. Wang, J. Szanyi, and C.H.F. Peden, 16th ICC, 07/04/2016, Beijing, China. Title: Fundamental studies of small-pore zeolites for NO<sub>x</sub> emission control in vehicle exhaust. Presented by Feng Gao. (invited presentation)

4. Gao, F., Y.L. Wang, J. Szanyi, and C.H.F. Peden, Post ICC conference, 07/09/2016, Dalian, China. Title: Using model Cu/Chabazite catalysts to understand ammonia selective catalytic reduction (NH<sub>3</sub>-SCR) mechanisms. Presented by Feng Gao. (invited presentation)

#### **Contributed Presentations**

1. Gao, F., Y.L. Wang, J. Szanyi, and C.H.F. Peden, 2016 ACS Fall Meeting. Title: Approaching rational design of Cu- and Fe/CHA SCR catalysts. Presented by Feng Gao.

### III.3 Enhanced High and Low Temperature Performance of NO<sub>x</sub> Reduction Catalyst Materials

#### Objectives

Identify approaches to significantly improve both the high and low temperature performance, and the stability of catalytic NO<sub>x</sub> reduction technologies via a pursuit of a more fundamental understanding of:

- The various roles for the multiple catalytic materials.
- The mechanisms for these various roles.
- The effects of high temperatures on the performance of these catalyst component materials in their various roles.
- Mechanisms for higher temperature NO<sub>x</sub> storage performance for modified and/or alternative storage materials.
- The interactions between the precious metals and the storage materials in both optimum NO<sub>x</sub> storage performance and long-term stability.
- Modes of thermal degradation of new generation chabazite (CHA) zeolite-based selective catalytic reduction (SCR) catalysts.
- The sulfur adsorption and regeneration mechanisms for NO<sub>x</sub> reduction catalyst materials.

#### Fiscal Year (FY) 2016 Objectives

- Complete Fe/SSZ-13 hydrothermal aging effects from imaging and spectroscopy
- Complete Fe loading effects in Fe/SSZ-13 zeolite catalysts
- Complete Cu, Fe-based co-cation SSZ-13 and beta zeolite catalysts

#### FY 2016 Accomplishments

One research thrust continued this year:

- Mechanisms for high and low temperature performance of CHA-based zeolites
  - Based on prior literature reports, several synthesis efforts were carried out at PNNL to prepare model SSZ-13 and beta-based catalysts.

**Feng Gao (Primary Contact),  
Janos Szanyi, Yilin Wang, Yong Wang,  
Charles H.F. Peden**

Institute for Integrated Catalysis  
Pacific Northwest National Laboratory (PNNL)  
PO Box 999 MSIN: K8-87  
Richland, WA 99354  
Phone: (509) 371-7164  
Email: feng.gao@pnnl.gov

DOE Technology Development Manager:  
Ken Howden

CRADA Partners:

- Neal Currier, Krishna Kamasamudram, Ashok Kumar, Junhui Li, Jinyong Luo, Randy Stafford, Alex Yezerets; Cummins Inc.
- Mario Castagnola, Hai-Ying Chen, Howard Hess; Johnson Matthey

- Catalysts were characterized after incorporation of Cu and Fe by nuclear magnetic resonance (NMR), Mössbauer, electron paramagnetic resonance, and Fourier transform infrared spectroscopies.
- Baseline reactivity measurements were performed on these catalysts in preparation for mechanistic studies of high and low temperature performance loss.

Three journal publications, one patent, and four public presentations (two invited) have resulted from this program this year. ■

#### Introduction

Two primary NO<sub>x</sub> aftertreatment technologies have been recognized as the most promising approaches for meeting stringent NO<sub>x</sub> emission standards for diesel vehicles within the Environmental Protection Agency's 2007/2010 mandated limits, NO<sub>x</sub> storage-reduction (NSR) and NH<sub>3</sub> SCR. Both have been commercialized in the United States for this application. Copper ion-exchanged small pore zeolite catalysts with a CHA structure have recently been shown to exhibit both remarkable activity and very high hydrothermal stability in the NH<sub>3</sub> SCR process.

The NSR (also known as the lean- $\text{NO}_x$  trap, LNT, or  $\text{NO}_x$  absorber) technology is based upon the concept of storing  $\text{NO}_x$  as nitrates over storage components, typically barium species, during a lean-burn operation cycle, and then desorbing and subsequently reducing the stored nitrates to  $\text{N}_2$  during fuel-rich conditions over a precious metal catalyst. However, with expected more stringent regulations, the continued viability of the NSR technology for controlling  $\text{NO}_x$  emissions from lean-burn engines such as diesels will require at least two specific, significant, and interrelated improvements. First, it is important to reduce system costs by, for example, *minimizing the precious metal content* while maintaining, even improving, performance and long-term stability. A second critical need for future NSR systems, as well as for  $\text{NH}_3$  SCR, will be significantly *improved higher and lower temperature performance* and stability. Furthermore, these critically needed improvements will contribute significantly to minimizing the impacts to fuel economy of incorporating these aftertreatment technologies on lean-burn vehicles. To meet these objectives will require, at a minimum, an improved scientific understanding of the following things:

- The various roles for the precious and coinage metals used in these catalysts
- The mechanisms for these various roles
- The effects of high temperatures on the active metal performance in their various roles
- Mechanisms for higher temperature  $\text{NO}_x$  storage performance for modified and/or alternative storage materials
- The interactions between the precious metals and the storage materials in both optimum  $\text{NO}_x$  storage performance and long-term stability
- The sulfur adsorption and regeneration mechanisms for  $\text{NO}_x$  reduction materials
- Materials degradation mechanisms in CHA-based  $\text{NH}_3$  SCR catalysts

The objective of this CRADA project is to develop a fundamental understanding of the above listed issues. Model catalysts that are based on literature formulations are the focus of the work being carried out at PNNL. In addition, the performance and stability of more realistic catalysts, supplied by the industrial CRADA partners, are being studied in order to provide baseline data for the model catalysts that are, again, based on formulations described in the open literature [1-6].

## Approach

In microcatalytic reactor systems, catalyst performance is evaluated in two separate fixed bed reactors under both steady-state and transient operation conditions. We have established reaction protocols, which evaluate the performance of samples after various pretreat (thermal aging) conditions. In this way, we could largely mimic performance of catalysts under on-road aging conditions.

Based on formulations and synthesis procedures described in the literature, PNNL has prepared model  $\text{NH}_3$  SCR catalysts. Activity and performance stability measurements were performed. State-of-the-art catalyst characterization techniques such as X-ray diffraction, Mössbauer, Fourier transform infrared spectroscopy, NMR, electron paramagnetic resonance, transmission electron microscopy (TEM)/energy-dispersive X-ray spectroscopy, Brunauer–Emmett–Teller/pore size distribution, and temperature programmed desorption/reaction were utilized to probe the changes in physicochemical properties of the PNNL-prepared model catalyst samples under deactivating conditions, e.g., thermal aging.

## Results

### Fe/SSZ-13 Hydrothermal Aging Effects from Imaging and Spectroscopy

The commercial success for Cu/CHA catalysts is due largely to their superb hydrothermal stability. For Fe/SSZ-13, a detailed understanding of its hydrothermal stability is also of vital importance when its application potential is concerned. It has been shown recently that even at a rather low Fe loading (Fe/Al = 0.2), a harsh steaming treatment at 800°C for 16 h in the presence of 10% water vapor imposed no damage to the structural integrity of Fe/SSZ-13. However, moderate SCR performance drop was noticed, especially at low reaction temperatures.

As shown in Figure 1, which the fresh sample is essentially featureless indicating well-dispersion of Fe-ions; in the age sample, lighter spots in the range of 1–2 nm are observed. These are Fe-oxide cluster aggregates formed during hydrothermal aging. Spectroscopic methods, including ultraviolet–visible spectroscopy and NMR, were also performed to gain a more complete picture on changes to the zeolite structure and the active sites during hydrothermal aging. These changes are successfully linked to catalytic performance.

### Fe Loading Effects in Fe/SSZ-13 Zeolite Catalysts

We have performed a systematic study on Fe loading effects to SCR and side reactions. By varying Fe loadings,

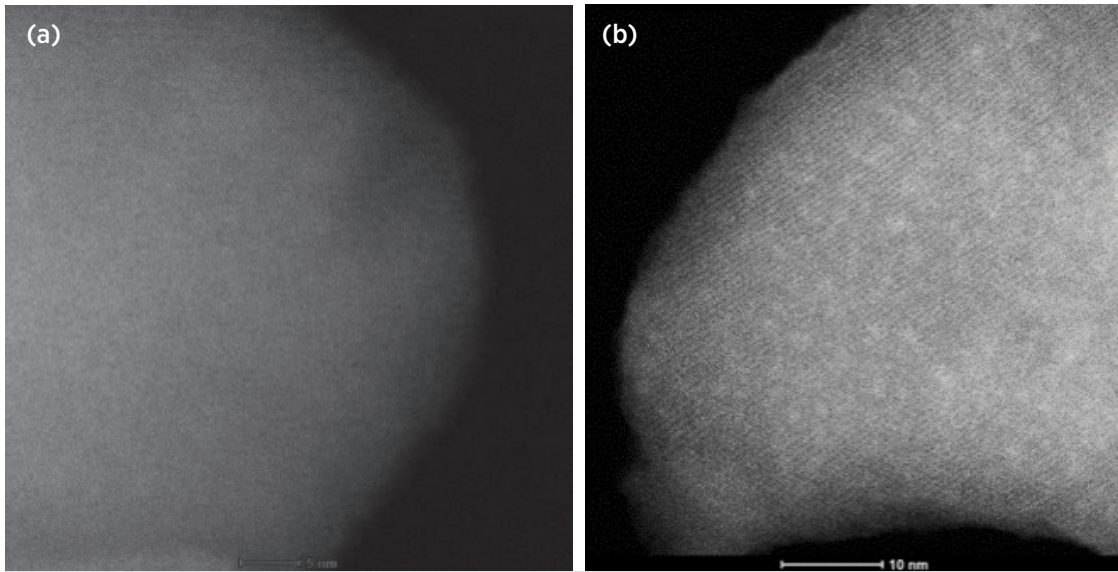


Figure 1. (a) TEM image of a fresh Fe/SSZ-13 sample, (b) TEM image of a Fe/SSZ-13 sample hydrothermally aged at 800°C for 16 h. Both samples have Si/Al = 12 and Fe loading 1.2 wt%.

it is possible to populate Fe sites with different nuclearity. This, in turn, influences catalytic performance. Based on these studies, a general picture is obtained that is schematically shown in Figure 2. Briefly, two key active sites are present in Fe/SSZ-13, monomeric  $[\text{Fe}(\text{OH})_2]^+$  and dimeric  $[\text{HO}-\text{Fe}-\text{O}-\text{Fe}-\text{OH}]^{2+}$ . The former is active at low temperatures and is more SCR selective. The latter is active at higher temperatures and is also responsible for side reactions.

### Cu, Fe-Based Co-Cation SSZ-13 and Beta Zeolite Catalysts

Comparative studies were performed on Cu, Fe, and Cu/Fe cocationated beta and SSZ-13 catalysts, focusing on

hydrothermal stability,  $\text{N}_2\text{O}$  formation and resistance to hydrocarbon poisoning. As shown in Figure 3, for beta zeolite, addition of Fe to a Cu catalyst greatly inhibits  $\text{C}_3\text{H}_6$  poisoning. For SSZ-13, this effect is not seen.

### Conclusions

PNNL and its CRADA partners from Cummins Inc. and Johnson Matthey have been carrying out a CRADA program aimed at improving the higher temperature performance and stability of candidate  $\text{NO}_x$  reduction technologies.

Model Fe/SSZ-13 catalysts were successfully synthesized. By using samples with various Fe loadings, detailed

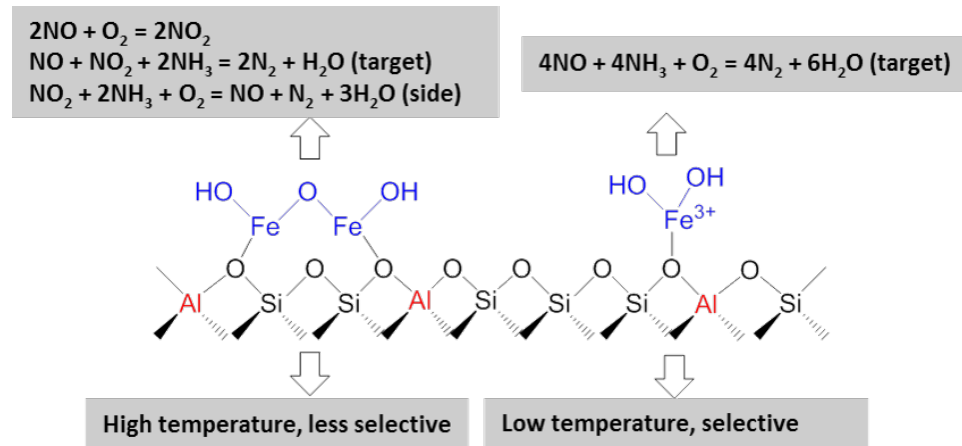


Figure 2. Schematics on the active centers and reactions that these active centers catalyze

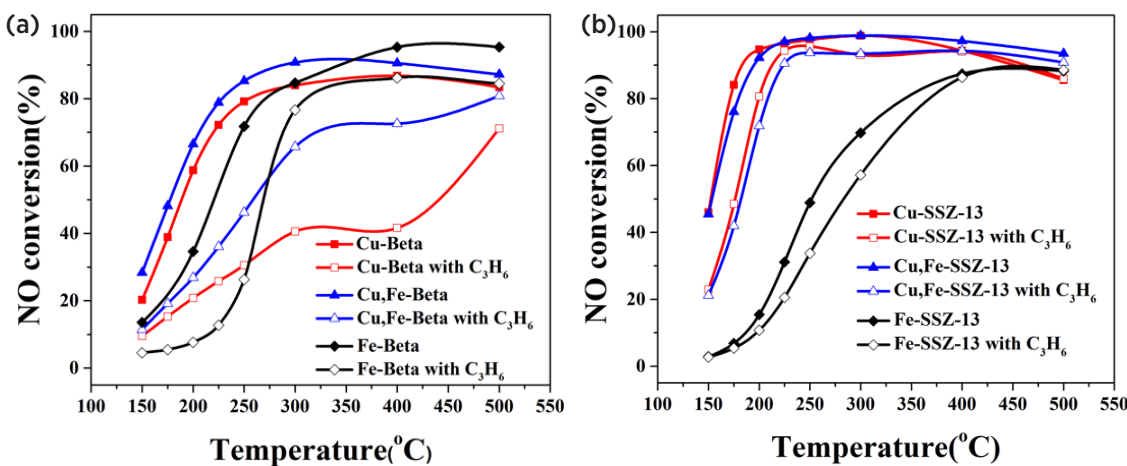


Figure 3. Effects of  $\text{C}_3\text{H}_6$  to SCR on Cu, Fe, Cu/Fe-beta (a) and Cu, Fe, Cu/Fe-SSZ-13 (b) catalysts. Reactant feed contains 350 ppm NO, 350 ppm  $\text{NH}_3$ , 300 ppm  $\text{C}_3\text{H}_6$  (when use), 14%  $\text{O}_2$ , 2.5%  $\text{H}_2\text{O}$  balanced with  $\text{N}_2$  at a gas hourly space velocity of  $200,000 \text{ h}^{-1}$ .

reaction kinetics and spectroscopic studies allow for the determination of key active centers in these catalysts. With the aid from microscopic imaging, it was further concluded that isolated Fe-ions agglomerate during hydrothermal aging to form Fe-oxides.

For Cu,Fe cocationated beta and SSZ-13 catalysts, synergy between the two active species has been found on  $\text{N}_2\text{O}$  formation and hydrocarbon poisoning resistance.

## References

1. J.H. Kwak, D. Tran, S.D. Burton, J. Szanyi, J.H. Lee, C.H.F. Peden, *Journal of Catalysis* **287** (2012) 203–209.
2. W.S. Epling, L.E. Campbell, A. Yezerets, A., N.W. Currier, J.E. Parks, *Catalysis Review—Science and Engineering* **46** (2004) 163.
3. F. Gao, E.D. Walter, N.M. Washton, J. Szanyi, C.H.F. Peden, *ACS Catalysis* **3** (2013) 2083–2093.
4. F. Gao, E.D. Walter, N.M. Washton, J. Szanyi, C.H.F. Peden, *Applied Catalysis B* **162** (2015) 501–514.
5. F. Gao, M. Kollar, R.K. Kukkadapu, N.M. Washton, Y.L. Wang, J. Szanyi, C.H.F. Peden, *Applied Catalysis B* **164** (2015) 407–419.
6. F. Gao, Y.L. Wang, M. Kollar, N.M. Washton, J. Szanyi, C.H.F. Peden, *Catalysis Today* **258** (2015) 347–358.

## Special Recognitions and Awards/ Patents Issued

1. C.H.F. Peden, F. Gao, Y. Wang, M. Kollar, J. Szanyi. “Catalysts for enhanced reduction of NOx gases

and processes for making and using same.” US 2016/0107119 A1.

## FY 2016 Publications/Presentations

### Publications

1. L. Righini, F. Gao, L. Liotti, J. Szanyi, C.H.F. Peden. “Performance and properties of K and  $\text{TiO}_2$  based LNT catalysts.” *Applied Catalysis B* **181** (2016) 862–873.
2. F. Gao, J. Szanyi, Y. Wang, B. Schwenzer, M. Kollar, C.H.F. Peden. “Hydrothermal Aging Effects on Fe/SSZ-13 and Fe/Beta  $\text{NH}_3$ –SCR Catalysts.” *Topics in Catalysis* **59** (2016) 882–886.
3. F. Gao, Y. Zheng, R.K. Kukkadapu, Y. Wang, E.D. Walter, B. Schwenzer, J. Szanyi, C.H.F. Peden. “Iron Loading Effects in Fe/SSZ-13  $\text{NH}_3$ –SCR Catalysts: Nature of the Fe Ions and Structure–Function Relationships.” *ACS Catalysis* **6** (2016) 2939–2954.

### Presentations

1. F. Gao, Y. Zheng, Y.L. Wang, J. Szanyi, Y. Wang, C.H.F. Peden. “Approaching Rational Design of Cu/CHA SCR Catalysts.” Presented by **Feng Gao** at the 2016 Annual CLEERS Workshop, Ann Arbor, MI, April 2016.
2. F. Gao, G.G. Muntean, J. Szanyi, C.H.F. Peden, N. Currier, A. Kumar, K. Kamasamudram, J. Li, J. Luo, A. Yezerets, M. Castagnola, H.Y. Chen, and H. Hess. “Enhanced High Temperature Performance of NOx Storage/Reduction (NSR) Materials.” Presented by **Feng Gao (Invited Speaker)** at the DOE Combustion and Emission Control Review, Washington, D.C., June 2016.

3. F. Gao, J. Szanyi, D. Mei, N.W. Washton, E.D. Walter, Y.L. Wang, Y. Wang, C.H.F. Peden. "Fundamental studies of small-pore zeolites for NOx emission control in vehicle exhaust" Presented by **Feng Gao (Invited Speaker)** at the 16th ICC, Beijing, China, July 2016.
4. F. Gao, Y. Zheng, Y.L. Wang, J. Szanyi, Y. Wang, C.H.F. Peden. "Approaching Rational Design of Cu/CHA SCR Catalysts." Presented by Feng Gao at the 2016 ACS Fall national meeting, Philadelphia, PA, August 2016.

## III.4 Thermally Stable Ultra-Low Temperature Oxidation Catalysts

### Overall Objectives

- Investigate a number of candidate low temperature oxidation catalysts as fresh materials, and after realistic laboratory and engine aging
- Obtain a better understanding of fundamental characteristics and various aging factors in both thermal and chemical aspects that impact the long-term performance of these candidate low temperature oxidation catalysts
- Provide an assessment of the appropriateness of the laboratory aging protocols in realistically reproducing the effects of actual engine aging conditions
- In this way, provide a viable pathway to commercialization of these very new and, thus, uncharacterized catalyst materials

### Fiscal Year (FY) 2016 Objectives

- Verify the effect of  $\text{SO}_2$  on the CO oxidation activity of highly active Cu/GMR6 low temperature CO oxidation catalyst
- Determine the deactivation mechanism by combined diffraction and spectroscopy measurements
- Verify the experimental findings by density functional theory (DFT) calculations on model Cu/ $\text{CeO}_2$  systems

### FY 2016 Accomplishments

- PNNL determined that sulfur poisoning causes irreversible deactivation of the Cu/GMR6 catalyst.
- The presence of  $\text{SO}_2$  in the simulated diesel exhaust initiates the formation of sulfates.
- The presence of sulfates influences both the active phase ( $\text{CuO}_2$ ) and the support (GMR6). Diffraction studies and DFT calculations revealed that sulfates accumulated on the ceria/zirconia support. Sulfates degrade the oxygen mobility of the support material. Sulfates on the support also affect the CuO, thereby weakening the interaction between CO and Cu+. Reduction in CO coverage causes activity decrease. ■

### János Szanyi (Primary Contact), Charles H.F. Peden

Institute for Intergrated Catalysis  
Pacific Northwest National Laboratory (PNNL)  
P.O. Box 999, MS K8-87  
Richland, WA 99354  
Phone: (509) 371-6524  
Email: janos.szanyi@pnl.gov

DOE Program Manager: Ken Howden  
Phone: (202) 586-3631  
Email: Ken.Howden@ee.doe.gov

CRADA Partners:  
Se H. Oh and Steven J. Schmieg, General Motors

### Introduction

New federally mandated Corporate Average Fuel Economy standards for light-duty vehicles in the United States will require a near doubling of the fuel economy by 2025. These new regulations are a direct response to the need to reduce emissions of greenhouse gases. To meet these challenges, automobile manufacturers are pursuing a variety of advanced stoichiometric and lean combustion to dramatically increase the efficiency of engine operation. These fuel efficient strategies result in significantly lower temperatures of exhaust gases while, at the same time, emissions regulations are also becoming more stringent. Exhaust gas temperatures from many of the new engine technologies are expected to be below 200°C for a considerable fraction of federal driving cycles. This presents an enormous challenge for today's vehicle emissions control systems.

What is needed to meet this "low temperature challenge" for vehicle emissions control systems are revolutionary solutions. The fundamental catalysis science community has identified a number of candidate catalyst formulations that provide for sufficient activity below 200°C [1]. A primary issue with many of these laboratory results is the absence of high temperature hydrothermal stability and poisoning by sulfur (in some studies the omission of  $\text{H}_2\text{O}$  from the simulated exhaust stream). General Motors Company and Battelle/PNNL have investigated a number of candidate low temperature oxidation catalysts as

fresh materials, and after realistic laboratory and engine aging. The studies performed in this cooperative research and development agreement (CRADA) led to a better understanding of fundamental characteristics and various aging and poisoning factors that impact the long-term performance of catalysts.

## Approach

This project focused on the characterization of catalyst materials used for low temperature catalytic oxidation reactions with special attention to the materials' sensitivities to  $\text{SO}_2$  in the simulated diesel exhaust. This information will aid the development of improved catalyst formulations and the understanding of the mechanisms for catalyst degradation of low temperature catalytic oxidation materials. General Motors provided both fresh and aged catalyst materials that were potentially useful for low temperature oxidation, and examined changes in the catalytic performance of these materials before and after the aging. Battelle provided state-of-the-art analytical techniques to investigate the surface and bulk properties of these catalysts, and the changes in these properties induced by the aging and poisoning process.

## Results

Ceria-based catalysts have long been known to be prone to sulfur poisoning, and the catalysts studied in this project were not exceptions either. We examined the effect of  $\text{SO}_2$  on the catalytic activity of Cu/GMR6 for the  $\text{CO} + \text{O}_2$  reaction (GMR6 is a commercial ceria/zirconia mixed oxide support containing Pr and La dopants, specifically developed for elevated temperature automotive applications). This study was conducted with the same reactant gas mixture composition as the other tests except that 1 ppm  $\text{SO}_2$  was also included in the gas mixture. The effect of sulfur on the CO oxidation activity of this catalyst was tested at both 175°C and 300°C. The change in CO conversion as a function of time-on-stream is displayed in Figure 1. The initial CO conversion over the catalysts at 175°C was ~60% but it decreased rapidly with exposure to the  $\text{SO}_2$ -containing reactant gas mixture. After 10 h on stream, the activity dropped to ~30%. When the reaction was carried out at 300°C, complete (100%) CO conversion was maintained in the first 5 h on stream, and then it decreased rapidly. After 14 h on stream, the CO conversion dropped to ~50%. At this point the catalyst was regenerated by removing  $\text{SO}_2$  from the reaction gas mixture and raising the temperature to 500°C. As  $\text{SO}_2$  was omitted from the reactant gas mixture, the CO conversion increased instantaneously to >90%. However, it did not reach 100% even after 2 h at 500°C.

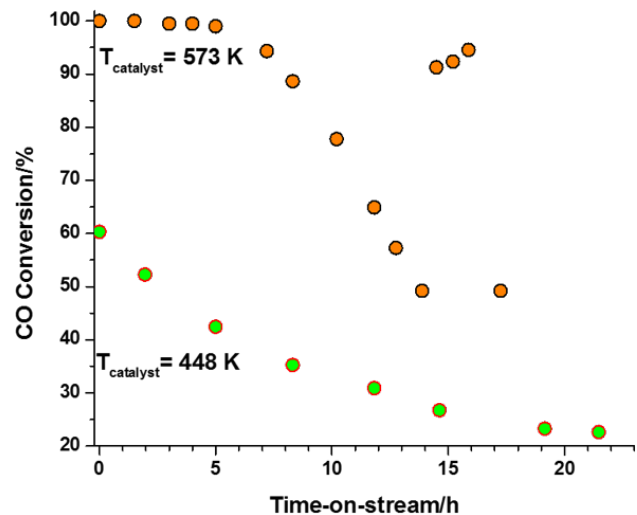


Figure 1. CO conversion as a function of time in a simulated diesel exhaust gas mixture (500 ppm CO, 260 ppm  $\text{C}_3\text{H}_8$ , 87 ppm  $\text{C}_3\text{H}_8$ , 200 ppm NO, 8%  $\text{O}_2$ , 8%  $\text{H}_2\text{O}$  and  $\text{N}_{\text{bal}}$ ).  $\text{SO}_2$ : 1 ppm for 21 h at 448 K ( $\approx 1.5 \text{ g SO}_2/\text{L}_{\text{monolith}}$ ); 1 ppm for 14 h at 573 K ( $\approx 1.0 \text{ g SO}_2/\text{L}_{\text{monolith}}$ ) at 175°C and 300°C

In order to investigate whether the sudden activity change was due to actual regeneration (i.e., sulfur removal) or just the increase in catalyst bed temperature, we cooled the sample back to 300°C and measured the CO oxidation activity with no  $\text{SO}_2$  in the feed. The CO oxidation activity of the catalyst dropped back to ~50%, suggesting that the activity increase seen at 500°C in the  $\text{SO}_2$ -free gas mixture was the result of increased catalyst bed temperature, and not the desulfation of the poisoned catalyst. (X-ray photoelectron spectroscopy analysis conducted on the S-poisoned Cu/GMR6 samples showed one  $\text{S} 2p_{3/2}$  feature at 169.0 eV consistent with the presence of sulfates.) Although these experiments clearly showed that the activity drop upon exposure to  $\text{SO}_2$ -containing gas mixture was caused by sulfate formation, it was not evident which component of the catalyst (i.e., CuO or ceria–zirconia [CZ]) was poisoned by sulfates. In order to address this question we conducted Fourier transform infrared spectroscopy measurements with CO as the probe molecule, and also in situ X-ray diffraction (XRD) measurements during reduction with CO at 300°C on both the fresh and S-poisoned catalysts. Fourier transform infrared spectroscopy spectra collected from the fresh and S-poisoned Cu/GMR6 catalysts after CO exposure are displayed in Figure 2. Both the fresh and S-poisoned catalysts exhibited CO adsorption, as strong vibrational features were recorded at 2,109–2,116  $\text{cm}^{-1}$  (fresh) and 2,142  $\text{cm}^{-1}$  (S-poisoned) upon exposure to CO. Interestingly, the position of this band differed significantly, depending on the presence (S-poisoned) or

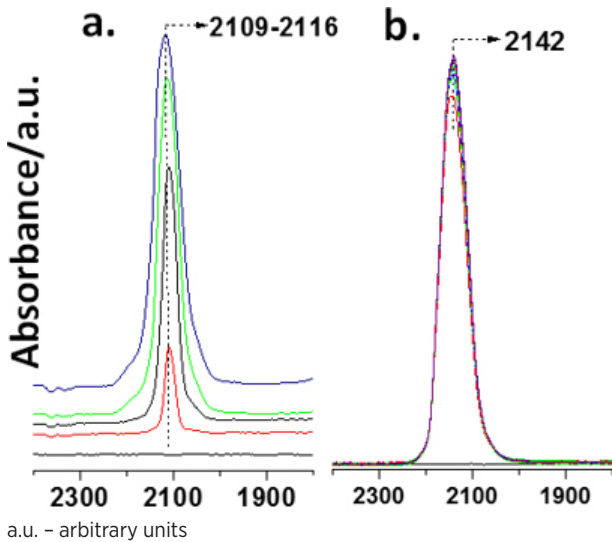


Figure 2. Infrared spectra collected from CO-exposed fresh (a) and sulfur-poisoned (b) catalyst at 25°C

absence (fresh) of sulfates on the catalyst. The blueshift of the vibrational feature of adsorbed CO on the S-poisoned catalyst indicates weaker interaction between CO and Cu, underlining the electronic influence of sulfates on the Cu adsorption center.

It is also interesting to note that strong carbonate features develop on the fresh catalyst upon CO exposure, while only very low intensity carbonate bands are observed on the S-poisoned sample. This observation may suggest that either the CO oxidation activity of the catalyst decreased by the modification of the Cu active phase due to sulfate formation, or the sulfates present on the CZ support prevent the formation of carbonates. In light of the activity data presented above the modification of the active Cu phase seems to be responsible for the suppressed reactivity of the S-poisoned Cu/GMR6 catalyst.

Experimental results discussed above suggest that sulfates were mostly formed on the CZ support, but strongly influenced the CO adsorption properties of the active Cu phase. The role of the CZ support is assumed to provide dissociated oxygen species to CO adsorbed on Cu, thus enhancing the CO oxidation activity of the active phase (Mars–van Krevelen mechanism). If sulfates bind to the CZ support strongly, they could prevent the support material to supply mobile oxygen for the CO oxidation reaction. Our previous experiments have shown that extensive CO oxidation can be achieved on Cu/GMR6 even in the absence of gas phase oxygen at 473 K, due to the presence of a large pool of highly mobile oxygen on/in the CZ support. If we assume that most of the oxygen used in CO oxidation in the absence of O<sub>2</sub> comes from

the CZ support, the lattice of the CZ has to expand as oxygen is removed from the structure [2]. To this end we carried out a series of experiments in which we exposed the catalyst support (GMR6), the fresh (Cu/GMR6), and S-poisoned catalysts (S-Cu/GMR6) to CO at 300°C in an in situ XRD cell and followed the variation in the unit cell (expansion of the unit cell) as a function of time. Prior to reduction, the samples were oxidized in O<sub>2</sub> flow at 300°C and purged with N<sub>2</sub>. A series of XRD patterns collected in situ from the fresh and S-poisoned Cu/GMR6 samples are shown in Figure 3. After oxidation at 300°C the XRD patterns of both samples indicate the presence of CuO and CZ phases only. After N<sub>2</sub> purge as the gas stream is switched to CO, CuO in the Cu/GMR6 sample was reduced very fast to Cu<sub>2</sub>O and then to metallic Cu. This reduction process was much slower over the S-Cu/GMR6 sample, although after extended period of reduction all the copper oxide was reduced to metallic Cu. When the gas stream was switched back to O<sub>2</sub> after the reduction with CO, metallic copper was reoxidized to CuO very fast in the Cu/GMR6 sample, while it was only re-oxidized to Cu<sub>2</sub>O in the S-poisoned sample. These observations clearly show the suppression of the redox properties of the Cu/GMR6 sample as a result of poisoning by sulfur.

The changes in the unit cell parameter of the CZ lattice as a function of time are summarized in Figure 4 for the GMR6 support material, as well as for the fresh and S-poisoned Cu/GMR6 catalysts. The results revealed that the increase in unit cell parameter as a result of reduction with CO at 300°C varied significantly for the different samples. The unit cell parameter for the GMR6 support increased rather slowly (in comparison to the Cu-containing samples) and it became constant only after ~200 min on stream. On the other hand, the expansion of the unit cell of the Cu/GMR6 sample was very fast, substantiating again the enhanced reduction of the CZ support by the presence of Cu. Beside the rate of unit cell parameter increase (i.e., rate of CZ reduction) the extent of the expansion was also dependent on the presence or absence of Cu. While the unit cell of the GMR6 support material increased by 0.030 Å, Cu/GMR6 increased by 0.041 Å. Thus, the extent of reduction of the CZ substrate was higher in the presence of Cu. Comparing the trends in the fresh and S-poisoned Cu/GMR6 samples it is evident that the extent of reduction is much lower in the S-Cu/GMR6 sample than in the fresh sample (the unit cell parameter only increased by 0.010 Å in the S-poisoned sample). The results of these experiments clearly show that sulfates formed on the CZ support strongly decrease the reducibility of the GMR6 support. (The large decrease in the mobility of lattice oxygens in the CZ support was also evidenced in the isotope exchange experiments [3] carried out on the S-poisoned sample in

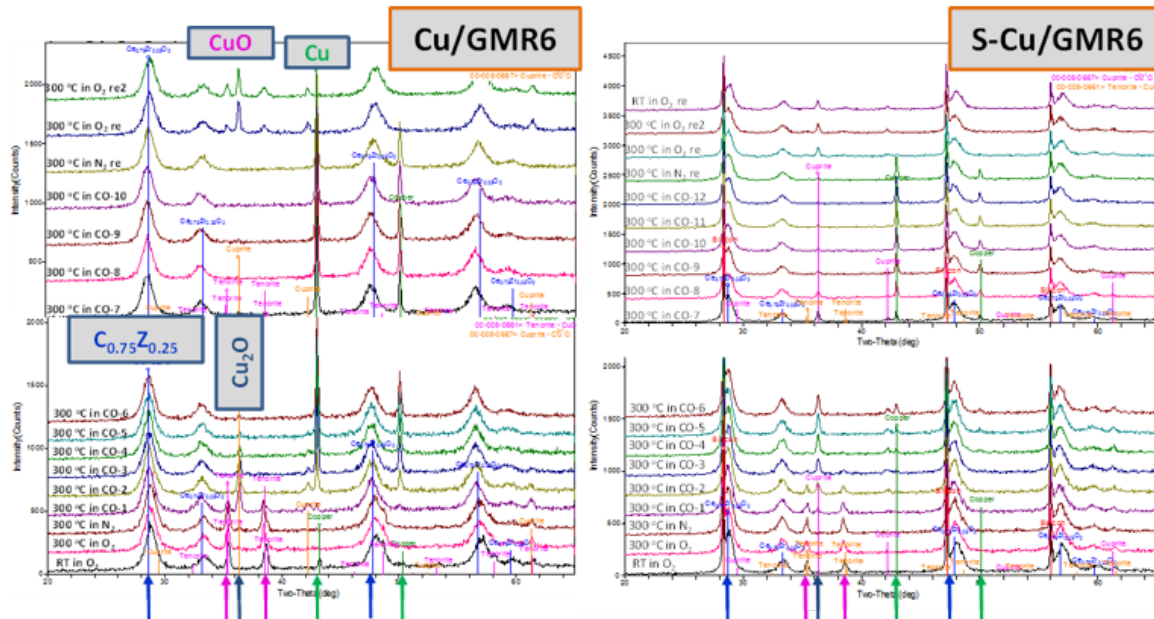


Figure 3. Series of XRD patterns recorded during in situ reduction of a fresh (a) and  $\text{SO}_2$ -exposed (b) Cu/GMR6 catalyst at 300°C under CO flow

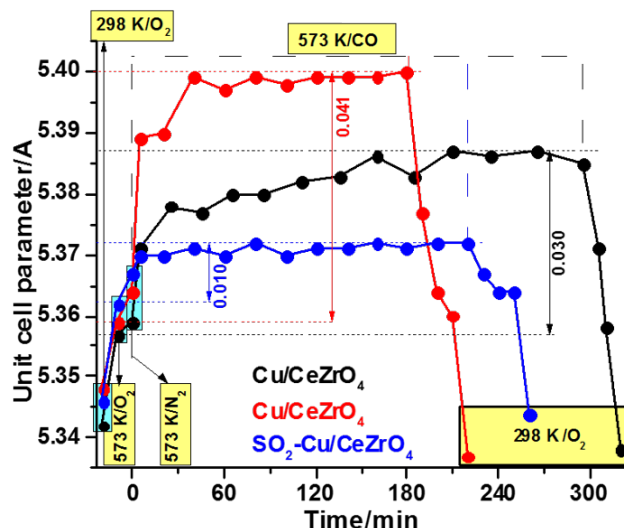


Figure 4. Variation of the unit cell parameter of the CZ lattice during CO reduction at 300°C (fresh GMR6 and Cu/GMR6 and  $\text{SO}_2$  exposed Cu/GMR6)

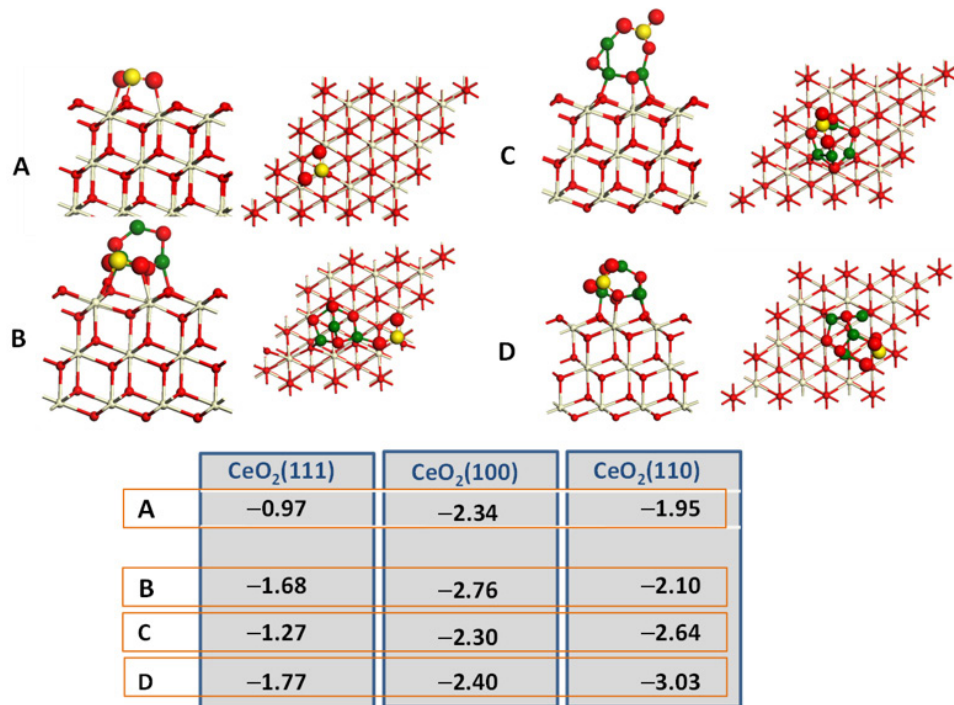
an identical manner we have reported in our prior report for Cu/GMR6. The extent of  $^{15}\text{N}^{18}\text{O}$  to  $^{15}\text{N}^{16}\text{O}$  isotope exchange was dramatically reduced in the S-Cu/GMR6 sample in comparison to the Cu/GMR6 one.)

The interaction of  $\text{SO}_2$  with different facets of  $\text{CeO}_2$  and  $(\text{CuO})_4/\text{CeO}_2$  was also evaluated by DFT calculations. The results summarized in Table 1 indicate that  $\text{SO}_2$  adsorption on  $\text{CeO}_2(100)$  and  $\text{CeO}_2(110)$  facets are

stronger than on  $\text{CeO}_2(111)$ . Furthermore, the presence of  $(\text{CuO})_4$  clusters enhances that stability of  $\text{SO}_2$  on all three  $\text{CeO}_2$  facets. The calculations also revealed that  $\text{SO}_2$  preferentially adsorbs at the  $(\text{CuO})_4/\text{CeO}_2$  interface, supporting our conclusion that the sulfates formed influence the electronic properties of CuO, and also retards the oxygen mobility (atomic oxygen supply) of the support around the active catalytic phase.

## Conclusions

- The activity of the Cu/GMR6 low temperature CO oxidation catalyst dramatically and irreversibly reduced when  $\text{SO}_2$  was present in the simulated diesel exhaust gas stream.
- X-ray photoelectron spectroscopy analysis revealed the formation of sulfates during catalytic measurements in the  $\text{SO}_2$ -containing gas mixture.
- Sulfates influence both the CuO active phase and the GMR6 support, although the CO adsorption capacity of the CuO did not change significantly but its binding strength did.
- The formation of sulfates on the GMR6 support reduced its ability to deliver active oxygen to the CO bound to CuO. DFT calculation revealed that sulfates prefer to bind at the interface of the CuO and GMR6.

**Table 1. DFT-calculated adsorption energies (eV) of SO<sub>2</sub> on different crystal facets of CeO<sub>2</sub> and CuO/CeO<sub>2</sub>.**

## References

1. Zammit M., C.L. DiMaggio, C.H. Kim, C. Lambert, G.G. Muntean, C.H.F. Peden, J.E. Parks, and K. Howden. "Future Automotive Aftertreatment Solutions: The 150°C Challenge Workshop Report." Pacific Northwest National Laboratory Report #PNNL-22815.
2. R. Ran, D. Weng, X. Wu, J. Fan, L. Wang, X. Wu, J. Rare Earths, 29, 1053, 2011.
3. J. Szanyi, J.H. Kwak, Chem. Comm. 50, 14998, 2014.

## FY 2016 Publications/Presentations

1. I. Heo, S.J. Schmiege, S.H. Oh, W. Li, J. Szanyi, C.H.F. Peden, and C.H. Kim. "Improved Thermal Stability of a Ceria-based Catalyst Containing Copper for Low Temperature CO oxidation under Simulated Diesel Exhaust Conditions." Appl.Catal. B: Environmental, to be submitted.
2. J. Szanyi, C.H.F. Peden, C.H. Kim, W. Li, S.H. Oh, and S.J. Schmiege. "Thermally Stable Ultra-Low Temperature Oxidation Catalysts." Presented by Janos Szanyi at Vehicle Technologies Program Annual Merit Review and Peer Evaluation Meeting, Washington, D.C., June 2016.

## III.5 Low Temperature Emissions Control

### Overall Objectives

- Develop emission control technologies that achieve >90% reduction of pollutants at low temperatures (<150°C) to enable fuel-efficient engines with low exhaust temperatures to meet new U.S. Environmental Protection Agency Tier 3 emission regulations that require ~80% less NO<sub>x</sub> and hydrocarbon emissions than current standards
- Identify advancements in technologies that will enable commercialization of advanced combustion engine vehicles
- Understand fundamental surface chemistry mechanisms that either enable or limit low temperature emission control

### Fiscal Year (FY) 2016 Objectives

- Investigate individual roles of the components in the CuO–Co<sub>3</sub>O<sub>4</sub>–CeO<sub>2</sub> (CCC) ternary oxide and potential synergies with standard emissions control components
- Identify impact of sulfur
- Expand studies of zeolite materials to include passive NO and hydrocarbon (HC) adsorber applications based on industry guidance

### FY 2016 Accomplishments

- Platinum group metal (PGM)-free mixed metal oxides
  - Identified new mixed metal oxide candidate (with University of South Carolina [USC]) that has improved HC activity (Sn-Mn-Ce and Mn-Ce)
  - Measured sulfur tolerance of CCC while also exploring mitigation strategies with PGM
- Support modifications for enhanced PGM activity
  - New core@shell technique employed to maximize ZrO<sub>2</sub> surface for PGM catalysis shown to yield improved activity especially for total hydrocarbon (THC)
  - Successfully implemented nano-on-nano technique with Pd dispersed on nanoparticles of Ce-Zr dispersed on Al<sub>2</sub>O<sub>3</sub>; high activity observed, approaching targets for some gases
- Trapping materials

**Todd J. Toops (Primary Contact),  
James E. Parks, Eleni Kyriakidou,  
Andrew Binder, Jae-Soon Choi**

Oak Ridge National Laboratory

2360 Cherahala Boulevard

Knoxville, TN 37932

Phone: (865) 946-1207

Email: [toopstj@ornl.gov](mailto:toopstj@ornl.gov)

DOE Technology Development Manager:

Ken Howden

- Determined key attributes of silver-zeolite HC trap; deep ion exchange and low Si to Al ratios
- Demonstrated NO adsorption on Pd/ZSM-5; impact of pretreatment temperature ■

### Introduction

Removing the harmful pollutants in automotive exhaust has been an intense focus of the automotive industry over the last several decades. In particular, the emissions regulations for fuel-efficient diesel engines that were implemented in 2007 and 2010 have resulted in a new generation of emissions control technologies. These catalysts usually reach 90% conversion of pollutants between 200°C and 350°C, but below these temperatures, the catalysts are relatively inactive. Consequently, more than 50% of pollutant emissions occur in the first 2–3 min of the transient drive cycle required for certification and under cold-start or idling conditions [1]. Thus, as emissions regulations become more stringent [2] meeting the emission regulations will require increased activity during this warm-up period. To further complicate matters, the increased Corporate Average Fuel Economy standards that will be implemented over the next decade will result in the introduction of more fuel-efficient engines [3]. Higher fuel efficiency will result in less heat lost to exhaust and lower exhaust temperatures, which further necessitates the need for increased emissions control activity at low temperatures [4]. With this in mind the U.S. DRIVE ACEC Tech Team has set a goal of achieving 90% conversion of CO, HC, and NO<sub>x</sub> at 150°C. Higher Pt and Pd loadings may help to increase the catalytic efficiency, but such methods are too expensive for long-term success. Thus, this project focuses on

developing new catalytic materials that are active at lower temperatures. In addition, other options to meet the emissions standards such as hydrocarbon and  $\text{NO}_x$  absorbers are being pursued; these adsorber materials can trap the pollutants at low temperature for later release and treatment at higher temperatures where catalysts are active.

## Approach

To reach the goal of 90% conversion at 150°C a multi-functional approach will be pursued. Currently, there is a large effort being pursued in Basic Energy Science programs that are focused on studying catalysts with very high activity regardless of the specific application. We initiate contact with these researchers to investigate their catalysts in the harsh conditions that are present in automotive exhaust, e.g.,  $\text{H}_2\text{O}$ ,  $\text{CO}_2$ , CO, HC,  $\text{NO}_x$  and hydrothermal aging above 800°C. Often these catalysts show exceptional activity in single component exhaust streams, but there is significant inhibition from other exhaust species. With this in mind, we are aiming to understand the limitations of each system, but also look for synergistic opportunities when possible. This includes using traps to limit exposure of inhibiting species to active catalysts until temperatures are more amenable. Also, mixing catalytic components where the catalysts are limited by different species will be explored. Our efforts will aim to understand the processes at a fundamental level and illustrate any benefits or shortcomings of each catalyst we study, while striving to find compositions that will achieve the very challenging goal of 90% conversion of CO,  $\text{NO}_x$ , and HC at 150°C. Improving this understanding of the potential advantages and limitations of catalysts will guide the reformulation of new catalysts.

## Results

Efforts this year continued in the study of the CCC catalyst which has shown excellent CO oxidation behavior [5] and synergistic chemistry when combined with PGM-based catalysts. A primary concern expressed by industry to us with this catalyst has been its sulfur tolerance. This year we implemented the ACEC guidelines for sulfur exposure which involves flowing 5 ppm  $\text{SO}_2$  at 300°C under reaction conditions for 5 h. The results shown in Figure 1a illustrate that the CCC catalyst loses activity precipitously at these conditions. Adding 1% Pt to the catalyst does little to regain its activity; however, when blended with physical mixture of  $\text{Pt}/\text{Al}_2\text{O}_3$  there are minimal activity losses. Figures 1b and 1c show the light-off profiles of the degreened, sulfated and desulfated catalysts (desulfation consisted of cycling between lean and rich operation at 600°C). In

these experiments, it is clear that the CCC is significantly impacted by the sulfur exposure and full recovery is not possible even after sulfation. However, the impact continues to be minimal when mixed with  $\text{Pt}/\text{Al}_2\text{O}_3$ . Efforts will continue in this physical mixture studies to understand if there is a synergistic benefit or if the CCC is still being deactivated and the reactivity is moving towards the  $\text{Pt}/\text{Al}_2\text{O}_3$  base case.

In efforts to explore other potential catalysts that are being developed through other National Science Foundation/Basic Energy Science funded programs, a collaboration was initiated with the USC. They had been studying another series of metal oxide catalysts containing varying levels of Sn, Mn, and Ce; additionally they were directly dispersing 1% Pd on these metal oxide catalysts [6]. While these samples showed excellent CO oxidation behavior, they were only employing relatively simple simulated exhaust streams (Figure 2a). For a full comparison, they sent samples to Oak Ridge National Laboratory, and we evaluated the samples under the ACEC protocols; specifically, the low temperature combustion diesel (LTC-D) protocol. Not surprisingly, the behavior was not as promising as initially hoped, but the  $\text{MnO}_x\text{--CeO}_2$  catalyst showed very good hydrocarbon activity (Figure 2b), which improved even further when Pd was added to the catalyst (Figure 2c). Overall this series of catalysts is not likely to be the primary solution, but understanding how these components interact with the exhaust constituents is important and can help guide future catalyst formulations. Mn in particular has shown a lot of promise in many different studies.

Other efforts in this project have focused on traditional PGM-based approaches while trying to improve the activity through modifications of the underlying support. Interactions between Pd and  $\text{ZrO}_2$  have been the primary target since the initial results showed great initial reactivity [7,8]. One of our approaches to improve the reactivity further is to expand the available surface area of the  $\text{ZrO}_2$  by fully covering the surface of a high surface area support with  $\text{ZrO}_2$ . As shown in Figure 3a, this was achieved through advanced synthesis technique. Pd is then deposited on this outer shell of  $\text{ZrO}_2$ . Reactivity results employing the ACEC LTC-D protocol illustrate improved reactivity and a catalyst durable to 900°C (Figures 3b and 3c). Another approach to enhance the reactivity is to disperse the Pd directly on islands of the idealized support. Here we employ either ceria or ceria-zirconia (Ce-Zr) 5 nm nanoparticles on a high surface area alumina support, and then deposit Pd preferentially on the nanoparticles as shown in Figure 4a with Ce-Zr. Again the reactivity of this sample is very good and offers significant improvement and durability over the initial

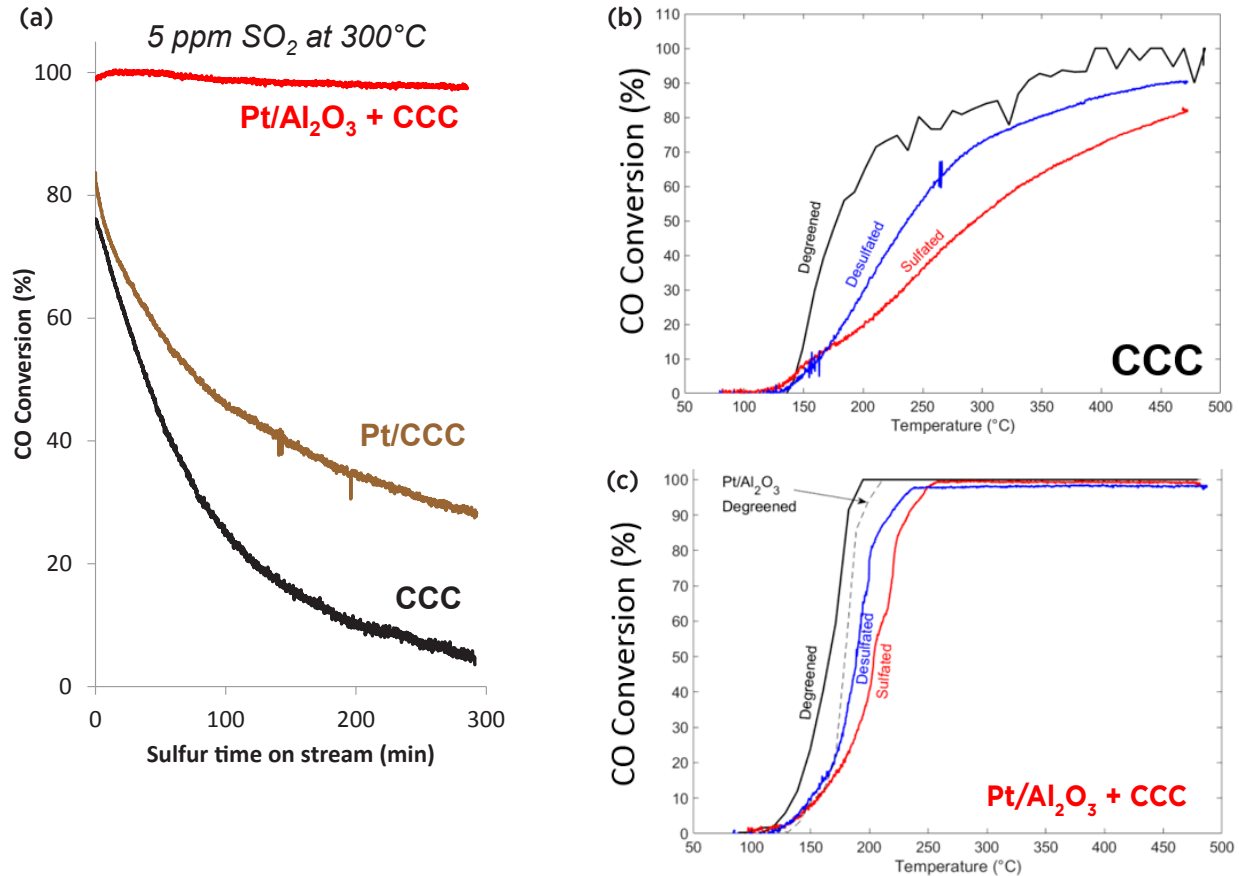


Figure 1. (a) Time-on-stream CO oxidation conversions during 5 ppm SO<sub>2</sub> poisoning in LTC-D stream conditions for various catalysts. CO conversion while ramping from 80°C to 500°C for (b) CCC and (c) Pt/Al<sub>2</sub>O<sub>3</sub> + CCC in the degreened, sulfated, and desulfated state.

Pd-Zr sample (Figures 4b, 4c, and 4d). Of particular interest with this sample is that propane (C<sub>3</sub>H<sub>8</sub>) starts to react at around 200°C, which is exceptionally low for this difficult to react HC. There is still room for improvement as the target of 90% conversion of CO and THC are not achieved; therefore, efforts will continue with this approach especially to get smaller initial deposition of Pd and investigation of Pt-Pd bi-metallic catalysts.

Investigating a potential method for capturing NO and HCs during low temperature operation during both cold-start and other low temperature exhaust conditions has been another area of study in this project. Initial efforts were focused on hydrocarbon adsorption using a BEA zeolite with varying loadings of ion-exchanged Ag in the sample (0–5%). Employing a protocol developed through discussions with Johnson Matthey, propylene adsorption was measured at 80°C for 3 min. In the presence of water vapor, the capture efficiency trends with increasing loading as expected (Figure 5a). However, capturing the HC is only part of the equation, as it is important to

release the pollutant at a temperature where the oxidation catalyst is active. Figures 5b and 5c show that the loading also influences the release characteristics as the higher loaded Ag materials result in higher temperature release. It should be noted that the hydrocarbon release is typically partially oxidized propylene and thus total hydrocarbons are reported along with CO and CO<sub>2</sub>. Although NO was being fed during this experiments, there was not significant adsorption observed. To aid with NO adsorption, another material was investigated based on recent reports [9,10], Pd ion-exchanged on ZSM-5. Two samples were prepared with differing calcination temperatures, 650°C and 750°C. These ion-exchanged Pd/ZSM-5 sample showed significant NO and HC adsorption at 80°C (Figures 6a and 6b). Furthermore, the release profile of the NO was such that the selective catalytic reduction catalyst would be active and urea injection would be possible to reduce the NO to N<sub>2</sub>.

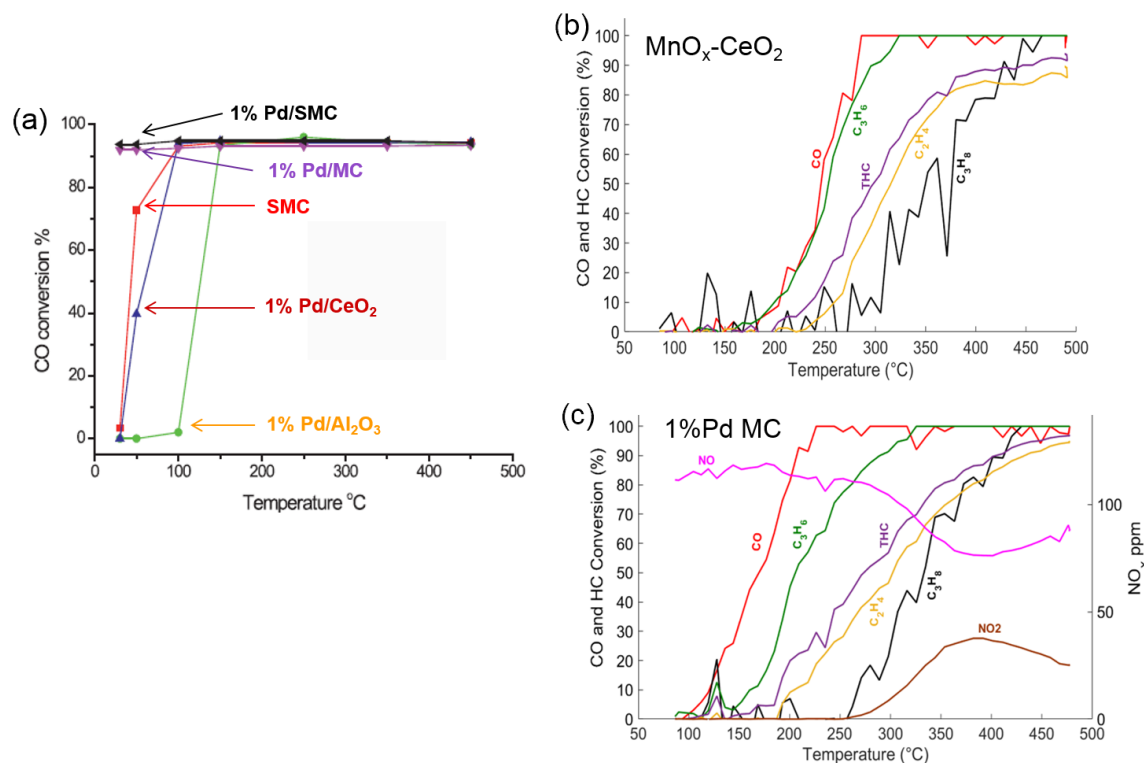


Figure 2. (a) Initial data from USC collaboration under simple reaction conditions (reproduced from Wang et al. [6]); 1%Pd/Sn-Mn-Ce Oxide (SMC), 1% Pd/Mn-Ce oxide (MC), SMC, 1% Pd/CeO<sub>2</sub>, and 1% Pd/Al<sub>2</sub>O<sub>3</sub>. Light-off curves under LTC-D protocol standards of the most promising candidate, MnO<sub>x</sub>-CeO<sub>2</sub>, (b) without and (c) with Pd.

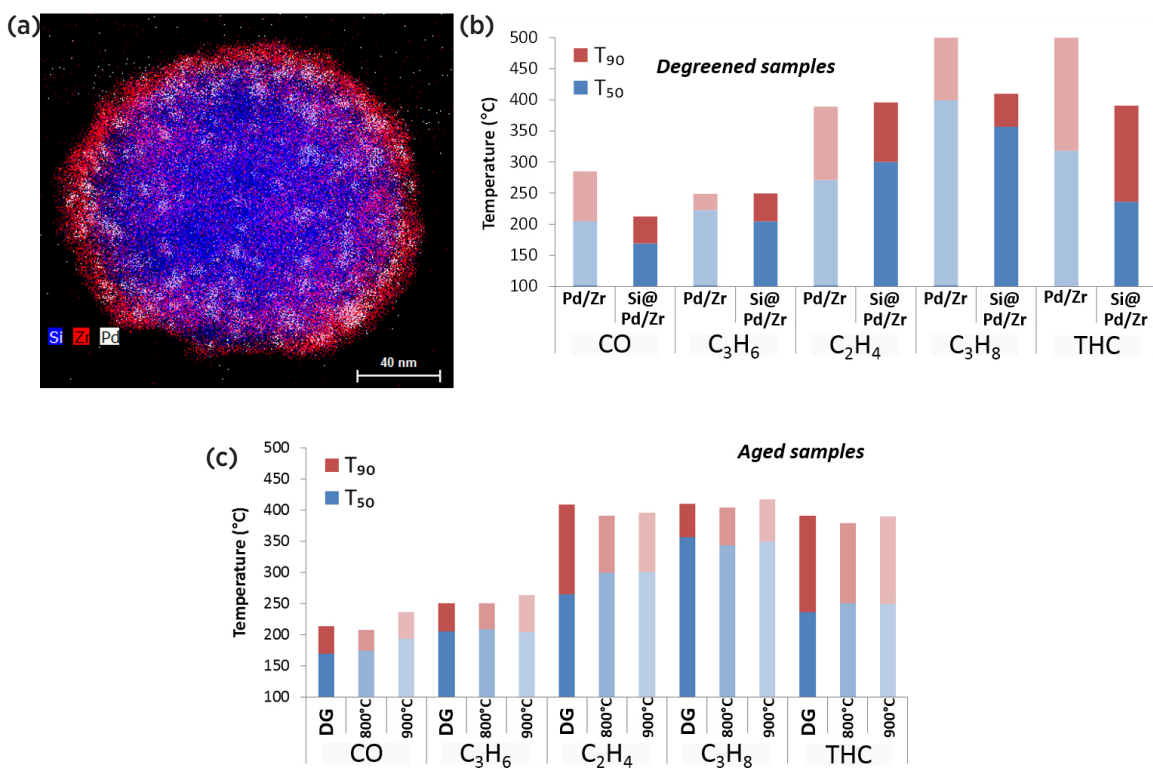


Figure 3. (a) Resulting catalyst from new synthesis technique with a complete ZrO<sub>2</sub> shell around a SiO<sub>2</sub> core with Pd dispersed only on the ZrO<sub>2</sub> (Si@Pd/Zr). Temperature of 50% and 90% conversion (T<sub>50</sub> and T<sub>90</sub>, respectively) for the (b) degreened (DG) and (c) aged PGM-based catalysts.

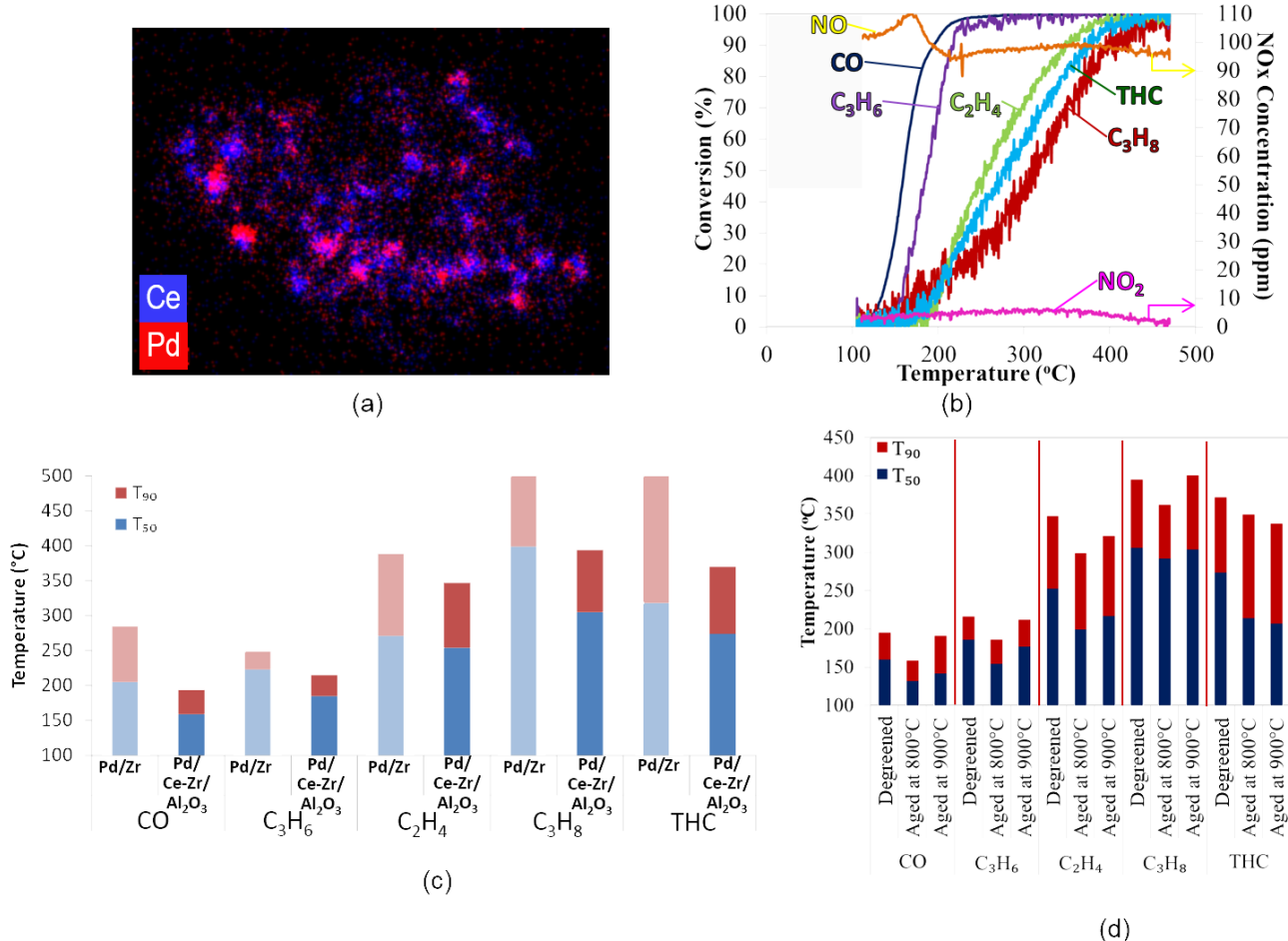


Figure 4. (a) Resulting catalyst from directed deposition of Pd on the Ce-Zr nanoparticles that have been dispersed on a high surface area alumina support. (b) Temperature programmed ramp illustrating reactivity of gases over the Pd/Ce-Zr/Al<sub>2</sub>O<sub>3</sub> sample. T<sub>50</sub> and T<sub>90</sub> for the (c) degreened and (d) aged PGM-based catalysts.

## Conclusions

All of the strategies being considered are focused on reducing criteria emissions at low temperatures. Although the 150°C target has not been achieved, there have been significant gains and improved understanding of how the samples are operating and what is limiting their performance. Achievements this year are summarized below:

- Measured sulfur tolerance of CCC; identified potential mitigation strategies with PGM physical mixture
- Identified new mixed metal oxide candidates (USC) that have improved HC activity
- New synthesis technique employed to maximize ZrO<sub>2</sub> surface for PGM catalysis shown to yield improved activity and durability especially for THC

- Successfully implemented nano-on-nano technique with nano-sized Pd dispersed on nanoparticles of Ce-Zr dispersed on Al<sub>2</sub>O<sub>3</sub>
  - High activity observed, approaching targets for some gases
- Determined key attributes of silver-alumina HC trap; deep ion exchange and low Si:Al
- Demonstrated NO adsorption on Pd/ZSM-5; assessed impact of pretreatment temperature

## Acknowledgment

The authors acknowledge the support from U.S. Department of Energy under Award DE-FE0011585. This research was partially conducted at the Center for Nanophase Materials Sciences, which is a DOE Office of Science User Facility. The elemental analysis data and micrographs presented in Figures 3 and 4 were obtained

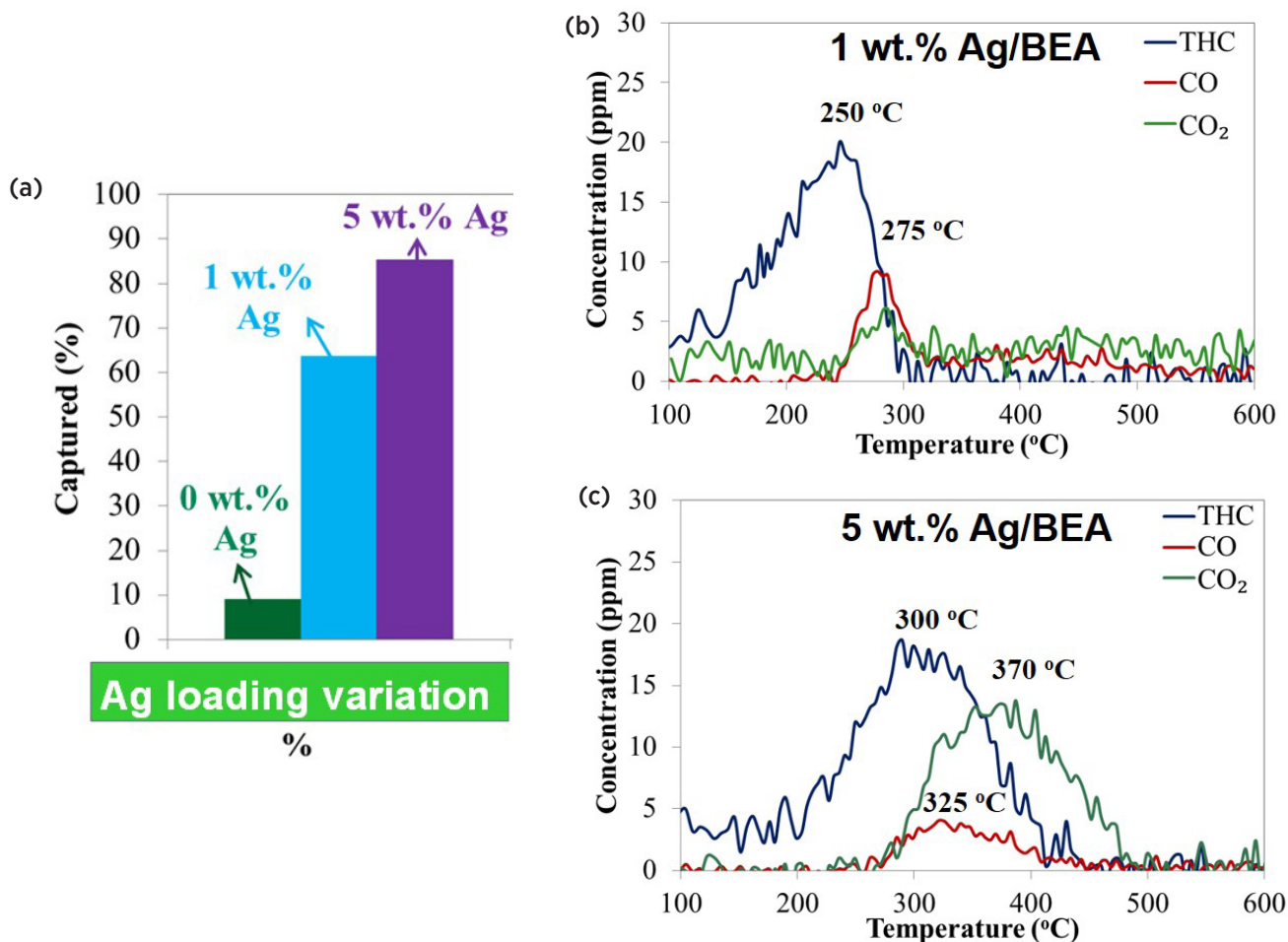


Figure 5. (a) Percentage of the propylene fed to the reactor adsorbed by the three BEA-based HC adsorbers at 80°C. Release profiles during the desorption phase of the study for (b) 1% Ag/BEA and (c) 5% Ag/BEA.

using instrumentation (FEI Talos F200X S/TEM) provided by the Department of Energy, Office of Nuclear Energy, Fuel Cycle R&D Program and the Nuclear Science User Facilities.

## References

1. Kašpar, J.; Fornasiero, P.; Hickey, N.; *Catal. Today* **2003**, 77, 419–449.
2. U.S. Environmental Protection Agency, *EPA-420-F-13-016a* **2013**, 1–4.
3. U.S. Environmental Protection Agency, Department of Transportation, National Highway Traffic Safety Administration, *Federal Register* **2012**, 77:199, 62623–63200.
4. Prikhodko, V.; Curran, S.; Parks, J.; and Wagner, R.; *SAE Int. J. Fuels Lubr.* **2013**, 6:2, 329–335.
5. Andrew J. Binder, Todd J. Toops, James E. Parks II, Sheng Dai, “Low Temperature CO Oxidation over Ternary Oxide with High Resistance to Hydrocarbon Inhibition,” *Angew. Chem. Int. Ed.* **54** (2015) 13263–13267.
6. C. Wang et al. *Catalysis Today* **258** (2015) 481–486.
7. Mi-Young Kim, Eleni A. Kyriakidou, Jae-Soon Choi, Todd J. Toops, Andrew J. Binder, Cyril Thomas, James E Parks II, Viviane Schwartz, Jihua Chen, Dale K. Hensley, “Enhancing Low-Temperature Activity and Durability of Pd-based Diesel Oxidation Catalysts Using ZrO<sub>2</sub> Supports,” *Applied Catalysis B: Environmental* **187** (2016) 181–194.
8. Mi-Young Kim, Jae-Soon Choi, Todd J. Toops, Eun-Suk Jeong, Sang-Wook Han, Viviane Schwartz, and Jihua Chen, “Coating Silica Support with Titania or Zirconia and Effects on Structure and CO Oxidation Performance of Platinum Catalysts,” *Catalysts* **3** (2013) 88–103; doi:10.3390/catal3010088.

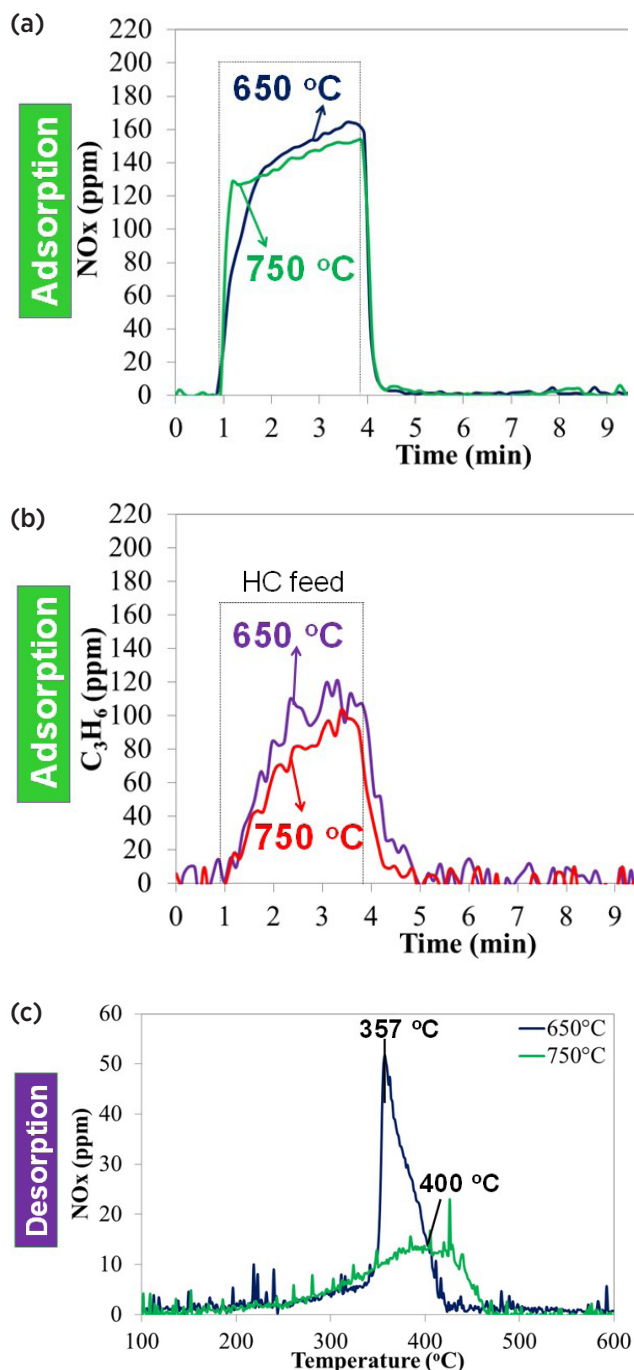


Figure 6. Percentage of the (a) NO and (b) propylene fed to the reactor adsorbed by Pd/ZSM-5 at 80°C; they were pretreated (calcined) at either 650°C or 750°C. (c) Release profile during the desorption phase of the study for total NO<sub>x</sub> for the Pd/ZSM-5 samples.

9. Yuichiro Murata, Tomoko Morita, Katsuji Wada, and Hiroshi Ohno, "NO<sub>x</sub> Trap Three-Way Catalyst (N-TWC) Concept: TWC with NO<sub>x</sub> Adsorption Properties at Low Temperatures for Cold-Start Emission Control," SAE Technical Paper, 2015-01-1002 (2015).

10. Hai-Ying Chen, Jillian E. Collier, Dongxia Liu, Loredana Mantarosie, Desirée Durán-Martín, Vladimír Novák, Raj R. Rajaram, David Thompsett, "Low Temperature NO Storage of Zeolite Supported Pd for Low Temperature Diesel Engine Emission Control," *Catal. Lett.* 146 (2016) 1706–1711.

## FY 2016 Publications/Presentations

1. Andrew J. Binder, Todd J. Toops, James E. Parks II, Sheng Dai, "Low Temperature CO Oxidation over Ternary Oxide with High Resistance to Hydrocarbon Inhibition," *Angew. Chem. Int. Ed.* 54 (2015) 13263–13267.
2. Andrew P. Wong, Eleni A. Kyriakidou, Todd J. Toops, and John R. Regalbuto, "The Catalytic Behavior of Pt-Pd Bimetallic Catalysts for Use as Diesel Oxidation Catalysts," *Catalysis Today* 267 (2016) 145–156.
3. Mi-Young Kim, Eleni A. Kyriakidou, Jae-Soon Choi, Todd J. Toops, Andrew J. Binder, Cyril Thomas, James E. Parks II, Viviane Schwartz, Jihua Chen, Dale K. Hensley, "Enhancing Low-Temperature Activity and Durability of Pd-based Diesel Oxidation Catalysts Using ZrO<sub>2</sub> Supports," *Applied Catalysis B* 187 (2016) 181–194.
4. Todd J. Toops, Eleni A. Kyriakidou, Andrew J. Binder, James E. Parks II, Jae-Soon Choi, "Low Temperature Emissions Control," DOE 2015 Annual Progress Report, March 2016, <http://energy.gov/sites/prod/files/2016/03/f30/FY2015%20Advanced%20Combustion%20Engine%20R%26D%20Annual%20Report.pdf>.
5. Chao Wang, Andrew J. Binder, Todd J. Toops, Jochen Lauterbach, Erdem Sasmaz, "Evaluation of Mn and Sn modified Pd-Ce based catalysts for low-temperature diesel exhaust oxidation," submitted to *Emissions Control Science and Technology*, September 2016.
6. (KEYNOTE) Todd J. Toops, James E. Parks, Eleni Kyriakidou, Andrew Binder, Jae-Soon Choi, Michael Lance, "Approaches to the challenges of treating emissions at low temperatures," PACIFICHEM, Honolulu, Hawaii, December 15, 2015.
7. (KEYNOTE) Todd J. Toops, "Approaches and Advances to the challenges of treating emissions at low temperatures," *Emissions 2015*, Troy, MI, June 23–24, 2015.
8. (INVITED) Todd J. Toops, "Approaches to the challenges of treating emissions at low temperatures," presentation to the Karlsruhe Institute of Technology, Karlsruhe, Germany, September 17, 2015.

9. (INVITED) Todd J. Toops, "Approaches to the challenges of treating emissions at low temperatures," presentation to the Politecnico di Milano, Milano, Italy, September 11, 2015.
10. Mi-Young Kim, Eleni A. Kyriakidou, Jae-Soon Choi, Todd J. Toops, Cyril Thomas, Andrew Binder, James E. Parks II, Viviane Schwartz, Jihua Chen, "Impact of  $ZrO_2$  Supports on the Durability and Low-Temperature Performance of Pd-Based Diesel Oxidation Catalysts," *24th North American Catalysis Society Meeting (NAM)*, Pittsburgh, PA, June 14–19, 2015.
11. Andrew J. Binder, Todd J. Toops, Raymond R. Unocic, James E. Parks II, Sheng Dai, "Inhibition-Resistant Ternary Oxide Catalyst for Low Temperature CO Oxidation in Automotive Exhaust," *24th North American Catalysis Society Meeting (NAM)*, Pittsburgh, PA, June 18, 2015.
12. Eleni A. Kyriakidou, Jae-Soon Choi, Mi-Young Kim, Todd J. Toops, James E. Parks II, "A Comparative Study of BEA-Zeolites for Hydrocarbon Trap Applications under 'Cold-Start' Conditions," *AIChE Annual Conference*, Salt Lake City, UT, November 2015.
13. Andrew J. Binder, Todd J. Toops, Raymond R. Unocic, James E. Parks II, Sheng Dai, "Inhibition-Resistant Ternary Oxide Catalyst for Low Temperature CO Oxidation in Automotive Exhaust," *14th Annual Fall Symposium of the Southeastern Catalysis Society*, Clemson, SC, September 28, 2015.
14. Eleni A. Kyriakidou, Jae-Soon Choi, Mi-Young Kim, Todd J. Toops, James E. Parks II, "A Comparative Study of ZSM-5 and Beta-Zeolites for Hydrocarbon Trap Applications under 'Cold-Start' Condition," *14th Annual Fall Symposium of the Southeastern Catalysis Society*, Clemson, SC, September 27, 2015.
15. Eleni A. Kyriakidou, Jae-Soon Choi, Todd J. Toops, James E. Parks II, "A Comparative Study of BEA-Zeolites for Hydrocarbon Trap Applications under 'Cold-Start' Conditions," *CLEERS Workshop*, Ann Arbor, MI, April 2016.
16. Eleni A. Kyriakidou, Todd J. Toops, Michael J. Lance, Andrew Binder, James E. Parks II, "Impact of Mixed Metal Oxides Supports on the Durability and Low-Temperature Performance of Pd-based Diesel Oxidation Catalysts," *CLEERS Workshop*, Ann Arbor, MI, April 7, 2016.
17. Andrew Binder, Todd J. Toops, Chao Wang, Erdem Sasmaz, James E. Parks II, "Evaluation of Mixed Oxide Catalysts for Lean Diesel Applications," *CLEERS Workshop*, Ann Arbor, MI, April 7, 2016.
18. Todd J. Toops, Eleni A. Kyriakidou, Jae-Soon Choi, Andrew Binder, James E. Parks II, "Impact of Mixed Metal Oxides Supports on the Durability and Low-Temperature Performance of Pd-based Diesel Oxidation Catalysts," *2016 CLEERS Workshop*, Ann Arbor, MI, April 6, 2016.

## III.6 Emissions Control for Lean-Gasoline Engines

### Overall Objectives

- Assess and characterize catalytic emission control technologies for lean-gasoline engines
- Identify strategies for reducing the costs, improving the performance, and minimizing the fuel penalty associated with emission controls for lean-gasoline engines
- Identify a technical pathway for a lean-gasoline engine to meet U.S. Environmental Protection Agency Tier 3 emission regulations with minimal fuel consumption and cost
- Demonstrate the fuel efficiency improvement of a low-emission, lean-gasoline engine relative to the stoichiometric gasoline engine case on an engine dynamometer platform

### Fiscal Year (FY) 2016 Objectives

- Characterize the performance of three-way catalyst (TWC) formulations for  $\text{NH}_3$  production during cold start conditions on a bench flow reactor
- Determine the effects of  $\text{NH}_3:\text{NO}_x$  ratio on passive selective catalytic reduction (SCR) performance on the engine research platform
- Characterize the dispersion of platinum group metals (PGM) on the TWC in the passive SCR system by accelerated aging on a bench flow reactor with aging conditions defined in collaboration with industry partners General Motors and Umicore

### FY 2016 Accomplishments

- Completed evaluation of a matrix of TWC formulations under cold start conditions, and demonstrated that  $\text{NH}_3$  can be produced at >80% efficiency beginning at  $150^\circ\text{C}$
- Determined that the optimal  $\text{NH}_3:\text{NO}_x$  ratio is 1.13 at TWC and SCR temperatures of  $470^\circ\text{C}$  and  $350^\circ\text{C}$ , respectively to achieve minimal  $\text{NO}_x$ ,  $\text{NH}_3$ , and  $\text{N}_2\text{O}$  tailpipe emissions
- With a scanning transmission electron microscope (STEM), measured the distribution of PGM particle sizes on TWCs aged for 25 h, 50 h, and 100 h with an accelerated aging protocol performed on the bench flow reactor
- Investigations of the impacts of sulfur, a known catalyst poison, on TWC function after hydrothermal aging were

**Jim Parks (Primary Contact),**

**Todd Toops, Josh Pihl,**

**Vitaly Prikhodko**

Oak Ridge National Laboratory

2360 Cherahala Blvd.

Knoxville, TN 37932

Phone: (865) 946-1283

Email: parksjeii@ornl.gov

DOE Technology Development Manager:

Ken Howden

Subcontractor:

University of South Carolina, Columbia, SC

conducted; studies demonstrated reversal of negative effects via desulfation techniques and are continuing in FY 2017 with other TWCs ■

### Introduction

Currently, the U.S. passenger car market is dominated by gasoline engine powertrains that operate at stoichiometric air-to-fuel ratios (sufficient fuel is mixed in air such that all of the oxygen in the air is consumed during combustion). Stoichiometric combustion leads to exhaust conditions suitable for TWC technology to reduce  $\text{NO}_x$ ,  $\text{CO}$ , and hydrocarbon emissions to extremely low levels. Operating gasoline engines at lean air-to-fuel ratios (excess air) enables more efficient engine operation and reduces fuel consumption; however, the resulting oxygen in the exhaust prevents the TWC technology from reducing  $\text{NO}_x$  emissions. It is relatively straightforward to operate an engine lean over a significant portion of the load and speed operating range; so, the largest challenge preventing fuel-saving lean combustion in gasoline applications is the control of emissions, primarily  $\text{NO}_x$ . This project addresses the challenge of reducing emissions from fuel-saving lean gasoline engines in a cost-effective and fuel-efficient manner to enable their market introduction.

### Approach

This project utilizes the full suite of capabilities available at Oak Ridge National Laboratory's National Transportation Research Center, including a lean-gasoline engine on an engine dynamometer, simulated exhaust flow

reactors for detailed catalyst evaluations under carefully controlled operating conditions, material characterization tools for catalyst analysis, and vehicle system level modeling. The combination of catalyst studies on flow reactor and engine platforms is a key component of the project approach. Prototype catalyst formulations are first studied on flow reactors to understand catalytic function and establish operating parameters in a controlled setting; then, select catalyst combinations are studied on the engine platform to characterize performance under realistic exhaust conditions. The engine studies also enable direct measurement of fuel consumption benefits from lean-gasoline engine operation as well as measurement of “fuel penalties” imposed by the emission control system to function properly.

The engine platform for the project is from a model year 2008 BMW 120i vehicle sold in Europe. The 4-cylinder, direct injection, naturally aspirated engine operates in multiple modes including lean (excess air) and stoichiometric combustion. The BMW 120i employs both a TWC for stoichiometric operation and a lean  $\text{NO}_x$  trap catalyst for  $\text{NO}_x$  reduction during lean operation. Although this engine and aftertreatment combination met the relevant emissions regulations in Europe, as configured its emissions are well above the current and pending U.S. emissions standards. Furthermore, the lean  $\text{NO}_x$  trap catalyst contains high levels of platinum group metals, which add significantly to the overall cost of the vehicle. The goal for this project is to identify emissions control technologies that could meet the U.S. Environmental Protection Agency Tier 3 emission standards, which require additional reductions of 70% for  $\text{NO}_x$  and 85% for hydrocarbons compared to the previous Tier 2 standard. In addition to the emissions goal, the project aims to maximize the fuel efficiency benefit from lean-gasoline engine operation and minimize system cost.

To date, the project has primarily focused on an emission control concept known as “passive SCR” [1–3]. The key to the approach is to generate  $\text{NH}_3$  over the TWC under slightly rich conditions and then store it on a downstream SCR. After returning to lean operation, the stored  $\text{NH}_3$  reduces  $\text{NO}_x$  that is not converted over the upstream TWC. In this manner, the TWC controls  $\text{NO}_x$  during stoichiometric and rich operation of the engine, and the SCR catalyst controls  $\text{NO}_x$  during lean-engine operation. This report highlights results from both engine and flow reactor experiments of passive SCR emission control catalysts and systems. The catalysts used in the system were either supplied or recommended by Umicore, a major catalyst supplier to the automotive industry. Frequent interaction occurred with collaborating partners Umicore and General Motors to guide project progress

and relevance. The University of South Carolina is also a collaborating partner on the project.

## Results

In FY 2015, flow reactor studies were conducted to quantify  $\text{NH}_3$  yield from a matrix of TWCs provided by Umicore in the temperature range of 300–650°C. Follow-up investigations specific to the low temperature performance of the TWCs were conducted in FY 2016. Low temperature performance is important for the cold start region of the regulation drive cycle where most emissions from the vehicle occur. In stoichiometric engine vehicles, exhaust temperatures are increased as rapidly as possible to attain TWC temperatures where  $\text{NO}_x$ ,  $\text{CO}$ , and hydrocarbons can be controlled (nominally around 250°C). For the lean-gasoline vehicle case, the potential to produce  $\text{NH}_3$  during cold start was studied by evaluating TWCs at low temperatures and over a range of air-to-fuel ratios. The objective was to determine if  $\text{NH}_3$  could be produced during cold start; if so, complete drive cycle fuel economy could be improved by reducing time at rich conditions for  $\text{NH}_3$  production after catalyst warm up.

Although five different TWC formulations were studied, the performance trends were similar for all catalysts. For this report, results from a commercial TWC with primarily Pd as the active catalyst will be shown; the catalyst is known as “Malibu-1” since it was obtained from the front portion of a super ultra-low emission vehicle Chevrolet Malibu. Figure 1 shows the conversion efficiency of several pollutant species by the Malibu-1 TWC during a temperature ramp from 100–600°C. NO and CO are the first species that the TWC is active at converting, with sharp increases in conversion below 150°C. Shortly after NO and CO “light-off” (a common term representing the temperature at which a catalyst is active),  $\text{NH}_3$  production begins and increases to 100% conversion before 200°C. Hydrocarbons (represented by  $\text{C}_3\text{H}_8$  in this study) are the last species to be actively converted on the catalyst during the temperature ramp. Note that  $\text{C}_3\text{H}_8$  is a difficult hydrocarbon to oxidize catalytically, so it represents a worst case scenario regarding hydrocarbon conversion. Importantly, the catalyst can produce  $\text{NH}_3$  at lower temperatures than hydrocarbons are converted. It is also important to note the production of  $\text{N}_2\text{O}$  in the temperature range of 100–150°C. Since  $\text{N}_2\text{O}$  is a greenhouse gas, it is not a desired product, but fortunately, it is only produced at low temperatures.

The results shown in Figure 1 were obtained with an equivalence ratio ( $\lambda$ ) of 0.97. Here  $\lambda$  is the ratio of actual air-to-fuel ratio to stoichiometric air-to-fuel ratio; so,  $\lambda < 1$  indicates rich combustion. The temperature ramp

shown in Figure 1 was repeated across a  $\lambda$  range of 0.95 to 1. In this manner, the optimal  $\lambda$  for producing  $\text{NH}_3$  while minimizing  $\text{N}_2\text{O}$  formation could be determined. Figure 2 shows the lowest temperatures at which  $\text{NH}_3$  is formed at >80% efficiency and  $\text{N}_2\text{O}$  is formed at less than 10% efficiency as a function of  $\lambda$ . A  $\lambda$  of 0.97 was found to be optimal for maximizing  $\text{NH}_3$  production while minimizing  $\text{N}_2\text{O}$  formation.

The selectivity to  $\text{N}_2\text{O}$  production was also studied in engine-based studies of the passive SCR system composed of the same Malibu-1 TWC plus a downstream SCR catalyst. Engine operation was controlled to alternate between lean ( $\lambda > 1$ ) and rich ( $\lambda < 1$ ) operation. The intent of the rich operation was to produce  $\text{NH}_3$  over the TWC for subsequent storage and use on the SCR catalyst for  $\text{NO}_x$  reduction during lean engine operation. Ideally, an average  $\text{NH}_3:\text{NO}_x$  ratio of 1 would be sufficient to reduce the  $\text{NO}_x$  to  $\text{N}_2$  over the SCR catalyst; however, some

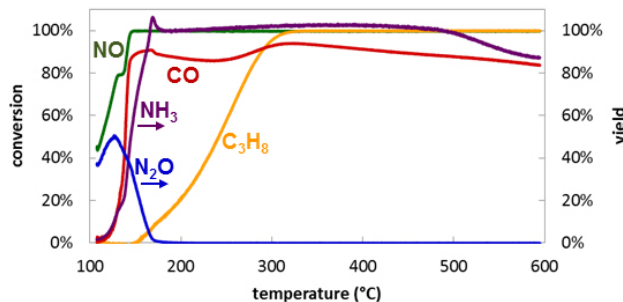


Figure 1. Conversion of NO, CO, and  $\text{C}_3\text{H}_8$  to  $\text{NH}_3$  and  $\text{N}_2\text{O}$  (expressed as yield relative to inlet NO) as a function of temperature during a temperature ramp for the Malibu-1 TWC at  $\lambda = 0.97$

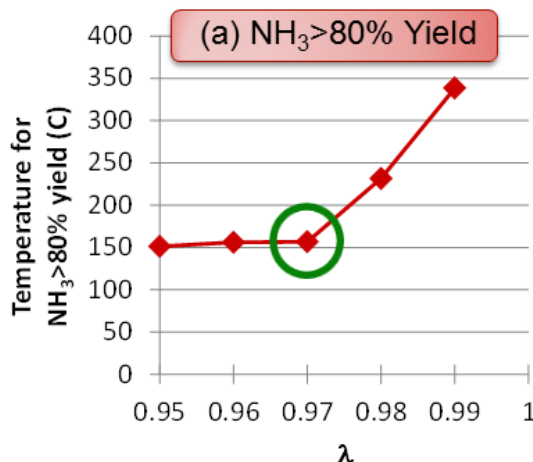


Figure 2. Lowest TWC temperature at which  $\text{NH}_3$  is formed at >80% yield (a) and  $\text{N}_2\text{O}$  is formed at <10% yield (b) as a function of  $\lambda$  during temperature ramps of the Malibu-1 TWC; green circles highlight the optimal  $\lambda$  to achieve maximum  $\text{NH}_3$  production with minimal  $\text{N}_2\text{O}$  formation at the lowest temperature

$\text{NH}_3$  is lost by oxidation on the SCR catalyst. During the study, the ratio of the time running slightly rich to the time running lean combustion of the engine was varied to produce different average  $\text{NH}_3:\text{NO}_x$  as measured downstream of the TWC (and upstream of the SCR catalyst). Figure 3 shows the  $\text{NO}_x$  conversion obtained by the system during the sweep of  $\text{NH}_3:\text{NO}_x$ .  $\text{NO}_x$  conversion increases with increasing  $\text{NH}_3:\text{NO}_x$ , with >99% conversion occurring at  $\text{NH}_3:\text{NO}_x = 1.13$ . For reference, the corresponding dose of  $\text{NH}_3$  as a function of the storage capacity of the SCR catalyst is also shown, and increases some with increasing  $\text{NH}_3:\text{NO}_x$  ratio while staying in the range of 20–40% of total  $\text{NH}_3$  storage capacity.

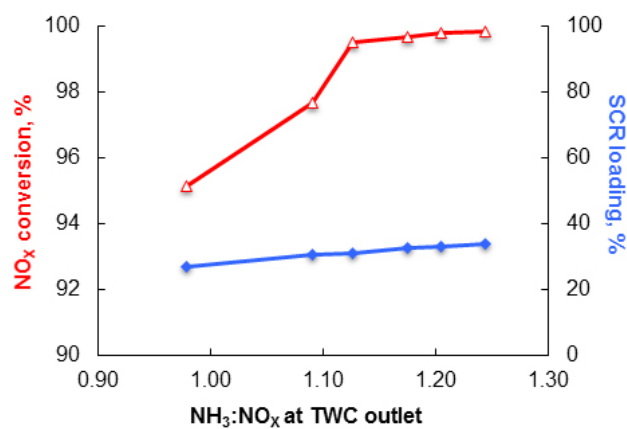
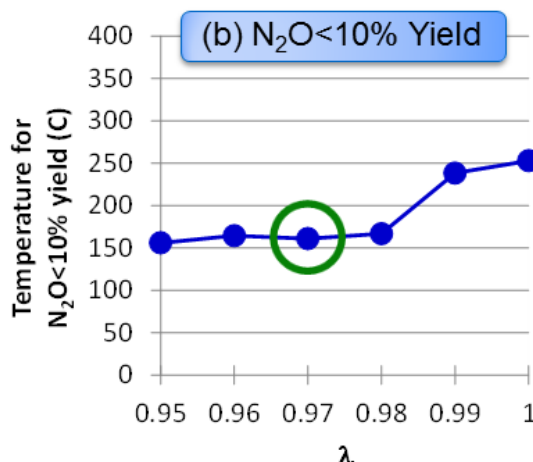


Figure 3.  $\text{NO}_x$  conversion as a function of  $\text{NH}_3:\text{NO}_x$  measured at the TWC outlet over engine lean-rich cycles in which the lean to rich periods were varied to control  $\text{NH}_3:\text{NO}_x$ . The corresponding  $\text{NH}_3$  loading on the SCR catalyst with each cycle as a function of total SCR  $\text{NH}_3$  storage capacity is also shown for reference.



Emissions of  $\text{NO}_x$ ,  $\text{NH}_3$ , and  $\text{N}_2\text{O}$  were monitored at the tailpipe (downstream of the SCR catalyst) during the sweep of  $\text{NH}_3:\text{NO}_x$  shown in Figure 3. Figure 4 shows the average concentrations over the lean–rich cycle as a function of  $\text{NH}_3:\text{NO}_x$ .  $\text{NO}_x$  emissions decrease as  $\text{NH}_3:\text{NO}_x$  increases, as expected. However,  $\text{NH}_3$  slip from the SCR catalyst can occur at the highest  $\text{NH}_3:\text{NO}_x$  ratios.  $\text{N}_2\text{O}$  is measured; however,  $\text{N}_2\text{O}$  levels do not vary much with changing  $\text{NH}_3:\text{NO}_x$ . It was observed that  $\text{N}_2\text{O}$  is primarily formed during the lean phase of engine operation over the SCR catalyst at a concentration of  $\sim 2$  ppm. Thus, the engine lean–rich cycling can be used to maximize  $\text{NO}_x$  conversion with minimal  $\text{NH}_3$  emissions, but SCR formulation improvements may be needed to further minimize  $\text{N}_2\text{O}$  emissions.

Another aspect of the project involves durability studies of the catalysts, which is important since regulations require catalyst performance up to full useful life (generally defined as 150,000 miles for a light-duty vehicle). Performance of the Malibu-1 TWC aged over a four-mode cycle including lean, rich, and stoichiometric conditions was characterized during FY 2015. In FY 2016, material analysis of the aged catalysts was conducted to understand the degradation mechanisms occurring during the aging process. TWC samples were imaged with a STEM at magnifications suitable to resolve individual Pd particles on the catalyst surface. X-ray emission analysis during STEM imaging was used to selectively image the Pd particles. Figure 5 shows the raw and Pd-specific STEM images of the catalyst. Images of the TWC at different aging times were analyzed to measure the distribution of Pd particle diameter; the results are shown in Figure 6. As expected, sintering of the Pd occurs with aging, with the largest change in particle size distribution occurring during

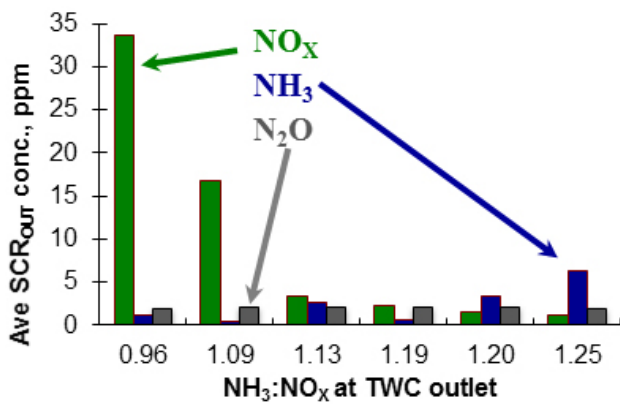


Figure 4. Lean–rich cycle average concentrations of  $\text{NO}_x$ ,  $\text{NH}_3$ , and  $\text{N}_2\text{O}$  measured at the SCR outlet position (tailpipe) as a function of  $\text{NH}_3:\text{NO}_x$  ratio for the same engine results shown in Figure 3

the first 25 h of aging. This was also the aging time frame over which the largest changes in catalyst performance occurred. Durability studies are continuing with investigations of the impact of sulfur, a known catalyst poison, on catalyst performance.

## Conclusions

Experimental research on the passive SCR approach to control  $\text{NO}_x$  emissions from lean-gasoline direct injection engines was conducted on both flow reactor and engine platforms. Conclusions are:

- $\text{NH}_3$  can be produced over the TWC during cold start conditions at temperatures near 150°C; cold start  $\text{NH}_3$

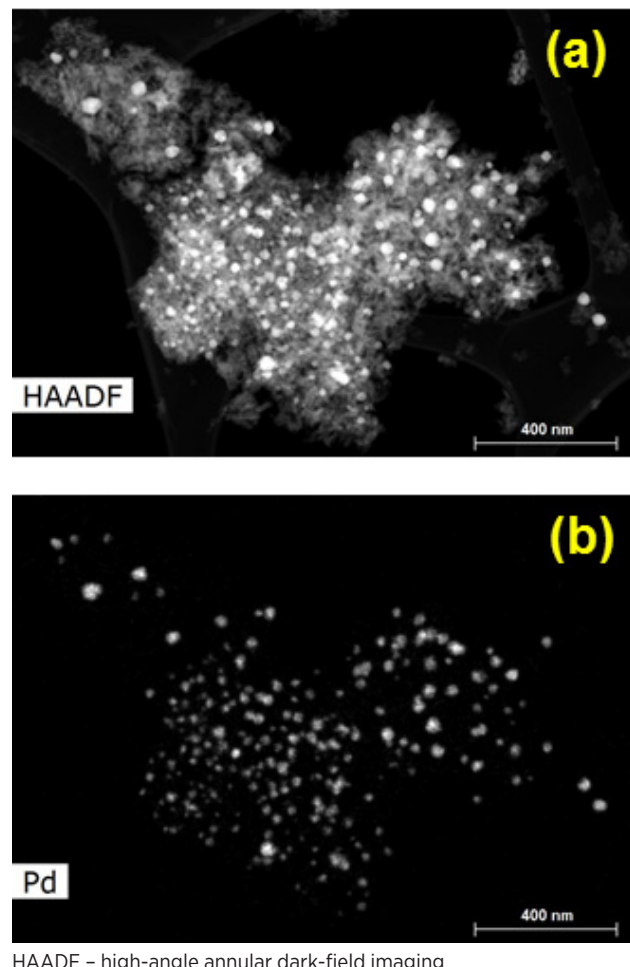


Figure 5. STEM images of the Malibu-1 TWC; image (a) is the raw STEM image and image (b) shows Pd only based on X-ray emission analysis mapping. Images were obtained using instrumentation (FEI Talos F200X STEM) provided by the Department of Energy, Office of Nuclear Energy, Fuel Cycle R&D Program and the Nuclear Science User Facilities. STEM images collected by Michael Lance (Oak Ridge National Laboratory).

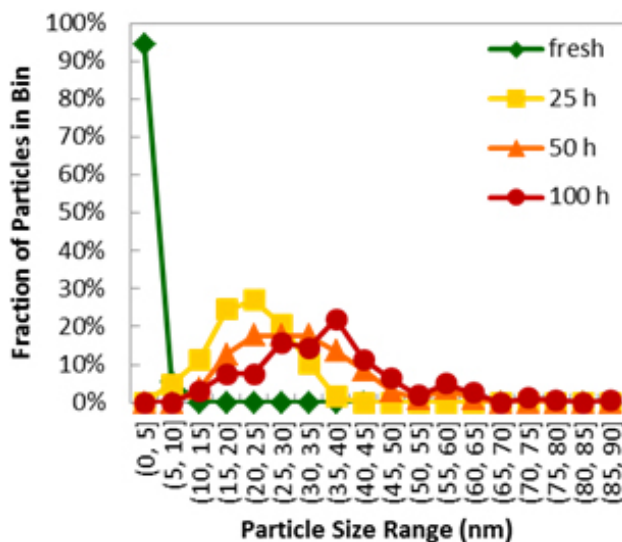


Figure 6. Histograms of the distribution of Pd particle sizes for the Malibu-1 TWC aged for different amounts of time with a four-mode accelerated aging protocol

production can help reduce rich engine operation after warm-up and thereby reduce the fuel penalty for  $\text{NH}_3$  production over a given drive cycle.

- Engine rich-lean cycling can be adjusted to maximize  $\text{NO}_x$  conversion and minimize  $\text{NH}_3$  slip to the tailpipe; a  $\text{NH}_3:\text{NO}_x$  of 1.13 was found to be optimal.  $\text{N}_2\text{O}$  formation occurs at low levels and is not affected significantly by varying  $\text{NH}_3:\text{NO}_x$ .
- Sintering of Pd was observed in accelerated aging studies and was typical of PGM catalysts. Most of the sintering occurs in the first 25 h of aging, after which changes in particle size distribution are less pronounced.

## References

1. Li, W., Perry, K., Narayanaswamy, K., Kim, C. et al., "Passive Ammonia SCR System for Lean-burn SIDI Engines," *SAE Int. J. Fuels Lubr.* 3(1):99–106, 2010, doi:10.4271/2010-01-0366.
2. Kim, C., Perry, K., Viola, M., Li, W. et al., "Three-Way Catalyst Design for Ureless Passive Ammonia SCR: Lean-Burn SIDI Aftertreatment System," *SAE Technical Paper* 2011-01-0306, 2011, doi:10.4271/2011-01-0306.
3. Guralp, O., Qi, G., Li, W., and Najt, P., "Experimental Study of  $\text{NO}_x$  Reduction by Passive Ammonia-SCR for Stoichiometric SIDI Engines," *SAE Technical Paper* 2011-01-0307, 2011, doi:10.4271/2011-01-0307.

## FY 2016 Publications/Presentations

1. Vitaly Prikhodko, James Parks, Josh Pihl, and Todd Toops, "Ammonia generation and utilization in a passive SCR (TWC+SCR) system on lean gasoline engine," *SAE International Journal of Engines* 9 2016-01-0934 (2016).
2. James E. Parks, John Storey, Vitaly Prikhodko, Melanie Debusk, Sam Lewis, "Filter-based control of particulate matter from a lean gasoline direct injection engine," *SAE Technical Paper Series* 2016-01-0937 (2016).
3. Alla Zelenyuk, Jacqueline Wilson, Dan Imre, Mark Stewart, George Muntean, John Storey, Vitaly Prikhodko, Samuel Lewis, Mary Eibl, and James Parks, "Detailed Characterization of Particulate Matter Emitted by Lean-Burn Gasoline Direct Injection Engine," *International Journal of Engine Research* [under review].
4. Vitaly Prikhodko, James E Parks, Josh A Pihl, and Todd J Toops, "Passive SCR for lean gasoline  $\text{NO}_x$  control: engine-based strategies to minimize fuel penalty associated with catalytic  $\text{NH}_3$  generation," *Catalysis Today* 267, pp. 202–209 (2016).
5. Jim Parks, Todd Toops, Josh Pihl, Vitaly Prikhodko, "Emissions Control for Lean Gasoline Engines," 2016 DOE Vehicle Technologies Office Annual Merit Review, Washington, DC, June 6–9, 2016. [available at <http://energy.gov/eere/vehicles/vehicle-technologies-office-annual-merit-review-presentations>]
6. Vitaly Prikhodko, Jim Parks, Josh Pihl, and Todd Toops, "Ammonia Generation and Utilization in a Passive SCR (TWC+SCR) System on Lean Gasoline Engine," *2016 CLEERS Workshop*, April 6–8, 2016. [available at <http://www.cleers.org/workshops/workshop2016/index.php>]
7. Vitaly Prikhodko, James Parks, Josh Pihl, and Todd Toops, "Ammonia generation and utilization in a passive SCR (TWC+SCR) system on lean gasoline engine," *2016 SAE World Congress*, April 12–14, 2016. [presentation associated with publication #1]
8. James E. Parks, John Storey, Vitaly Prikhodko, Melanie Debusk, Sam Lewis, "Filter-based control of particulate matter from a lean gasoline direct injection engine," *2016 SAE World Congress*, April 12–14, 2016. [presentation associated with publication #2]

## III.7 Cummins-ORNL SmartCatalyst CRADA: NO<sub>x</sub> Control and Measurement Technology for Heavy-Duty Diesel Engines

### Overall Objectives

- Understand the fundamental chemistry of automotive catalysts
- Identify strategies for enabling self-diagnosing catalyst systems
- Address critical barriers to market penetration

### Fiscal Year (FY) 2016 Objectives

- Compare impact of two separate field ageing experiences on catalyst performance
- Apply spatially resolved capillary inlet mass spectrometry (SpaciMS) data to critically assess a predictive selective catalytic reduction (SCR) catalyst model
- Mine cooperative research and development agreement (CRADA) data and insights for catalyst state assessment methodologies

### FY 2016 Accomplishments

- Spatially distributed performance of two separate field-aged catalyst samples assessed relative to each other and the same commercial catalyst in the degreened (DG) state
- Cummins predictive SCR model tuned and assessed via intra-catalyst SpaciMS data
- Practical method for catalyst state assessment demonstrated
- Two archival publications, one journal cover feature, and one oral presentation ■

### Introduction

A combination of improved technologies for control of NO<sub>x</sub> and particulate emissions are required to efficiently meet increasingly stringent emission regulations. This CRADA section focuses on catalyst technologies.

Improved catalyst system efficiency, durability, and cost can be achieved through advanced control methodologies based on continuous catalyst state monitoring. The overarching goal of this CRADA section is to enable

**Bill Partridge<sup>1</sup> (Primary Contact),  
Neal Currier<sup>2</sup>, Saurabh Joshi<sup>2</sup>,  
Mariam Salazar<sup>1</sup>,  
Krishna Kamasamudram<sup>2</sup>,  
Alex Yezers<sup>2</sup>**

<sup>1</sup>Oak Ridge National Laboratory (ORNL)

2360 Cherahala Blvd.

Knoxville, TN 37932

Phone: (865) 946-1234

Fax: (865) 946-1354

Email: partridgewp@ornl.gov

<sup>2</sup>Cummins Inc.

Columbus, IN 47201

DOE Technology Development Manager:

Ken Howden

self-diagnosing or smart catalyst systems. These are enabled by basic and practical insights into the transient distributed nature of catalyst performance, improved catalyst models, insights suggesting control methodologies, and instrumentation for improved control. Development and application of enhanced diagnostic tools is required to realize these technology improvements.

### Approach

The CRADA applies the historically successful approach of developing and applying minimally invasive advanced diagnostics to resolve spatial and temporal function and performance variations within operating catalysts. Diagnostics are applied to study the detailed nature and origins of catalyst performance variations; this may be spatial and temporal variations unique to each catalyst function during operating and how these vary with ageing. This detailed information is applied to understand how catalysts function and degrade, develop device and system models, and develop advanced control strategies.

### Results

In FY 2016, the CRADA focused on comparing the impact of two separate normal field-ageing events via

assessing the intra-catalyst distributed performance of a field-aged (FA) commercial copper-containing silicoaluminophosphate (Cu/SAPO-34) SCR catalyst under standard SCR conditions and comparing to that of the same catalyst in a DG state previously characterized in the CRADA. The data was also used to assess a predictive catalyst model. Moreover, the data was mined for insights regarding catalyst state assessment, and a practical method for on-road application was demonstrated.

### **Assessing Impact of Field Ageing on the Distributed Performance of a Commercial Catalyst**

The distributed performance of a second field-aged sample (FA-2) was evaluated by comparison to that of a previously investigated sample FA-1. The FA-1 and FA-2 samples are both commercial Cu/SAPO-34 samples of the same formulation, but which were applied on different vehicles; they both have normal field performance. Although there is value in controlled ageing, e.g., where histograms of specific thermal exposure are known, there is similar value in field-aged samples that have been exposed to uncontrolled real-world, in-use conditions. This is the nature of the FA-1 and FA-2 samples, and is valuable for critically assessing the performance of Cummins' predictive catalyst models. Comparison of a second field-aged sample provides insights regarding how broadly the findings from the FA-1 analysis can be applied.

The spatially distributed performances of the FA samples are compared to that of the same catalyst in the DG state in Figure 1. Figures 1a and 1b show the impact of ageing on distributed SCR conversion and total  $\text{NH}_3$  capacity (TC). In general FA degrades both conversion and capacity, in a proportional way, i.e., the greater conversion of FA-2 vs. FA-1 is consistent with its greater TC. Figures 1c and 1d show the impact of ageing on distributed capacity components; TC, dynamic capacity (DC), and unused capacity (UC), where DC is the capacity under SCR conditions, and there is a balance between TC and the sum of DC and UC. The impact of field ageing on the distributed capacity components is generally similar for the two FA samples relative to the DG performance. Specifically FA reduces TC and UC with a lesser impact on the DC distribution. By degrading SCR conversion, FA causes higher  $\text{NH}_3$  concentrations to exist deeper into the catalyst causing the DC–TC separation point to correspondingly shift (shift in the orange circled point in Figure 1c and 1d). The similar correlations between the capacity components for the various catalyst states is consistent with using UC as a basis to measure catalyst state and associated state-dependent parameters for updating a predictive model throughout the catalyst's

life. The nature of the shifting DC–TC separation point with ageing is consistent with the operando isotherms shown in Figure 1e. These isotherms are measured under SCR conditions, and specifically with both  $\text{NO}_x$  and  $\text{NH}_3$  present, vs. more traditional isotherm conditions involving  $\text{NH}_3$  adsorption at varying partial pressures in the absence of  $\text{NO}_x$ . The isotherm is consistent with Langmuir adsorption on two sites. Figure 1e shows that the isotherm shape is approximately the same at a given temperature for the three catalyst states, DG, FA-1, and FA-2. This indicates that field ageing does not selectively impact a single of the two adsorption sites, but rather proportionally impacts the two sites. Thus, although field ageing reduces the TC,  $\text{NH}_3$  adsorption occurs in the same way. As such, the same adsorption model can be used for a range of catalyst states, requiring only a scalar factor to account for the TC loss. This was similarly apparent from the results in Figures 1c and 1d showing similar relation between the capacity components for the various catalyst states scaled by the varying TC.

### **Assessing Distributed Intra-Catalyst Performance of a Predictive SCR-Catalyst Model**

A predictive model which can accurately determine the internal distributed catalyst properties over a range of catalyst states has broad applicability for enabling advanced engine catalyst system performance throughout the design, development, and life of that system; i.e., such models enhance design tools resulting in more reliable analysis-led design, which in turn results in faster and lower-cost development and improved component specification (e.g., size, cost). Versions of these predictive models can be used in field-deployed systems resulting in improved on-board diagnostics (OBD), control, efficiency, and durability. Cummins has developed such a predictive catalyst performance model based on in-house effluent performance of the DG catalyst. There are many ways to structure the internal workings of this predictive model, and many parameters to fit. The CRADA data presented in Figure 1 was used to critically assess the performance of Cummins' predictive model with respect to determining distributed intra-catalyst performance and field ageing impacts. Figure 2 compares the experimentally measured intra-catalyst performance distributions for the catalyst in the DG and FA-2 states to those resulting from Cummins' predictive model. While the model was developed based on effluent measurements from the DG sample, only the SCR pre-exponential factor was modified for fitting the FA-2 experimental results. This factor is proportional to site density and the modified value reflects FA-induced site loss. Figure 2 shows that the model can accurately predict intra-catalyst conversion distributions over a range

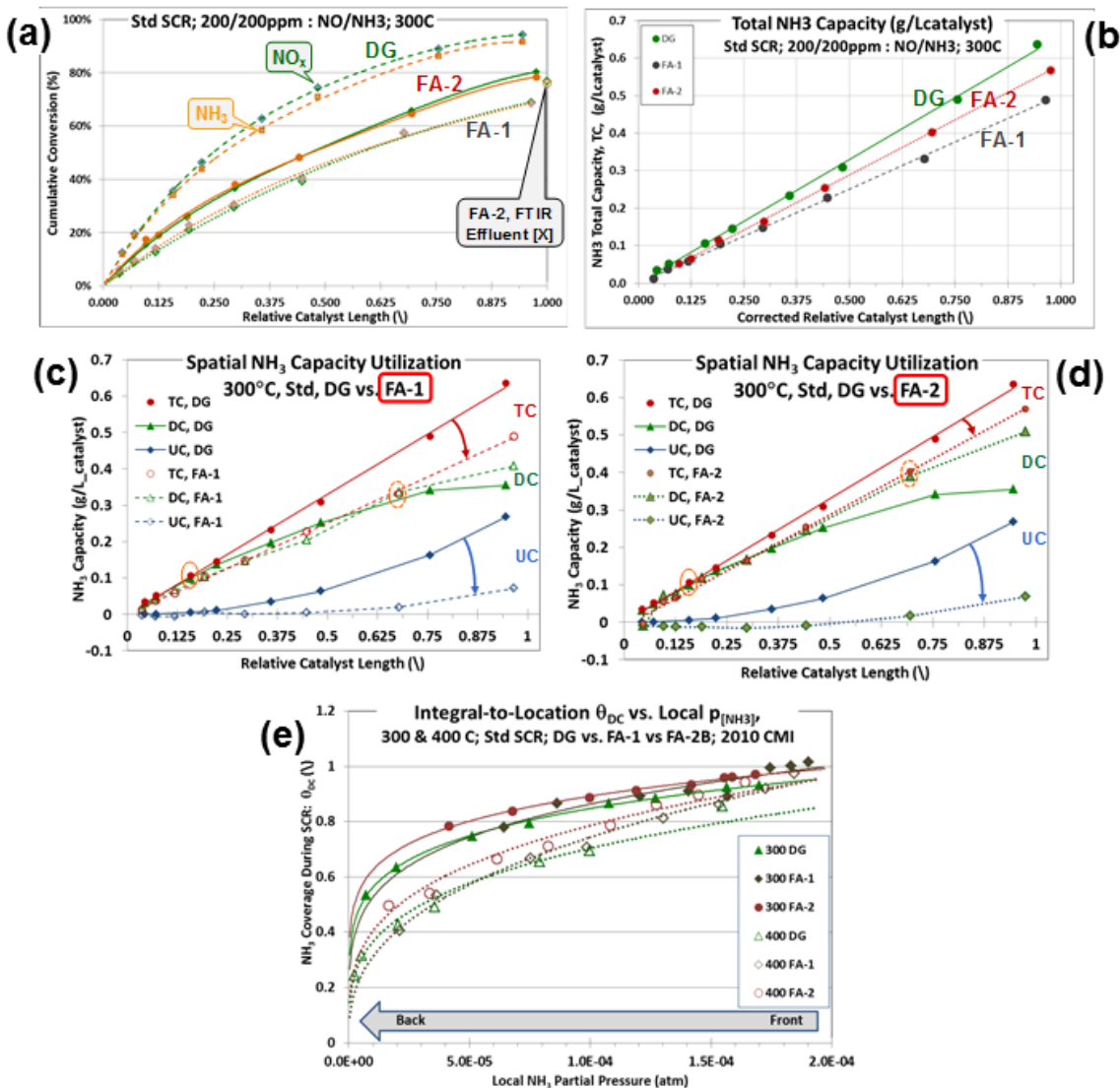


Figure 1. Impact of FA-1 and FA-2 relative to the DG catalyst state on (a) distributed  $NO_x$  and  $NH_3$  conversion, (b) total  $NH_3$  capacity; (c & d) distributed  $NH_3$  capacity components; total, dynamic, and unused; and (e) adsorption energetics, as measured by operando isotherms. Dynamic capacity is that under SCR conditions, and TC is the sum of DC and UC. Operando isotherms refers to isotherms measured with the catalyst under SCR conditions vs. with  $NH_3$  exposure in the absence of  $NO_x$ .

of values for the two catalyst states. This is particularly significant at 300°C, near peak performance where effluent conversions are at or near 100%. Similarly, the model does an excellent job predicting the distributed  $NH_3$  capacity utilization in the two states. Specifically, the model accurately reflects the various relationships between the capacity components observed with the experimental data, and supports the concept of a UC-based measure of catalyst state and state-related parameter determination. Possibly, with additional work, the modified pre-exponential factor used to fit the base DG-developed model to the FA-2 data could be determined from such a measurement. The fidelity of the predictive

model gives the CRADA team confidence in using it to design OBD parts and reduce catalyst design margins.

### Methodology for On-Road Catalyst State Assessment

Measurements to determine catalyst state are needed to optimize on-board diagnostics and through-life catalyst performance. Such measurements can quantify the impact of various ageing processes on specific catalyst functions and be used in conjunction with predictive catalyst performance models to enable advanced OBD and adaptive control, e.g., age-dependent model parameters can be determined based on the catalyst

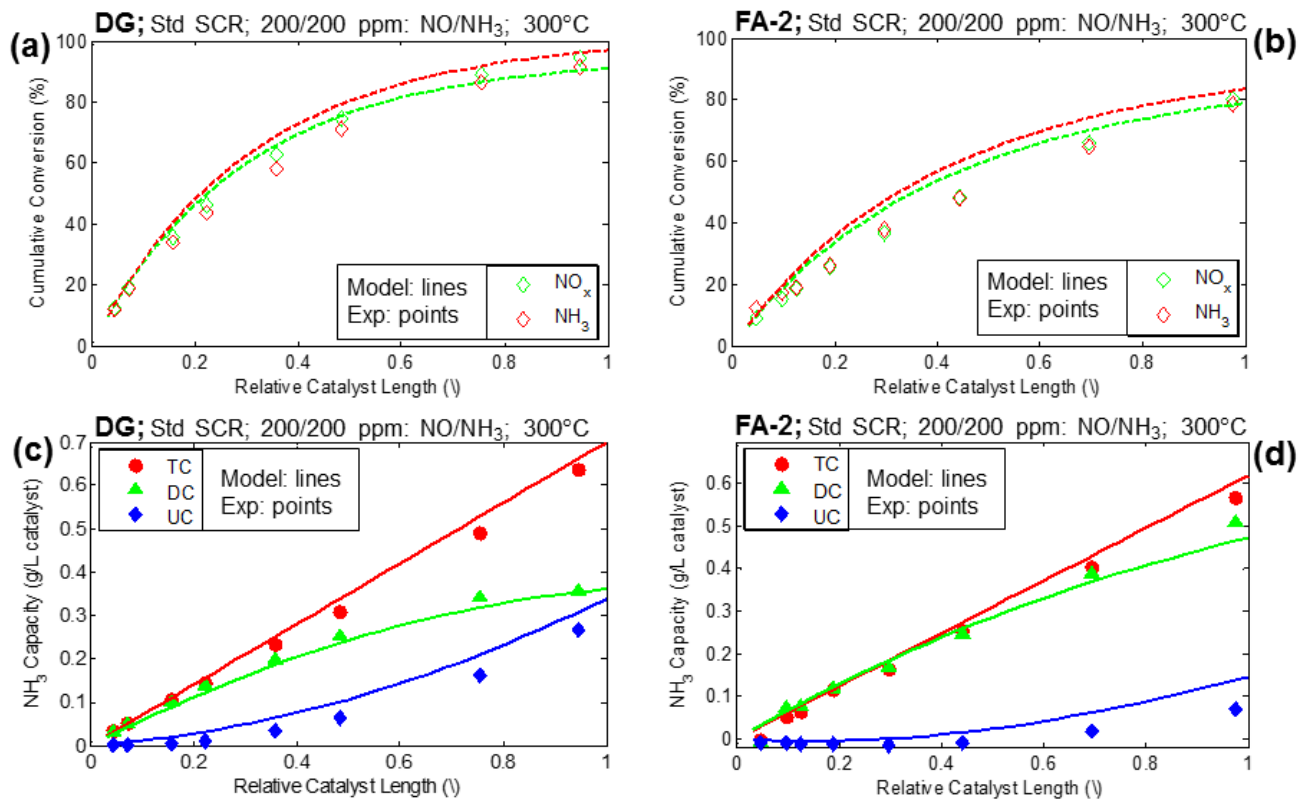


Figure 2. Comparison of predictive model distributed intra-catalyst performance results with experimental measurements

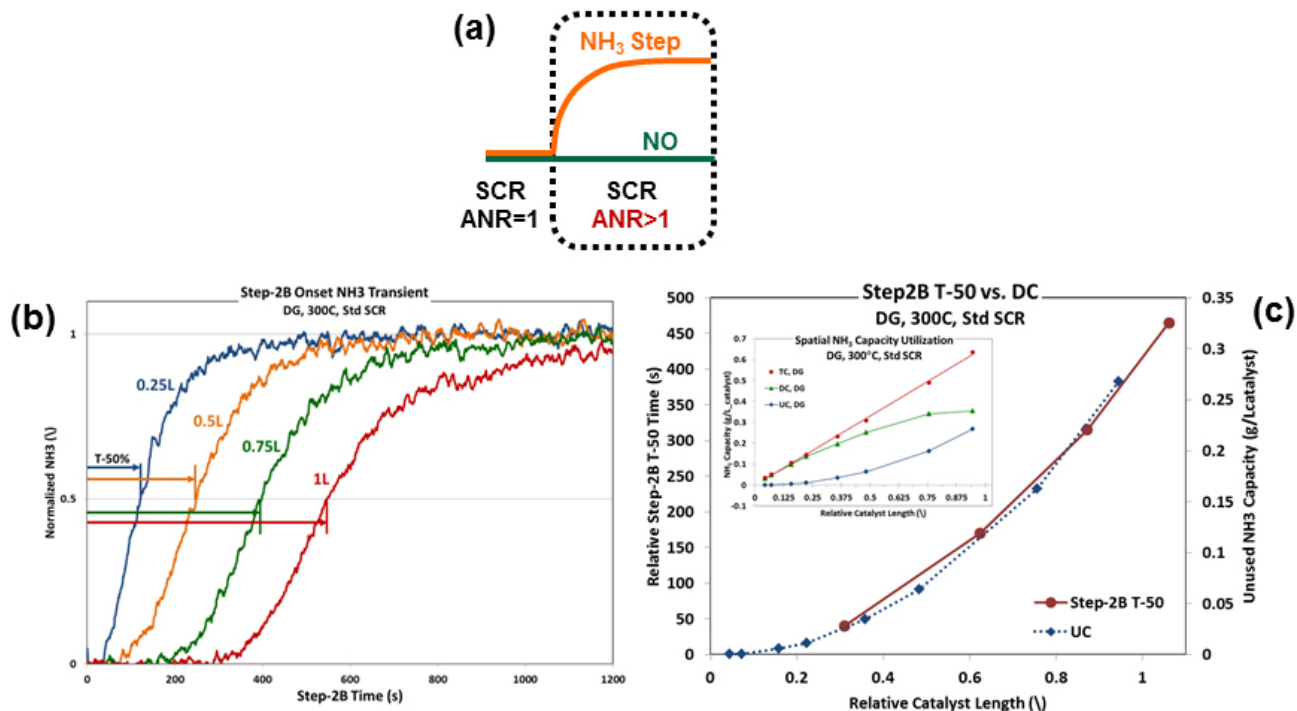
state measurements. While the four-step protocol (4SP) used to acquire the data of Figure 1 is valuable for detailed laboratory studies, it is not practical for on-road determination of catalyst performance; an alternate practical method is needed for detecting UC variations in on-road applications. Figure 3a shows a step in ammonia-to- $\text{NO}_x$  ratio (ANR), that was used to demonstrate practical determination of UC variations and catalyst state sensing. The SCR ANR = 1 portion in Figure 3a is equivalent to Step 2 of the 4SP where the DC values in Figure 1 are determined, and thus the same DC exists in the two experiments. Unused capacity exists when DC is less than TC (Figures 1c and 1d), and in such cases adding additional  $\text{NH}_3$  via an ANR step will populate some of this UC. Ammonia used to populate UC will be missing from the ANR step, producing a non-step loading profile as shown by the  $\text{NH}_3$  curve in Figure 3a. Specifically, the shape of the  $\text{NH}_3$  step during the ANR transient can be used to quantify UC. In practice, the nature of this loading curve can be used to determine variations in UC. In actuality, an ANR step will also increase TC and so the nature of the loading curve will reflect both UC and a TC change.

Figure 3b shows normalized  $\text{NH}_3$  transients associated with an inlet ANR step, measured at  $\frac{1}{4}$ ,  $\frac{1}{2}$ ,  $\frac{3}{4}$  and 1L along

the catalyst length for the commercial SCR catalyst in the DG state under standard SCR at 300°C. The indicated spatial locations in Figure 3b are nominal values. One method of characterizing the transient curves is via the 50% rise time (T-50). The T-50 monotonically increases along the catalyst axis; this is consistent with the general UC trend shown in Figures 1c and 1d. Figure 3c compares the UC distribution as determined by the 4SP (inset and blue dotted curve in Figure 3c) and the ANR step (see red curve in Figure 3c), and demonstrates that the curves are correlated. Specifically, the practical ANR step method is able to replicate UC spatial trends measured by the complex laboratory 4SP. While this practical method was demonstrated via effluent T-50 response to an ANR step, other transient probes (e.g.,  $\text{NO}_x$  pulse via load transient) and measures are possible and the ultimate realization would be to use a transient that naturally exists in the drive cycle. This provides a practical pathway for on-road catalyst state assessment for improved operation throughout the device life which could enhance efficiency, conversion performance and durability.

## Conclusions

- Impacts of normal field ageing are broadly applicable to different specific field-ageing experiences.



L – catalyst length

Figure 3. (a) An ANR step during continuous SCR provides a practical method for assessing UC via the shape of the effluent NH<sub>3</sub> response. (b) Normalized NH<sub>3</sub> transient during the ANR step at various locations along the catalyst and measured 50% rise time, T-50. (c) Comparison of UC and T-50 spatial distributions.

- FA degrades both conversion and NH<sub>3</sub> capacity in a proportional way
- FA degrades TC, but NH<sub>3</sub> adsorption occurs in same way
  - FA does not selectively impact one NH<sub>3</sub> capacity site over the other
  - The same NH<sub>3</sub> adsorption model can be used throughout catalyst life
- Cummins, predictive model accurately predicts the intra-catalyst distributed performance of the commercial Cu/SAPO-34 SCR catalyst in the DG and FA states
- Measuring catalyst effluent response to an input transient provides a practical methodology for on-road catalyst state assessment
  - Applicable for enhancing through-life catalyst performance
- The effectiveness of the CRADA approach for broadly advancing catalyst technology was demonstrated
  - Detailed information regarding distribution, network and sequence of reactions

- Applications to understanding how catalyst functions
- Applications to structuring catalyst models, determining model parameters, and tuning and validating models
- Insights for practical catalyst state assessment and control strategies

## FY 2016 Publications/Presentations

Two archival publications (AP), one cover feature (CF), and one oral presentation (OP)

1. Kevin Morgan, et al. (2016). ACS Catalysis 6, 1356–1381. **Invited, Cover Feature**, DOI:10.1021/acs.catal.5b02602; (AP, CF).
2. Maria Pia Ruggeri, et al. (2016). Topics in Catalysis 59:10-12 (2016) 907–912; doi.org/10.1007/s11244-016-0567-1 (AP).
3. W.P. Partridge, et al. 2016 DOE Vehicle Technologies Program Annual Merit Review, Washington, DC, June 9, 2016. [http://energy.gov/sites/prod/files/2016/06/f32/ace032\\_partridge\\_2016\\_o.pdf](http://energy.gov/sites/prod/files/2016/06/f32/ace032_partridge_2016_o.pdf) (OP)

## III.8 Ash-Durable Catalyzed Filters for Gasoline Direct Injection (GDI) Engines

### Overall Objectives

- Understand performance of three-way catalyst (TWC) coated gasoline particulate filters (GPFs) with variation of filter/coating design parameters
- Propose an ideal combination of filter/coating design parameters that benefits TWC performance and backpressure increase under engine oil-derived aging conditions

### Fiscal Year (FY) 2016 Objectives

- Evaluate TWC/GPF performance with different filter/coating designs for gaseous and particulate emissions
- Examine if TWC inner-coated GPFs are deactivated with engine oil-derived ash
- Investigate ash distribution in field- and lab-aged GPFs
- Initiate research on ash chemistries that affect TWC functionality with chemical attack/physical block

### FY 2016 Accomplishments

- Demonstrated the effects of TWC coating levels on initial TWC/GPF performance in terms of gaseous emissions conversions
- Improved the method to evaluate TWC performance with aging from the measurement of light-off temperatures
- Examined gaseous emissions conversions with varying oxygen–fuel equivalence ratio (lambda)
- Initiated ash distribution analyses of lab- and field-aged GPFs
- Proposed ash formation mechanism by analyzing ash nanoparticles under scanning transmission electron microscopy–energy dispersive X-ray spectroscopy (STEM-EDS) ■

### Introduction

Gasoline direct injection (GDI) engines, which feature direct injection of gasoline fuel into engine cylinders typically at high compression ratio, offer low fuel consumption and high power output. Although these benefits of GDI engines contribute to their increasing

**Hee Je Seong (Primary Contact),  
Seungmok Choi**

Argonne National Laboratory

9700 South Cass Avenue

Argonne, IL 60439

Phone: (630) 252-9239

Email: hseong@anl.gov

DOE Technology Development Manager:

Ken Howden

market share for passenger vehicles, their high particulate emissions will need to be significantly reduced to comply with future regulations. To achieve this goal, GPFs have been developed for GDI engines, like diesel particulate filters (DPFs) for diesel engines. Despite the similarity in function of GPFs and DPFs, however, GPFs require high porosity filters compared to DPFs to minimize backpressure sensitivity as GDI engines present high exhaust temperatures. In addition, GPFs can act as four-way catalysts that remove  $\text{NO}_x$ , CO, and hydrocarbons as well as particulates, with the incorporation of TWC into GPFs. As metal additives from engine oil are produced and eventually accumulated in GPFs with vehicle mileage, it is of great interest if TWC performance will be degraded with increased ash loading as known to occur in TWC-coated monoliths equipped in conventional gasoline engines.

### Approach

This project aims at detailing the impact of ash loading on TWC/GPF performance in variation of TWC coating level, GPF design and other parameters, ultimately proposing optimized design parameters of TWC coating and GPF designs when ash-derived chemical aging is concerned. Advanced prototype TWC/GPFs with different coating levels and filter types are prepared and their performance is examined with ash loading in terms of pressure drop, number and mass filtration efficiencies, and gaseous emissions conversion. Also, in order to find potential aging factors in TWC/GPFs, ash distributions in aged filter are analyzed by elemental mapping of wall microstructures and by X-ray microtomography. Moreover, interactions between catalysts and ash elements (in particular, phosphorus) and filter porosities are further

examined. In addition, metal additive-dependent ash chemistries are explored to detail potential ash-inhibiting factors by transmission electron microscopy and Advanced Photon Source facilities.

## Results

As a TWC is incorporated into the high porosity GPF wall, GPF performance, which is represented by pressure drop and filtration efficiency, was appreciably impacted with the TWC coating level, as noted in the 2015 report. To better understand its influence on initial TWC performance, two high porosity filters, HP300/8 (300 cells/in<sup>2</sup> and a wall thickness of 0.008 in) and HP200/12 (200 cells/in<sup>2</sup> and a wall thickness of 0.012 in), were selected for TWC coatings of 25 g/L, 50 g/L, and 100 g/L, while the amount of active platinum group metals (PGMs) remained constant at 0.5 g/L for the different coating levels. TWC performance was evaluated with respect to light-off temperatures (T50, the temperature where gaseous emissions conversions of 50% are achieved). The results for both GPFs are consistent as shown in Figure 1; T50 was lowered with increased TWC coating, indicating that the lower TWC coating is more efficient. Since active PGM catalysts are increasingly available with the decreased TWC coating when the PGM amount is identical, the lower TWC coating seems to be more active. In consideration of TWC performance as well as pressure drop and filtration efficiency from the 2015 result, the TWC coatings of 25 g/L and 50 g/L are favorable for the optimized coating level.

The effects of ash loading on TWC performance were explored for HP200/12 up to the ash loading of 20 g/L. As examined above, T50 was measured with increased ash loading, as found in Figure 2. Although the impact of ash loading appeared to be minor from the 2015 result, it was more apparent from the measurements of T50;

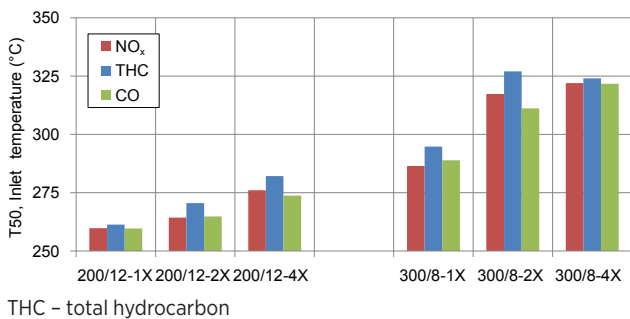


Figure 1. Light-off temperatures (T50) of TWC/GPFs in variation of TWC coatings and filter types. 1X, 2X, and 4X represent TWC coating levels of 25 g/L, 50 g/L, and 100 g/L, respectively.

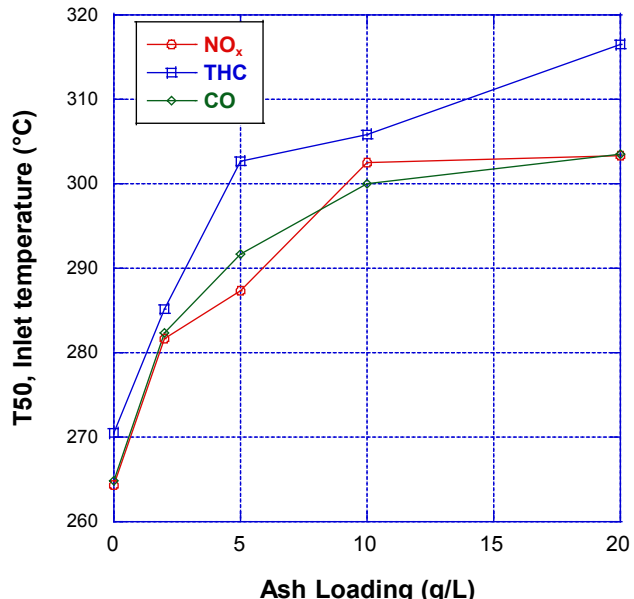


Figure 2. Light-off temperatures (T50) of 200/12-2X with respect to ash loading

T50 increased gradually with ash loading, so T50 with ash loading of 20 g/L was delayed by approximately 40°C, compared to that with no ash loading, confirming that the inner-wall coated TWC was also deactivated with ash loading, as noted in the conventional TWC coated on surface monolith. Detailed conversions of NO<sub>x</sub>, THC, and CO were further examined at the inlet temperatures of 280°C, 350°C, and 430°C with varying lambda (NO<sub>x</sub> conversions are presented in Figure 3). The NO<sub>x</sub> conversions were significantly lowered at the inlet temperature of 280°C with ash loading, whereas they were marginally reduced at the inlet temperatures of 350°C and 430°C. For CO and THC, the reductions in conversions were noticeable only at 280°C. When it comes to gaseous emissions under transient modes, therefore, there would be increased gaseous emissions in the low temperature range with ash-derived TWC deactivation. This result suggests that fast warming-up of the TWC/GPF undermines the effect of TWC deactivation.

Ash distribution in conventional TWC-coated monoliths is known to provide valuable information of the deactivation mechanism in aged TWC. Accordingly, the research of ash distribution was initiated in two ways: X-ray computed tomography scans for ash accumulation throughout filters, and SEM-EDS and X-ray fluorescence tomography for elemental mapping analysis in filter walls. X-ray computed tomography scans were performed for field- and lab-aged filters. The field-aged filter taken from a vehicle with 100,000 miles showed relatively low ash

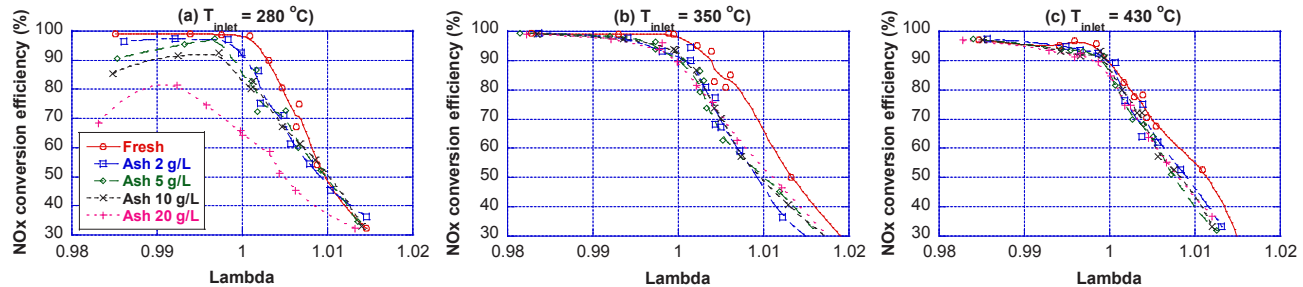


Figure 3.  $\text{NO}_x$  conversion efficiencies with respect to lambda under different inlet temperatures

loading throughout the filter, concentrated only on the rear side as noted in Figure 4. The result is consistent with other reports displaying slight ash plugs, compared to those in DPFs. Elemental mapping analyses of aged filters presented that primary ash-derived elements such as Ca, Zn, and P were deposited on the surface walls. And, S and P were also observed inside the walls, but this is yet to be further investigated. As P is known to interact with  $\text{CeO}_2$  in TWCs for conventional TWC-coated monoliths, resulting in decreased TWC performance, P– $\text{CeO}_2$  interaction and other deactivation factors will be further detailed in FY 2017.

Several reports have discussed ash chemistries in conventional TWC coatings and DPFs, but their characterization was rather focused on agglomerated ash particles taken from remains in TWC coatings and DPFs as well as in sump oil. Therefore, researchers have not paid much attention to ash formation processes in nanoscale, partly because stand-alone ash nanoparticles are not observable in normal operating conditions. With the application of accelerated engine oil dosage, a number of nanoparticles in the sub-30-nm range could be separately analyzed by using STEM. Figure 5a shows that these nanoparticles appeared to be single primary particles and aggregates with several primary particles. STEM-EDS analyses were performed to detail elemental information of nanoparticles. Careful examinations clearly showed that these nanoparticles contained C, Ca, and P in every case, regardless of their size, as exemplified in Figure 5b. Zn was sometimes present with these elements, but such cases were not often observed. Since C originated from soot and Ca, P, and Zn were derived from engine oil, it is presumed that soot and ash elements form chemical compounds in nanoscale during the combustion process. Since engine oil consumption is extremely low in normal operating conditions, it is understood that ash nanoparticles transport with abundant soot particles as attachments and they are trapped in GPFs along with soot. Because soot is burned off during the regeneration process of filters, ash particles will accumulate in filter pores and

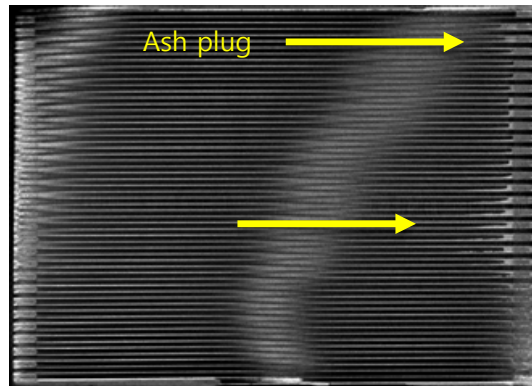


Figure 4. X-ray computed tomography result of a field-aged filter

eventually in filter walls, resulting in increasing pressure drop across filters.

## Conclusions

- Initial  $\text{NO}_x$ , THC, and CO conversions were observed to decrease in a low temperature range with increased TWC coating level under the identical PGM amount, probably because of reduced availability of active catalysts.
- The light-off temperatures of  $\text{NO}_x$ , THC, and CO increased gradually with increased ash loading, indicating that TWC performance was retarded in a low temperature range with ash loading.
- While the negative impact of ash loading on THC and CO conversions was minor over 350°C, its effect on  $\text{NO}_x$  conversions was more apparent.
- Slight ash plugs were observed in the filter back side for a field-aged filter.
- Initial elemental mapping analysis proposes the penetration of P and S into filter walls.

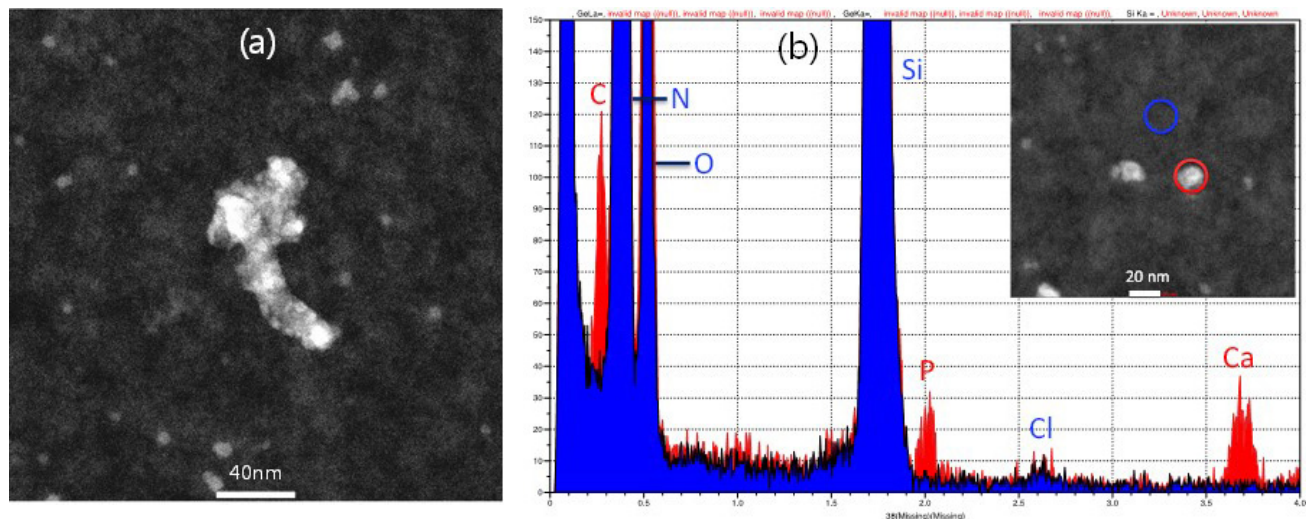


Figure 5. (a) STEM image of ash and soot particles, and (b) STEM-EDS analysis of an ash nanoparticle. Red peaks are from an ash nanoparticle, while blue peaks are from background.

- Ash nanoparticles, which appeared to be single or agglomerated, contained C, Ca, and P, regardless of particle size, suggesting that soot and metallic elements from engine oil form ash compounds in nanoscale during the combustion process.

## FY 2016 Publications/Presentations

1. Seungmok Choi and Heeje Seong, “Lube oil-dependent ash chemistry on soot oxidation reactivity in a gasoline direct-injection engine,” *Combustion and Flame*, 2016, 174, 68–76.
2. Luxi Li, Seungmok Choi, Hee Je Seong and Stefan Vogt, “X-ray fluorescence microscopy analyses of three-way catalyst aging and deactivation in gasoline particulate filter application,” *2016 Microscopy & Microanalysis*, July 24–28, Columbus (Ohio, USA), 2016.
3. Heeje Seong and Seungmok Choi, “Fundamental understanding of particulates from gasoline direct injection (GDI) engines and their mitigation using gasoline particulate filters (GPF),” *2016 International Conference on Advanced Automotive Technology*, July 7–8, Gwangju (S. Korea), 2016.
4. S. Choi, H. Seong, J. Williams, J. Seo and C. In, “Analysis of TWC coated prototype gasoline particulate filter (GPF) – TWC washcoat level and soot/ash loading impacts on filtration and gaseous emissions conversion,” *SAE 2016 World Congress & Exhibition*, April 12–14, Detroit (MI, USA), 2016.
5. H. Seong, S. Choi, J. Williams, J. Seo, C. In, B. Lam and H. Shao, “Soot oxidation impacted by engine oil-derived ash from a gasoline direct injection engine,” *2016 Cross-Cut Lean Exhaust Emissions Reduction Simulations (CLEERS) Workshop*, April 6–8, Ann Arbor (MI, USA), 2016.
6. S. Choi, H. Seong, J. Williams, J. Seo, C. In, B. Lam and H. Shao, “Analysis of ash loading impact on prototype gasoline particulate filters,” *2016 CRC World Emissions Workshop*, March 13–16, Newport Beach (CA, USA), 2016 (poster).

## III.9 Fuel-Neutral Studies of PM Transportation Emissions

### Overall Objectives

- Systematic particulate characterization with single-cylinder test engines, guided by industry
- Seek to shorten development time of filtration technologies for future engines
- Develop modeling approaches relevant to the likely key challenge for gasoline particulate filtration: high number efficiency at high exhaust temperatures

### Fiscal Year (FY) 2016 Objectives

- Finish analysis and publication of particulate characterization data from third cooperative test campaign at the University of Wisconsin-Madison ERC
- Continue development of the Exhaust Filtration Analysis (EFA) apparatus for both low and high temperature filtration experiments
- Perform filtration experiments with a variety of filter substrates, covering a range of porosity and pore size

### FY 2016 Accomplishments

- Assembled a large set of consistent filtration data, using a number of different filter materials and covering a range of engine operating conditions
- Developed a simple straight cylindrical pore filter model that qualitatively predicted many of the trends observed in the data
- Performed three-dimensional (3D) flow simulations in filter wall reconstructions from micro X-ray computed tomography (CT) data and compared to experimental results
- Began development of constricted tube unit collector filtration models, which may offer some advantages over the more commonly used spherical unit collector models ■

### Introduction

Technologies such as SIDI offer the possibility of dramatically increasing the fuel efficiency of engines that run on gasoline and associated fuel blends, but this increased efficiency can come at the price of higher NO<sub>x</sub> and/or particulate emissions. As global fuel economy standards increase and emissions limits continue to tighten, major manufacturers are considering exhaust

### Mark Stewart (Primary Contact), Alla Zelenyuk

Pacific Northwest National Laboratory (PNNL)  
902 Battelle Boulevard  
Richland, WA 99352  
Phone: (509) 375-2179  
Email: mark.stewart@pnnl.gov

DOE Technology Development Manager:  
Ken Howden

Subcontractor:  
University of Wisconsin-Madison Engine Research Center (ERC), Madison, WI

filtration for gasoline vehicles, with some deployments anticipated in Europe over the coming year. Exhaust filter manufacturers are now offering products designed specifically for advanced combustion engines, including SIDI. Understanding the fundamental relationships between filter substrate characteristics and ultimate system performance will be critical as manufacturers consider various options moving forward.

### Approach

General Motors Research has provided components and guidance to develop advanced gasoline research engines at the University of Wisconsin-Madison ERC. These research engines have been configured to run with a variety of fuels over a wide range of operating conditions. Three campaigns of joint experiments conducted by the ERC and PNNL have generated an extensive set of data on particulate size, shape, and composition, using standard gasoline and various ethanol blends. An array of commercial instruments was used to characterize particle size and mass distributions, along with SPLAT II [1], a single particle mass spectrometer developed at PNNL. SPLAT II provides composition and vacuum aerodynamic diameter measurements for individual particles, which can be combined with data from standard instruments to elucidate characteristics including soot particle morphology and primary particle size.

The EFA system at the University of Wisconsin-Madison [2] allows fundamental filtration experiments to be conducted in realistic exhaust streams by using flat wafer samples of filter substrates. Detailed characterization of a

number of porous ceramic materials used in the filtration tests, through techniques including mercury porosimetry and micro X-ray CT, was used to understand the differences between the various products. Less commonly used characterization techniques, including capillary flow porometry and liquid extrusion porosimetry, are also being explored. Insight from fundamental experiments, filter characterization, and micro-scale modeling will ultimately be incorporated into new empirical expressions and improved device-scale models that can be used by original equipment manufacturers to optimize engine and exhaust systems in future high-efficiency vehicles.

## Results

Particulate matter in vehicle exhaust comprises a complex mixture of particles with various sizes, compositions, and morphologies. Since the SPLAT II instrument provides mass spectra for individual particles, particles may be binned into a number of different classes. Figure 1 shows how the proportions of four different particle classes from the single-cylinder SIDI test engine running on E20 (20% ethanol, 80% gasoline blend) fuel vary over a number of different end of injection (EOI) times. Note that the scale begins at 50%, so fractal soot makes up the majority of the particles observed. The other particle types are all compact (non-fractal). Metallic particles are associated with engine wear. Ash particles are dominated by oxides, largely from lube oil components. Compact organic particles are separate from the organic content that is integrated with the fractal soot particles.

Figure 2 shows a comparable breakdown for pure ethanol fuel (E100). Note the change in scale. With clean-burning ethanol, total particle numbers are much smaller, and the “baseline” particles associated with lube oil and engine wear emerge to dominate particle counts. These results show just one example of the many ways in which such techniques can be used to understand the nature and origin of exhaust particulates.

The low temperature EFA apparatus was improved, with a new gasket material to avoid spurious particulate formation during filtration experiments. Several iterations were also carried out in the development of a high temperature filter holder, with promising preliminary results. Detailed filter performance data was gathered for a wide variety of ceramic filter specimens. Figure 3 from Viswanathan [3] shows data from one example study of two filter substrates with similar porosity and average pore size. C1 is a cordierite substrate with a porosity of 43% and a median pore diameter of 12 microns. A2 is aluminum titanate with a porosity of 43% and a median pore diameter of 11.4 microns. The A2 substrate has a

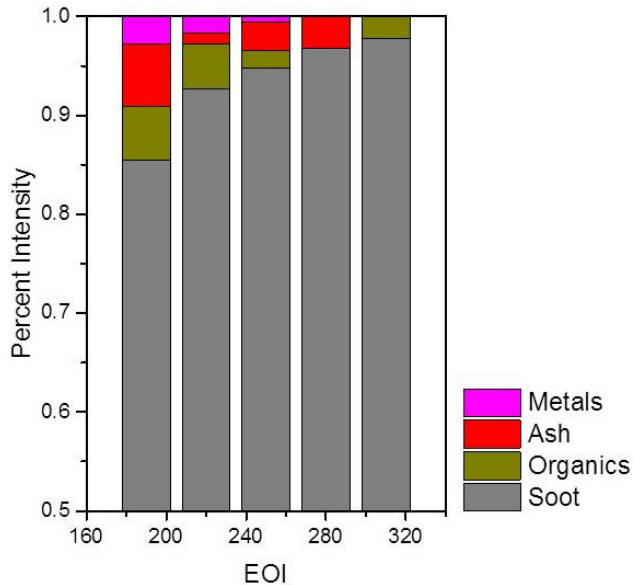


Figure 1. Proportions of various classes of exhaust particles from a SIDI test engine burning E20 fuel

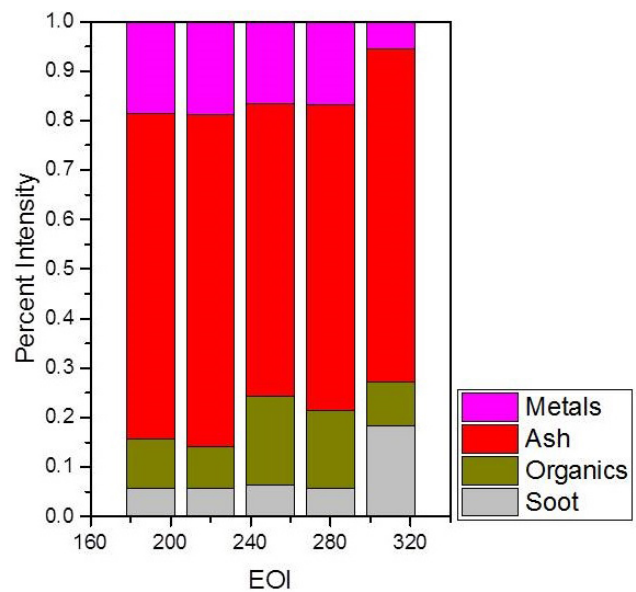


Figure 2. Proportions of various classes of exhaust particles from a SIDI test engine burning E100 fuel

narrower pore size distribution as measured by mercury porosimetry, and a somewhat higher (~12%) permeability. Figure 3 shows that the penetration of larger particles through the two filter materials at a filtration velocity of 2.75 cm/s is similar. However, small particles, which make up the majority of SIDI exhaust particulate matter (PM) on a number basis, penetrate the C1 material to

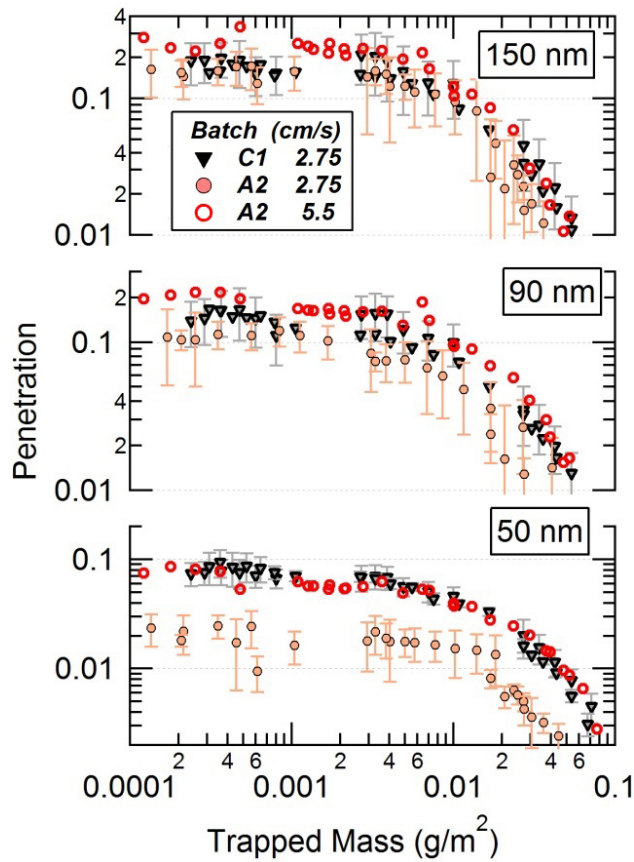


Figure 3. Change of penetration of 50-nm, 90-nm, and 150-nm particles as a function of trapped mass for filters C1 and A2 at 2.75 cm/s and 5.5 cm/s

a significantly greater extent. Filtration velocity can be doubled to 5.5 cm/s through the A2 material to achieve similar removal efficiency to that achieved by the C1 material at 2.75 cm/s. The observed dependence of filtration efficiency of small particles on flow velocity is consistent with theory. Removal efficiency for all particle sizes rapidly increases as small amounts of soot accumulate in the filter walls.

Figure 4 shows X-ray CT images from filter wall cross sections of the two materials, which have visibly different textures. The broader pore size distribution in C1 is apparent. The CT data exemplified in Figure 4 was used to generate 3D reconstructions of small segments of the filter walls, shown in Figure 5. These reconstructions were then used to perform lattice Boltzmann simulations of the flow fields through the clean filters.

Figure 6 shows streamlines through the two materials, with flow moving downward through the filter wall thickness. Color indicates local velocity along the streamlines. It is apparent that there are more discrete flow paths through the A2 material, so that flow is

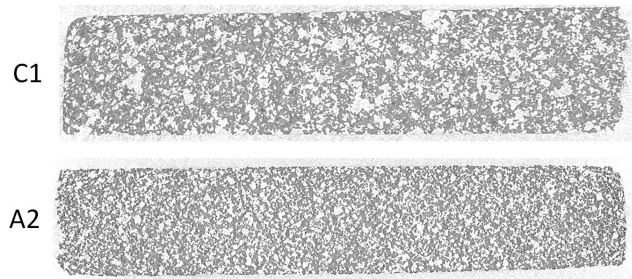


Figure 4. X-ray CT images of C1 and A2 filter wall cross sections

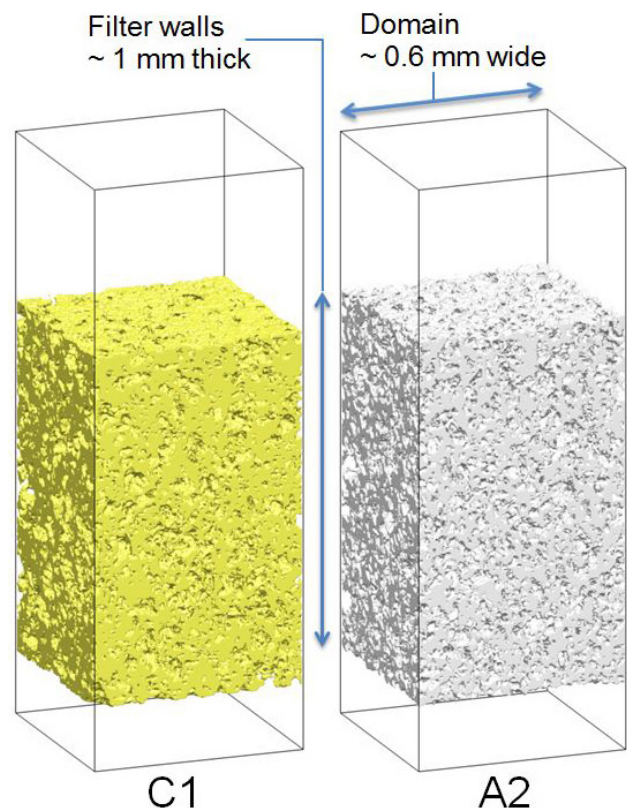


Figure 5. 3D reconstructions of porous C1 and A2 filter walls

distributed more evenly. Average velocities are lower. Gas flowing through C1 must pass through relatively fewer bottlenecks, resulting in higher local velocities. It has been previously postulated that narrow pore size distributions are associated with better pore connectivity [4]. More even flow distribution leads to lower interstitial velocities and exposure of the flowing gas to more surface area within the filter wall, both of which promote removal of small particles by diffusion.

Work continued in 2016 to explore new alternatives in filter modeling. A simple filter model based on straight cylindrical pores was developed using capillary flow

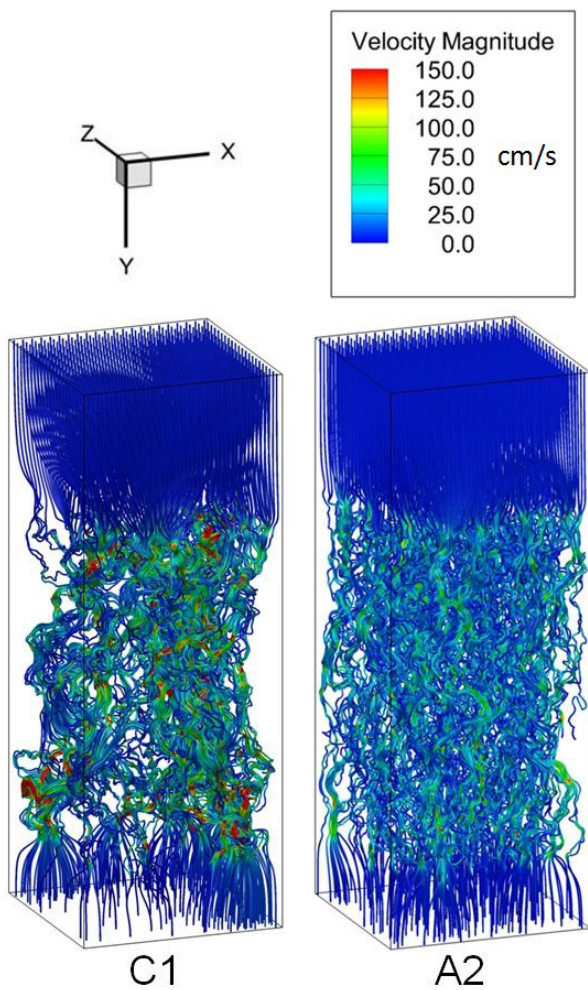


Figure 6. Streamlines for flow through C1 and A2 filter walls

porometry measurements. Despite many simplifying assumptions, this model correctly predicted many of the trends observed in the filtration data [3]. A more sophisticated restricted tube unit collector model [5] was developed and predictions were compared to those made by the standard spherical unit collector model [6] and by the heterogeneous multi-scale filtration model developed at the University of Wisconsin-Madison. Efforts are currently under way to incorporate experimental measurements, analysis of X-ray CT data, and insight from 3D flow simulations into the device-scale unit collector models.

## Conclusions

- Various particle types are present in exhaust in different proportions under different engine operating conditions and with different fuels.

- Carbonaceous soot typically dominates under conditions where large numbers of particles are generated.
- Cleaner burning fuels and operating conditions still produce small amounts of soot, along with compact organic, metallic, and ash particles.
- The improved EFA apparatus yields consistent, repeatable backpressure and filtration data for a wide range of filter materials, fuels, and engine operating conditions.
- Small amounts of soot or ash accumulated in filter walls have a dramatic effect on filtration performance.
- Pore connectivity is an important feature in determining performance of filter substrates.
  - Relative differences in connectivity indicated by established metrics for width of pore size distributions agree qualitatively with observations from filter experiments and 3D flow simulations.
- Based on the data collected, a combination of high filter porosity, small median pore size, and narrow pore size distribution are the most attractive characteristics for removal of small particles with moderate backpressure.
- It is difficult to quantitatively predict the evolution of backpressure, mass filtration efficiency, and number filtration efficiency as soot accumulates in exhaust filters using existing unit collector models.

## References

1. Zelenyuk, A.; Yang, J.; Choi, E.; Imre, D. "SPLAT II: An Aircraft Compatible, Ultra-Sensitive, High Precision Instrument for In-Situ Characterization of the Size and Composition of Fine and Ultrafine Particles," *Aerosol Sci Tech* 2009, 43, (5), 411–424.
2. Viswanathan, S., S. Sakai, and D. Rothamer. "Design & Evaluation of an Exhaust Filtration Analysis (EFA) System," *SAE Technical Paper 2014-01-1558*, 2014 SAE World Congress and Exhibition. Detroit, MI.
3. Viswanathan, S. *Experimental investigation of deep-bed filtration of spark-ignited, direct-injection engine exhaust using ceramic particulate filters*. Doctoral dissertation. University of Wisconsin-Madison, 2016.
4. Merkel, G.A., W.A. Cutler, T. Tao, A. Chiffey, P. Phillips, M.V. Twigg and A. Walker (2003). New cordierite diesel particulate filters for catalyzed and non-catalyzed applications. 9th Diesel Engine Emissions Reduction Conference, Newport, Rhode Island.

5. Tien, C. and Payatakes, A., "Advances in deep bed filtration," AIChE J., no. 5, pp. 737–759, 1979.
6. Konstandopoulos, A.G. and Johnson, J.H., "Wall-Flow Diesel Particulate Filters — Their Pressure Drop and Collection Efficiency," SAE Tech. Pap. 890405, 1989.

## FY 2016 Publications/Presentations

1. Viswanathan, S., Rothamer, D., Fansler, T., Foster, D., Zelenyuk, A., Bell, D. and Stewart, M.L. "Evolution Of Deep Bed Filtration Of Engine Exhaust Particulates With Trapped Mass." International Journal of Engine Research. (accepted for publication)
2. Viswanathan, S., Rothamer, D., Zelenyuk, A., Stewart, M.L., and Bell, D. "Experimental investigation of the effect of inlet particle properties on the capture efficiency in an exhaust particulate filter." Journal of Atmospheric Sciences. (in preparation)
3. Viswanathan, S. *Experimental investigation of deep-bed filtration of spark-ignited, direct-injection engine exhaust using ceramic particulate filters*. Doctoral dissertation. University of Wisconsin-Madison, 2016.

## Acknowledgements

General Motors Corporation: Kushal Naranayashwamy, Paul Najt, Arun Solomon, Wei Li

University of Wisconsin-Madison: David Rothamer, Chris Rutland, Sandeep Viswanathan, Jonathan Molina, Yangdongfeng Yang, Andrea Shen, Todd Fansler, Stephen Sakai, Michael Andrie

PNNL: Jacqueline Wilson, David Bell, Jie Bao

A portion of the research described was performed at Environmental Molecular Sciences Laboratory, a national scientific user facility sponsored by the Department of Energy's Office of Biological and Environmental Research and located at Pacific Northwest National Laboratory.

## III.10 Next-Generation SCR Dosing System Investigation

### Overall Objectives

- Help fuel-efficient lean gasoline and diesel engines meet the current and future emission regulations with effective, inexpensive, and reliable  $\text{NO}_x$  emission control technologies
- Help develop the next generation selective catalytic reduction (SCR) dosing system for improved low-temperature performance, convenient handling and distribution of ammonia carriers, and reduced overall system volume, weight, and cost

### Fiscal Year (FY) 2016 Objectives

- Synthesize novel composites that enhance ammonia storage capacity
- Quantify and mitigate solid material volume change during charge and discharge
- Quantify amount of HCl gas generated during ammonia release
- Develop pathways to mitigate HCl during ammonia release

### FY 2016 Accomplishments

- Completed detailed evaluation of 15 compositions
- Developed composites that mitigate volume expansion issues from 350 vol% to 19 vol%
- Quantified HCl generated during ammonia release
- Evaluated composites and mitigated HCl generated from ~600 ppm to <1 ppm HCl ■

### Introduction

Lean burn gasoline and diesel engines can offer substantially higher fuel efficiency, good driving performance, and reduced carbon dioxide emissions compared to stoichiometric gasoline engines. Various catalyst technologies have been developed to remove the pollutants from these engines. For example, a three-way catalyst is used to remove hydrocarbons, CO, and  $\text{NO}_x$  from gasoline engines during the stoichiometric conditions. During the lean burn conditions, a three-way catalyst or a diesel oxidation catalyst is used to control hydrocarbons and CO emissions.  $\text{NO}_x$  is removed by either lean  $\text{NO}_x$  trap catalyst that can store  $\text{NO}_x$  under lean conditions and reduce  $\text{NO}_x$  under rich conditions, or SCR

### Abhi Karkamkar (Primary Contact), Chinmay Deshmane

Pacific Northwest National Laboratory (PNNL)  
902 Battelle Boulevard  
Richland, WA 99352  
Phone: (509) 372-4973  
Email: abhi.karkamkar@pnnl.gov

DOE Technology Development Manager:  
Ken Howden

that can selectively remove  $\text{NO}_x$  with a reducing agent. Among the  $\text{NO}_x$  reduction catalyst technologies, SCR offers a number of advantages including excellent  $\text{NO}_x$  reduction efficiency over a wide range of temperatures and overall lower system cost. In fact, the SCR technology using  $\text{NH}_3$  as a reductant has been proven effective and used commercially for the removal of  $\text{NO}_x$  emissions from stationary sources since the 1970s. Currently, SCR is being used to meet the  $\text{NO}_x$  emission standards for diesel engines in Europe and North America, and also being considered for meeting the future  $\text{NO}_x$  emission standards for lean burn gasoline engines.

The major challenges with automotive emissions are:

- The discrepancy between legislation and real driving emissions.
- Air quality targets are not met globally.
- $\text{NO}_x$  concentration in cities are of particular concern.
- Efficient engines and low exhaust temperature.
- Existing limitations of liquid SCR must be resolved robustly.

Because of the challenges associated with storage, handling, and transportation of ammonia on a vehicle, aqueous urea solutions (e.g., Diesel Exhaust Fluid, AdBlue) have been developed as an ammonia storage compound for mobile applications. When the aqueous urea solution is sprayed into the exhaust gas stream, urea is decomposed to release ammonia, which then reduces  $\text{NO}_x$  over the downstream SCR catalyst. Although aqueous urea solution technology has enabled automakers and engine manufacturers to meet the current  $\text{NO}_x$  emission standards, this process of releasing ammonia

requires a hot exhaust gas and sufficient mixing, creating challenges for low temperature  $\text{NO}_x$  emission control and aftertreatment system packaging. For these reasons, alternative technologies have been developed as ammonia sources (e.g., solid urea, ammonium carbamate, metal ammine chloride) during the past few years. These technologies promise more convenient handling and distribution of ammonia sources, and help maximize the low-temperature performance of SCR catalysts and reduce the overall system volume and weight.

However, none of these alternative technologies can be successfully implemented without the industry consensus. Therefore, the United States Council for Automotive Research SCR work group, which is comprised of representatives from General Motors, Ford, and Chrysler, has decided to investigate the potential alternative ammonia carriers, define common standard vehicle interfaces, and address personal and environmental safety concerns with part suppliers and chemical companies.

## Approach

PNNL and the United States Council for Automotive Research explored methods to improve or optimize the properties of solid state ammonia storage materials based on the information collected during the first year. This FY the project focused on ways to develop experimental protocols to quantify and mitigate solid material volume change during charge and discharge. The project also developed methods to quantify the amount of HCl gas generated during ammonia release and pathways to mitigate them. PNNL synthesized several composites of metal salts with additives by a combination of wetness incipient, co-precipitation, and ion exchange. Anhydrous ammonia was used for sorption.

Generation of HCl was measured by the use of Draeger tubes and was optimized to sample mass and ammonia released. Volume expansion studies were measured using a 1 cc syringe by measuring the volume and mass before and after ammonia sorption.

## Results

The most promising materials (metal ammine salts) have two critical challenges:

- Evolution of highly corrosive and toxic HCl gas during ammonia release
- A significant volume change (as high as 350%) during ammonia loading and release

Both these challenges severely hamper practical utilization of these materials in passenger vehicles.

## Volume Expansion Studies

The volumetric expansion of these materials during ammonia charging and discharging were investigated to provide a preliminary understanding of challenges associated with design of storage vessels. Due to drastic differences in the density of salts and their complexes with ammonia, a huge volume expansion occurs upon ammonia sorption. PNNL has synthesized composites that minimize these drastic volume expansions without a significant loss in ammonia content. Table 1 summarizes the volume expansion of these samples. The primary additives that were identified were mesoporous silica and carbon materials with pore sizes ranging from 3 nm to 30 nm. Volume expansions as high as 360 vol% were measured in pristine materials upon ammonia sorption. The composites synthesized were able to mitigate this enormous expansion to as low as 19 vol%. This mitigates several issues and allows for increased packing efficiency resulting in high volumetric capacity of ammonia. Figure 1 shows the sample volumes before and after ammonia addition.

**Table 1. Volumetric expansion of pristine material and composites upon ammonia sorption**

Material	Ratio	Volume change (%)
X: $\text{MgCl}_2$	0:1	-
X: $\text{Mg}(\text{NH}_3)_6\text{Cl}_2$	0:1	264
X: $\text{Mg}(\text{NH}_3)_6\text{Cl}_2$	1:1	29
X: $\text{Mg}(\text{NH}_3)_6\text{Cl}_2$	1:2	34
X: $\text{Mg}(\text{NH}_3)_6\text{Cl}_2$	1:3	52

## HCl Quantification and Mitigation

Reviewers identified generation of toxic and corrosive HCl as a major issue with metal salts. This was not identified as an issue at lower temperatures (200°C) at which most of the ammonia release occurs. However, at elevated temperatures HCl generation was observed (>350°C). The amount of HCl generated was quantified at ~600 ppm per gram of  $\text{NH}_3$  released. Further studies revealed that the presence of water enhanced HCl generation. Several composites materials were screened to identify compositions that would mitigate HCl generation. Compositions containing 50 wt% additive to 20 wt% additive were screened. The additives resulted in a decrease in gravimetric capacity of the material. However, no HCl was generated during ammonia release from these composites. The composites were tested under several

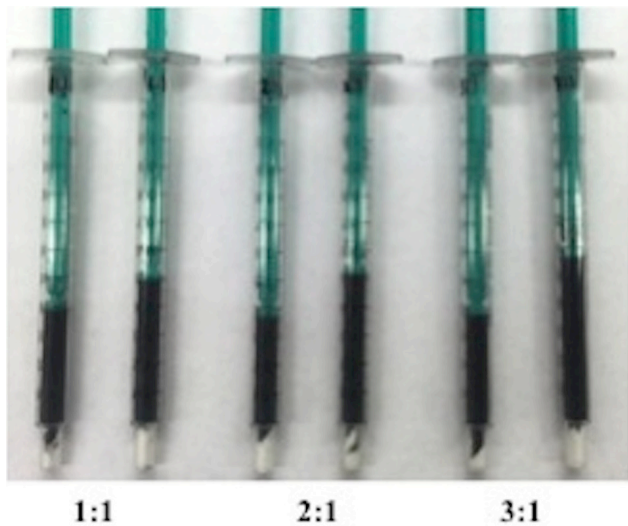


Figure 1. Change in volume of samples upon exposure to ammonia

harsh conditions such as high temperature (400–600°C) and extended periods as long as 72 h. Table 2 summarizes results of the amount of HCl generated and the test conditions.

## Conclusions

- Metal ammine complexes have significantly higher gravimetric and volumetric capacity over aqueous urea compositions.
- Volume change upon ammonia capture and release is a challenge for reactor design and preliminary results suggest that novel composites have been synthesized and evaluated to minimize the volume expansion.
- HCl generation was quantified and mitigated by synthesizing and evaluating the performance of novel composites synthesized by PNNL.

## References

1. Johannessen T., “Emissions solutions for optimal DeNOx in real driving conditions,” Integer Emissions Summit Asia Pacific 2016.
2. Fulks, G., Fisher, G., Rahmoeller, K., Wu, M. et al., “A Review of Solid Materials as Alternative Ammonia Sources for Lean NOx Reduction with SCR,” SAE Technical Paper 2009-01-0907, 2009, doi:10.4271/2009-01-0907.

**Table 2. HCl outlet concentration as a function of ammonia release temperature for magnesium chloride and novel composites developed and tested at PNNL**

Material	Temp* (°C)	Amount of HCl (ppm)
MgCl <sub>2</sub>	400	580
Mg(NH <sub>3</sub> ) <sub>6</sub> Cl <sub>2</sub>	250	20
Mg(NH <sub>3</sub> ) <sub>6</sub> Cl <sub>2</sub> :X (1:1)	400	<1
Mg(NH <sub>3</sub> ) <sub>6</sub> Cl <sub>2</sub> :X (1:1)	400	<1
Mg(NH <sub>3</sub> ) <sub>6</sub> Cl <sub>2</sub> :X (2:1)	250	<1
Mg(NH <sub>3</sub> ) <sub>6</sub> Cl <sub>2</sub> :X (3:1)	250	<1

3. Lysgaard, Steen, et al. “Resolving the stability and structure of strontium chloride amines from equilibrium pressures, XRD and DFT.” *International Journal of Hydrogen Energy* 37.24 (2012): 18927–18936.

## Acknowledgements

United States Council for Automotive Research Partners

- General Motors: Yong Miao
- Ford: Jafar Shaikh
- Chrysler: Mike Zammit

## III.11 Metal Oxide-Based Nano-array Catalysts for Low Temperature Diesel Oxidation

### Overall Objectives

- Synthesize, characterize, and develop a new class of cost-effective and high performance metal oxide nanostructure array (nano-array)-based monolithic catalysts for hydrocarbon (HC) oxidation under lean burn conditions at low temperatures (<150°C)

### Fiscal Year (FY) 2016 Objectives

- Synthesize various metal oxide nano-arrays and porous materials (e.g., transition metal oxides, perovskites) onto monolithic cordierite substrates with high surface area, well-defined structure, and composition
- Demonstrate low cost, stable, and efficient nano-array-based monolith catalysts for low temperature diesel oxidation
- Optimize the nano-array-based monolithic catalysts with selective structure, composition, loading, and good catalytic activities toward low temperature oxidation
- Optimize the composition and loading of the porous materials on honeycomb monolithic substrate with good thermal and hydrothermal stabilities, and catalytic activities for low temperature oxidation
- Formulate and assemble large-scale nano-array-based monolithic catalysts ready for selective transient tests and engine tests

### FY 2016 Accomplishments

- Demonstration of ZnO/perovskite/Pt core-shell metal oxide nano-array catalysts with tunable propane oxidation activities
- Demonstration of TiO<sub>2</sub>/Pt nano-array catalysts with good low temperature CO and C<sub>3</sub>H<sub>6</sub> oxidation performance under U.S. DRIVE protocolled low temperature combustion diesel (LTC-D) simulated exhaust gas conditions
- Demonstration of TiO<sub>2</sub>/Pt nano-array catalysts with promising low temperature CO, C<sub>2</sub>H<sub>4</sub>, and C<sub>3</sub>H<sub>6</sub> oxidation performance in U.S. DRIVE protocolled conventional diesel combustion (CDC) simulated exhaust gas conditions
- Hydrothermal durability evaluation of various metal oxide nano-array-based monolithic catalysts

**Pu-Xian Gao<sup>1</sup> (Primary Contact),  
Steven L. Suib,<sup>1</sup> Todd Toops,<sup>2</sup>  
Yanbing Guo,<sup>1,3</sup> Thomas Pauly<sup>4</sup>**

<sup>1</sup>University of Connecticut  
97 North Eagleville Road  
Storrs, CT 06269-3136  
Phone: (860) 486-9213  
Email: puxian.gao@uconn.edu

<sup>2</sup>Oak Ridge National Laboratory  
2360 Cherahala Blvd.  
Knoxville, TN 37932

<sup>3</sup>3D Array Technology, LLC  
300 South Street  
Vernon, CT 06066

<sup>4</sup>Umicore Autocat. USA, Inc.  
Auburn Hills, MI 48326

DOE Technology Development Manager:  
Ken Howden

NETL Project Manager:  
Ralph Nine

- Formulation and assembly of large-scale nano-array-based monolithic catalysts for selective transient cyclic tests and engine tests ■

### Introduction

Clean and fuel-efficient low temperature combustion (LTC) is preferred in the latest development of various combustion-based energy devices, prompting the need of various LTC strategies including the low cost, efficient, and robust catalytic emission control devices. Despite the reduced NO<sub>x</sub> emissions and increased fuel efficiency through adopting LTC modes, new challenges arise. These include, for instance, the increased HC and CO emissions and different HC species that may be generated through these new techniques [1]. Although the research and development on efficient engine technologies, such as homogenous charge compression ignition and premixed charge compression ignition [2] in the LTC regime, have been in a fast-developing stage, the compatible catalytic aftertreatment technologies that operate efficiently

at temperatures lower than 150°C are still lacking in industry. For example, at temperatures below 150°C, traditional diesel oxidation catalysts (DOCs) become inefficient due to the higher light-off temperature needed to activate the oxidation of CO and HCs into CO<sub>2</sub> and H<sub>2</sub>O, as well as NO oxidation into NO<sub>2</sub> for downstream NO<sub>x</sub> removal devices such as selective catalytic reduction structured catalysts. In this project, we will address these issues using our nano-array monolithic catalyst technology, i.e., in situ growth of nano-array-based catalysts on monoliths to reduce catalyst material usage, improve and demonstrate their low temperature catalytic oxidation activity and selectivity through size, shape, structure, and composition control over the nano-arrays.

## Approach

Low cost and green wet chemical methods are used to synthesize metal oxide nano-arrays on honeycomb substrates, followed by various porous coatings and platinum group metal loading through sol-gel-based processes [3]. Post thermal annealing is used to improve the crystallinity and stoichiometry of nano-array-based structures. Structure, morphology, and chemical characterization are carried out using X-ray diffraction, transmission electron microscopy (TEM), scanning electron microscopy (SEM), and energy-dispersive X-ray spectroscopy. Catalyst evaluation is conducted using temperature-programmed reduction, temperature-programmed desorption, and temperature-programmed oxidation; benchtop tube reactor kinetics testing

involving Fourier transform infrared spectrometry and gas chromatography–mass spectrometry; and thermal and hydrothermal aging testing.

## Results

By using the patent pending technology developed at the University of Connecticut, a broad spectrum of metal oxide-based nano-arrays including ZnO [4], TiO<sub>2</sub> [5], CeO<sub>2</sub>, MnO<sub>2</sub> [6], NiO, and Co<sub>3</sub>O<sub>4</sub> [7] have been successfully grown onto cordierite honeycomb substrates (Figure 1).

### ZnO/Perovskite Nano-Array Catalysts

Platinum and strontium have been successfully incorporated into materials by tuning elemental species and compositions of the sol-gel solution, and the as-prepared nano-array was denoted as Pt/LSMO (platinum-doped lanthanum strontium manganese oxide). Pt nanoparticles were dispersed uniformly either in the bulk or on the surface of perovskites. Microwave irradiation was used in the dip coating process to promote the uniformity of perovskites across the channel length, allowing higher perovskite loading without deteriorating the core-shell nanostructure. On the other hand, acid treatment provides a new route to manipulate the nanostructure of catalysts. Pt incorporated perovskite nanotube arrays were successfully obtained by acidic removal of ZnO nanorods and are denoted as Pt/LMO (platinum-doped lanthanum manganite). The as-obtained perovskite nanotube arrays possess a porous structure

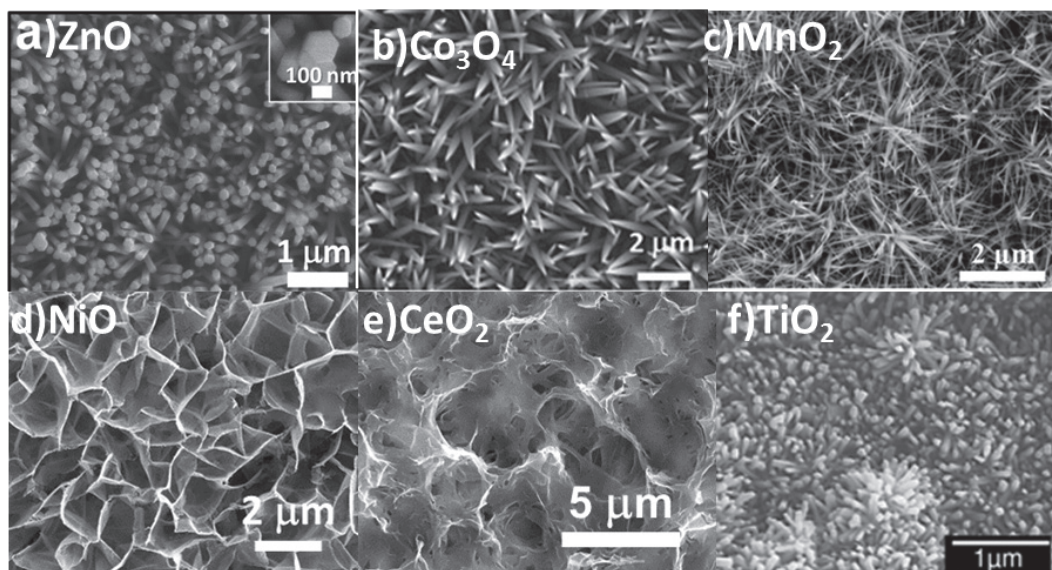


Figure 1. SEM images of several metal oxide nanostructures/cordierite honeycomb monolith developed in our lab: (a) ZnO nanorod [4], (b)Co<sub>3</sub>O<sub>4</sub> nanowire [7], (c) MnO<sub>2</sub> nanowire [6], (d) NiO nano-network, (e) CeO<sub>2</sub> nano-network, and (f)TiO<sub>2</sub> nanorod [5]

and enhanced surface area compared to ZnO/perovskite core-shell nano-arrays.

Pt-ZnO/LSMO nanorod array and Pt/LMO nanotube arrays have been successfully obtained via microwave assisted dip coating and diluted acid treatment (Figures 2a–2d). Propane oxidation was employed as the probe reaction to evaluate the catalytic performance of the monoliths (Figures 2e and 2f). During the test, the inlet gas was composed of 0.8% propane and 8% oxygen balanced with nitrogen with a flow rate of 200 mL/min. The space velocity was 60,000 h<sup>-1</sup>. With rival Pt loading, 0.001Pt-ZnO/LSMO exhibits a lower light-off temperature T<sub>90</sub> (90% conversion temperature) of 60°C than ZnO/LSMO (no Pt incorporated). The catalytic activity increases with Pt concentration, indicated by a decrease of ~200°C in T<sub>90</sub> for the sample 0.1Pt-ZnO/LSMO as compared with the sample 0.001Pt-ZnO/LSMO. The exceptional low temperature activity enhancement can be attributed to the catalytically active PtO<sub>x</sub> species on nano-arrays. Additionally, Pt-perovskite co-deposition can improve the dispersion of Pt nanoparticles and form Pt-perovskite interfaces, which play an important role in improving low temperature activity and stabilizing the active sites.

Meanwhile, Pt/LMO nanotube arrays show (~40°C) lower light-off temperature and (120°C) lower T<sub>90</sub> than Pt-ZnO/LMO nanorod arrays, which indicates a significant activity boost enabled by acid removal of ZnO nanorods. This activity enhancement can be attributed to the surface area increase of porous nanotube arrays, which give rise to stronger gas-solid phase interactions in propane oxidation reactions. On the other hand, the acid treatment also regulates the oxidation state of Mn in the perovskite and increases the surface adsorbed oxygen population [8], which can be closely correlated to the catalytic performance improvement for Pt/LMO nanotube arrays.

### Pt/TiO<sub>2</sub> Nano-Arrays for CO and C<sub>3</sub>H<sub>6</sub> Oxidation

Mesoporous rutile TiO<sub>2</sub> nano-arrays were directly integrated with cordierite honeycomb monoliths using our newly developed solvothermal procedure. As shown in the SEM images (Figures 3a and 3b), the TiO<sub>2</sub> nanoarrays with characteristic diameters of ~50–150 nm were uniformly grown on the monolith substrate with a thickness of ~3 μm. Notably, the TiO<sub>2</sub> nano-array/cordierite sample has an extremely high specific surface area, reaching ~100 m<sup>2</sup>/g (including cordierite substrate), allowing high noble metal dispersion and improving metal–support interactions. Platinum was loaded on the

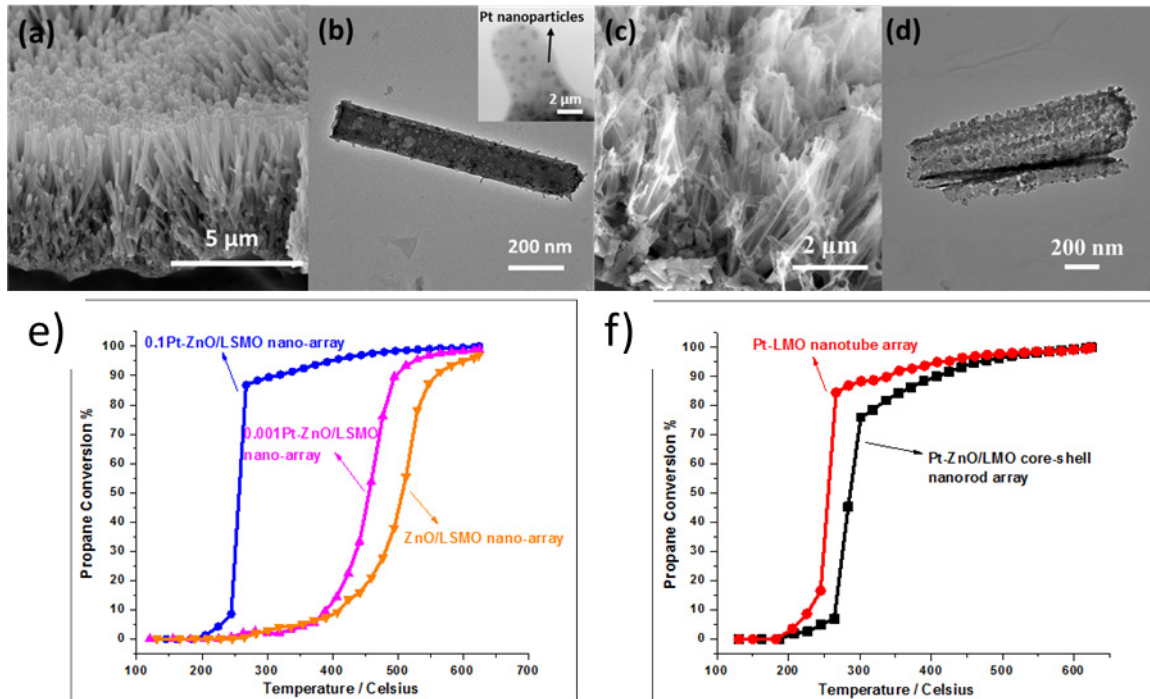


Figure 2. (a) Cross-sectional view SEM image and (b) TEM image of Pt incorporated ZnO/La<sub>0.8</sub>Sr<sub>0.2</sub>MnO<sub>3</sub> nano-array catalyst; (c) cross-sectional view SEM image and (d) TEM image of Pt incorporated LaMnO<sub>3</sub> nanotube array catalyst, and catalytic C<sub>3</sub>H<sub>6</sub> oxidation conversion of (e) Pt-ZnO/LSMO nanorod array catalysts and (f) comparison of Pt/LMO nanotube and Pt-ZnO/LMO nanorod array catalysts

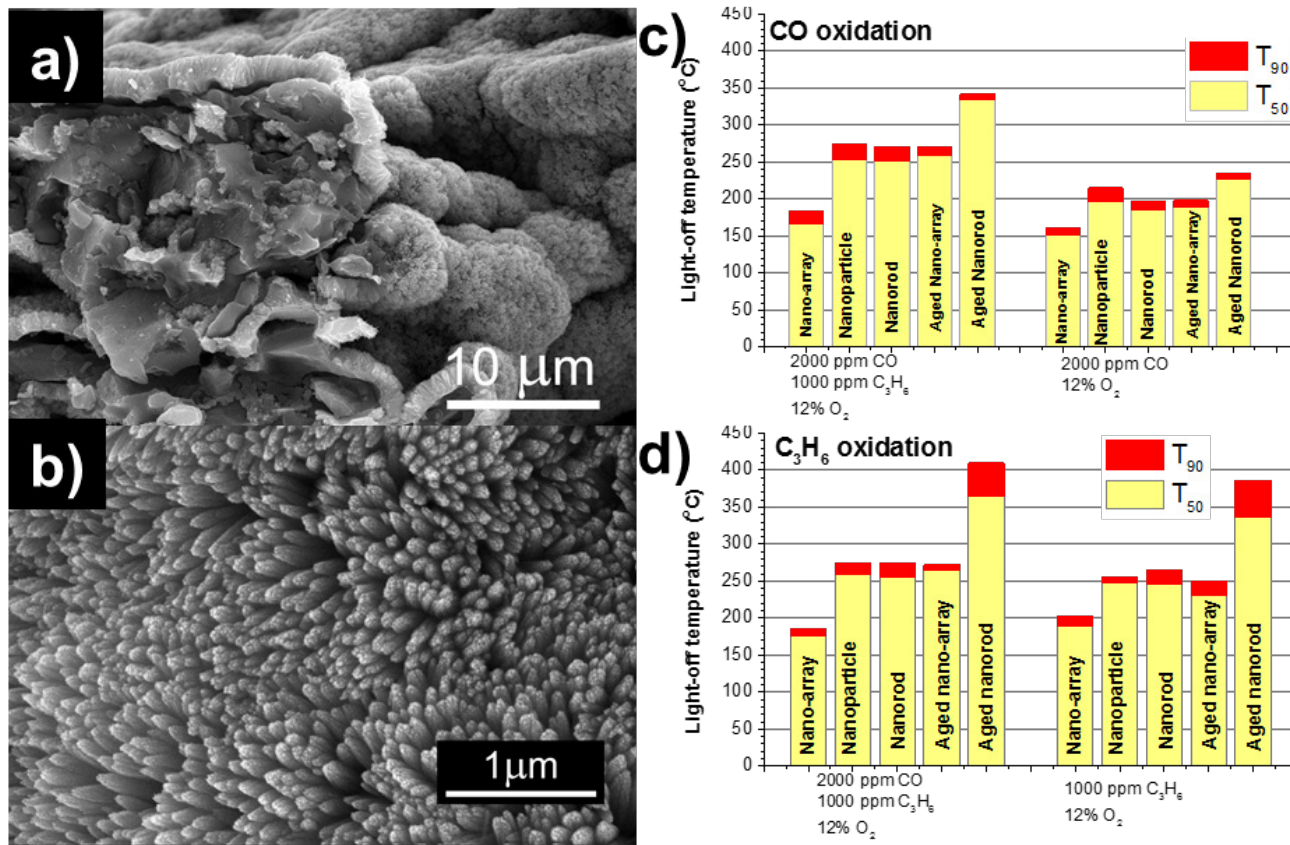


Figure 3. SEM images of rutile  $TiO_2$  grown on cordierite monolith (a, b); light-off temperatures ( $T_{50}$  and  $T_{90}$ ) for CO oxidation (c) and  $C_3H_6$  oxidation (d) at a space velocity of 30,000  $h^{-1}$  for  $Pt/TiO_2$  nano-array and wash-coat-based samples. To evaluate the hydrothermal stability, samples were aged at 700°C for 100 h in a gas stream containing 10%  $O_2$ , 5%  $CO_2$ , 5%  $H_2O$ , and balanced with  $N_2$ .

$TiO_2$  nano-array/cordierite monoliths using microwave-assisted dip coating to make functional DOC devices. CO and propylene ( $C_3H_6$ ) oxidation were employed as the probe reactions to evaluate DOC activity of  $Pt/TiO_2$  nano-array catalysts in both individual and mixtures of CO and  $C_3H_6$ . The concentrations of CO and  $C_3H_6$  were chosen to reflect the concentration of CO and total hydrocarbons in LTC-D simulated exhaust. The compositions of the feeding gas mixtures for different tests are: (1) CO: 2,000 ppm,  $C_3H_6$ : 1,000 ppm,  $O_2$ : 12%; (2) CO: 2,000 ppm,  $O_2$ : 12%; and (3)  $C_3H_6$ : 1,000 ppm,  $O_2$ : 12% and all balanced by  $N_2$ . During the test, the feeding gases flowed through the monolith catalysts at a flow rate of ~500 SCCM, equivalent to a space velocity of 30,000  $h^{-1}$ . Additionally, wash-coat-based samples employing similar loadings of Pt and  $TiO_2$  nanopowders (either anatase  $TiO_2$  nanoparticles or rutile  $TiO_2$  nanorods), were used as references to highlight the advantages of the nano-array structures.

The nano-array sample showed an excellent catalytic activity for both CO and  $C_3H_6$  oxidation. As shown in

Figure 3c, the temperature  $T_{90}$  for CO oxidation for  $Pt/TiO_2$  nano-array is only 152°C, very close to the 150°C target, and much lower than that for the wash-coat-based samples (197°C and 185°C). The  $Pt/TiO_2$  nano-arrays also showed much better catalytic activity for  $C_3H_6$  oxidation than the wash-coat-based samples. The temperature  $T_{90}$  for  $C_3H_6$  oxidation for the nano-array sample is almost 60°C lower than that for wash-coat samples. We believe that the outstanding performance of the nano-array samples is due to the unique nano-array structure that enhances gas–solid interactions [3] and gives better metal dispersion, thus providing more active sites with the same amount of Pt.

In addition to the exceptional catalytic activity in the oxidation of individual gasses, the nano-array sample showed higher resistance to the inhibition effects in the mixture gas of CO and  $C_3H_6$ . There is competition between CO and  $C_3H_6$  for the active sites on platinum group metal-based catalysts [9], thus shifting the light-off temperatures for oxidation of each component to a higher

temperature. We observed a shift of only 14°C in  $T_{90}$  for CO oxidation for the nano-array sample when tested in a mixture of CO and  $C_3H_6$ . Meanwhile, the wash-coat-based samples exhibited more severe inhibition effects with an increase of 56°C and 66°C for anatase nanoparticles and rutile nanrod-based samples, respectively.

The nano-array sample also showed excellent hydrothermal stability. After being hydrothermally aged at 700°C for 100 h in a gas stream composing of 5%  $CO_2$ , 5%  $H_2O$ , 10%  $O_2$ , and balanced by  $N_2$ , the nano-array sample still showed a comparable performance to fresh wash-coat-based samples. On the other hand, the nanorod samples demonstrated a significant decrease in reactivity, especially for  $C_3H_6$  oxidation. The temperature  $T_{90}$  for  $C_3H_6$  oxidation for the nanorod sample is ~137°C higher than that for the nano-array sample.

We have successfully evaluated selective nano-array catalysts using the standardized CDC and LTC-D methods provided by the Advanced Combustion and Emissions Control Tech Team (Table 1).

Using the nano-array-based monolithic catalysts such as  $TiO_2/Pt$ , as shown in Figure 4a, promising alkene and CO oxidation performance have been achieved under CDC exhaust conditions [10]. The reactor gas flow was

adjusted to achieve a space velocity of either 30,000  $h^{-1}$  or 60,000  $h^{-1}$ . Initial Fourier transform infrared spectroscopy testing results (Figure 4b) of the CDC protocol runs at 60,000  $h^{-1}$  on the  $Pt/TiO_2$  sample showed very good activity (with  $T_{90} < 200^\circ C$ ) for CO, propene, and ethene but poor propane oxidation activity. This was due to the possible suppression effect from oxygen coverage competition with HCs on the catalytic active sites under low propane/oxygen concentration ratio revealed in our probe reaction study, which is consistent with recent report on  $Pt/Al_2O_3$  wash-coated catalysts. On the other hand, the LTC-D protocol evaluation of Pt, Pd, and Pt/Pd catalysts impregnated or dip coated onto grown  $TiO_2$  supports showed good low temperature conversion of both CO and total HCs over Pt/Pd samples. CO oxidation over the best samples even approached the  $T_{90} = 150^\circ C$  goal set by the automotive industry. More intensive evaluation is ongoing over the  $TiO_2$  and other promising material systems.

## Conclusions

In FY 2016, main accomplishments are listed as follows:

- Demonstration of  $ZnO$ /perovskite/Pt core-shell metal oxide nano-array catalysts with tunable propane oxidation activities

**Table 1. CDC and LTC-D Protocols Provided by the Advanced Combustion and Emissions Control (ACEC) Technical Team**

	ACEC CDC	ACEC LTC-D
$H_2O$	6%	6%
$CO_2$	6%	6%
$O_2$	12%	12%
CO	500 ppm	2000 ppm
NO	200 ppm	100 ppm
$C_3H_6$	156 ppm	333.3 ppm
$C_3H_8$	52 ppm	111 ppm
$C_2H_4$	389 ppm	833.5 ppm
$H_2$	100 ppm	400 ppm
Space Velocity	$30,000\ h^{-1}$ / $60,000\ h^{-1}$	$30,000\ h^{-1}$
Degreening	$700^\circ C$ 4 h in $O_2$ , $H_2O$ , $CO_2$	$700^\circ C$ 4 h in $O_2$ , $H_2O$ , $CO_2$
Pretreatment	$600^\circ C$ 20 min in $O_2$ , $H_2O$ , $CO_2$	$600^\circ C$ 20 min in $O_2$ , $H_2O$ , $CO_2$

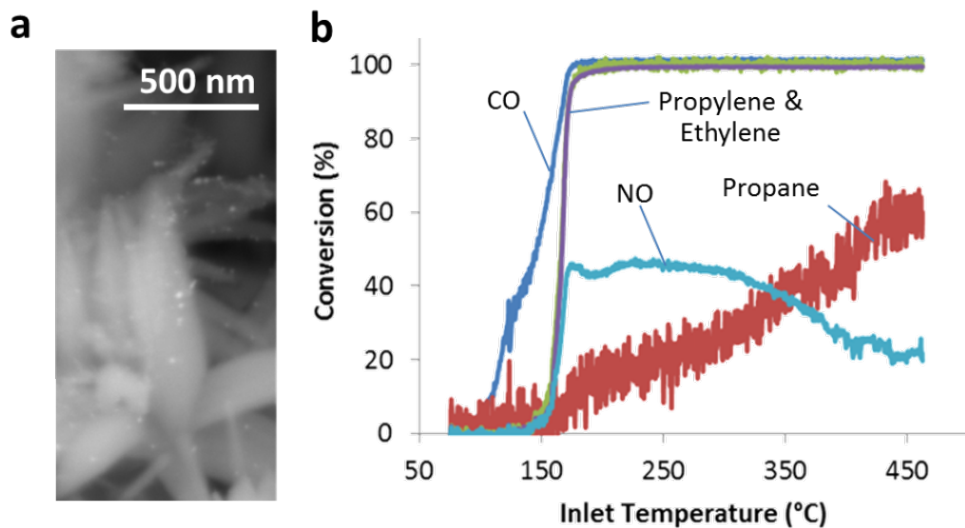


Figure 4. (a) Angular back scattering SEM images of Pt/TiO<sub>2</sub> nano-array rooted on cordierite monolith, white spots: Pt nanoparticles on TiO<sub>2</sub> nanorods; (b) light-off curves of Pt/TiO<sub>2</sub> nano-array-based monolithic catalysts tested under CDC conditions

- Demonstration of TiO<sub>2</sub>/Pt nano-array catalysts with promising low temperature CO and C<sub>3</sub>H<sub>6</sub> oxidation performance at dry conditions
- Demonstration of TiO<sub>2</sub>/Pt nano-array catalysts with promising low temperature CO, C<sub>2</sub>H<sub>4</sub>, and C<sub>3</sub>H<sub>6</sub> oxidation performance in U.S. DRIVE protocaled CDC simulated exhaust gas conditions
- Hydrothermal durability evaluation of various metal oxide nano-array-based monolithic catalysts

## References

1. Zheng, M.; Asad, U.; Reader, G.T.; Tan, Y.; Wang, M., "Energy efficiency improvement strategies for a diesel engine in low-temperature combustion," **International Journal of Energy Research** 2009, 33 (1), 8–28.
2. Jacobs, T. J.; Assanis, D.N., "The attainment of premixed compression ignition low-temperature combustion in a compression ignition direct injection engine," **Proceedings of the Combustion Institute** 2007, 31 (2), 2913–2920.
3. Guo, Y.; Ren, Z.; Xiao, W.; Liu, C.; Sharma, H.; Gao, H.; Mhadeshwar, A.; Gao, P.-X., "Robust 3-D configurated metal oxide nano-array based monolithic catalysts with ultrahigh materials usage efficiency and catalytic performance tunability," **Nano Energy** 2013, 2 (5), 873–881.
4. Xiao, W.; Guo, Y.; Ren, Z.; Wrobel, G.; Ren, Z.; Lu, T.; Gao, P.-X., "Mechanical-Agitation-Assisted Growth of Large-Scale and Uniform ZnO Nanorod Arrays within 3D Multichannel Monolithic Substrates," **Crystal Growth & Design** 2013, 13 (8), 3657–3664.
5. Guo, Y.; Liu, G.; Ren, Z.; Piyadasa, A.; Gao, P.-X., "Single crystalline brookite titanium dioxide nanorod arrays rooted on ceramic monoliths: a hybrid nanocatalyst support with ultra-high surface area and thermal stability," **CrystEngComm** 2013, 15 (41), 8345–8352.
6. Chen, S.-Y.; Song, W.; Lin, H.-J.; Wang, S.; Biswas, S.; Mollahosseini, M.; Kuo, C.-H.; Gao, P.-X.; Suib, S.L., "Manganese Oxide Nanoarray-Based Monolithic Catalysts: Tunable Morphology and High Efficiency for CO Oxidation," **ACS Applied Materials & Interfaces** 2016, 8 (12), 7834–7842.
7. (a) Ren, Z.; Guo, Y.; Zhang, Z.; Liu, C.; Gao, P.-X., "Nonprecious catalytic honeycombs structured with three dimensional hierarchical Co<sub>3</sub>O<sub>4</sub> nano-arrays for high performance nitric oxide oxidation," **Journal of Materials Chemistry A** 2013, 1 (34), 9897–9906; (b) Ren, Z.; Botu, V.; Wang, S.; Meng, Y.; Song, W.; Guo, Y.; Ramprasad, R.; Suib, S.L.; Gao, P.-X., "Monolithically Integrated Spinel M<sub>x</sub>Co<sub>3-x</sub>O<sub>4</sub> (M=Co, Ni, Zn) Nano-array Catalysts: Scalable Synthesis and Cation Manipulation for Tunable Low-Temperature CH<sub>4</sub> and CO Oxidation," **Angewandte Chemie** 2014, 53, 7223–7226.
8. Si, W.; Wang, Y.; Peng, Y.; Li, J., "Selective Dissolution of A-Site Cations in AB<sub>3</sub>O<sub>9</sub> Perovskites: A New Path to High-Performance Catalysts," **Angewandte Chemie** 2015, 127 (27), 8065–8068.

9. Binder, A.J.; Toops, T.J.; Unocic, R.R.; Parks, J.E.; Dai, S., "Low-Temperature CO Oxidation over a Ternary Oxide Catalyst with High Resistance to Hydrocarbon Inhibition," **Angewandte Chemie** 2015, 127 (45), 13461–13465.
10. Du, S.C.; Tang, W.X.; Guo, Y.B.; Binders, A.; Kyriakidou, E.; Toops, T.; Wang, S.B.; Ren, Z.; Hoang, S.; Gao, P.-X., "Understanding low temperature oxidation activity of nano-array based monolithic catalysts: from performance observation to structural and chemical insights," **Emission Control Science and Technology**, 2016, DOI 10.1007/s40825-016-0054-y.

## FY 2016 Publications/Presentations

### Publications

1. W. Tang, Z. Ren, X. Lu, S. Wang, Y. Guo, S. Hoang, S.C. Du, and P.X. Gao, "Scalable fabrication of spinel structured  $Mn_xCo_{3-x}O_4$  nano-sheet array based monolithic catalysts for low temperature catalytic propane oxidation," *Chemical Engineering Journal*, 2016, submitted.
2. S.C. Du, W.X. Tang, Y.B. Guo, A. Binders, E. Kyriakidou, T. Toops, S.B. Wang, Z. Ren, S. Hoang, and P.X. Gao, "Understanding low temperature oxidation activity of nano-array based monolithic catalysts: from performance observation to structural and chemical insights," *Emission Control Science and Technology*, 2016, DOI 10.1007/s40825-016-0054-y.
3. W.X. Tang, P.X. Gao, "Nanostructured  $CeO_2$ : preparation, characterization, and application in energy and environmental catalysis," *MRS Communication*, 2016, doi: 10.1557/mrc.2016.52. (invited review)
4. W. Song, Z. Ren, S.Y. Chen, S. Suib, P.X. Gao, et al., "Ni and Mn-Substituted Mesoporous  $Co_3O_4$ : an Ultra Stable Bifunctional Catalyst with Surface Structure Dependent Activity for Oxygen Reduction Reaction and Oxygen Evolution Reaction," *ACS Materials & Interfaces*, 2016, DOI: 10.1021/acsami.6b06103.
5. S. Hoang, and P.X. Gao, "Nanowire Array Structures for Photocatalytic Energy Conversion and Utilization: A Review of Design concepts, Assembly and Integration, and Function Enabling," *Adv. Energy Mater.* 2016, DOI: 10.1002/aenm.201600683. (invited review)
6. S.B. Wang, Z. Ren, Y.B. Guo, P.X. Gao, "Nano-array integrated monolithic devices: toward rational materials design and functional performance by scalable self-assembly of nanostructures," *CrystEngComm*, 2016, 18, 2980–2993. (invited highlight, inside cover)
7. S.Y. Chen, W. Song, H.-J. Lin, S. Wang, S. Biswas, M. Mollahosseini, C.-H. Kuo, P.X. Gao, S. Suib,

"Manganese Oxide Nanoarray-Based Monolithic Catalysts: Tunable Morphology and High Efficiency for CO Oxidation," 2016, *ACS Materials & Interfaces*, 8 (12), 7834–7842.

8. Z. Ren, Z. Wu, W. Song, W. Xiao, Y.B. Guo, J. Ding, S.L. Suib, & P.X. Gao, "Low Temperature Propane Oxidation over  $Co_3O_4$  based Nano-array Catalysts: Ni Dopant Effect, Reaction Mechanism and Structural Stability," *Appl. Catal. B*, 2015, DOI: 10.1016/j.apcatb.2015.04.021.

### Presentations

1. P.X. Gao, Metal Oxide Nano-array based Monolithic Catalysts for Low Temperature Emission Control, American Chemical Society (ACS) Fall National Meeting, Philadelphia, PA, August 23, 2016.
2. P.X. Gao, Metal oxide based heterostructure nanowire arrays for multi-mode chemical sensors at elevated temperature, American Chemical Society (ACS) Fall National Meeting, Philadelphia, PA, August 24, 2016. (invited talk)
3. P.X. Gao, Metal Oxide based Nano-array Catalysts for Low Temperature Diesel Oxidation, DOE Vehicle Technology Program Annual Merits Review Meeting, Washington, D.C., June 9, 2016.
4. P.X. Gao, Metal Oxide Nano-array based Monolithic Catalysts for Low Temperature Diesel Oxidation, DOE CLEERS Workshop, Ann Arbor, MI, April 7, 2016.
5. P.X. Gao, Scalable and hierarchical nanostructure ensembles for high temperature energy and environmental applications, TMS 2016 145th Annual Meeting, Nashville, TN, February 14–18, 2016.
6. P.X. Gao, Scalable Nanomaterials Integration toward Ultrahigh Efficiency, Robustness, and Multi-functionality: An example of Nano-array based Catalytic Converters, International Conference on Advanced Ceramics and Composites 2016, Daytona Beach, FL, January 26, 2016.
7. P.X. Gao, Scalable heterogeneous nanostructure integration for multimode gas sensing at high temperature, MRS Fall Meeting, Boston, MA, November 29–December 4, 2015.

### Special Recognitions and Awards/ Patents Issued

1. S.Y. Chen, J.K. He, P.X. Gao and S. Suib, Fabrication of manganese oxide based nanorod arrays on 3D substrates, University of Connecticut Invention Disclosure, 2016, submitted.

## III.12 NSF/DOE Advanced Combustion Engines: Collaborative Research: GOAL! Understanding NO<sub>x</sub> SCR Mechanism and Activity on Cu/Chabazite Structures throughout the Catalyst Life Cycle

### Overall Objectives

- Synthesize copper ion-exchanged aluminosilicate zeolite (Cu-SSZ-13) catalysts with well-defined numbers and types of active sites
- Use operando spectroscopy to simultaneously observe the catalyst surface and reaction intermediates and measure selective catalytic reduction (SCR) rates, under various reaction conditions
- Correlate experimental observations with first principles models to determine mechanisms, rate laws, and predictive structure–function–activity relationships
- Integrate experiment and computation to characterize and quantify catalyst response to sulfur poisoning and to develop strategies to mitigate poisoning

### Fiscal Year (FY) 2016 Objectives

- Contrast standard SCR turnover rates (per Cu) across a range of Cu-exchanged zeolite frameworks and across a range of Cu loadings
- Develop validated spectroscopic (ultraviolet [UV]-visible and X-ray) methods for detecting and quantifying Cu sites
- Develop synthetic methods that permit control over Cu(II)/Cu(II)OH site ratios
- Develop insights into SCR mechanism and relationship to Cu site types

### FY 2016 Accomplishments

- Showed that Cu exchange sites exist as NH<sub>3</sub>-solvated ions at 200°C standard SCR conditions and that NH<sub>3</sub> solvation mobilizes Cu ions
- Showed that standard SCR rates (per Cu) at 200°C are independent of Cu loading, Cu speciation, and zeolite framework type at commonly used Cu loading levels
- Developed infrared and UV-visible spectroscopies as a means to distinguish Cu(II) and Cu(II)OH exchange sites

**Fabio H. Ribeiro (Primary Contact), W. Nicholas Delgass, Rajamani Gounder, William F. Schneider, Jeffrey T. Miller, Aleksey Yezers, Jean-Sabin McEwen, Charles H. Peden.**

Purdue University  
School of Chemical Engineering  
480 Stadium Mall Dr.  
West Lafayette, IN 47907  
Phone: (765) 494-7799  
Email: fabio@purdue.edu

DOE Technology Development Manager:  
Ken Howden

- Developed synthetic methods to prepare SSZ-13 zeolites with tunable framework Al distribution and corresponding variations in Cu(II)/Cu(II)OH site ratios
- Developed models to correlate features in Cu X-ray spectra with Cu coordination and oxidation state
- Showed that at low Cu loadings, standard SCR rates at 200°C vary with the square of Cu density, implicating a Cu dimer as transient SCR intermediate ■

### Introduction

NO<sub>x</sub> compounds contribute to acid rain and photochemical smog and have been linked to respiratory ailments. NO<sub>x</sub> emissions regulations continue to tighten, driving the need for high performance, robust control strategies. The goal of this project is to develop a molecular-level understanding of the function of Cu-SSZ-13 and copper-containing silicoaluminophosphate (Cu/SAPO-34) materials that catalyze NO<sub>x</sub> SCR with NH<sub>3</sub>.

### Approach

An approach that tightly integrates five tasks take advantage of state-of-the-art experimental and

computational catalytic capabilities, which is necessary to develop robust descriptions of SCR catalyst systems.

- **Task 1 – Simulation:** Density functional theory (DFT) models are used to predict the structure, spectroscopy, and reactivity of various candidate Cu sites in SSZ-13 and SAPO-34 catalysts. These results are used as the basis of microkinetic models.
- **Task 2 – Kinetics:** Reaction rates are measured as a function of reaction conditions and catalyst composition. Two dedicated reactors that are automated and can work unattended are used.
- **Task 3 – Synthesis:** SSZ-13 and SAPO-34 samples are synthesized with systematically varying Si, Al, P, and Cu content and distribution, in order to use as model catalysts in characterization and kinetic studies.
- **Task 4 – Spectroscopies:** Mechanistic hypotheses are generated from the kinetic and theoretical work are addressed using operando spectroscopies and isotopic transient studies. X-ray absorption spectroscopy directly probe Cu oxidation state, key information in relating structure and function.
- **Task 5 – Applications:** A critical element is regular communication and face-to-face meetings with collaborators at Cummins to ensure that research follows a path that maximizes the impact on advances in engine efficiency.

## Results

Three significant outcomes have emerged from this project, summarized in Figure 1. These include demonstration that: (1) SCR occurs on isolated, exchanged Cu ions in SSZ-13; (2) SCR involves a redox cycle between Cu(II) and Cu(I) states, reduction involves NH<sub>3</sub> and NO, and oxidation involves both NO and O<sub>2</sub>; and (3) Cu(II) ions can appear in two forms, a Cu(II) ion charge-compensated by two framework Al in a six-membered ring (“Z<sub>2</sub>Cu”), and a Cu(II)OH ion charge-compensated by one framework Al (“ZCuOH”). Year 3 efforts have seen several additional technical advances.

New synthetic methods were developed to prepare SSZ-13 zeolites with tunable framework Al distribution. These methods permit the number of Cu(II) and Cu(II)OH sites at a given Si:Al ratio to be varied. As demonstration, Cu-SSZ-13 samples with only one or the other type of sites were prepared and validated through titrations of residual protons following Cu exchange. These model systems are useful for comparing and contrasting the contributions of these sites to SCR, to hydrothermal stability, and to sulfur tolerance.

UV-visible spectroscopy is potentially a powerful means for distinguishing Z<sub>2</sub>Cu from ZCuOH. Figure 2 shows that the observed spectra on samples prepared to contain predominantly one or the other type of site are indeed different. To assign these two, the UV-visible spectra were

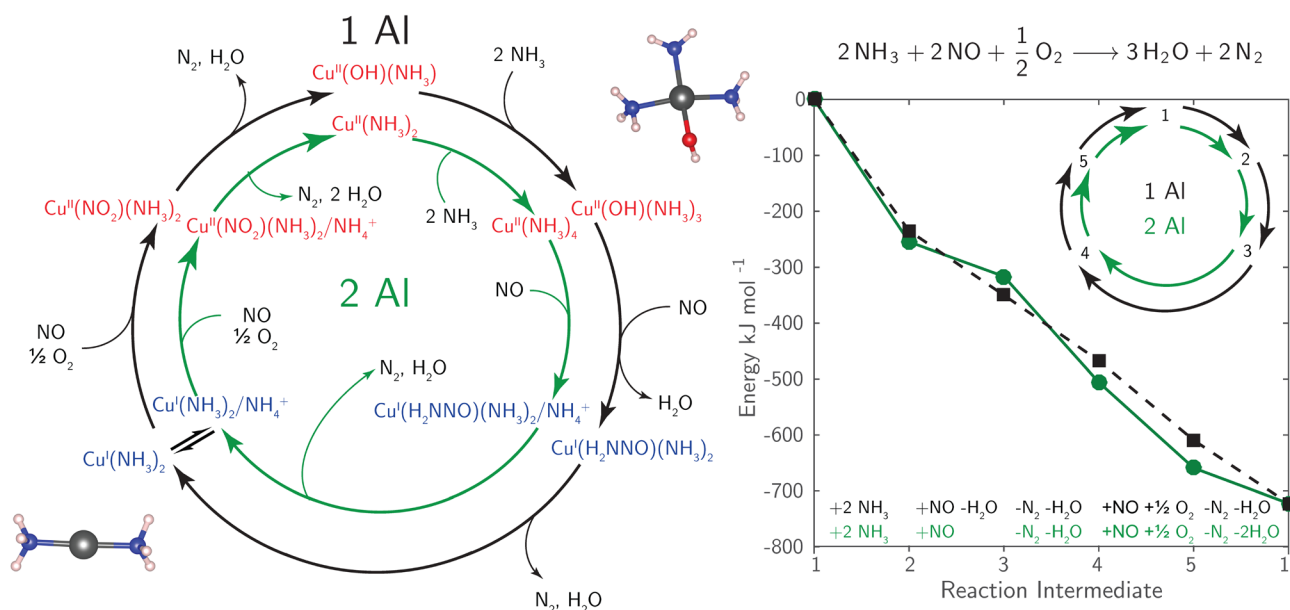
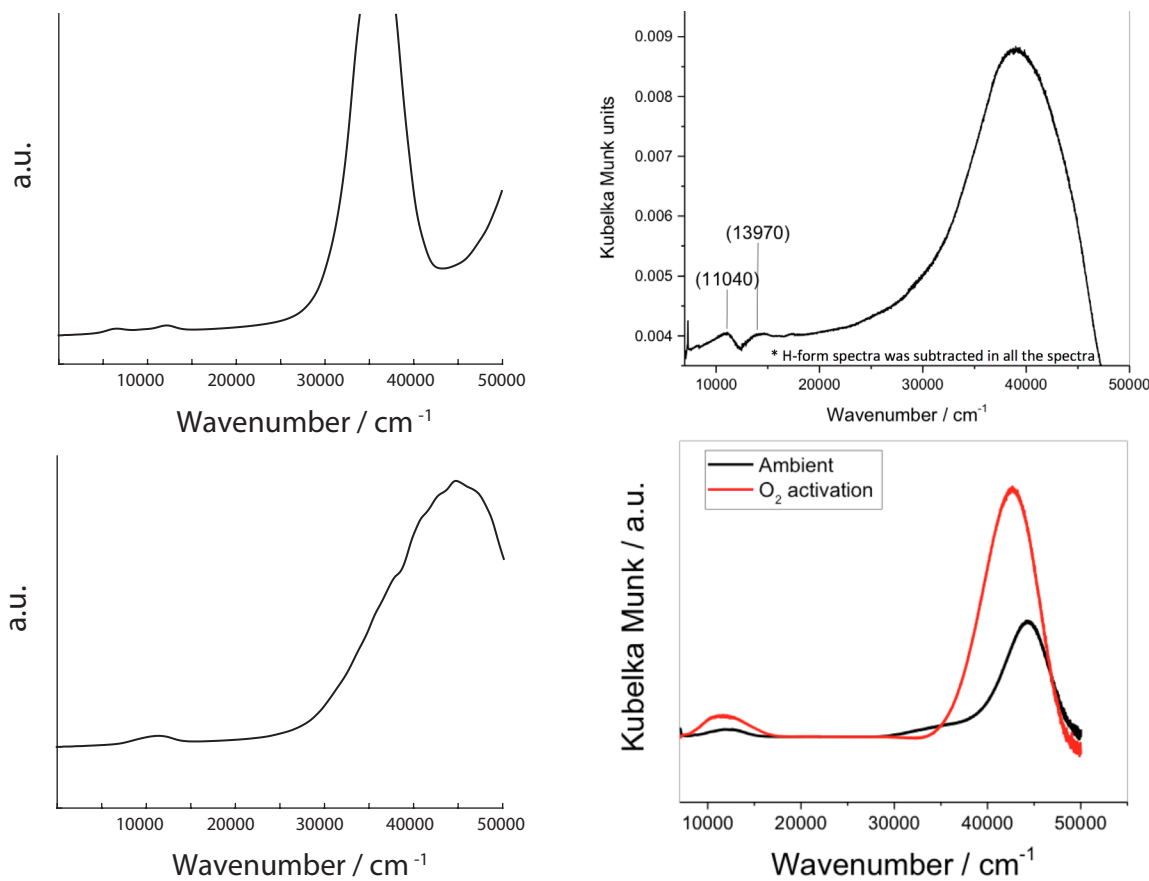


Figure 1. (Left) Proposed parallel standard SCR cycles for NH<sub>3</sub> solvated Cu ions near 1 Al (black) or 2 Al (green). (Right) HSE06-TSvdw-computed reaction energies along each step of the proposed cycles. 1–5 correspond to the intermediates in the left panel. Listed are the molecules consumed (+) and generated (–) between each intermediate.

computed from first principles. The spectra are found to be a product both of differences in the Cu site structure and their mobility within the exchange site. The results decouple the UV-visible fingerprints of these sites from new ones that appear at higher Cu loading.

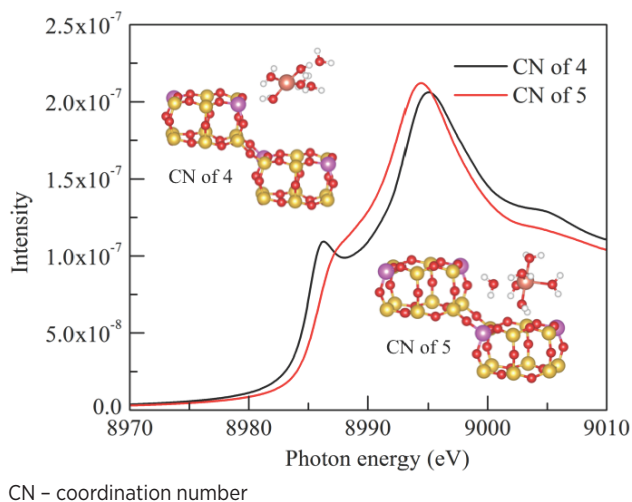
The X-ray absorption near edge structure (XANES) and the X-ray emission spectroscopy (XES) features were modeled to aid in identification of reactants, intermediates and products at the active sites during the SCR reaction. Models show that the intensities of some of the XANES spectral features are sensitive both to the Cu oxidation state and to the number of solvating species ( $\text{NH}_3$  or  $\text{H}_2\text{O}$ ) around the Cu (Figure 3). As for the modeling of the XES, the calculations confirmed, in agreement with the experimental results that are available in the literature, that this technique is a sensitive probe of the nature of the ligands. In particular, our modeling results show that it is possible to distinguish Cu–N and Cu–O bonds with this technique.

Experiments on Cu-SSZ-13 samples containing only isolated Cu(II) ions but at very low Cu densities revealed that 200°C standard SCR rates depend quadratically, rather than linearly, on the Cu density and that apparent  $\text{O}_2$  orders decrease systematically with increasing Cu density (Figure 4). One possible interpretation of these results is that two Cu ions pair during a part of the SCR cycle that is sensitive to the  $\text{O}_2$  pressure. X-ray observation of Cu oxidation states suggest that this pairing may be associated with both the oxidation of Cu(I) to Cu(II) and increase in Cu coordination from two to four. DFT calculations show that two  $\text{NH}_3$ -solvated Cu(I) ions combine with apparently no activation energy to form an  $\text{O}_2$ -bridged dimer and ultimately oxidize Cu(I) to Cu(II), and further that these  $\text{NH}_3$ -solvated Cu(I) ions are mobile within the SSZ-13 lattice. These results both explain the observed rate dependence on Cu(I) density and further highlight the importance of  $\text{NH}_3$ -solvation in facilitating Cu(I) mobility.



a.u. – arbitrary units

Figure 2. Simulated (left) and observed (right) UV-visible spectra of the ZCuOH model and sample (top) and  $\text{Z}_2\text{Cu}$  model and sample (bottom).



CN – coordination number

Figure 3. Recent modeling results of the Cu K-edge XANES in Cu-SSZ-13 show that the intensity and edge position does not only depend on the oxidation state of Cu, but also its coordination environment.

## Conclusions

- A combined experiment and molecular-level modeling approach has elucidated the nature of the Cu active sites and key elements of the SCR mechanism.
- Synthetic methods have been developed to control the types of active sites present and spectroscopic techniques to observe those sites.
- At temperatures at or below 200°C, Cu sites are  $\text{NH}_3$ -solvated and mobile. The mobility of Cu may play a critical role in the SCR mechanism.

## FY 2016 Publications/Presentations

1. C. Paolucci, A.A. Parekh, I. Khurana, J.R. Di Iorio, H. Li, J.D. Albarracin Caballero, A.J. Shih, T. Anggara, W.N. Delgass, J.T. Miller, F.H. Ribeiro, R. Gounder, and W.F. Schneider. “Catalysis in a Cage: Condition-Dependent Speciation and Dynamics of Exchanged Cu Cations in SSZ-13 Zeolites,” *Journal of the American Chemical Society* 138 (2016) 6028-6048.
2. J.R. Di Iorio and R. Gounder, “Controlling the isolation and pairing of aluminum in chabazite zeolites using mixtures of organic and inorganic structure-directing agents,” *Chemistry of Materials* 28 (2016) 2236–2247.
3. C. Paolucci, J.R. Di Iorio, F.H. Ribeiro, R. Gounder, and W.F. Schneider, “Catalysis Science of  $\text{NO}_x$  Selective Catalytic Reduction with Ammonia over Cu-SSZ-13 and Cu-SAPO-34,”

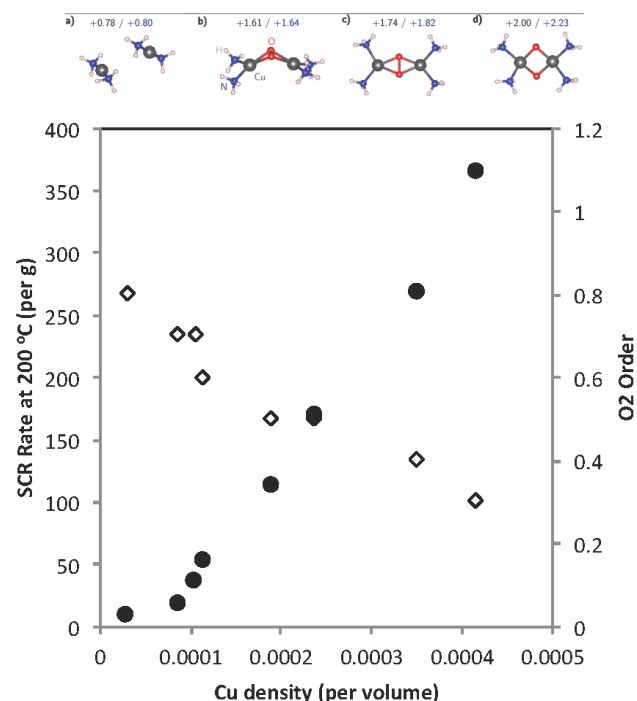


Figure 4. (top) Schematic of  $\text{Cu}(\text{I})(\text{NH}_3)_2$  dimerization in presence of  $\text{O}_2$ . (bottom) Dependence on SCR rate (per g) on Cu density in Cu-SSZ-13 and corresponding  $\text{O}_2$  orders.

*Advances in Catalysis* 59 (2016) 1-107, in press, DOI: 10.1016/bs.acat.2016.10.002.

4. V.J. Cybulskis, F.H. Ribeiro, R. Gounder, “Using a Hands-On Hydrogen Peroxide Decomposition Activity to Teach Catalysis Concepts to K-12 Students,” *Journal of Chemical Education* 93 (2016) 1406–1410.
5. T. Anggara, C. Paolucci, and W.F. Schneider. “Periodic DFT Characterization of  $\text{NO}_x$  Adsorption in CuExchanged SSZ-13 Zeolite Catalysts,” *Journal of Physical Chemistry C* (2016) in press, DOI: 10.1021/acs.jpcc.6b07972.
6. R. Zhang, K. Helling and J.-S. McEwen. “Ab initio X-ray Absorption Modeling of Cu-SAPO-34: Characterization of Cu Exchange Sites Under Different Conditions,” *Catalysis Today* 267 (2016) 28–40.
7. R. Zhang, J. Szanyi, F. Gao and J.-S. McEwen. “The Interaction of Reactants, Intermediates and Products with Cu ions in Cu-SSZ-13  $\text{NH}_3$  SCR Catalysts: An Energetic and Ab Initio X-ray Absorption Modeling Study,” *Catalysis Science and Technology* 6 (2016) 5812–5829. Featured on the inside cover of issue with a DOI of 10.1039/C6CY90075E.

8. R. Zhang and J.-S. McEwen. "Local Environment Sensitivity of the Cu K-edge XANES Features in Cu-SSZ-13: An Analysis from First Principles," *Journal of Physical Chemistry Letters* (2016) submitted.
9. W.F. Schneider (2016). *First Principles Models of Heterogeneity in Catalysis*. American Chemical Society National Meeting. San Diego, CA.
10. W.F. Schneider (2015). *Molecular Elucidation of NO<sub>x</sub> Selective Catalytic Reduction in Cu-SSZ-13*. Pacificchem. Honolulu, HI.
11. W.F. Schneider (2016). *Operando Computations for Discovery in Heterogeneous Catalysis*. Midwest Theoretical Chemistry Conference. Pittsburgh, PA.
12. J.R. Di Iorio (2016). *Controlling the Isolation and Pairing of Aluminum in Chabazite Zeolites Using Mixtures of Organic and Inorganic Structure-Directing Agents*. Michigan Catalysis Society Spring Symposium. Midland, MI.
13. J.R. Di Iorio (2016). *Controlling the Isolation and Pairing of Aluminum in Chabazite Zeolites Using Mixtures of Organic and Inorganic Structure-Directing Agents*. Catalysis Club of Chicago Spring Symposium. Naperville, IL.
14. R. Gounder (2016). *Synthetic methods to control framework aluminum distribution in chabazite zeolites and consequences for NO<sub>x</sub> selective catalytic reduction with ammonia*. American Chemical Society National Meeting. San Diego, CA.
15. R. Gounder (2016). *Structural and Kinetic Changes to Small-Pore Cu-Zeolites After Hydrothermal Treatment and NO<sub>x</sub> SCR with Ammonia*. DOE Cross-Cut Lean Engine Emissions Reduction Simulations (CLEERS) Workshop, Ann Arbor, MI.
16. R. Gounder (2016). *New Insights into the Mechanisms and Active Site Requirements of Low Temperature NO<sub>x</sub> SCR with Ammonia on Cu-SSZ-13 Zeolites*. DOE Cross-Cut Lean Engine Emissions Reduction Simulations (CLEERS) Workshop, Ann Arbor, MI.
17. R. Gounder (2016). *Controlling the Al Distribution and Cu Speciation and Proximity in Cu-SSZ-13 Zeolites: Consequences for NO<sub>x</sub> SCR Catalysis*. Catalysis Club of Philadelphia Spring Symposium, Newark, DE.
18. R. Gounder (2016). *Catalysis in a Cage: The Dynamic Nature of Active Sites in Cu-SSZ-13 During NO<sub>x</sub> SCR with Ammonia*. International Symposium on Catalytic Conversion of Energy and Resources (ISCCER), Seoul, South Korea.
19. A. Shih (2016). *Understanding the Nature and Speciation of the Active Sites on Cu-SSZ-13 During the Selective Catalytic Reduction of NO<sub>x</sub>*. ISCRE 24, Minneapolis, MN.
20. I. Khurana (2016). *Automotive NO<sub>x</sub> Abatement by NH<sub>3</sub> Selective Catalytic Reduction (NH<sub>3</sub>-SCR) on Copper-Exchanged Zeolites*. Catalysis Club of Chicago Spring Symposium, Naperville, IL.
21. F.H. Ribeiro (2016). *On the Reaction Mechanism and the Nature of the Active Site for Standard, Selective Catalytic Reduction of NO<sub>x</sub> on Cu/SSZ-13 Zeolites*. American Chemical Society National Meeting. San Diego, CA.
22. F.H. Ribeiro (2016). *On the Reaction Mechanism and Nature of Active Sites for the Selective Catalytic Reduction (SCR) of NO<sub>x</sub> with NH<sub>3</sub> on Cu/SSZ-13 Zeolites*. International Congress on Catalysis, Beijing, China.
23. J.-S. McEwen, R. Zhang, K. Helling, J. Szanyi, F. Gao (2015). *Spectroscopic Properties of Cu in Cu-SSZ-13 and Cu-SAPO-34 During the Selective Catalytic Reduction of NO<sub>x</sub> with NH<sub>3</sub>: Atomic and Electronic Study From First Principles*, AIChE Meeting, Salt Lake City, UT.
24. E. Anderst, R. Zhang, F. Gao, J. Szanyi, J.-S. McEwen (2015). *NO and NH<sub>3</sub> Adsorption on Fe-SSZ-13: Insights Using DFT Calculations*, AIChE Meeting, Salt Lake City, UT.
25. R. Zhang, H. Li, J. Szanyi, F. Gao, C. Paolucci, T. Anggara, H. Li, W. Schneider and J.-S. McEwen (2016). *Multiple H<sub>2</sub>O and NH<sub>3</sub> Adsorbed on Cu-SSZ-13: XANES and XES Study from First Principles*. 2016 Symposium of the Pacific Northwest Chapter of the American Vacuum Society, PNNL, WA.

## FY 2016 Special Recognitions and Awards/Patents Issued

1. Best Poster Award at Gordon Research Conference on Catalysis, Colby-Sawyer, New Hampshire, June 2016 (C. Paolucci).
2. AIChE CRE Division Travel Award, San Francisco, CA, November 2016 (J. R. Di Iorio).
3. Dow Chemical Company Travel Award for the ISCRE 24 Meeting, Minneapolis, MN, June 2016 (A. Shih).

## III.13 Tailoring Catalyst Composition and Architecture for Conversion of Pollutants from Low Temperature Diesel Combustion Engines

### Overall Objectives

- Predict binary and ternary metal alloy catalyst compositions for enhanced CO, NO, and hydrocarbons (HC) oxidation from first principles density functional theory (DFT) and verify through kinetic and mechanistic studies
- Develop enhanced low temperature CO, HC, and NO oxidation catalysts through zoning and profiling of metal and ceria components
- Develop zoned and layered catalysts that exploit the coupling between in situ NH<sub>3</sub> generation and NO<sub>x</sub> reduction
- Develop reactor models of these catalysts with active site gradients to elucidate the effects of catalyst architecture on performance for the oxidation and reduction catalysts

### Fiscal Year (FY) 2016 Objectives

- Prediction of ternary (surface) alloys from DFT
- Fabrication of diesel oxidation catalysts (DOCs) with axial and radial active site distributions
- Characterization of zoned and layered lean NO<sub>x</sub> trap selective catalytic reduction (LNT/SCR) catalyst performance
- Review of tailor-designed catalysts with catalyst suppliers

### FY 2016 Accomplishments

- A micro-kinetic model was developed that could predict experimentally observed inverse hysteresis behavior during co-oxidation of CO and propylene.
- A zoned catalyst design is predicted to lower the temperature required for 90% conversion by 40°C.
- DFT calculations predict a bimetallic catalyst that avoids NO<sub>2</sub> oxidation of CO and hydrocarbons, such that higher NO<sub>2</sub> yields can be achieved at lower temperature.

**William Epling (Primary Contact),  
Vemuri Balakotaiah, Lars Grabow,  
Michael Harold, and Dan Luss**

University of Houston  
4800 Calhoun Rd.  
Houston, TX 77002  
Phone: (713)743-4234  
Email: wsepling@uh.edu

DOE Technology Development Manager:  
Ken Howden

Subcontractor:  
Oak Ridge National Laboratory, Knoxville, TN

- Using rapid cycling of reductant via a NO<sub>x</sub> storage/reduction process, NO<sub>x</sub> reduction could be achieved 50°C lower than under conventional cycling modes. ■

### Introduction

Diesel engines are more fuel efficient than their gasoline counterparts, but even so, increases in fuel economy are needed. Coincidentally, environmental policies require significant decreases in tailpipe NO<sub>x</sub>, HC, CO, CO<sub>2</sub>, and particulate matter (PM) emissions from diesel engines. To meet these emissions regulations and fuel economy demands, the diesel engine community has developed low temperature combustion (LTC) engines.

Most past research and development effort has focused on NO<sub>x</sub> and PM emissions control from conventional diesel engines. Current diesel aftertreatment systems contain catalysts in series, including a DOC, followed by some combination of a NO<sub>x</sub> storage/reduction catalyst, an SCR catalyst and a diesel particulate filter. Although the relatively low temperature of conventional diesel engine exhaust is already a challenge, LTC engines have persistently lower exhaust temperatures. While NO<sub>x</sub> and PM emissions are reduced, there are substantially higher levels of CO and HC emissions. These trends put significantly more emphasis on the activity of the oxidation catalyst and low temperature NO<sub>x</sub> reduction performance.

## Approach

Computational catalyst screening is being used to predict optimal metal alloy compositions for DOCs. The approach requires DFT derived binding energies and activation barriers, which are subsequently reduced to a minimum set of reactivity descriptors. The use of descriptors allows subsequent combinatorial screening of binary and ternary metal alloys using high performance computing infrastructure. The data obtained from reactor studies is being used as a source for the DFT studies, as well as for the micro-kinetic and reactor models being developed. The key is evaluating the impact of metal ratios and loading on oxidation reactions.

$\text{NO}_x$  reduction at low temperatures is also challenging, particularly with the inability to use urea as an  $\text{NH}_3$  source, since urea will not hydrolyze at some LTC exhaust temperatures. Layered  $\text{NO}_x$  reduction catalysts are being utilized to take advantage of in situ  $\text{NH}_3$  formation and the inherent reductants in the exhaust ( $\text{H}_2$ ,  $\text{CO}$ , and  $\text{HC}$ ).

## Results

### Modeling Efforts

A micro-kinetic model was developed that predicts experimentally observed inverse hysteresis behavior during co-oxidation of  $\text{CO}$  and propylene over a DOC. The reason for inverse hysteresis behavior is the formation of several surface intermediates during extinction, or when the feed gas temperature drops. These surface intermediates compete with  $\text{CO}$  for adsorption on active sites and therefore reduce available reaction sites and the light-off activity of  $\text{CO}$  during this temperature ramp down phase. This results in inverse hysteresis.

Although the micro-kinetic model provides more details since it contains reaction steps as part of the mechanism, a global kinetic model can be useful because of the smaller amount of computational effort required. Therefore, the results obtained using a global kinetic model was compared with the results obtained using a micro-kinetic model. Figure 1 compares the global kinetic model and the detailed model for 1%  $\text{CO}$  oxidation at two different ramp rates. It can be observed from Figure 1 that light-off temperature during ramp-up phase is nearly the same for both the global and detailed models for the case of a ramp rate of 1 K/min. The slight difference in the light-off temperature for the 10 K/min ramp rate is attributed to the transport delay associated with the faster ramp rate. In both cases (1 K/min and 10 K/min), the extinction temperature for the detailed model is quite different from the extinction temperature predicted using the global kinetic model. The global kinetic model originates through the assumption that the surface reaction step is rate limiting. However, the desorption of  $\text{CO}$  is rate limiting during the ramp down phase. This is the reason for the different extinction temperatures predicted by the global and detailed models.

DFT was used to predict bimetallic alloy surfaces that lead to improved  $\text{NO}$  oxidation in the presence of  $\text{CO}$  and hydrocarbon species. Specifically, it is known that  $\text{NO}$  oxidation occurs, but  $\text{NO}_2$  as a strong oxidant is quickly consumed in oxidizing any  $\text{CO}$  and hydrocarbons, until their complete oxidation (100% conversion) is achieved. DFT predicts that a bimetallic  $\text{Pd}/\text{Ag}$  catalyst does not catalyze the reaction between  $\text{NO}_2$  and the reductants, which would result in improved  $\text{NO}_2$  levels exiting the upstream diesel oxidation catalyst. This is ultimately beneficial for downstream  $\text{NO}_x$  control devices.

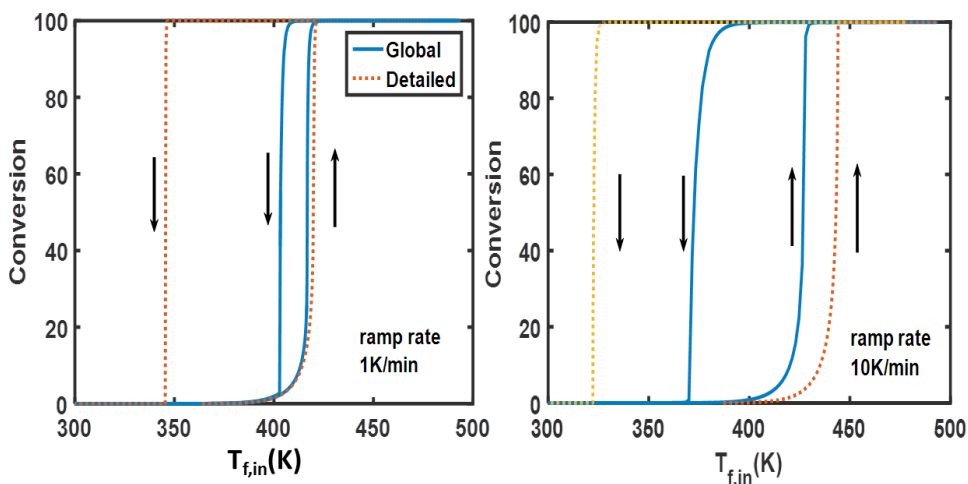


Figure 1. Comparison of hysteresis behavior in global and micro-kinetic models for CO oxidation

## Experimental Efforts

There have been three main areas of accomplishment over the last year. First, coupled homogeneous and heterogeneous hydrocarbon oxidation reactions were demonstrated under conditions relevant in diesel engine exhaust. In testing model DOCs to treat exhaust from low temperature combustion vehicle engines, the simulated exhaust conditions were such that not only did the assumed heterogeneous catalyzed reactions occur, but homogeneous, gas-phase did also. This is exemplified in Figure 2, where in an empty reactor dodecane oxidation was observed, as was NO<sub>2</sub> formation under conditions relevant to diesel exhaust. When homogeneous oxidation occurred, NO was readily oxidized to NO<sub>2</sub> and the larger hydrocarbon species were partially oxidized to aldehyde, alcohol, and alkene intermediates. The homogeneous oxidation potential of several hydrocarbons were compared in the absence and presence of a model oxidation catalyst. Of the hydrocarbons evaluated, diethyl ether led to the best NO to NO<sub>2</sub> oxidation in terms of temperature and extent of conversion, and it did not inhibit oxidation of other hydrocarbon species. The clear evidence of homogeneous reactions occurring within the monolith catalyst channels, and formation of associated reaction intermediates, may impact reactions that would normally be considered isolated to the catalyst surface. These findings demonstrate that in modeling such reactions, the homogeneous reactions

need to be considered and may influence future catalyst design, especially considering the importance of NO<sub>2</sub> for downstream selective catalytic reduction and particulate filter catalyst systems.

Second, the extensive inhibition of hydrocarbon and CO oxidation when mixtures of the two are used was investigated. CO and propylene oxidation were studied, as representative LTC exhaust components, over model bimetallic Pt-Pd/γ-Al<sub>2</sub>O<sub>3</sub> catalysts. During CO oxidation tests, monometallic Pt suffered the most extensive inhibition, which was correlated to a greater extent of dicarbonyl species formation. Pd and Pd-rich bimetallics were inhibited by carbonate formation at higher temperatures. The 1:1 and 3:1 Pt:Pd bimetallic catalysts did not form the dicarbonyl species to the same extent as the monometallic Pt sample, and therefore did not suffer from the same level of inhibition. Similarly, they also did not form carbonates to as large an extent as the Pd-rich samples and were therefore not as inhibited from this intermediate surface species at higher temperature. The Pd-rich catalysts were relatively poor propylene oxidation catalysts; and partial oxidation product accumulation deactivated these catalysts. Byproducts observed include acetone, ethylene, acetaldehyde, acetic acid, formaldehyde, and CO. For CO and propylene co-oxidation, the onset of propylene oxidation was not observed until complete CO oxidation was achieved, and the bimetallics showed higher activity. This was again related to less extensive poisoning, less dicarbonyl species formation and less overall partial oxidation product accumulation.

Third, samples have been fabricated with zones of different precious metal (Pt and Pd) ratios. Based on our experiments and subsequent modeling, >90% conversion can be achieved at lower temperatures when the catalyst is zoned. We predict a 40°C difference in achieving >90% conversions. This aspect is being proven at this stage with further experimentation. We have established a non-disclosure agreement with a catalyst supplier so that best practices in fabrication can be achieved.

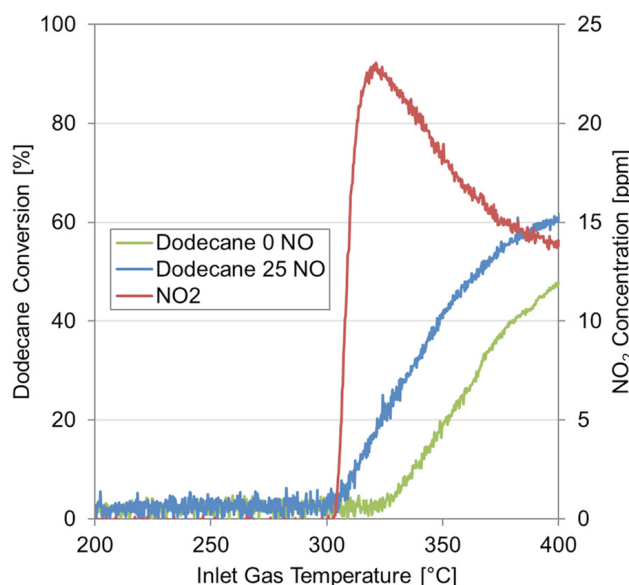


Figure 2. Homogeneous dodecane oxidation and NO<sub>2</sub> formation in an empty quartz tube reactor. Experimental conditions: 250 ppm C<sub>12</sub>H<sub>26</sub>, 0/25 ppm NO, 5% CO<sub>2</sub>, 5% H<sub>2</sub>O, and 10% O<sub>2</sub> in balance N<sub>2</sub>.

## Conclusions

- Oxidation hysteresis behavior can be predicted using a microkinetic model.
- A global model was unable to predict CO oxidation extinction behavior, whereas a microkinetic model was.
- When multiple reactions are occurring over the same catalyst, a zoning approach can be used to minimize the amount of catalyst or improve overall performance in terms of conversions.

- A significant improvement in  $\text{NO}_x$  reduction can be achieved with rapid cycling between the lean and rich phases of a  $\text{NO}_x$  storage reduction cycle.

## FY 2016 Publications/Presentations

1. L.C. Grabow, Q. Yuan, H.A. Doan and S.R. Brankovic, “Novel 2D RuPt Core-Edge Nanocluster Catalyst for CO Electro-oxidation,” *Surface Science* 640(2015)50.
2. M.J. Hazlett and W.S. Epling, “Spatially resolving CO and  $\text{C}_3\text{H}_6$  oxidation reactions in a  $\text{Pt}/\text{Al}_2\text{O}_3$  model oxidation catalyst,” *Catalysis Today* 267(2016)157.
3. R. Raj, M.P. Harold and V. Balakotaiah, “Steady-state and dynamic hysteresis effects during lean co-oxidation of CO and  $\text{C}_3\text{H}_6$  over  $\text{Pt}/\text{Al}_2\text{O}_3$  monolithic catalyst,” *Chemical Engineering Journal* 281(2015)322.
4. R.K. Dadi, D. Luss and V. Balakotaiah, “Bifurcation features of mixtures containing CO and hydrocarbons in diesel oxidation catalyst,” *Chemical Engineering Journal* 304(2016)941.
5. R.K. Dadi, D. Luss and V. Balakotaiah, “Dynamic hysteresis in monolith reactors and hysteresis effects during co-oxidation of CO and  $\text{C}_2\text{H}_6$ ,” *Chemical Engineering Journal* 297(2016)325.
6. Y. Zheng, M. Li, M.P. Harold, and D. Luss, “Enhanced Low-temperature NOx Conversion by High-Frequency Hydrocarbon Pulsing on a Dual Layer LNT-SCR Catalyst,” *SAE Journal* 2015-01-0984.
7. Y. Zheng, M.P. Harold and D. Luss, “Effects of CO,  $\text{H}_2$ , and  $\text{C}_3\text{H}_6$  on Cu-SSZ-13 Catalyzed  $\text{NH}_3$  Based Selective Catalytic Reduction,” *Catalysis Today* 264(2016)44.
8. Y. Zheng, M.P. Harold, and D. Luss, “Rapid Propylene Pulsing for Enhanced Low Temperature NOx Conversion on Combined LNT-SCR Catalysts,” *Catalysis Today* 267(2016)192.

## Special Recognitions and Awards/ Patents Issued

1. Yuying Song received the Colt Refining Award from the International Precious Metals Institute.

## III.14 Low Temperature NO<sub>x</sub> Storage and Reduction Using Engineered Materials

### Overall Objectives

- Improve the low temperature performance of catalyst-based NO<sub>x</sub> mitigation systems by designing materials which can function as either passive NO<sub>x</sub> adsorbers (PNAs) or low temperature lean NO<sub>x</sub> trap (LNT) catalysts
- Develop materials capable of storing NO<sub>x</sub> at low temperatures (<200°C); these materials should also readily release NO<sub>x</sub> at higher temperatures (>200°C) under lean conditions, at which point the NO<sub>x</sub> can be reduced by a downstream selective catalytic reduction SCR catalyst
- Develop materials for LNT applications which can store NO<sub>x</sub> at low temperatures but which form thermally stable nitrites/nitrates under lean conditions

### Fiscal Year (FY) 2016 Objectives

- Complete microreactor and diffuse reflectance infrared Fourier transform spectroscopy (DRIFTS) studies on Ce<sub>0.2</sub>Zr<sub>0.8</sub>O<sub>2</sub> promoted by Pt and Pd
- Evaluate the NO<sub>x</sub> storage and release performance of Pd-promoted mixed oxides by microreactor and in situ DRIFTS methods
- Prepare monolith samples by washcoating the most promising PNA powder materials onto cores taken from cordierite substrates
- Evaluate the monolith core samples using facilities at Ford Motor Co. and Oak Ridge National Laboratory (including the use of spatially resolved capillary inlet mass spectrometry)
- Complete project reporting

### FY 2016 Accomplishments

- The majority of work in the past year focused on a set of samples which show particular promise for PNA applications. Based on this work, a joint University of Kentucky and MEL Chemicals patent application is in preparation and will be submitted shortly.
- Bench reactor studies were performed on 0.9% Pt-0.9% Pd/Ce<sub>0.2</sub>Zr<sub>0.8</sub>O<sub>2</sub>, both before and after hydrothermal aging. For the fresh material, high NO<sub>x</sub> storage efficiency (90%) was obtained at short storage times

**Mark Crocker (Primary Contact),  
Yaying Ji, Samantha Jones**

University of Kentucky Center for Applied Energy Research

2540 Research Park Drive

Lexington, KY 40511

Phone: (859) 257-0295

Email: mark.crocker@uky.edu

DOE Technology Development Manager:  
Ken Howden

Subcontractors:

- MEL Chemicals, Flemington, NJ (John Darab)
- Oak Ridge National Laboratory (Fuels, Engines and Emissions Research Center), Oak Ridge, TN (Jae-Soo Choi)

Partners:

Ford Motor Co., Dearborn, MI (Christine Lambert)

(<2 min). Hydrothermal aging induced a 10% drop in NO<sub>x</sub> storage efficiency (NSE), while NO<sub>x</sub> desorption efficiency (NDE) of ca. 80% was achieved both before and after hydrothermal aging upon ramping the temperature to 350°C.

- CO exerted almost no impact on NSE at 160°C but significantly improved NO<sub>x</sub> storage performance at 120°C and 80°C. However, C<sub>2</sub>H<sub>4</sub> exerted a negligible impact on NSE regardless of storage temperature.
- DRIFTS measurements indicated that both nitrate and nitrite species were generated on 0.9% Pt-0.9% Pd/Ce<sub>0.2</sub>Zr<sub>0.8</sub>O<sub>2</sub> during NO storage. However, more nitrate species were generated relative to nitrite after hydrothermal aging. ■

### Introduction

The use of a PNA device in combination with a urea SCR catalyst is an attractive option for the abatement of cold-start diesel NO<sub>x</sub> emissions which to date has been little explored. In this system the PNA adsorbs NO<sub>x</sub> emitted from the engine during cold starts, and then releases the NO<sub>x</sub> at higher temperatures, e.g., ≥200°C. At this point the

SCR catalyst is sufficiently warm to function efficiently, while the temperature is also high enough to permit stoichiometric injection of urea. By developing materials tailored for this purpose, this project intends to fully develop this concept. Insights gained in this work should also aid the development of materials suitable for low temperature  $\text{NO}_x$  storage–reduction, as applied in LNT catalysts. This work will be of benefit to both urea SCR and LNT–SCR  $\text{NO}_x$  reduction systems and will directly address the emission control research and development tasks pertaining to  $\text{NO}_x$  control outlined in the DOE Vehicle Technologies 2011–2015 Multi-Year Program Plan.

## Approach

The overarching goal of this proposal is to improve the low temperature performance of catalyst-based  $\text{NO}_x$  mitigation systems. Towards this goal, we are employing a two-pronged approach which may be summarized as follows:

- The development of PNAs. We will develop materials capable of storing  $\text{NO}_x$  at low temperatures ( $<200^\circ\text{C}$ ), either as nitrite ( $\text{NO}_2^-$ ) and/or as nitrate ( $\text{NO}_3^-$ ), and which readily release  $\text{NO}_x$  at higher temperatures ( $>200^\circ\text{C}$ ) under lean conditions, at which point the  $\text{NO}_x$  can be reduced by a downstream SCR catalyst (with urea injection downstream of the  $\text{NO}_x$  adsorber providing the necessary reductant).
- The design of materials for improved low temperature  $\text{NO}_x$  storage and reduction. Building on knowledge generated in the first activity, materials will be developed which can store NO at low temperatures but which form thermally stable nitrites/nitrates.

## Results

The majority of work in the past year focused on a set of samples which show particular promise for PNA applications. As a result of these studies, the University of Kentucky and MEL Chemicals decided to file a joint patent application. This application is ongoing, such that the pertinent results cannot be disclosed at present.

In other work, one of the more promising catalysts identified to date, Pt-Pd/Ce<sub>0.2</sub>Zr<sub>0.8</sub>O<sub>2</sub> (0.9 wt% Pt and 0.9 wt% Pd), was coated onto monolith cores and evaluated on a bench reactor. As shown in Figure 1, NSE of  $>90\%$  was obtained for the first 2 min of storage, which then decreased with increasing storage time. Hydrothermal aging at  $750^\circ\text{C}$  resulted in a ca. 10% drop in NSE. However, regardless of aging, over 80% NDE was achieved over the catalyst during ramping to  $350^\circ\text{C}$ .

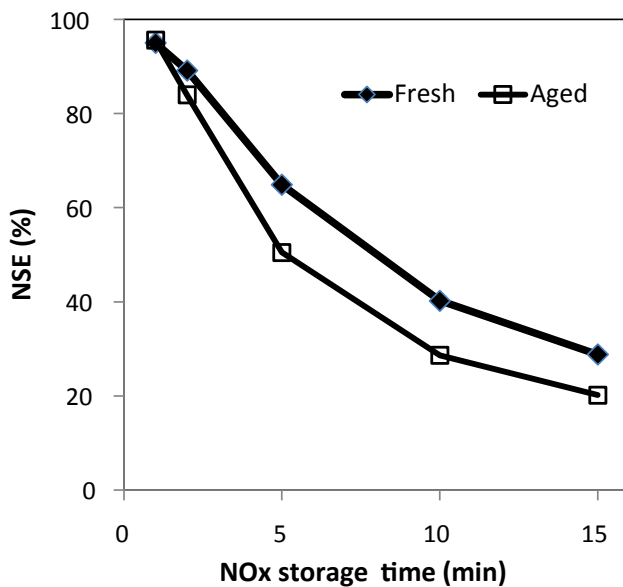
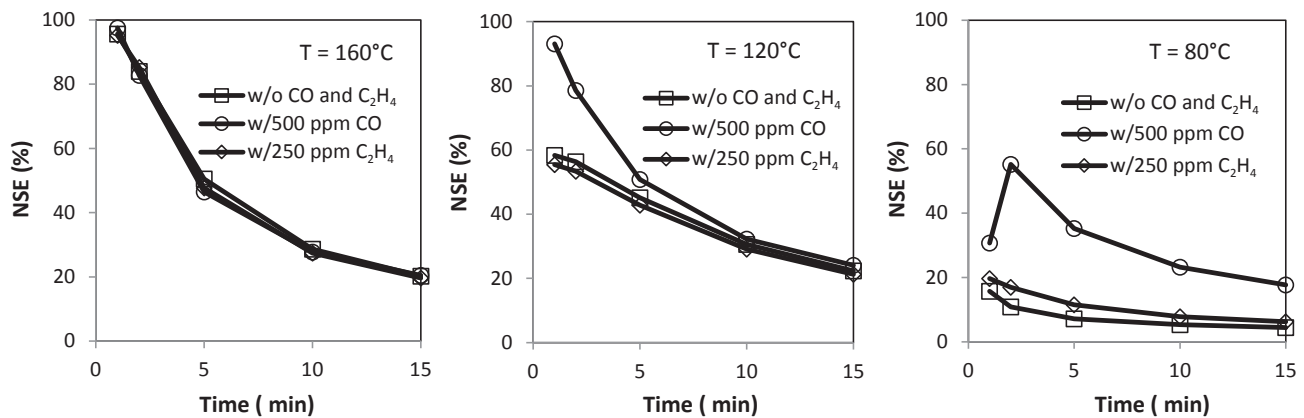


Figure 1. NSE at  $160^\circ\text{C}$  for fresh and aged Pd-Pd/Ce-Zr. Feed gas: 100 ppm NO, 10% O<sub>2</sub>, 5% CO<sub>2</sub>, 5% H<sub>2</sub>O, He as balance; gas hourly space velocity (GHSV) = 30,000 h<sup>-1</sup>.

More detailed studies were carried out on the hydrothermally (HT) aged catalyst. Figure 2 compares the NSE at three different temperatures under different conditions. Similar to earlier results obtained for powder samples, the storage temperature was found to significantly impact  $\text{NO}_x$  storage performance, higher NSE being obtained for the first 2 min at  $160^\circ\text{C}$  compared to at  $120^\circ\text{C}$  and  $80^\circ\text{C}$ . In addition, the effect of other exhaust gas components on NO storage was examined. CO exerted a negligible impact at  $160^\circ\text{C}$ , although a significant improvement in NSE was obtained at  $120^\circ\text{C}$  for the first 2 min, as well as during the entire storage phase at  $80^\circ\text{C}$ . This finding is similar to observations made by our project partner, Ford, and can be rationalized on the basis that CO either aids NO storage via the formation of isocyanates and/or is able to reduce the precious metals, thereby promoting NO adsorption. In contrast, C<sub>2</sub>H<sub>4</sub> had almost no impact during the storage phase regardless of storage temperature. Moreover, the addition of CO and C<sub>2</sub>H<sub>4</sub> to the gas feed during NO storage had no effect on subsequent  $\text{NO}_x$  desorption behavior.

The impact of inlet NO concentration on  $\text{NO}_x$  storage and desorption performance was also investigated for the HT-aged catalyst. As displayed in Figure 3, NSE decreased with increasing inlet NO concentration as evidenced by a drop in NSE of ca. 30% during the first minute of storage when the NO concentration was increased from 100 ppm to 300 ppm. However, there was almost no effect on the NDE during subsequent  $\text{NO}_x$ –temperature programmed



w/ - with; w/o - without

Figure 2. NSE obtained at three different temperatures over HT-aged Pd-Pd/Ce-Zr. Feed gas: 100 ppm NO, 10% O<sub>2</sub>, 5% CO<sub>2</sub>, 5% H<sub>2</sub>O, with and without CO (or C<sub>2</sub>H<sub>4</sub>), He as balance; GHSV = 30,000 h<sup>-1</sup>.

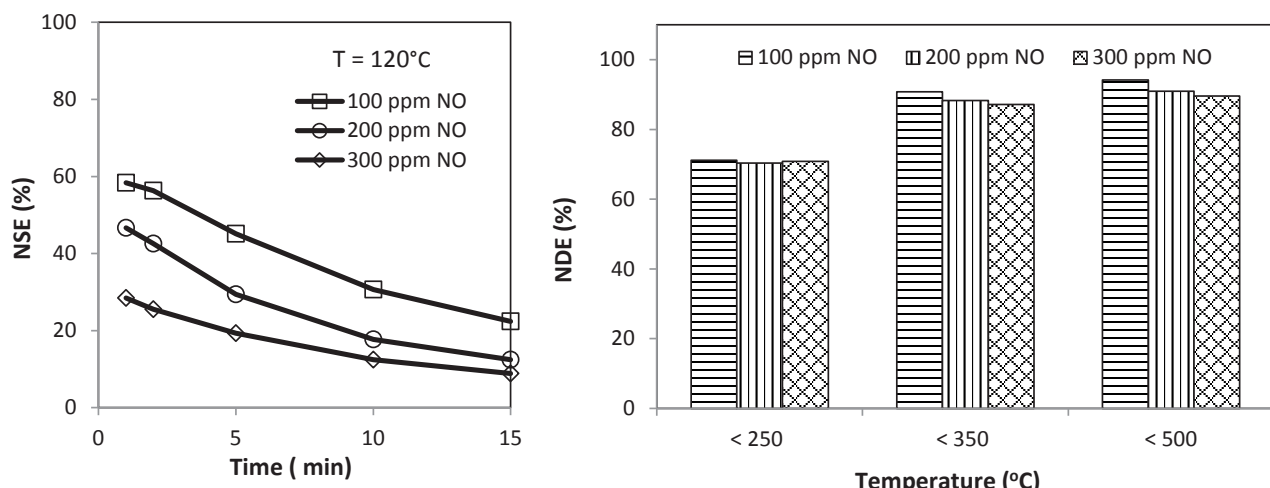


Figure 3. Effect of inlet NO concentration on NSE at 120°C and subsequent NDE over the HT-aged Pd-Pd/Ce-Zr. Feed gas: 100 ppm (200 ppm or 300 ppm) NO, 10% O<sub>2</sub>, 5% CO<sub>2</sub>, 5% H<sub>2</sub>O, He as balance; GHSV = 30,000 h<sup>-1</sup>.

desorption (NO<sub>x</sub>-TPD). NSE at three different locations in the HT-aged core sample was determined using spatially resolved capillary inlet mass spectrometry (Figure 4). Comparison of NSE at different locations indicated that NO<sub>x</sub> storage proceeds in chromatographic-type fashion, NSE increasing with the core length. After hydrothermal aging NSE was reduced throughout the catalyst although more produced reduction was observed in the rear one-third of the catalyst for reasons that are not yet apparent.

To gain insights into the surface chemistry involved during NO<sub>x</sub> storage and desorption, DRIFTS measurements were performed on the fresh and HT-aged Pt-Pd/Ce-Zr catalyst. As shown in Figure 5, during NO<sub>x</sub> storage in the presence of O<sub>2</sub> both nitrate (>1,500 cm<sup>-1</sup>) and nitrite (1,500–1,400 cm<sup>-1</sup>) species were formed almost simultaneously on the fresh sample. However, the nitrite

species grew in more strongly than the nitrate with time and became the dominant species after 20 min. In the case of the HT-aged sample, nitrite formation was less significant as compared to nitrate bands, the catalyst surface being dominated by monodentate nitrate species giving rise to bands between 1,550 cm<sup>-1</sup> and 1,500 cm<sup>-1</sup>. During subsequent NO<sub>x</sub>-TPD, nitrite species disappeared by 300°C, while the nitrate bands first increased in intensity and then started to decrease around 400°C. Residual nitrate species remained on the surface at 500°C for both the fresh and aged samples.

## Conclusions

- Bench reactor studies on 0.9% Pt-0.9% Pd/Ce<sub>0.2</sub>Zr<sub>0.8</sub>O<sub>2</sub> indicated that prior to hydrothermal aging, high NSE (>90%) was obtained at short storage times (<2 min).

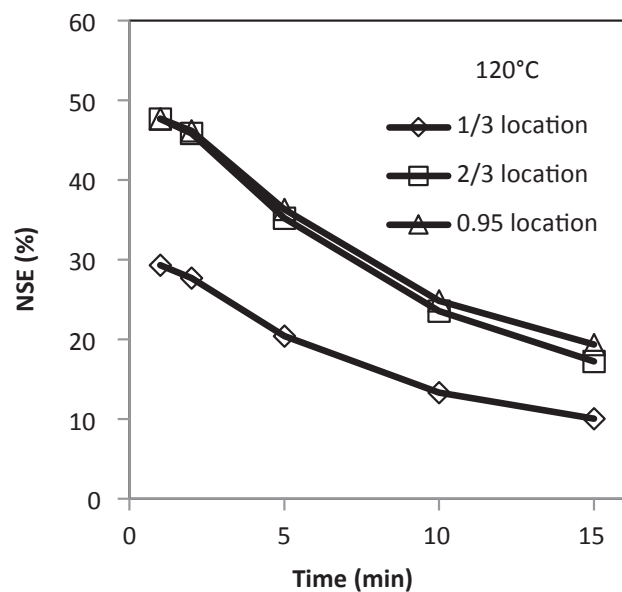


Figure 4. NO<sub>x</sub> storage efficiency as a function of core length for HT-aged Pt-Pd/Ce-Zr. Feed gas as for Figure 1.

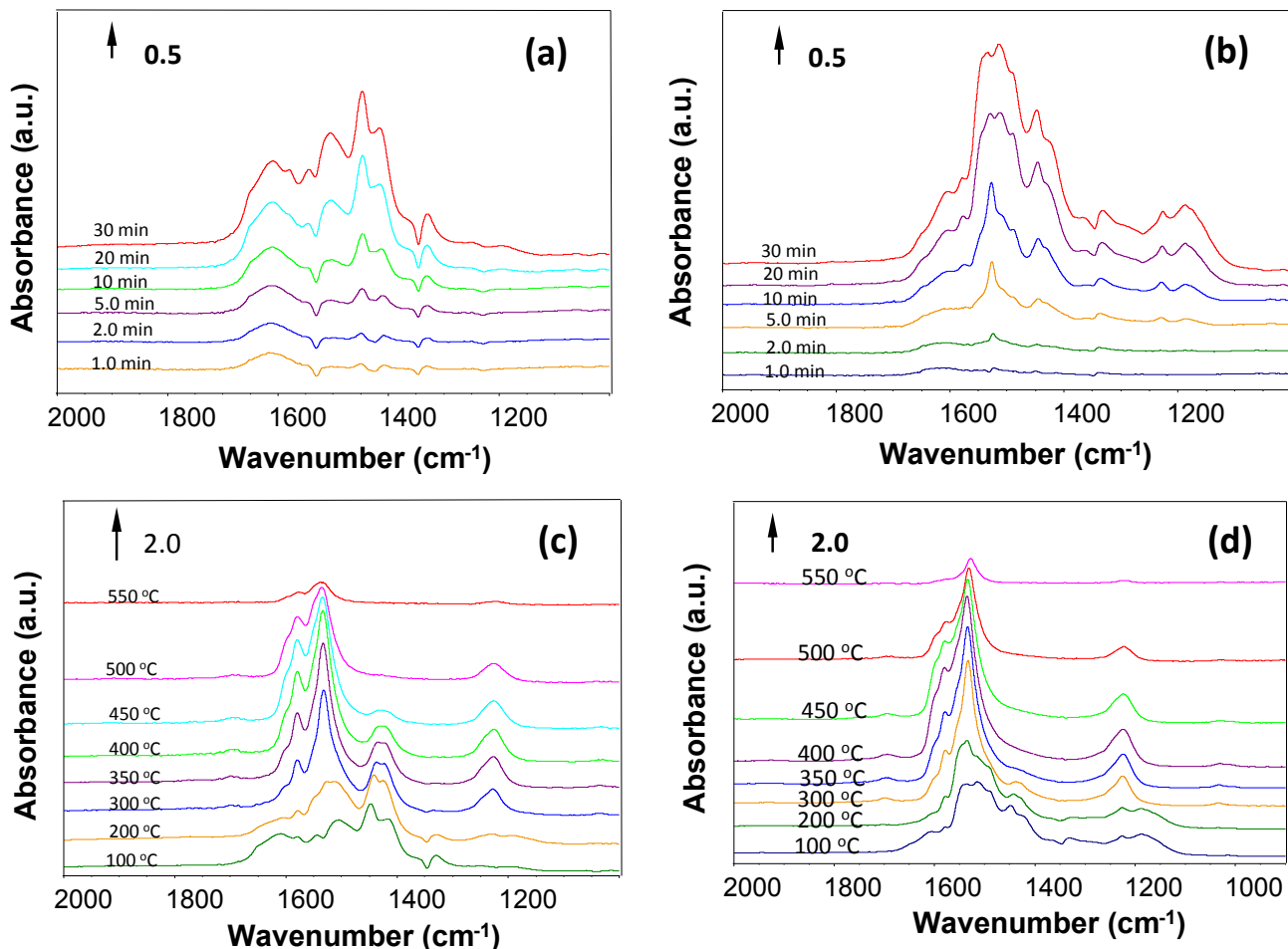


Figure 5. DRIFT spectra acquired during NO<sub>x</sub> storage at 100°C and subsequent NO<sub>x</sub>-TPD over Pd-Pt/Ce-Zr: (a) NO<sub>x</sub> storage on the fresh sample; (b) NO<sub>x</sub> storage on the HT-aged sample; (c) NO<sub>x</sub>-TPD for the fresh sample; (d) NO<sub>x</sub>-TPD for the HT-aged sample

Hydrothermal aging at 750°C induced a 10% drop in NSE, although NDE remained unchanged, ca. 80% of stored NO<sub>x</sub> being desorbed upon ramping the temperature to 350°C.

- Addition of CO to the feed gas during NO<sub>x</sub> storage exerted almost no impact on NSE at 160°C but significantly improved NO<sub>x</sub> storage performance for the first 2 min at 120°C and for the entire storage phase at 80°C. In contrast, the presence of C<sub>2</sub>H<sub>4</sub> exerted a negligible impact on NSE, regardless of storage temperature.
- DRIFTS measurements demonstrated that both nitrate and nitrite species were observed during NO<sub>x</sub> storage regardless of hydrothermal aging. However, more nitrate species (monodentate nitrate) were generated relative to nitrite species after hydrothermal aging.
- Overall, Pt-Pd/Ce<sub>0.2</sub>Zr<sub>0.8</sub>O<sub>2</sub> is indicated to be an interesting candidate for PNA applications.

## FY 2016 Publications/Presentations

1. S. Jones, Y. Ji, M. Crocker, "Ceria-Based Catalysts for Low Temperature NO<sub>x</sub> Storage and Release," *Catal. Lett.*, 146 (2016) 909.
2. Z. Zhang, M. Crocker, L. Yu, X. Wang, C. Shi, "Non-thermal plasma-assisted NO<sub>x</sub> storage and reduction over cobalt-containing Pd catalyst using H<sub>2</sub> and/or CO as reductants," *Catal. Today*, 258 (2015) 175.
3. S. Jones, Y. Ji, A. Bueno-Lopez, V. Song, M. Crocker, "CeO<sub>2</sub>-M<sub>2</sub>O<sub>3</sub> Passive NO<sub>x</sub> Adsorbers for Cold Start Applications," submitted to *Emission Control Sci. Technol.*
4. Y. Ji, D. Xu, S. Bai, U. Graham, M. Crocker, B. Chen, C. Shi, D. Harris, D. Scapens, J. Darab, "Pt- and Pd-promoted CeO<sub>2</sub>-ZrO<sub>2</sub> for passive NO<sub>x</sub> adsorber applications," submitted to *Ind. Eng. Chem. Res.*
5. Y. Ji, M. Crocker, J.-S. Choi, D.W. Brookshear, J. Darab, D. Scapens, D. Harris, Promotion of Ce-Zr mixed oxide with Pt and Pd for low-temperature NO<sub>x</sub> adsorption, oral presentation CATL 161, 252nd ACS National Meeting, Philadelphia, PA, August 21–25, 2016.
6. Y. Ji, S. Bai, D. Xu, M. Crocker, J. Darab, D. Harris, "Pt- and Pd-promoted Ce-Zr Mixed Oxide for Low Temperature NO<sub>x</sub> Adsorption," poster presentation, 2016 CLEERS Workshop, Ann Arbor, MI, April 6–8, 2016.
7. S. Jones, Y. Ji, M. Crocker, A. Bueno Lopez, "CeO<sub>2</sub>-M<sub>2</sub>O<sub>3</sub> Passive NO<sub>x</sub> Adsorbers for Cold Start Applications," oral presentation, 2016 CLEERS Workshop, Ann Arbor, MI, April 6–8, 2016.

## Special Recognitions and Awards/Patents Issued

1. D. Scapens, D. Harris, J.G. Darab, M. Crocker, Y. Ji, patent application pending.

## IV. High-Efficiency Engine Technologies

The Vehicle Technologies Office funds the research, development, and integration of prototype engine/powertrain designs into passenger and commercial vehicle platforms to validate performance, fuel economy improvements, and compliance with future emissions standards. Under cost-shared contract awards, competitively selected teams of engine and original equipment manufacturers and their suppliers focus on developing and testing innovative technologies for engines and powertrains that can increase fuel economy, reduce cost, and address technical barriers currently inhibiting the wider use of advanced engine technologies in the light- and heavy-duty vehicle markets. Projects validate technologies developed at the engine and vehicle level to help ensure that these innovations can advance into broad commercial use at a scale needed to reduce the nation's transportation fuel consumption and greenhouse gas emissions.

Two initiatives, SuperTruck and Advanced Technology Powertrains, focused on improving the fuel economy of commercial vehicles (heavy-duty trucks) and passenger vehicles (cars and light trucks), respectively. Both initiatives accomplished their FY 2015 goals, and new goals were set for FY 2020. In FY 2016, the SuperTruck II projects were initiated to focus on cost-effective measures to improve the efficiency of Class 8 long-haul freight trucks by 100%; engine efficiency is expected to contribute as much as 30%. The Advanced Technology Powertrain projects continued to focus on increasing the fuel economy of passenger vehicles by 35% to 50% (compared to a 2009 baseline vehicle) using an engine/powertrain-only approach.

Enabling technologies development projects focus on approaches such as, but not limited to, variable compression ratio, variable valve timing and lift, boosting systems, high-energy ignition, alternative cylinder head and piston designs, thermal barrier coatings, waste energy recovery, and sensors for engine control systems and for engine diagnostics to achieve the efficiency, performance, and emissions requirements for advanced combustion engines/powertrains. New types of sensors are required for sophisticated feedback systems in support of complex and precise engine and emission controls. NO<sub>x</sub> and particulate matter sensors, and catalyst diagnostic sensors are essential for effective control of advanced engine aftertreatment systems.

Work is coordinated with the Vehicle Systems Program for integration of computational models for the engine combustion and aftertreatment subsystems into a vehicle simulation model that will enable optimization of the engine/powertrain system to ascertain potential contribution to the fuel economy improvement targets.

## IV.1 Volvo SuperTruck Powertrain Technologies for Efficiency Improvement

### Overall Objectives

- Identify concepts and technologies that have potential to achieve 55% brake thermal efficiency (BTE) on a heavy-duty diesel engine; perform thorough analysis of the limiting factors and potential areas for improving the engine's efficiency using analytical simulations, including research into alternative thermodynamic cycles, advanced component design, effects of fuel formulation and new engine designs, as well as development of more advanced combustion modeling tools
- Demonstrate a heavy-duty diesel engine capable of achieving 50% BTE at the end of the SuperTruck project

### Fiscal Year (FY) 2016 Objectives

- Validate a suite of simulation tools to model new combustion concepts and unconventional operating conditions
- Complete the single-cylinder engine to demonstrate the combustion systems designed for the various 55% engine concepts
- Complete a validation study to demonstrate a linkage between the engine simulations, advanced combustion simulations, injector spray modeling, and single-cylinder experimental engine
- Complete the Phase 2 engine and demonstrate 50% BTE on simulated road cycles in the test cell

### FY 2016 Accomplishments

- Simulation tools have been refined and used together to lead design decisions and make accurate predictions of new combustion regimes required for the 55% BTE target.
- Computational fluid dynamics (CFD) combustion models have been validated against one-cylinder engine test data with Primary Reference Fuel 87 surrogate fuel.
- The design of concepts achieving 55% BTE have been progressed and simulated, and practical implementations have been identified.
- The engine installed in the SuperTruck demonstrator was previously proven capable of stable operation at

**Pascal Amar (Primary Contact),  
Richard Morton, Arne Andersson,  
John Gibble, Andre Boehman,  
Dan Haworth, Jacqueline O'Connor**

Volvo Group Trucks North America

13302 Pennsylvania Avenue

Hagerstown, MD 21742

Phone: (301) 790-5400

Email: pascal.amar@volvo.com

DOE Technology Development Manager:

Roland Gravel

NETL Project Manager:

Ralph Nine

Subcontractor:

Pennsylvania State University, State College, PA

48% BTE without waste heat recovery. An upgraded Rankine cycle waste heat recovery system was demonstrated in a test cell, with the complete engine achieving 50% BTE, and produced power as expected on simulated road cycles.

- Gas jet modeling has been able to shed new insight on the physics of multiple injections, interaction between adjacent injection plumes, and jet–wall interactions. This technique has been able to help validate CFD predictions and guide selection of different combustion bowls.
- A novel “wave piston” combustion system, which was developed earlier in this project, has moved into production at Volvo, providing both improved fuel economy and lowered emissions. ■

### Introduction

Designing engines that will achieve ambitious efficiency and emissions goals requires the use of tools capable of simulating new engine operation regimes. Volvo and its partners are taking a holistic approach in improving the tools that guide engine design by employing new methods of simulating advanced and unconventional operating conditions, carrying out tests to validate these simulations and further characterize their results, applying

these developments to the design process, and improving methods of simulating other aspects of engine operation.

A new gas jet visualization laboratory has been commissioned at Penn State University to study fuel injection sprays interacting with piston geometry. This has been incorporated into the collaboration between Volvo and its partners at Penn State University, which includes CFD development as well as the gas jet tests, and the University of Michigan, where engine tests will be used to characterize strategies and validate simulations.

The advanced modeling capabilities these improvements provide have enabled Volvo engineers to design an advanced concept engine that exceeds 55% BTE in GT-POWER simulations.

## Approach

Alternative advanced engine concepts have been described in previous quarterly reports and are currently under evaluation numerically. The concepts incorporate over-expansion, extreme peak cylinder pressure with more efficient compression, partial thermal insulation, and friction reduction. These conditions are well outside of current practice, which leads to significant uncertainty in the accuracy of standard analytical approaches.

Volvo, together with its academic and industry partners, have taken a broad approach to advancing the predictive capabilities for these conditions by supporting advances in chemical reaction modeling, computational efficiency of in-cylinder CFD, and visualization techniques for injector spray modeling. These new methods were assembled into a systematic process along with more conventional one-dimensional (1-D) and three-dimensional (3-D) CFD tools to provide robust predictions, then were validated on a single-cylinder research engine. The design process and tool verification effort consisted of a feedback loop between various simulations and experiments. Figure 1 provides an overview of this process.

In a step-wise procedure, the Volvo team utilized both 1-D complete engine and 3-D combustion and gas flow simulations to work in parallel to develop a series of broad spectrum design of experiments (DOEs) that were used to validate and facilitate downstream lab and bench level tests. These DOEs were filtered for key engine operating parameters that can be verified using conventional engine test cell data, backed with previously calibrated simulations. As these DOEs were post-processed, they were evaluated for consistency and agreement with expected trends towards the 55% BTE goal, where a selected group of parameter values were used to further develop tools, experiments, and hardware

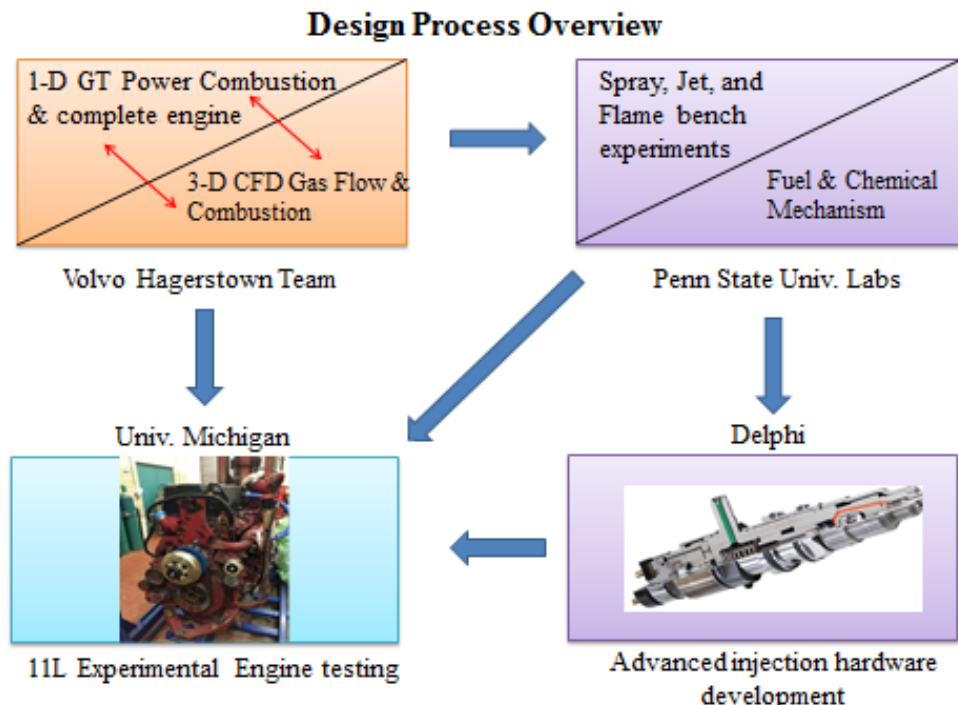


Figure 1. Feedback loop depiction of the design process through experimental and simulation collaboration between partners

downstream. The results of the detailed 3-D parameter analysis aided in the selection of engine hardware, which was then validated in an engine test cell.

## Results

Comprehensive 1-D engine performance screening was carried out in order to investigate the BTE potential of the current Volvo 55% BTE engine concept. A number of key engine speed points varying from 900 rpm to 1,800 rpm were simulated by sweeping the air–fuel equivalence ratio, exhaust gas recirculation rate, rail pressure, and injection timing, respectively, as shown in Figure 2.

A number of these DOE studies were performed to explore the parameter space and down-select conditions to further reduce the number of cases to explore using higher fidelity tools. This simulation process was done using Volvo in-house multidimensional CFD modeling, including spray modeling and combustion modeling. A transported probability density function (PDF) method was implemented to account for unresolved turbulent fluctuations in composition and temperature. While the merits of PDF methods have been amply demonstrated in laboratory turbulent flames, applications to practical combustion systems have been limited.

One important finding from the PDF-based modeling work pertains to the differences in the relative importance of different physical processes in soot formation between atmospheric pressure combustion versus high-pressure turbulent combustion. Compared to atmospheric pressure and flames, where most soot modeling and experimental studies have been done, it has been found that at engine-relevant pressures, computed soot volume fractions are relatively less sensitive to the kinetic rates in the soot

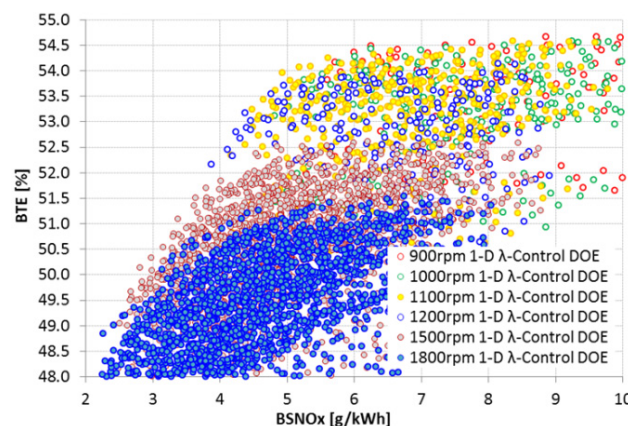


Figure 2. Trade-offs of BTE vs. brake specific  $\text{NO}_x$  (BSNOx) from 55% BTE engine performance screening based on air–fuel equivalence ratio ( $\lambda$ ) sweep

models, because the rates are so fast, and that the rate-limiting processes are turbulent transport and mixing. Accurate accounting for unresolved turbulent fluctuations in composition and temperature is essential.

A series of schlieren and acetone tracer planar laser-induced fluorescence (PLIF) experiments were conducted to determine the optimal bowl geometry and nozzle configuration for effective in-cylinder mixing. Optimal mixing was determined using a metric of “air utilization,” or how well the jet fluid mixes with the ambient fluid. The mixing was determined both by concentrations from the PLIF measurements and quantification of the spatial extent of the jet fluid; for a given injection schedule, a larger spatial extent of the jet fluid indicates better fluid mixing and air utilization. Two bowl shapes were tested in two different configurations, allowing for measurement of different flow processes. First, the bowl shapes were extruded into a two-dimensional block, shown in Figure 3, which allowed for schlieren imaging of the jet flow along the contour of the bowl wall.

Second, the bowl shapes were rotated to make a sector of the bowl, and the flow along the bowl was imaged from two angles using acetone-PLIF. This configuration is shown in Figure 4, where the bowl sector has a mounting plate attached to it on the top right of the figure. Both the bowl shapes in Figure 3 and Figure 4 were fabricated using a 3-D printer and are made from dark-colored plastic to reduce laser reflections.

## Conclusions

The outcome of this work is an improved design methodology for exploring advanced combustion strategies that result in ultra-high efficiency and low

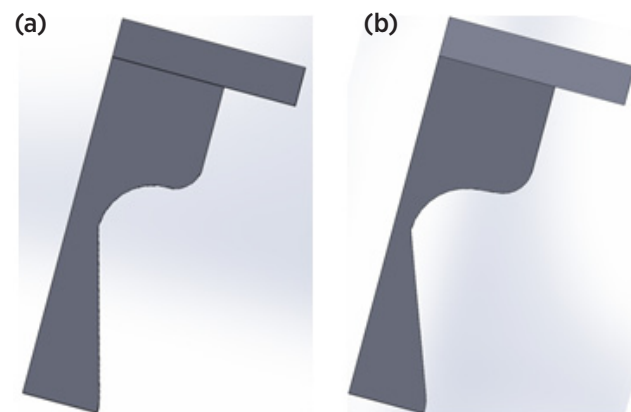


Figure 3. Two-dimensional extrusions of (a) Bowl 1 and (b) Bowl 3 used for schlieren imaging of jet interaction with bowl shape

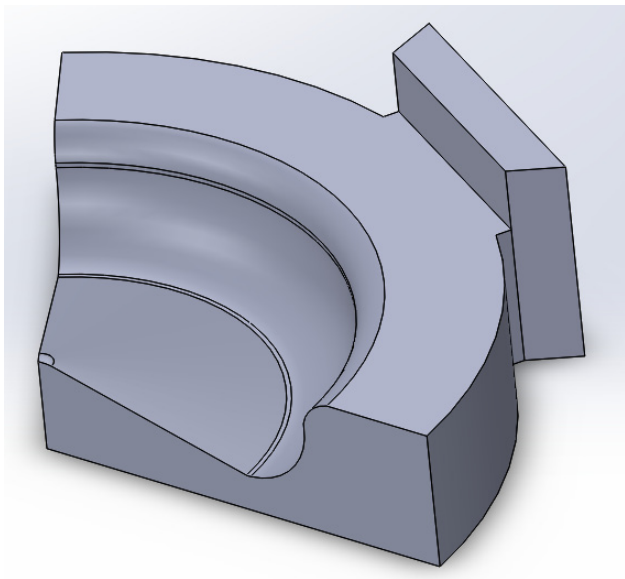


Figure 4. Three-dimensional rotation of Bowl 1 used for acetone-PLIF imaging of jet interaction with bowl surfaces

emissions combustion. The unique combination of 1-D and 3-D simulation, scaled experiments, and engine testing is used to design and understand combustion processes in new engine geometries and at high-efficiency engine operating conditions. These methods were used to refine the piston bowl design and helped to identify combustion strategies that would reach the design goal of 55% BTE. Engine testing throughout this process has helped to validate models and provide insight into the impact of design choices on engine performance.

## FY 2016 Publications/Presentations

1. Borz, M., Kim, Y., and O'Connor, J., "The Effects of Injection Timing and Duration on Jet Penetration and Mixing in Multiple-Injection Schedules," SAE Technical Paper 2016-01-0856.
2. Han, J., V.B. Kalaskar, D. Kang, D.C. Haworth, A.L. Boehman, "A Computational and Experimental Study of Ignition Behavior of Gasoline Surrogate Fuels Under Low-Temperature Combustion Conditions," 2016 Spring Technical Meeting of the Eastern States Section of the Combustion Institute, Princeton, NJ, March 13–16, 2016.
3. Han, J., V.B. Kalaskar, D. Kang, D.C. Haworth, A.L. Boehman, "Ignition Behavior of Gasoline Surrogate Fuels Under Low-Temperature Combustion Conditions," International Multidimensional Engine Modeling User's Group Meeting at the SAE Congress, Detroit, MI, April 11, 2016.

4. Kalaskar, V., D. Kang, A.L. Boehman, "Impact of Fuel composition and intake pressure on lean autoignition of gasoline surrogates in a CFR engine" in preparation for submission to *Combustion and Flame*, 2017.
5. Lundgren, M., "Optical study on combustion transition from HCCI to PPC with gasoline compression ignition in a HD engine," SAE Technical Paper 2016-01-0768.
6. Martin, J., C. Sun, A. Boehman, and J. O'Connor, "Experimental Study of Post Injection Scheduling for Soot Reduction in a Light-Duty Turbodiesel Engine," SAE Technical Paper 2016-01-0726.
7. O'Connor, J., M. Borz, J. Han, C. Paul, D. Ruth, A. Imren, D. Haworth, J. Martin, C. Sun, A. Boehman, K. Heffelfinger, J. Li, S. McLaughlin, R. Morton, A. Andersson, A. Karlsson, "Optimization and Verification of an Advanced Combustion Strategy Towards 55% BTE for the DOE/Volvo SuperTruck Program," SAE technical paper (submitted).
8. Ruth, D., J. O'Connor, "Development and Verification of Reduced-Order Model for Diesel Spray Penetration and Spreading during Wall Impingement," SAE Technical Paper (submitted).
9. Sun, C., D. Kang, S.V. Bohac, and A.L. Boehman. "Impact of Fuel and Injection Timing on Partially Premixed Charge Compression Ignition Combustion," *Energy & Fuels*, **30**, 4331–4345 (2016).
10. Meghan Borz, (2016) "Gas jet studies for the characterization of advanced injection schedules and bowl designs in diesel engines," MS Thesis, The Pennsylvania State University.
11. Daniel Ruth, (2016) "Assessment of the use of models for diesel sprays and the gas jets used to study them," Schreyer Honors Thesis, The Pennsylvania State University.

## Special Recognitions & Awards/ Patents Issued

1. Dan Ruth (2015) Dr. John P. Karidis Department Head's Award for Research Achievement in Mechanical Engineering, The Pennsylvania State University.

## IV.2 Navistar SuperTruck Advanced Combustion Development

### Overall Objectives

- Through advanced engine technologies, to develop a heavy-duty diesel engine capable of achieving 50% or better brake thermal efficiency (BTE) on a dynamometer under a load representative of a level road at 65 mph

### Fiscal Year (FY) 2016 Objectives

- Meeting ST1 program goals
- Combustion optimization
- Parasitic reduction
- Dual-fuel investigation
- Conjugate heat transfer modeling

### FY 2016 Accomplishments

- Deliver the engine calibrations for ST1 vehicle testing
- Complete the demonstration of greater than 50% BTE on a dynamometer
- Examine in-cylinder combustion process to identify opportunities for 55% BTE
- Develop detailed friction models for valvetrain and cranktrain in GT-POWER
- Complete low pressure exhaust gas recirculation (LP EGR) evaluation for  $\text{NO}_x$  reduction with no negative impact on BTE
- Complete the evaluation of three parasitic reduction technologies
- Complete the dual-fuel investigation with LP EGR
- Advance the conjugate heat transfer (CHT) modeling for in-cylinder heat transfer simulation ■

### Introduction

The overall goal of this project is to develop and demonstrate a 50% total increase in vehicle freight efficiency measured in ton-miles per gallon. This overall goal will be achieved through efficiency improvements in advanced vehicle systems technologies and advanced engine technologies. At least 20% of this improvement

**Russell Zukouski (Primary Contact),  
James Cigler (Chief Engineer),  
Gengxin Han, James Park,  
Raj Kumar, Ryan Vojtech,  
Jasmeet Singh, Matthew Taylor,  
Jason Chen, Yan Wang, Peirong Jia,  
Jincai Zheng, Andrew Ickes,  
Thomas Wallner, Sibendu Som,  
Riccardo Scarcelli, Prithwish Kundu,  
Reed Hanson**

Navistar, Inc.  
2701 Navistar Drive  
Lisle, IL 60531  
Phone: (331) 332-2908  
Email: russ.zukouski@navistar.com

DOE Technology Development Manager:  
Roland Gravel  
NETL Project Manager:  
Ralph Nine

will be through the development of a heavy-duty diesel engine capable of achieving 50% BTE in an engine on the dynamometer. In addition, a pathway to a 55% BTE engine is part of the deliverables of the ST1 program.

### Approach

In order to develop an engine with 50% BTE incorporating the compliance with prevailing U.S. Environmental Protection Agency emissions standards, certain advanced engine technologies need to be applied in order to help attain higher efficiency through combustion optimization by maximizing work extraction from the combustion process and minimization of thermal and parasitic losses. The following are major technology areas being pursued during FY 2016:

- Parametric studies for combustion optimization, both engine testing and three-dimensional (3D) simulation
- Parasitic reduction and friction modeling
- Further assessment of dual-fuel combustion with LP EGR

- Overall in-cylinder thermal management modeling

## Results

### Achieved >50% BTE

For the final ST1 vehicle testing, the engine calibration was optimized for emissions test cycle  $\text{NO}_x$  production with minimum drive cycle fuel consumption. The brake specific fuel consumption (BSFC) improvement of this calibration over the model year 2009 baseline engine is significant, greater than 10% at selected modal points, which focused on the expected drive cycle operation, Figure 1. In addition, greater than 50% BTE was demonstrated at Bosch in conjunction with an Organic Rankine Cycle system.

### Combustion Optimization – Heat Release Rate (HRR) and Compression Ratio (CR)

A key to further improve BTE is to reduce the combustion duration, i.e., faster HRR. Figure 2 shows the HRR of three different injector nozzles which is an attempt to affect the fuel atomization and penetration. The best BTE is produced by the blue curve, which is approximately 0.5% higher than the orange curve and 0.85% better than the green one. Evident in each case, the initial drop of HRR is due to the phase change of the liquid fuel, resulting in an ignition delay. Due to the relatively long duration of conventional diesel combustion, a portion of the heat release occurs before top dead center (TDC) for demonstrated high efficiency injection timing cases. The ability to shorten the duration of HRR for fixed fuel—energy input will reduce the amount of heat release that occurs before TDC. To avoid the peak cylinder pressure exceeding the mechanical limit of the power cylinder, in addition to shorten the duration, the shape of the HRR must be optimized too.

A combustion bowl of 15% higher CR than the ST1 baseline was tested on an engine with a high efficiency turbocharger to investigate the opportunity of higher CR for BTE improvement. EGR valve sweeps were conducted to vary the air flow and  $\text{NO}_x$  levels. The test results show no significant BTE benefit of the increased CR. The BTE is the net of the cycle work and friction loss. The peak cylinder pressure is higher with the increase of CR for this test, however, such increase of cylinder pressure could lead to more friction losses in the valvetrain and cranktrain as a result of increased bearing loading.

### Friction Modeling

Detailed valvetrain and cranktrain friction models based on the physical principles were assembled in GT-POWER to more accurately represent the friction resulting from component and performance changes. With the integration with detailed engine model, the friction models was used to investigate effects of valve timing, oil properties, surface roughness, and engine speeds on the friction power loss. Friction power increases roughly linearly

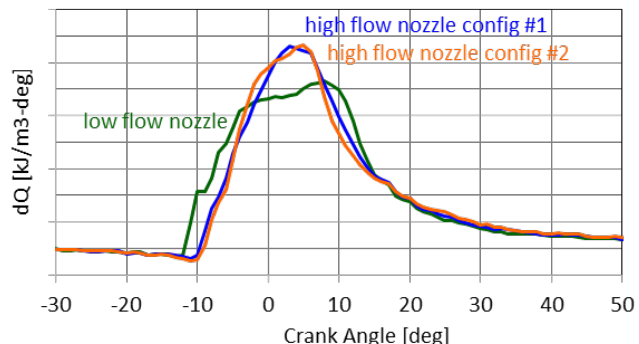


Figure 2. Comparison of HRR of three nozzle configurations

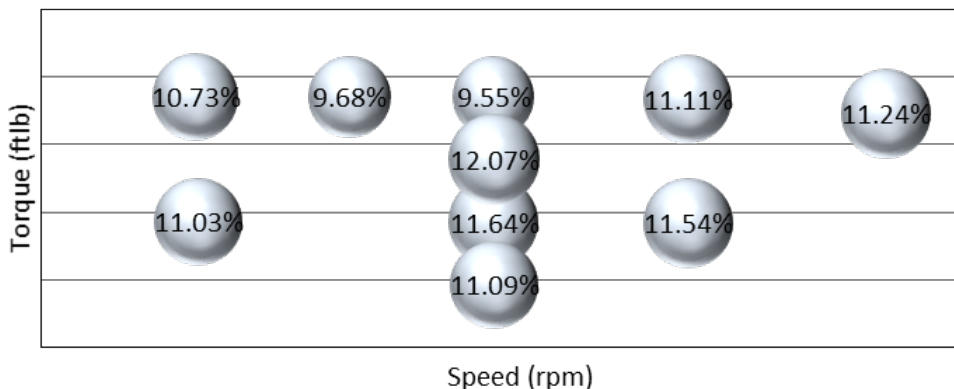


Figure 1. ST1 BSFC improvement over the model year 2009 engine

with cylinder pressure. The simulation shows that a new cam with early intake valve closing would increase peak cylinder pressure, resulting in higher friction loss. Figure 3 shows that the major contribution of friction power loss comes from the cranktrain, which includes crankshaft main bearings, connecting rod large-end and small-end bearings, piston rings, and piston skirts. Further analysis shows that the connecting rod small-end bearings are vulnerable to the mixed lubrication at low engine speeds. The mixed lubrication occurs when the minimum oil film thickness is less than  $2\times$  of the surface roughness.

### 3D Simulation—Swirl Ratio on HRR

To identify if there is room for further improvement of HRR, the effect of swirl on the ST1 engine was investigated with 3D simulation. Two cylinder heads were compared. The key in-cylinder fluid dynamic characteristics are swirl ratio and tumbling. For both cylinder heads, the difference of swirl ratio was about 1.1 before TDC. This difference was reduced to 0.5 during the combustion, Figure 4. The simulation also shows that, with the ST1 combustion bowl, the difference of tumbling is at a minimum after the start of injection. The simulation shows that there is basically no difference in the HRR of these two heads.

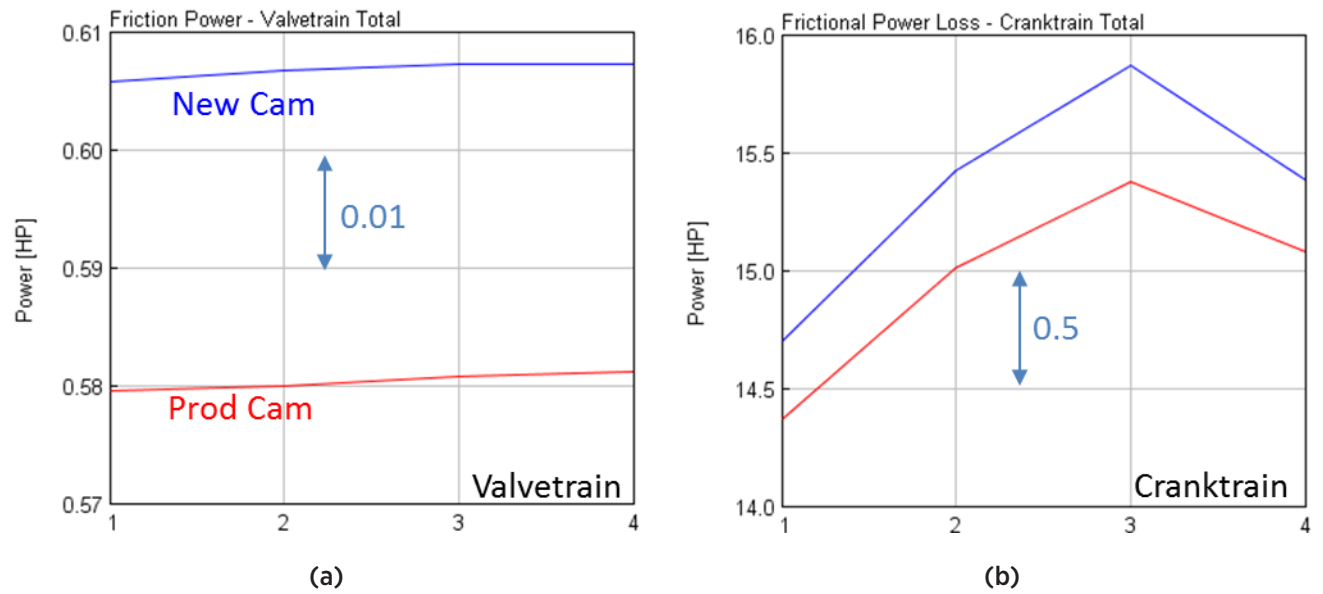


Figure 3. Effects of valves timing on friction power loss: (a) valvetrain and (b) cranktrain

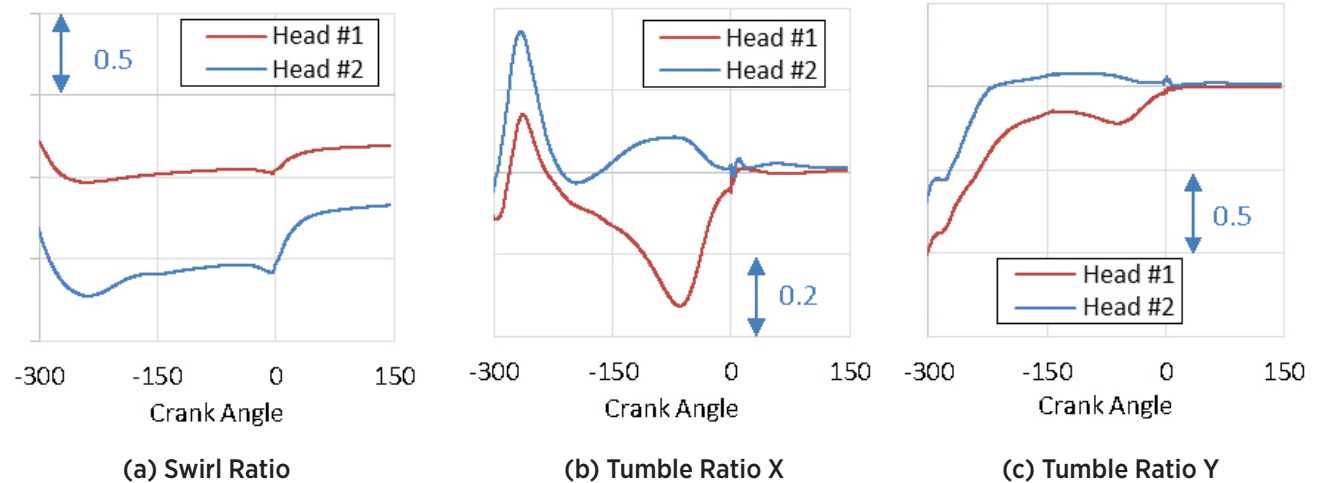


Figure 4. In-cylinder fluid dynamic characteristics of two cylinder heads

## NO<sub>x</sub> Reduction with LP EGR

An LP EGR system was set up for NO<sub>x</sub> reduction without negative impacts on the fuel economy. An existing two-stage EGR cooler was used for the EGR cooling. The EGR was taken from the downstream of the turbine without a diesel particulate filter and then delivered to mix with fresh air before the compressor. At speed in Figure 5, the LP EGR achieved significant NO<sub>x</sub> reduction with no negative impact to BSFC than the high pressure exhaust gas recirculation (HP EGR) at the same engine condition. Proper coordination of LP and HP EGRs for a given turbocharger system would provide wider calibrations for NO<sub>x</sub> emissions control without sacrificing the fuel economy than using the HP EGR alone.

## Parasitic Reduction Evaluation

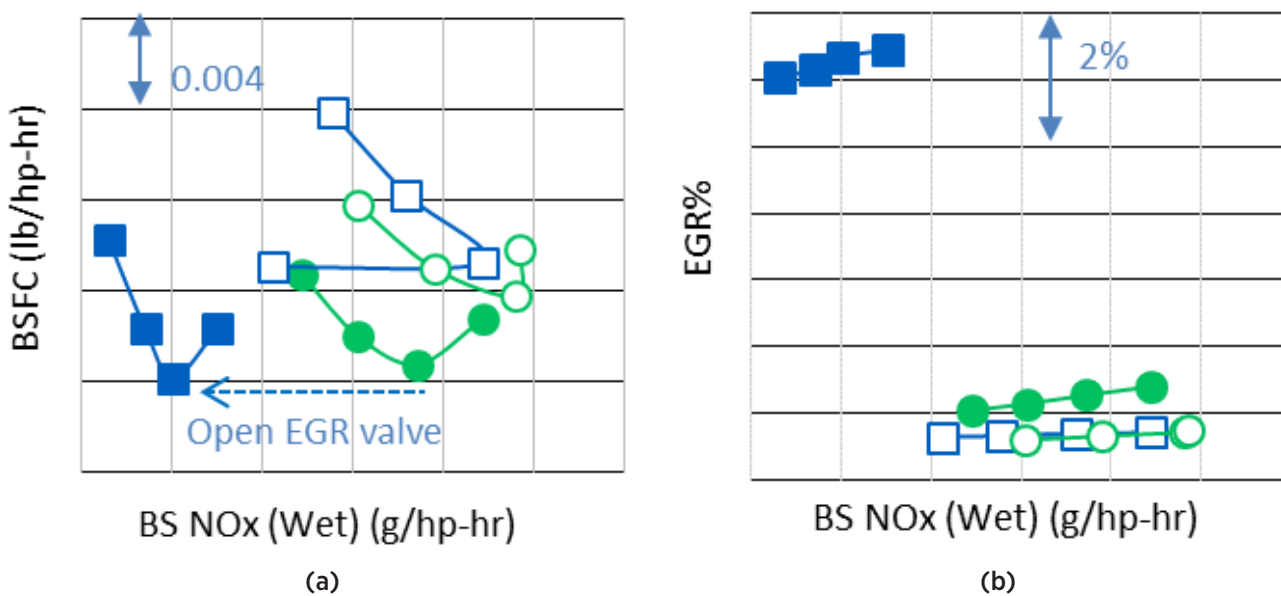
Parasitic reduction is important to the improvement of BTE. In addition to what have been evaluated previously, electrical low pressure fuel pump, low viscosity blend oil, and isentropic gears were evaluated this year. An electrical low pressure fuel pump would allow the adjustment of low pressure fuel flow when demand is less than the maximum for a given engine speed, thus, providing an opportunity to reduce the friction mean effective pressure (FMEP) due to the mechanical, low pressure pump. However, the testing shows no significant BSFC or FMEP improvement with the electrical pump. The testing of a low viscosity oil shows that the FMEP reduction is minimum at the operating conditions of interest as compared to the baseline 10W30 oil. Isotropic

Superfinish gears with reduced surface roughness were evaluated for friction reduction. The testing shows a small decrease of FMEP with the isotropic gears and such gears were used in the SuperTruck vehicle demonstrator engine.

## Dual-Fuel Combustion at Argonne National Laboratory (ANL)

ANL is Navistar's SuperTruck partner for dual-fuel investigations. The engine was rebuilt with a piston optimized for dual-fuel combustion featuring a reduced CR (17:1) to allow an increase in the reactive fuel mixture. The BTE of conventional diesel operation at the same operating condition decreases 1% due to the change of CR. Natural gas–diesel (NG/D) dual-fuel combustion peak efficiency at the selected operating point was slightly lower than what achieved with the higher CR engine configuration.

An LP EGR system was then implemented to provide an assessment of the NO<sub>x</sub>–BTE impact of such a system with the existing turbocharger sizing and efficiency levels extending the evaluation of the dual fuel efficiency potential. The system takes the exhaust from downstream to the turbine outlet and recycling into the intake system upstream of the compressor. A stock two-stage EGR cooler was used for the LP EGR cooling. The maximum EGR rate achievable was 14% without change of exhaust backpressure. Conventional diesel combustion as well as NG/D and E85 (85% ethanol, 15% gasoline blend)–diesel dual-fuel combustion were carried out at two EGR levels,



BS – brake specific

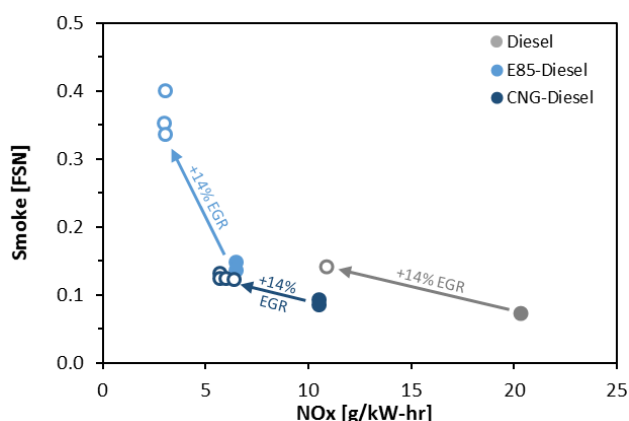
Figure 5. Effects of LP EGR on BSFC and NO<sub>x</sub> emissions at Navistar. Open symbols are HP EGR data; solid symbols are corresponding LP EGR data.

0% and 14%. Approximately 50% reduction in  $\text{NO}_x$  was observed along with the corresponding increase in soot emissions with the use of LP EGR. The key difference is the baseline  $\text{NO}_x$  level of each fuel. The  $\text{NO}_x$  level of conventional diesel combustion is about twice that of NG/D dual-fuel combustion, and four times of E85/D dual-fuel combustion (Figure 6).

### ANL 3D CHT Modeling

Heat transfer across engine boundaries has a significant impact on the performance and efficiency of any engine. 3D CHT modeling work was performed by ANL with the cooperation of Convergent Science, Inc. The computational domain consists of the in-cylinder combustion volume interfaced with the solid piston region. The intake and exhaust manifolds were also included along with the valves for open cycle simulations. The piston is bifurcated into four different boundaries in order to account for the spatial variation in temperature boundary conditions. The liner temperature varies along axis. The liquid spray was modeled using the Lagrangian approach. A supercycling interval of 1 crank angle degree was used to save computation time. The simulation results were validated and results showed that the overall errors from the temperature predictions of the solid domain were less than 5% of the measured values.

The results from the CHT model were used to explore parameters of engine design that influence heat transfer and efficiency. The effect of the spray angle was found to play a significant role in the overall heat loss from the engine. The heat loss analysis with open cycle simulations and CHT models were carried out for different spray angles. The result indicates that the spray angle needs to be considered while optimizing a piston bowl geometry with the heat loss being a merit function.



FSN – Filter Smoke Number; CNG – compressed natural gas

Figure 6. Comparison of dual-fuel combustion without EGR and with 14% LP EGR

### Conclusions

- The ST1 goal of 50% BTE was achieved with the integration of advanced engine technologies and Organic Rankine Cycle system.
- The shape of HRR could be used to gauge the combustion improvement. Injection rate shape is one of the key parameters to the HRR.
- Lubrication plays an important role to the friction reduction. The connecting rod small-end bearing was identified as vulnerable to the mixed lubrication at low speeds.
- LP EGR could be an effective way for significant  $\text{NO}_x$  reduction but no negative impact to the BSFC.
- Further in-cylinder thermal management investigation is important to achieve the 55% BTE goal of ST2 program.

### FY 2016 Publications/Presentations

- Hanson R., Ickes A., Wallner T., "Use of Adaptive Injection Strategies to Increase the Full Load Limit of RCCI Operation," ASME J. Eng. Gas Turbines Power. 2016;138(10):102802-102802-10. doi:10.1115/1.4032847.
- Hanson, R., Ickes, A., and Wallner, T., "Comparison of RCCI Operation with and without EGR over the Full Operating Map of a Heavy-Duty Diesel Engine," SAE Technical Paper 2016-01-0794, 2016, doi:10.4271/2016-01-0794.
- Kassa, M., Hall, C., Ickes, A., and Wallner, T., "Cylinder-to-Cylinder Variations in Power Production in a Dual Fuel Internal Combustion Engine Leveraging Late Intake Valve Closings," SAE Int. J. Engines 9(2):1049–1058, 2016, doi:10.4271/2016-01-0776.
- Kassa, M., Hall, C., Ickes, A., and Wallner, T., "Feedforward Control of Fuel Distribution on Advanced Dual-Fuel Engines with Varying Intake Valve Closing Timings," SAE Technical Paper 2016-01-2312, 2016, doi:10.4271/2016-01-2312.
- Kundu, P., Scarcelli, R., Som, S., Ickes., A., Wang, Y., Kiedaisch, J., and Kumar, R., "Modeling Heat Loss through Pistons and Effect of Thermal Boundary Coatings in Diesel Engine Simulations using a Conjugate Heat Transfer Model," SAE Technical Paper 2016-01-2235, 2016, doi:10.4271/2016-01-2235.
- Ickes, A., "Diesel-Natural Gas RCCI Strategies for High Efficiency," Presented to the USCAR U.S. Drive Advanced Engine & Emissions Control (ACEC) Technical Team, Dearborn, MI, March 10, 2016.

## IV.3 Ultra-Efficient Light-Duty Powertrain with Gasoline Low Temperature Combustion

### Overall Objectives

The project will develop, implement, and demonstrate a low temperature combustion scheme called Gasoline Direct-Injection Compression Ignition (GDCI). The project will demonstrate a 35% fuel economy improvement over the baseline vehicle while meeting Tier 3 emissions levels.

### Fiscal Year (FY) 2016 Objectives

- Map and evaluate Gen2 GDCI engine on dynamometer
- Build vehicle to Gen1.8 configuration of engine and controls
- Refine calibration and test Gen1.8 vehicle
- Build vehicle with Gen2 GDCI engine and controls
- Develop Gen2 GDCI controls
- Simulate Gen3 GDCI engine, systems, and controls
- Design Gen3 GDCI engine
- Develop Gen3 GDCI aftertreatment
- Begin the build of the Gen3 GDCI engines

### FY 2016 Accomplishments

- Gen1 vehicle fuel economy testing issues resolved
- Designed and implemented improvements to engine controls and calibration on Gen1.8 vehicle for improved fuel economy and emissions
- Gen1.8 vehicle testing completed with Hydrocarbon Trap aftertreatment system
- Characterized and evaluated the fuel economy, emissions, and performance of Gen2 GDCI engine on dynamometer
- Performed detailed emissions characterization of the Gen2 GDCI engine at Delphi with Oak Ridge National Laboratory.
- Gen2 vehicle update completed and started break-in and steady-state calibration development
- Designed and fabricated new Gen3 GDCI engines for dynamometer and vehicle testing

**Keith Confer (Primary Contact),  
Dr. Peter Olin, Mark Sellnau**

Delphi  
3000 University Drive  
Auburn Hills, MI 48326  
Phone: (810) 247-2890  
Email: keith.confer@delphi.com

DOE Technology Development Manager:  
Ken Howden

NETL Project Manager:  
Ralph Nine

#### Subcontractors:

- Douglas Ball, Umicore, Auburn Hills, MI
- Dr. John Storey, Oak Ridge National Laboratory, Oak Ridge, TN

- Packaged the Gen3 powertrain, new thermal management and new aftertreatment in the test vehicle
- Developed the Gen3 aftertreatment system using simulation ■

### Introduction

Low temperature combustion schemes have the potential to provide significant fuel economy benefit. GDCI is a particular approach to realizing low temperature combustion operation. GDCI is currently a moderately mature combustion technology, due in large part to advances made during a previous program funded through the Department of Energy Advanced Technology Powertrain (ATP) opportunity and led by Delphi (ATP contract DE-EE0003258).

The current project is addressing a number of technical risks and issues that must be overcome for GDCI to become a production-viable technology. These are (1) further refinement of the GDCI combustion system to achieve near-ideal air-fuel mixture preparation for high efficiency and low hydrocarbons (HC) and CO emissions, (2) demonstration of low temperature combustion transient control with high exhaust gas recirculation levels during real-world transient driving maneuvers and over a

broader range of ambient conditions, and (3) development of an aftertreatment system that is effective in dealing with the low temperature challenges of a highly efficient engine.

The ultimate deliverable for this project will be a vehicle that will demonstrate a 35% fuel economy improvement over a baseline vehicle with a port fuel injection engine, while simultaneously meeting Tier 3 emissions levels.

## Approach

This project will substantially expand upon the existing success of GDCI combustion. Further combustion optimization, supported by component development, will focus on improved brake thermal efficiency and reduced emissions. A key focus area is continued development of the injection process and fuel sprays to reduce engine-out HC and CO, which are especially challenging for low temperature combustion, while also improving thermal efficiency. Controls development will improve ignition and combustion control, with an emphasis on transient operation and cold starting. System and controls optimization work will provide robust operation over an expanded range of operating conditions, including ambient temperature and variations in gasoline composition. To meet stringent Tier 3 emission targets, a new aftertreatment system will be developed in combination with advanced controls and fast warm-up strategies to deliver an optimized solution for GDCI.

Initial work on this project leveraged the development vehicle from the ATP1 project. That vehicle was used as an initial test bed in the development of a high performance exhaust aftertreatment system for GDCI as well as to develop calibration refinements for improved exhaust emissions and fuel efficiency.

Samples of the new GDCI development level engine, called Gen2.0 GDCI, are being used to develop refined controller hardware, including improved sensor, actuator, and control algorithms. The Gen2.0 engine was retrofitted into the development vehicle and is being used for controls refinement and calibration of GDCI. Development of the final demonstration vehicle, control systems, aftertreatment, and Gen3 GDCI engine are all based on the work done on the Gen2.0 engine.

A Gen3.0 version of the GDCI engine was designed and is being built specifically for this project based on experience from the earlier engines. This engine, when combined with refined control systems and project specific exhaust aftertreatment, is planned to meet Tier 3 emissions levels. The culmination of the project will be realized with the GDCI Gen3.0 demonstration

vehicle which will demonstrate a 35% fuel economy improvement along with Tier 3 emissions levels.

Modeling and simulation work is being used throughout the program, including finite element modeling for component development, engine and vehicle simulations to determine requirements and estimate benefits for the implemented technologies, and computational fluid dynamics to support fuel spray development and combustion development.

## Results

### Engine Controls

Controls work over the past year has focused on calibration mapping, vehicle transient control, and improved fuel economy and emissions for the Gen1.8 vehicle and electronic controls development and algorithm development for system architecture upgrades for the Gen2.0 GDCI vehicle.

### Demonstration Vehicle

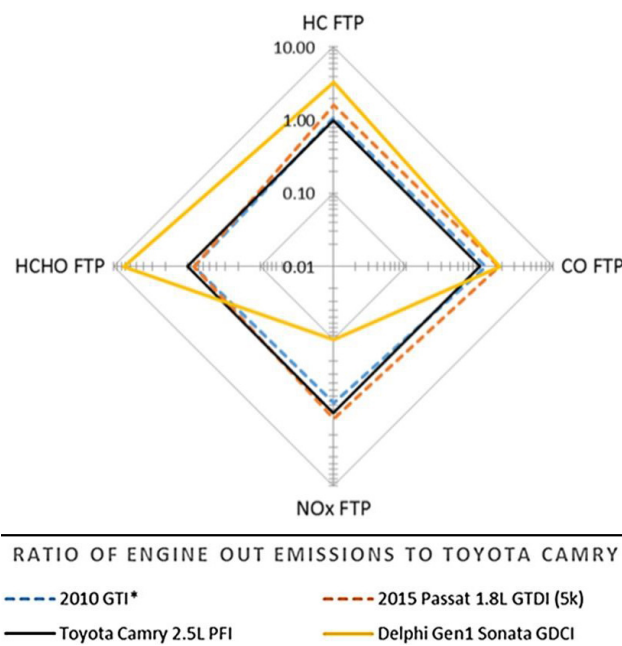
Delphi demonstrated 32% combined fuel economy improvement of the Gen1.8 vehicle over the baseline vehicle (30% Highway Fuel Economy Test, 33% Environmental Protection Agency III). The Gen1.8 vehicle also demonstrated reduced HC, CO, and NO<sub>x</sub> emissions relative to the Gen1 vehicle, but did not meet Tier 3 requirements. Engine-out data was also established over the Federal Test Procedure (FTP) cycle for both emissions and temperatures and compared to traditional spark ignition gasoline engines (see Figures 1 and 2). This data was used for the design of the Gen3 level hardware.

### Emissions Characterization of Gen2 GDCI Engine with Oak Ridge National Laboratory

Detailed tests were performed on the Gen2 dynamometer engine at five speed-load conditions to characterize engine-out and tailpipe emissions. Results include HC speciation, and elemental and organic particulate both before and after an oxidation catalyst, particle size spectra data, and nitrogen species.

### Gen3 Engine Design and Build

Design work was completed for the Gen3 engines and all components are on track for first builds in the fourth quarter of 2016. The engine features improvements to the fuel injection, thermal management, boost, exhaust gas recirculation, cold start, and aftertreatment systems. A key design change is the stroke-to-bore ratio of the engine, which was increased to 1.34 by increasing the stroke. This increases the top dead center clearance in the cylinder and enables late injections without wetting piston or liner surfaces. New injectors and sprays are matched



PFI - port fuel injection; GTDI - gasoline turbocharged direct injection

Figure 1. Vehicle level GDCI engine-out emissions compared to spark ignition engine results (spark ignition data compliments of Umicore)

with the Gen3 piston bowl through computational fluid dynamics optimization. For fast cold starts at any ambient temperature, an electric intake air heater was designed and positioned just upstream of the intake valves. A photo of the Gen3 mockup engine is shown in Figure 3.

### Gen3 Vehicle Packaging

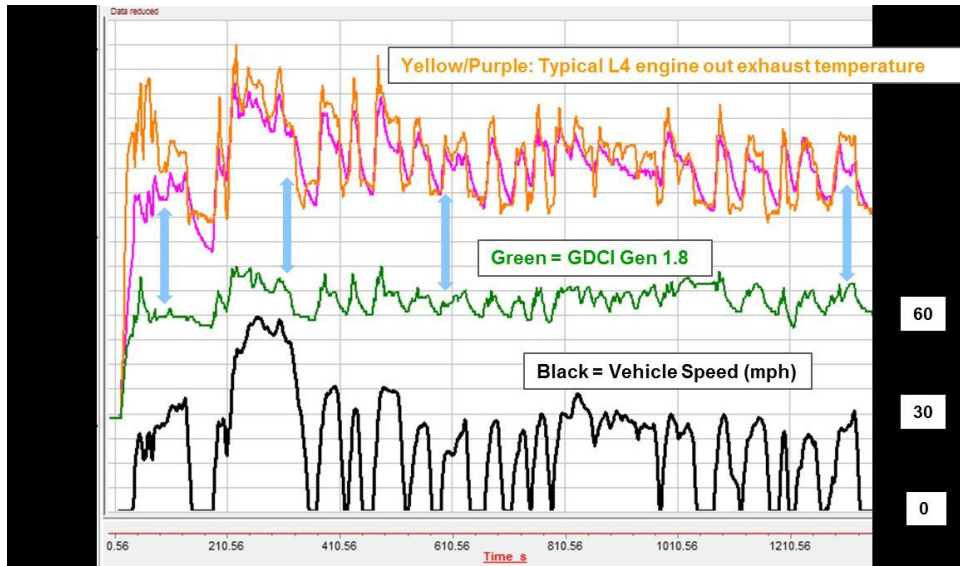
The entire powertrain was packaged in the test vehicle (see Figure 4).

### Aftertreatment for Tier 3 Bin 30.

An all new aftertreatment system was designed for the Gen3 GDCI engines to meet stringent Tier 3 Bin 30 emissions targets. Figure 5 shows the schematic of this system, which includes a pre-turbocharger catalyst, a hydrocarbon trap with oxidation catalyst, a catalysed gasoline particulate filter, and a selective catalytic reduction system. The design features good heat conservation due to the integral exhaust manifold and very compact system layout. Space velocities were reduced for improved conversion efficiencies.

### Conclusions

- The Gen1.8 vehicle configuration is capable of 32% combined fuel economy improvement over the baseline vehicle.



L4 – inline four cylinder

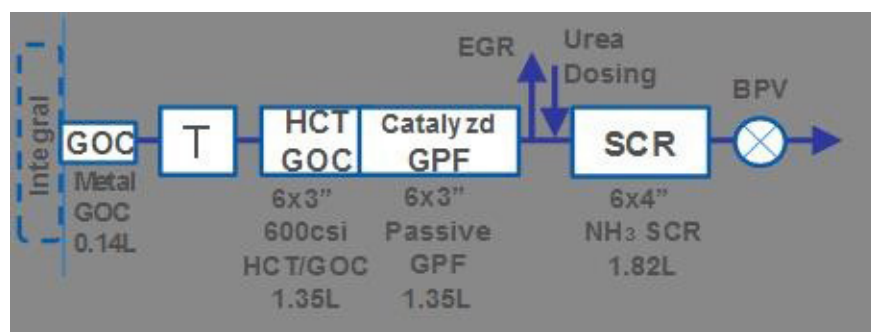
Figure 2. Vehicle level GDCI engine-out temperatures compared to spark ignition engine results



Figure 3. Gen3 engine mockup



Figure 4. Gen3 engine mockup in test vehicle



EGR – exhaust gas recirculation; BPV – bypass valve

Figure 5. Gen3 aftertreatment system schematic: turbocharger (T), pre-turbocharger catalyst, hydrocarbon trap (HCT) with oxidation catalyst (GOC), catalyzed gasoline particulate filter (GPF), selective catalyst reduction system (SCR)

- The Gen1.8 vehicle configuration is capable of reduced HC, CO, and NO<sub>x</sub> emissions (relative to the Gen1 vehicle), but not meeting Tier 3 requirements.
- Vehicle level engine-out emissions for GDCI are comparable to engine-out emissions for gasoline spark ignition engines.
- Vehicle level engine-out temperatures for GDCI are significantly lower than exhaust temperatures of gasoline spark ignition engines and represent the major challenge to meeting future emission regulations.
- The new Gen3 GDCI engine, with advancements for most engine subsystems, is expected to significantly improve brake specific fuel consumption, emissions, and output.

- The aftertreatment system and the fast cold start system developed for the Gen3 GDCI engine show potential to meet stringent United States 2025 Tier 3 Bin 30 standards.

## FY 2016 Publications/Presentations

1. *“Development of Electrical-Electronic Controls for a Gasoline Direct Injection Compression Ignition Engine,”* Johnson et al., SAE 2016-01-0614, SAE World Congress, April 2016.
2. *“Second Generation GDCI Multi-cylinder Engine for High Fuel Efficiency and US Tier 3 Emissions,”* Sellnau et al., SAE 2016-01-0760, SAE World Congress, April 2016.

3. 2016 DOE Vehicle Technologies Review: *ACE094 Merit Review DE-EE0006839* presentation given by Keith Confer, Washington, D.C. on June 9, 2016.
4. “*Advancement of GDCI Technology for US 2025 CAFE and Tier 3 Emissions*,” Presented by Mark Sellnau at ASME Fall ICE Conference, Greenville, South Carolina, USA on October 11, 2016.

## IV.4 Improved Fuel Efficiency Through Adaptive Radio Frequency Controls and Diagnostics for Advanced Catalyst Systems

### Overall Objectives

- Develop radio frequency (RF) sensors and evaluate RF sensing feasibility for selective catalytic reduction (SCR), three-way catalyst (TWC), and hydrocarbon trap applications
- Develop systems and implementation strategies for the most promising applications to enable low-cost and robust emission controls for dilute gasoline, clean diesel, and low temperature combustion engines
- Demonstrate and quantify improvements in fuel consumption and emissions reduction through the use of RF sensing in engine and vehicle tests with industry and lab partners

### Fiscal Year (FY) 2016 Objectives

- Develop RF sensor prototype hardware and software to enable bench reactor studies, and supply measurement systems to project partners for testing
- Evaluate RF sensing feasibility for specific catalyst formulations to monitor stored gas species and interactions with the catalyst/washcoat
- Identify and quantify potential error sources on the RF signal
- Develop application-specific sensor calibration functions and evaluate RF sensor performance for each catalyst application

### FY 2016 Accomplishments

- Developed RF sensor hardware and software, including custom antennas for catalyst bench tests as well as full-size, heavy-duty system applications
- Setup and conducted catalyst bench reactor studies to evaluate RF sensing feasibility for specific catalyst systems and formulations
- Initiated fleet vehicle RF sensor evaluations with full-size SCR systems ahead of schedule and with more vehicles than originally planned

### Alexander Sappok (Primary Contact), Leslie Bromberg, Paul Ragaller

Filter Sensing Technologies, Inc.

7 Bow Street

Malden, MA 02148

Phone: (617) 379-7330

Email: alexander.sappok@ctscorp.com

DOE Technology Development Manager:

Roland Gravel

NETL Project Manager:

Jason Conley

Subcontractors:

- Corning, Inc., Corning, NY
- Oak Ridge National Laboratory, Knoxville, TN

- Investigated error sources, quantified their potential impacts on the RF sensor accuracy, and developed sensor correction methods where necessary
- Developed initial RF sensor calibration functions and evaluated sensor performance through bench reactor tests with carefully controlled gas compositions ■

### Introduction

The transportation sector is responsible for 28% of the United States' energy consumption, of which over 93% is derived from petroleum sources [1]. Advanced combustion engines could significantly reduce petroleum consumption; however, emissions limits must still be achieved. A number of advanced combustion engines are presently being developed and include lean gasoline, clean diesel, and low temperature combustion modes. However, aftertreatment systems remain a barrier for advanced combustion engines to achieve their full fuel efficiency potential and market adoption (limited by efficacy and cost) [2]. This project directly addresses these challenges by developing an RF sensor and control system, for improved monitoring and control of advanced catalyst systems to reduce engine fuel consumption while still meeting emissions requirements. Direct RF catalyst

state measurements provide a path to lower costs, reduced fuel penalty and improved emissions control, not possible with current technologies, and could be applied to all of the advanced combustion modes being developed by DOE and its partners.

Diesel combustion engines dominate heavy-duty applications, but high NO<sub>x</sub> conversion efficiency (and associated lower fuel consumption) is limited by uncertainties in the SCR ammonia inventory utilizing conventional gas sensors and model-based approaches. Similarly, lean gasoline engines employing passive SCR rely on the generation of ammonia over the TWC during periods of rich operation which consumes additional fuel. Finally, low temperature combustion modes require means for storing emissions during start-up, and managing those inventories on storage traps. The RF-based sensing approach investigated in this program provides a unique, direct measurement of the catalyst storage state to enable improved controls. This approach is in contrast to conventional methods using upstream and downstream electrochemical gas sensors to indirectly infer the state of the catalyst.

Work in the first year of this program (since project inception) developed the RF sensing hardware along with the catalyst samples, which were provided to project partners for bench reactor testing. The results confirmed direct measurement of ammonia storage on the SCR catalyst with RF sensing and further quantified potential system noise factors. A custom reactor setup was developed, which allowed for benchmarking of the RF measurements of ammonia storage relative to estimates based on commercial NO<sub>x</sub> and NH<sub>3</sub> sensors. RF simulations were also developed and applied to understand the electric field distributions within the catalyst and provide insight into the spatial sensitivity of the RF measurements. Fleet testing with heavy-duty and medium-duty diesel vehicles operating on urban drive cycles in New York City was also initiated. The fleet testing will provide over 18 months of real-world data with RF sensors on SCR-equipped diesel vehicles. In parallel, bench reactor feasibility studies with TWCs and low-temperature trap applications will continue into the second year of the program, which will culminate with implementation of the RF sensor on a range of engine and vehicle applications to quantify improvements in efficiency and emissions reduction through improved catalyst controls.

## Approach

The approach taken in this project is to identify, address, and overcome key technical challenges to successful RF sensor implementation early on, by leveraging

knowledge gained from past research and development efforts conducted by Filter Sensing Technologies (now CTS Corporation) and in collaboration with national laboratories, industry, and academia [4–7]. The previous work, focused on monitoring soot and ash levels on ceramic particulate filters, not only resulted in successful development and demonstration of the RF sensing technology, but also subsequent commercialization of the sensor by CTS. Following on the success of this model, the approach and structure of this program seeks to extend the understanding gained from measuring particulate matter trapped on filters to gas species stored on catalysts.

The expected project outcomes are twofold. The first phase will evaluate the feasibility of RF sensing for several catalysts: (1) NH<sub>3</sub> storage on SCR (passive SCR and urea SCR); (2) oxygen storage on TWC; (3) NH<sub>3</sub>, particulate matter, and ash on combined SCR filters; and (4) hydrocarbon storage on traps. The results will provide a comprehensive evaluation of the key hurdles and technology readiness for each application. The second phase will focus on SCR, the most promising near-term application. Engine and vehicle evaluations of SCR and SCR + filter for lean gasoline and diesel will position the RF sensing technology for commercial deployment following this program. The results of the engine and vehicle tests will quantify gains in fuel efficiency and catalyst performance relative to the current state-of-the-art to directly address the barriers to advanced combustion engine implementation identified by DOE.

## Results

The RF sensor, including the control unit and antenna, is shown in Figure 1. The sensor enables fast response vector measurements (amplitude and phase) over a broad frequency range. Single or dual antenna operation is possible, and measurement output is provided over a Controller Area Network. The measurement probe (antenna) is of similar size and form factor to a conventional exhaust temperature sensor and the subject of a previous patent application. The system is designed for on-vehicle operation but may also be controlled by a personal computer for laboratory applications.

High frequency measurements with the catalyst core samples were conducted using a laboratory network analyzer to accurately characterize the dielectric properties of the materials and provide a large dynamic range. Figure 2a shows the antennas that were fabricated specifically for the bench reactor measurements for installation in the catalyst core sample cavities shown in Figure 2b. The cavities, a custom design, enable efficient testing on the bench reactor and are utilized by all of the test partners in this program as a common test platform.

The internal cavity configuration is shown in Figure 2c, which is designed to simulate (on a small scale) the same overall system configuration as the full-size catalyst system.

For a commercial SCR, Cummins 2015 8.9-L ISL platform was selected as the standard SCR catalyst for this program. Core samples, as shown in Figure 2b, were



Figure 1. RF sensor control unit and antennas for full-size system testing

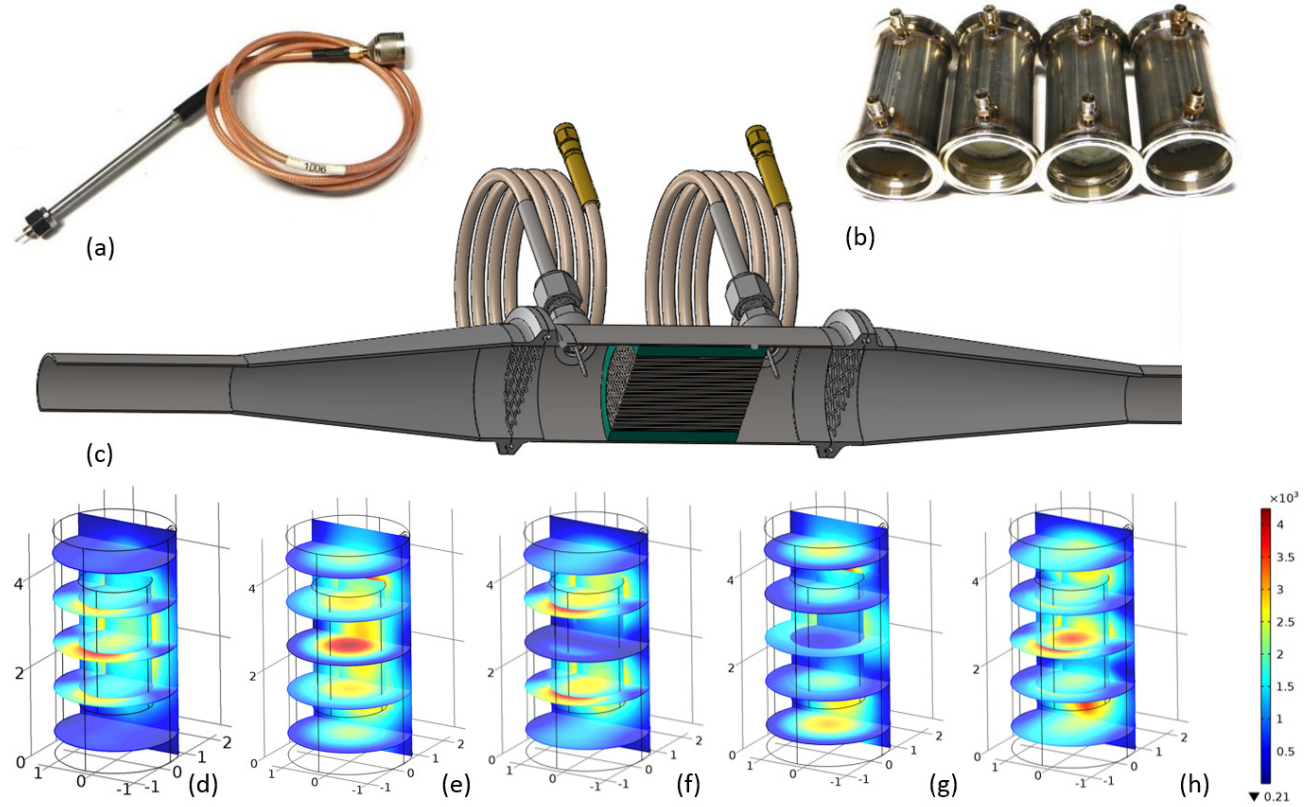


Figure 2. (a) Custom-designed RF antennas for catalyst core sample testing, (b) fabricated core sample housings, (c) full core sample assembly, and (d-h) simulated electric field distribution within core sample for several resonant modes

harvested from a full-size commercial SCR catalyst for the bench reactor testing in Phase I. The same catalyst will also be used with the heavy-duty engine testing at Corning in Phase II, thereby enabling the results from the bench reactor testing to be applied to the full-size engine evaluations in this program.

RF simulations were also developed and applied to understand the electric field profiles associated with the specific resonant modes utilized for the measurements. Figures 2d–2h present examples of the simulation output. Regions in red and orange denote localized areas with high electric field. Sensitivity of the RF measurements to detect changes in the loading state of the catalyst are greatest in regions of high electrical field. The simulation results were applied to guide the development of the measurement setup in the first phase of this program, and will further be utilized to guide the analysis and interpretation of the measurement results particularly as they relate to the spatial variations within the catalyst.

The bench reactor developed and commissioned for this program at Filter Sensing Technologies is shown in Figure 3. Parallel bench reactor studies are underway at Oak Ridge National Laboratory in this program. As

shown in Figure 3, the Filter Sensing Technologies reactor setup is designed to represent the same system mechanization currently found on conventional production SCR systems, which consist of  $\text{NO}_x$  sensors at

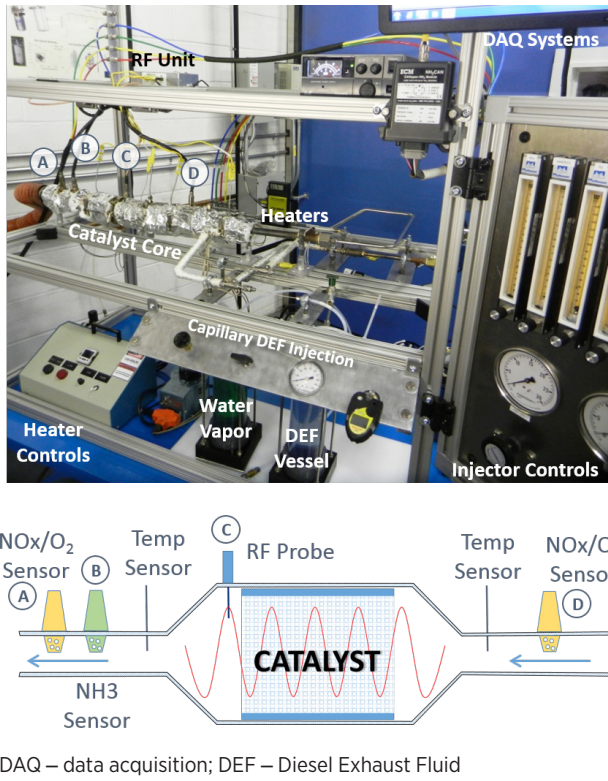


Figure 3. Catalyst bench reactor setup showing details of  $\text{NO}_x$  and ammonia sensor installations as well as RF antenna installed in catalyst core sample

the catalyst inlet and outlet as well as an ammonia sensor to provide closed loop control of the SCR. The setup allows for benchmarking of direct RF-based ammonia storage control relative to conventional control strategies utilizing upstream and downstream electrochemical gas sensors. The bench system in Figure 3 is capable of automated operation, temperature control from ambient to  $600^\circ\text{C}$ , synthetic gas and water vapor mixture preparation, and the introduction of either gaseous ammonia or the injection of urea through a capillary-based injection system. Bench testing at Oak Ridge National Laboratory, conducted in parallel, further provides Fourier transform infrared and spatially resolved mass spectrometry measurement capabilities to very accurately quantify catalyst storage levels for RF sensor calibration.

In addition to bench testing, several RF systems were installed on SCR-equipped vehicles operated by the New York City Department of Sanitation as part of a long-term test campaign. These systems, shown in Figure 4a, were set up to run continuously during normal vehicle operation in both single and dual antenna configurations. Further, Figures 4b and 4c illustrate the mounting location of the control unit as well as the RF antennas, respectively. The fleet testing will continue for the duration of this program and includes heavy-duty Volvo/Mack MP-7 engine-equipped vehicles and a medium-duty Cummins ISB-equipped vehicle.

Additional RF sensor evaluations included an assessment of the measurement response to various noise sources. Figure 5a illustrates RF sensor response to the injection of urea and Figure 5b shows the response to injection of

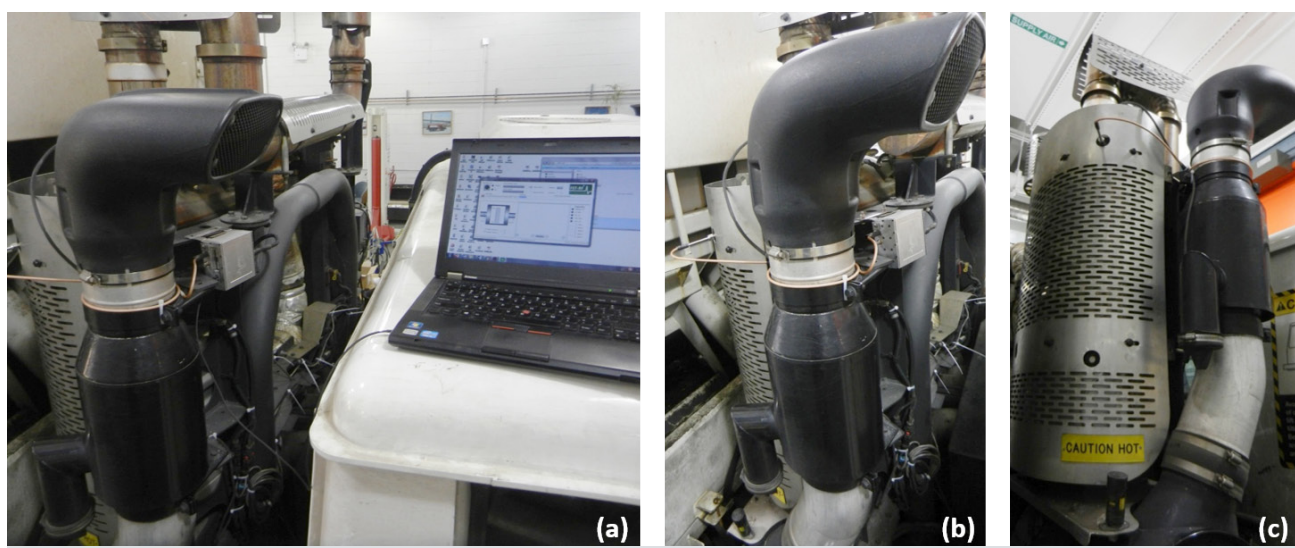


Figure 4. (a) RF sensor installation on heavy-duty fleet vehicles, (b) details of sensor control unit mounting, and (c) antenna positions on SCR catalyst

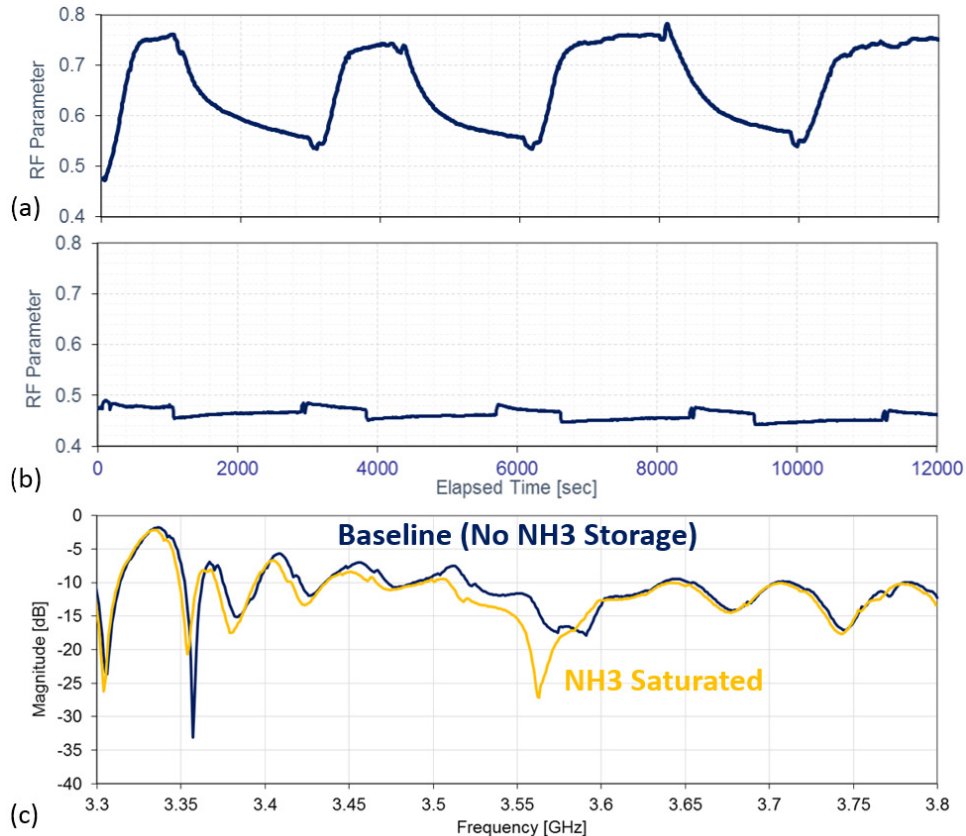


Figure 5. (a) RF sensor response to ammonia storage following urea injection, (b) sensor response to water injection at the same rate, and (c) RF resonance curves corresponding to fresh and fully ammonia saturated catalyst

pure water at the same rate into the bench reactor system. Additionally, a portion of the full RF spectrum is shown in Figure 5c for the case with no ammonia storage on the SCR catalyst and the case with full ammonia saturation of the catalyst. It can be seen from these figures that water has a negligible effect on the RF signal, especially when compared with the effect of ammonia.

Ammonia storage measurements based on the RF sensor are presented in Figure 6 which shows the RF response to ammonia injection upstream of the catalyst at 300°C and a flow rate of 60,000 hr<sup>-1</sup>. The experiments were conducted in the absence of NO<sub>x</sub> and show the inlet and outlet NO<sub>x</sub> sensors' cross-sensitivity to the ammonia. The tests were conducted to complete catalyst saturation and ammonia slip through the catalyst is readily observed. In addition, the difference between the inlet and outlet gas sensor measurements is due to ammonia oxidation.

The RF sensor measurements are further consistent with the general trends in the gas sensor response

shown in Figure 6. Ammonia storage on the SCR catalyst is observed by the increase in in the RF sensor measurements at the start of the test. Ammonia slip, as measured by the downstream NO<sub>x</sub> sensor (due to ammonia cross-sensitivity), also corresponds to the inflection point in the RF sensor response. Catalyst saturation is evident in the flat response of the RF sensor and is further consistent with the steady response of the outlet NO<sub>x</sub> sensor as well. The RF sensor also shows ammonia desorption from the catalyst at the end of the experiment when feedgas ammonia injection was terminated. The results of this first project phase thus confirmed the feasibility to monitor ammonia storage on the SCR catalyst using RF sensing. Ongoing work includes measurements of oxygen storage on TWCs and hydrocarbon storage on low temperature traps.

## Conclusions

Work in the first year of this program has already resulted in significant progress toward achieving the overall

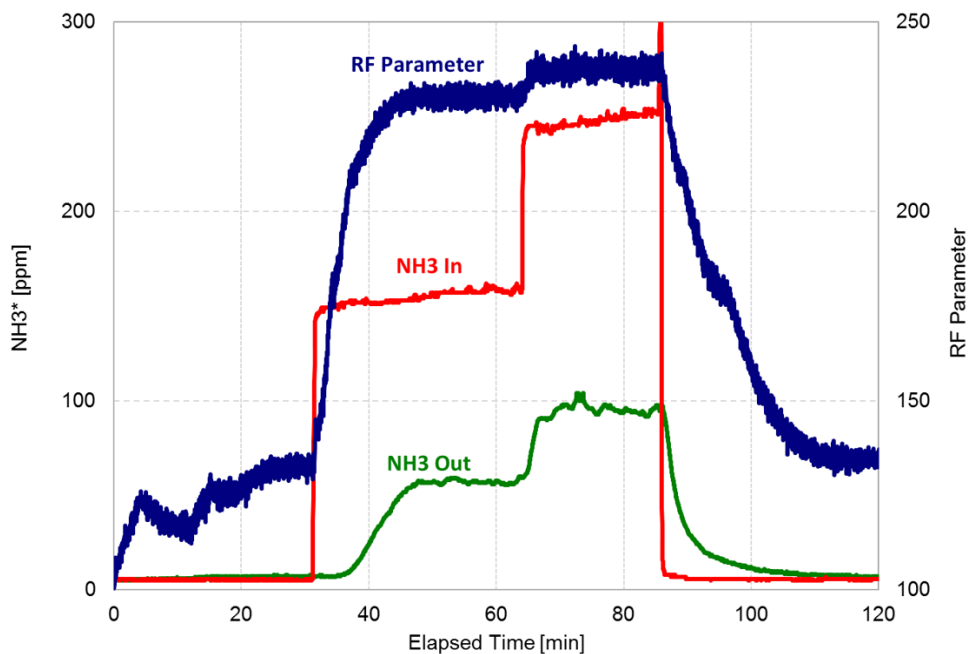


Figure 6. Ammonia storage measured via RF sensing at 300°C and flow rate of 60,000 hr<sup>-1</sup> on SCR catalyst core sample and comparison with conventional NO<sub>x</sub> sensor response

project objectives. Specific accomplishments are the following:

- Developed RF sensor control units, antennas, and software including custom systems for small-scale catalyst bench tests as well as full-size, heavy-duty applications
- Setup catalyst bench reactor systems and conducted studies to evaluate RF sensing feasibility for specific catalyst systems and formulations relative to measurements from conventional electrochemical gas sensors
- Initiated fleet vehicle RF sensor evaluations with full-size SCR systems ahead of schedule with several heavy-duty and medium-duty vehicles in New York City
- Investigated error sources, including water injection, and quantified their potential impacts on the RF sensor accuracy, which were found to be minimal for normal operating conditions
- Developed initial RF sensor calibration functions and confirmed the feasibility of monitoring ammonia storage levels on Cu-based SCR catalysts with RF
- The results to date demonstrate considerable potential for direct RF feedback control of the catalyst storage state to optimize the combined engine and

aftertreatment system and address key barriers to the increased adoption of efficient and cost-effective advanced combustion engines

## References

1. U.S. Department of Energy, Energy Information Administration. Annual Energy Outlook 2012. 2012.
2. U.S. Department of Energy, “Freedom Car and Vehicle Technologies Program, Multi-Year Program Plan 2011-2015,” Office of Energy Efficiency and Renewable Energy, 2010.
3. U.S. DRIVE, “Advanced Combustion and Emission Control Technical Team Roadmap,” 2013.
4. Sappok, A., Ragaller, P., Bromberg, L., Prikhodko, V., Storey, J., and Parks, J., “Real-Time Engine and Aftertreatment System Control Using Fast Response Particulate Filter Sensors,” SAE 2016-01-0918, 2016.
5. Ragaller, P., Sappok, A., Bromberg, L., Gunasekaran, N., Warkins, J., and Wilhelm, R., “Lifetime Particulate Filter Soot and Ash Measurements using Radio Frequency Sensors and Potential for Improved Filter Management,” SAE 2016-01-0943, 2016.
6. Nanjundaswamy, H., Nagaraju, V., Wu, Y., Koehler, E., Sappok, A., Ragaller, P., and Bromberg, L., “Advanced RF Particulate Filter Sensing and Controls for Efficient

Aftertreatment Management and Reduced Fuel Consumption," SAE 2015-01-0996, 2015.

7. Sappok, A. and Bromberg, L., "Radio Frequency Diesel Particulate Filter Soot and Ash Level Sensors: Enabling Adaptive Controls for Heavy-Duty Diesel Applications," SAE Int. J. Commer. Veh. 7(2):468–477, 2014, doi:10.4271/2014-01-2349.

## Special Recognitions and Awards/ Patents Issued

1. ASME Internal Combustion Engine Division Student Presentation Award, "Direct Measurements of Ammonia Storage on Selective Catalytic Reduction (SCR) Systems using Radio Frequency Methods," ASME, Greenville, SC, 2016.

## IV.5 Affordable Rankine Cycle

### Overall Objectives

- Quantify the available energy in the engine exhaust and engine coolant for waste heat recovery (WHR) system
- Optimize the WHR architecture through optimized number of heat exchangers and optimized expander design with optimized engine coolant composition
- Demonstrate 5% fuel economy improvement from affordable Rankine cycle (ARC) system

### Fiscal Year (FY) 2016 Objectives

- Quantify the total available exergy in engine exhaust and engine coolant
- Develop and optimize the engine coolant, expander, and WHR components to achieve the program targets
- Demonstrate the affordable Rankine architecture for 5% fuel economy improvement through analytical model

### FY 2016 Accomplishments

- Completed engine baseline experiments and analyzed the potential WHR architecture and boundary conditions of ARC system
- Evaluated the ARC system benefits based on WHR analysis
- Attained the technical target of 5% fuel economy improvement from ARC architecture through preliminary analytical modeling
- ARC system components (expander, working fluid, heat exchanger, and working fluid pump) have been identified
- Completed Roots expander computational fluid dynamics (CFD) analysis for ARC specifications and concluded the need for an alternative positive displacement expander technology for ARC demonstration
- Evaluated the engine coolant feasibility of WHR working fluid using laboratory-scale coolant degradation analysis ■

### Introduction

Nearly 30% of fuel energy is not utilized and wasted in engine exhaust. Organic Rankine Cycle (ORC)-based

### Swami Subramanian

Eaton

26201 Northwestern Hwy.

Southfield, MI 48076

Phone: (248) 226-1754

Email: [swaminathan@eaton.com](mailto:swaminathan@eaton.com)

DOE Technology Development Manager:

Roland Gravel

NETL Project Manager:

Ralph Nine

Subcontractors:

- Modine, Racine, WI
- Purdue University, West Lafayette, IN
- Mississippi State University, Starkville, MS
- Kettering University, Flint, MI
- AVL, Plymouth, MI
- Argonne National Laboratory, Lemont, IL

Program Partners:

- Shell Global Solutions (US) Inc., Houston, TX
- PACCAR Inc., Mount Vernon, WA

WHR systems offer a promising approach on waste energy recovery and improving the efficiency of heavy-duty diesel engines. Major technological barriers in the ORC WHR system is the system cost and high conflict waste heat recovery working fluids. More than 40% of the system cost is from the additional heat exchangers (recuperator, condenser, and tail pipe boiler). The secondary working fluid loop designed in the ORC system is either flammable or environmentally sensitive. Eaton Corporation's comprehensive project will develop and demonstrate affordable Rankine cycle technology to reduce the cost of implementing ORC-based WHR systems to heavy-duty diesel engines while utilizing safe working fluids.

Eaton's solution is to adapt a cost effective two-phase flow capable expander. Since the engine coolant is proposed as the waste heat recovery working fluid, it provides significant advantages compared to the

conventional flammable fluids or refrigerants used currently. In particular, some of the advantages include coolant energy waste heat recovery, no additional working fluid loop, no separate condenser, and no recuperator. This configuration will enable faster commercialization of WHR technology capable of improving engine fuel efficiency and total power output (performance). The ARC system to be demonstrated during this project will be validated using engine dynamometer testing with a PACCAR MX-13 heavy-duty diesel engine.

## Approach

The present work has been structured to baseline the 13-L heavy-duty diesel engine, and characterize and quantify the potential waste energy sources for the development of thermodynamic models. The impact of various WHR heat exchanger layouts on system performance will be assessed, leading to specifications of WHR components. The expander development will utilize CFD analysis, bench testing, calibration, and validation to maximize efficiency and durability. The developed expander for the ARC system will be tested on an engine operated over the selected speed and load conditions of the baseline engine representing key on-road engine operating conditions. These results will be compared to the baseline engine data at the same  $\text{NO}_x$  emission levels to provide a back to back demonstration of the expander technology and impact on fuel efficiency and engine system performance.

## Results

### ARC System Performance Prediction

Engine baseline testing, WHR analysis, and a simple thermodynamic model of ARC architecture development have been completed. Table 1 shows the ARC system performance predictions for selected truck operating conditions. Working fluid pump and expander efficiency

have been assumed as 60% for this analysis. This configuration contains an exhaust gas recirculation and a tail pipe heat exchanger in a parallel arrangement. Working fluid quality is maintained well below 0.5 to avoid coolant degradation. The fuel economy improvement target has been achieved for all of the operating conditions.

### Roots Expander Analysis

CFD analysis has been completed with the ARC boundary conditions. Results have shown that low volumetric flow rate results in the Roots expander operating at low efficiency. Analytical investigations to alter the porting and introduction of liquid to achieve viscous sealing and different rotor profiles have been completed. These approaches resulted in incremental improvements in efficiency and power generation compared to the baseline design but the program targets were still unable to be met. Pivoting to an alternative positive displacement expander is the prime path and preliminary analysis results show that the system performance targets can be achieved.

### Engine Coolant Feasibility and Development

Shell is developing a working fluid (commercially available existing engine coolant with minor additive modifications) that is applicable for WHR. An existing engine antifreeze/coolant (Shell ROTELLA® ELC-NF) was used as a baseline and tested for its feasibility and thermal stability under simulated WHR conditions.

Figure 1 shows the engine coolant (two components) behavior from saturation liquid to saturation vapor. This explains that engine coolant is a zeotropic mixture. We can possibly run the WHR system without vaporizing the glycol component. Theoretical results were confirmed with preliminary experimental analysis (shown in Figure 2). Figure 2 shows the enthalpy change of engine coolant with respect to temperature. It's derived from

**Table 1. ARC System WHR Analysis and Performance Predictions**

	A25	A50	A75	A100
Net Work Output from ARC (kW)	1.95	4.40	7.01	10.26
ARC Efficiency	7.56%	7.80%	7.89%	7.91%
Fuel Economy Improvement	<b>5.02%</b>	<b>5.66%</b>	<b>6.02%</b>	<b>6.74%</b>
Total Heat Input to ARC (kW)	25.76	56.45	88.91	129.70
Expander inlet volume flow (cc/s)	1331.10	3073.80	4916.30	7.19E+03
Volume ratio	8.27	7.94	7.87	7.87

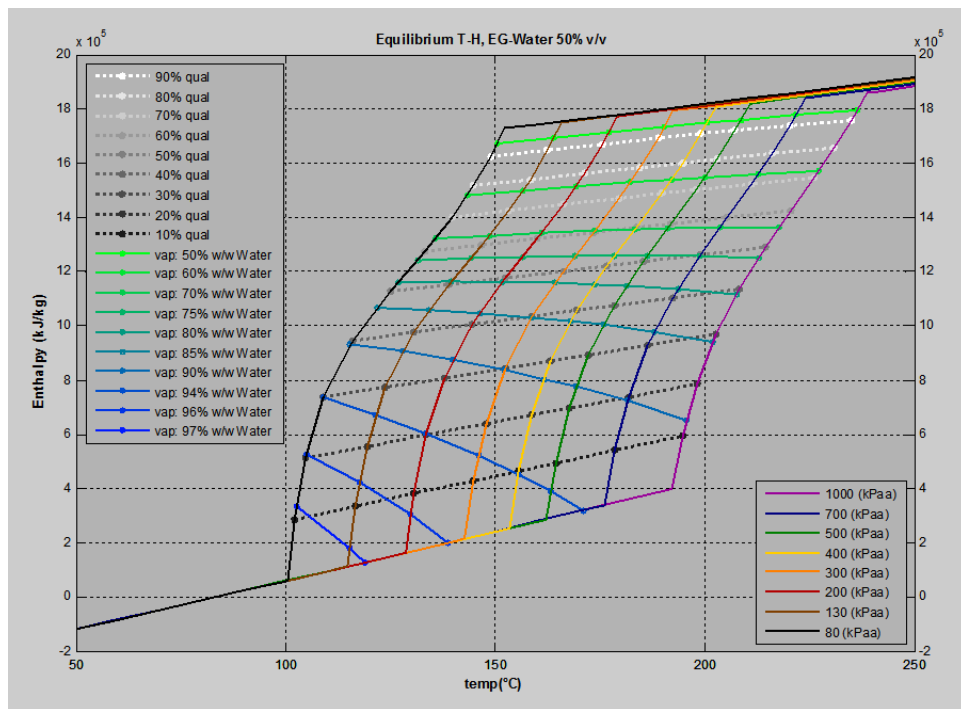
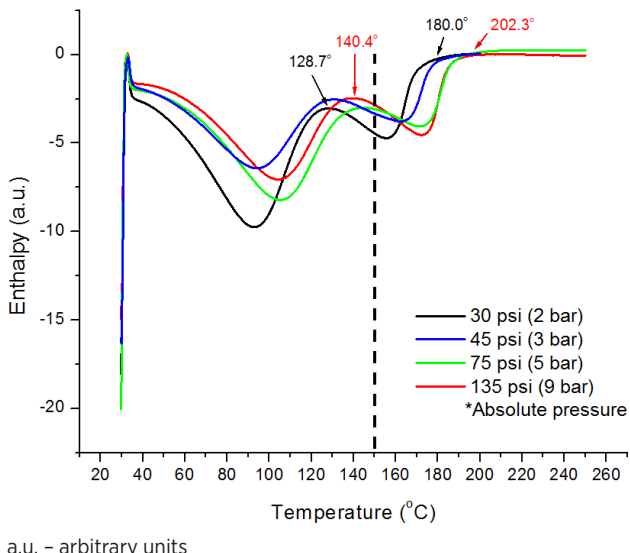


Figure 1. Enthalpy–temperature diagram for a 50:50 water–glycol mixture from the National Institute of Standards and Technology Reference Fluid Thermodynamic and Transport Properties Database



a.u. – arbitrary units

Figure 2. Engine coolant evaporation-enthalpy diagram (experimental)

laboratory-scale experiments at Shell. Direct comparison of Figures 1 and 2 give us the information of glycol–water vaporization behavior at different pressures. For example evaluation at 2 bar pressure (red line in Figure 1 and black line in Figure 2) from both figures reveal that the boiling process starts at 128.7°C and continues until 180°C.

Temperature glide of  $\sim 51^\circ\text{C}$  is noted from saturated liquid to saturated vapor. Around 150°C, nearly 80% of vapor is contributed by water at the quality of 0.5 (50% of the total mixture is in vapor condition). It has been proven that the coolant (50:50, ethylene glycol–water mixture) can go through water liquid–gas phase transition extracting extra heat from the WHR device.

Rotating pressure vessel oxidation testing shows that the glycol degraded at elevated temperatures. The depletion not only causes overheating of the cooling system and localized hot spots, but compromises the coolant's anti-corrosion attributes due to the relatively low pH of products derived from glycol decomposition, such as glycolates and formic acid. Three different antioxidants (ascorbic acid, citric acid, sucrose acetoisobutyrate) have been selected to mitigate the coolant degradation.

## Heat Exchanger Design and Development

Baseline results helped define the heat exchanger specifications for the 13-L diesel engine (ARC demo). Preliminary sizing work of the exhaust gas recirculation boiler and tailpipe boiler for the 13-L heavy-duty engine has been completed. Both heat exchangers were analyzed for A25, A50, A75, and A100 vehicle operating conditions. Two different design options of the exhaust gas recirculation boiler were analyzed. Design Option 1

is a drop-in replacement for the current exhaust gas recirculation cooler (~600-mm length). In this case, the cooled exhaust gas outlet temperatures were higher by 10°C to 20°C compared to the target requirements. The team is working on understanding the impact of 10°C to 20°C higher exhaust temperatures on base engine brake thermal efficiency. Design Option 2 is a configuration whereby the heat exchanger length is 1.5 times higher than Design Option 1, which reduced the exhaust temperature gap to 10°C.

### **Expander Model Development**

Leakage flow is one of the main aspects of the expander mechanistic model. In particular, the prediction of a binary mixture leakage flow under two-phase flow conditions is a challenging task. A detailed flow model has been established to analyze the impact of boundary conditions, such as temperature and pressure upstream and downstream the leakage path as well the gap size for the prediction of leakage mass flow rate. The conservations of mass, energy, and momentum are applied to derive a set of differential equations that describe the flow in the control volume. The mass flow rate predicted by the detailed compressible flow model, differs significantly from the one predicted by a simplified isentropic nozzle flow model, due to the presence of friction. This fact suggests that the isentropic nozzle flow model (more computationally efficient) needs to be corrected to account for friction. The possibility of creating a certain volume ratio by increasing the twist angle was investigated. It has been established that higher twist angles reduce the blowhole, however the required internal volume ratio could not be achieved. We conclude that a male–female rotor combination as seen in the twin-screw profile would allow the required volume ratio to be achieved.

### **Heat Exchanger Model Development**

Heat exchangers influence the transient behavior of ORC systems significantly. The finite volume method and moving boundary method have been studied to identify the appropriate approach for ARC model development. The finite volume method divides heat exchangers into a number of fixed control volumes and the moving boundary segments heat exchangers depending on

thermodynamic phase of the working fluid (sub-cooled liquid, two-phase, and superheated vapor) and moves control volumes as the length of each phase changes. The moving boundary methodology solves fewer equations due to a reduced number of control volumes. Both modeling approaches were validated with experiment data during this performance period. Standard (MATLAB) equation solvers were used for steady and transient heat exchanger models. The steady-state model predictions are very close to the measurements.

### **Conclusions**

The ARC modeling promises 5% fuel economy benefits. Engine coolant has been established as a potential WHR working fluid and thermal stability improvements are in progress. The program fuel economy targets will not be achieved with the Roots expander due to the system low volumetric flow rates. Alternative positive displacement expander technologies are being pursued to enable successful demonstration of the ARC system. WHR components (expander and heat exchanger) in ARC plant model is in progress.

### **FY 2016 Publications/Presentations**

1. AMR 2016 Report.

### **Special Recognitions and Awards/ Patents Issued**

1. Patent Application #62360769, Rankine Waste Heat Recovery Control Using Zeotropic Mixture.

## IV.6 High Efficiency Variable Compression Ratio Engine with Variable Valve Actuation and New Supercharging Technology: VCR Technology for the 2020 to 2025 Market Space

### Overall Objectives

The primary objective of this project is to develop a high-efficiency variable compression ratio (VCR) engine having variable valve lift (VVL) technology and an advanced high-efficiency supercharger to obtain up to a 40% improvement in fuel economy when replacing current production V8 engines with the new small displacement VCR engine.

- Target power range: 281 hp to 360 hp
- Target light and medium load efficiency: 230 g/kWh

### Fiscal Year (FY) 2016 Objectives

- Design and build of the VCR 2.0 prototype engine

### FY 2016 Accomplishments

- The variable compression ratio hardware was built and assembled. There are no issues with the VCR mechanical assembly. ■

### Historical Background

VCR technology in spark-ignition engines was initially pursued to improve part-load engine efficiency where the knock tendency is low. Naturally aspirated variable compression ratio engines were built by Volkswagen in the 1980s that showed a reduction in brake specific fuel consumption of approximately 12%. In the 1990s, Charles Mendler was awarded the landmark patent number 5,819,702 for combining VCR with boosting and downsizing, an approach that showed potential for more than doubling the fuel economy improvement. All major spark-ignition VCR engine development programs now use this approach. Infiniti recently announced that it will introduce VCR technology in a model year 2018 QX50. The vehicle will be the first mass market application of technology claimed in the Mendler patent.

Major advances in engine and VCR technology have occurred since the first spark-ignition boosted VCR engine prototypes were built. VCR engines currently under development now have 50% higher brake mean effective pressure (BMEP) levels and enable greater

### Charles Mendler

ENVERA LLC  
Mill Valley, CA 94941  
Phone: (415) 381-0560  
Email: CMendler@VCREngine.com

DOE Technology Development Manager:  
Roland Gravel

NETL Project Manager:  
Ralph Nine

#### Subcontractors:

- Eaton Corporation (variable valve control), Marshall, MI
- Eaton Corporation (supercharging), Southfield, MI

improvements in vehicle mileage to be achieved through engine downsizing. Internal engine friction losses have also been reduced, and are now similar to those of non-VCR engines. Mass production cost is now a selling point for the VCR, as spark-ignition in-line four-cylinder VCR engines have a lower production cost than V6 engines of similar power, diesel engines, and hybrid powertrains.

### Introduction

Engine downsizing is a leading global strategy for improving vehicle fuel economy. Under normal driving conditions very little power is demanded of a vehicle's engine. The smaller the engine, the higher its efficiency at these small power levels. Accordingly, there is a global trend towards making engines smaller to increase vehicle mileage.

Turbo and supercharging may be employed so that the small engine produces the same power and torque of the larger engine being replaced. Today in Europe about half of all new gasoline engines are turbocharged.

With an increase in boost pressure, engine compression ratio (CR) must be lowered and/or spark timing retarded to prevent detonation or pre-ignition of the fuel-air

mixture. This lowering of CR reduces engine efficiency at the small power levels where high efficiency is most needed. VCR technology solves this problem by enabling a very high CR to be used at small power levels and a low CR used only when needed at high power levels. Fuel economy benefits can be further increased with VVL and use of the Atkinson cycle at small power levels.

The potential gains in mileage are large. GT-POWER computer modeling indicates that a boosted four-cylinder VCR engine can deliver the power and torque of a V8, while improving the mileage of a full-size pickup truck by about 40%.

## Approach

The current program includes three phases. In Phase 1 the general feasibility of attaining performance goals was assessed. This included a detailed assessment of boosting system options using GT-POWER modeling, and down selection of the boosting system approach to be used for the program. Mechanical durability and functionality of the VCR 2.0 VCR mechanism was also evaluated. In Phase 2 the VCR engine was designed, including the VCR crankcase, VVL equipped cylinder head, and advanced supercharging installation. Phase 2 also includes engine build. In Phase 3 the engine will receive baseline calibration, optimization, and testing of program target parameters. The current program builds on earlier development efforts, including a VCR crankcase and actuator development conducted with the National Energy Technology Laboratory/DOE, and a 1.8-L VCR engine built for Oak Ridge National Laboratory for combustion research.

## Results

Both within and outside of the current program, boosting technologies are being developed that can deliver 25 bar to 30 bar BMEP engine torque values. It is assumed that when the VCR technology enters the market place circa 2020, boosting technology will be more advanced, and continuing to improve. Envera is developing the VCR 2.0 engine to support these high BMEP and torque values.

Optimum CR values were investigated using GT-POWER computer modeling and engine dynamometer testing. Historical and current analysis indicates that a maximum CR of at least 16.5:1 is desirable, with some additional gains in efficiency up to a CR of about 18:1. These results assume use of the Atkinson cycle. The optimum minimum CR is between 8.0 and 8.5:1. The low CR has a number of benefits:

- Prevention of detonation at high torque values

- Lower octane fuel requirement
- Lower intercooler effectiveness requirement
- Lower peak cylinder pressure and lower mechanical loading
- Lower combustion rate of pressure rise to comply with original equipment manufacturer noise, vibration, and harshness guidelines
- Improved turbocharger performance

Engine proportions were selected for maximizing fuel economy. Analysis indicated that bore to stroke ratio should be between 0.91 and 0.87 and cylinder displacement should be approximately 600 cc. The Envera VCR 2.0 prototype will use the General Motors 2.5-L Ecotec cylinder head. The Envera VCR 2.0 crankcase will also accept the Ford 2.3-L cylinder head. Table 1 shows VCR travel needed for two different engine options. VCR travel is the change in distance between the crankshaft and cylinder head with change of CR.

The table shows that a VCR travel range of about 7.0 mm is needed. Additional gains can be realized with a travel range up to 8.5 mm. Atkinson cycle engines attain high efficiency by combining a high mechanical compression ratio and late intake valve closing. VCR enables Atkinson cycle efficiency benefits to be increased by providing a higher mechanical compression ratio during light-load driving conditions. The Envera VCR 2.0 mechanism is one of the few variable compression ratio mechanism options that provides the desired VCR travel range. Another advantage of the Envera VCR 2.0 mechanism is that near-stock internal engine friction losses can be achieved. The mechanism is capable of supporting 30 bar BMEP and 7,000 rpm.

The Envera VCR 2.0 engine is shown in Figure 1. Figure 2 is a detailed view that shows how the VCR mechanism works. Figure 2 shows an iron cylinder jug retained in an aluminum crankcase by two control shafts. The two control shafts are geared together so that they rotate in the same direction to adjust compression ratio. The control shafts have eccentrically mounted journals. Rotating the control shafts causes the journals to orbit causing the iron cylinder jug to move relative to the aluminum crankcase and adjust compression ratio. The control shaft bearings in the iron cylinder jug (bronze in color) do not rotate and are held in place with fasteners.

The VCR 2.0 crankcase was engineered to support 30 bar BMEP engine operation. The iron cylinder jug was developed using finite element analysis to minimize distortion when combustion forces are applied. The iron

**Table 1. VCR Travel Distance Needed for Optimum Engine Efficiency and Engine Performance**

TABLE 1: VCR Travel Needed		GM 2.5L Ecotec Stock	Envera VCR 2.0 - 2.5L BUILD	
			Full CR	Reduced CR
			Range	Range
Bore	mm	88.00	88.00	88.00
Stroke	mm	101.00	101.00	101.00
Bore/Stroke		0.871	0.871	0.871
Cylinder displacement	cc	614.3	614.3	614.3
Cylinders		4	4	4
Engine displacement	L	2457	2457	2457
CR				
Max		11.30	18.00	16.50
Min			8.00	8.50
Chamber volume, d				
Max CR	cc	59.64	36.13	39.63
Min CR	cc		87.76	81.91
Change in volume	cc		51.62	42.27
VCR Travel, T	mm		<b>8.49</b>	<b>6.95</b>

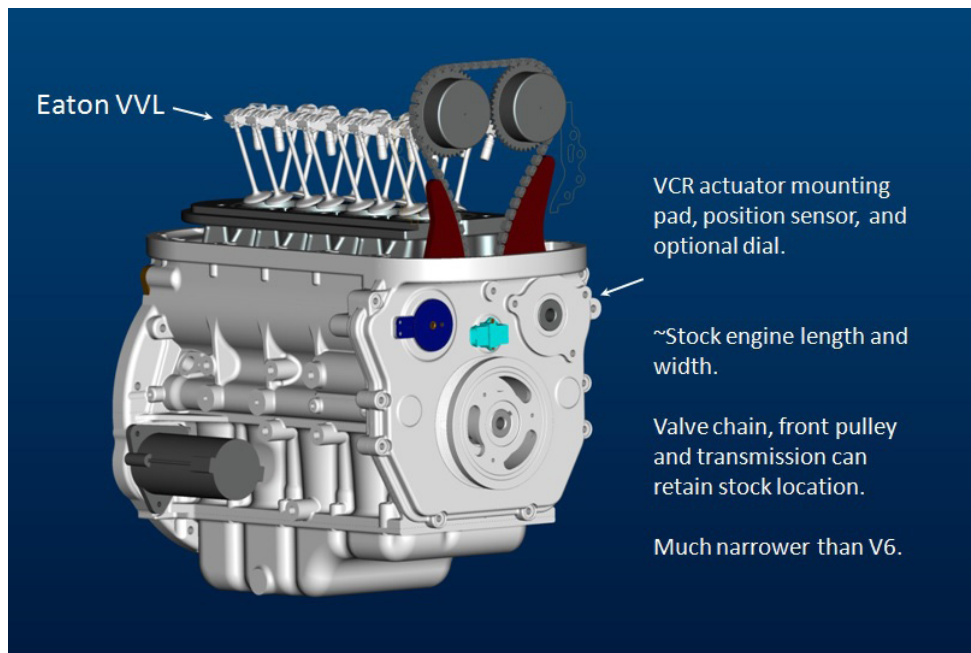


Figure 1. The Envera VCR 2.0 variable compression ratio engine

jug is stiffer than the stock aluminum crankcase and can be used for diesel or gasoline engine builds. The aluminum crankcase was also developed using finite element analysis for high stiffness and strength values.

The VCR 2.0 mechanism doesn't add mass to the cranktrain. High engine speeds and loads can be attained with conventional and reliable cranktrain technology.

The VCR 2.0 engine can be operated at speeds over 7,000 rpm. Additionally, the Envera VCR 2.0 mechanism doesn't increase engine internal friction losses or increase oil pump power consumption.

The VCR 2.0 build includes larger connecting rod bearings and a larger flywheel bolt flange to support 600 N·m torque values. These changes are not part of

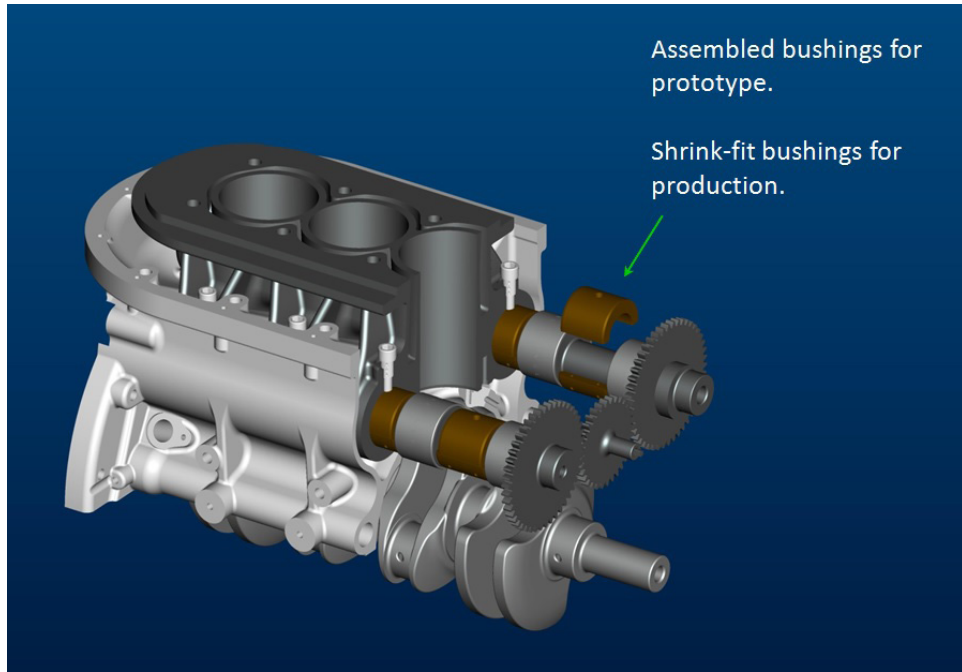


Figure 2. Detailed view of the Envera VCR mechanism

the VCR mechanism but do add some weight to the cranktrain.

Referring now to Figure 1, a major advantage of the VCR 2.0 design is that near-stock engine length can be retained. The short engine length will enable the engine to be used in a broad range of vehicle models. The stock cylinder head and stock valve chain location of the General Motors 2.5-L Ecotec engine are used. The VCR crankcase can also be designed to have a high degree of commonality with the stock crankcase to minimize development and manufacturing costs.

## Conclusions

Turbo and supercharging technology is advancing on multiple fronts to levels that will support 25 bar to 30 bar BMEP engine load values. These advances greatly escalate the value of VCR technology as high compression ratio values are needed for fuel efficiency and low compression ratio values are needed for high BMEP (high torque) conditions.

The Envera VCR 2.0 engine is being developed to support boosting technology projected to be available in the 2020 to 2025 market space and beyond. The Envera VCR 2.0 VCR mechanism has the large VCR travel distance and mechanical robustness needed for engines operating at high BMEP levels.

Another advantage of the Envera VCR 2.0 mechanism is that near-stock internal engine friction losses can be achieved. The Envera VCR 2.0 mechanism is also fully capable of supporting the 7,000 rpm target engine speed. A major advantage of the VCR 2.0 design is that near-stock engine length can be retained. The short engine length will enable the engine to be used in a broad range of vehicle models.

## FY 2016 Publications/Presentations

1. DOE Annual Merit Review presentation, June 9, 2016.

## IV.7 Lean Miller Cycle System Development for Light-Duty Vehicles

### Overall Objectives

- Demonstrate a new combustion concept combining lean stratified operation with Miller cycle in a gasoline engine
- Integrate with engine downsizing, advanced thermal management, 12-V stop/start, friction reduction mechanisms, and a lean aftertreatment exhaust system
- Demonstrate a vehicle with a fuel economy improvement of more than 35% over an existing production baseline vehicle while meeting Tier 3 emissions standards

### Fiscal Year (FY) 2016 Objectives

- Baseline the single-cylinder engine (SCE) on dynamometer
- Optimize the “multi-hole” combustion system design on the SCE
- Design initial multi-cylinder engine (MCE) and vehicle system architecture
- Develop the overall system architecture using one-dimensional (1D) and three-dimensional (3D) simulations

### FY 2016 Accomplishments

- Successfully demonstrated baseline homogeneous stoichiometric targets for the SCE
- Optimized piston, port, and injector spray details to achieve the target spray that avoids collapse
- Demonstrated viable fuel consumption levels during stratified operation at the NO<sub>x</sub> target of 10 g/kg fuel
- Developed and calibrated computational fluid dynamics (CFD) models to support understanding of the cylinder spray, mixing, and combustion phenomena, and guide design changes
- Developed boost and aftertreatment system using 1D models to address the challenges of low-temperature lean exhaust, and define SCE boundary conditions
- Analyzed the overall system cost for commercial viability

### David P. Sczomak (Primary Contact), Arun Solomon

General Motors LLC  
800 N. Glenwood Ave.  
Pontiac, MI 48340  
Phone: (586) 634-9858  
Email: david.sczomak@gm.com

DOE Technology Development Manager:  
Ken Howden  
NETL Project Manager:  
Ralph Nine

- Designed the initial MCE for dynamometer testing, including advanced thermal management ■

### Introduction

In order to accomplish the government objective of achieving breakthrough thermal efficiencies while meeting U.S. Environmental Protection Agency emission standards, this project focuses on combining two enabling technologies in a gasoline engine: lean combustion and Miller cycle. Lean combustion requires a more complex exhaust aftertreatment system than a traditional three-way catalyst system. The Miller cycle concept provides knock mitigation, increased expansion of combustion gases to extract additional work, reduced pumping losses, and increased efficiency.

The objective of the project is to research, develop and demonstrate the new Lean Miller Cycle combustion concept. The Lean Miller Cycle strategy will be integrated with engine downsizing, advanced thermal management, stop/start, and friction reduction to maximize efficiency to achieve a 35% improvement in fuel economy over a production baseline vehicle. A lean aftertreatment exhaust system will be developed to meet Tier 3 emissions standards. The overall system will be demonstrated in a vehicle.

### Approach

The challenges of the combustion and aftertreatment will be addressed systematically. The first step is SCE testing

which establishes the requirements for the combustion system. This central injection, lean combustion system requires very high levels of exhaust gas recirculation (EGR) to mitigate  $\text{NO}_x$  emissions; such a highly “dilute” system presents a combustion challenge. CFD is being used to analyze in-cylinder flows and spray interaction and design options for optimizing thermodynamic efficiency. This highly dilute system also presents a boost and aftertreatment challenge due to the low temperature lean exhaust and potential high cost of components. 1D modeling is being used to investigate options for boost, EGR, and exhaust aftertreatment systems and provide realistic boundary conditions for the SCE testing.

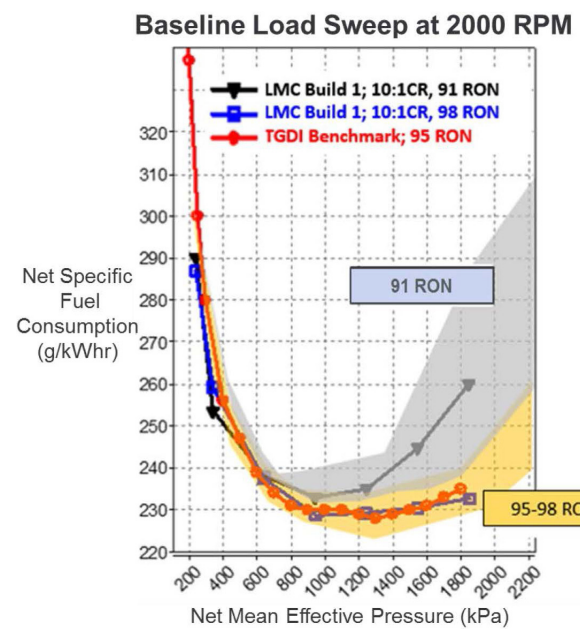
These fundamentals will then be integrated into an MCE and aftertreatment system. The engine will be optimized and calibrated on an engine dynamometer. The final demonstration will be in a vehicle, where emissions, drivability, and performance will be confirmed. Decision gates are set up annually to assess progress and determine whether or not to continue the investigation.

## Results

Significant progress was made in optimizing the Lean Miller Cycle system on the SCE. Results relative to the milestones are summarized below.

### Single-Cylinder Baseline Engine Testing Completed

Baseline testing of the single-cylinder engine was completed in homogeneous stoichiometric mode, at a 10:1 compression ratio (CR). Results compared favorably to baseline reference scatter-bands, as shown in Figure 1. This milestone is complete.



LMC – Lean Miller Cycle; RON – Research Octane Number;  
TGDI – turbo gasoline direct injection

Figure 1. Baseline test results

### 1D and 3D Simulations

1D modeling was used to determine realistic boundary conditions for the single-cylinder engine and evaluate options for the boost system. A summary of the boost options and selection criteria is shown in Table 1. A turbocharger, supercharger, and super-turbo combinations were assessed. It was determined that a variable speed supercharger would provide the best fuel consumption in the light load regime. In addition, an electrically assisted version was investigated, and offers some advantages in

Table 1. Boost System Evaluation Matrix

Option	Pros	Cons
Single Supercharger	<ul style="list-style-type: none"> <li>Highest exhaust enthalpy for cat</li> <li>Boost independent of exhaust enthalpy</li> <li>Compatibility with EGR</li> <li>Medium cost</li> </ul>	<ul style="list-style-type: none"> <li>Parasitics</li> <li>May require variable speed</li> </ul>
Super-Turbo or Turbo-Super	<ul style="list-style-type: none"> <li>Potential to meet flow requirements</li> </ul>	<ul style="list-style-type: none"> <li>Low exhaust enthalpy for boost</li> <li>Enthalpy loss for aftertreatment</li> <li>Parasitics</li> <li>Complexity / Cost</li> </ul>
Turbo-Turbo	<ul style="list-style-type: none"> <li>Potential to meet flow requirements</li> <li>Eliminates drive parasitic</li> </ul>	<ul style="list-style-type: none"> <li>Low exhaust enthalpy for boost</li> <li>Highest enthalpy loss for aftertreatment</li> <li>Complexity</li> <li>Risks w/ low pressure EGR</li> <li>Complexity / Cost</li> </ul>
Single Turbo	<ul style="list-style-type: none"> <li>Efficient / Simple</li> <li>Lowest cost</li> </ul>	<ul style="list-style-type: none"> <li>Limited flow and boost</li> <li>Risks w/ low pressure EGR</li> <li>Low exhaust enthalpy</li> </ul>

overall in-vehicle fuel consumption. The synergy of the Lean Miller Cycle system with an electric assist boost system continues to be assessed.

An aftertreatment model was developed to evaluate scenarios for active, passive, and mixed-mode aftertreatment strategies. Regions for lean stratified and stoichiometric (Miller) operation can be evaluated for optimum fuel economy. It also helps determine scheduling of urea and/or passive ammonia reductant generation required for lean  $\text{NO}_x$  reduction.

CFD modeling was used extensively to explain the in-cylinder spray, combustion, and mixing phenomena. Figure 2 shows an example where an issue with the piston bowl shape was identified. Improving the piston bowl geometry significantly reduced rich zones and improved combustion. In addition, intake port designs and injection strategies were investigated. This activity is continuing.

### Single Cylinder Development with Multi-Hole Head and Piston, Injector, Plug Optimization

This was the major focus of development. Several pistons bowls with compression ratios up to 12:1 were investigated. An injector matrix was developed to investigate the impact of spray hole and seat configurations. Intake ports with low and high tumble levels were developed and evaluated in both stratified

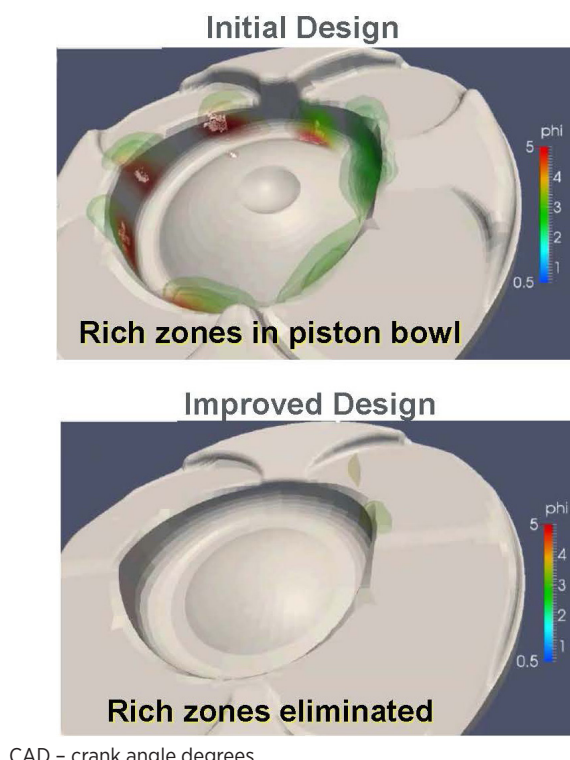


Figure 2. CFD analysis of piston bowl

lean and homogeneous stoichiometric operating regimes. By optimizing the injection strategy, good lean stratified performance appears feasible with higher tumble. This suggests that a “medium tumble” cylinder head may perform best and is planned for follow-up testing. Imaging of the sprays were made in spray vessels at both ambient and elevated pressure and temperature conditions. Twenty-four injector variants were subsequently tested on the SCE. In parallel, CFD analysis was utilized to understand the fundamental in-cylinder performance and to guide design improvements. Figure 3 shows images from the General Motors spray lab that show both liquid (Mie scatter) and vapor (Schlieren) phases of the sprays. This capability assisted the development of sprays that did not collapse under late injection lean stratified conditions. The projected brake thermal efficiency at a  $\text{NO}_x$  level of 10 g/kg fuel shows the potential to exceed the DOE target values, as shown in Figure 4. This work is continuing.

### Single-Cylinder Development Testing with Piezo Injector

The piezo injector variant was a risk mitigation option in the plan. Because the multi-hole injectors with optimized laser holes are showing promise of meeting combustion targets, this option was not exercised.

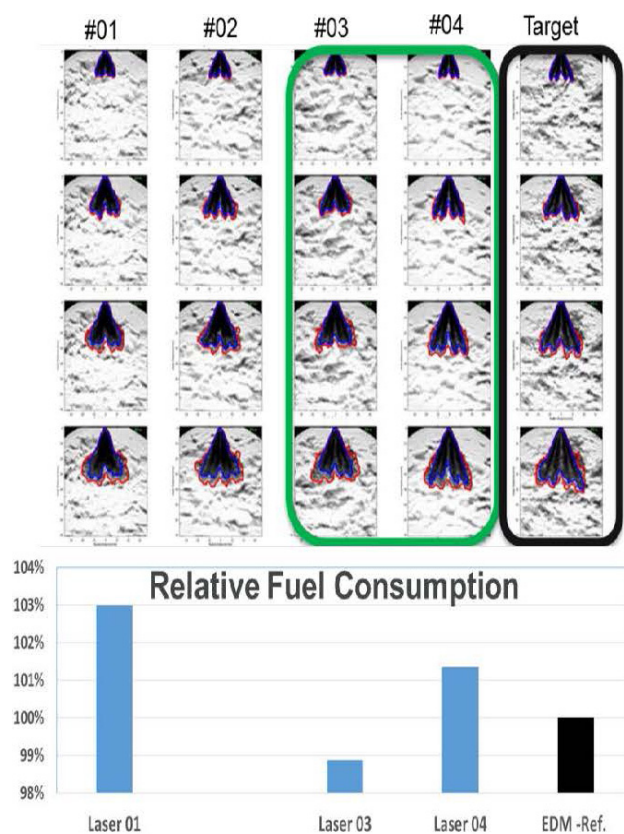


Figure 3. Impact of spray designs

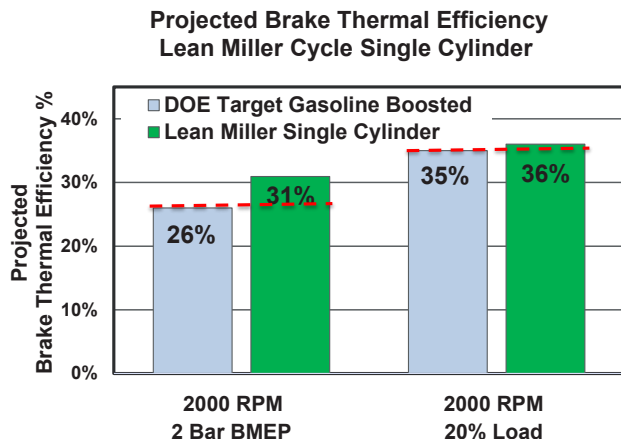


Figure 4. Single-cylinder efficiency status

### Design of Multi-Cylinder Engine

Water jackets for cylinder liner and cylinder head were designed with a targeted cooling approach using 3D modeling to optimize heat transfer. The design of all major engine systems is nearly complete, as shown in Figure 5. The initial aftertreatment and boost system concepts have also been designed.

### Conclusions

- The Lean Miller Cycle system scope of work includes analysis, single-cylinder, multi-cylinder, and vehicle development. It will include full aftertreatment and controls development to meet performance targets and Tier 3 emission standards.
- The SCE was successfully baselined.
- SCE testing showed promising results with multi-hole injectors. Injector, piston, and intake port designs have been the focus. Additional work is required to verify the final port and chamber designs, and to improve robustness.

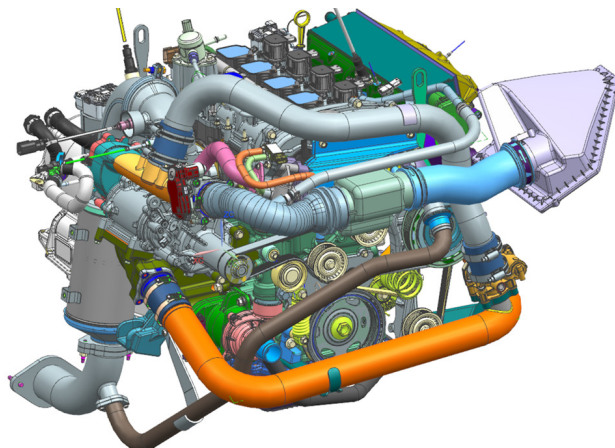


Figure 5. Multi-cylinder engine design

- The multi-cylinder design is nearly complete and is feasible for the vehicle installation.
- Options for lean and low-temperature aftertreatment and the boost system have been defined.
- 1D and 3D modeling have been used to guide combustion, boost, and aftertreatment design.
- The gate decision for initiation of multi-cylinder hardware procurement is planned for the second quarter of 2017.

### FY 2016 Publications/Presentations

- 2016 Annual Merit Review presented on June 9, 2016.

### Special Recognitions and Awards/ Patents Issued

- Three patent applications have been filed for this project since inception.

## IV.8 Enabling Technologies for Heavy-Duty Vehicles – Cummins 55% BTE

### Overall Objectives

- Use a diesel engine system to demonstrate in a test cell peak engine system efficiency of 55% brake thermal efficiency (BTE)
- Develop and demonstrate an advanced, highly integrated combustion and aftertreatment system to achieve 2010 emissions compliance

### Fiscal Year (FY) 2016 Objectives

- Design a high efficiency variable flow and pressure lube pump
- Design and develop air handling controls system for dual loop exhaust gas recirculation (EGR) architecture
- Integrate and control a high efficiency variable flow and pressure lube pump
- Design an optimized waste heat recovery turbine expander for best operating point

### FY 2016 Accomplishments

- Designed, procured, and tested a high efficiency variable flow and pressure lube pump
- Designed, developed, and tested an air handling controls system for dual loop EGR architecture
- Designed, developed, and tested a low parasitic valvetrain system incorporating roller bearing elements and lightweight components
- Designed, developed, and tested an optimized exhaust manifold for pulsation utilization
- Designed and developed a low heat transfer power cylinder system
- Designed, developed, and tested an optimized low friction power cylinder system ■

### Introduction

The successful development of a high efficiency diesel engine system could significantly reduce petroleum usage in the United States and provide energy security for the future. The program's efforts directly address the Vehicle Technologies Office's goal of achieving 55% BTE and

### Lyle Kocher

Cummins Inc.  
1900 McKinley Avenue  
Columbus, IN 47201-6414  
Phone: (812) 377-2507  
Email: lyle.e.kocher@cummins.com

DOE Technology Development Manager:  
Roland Gravel

NETL Project Manager:  
Ralph Nine

prevailing emissions compliance. The program accelerates the development of the high efficiency enabling technologies to shorten their time to market.

The landscape of advanced heavy-duty engines includes both high temperature diffusion combustion and low temperate premixed combustion. The low temperature combustion (LTC) engines are capable to demonstrate low engine-out constituent emissions and high thermal efficiencies. The high thermal efficiency is predominately due to a short combustion duration and low in-cylinder heat loss from the distributed premixed reactions. However, LTC engines suffer from controllability issues due to the lack of a direct combustion trigger and knock issues due to fuel and temperature stratification in the cylinder. These barriers currently prohibit LTC engines from entering the heavy-duty market. High temperature combustion engines are easily controllable and do not suffer from knock but emit higher levels of constituent emissions such as  $\text{NO}_x$  and particulate matter. The emissions can be treated through the application of low pressure EGR and a close-coupled selective catalytic reduction on filter catalyst system. Efficiency improvements for the high temperature combustion engines can be achieved by mimicking the best traits of an LTC engine, short combustion duration and low in-cylinder heat loss.

### Approach

The approach integrates advances in the areas of combustion, engine design, waste heat recovery, fuel injection, turbocharging, and aftertreatment to provide

an optimized and integrated total system. Achieving 55% BTE will require virtually all engine systems to be improved with thorough effort placed on the interaction between the systems. When examining the entire system, opportunities can be created to take advantage of technologies to benefit multiple engine systems. Starting with the combustion system, a low heat rejection combustion chamber is desired to minimize the in-cylinder heat losses. The low heat rejection design will be achieved through piston material changes to low thermal conductivity materials and use of thermal barrier coatings. The low heat transfer (LHT) piston will operate with higher surface temperatures and thus have lower in-cylinder heat losses. Additionally, the LHT piston will be able to operate with reduced piston oil cooling flow. This represents a savings of up to 40% of the lube flow and will allow a smaller, lower parasitic lube pump to be utilized. The LHT pistons will also have higher exhaust temperatures for better aftertreatment performance. Similar symbiotic system level opportunities are available through the use of a close-couple aftertreatment system and the addition of a low pressure EGR loop. An integrated system designed to opportunistically take advantage of these interactions is critical to achieving the overall efficiency goals.

## Results

### Low Heat Transfer Power Cylinder System

A low heat rejection combustion system was designed to reduce in-cylinder heat transfer. The design includes application of LHT materials to combustion surfaces, reduction and/or elimination of piston oil cooling and higher coolant operating temperature. Conjugate heat transfer analysis has been performed to maximize the benefit of a LHT combustion system while maintaining temperatures to below mechanical limitations of the selected materials. The temperatures for the LHT piston designs are shown in Figure 1 for a cruise power

condition. Figure 1 illustrates a substantial increase in piston surface temperature that will reduce the heat transfer losses in-cylinder.

Challenges in the implementation of a low heat rejection combustion system are expected. The typical observations of a lower peak heat release rate and a slower late cycle oxidation have been documented previously. Combustion modeling efforts are being directed to design a combustion system specifically for a low heat rejection engine to mitigate the combustion degradation observed experimentally.

### Pulse Capture Exhaust Manifold

The program is evaluating the addition of a low pressure EGR loop to the system. Unlike a high pressure EGR loop, which requires higher exhaust manifold pressure to drive EGR, a low pressure EGR loop system can conserve the exhaust pulse energy to drive the turbine and pull EGR from after the diesel particulate filter. This results in the turbine seeing higher engine flows and creating more power to drive the compressor. The exhaust manifold design is critical to minimizing the losses between the exhaust port and the turbine inlet. An optimized exhaust manifold was designed and procured to conserve the exhaust pulse energy and increase turbine efficiency. The exhaust manifold design is shown in Figure 2.

### Fuel Injection System

Conventional diesel combustion is a diffusion (or mixing) controlled combustion event meaning that the fuel is burned as soon as it has a chance to mix with entrained air to an ignitable equivalence ratio. In order to increase the rate at which the fuel is burned, the fuel needs to be introduced into the cylinder at an increased rate while ensuring that enough air can be entrained into the fuel jet for proper combustion. However, increased fuel flow through injectors has typically resulted in cavitation of the injector nozzles due to the high velocities in the

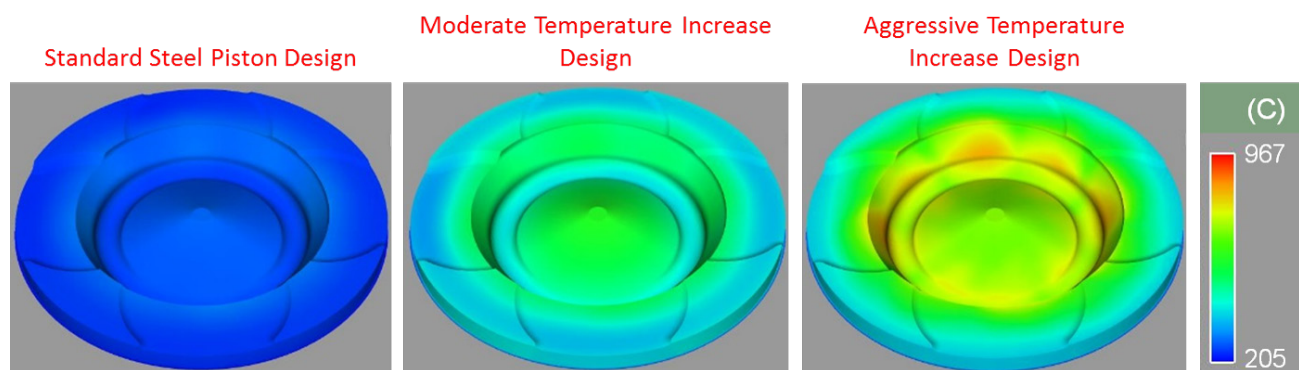


Figure 1. Conjugate heat transfer analysis of LHT piston designs at cruise power condition



Figure 2. Pulse capture exhaust manifold design

nozzle holes causing low pressure zones that encourage vapor formation. Additionally, high flow injectors tend to operate for longer periods of time with the injector needle being ballistic (i.e., the needle is opened to a position where it does not rest on a mechanical stop). Therefore, coupled design and analysis was performed to create fuel injectors with the desired fuel injection rate shape characteristics that are robust to cavitation and have acceptable shot-to-shot variability. The injector design is continuing to evolve as the low heat transfer combustion system is being developed.

### Friction and Parasitic Reductions

Substantial hardware improvements have been developed to minimize parasitic losses from the engine. The accessory load pumps, such as the water and lube, are traditionally fixed flow pumps that consume the same amount of input power at part load engine conditions as full load engine conditions. The flows from both the water and lube pump can be significantly reduced under part load conditions. The approach is to integrate variable flow pump technologies that can achieve lower flows without greatly affecting pump efficiencies and engine durability. The newly designed lube pump is expected to provide a 0.35 kW friction power savings under cruise conditions when coupled with the lube flow reduction efforts. The newly designed water pump is expected to provide a 0.5 kW friction power savings under cruise conditions when coupled with the water flow reduction efforts.

A valvetrain design concept was created to incorporate roller bearing elements and weight savings where possible to reduce the valvetrain parasitic loss. A key benefit of the roller bearing valvetrain design is the reduction in required oil flow to the overhead, which can be provide additional savings in the lube pump work. The parasitic savings of the rollerized valvetrain have been demonstrated on a motoring cylinder head test rig. Figure 3 shows the friction power savings with hot engine oil as a function of the camshaft speed. The rollerized

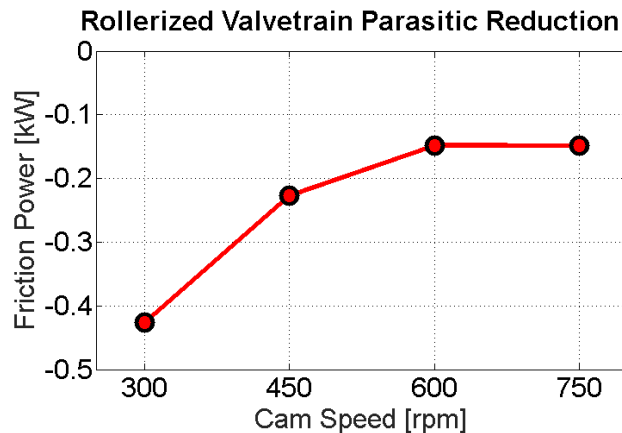


Figure 3. Rollerized valvetrain parasitic reduction

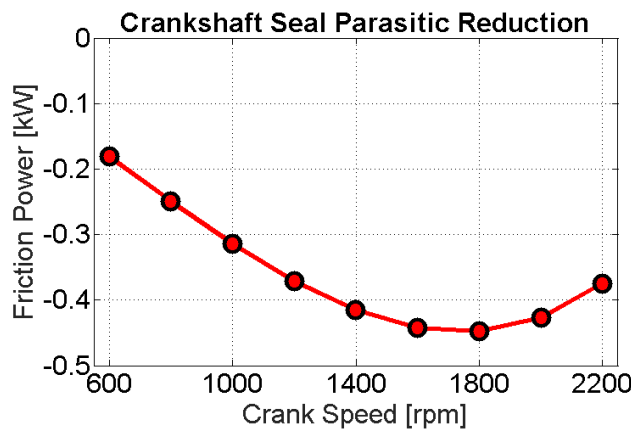


Figure 4. Crankshaft seals friction reduction

valvetrain concept is expected to provide a 0.2 kW friction power savings under cruise conditions.

New designs from suppliers for the front and rear main crankshaft seals were evaluated in the motoring test laboratory. Optimized seals were selected for demonstration engine testing. Figure 4 shows the parasitic reduction with hot engine oil of the new crankshaft seals over the production seals as a function of engine crankshaft speed. The crankshaft seals are expected to provide a 0.3 kW friction power savings under cruise conditions.

The engine will additionally utilize low tension compression and oil rings and diamond like carbon coatings. The cylinder liners have an improved surface finish to further reduce friction. The ring pack, like all the other low parasitic technologies being developed, still require more extensive durability testing to ensure the hardware is robust over the life of the engine.

## Conclusions

The Cummins 55% BTE program has successfully completed the first year of the two-year program. The following conclusions have come from the first year:

- A low parasitic engine system incorporating roller bearing elements, lightweight components, variable flow pumps, low friction seals, and optimized rings can provide a significant parasitic reduction benefit.
- A low heat transfer power cylinder system can provide necessary surface temperatures to realize efficiency improvement but additional work is required to mitigate combustion degradation.

## V. Solid State Energy Conversion

Along with high efficiency engine technologies and emission control, the Vehicle Technologies Office (VTO) is supporting research and development to increase vehicle fuel economy by recovering energy from engine waste heat. In current gasoline vehicles, only about 30% of the fuel's energy is used to drive the wheels; in contrast, more than 70% is lost as waste heat in the exhaust gases and to engine coolant. Recovering energy from the engine exhaust could improve the overall vehicle fuel economy by more than 5%. In FY 2016 VTO continued research and development of thermoelectric generators that can directly convert energy from the hot engine exhaust into electricity to power vehicle auxiliary loads and accessories. To enable further developments in this area, VTO also supported research into materials for energy recovery systems and materials by design for thermoelectric applications.

# V.1 Gentherm Thermoelectric Waste Heat Recovery Project for Passenger Vehicles

## Overall Objectives

- A detailed production cost analysis for a thermoelectric generator (TEG) for passenger vehicle volumes of 100,000 units per year and a discussion of how costs will be reduced in manufacturing
- A 5% fuel economy improvement by direct conversion of engine waste heat to useful electric power for light-duty vehicle (LDV) application; for light-duty passenger vehicles, the fuel economy improvement must be measured over the US06 Supplemental Federal Test Procedure cycle
- Confirmatory testing of the hardware to verify its performance in terms of fuel economy improvement
- Build scaled-up TEG for the U.S. Army Tank Automotive Research and Development Engineering Center Bradley Fighting Vehicle (BFV)

## Fiscal Year (FY) 2016 Objectives

- Vehicle level testing

## FY 2016 Accomplishments

- Final vehicle level integration and testing
- Completed project and submitted final report ■

## Introduction

The focus of this project is the development of a simple and reliable device that would enable recovery of otherwise wasted exhaust gas energy. Recovered thermal energy is directly converted into electricity using a solid state device, a TEG. The primary objective of this program is to design and implement TEG devices which demonstrate 5% fuel economy improvement for passenger or LDVs. In FY 2015 we have demonstrated a device design for both LDVs and heavy-duty vehicles (HDVs). The device developed for HDV applications was tested at Tenneco's R&D center and showed the potential to generate up to 1.8 kW of electricity and provide a fuel economy improvement of up to 1.5%. In FY 2016 we have integrated devices in two passenger vehicles and on the US06 cycle demonstrated up to 1.2% increase in fuel efficiency using this technology.

**Vladimir Jovovic (Primary Contact)<sup>1</sup>,  
D. Lock<sup>1</sup>, C. Haefele<sup>2</sup>, M. Miersch<sup>3</sup>**

<sup>1</sup>Gentherm Inc.  
1321 Mountain View Circle  
Azusa, CA 91702  
Phone: (626) 208-3460  
Email: Vladimir.jovovic@gentherm.com

<sup>2</sup>BMW AG  
Research and Innovation Center  
Knorrstraße 147  
80788 Munich, Germany

<sup>3</sup>Tenneco GmbH  
Luitpoldstrasse 83  
67480 Edenkoben, Germany

DOE Technology Development Manager:  
Gurpreet Singh

NETL Project Manager:  
Carl Maronde

Subcontractors:

- BMW, Palo Alto, CA and Munich, Germany
- Ford Motor Company, Dearborn, MI
- Tenneco GmbH, Grass Lake, MI and Edenkoben, Germany

## Approach

Gentherm began work in October 2011 to develop a Thermoelectric Waste Energy Recovery System for passenger vehicle applications. Partners in this program were BMW and Tenneco. Tenneco, in the role of Tier 1 supplier, developed the system-level packaging of the thermoelectric power generator. As the original equipment manufacturer, BMW Group demonstrated the TEG system in their vehicle in the final program phase. Gentherm demonstrated the performance of the TEG in medium-duty vehicles (MDVs) and HDVs. Technology developed and demonstrated in this program showed the potential to reduce fuel consumption by 1% in MDV and HDVs. In passenger vehicles on the US06 cycle this fuel saving potential is 1%. On the Worldwide Harmonized

Light Vehicles Test Procedure (WLTP) cycle or Federal Test Procedure (FTP-75), this potential drops down below 0.5% due to low mass flows and low temperatures of exhaust gasses.

## Results

In this project, a team consisting of Gentherm, BMW and Tenneco demonstrated the ability to produce, integrate, and test a reliable thermoelectric power generation device for passenger vehicle applications. The goal of this program was to demonstrate the ability to reduce vehicle fuel consumption by 5% in the US06 cycle. This goal was not reached as the team demonstrated 1% energy savings.

In addition, a team consisting of Gentherm and Tenneco worked on development of a HDV waste heat recovery device under contract with the Department of Energy and the U.S. Army Tank Automotive Research Development and Engineering Center. The goal of this part of the project was to demonstrate the ability to produce between 1 kW and 2 kW of electric power from the energy recovered from the exhaust of a BFV. This goal was fully reached and the team demonstrated an autonomous device generating 1.8 kW of power from the BFV's exhaust. The device is shown in Figure 1.

To reduce development time, both devices were designed using the same active power generation component. The basic building block used in both devices is a thermoelectric cartridge: a power conversion device developed by Gentherm and shown in Figure 2. Gentherm has developed methods of manufacturing these devices, test methodologies, and performance models. A combination of one-dimensional and three-dimensional models was used to evaluate performance and structural stability of components.



Figure 1. Demonstration of an HDV TEG. Device produces up to 1.8 kW of electric power using the exhaust heat of a 14.8-L diesel engine.

The role of the Tier 1 exhaust supplier, Tenneco, was to design and build the complete thermoelectric power generation unit, applying technologies developed in packaging catalytic converters, particulate filters, and other exhaust components. Tenneco used one-dimensional and three-dimensional modeling tools to predict system level performance and to design structural components of the TEG. As the TEG is a new component, structural integrity was verified following protocols similar to those used in development of active exhaust components such as catalytic converters.

BMW was the only original equipment manufacturer in this program. The role of BMW was to define packaging space and provide advice on system level requirements. In the final stage of this program, BMW performed vehicle level tests and evaluated the effect of integration of the TEG on fuel efficiency. Generators installed, Figure 3, in the BMW X3 showed a neutral effect on fuel efficiency. Figure 4 shows power output of the TEG installed in the BMW X3 and tested on the WLTP cycle. Peak power is limited to 120 W. Alternative installation of the TEG in a MDV demonstrated the ability to generate over 1.1 kW of electricity when tested on the US06 cycle. Results are shown in Figure 5. The tested vehicle was Gentherm's Ford F-350 MDV. For this demonstration Gentherm developed separate dual-zone radiator, electric water pump with control system, direct current-to-direct current power converter, exhaust system, and integrated two TEGs that were jointly developed by Tenneco and Gentherm. In this vehicle, the TEG installation resulted in fuel efficiency improvement of 1.2% and emission reduction of more



Figure 2. Lower left corner: thermoelectric power generation cartridge developed by Gentherm. Top: passenger vehicle thermoelectric power generation system developed by Gentherm and Tenneco. These devices were used to demonstrate system level performance in BMW and Gentherm vehicles (Ford F-350).

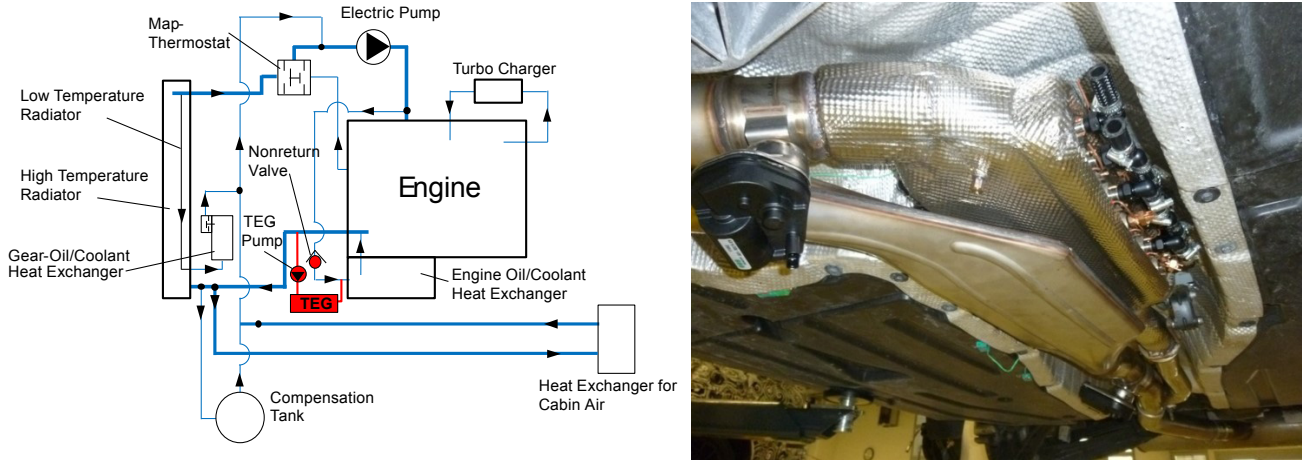


Figure 3. Installation of TEG in a BMW X3. Left: system level boundary diagram. Right: installation in mid-muffler position.

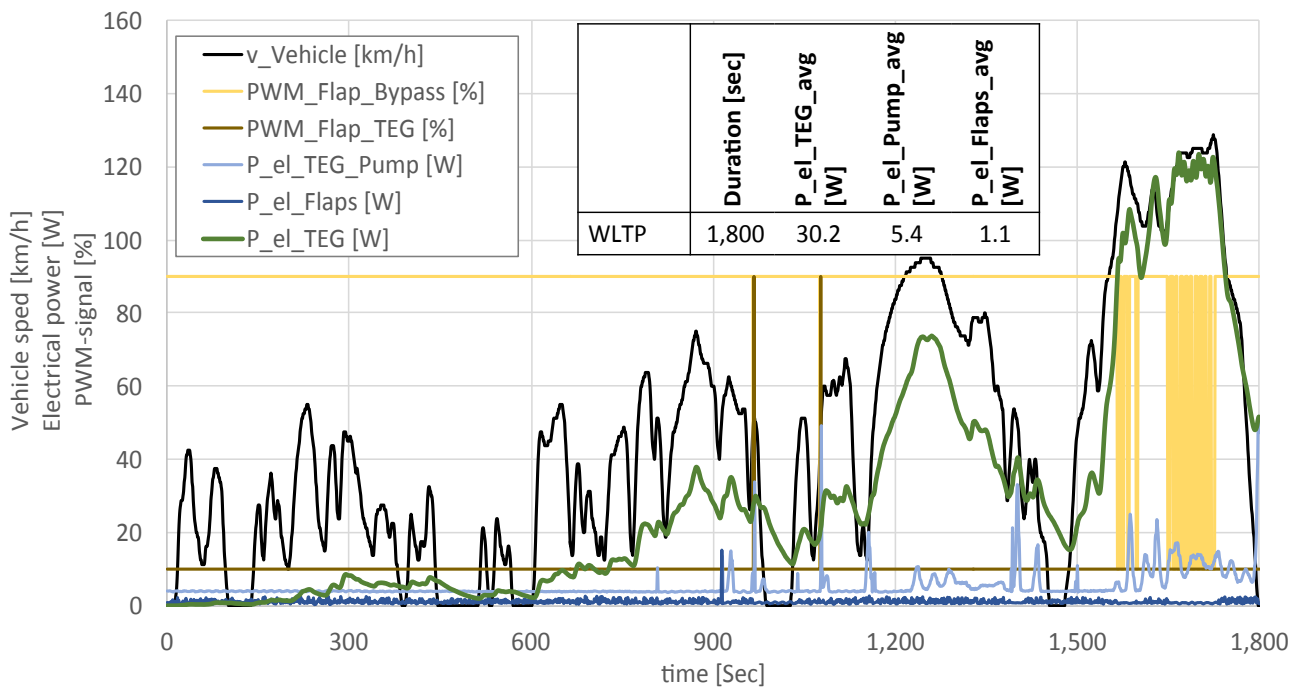


Figure 4. Test results from the BMW X3. Vehicle velocity, TEG power output, power consumption of TEG auxiliaries (flaps, pump), and pulse-width modulation (PWM) signals of the exhaust flaps over the WLTP cycle.

than 9 gCO<sub>2</sub>/mi. The major difference between the two demonstration vehicles was the position of the TEG. In the F-350, the TEG was installed closely coupled to the catalytic converter. The device installed in BMW X3 was in a mid-muffler position which resulted in up to 200°C lower exhaust gas temperatures entering the TEG.

In an HDV application, Gentherm and Tenneco demonstrated the ability to generate 1.8 kW of electricity from a moderately sized TEG system. This TEG system was undersized for this application, it uses only ~20% of

the available heat. This means that a properly sized TEG could generate up to 3 kW of electricity in this type of application.

In the development of the manufacturing process we focused on low-cost, high-yield technologies. Processing of thermoelectric materials requires fine control of ambient conditions and process parameters such as sintering temperatures. All thermoelectric materials are very sensitive to oxidation, contamination by impurities, and phase separation. For this reason we have selected

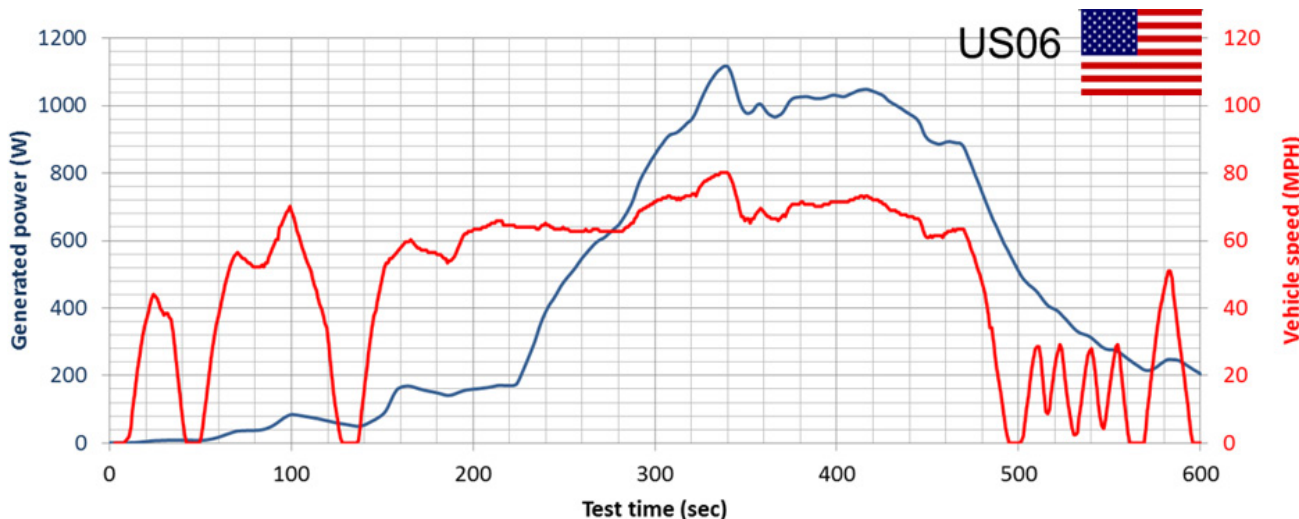


Figure 5. Ford F-350 results from the US06 drive cycle. TEG power output and vehicle speed in the US06 cycle. Peak power is 1,160 W and average power output is 470 W.

spark plasma sintering as our sintering process. As part of this project, we have developed a process to manufacture net-shaped thermoelectric elements using materials from the Skutterudite family. Both p- and n-type materials are produced with highly repeatable physical characteristics. The thermoelectric figure of merit,  $zT$ , is the best indication of material quality as it directly correlates to the efficiency with which thermoelectric materials convert heat to electricity. Based on in-process sampling of materials produced at Gentherm, we have peak  $zT$  values of 0.8 to 0.9 for p-type materials and 0.9 to 1.1 for n-type materials. The range shows our observed deviation in material properties in the past 12 months. Our manufacturing process is reliable, repeatable, and results in very low material loss. Yields are as high as 85%. Further improvements and automation of equipment could bring yields in the range of 92–95%. To demonstrate our ability to produce materials at a high rate, Gentherm has developed and installed automated equipment for handling of thermoelectric materials.

The major benefit of the scientific research and engineering development conducted in this program is in the systematic evaluation of cost drivers in manufacturing of thermoelectric elements and careful evaluation of performance of thermoelectric devices at the vehicle level. Analysis of conventionally accepted methods of manufacturing thermoelectric elements—ingot manufacturing followed by dicing, polishing and metallization—shows inherently low yields and high costs of material handling. The approach developed in this program focuses on net shape manufacturing and yield increase. Reduction of processing steps and material waste is the only approach which will result in

a commercially viable TEG system. At the device and vehicle level we have demonstrated the ability to generate significant power in MDVs and HDVs. Appropriately integrated devices can reduce fuel consumption by up to 2%. Measured power outputs in the systems demonstrated here is 1–2 kW of electricity. Fuel efficiency improvement in LDVs is much harder. Vehicle level performance analysis, a methodology developed by BMW, takes into account all impacts of the TEG on vehicle performance. Considering the modest heat potential of high efficiency engines, a TEG installed in a mid-muffler position has neutral effect on fuel efficiency.

## Conclusions

The team has completed the program with the following results:

- Delivered a method of producing high performance thermoelectric materials
- Developed automated equipment for handling of thermoelectric materials
- Manufactured seven fully functional and two partial TEG devices for LDV testing
- Performed LDV TEG bench tests at Gentherm, Tenneco, and the National Renewable Energy Laboratory
- Installed LDV TEGs in Gentherm and BMW vehicles and performed system level tests at Gentherm and BMW
- Built an HDV TEG for a BFV

## V.2 Development of Cost-Competitive Advanced Thermoelectric Generators for Direct Conversion of Vehicle Waste Heat into Useful Electrical Power

### Overall Objectives

- Overcome major obstacles to the commercialization of automotive thermoelectric generator (TEG) systems
- Develop a cost competitive TEG system including all necessary vehicle controls and electrical systems that are fully integrated into a light-duty vehicle
- Demonstrate fuel economy (FE) improvement over relevant Environmental Protection Agency test

### Fiscal Year (FY) 2016 Objectives

- Design a compact integrated heat exchanger-thermoelectric converter (TEC) system, perform all necessary finite element analysis on the generator system to verify it's robust to thermomechanical stress, and perform preliminary computational fluid dynamics simulations to ensure uniform flow distribution within the generator subunits and to verify that the system remains well below back pressure limits
- Perform proof of concept studies on all new materials and processes that will be required to execute the build of the redesigned generator and validate that they will scale to the system level and that they are compatible with all assembly procedures
- Design and deliver all necessary fixtures and alignment jigs to begin assembly of a full-size generator prototype
- Finalize controls development and integration plan to interface the generator with both the coolant and exhaust systems, including the required valves and routing schemes
- Build and characterize a demonstration vehicle that will accept the newly designed thermoelectric generator for the final stage of testing and FE improvement measurements.
- Obtain, test, and modify as needed the low cost direct current to direct current (DC-to-DC) converters for conditioning TEG power output for introduction into the vehicle, and validate that the power coming out of the DC-to-DC converter will automatically unload the alternator

**James R. Salvador (Primary Contact),  
Norman K. Bucknor, Kevin Rober,  
Edward R. Gundlach, and  
Aida Rodriguez**

General Motors  
30500 Mound Rd. MC 480-106-RA3  
Warren, MI 48090  
Phone: (517) 862-1376  
Email: james.salvador@gm.com

DOE Technology Development Manager:  
Gurpreet Singh

NETL Project Manager:  
Carl Maronde

Subcontractors:

- Brookhaven National Laboratory, Upton, NY
- Dana Canada Corp., Oakville, Ontario, Canada
- Delphi Electronics and Safety, Kokomo, Indiana
- Eberspaecher, Novi, MI
- Jet Propulsion Laboratory, Pasadena, CA
- Marlow Industries (II-VI), Dallas, TX
- University of Michigan, Ann Arbor, MI
- Oak Ridge National Laboratory, Oak Ridge, TN
- Purdue University, West Lafayette, IN
- University of Washington, Seattle, WA

### FY 2016 Accomplishments

- We have developed and implemented a method for printing dielectric thick films directly onto the surface of stainless steel heat exchangers. These films are thermomechanically robust at the full generator scale to thermal up and down shocks and effectively isolate the current carried in the thermoelectric converter system from the heat exchangers.

- We have developed a diffusion bonding technique to attach metal standoffs to skutterudite elements. The bonds are low in both electrical and thermal losses, and they are highly mechanically robust. We have been able to produce several thousand elements with this configuration and have tested them in both small and generator-sized arrays.
- Developed a high pressure, low temperature method to join the thermoelectric (TE) elements to the printed dielectric/thick film metal layer. The process will not require atmospheric isolation and has been demonstrated to make highly robust joints between the hot side attachment point and the elements. This joining technology results in low contact resistance and has been demonstrated at the generator level.
- We have finalized the subunit and system level design of the final TEG prototype. We have built the hot side heat exchangers (HHXs) and have begun fabrication of the cold side heat exchangers, which will be completed in December 2016; all other parts are now on-hand. The newly designed generator offers significant increases in both gravimetric and volumetric energy density while greatly reducing system costs by eliminating dielectric plates and load bearing heat exchanger assemblies.
- We have designed and fabricated all fixtures, screens, and alignment jigs required to build the final generator prototype.
- We have acquired, modified, and begun baseline testing on the demonstration vehicle. Cooling lines have been run, the exhaust system has been modified, and auxiliary components for the cooling system have been acquired and installed.
- We have acquired, tested, and, based on the test results, modified commercially available DC-to-DC converters for the final generator testing.
- Using a combination of validated TEG models and vehicle unified models, we have estimated the FE impacts of the generator. We have assessed the value of the off-cycle credits and have determined the likely total gCO<sub>2</sub>/mile reduction for a full-size truck. These results will establish the target system and integration costs that would make a compelling business case for technology adoption. ■

## Introduction

The development of a practical and fully integrated TEG for a production vehicle will be a significant step toward reducing energy consumption and lowering emissions associated with the U.S. transportation

sector. Considerable innovation, however, is needed to overcome the major obstacles to TEG technology commercialization. The economics of TEG technology implementation for passenger vehicles are challenging and will likely require the combination of off-cycle credits and on-cycle fuel savings in order to make a compelling business case for adoption. Our work on automotive TEGs has been refocused over the last year, and we are now centered on several key tasks: (1) validation of low temperature and high pressure silver sinter joining; (2) optimization and implementation of stainless steel dielectric coatings with long-term thermal stability; (3) accelerating novel routes to high volume production for successful market introduction of skutterudite materials and TE converters; (4) assessing the potential FE improvements the TEG can provide, and establishing a system cost based on these projected benefits; and (5) designing and building TEG subunits with drastically better volumetric and gravimetric power densities through the pursuit of a highly integrated component approach. At the completion of this four-year project, we will have created a potential supply chain for automotive TEG technology and identified manufacturing and assembly processes for large-scale production of TE materials and components that include scale-up plans for the production of 100,000 TEG units per year.

## Approach

Our current project builds on prior DOE-funded work with new goals for moving advanced TE materials and system fabrication from the laboratory-scale to mass production and for developing a fully integrated and viable TEG design suitable for commercialization by the automotive industry. We have made significant advances in TE material performance through collaborative research and development for more than a decade, and our TE material research partners all have extensive accomplishments in advanced TE technology. Our project team's expertise includes: (1) TE material research, synthesis, and characterization [1]; (2) thermal and electrical interfaces and contacts [2]; and (3) skutterudite-based TE element and module fabrication and testing [1,3]. We are working on improving the performance of TE materials simultaneously with the development of high volume methods for both TE material synthesis and TEC production. Further, our team has considerable expertise in heat exchanger design, computational fluid dynamics, and packaging of automotive exhaust systems that includes the design and commercialization of several exhaust gas heat exchangers for other waste heat recovery applications. We will rely on these core competencies as we develop TEG heat exchanger designs that optimize heat extraction for maximum TE conversion of heat

into usable electrical power. We are developing and implementing effective strategies for heat exchanger and TEC integration and power management that are crucial to manufacturability and system efficiency. We are leveraging the team's expertise in hybrid electric vehicle technology and integrated circuits to both design an electrical subsystem for the TEG and develop integrated circuit solutions in TE interconnections and TEC output power management hardware. Our focus is on durability and low-cost assembly strategies.

## Results

In the last year, we have undertaken and completed a total redesign of the generator subunits and system. We have retained the modular nature of the system using a plurality of these subunits to accommodate adoption over a wide variety of engine sizes. We have opted to integrate the HHX and the TEC dielectric by developing a method to print and fire a high-temperature, stable glass-ceramic coating on the surface of the HHX. Onto this coating we can print and fire metallic thick films that create anchor points for the attaching the TE elements. This approach eliminates the interface found in a conventional TEG design that needs high levels of compressive force to achieve good thermal contact between the HHX and the opposing surface of the TE modules. Eliminating this allows us to evenly distribute the TE elements over the HHX surface, leading to more uniform temperature distribution. Further, eliminating the clamping requirements reduced the size of the HHX by 40% to 50% without loss of effectiveness and reduced the weight of the cold side heat exchanger by more than 90%. Figure 1a shows a computer-aided drafting (CAD) rendering of the redesigned subunit including the heat exchanger, the printed dielectric and metallic thick films, the TE element array, and the isolation shield. Figure 1b is a picture of a HHX that has been coated with high temperature dielectric and metallic thick films. Figure 1c shows the overall generator design with five subunits. This approach to TEG integration was a new idea for us, and it required several aspects be proven out, first at the coupon level and then at a full subunit-scale.

We have demonstrated that the dielectric coating and accompanying metallic thick films are chemically stable at high temperature (600°C) and that the coatings can be applied to the full heat exchanger area while retaining their electrically insulating nature and remaining robust to thermal shock. We have further demonstrated that the TE elements can be joined to this coating using low temperature (250°C) and high pressure (10 MPa) sintering conditions. Figure 2a shows an array of 520 skutterudite TE elements after the joining operation. Figure 2b

shows the same array after the cold side circuit has been attached. Alternating current resistance measurements performed on the entire array finds it to be 390–400 mΩ, and this is within 7% or 8% of the value predicted for just the TE materials in the array. We can conclude that

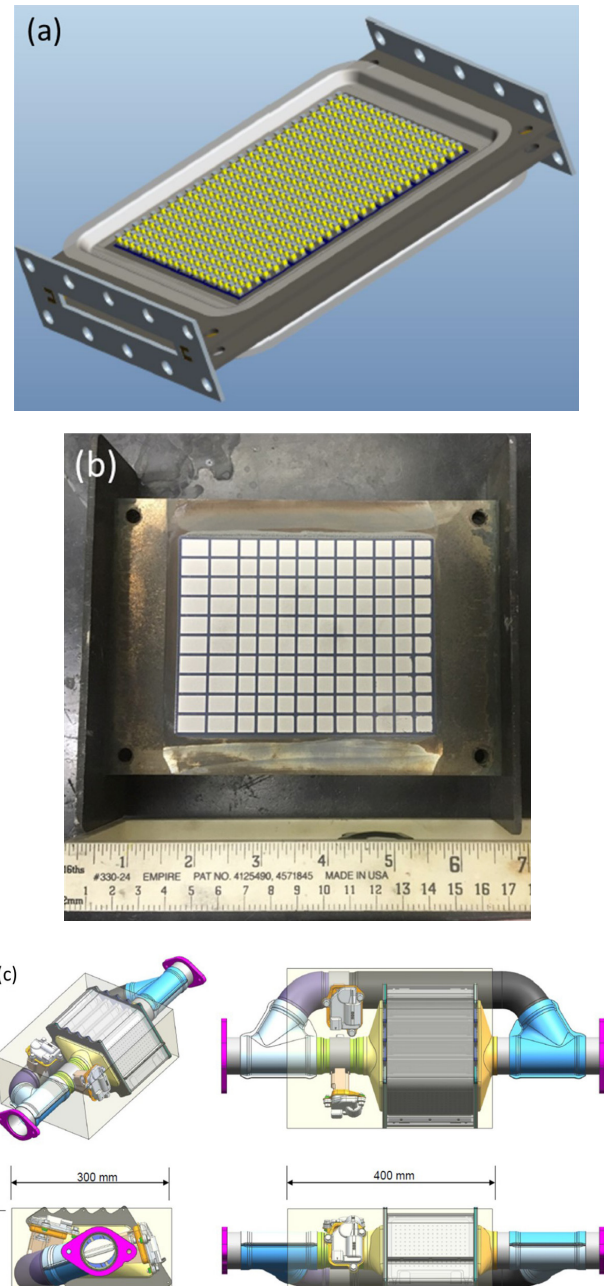


Figure 1. (a) CAD rendering of the HHX with dielectric coating and TE element array shown. (b) Photograph of the HHXs with the dielectric and metal thick films deposited on the surface. (c) CAD rendering of the TEG system composed of five subunits, the inlet and outlet manifolds for the exhaust gas, and the bypass channel.

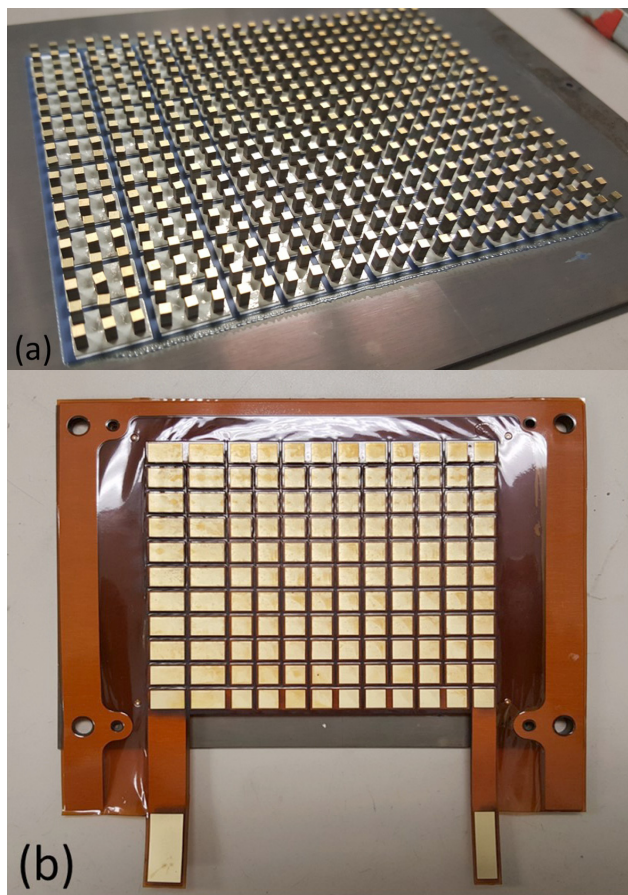


Figure 2. (a) Photograph of a heat exchanger plate section that is the subunit size. The photo shows a 520-element array after they have been affixed to the deposited metal interconnects. (b) Photograph of the same array after the cold side interconnecting circuit has been attached.

the electrical contact resistance with the array is small and that the joining technique we have developed in the last year is suitable for this application. We continue to fabricate the cold side heat exchangers and several other components to complete the prototype build. In step with this build is cost modeling and analysis to establish the range of system costs.

In the past year, we have acquired a demonstration vehicle for TEG integration, we have modified it to accept the generator system, and we have conducted a baseline analysis of the coolant and exhaust gas temperatures and flowrates. We used these measured values as inputs to our validated generator model to assess the power output over the Environmental Protection Agency test cycles including the Federal Test Procedure (FTP) city and highway cycles and the US06 Supplementary FTP cycle. The projected power output for these cycles is shown in

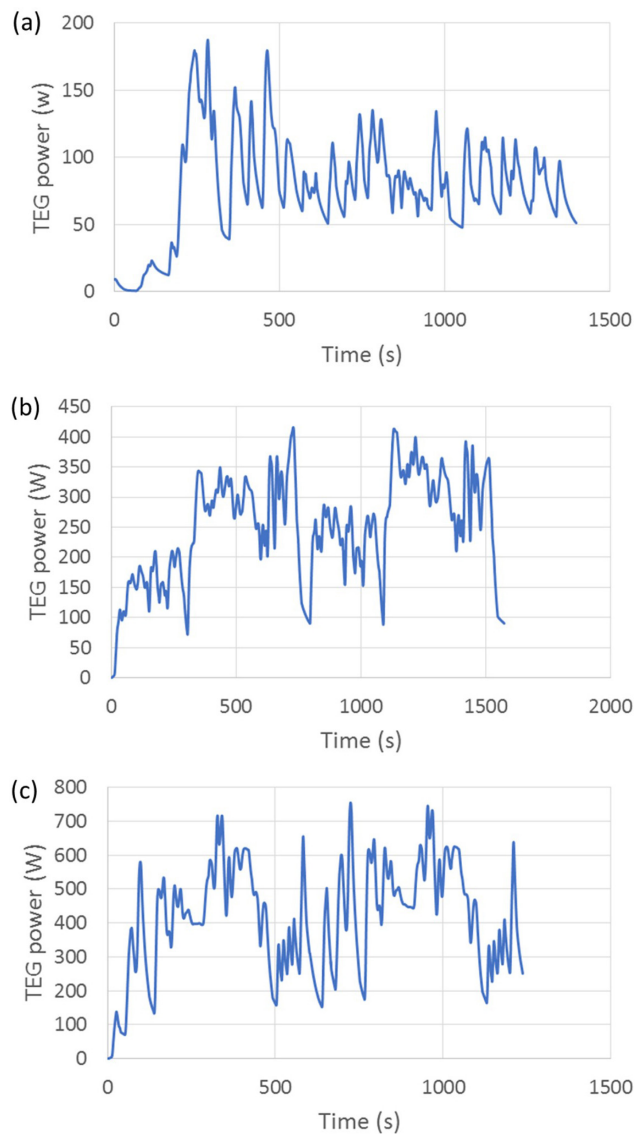


Figure 3. Plots of expected power out of the TEG after power conditioning via DC-to-DC converter for the (a) FTP-75 city cycle, (b) FTP-75 highway cycle, and (c) the US06 cycle. For both the FTP highway and US06, two cycles are shown. The first is a preparatory cycle, and the second is the test cycle.

Figures 3a, 3b, and 3c, respectively. In all cases, a 20% loss has been imposed to account for the efficiencies of the DC-to-DC converter. Using a unified vehicle model, the computed power output of the TEG was input as a supplemental power to the vehicle electrical bus, and the reduction in fuel consumption was estimated.

## Conclusions

- We have completely redesigned our TEG system to achieve much more highly integrated functionality to

improve gravimetric and volumetric energy density while significantly reducing cost.

- The high heat flux from the heat exchangers reduced TE materials requirements by 50%. This is enabled by integrating the heat TE converter system directly into the heat exchanger system.
- We have evaluated the dielectric and metallic thick films and find them to be chemically stable at high temperature and capable of effectively isolating current carried in the TE converter array from the heat exchangers. The joining between the TE elements and the cold side circuit and hot side interconnects is highly mechanically robust.
- Integrated TEG–vehicle modelling indicates that the TEG will improve FE by 0.23 mpg combined, based on the electrical power provided. Active thermal warm-up will increase its effectiveness to decrease CO<sub>2</sub> emissions and improve FE.

## References

1. (a) X. Shi, H. Kong, C.P. Li, C. Uher, J. Yang, J.R. Salvador, H. Wang, L. Chen, W. Zhang, *Appl. Phys. Lett.* 2008, 92, 182101; (b) X. Shi, J. Yang, J.R. Salvador, M.F. Chi, J.Y. Cho, H. Wang, G.Q. Bai, J.H. Yang, W.Q. Zhang, L.D. Chen, *J. Amer. Chem. Soc.* 133(20), 7837 (2011).
2. Purdue’s thermal resistance measurements using a photoacoustic technique showed thermal resistances as low as 1.7 mm<sup>2</sup> kW<sup>-1</sup> for bonded VACNT films 25–30 μm in length and 10 mm<sup>2</sup> kW<sup>-1</sup> for CNTs up to 130 μm in length. See: R. Cross, B.A. Cola, T.S. Fisher, S. Graham, *Nanotechnology*, 2010, 21, 445705.
3. T. Caillat “Advanced High-Temperature Thermoelectric Devices” DOE Thermoelectrics Applications Workshop, San Diego, 29 September 2009.
2. Invited Talk: J.R. Salvador. Overview of Thermoelectric Module Measurements at DARPA MATRIX Workshop, Arlington VA, December 9, 2015.
3. Invited Talk: J.R. Salvador et.al. Skutterudites, Materials Modules and Systems Invited Talk at 251st American Chemical Society National Meeting, San Diego, CA, March 16, 2016.
4. Invited Talk: A. Thompson, J. Sharp, J.R. Salvador and Hsin Wang Interagency Workshop on Metrology, Standards, and Data Validation for Energy Conversion Materials, NIST Gaithersburg, MD, November 20, 2015.
5. H. Wang, M.J. Kirkham, T.R. Watkins and E.A. Payzant, J.R. Salvador, A.J. Thompson and J. Sharp, David Brown and David Miller, Neutron and X-ray Powder Diffraction Study of Skutterudite Thermoelectrics, Powder Diffraction, Powder Diffraction, 31(1) pp16–22, March 2016.
6. B. Duan, J. Yang, J.R. Salvador, Y. He, B. Zhao, S.Y. Wang, P. Wei, F.S. Ohuchi, W.Q. Zhang, R.P. Hermann, O. Gourdon, S.X. Mao, Y. Cheng, C. Wang, J. Li, P. Zhai, X.F. tang, Q. Zhang, and J. Yang, Electro Negative Guests in CoSb<sub>3</sub>, *Energy and Environmental Science* DOI: 10.1039/c6ee00322b.
7. S. Wang, P. Wie, B. Duan, J. Yang, J.R. Salvador, and J. Yang, High performance n-type YbxCo4Sb12: from partially filled skutterudites towards composite thermoelectrics, *Nature Asia Materials* doi: 10.1038/am.2016.77.
8. Huang, S., and Xu, X., 2016, Parametric Optimization of Thermoelectric Generators for Waste Heat Recovery, *J. of Electronic Materials*, DOI: 10.1007/s11664-016-4740-x.
9. X. Shi, J. Yang, Lijun Wu, J.R. Salvador, W.L. Villaire, C. Zhang, D. Haddad, J. Yang, Y. Zhu, and Q. Li, Band Structure Engineering and Thermoelectric Properties of Charge-Compensated Filled Skutterudites, *Scientific Reports*, *Sci. Rep.* 5, 14641; doi: 10.1038/srep14641 2015.

## FY 2016 Publications/Presentations

1. Invited Talk: H. Wang and K. Leonard, Effect of High Fluence Neutron Irradiation on Transport Properties of Thermoelectrics, International Thermoelectrics Conference (ICT2016) Wuhan, China, May 29 – June 2, 2016

## VI. Index of Primary Contacts

### A

Agrawal, Ajay K.	195
Amar, Pascal	289

### B

Busch, Stephen	21
----------------	----

### C

Carrington, David B.	81
Ciatti, Stephen A.	92
Confer, Keith	298
Crocker, Mark	283
Curran, Scott J.	104

### D

Dec, John E.	36
Dibble, Robert W.	140

### E

Edwards, K. Dean	88
Ekoto, Isaac W.	42
Epling, William	279

### F

Filipi, Zoran	157
---------------	-----

### G

Gao, Feng	227
Gao, Pu-Xian	267
Genzale, Caroline L.	208
Goldsborough, S. Scott	63

### H

Haworth, Daniel C.	164, 175
--------------------	----------

**I**

Ihme, Matthias ..... 136

**J**

Jovovic, Vladimir ..... 327

**K**

Karkamkar, Abhi ..... 264

Kaul, Brian C. ..... 100

Kim, Seung Hyun ..... 199

Kocher, Lyle ..... 322

Kokjohn, Sage ..... 190

**L**

Lee, Chia-Fon F. ..... 172, 179

Lee, Seong-Young ..... 125, 183

Lu, Tianfeng ..... 150

**M**

McNenly, Matthew ..... 76

Mendler, Charles ..... 314

Musculus, Mark P.B. ..... 26

**O**

Ofelelein, Joseph C. ..... 59

**P**

Parks, Jim ..... 245

Partridge, Bill ..... 115, 250

Pfefferle, Lisa ..... 167

Pickett, Lyle M. ..... 32

Pihl, Josh ..... 214

Pitz, William J. ..... 68

Powell, Christopher F. ..... 54

**R**

Ribeiro, Fabio H.....	274
Ryan, Emily .....	203

**S**

Salvador, James R .....	331
Sappok, Alexander .....	303
Scarcelli, Riccardo .....	96
Sczomak, David P .....	318
Seong, Hee Je .....	255
Som, Sibendu .....	46
Stewart, Mark .....	259
Subramanian, Swami .....	310
Szanyi, János.....	232
Szybist, James P.....	109

**T**

Toops, Todd J.....	119, 237
Toulson, Elisa .....	145

**W**

Wang, Yong.....	220
White, Christopher .....	131
Whitesides, Russell.....	72

**Z**

Zukouski, Russell .....	293
-------------------------	-----

## VII. Project Listings by Organization

### Argonne National Laboratory

II.6	Advancements in Fuel Spray and Combustion Modeling with High Performance Computing Resources . . . . .	46
II.7	Fuel Injection and Spray Research Using X-Ray Diagnostics . . . . .	54
II.9	RCM Studies to Enable Gasoline-Relevant Low Temperature Combustion . . . . .	63
II.15	Use of Low Cetane Fuel to Enable Low Temperature Combustion . . . . .	92
II.16	High Efficiency GDI Engine Research . . . . .	96
III.8	Ash-Durable Catalyzed Filters for Gasoline Direct Injection (DGI) Engines . . . . .	255

### Boston University

II.38	Development and Multiscale Validation of Euler-Lagrange-Based Computational Methods for Modeling Cavitation Within Fuel Injectors . . . . .	203
-------	---	-----

### Clemson University

II.28	NSF/DOE Partnership on Advanced Combustion Engines: Thermal Barrier Coatings for the LTC Engine – Heat Loss, Combustion, Thermal vs. Catalytic Effects, Emissions, and Exhaust Heat . . . . .	157
-------	---	-----

### Cummins Inc.

IV.8	Enabling Technologies for Heavy-Duty Vehicles – Cummins 55% BTE . . . . .	322
------	---	-----

### Delphi

IV.3	Ultra-Efficient Light-Duty Powertrain with Gasoline Low Temperature Combustion . . . . .	298
------	--	-----

### Eaton

IV.5	Affordable Rankine Cycle . . . . .	310
------	------------------------------------	-----

### Envera LLC

IV.6	High Efficiency Variable Compression Ratio Engine with Variable Valve Actuation and New Supercharging Technology: VCR Technology for the 2020 to 2025 Market Space . . . . .	314
------	--	-----

### Filter Sensing Technologies, Inc.

IV.4	Improved Fuel Efficiency Through Adaptive Radio Frequency Controls and Diagnostics for Advanced Catalyst Systems . . . . .	303
------	--	-----

### General Motors

IV.7	Lean Miller Cycle System Development for Light-Duty Vehicles . . . . .	318
V.2	Development of Cost-Competitive Advanced Thermoelectric Generators for Direct Conversion of Vehicle Waste Heat into Useful Electrical Power . . . . .	331

**Gentherm**

V.1	Gentherm Thermoelectric Waste Heat Recovery Project for Passenger Vehicles	327
-----	--	-----

**Georgia Institute of Technology**

II.39	Development and Validation of a Turbulent Liquid Spray Atomization for Submodel for Diesel Engine Simulations	208
-------	---	-----

**Lawrence Livermore National Laboratory**

II.10	Chemical Kinetic Models for Advanced Engine Combustion	68
II.11	Model Development and Analysis of Clean and Efficient Engine Combustion	72
II.12	Improved Solvers for Advanced Combustion Engine Simulation	76

**Los Alamos National Laboratory**

II.13	2016 KIVA-hpFE Development: A Robust and Accurate Engine Modeling Software	81
-------	--	----

**Michigan State University**

II.26	Progress Report: NSF/DOE Partnership on Advanced Combustion Engines – Modeling and Experiments of a Novel Controllable Cavity Turbulent Jet Ignition System.	145
-------	--	-----

**Michigan Technological University**

II.22	Ignition and Combustion Characteristics of Transportation Fuels under Lean-Burn Conditions for Advanced Engine Concepts	125
II.34	Evaporation Submodel Development for Volume of Fluid (eVOF) Method Applicable to Spray-Wall Interaction Including Characteristics with Validation	183

**Navistar, Inc**

IV.2	Navistar SuperTruck Advanced Combustion Development	293
------	---	-----

**Oak Ridge National Laboratory**

II.14	Accelerating Predictive Simulation of Internal Combustion Engines with High Performance Computing	88
II.17	High Dilution Stoichiometric Gasoline Direct-Injection (GDI) Combustion Control Development	100
II.18	High Efficiency Clean Combustion in Light-Duty Multi-Cylinder Engines	104
II.19	Stretch Efficiency – Exploiting New Combustion Regimes	109
II.20	Cummins-ORNL Combustion CRADA: Characterization and Reduction of Combustion Variations	115
II.21	Neutron Radiography of Advanced Transportation Technologies	119
III.1	Joint Development and Coordination of Emission Control Data and Models: Cross-Cut Lean Exhaust Emissions Reduction Simulations (CLEERS) Analysis and Coordination	214
III.5	Low Temperature Emissions Control	237
III.6	Emissions Control for Lean-Gasoline Engines	245

## **Oak Ridge National Laboratory (Continued)**

III.7	Cummins-ORNL SmartCatalyst CRADA: NO <sub>x</sub> Control and Measurement Technology for Heavy-Duty Diesel Engines .....	250
-------	--	-----

## **The Ohio State University**

II.37	Development of a Physics-Based Combustion Model for Engine Knock Prediction .....	199
-------	---	-----

## **The Pacific Northwest National Laboratory**

III.2	CLEERS Aftertreatment Modeling and Analysis .....	220
III.3	Enhanced High and Low Temperature Performance of NO <sub>x</sub> Reduction Catalyst Materials .....	227
III.4	Thermally Stable Ultra-Low Temperature Oxidation Catalysts .....	232
III.9	Fuel-Neutral Studies of PM Transportation Emissions .....	259
III.10	Next-Generation SCR Dosing System Investigation .....	264

## **Pennsylvania State University**

II.29	Radiation Heat Transfer and Turbulent Fluctuations in IC Engines – Toward Predictive Models to Enable High Efficiency .....	164
II.32	Development and Validation of Predictive Models for In-Cylinder Radiation and Wall Heat Transfer .....	175

## **Purdue University**

III.12	NSF/DOE Advanced Combustion Engines: Collaborative Research: GOALI: Understanding NO <sub>x</sub> SCR Mechanism and Activity on Cu/Chabazite Structures Throughout the Catalyst Life Cycle .....	274
--------	--	-----

## **Sandia National Laboratories**

II.1	Light-Duty Diesel Combustion .....	21
II.2	Heavy-Duty Low-Temperature and Diesel Combustion & Heavy-Duty Combustion Modeling .....	26
II.3	Spray Combustion Cross-Cut Engine Research .....	32
II.4	Low-Temperature Gasoline Combustion (LTGC) Engine Research .....	36
II.5	Gasoline Combustion Fundamentals .....	42
II.8	Large Eddy Simulation Applied to Advanced Engine Combustion Research .....	59

## **Stanford University**

II.24	Development of a Dynamic Wall Layer Model for LES of Internal Combustion Engines .....	136
-------	--	-----

## **University of Alabama**

II.36	Development and Validation of Physics-Based Sub-Models of High Pressure Supercritical Fuel Injection at Diesel Conditions .....	195
-------	---	-----

## University of California, Berkeley

II.25	Collaborative Research: NSF/DOE Partnership on Advanced Combustion Engines: Advancing Low Temperature Combustion and Lean Burning Engines for Light- and Heavy-Duty Vehicles with Advanced Ignition Systems and Fuel Stratification . . . . .	140
-------	---	-----

## University of Connecticut

II.27	Collaborative Research: NSF/DOE Partnership on Advanced Combustion Engines: A Universal Combustion Model to Predict Premixed and Non-Premixed Turbulent Flames in Compression Ignition Engines . . . . .	150
III.11	Metal Oxide-Based Nano-Array Catalysts for Low Temperature Diesel Oxidation . . . . .	267

## University of Houston

III.13	Tailoring Catalyst Composition and Architecture for Conversion of Pollutants from Low Temperature Diesel Combustion Engines . . . . .	279
--------	---	-----

## University of Illinois at Urbana-Champaign

II.31	Micro-Jet Enhanced Ignition with a Variable Orifice Fuel Injector for High Efficiency Lean-Burn Combustion . . . . .	172
II.33	Model Development for Multi-Component Fuel Vaporization and Flash Boiling . . . . .	179

## University of Kentucky

III.14	Low Temperature NO <sub>x</sub> Storage and Reduction Using Engineered Materials . . . . .	283
--------	--	-----

## University of New Hampshire

II.23	A Comprehensive Investigation of Unsteady Reciprocating Effects on Near-Wall Heat Transfer in Engines . . . . .	131
-------	---	-----

## University of Wisconsin

II.35	Development and Validation of a Lagrangian Soot Model Considering Detailed Gas Phase Kinetics and Surface Chemistry . . . . .	190
-------	---	-----

## Volvo Group Trucks North America

IV.1	Volvo SuperTruck Powertrain Technologies for Efficiency Improvement . . . . .	289
------	---	-----

## Yale University

II.30	Sooting Behavior of Conventional and Renewable Diesel Fuel Compounds and Mixtures . . . . .	167
-------	---	-----

(This page intentionally left blank)



Energy Efficiency &  
Renewable Energy

For more information, visit: [energy.gov/eere/vehicles](http://energy.gov/eere/vehicles)

DOE/EE-1506 • July 2017